Changes in tropical ecosystem productivity as a result of altered climate and fire regimes



Francisco Navarro Rosales

Wolfson College

University of Oxford

A thesis submitted for the degree of

Doctor of Philosophy

Hilary Term 2026

This thesis is dedicated to my mother, Magdalena Rosales Jerez.

For her unwavering love and support for me and my sister.

Thank you for always taking care of us,

And for helping shape the person I have become.

And to the memory of Marcelo Leandro Feitosa de Andrade,

Analista Ambiental, chefe e brigadista da Estação Ecológica da Serra das Araras.

For his friendship and hospitality, and for his dedication to social and environmental leadership.

Thank you, Marcelo. We will continue forward; this is but part of your legacy.

Abstract

Tropical forests and savanna ecosystems play a fundamental role in maintaining and supporting biological diversity and ecosystem services. Tropical ecosystems regulate climatic processes by actively sequestering atmospheric carbon into plant structures, a process known as net primary productivity (NPP). However, anthropogenic impacts are increasingly threatening long-term carbon stability across tropical regions. In this context, understanding how shifting climates and fire regimes affect productivity dynamics will allow for better management strategies that optimise climate mitigation and ecosystem conservation under global change. Focusing on Brazilian Cerrado savannas and Bornean dipterocarp rainforests and taking advantage of long-term monitoring datasets, this thesis studies NPP responses to extreme climate events and altered fire regimes, investigating how these changes are influenced by plant functional traits. This objective was addressed in three data chapters. In **Chapter 3 (Research Paper 1)**, I investigate how annual, biennial and triennial fires influence different productivity and respiration fluxes within Cerrado savannas. Individual fluxes were then scaled up to ecosystem-level impacts on productivity and plant carbon expenditure. Repeatedly burning Cerrado vegetation limits woody encroachment and reduces NPP, carbon use efficiency and carbon uptake. Overall, more intense fires had stronger impacts on productivity. In **Chapter 4 (Research Paper 2)**, I focused on woody stem productivity dynamics of Cerrado vegetation in more detail, using tree inventory and functional trait data to reveal that generalist species dominate ecosystem NPP under fire suppression, but are replaced by savanna specialists after burning. After intense fires, bark protection and light-adapted photosynthesis maintain woody stem productivity. In **Chapter 5 (Research Paper 3)**, I sought to explore whether productivity-stressor-trait interactions remain comparable across ecosystems and drivers of change, investigating stem NPP responses to long-term climate variation in lowland dipterocarp forests. Extremes of temperature and drought constrained productivity in old-growth forests. In the logged forest, faster photosynthetic rates and higher concentrations of foliar nitrogen were associated with more productive species that were more sensitive to heat and drought extremes. This thesis shows that the productivity of lowland dipterocarp rainforests and Cerrado savannas is strongly influenced by changing climate and fire regimes. In both ecosystems, traits associated with stress tolerance and resource acquisition play an important role in supporting NPP dynamics in a context of global change. Photosynthetic rates are identified as useful predictors of NPP across environmental contexts, and periodic burning and enrichment planting are revealed to be efficient strategies for restoring carbon cycling and ecosystem functioning in savannas and forests, respectively.

Resumo

As florestas e as savanas desempenham um papel fundamental no suporte da biodiversidade e dos serviços ecossistêmicos. Esses ecossistemas tropicais regulam as mudanças climáticas ao absorver carbono atmosférico em estruturas vegetais, um processo conhecido como produtividade primária líquida (PPL). No entanto, a estabilidade do carbono em ecossistemas tropicais está cada vez mais ameaçada. Nesse contexto, uma melhor compreensão dos impactos das mudanças do clima e dos regimes de fogo na produtividade vegetal permitirá desenvolver melhores estratégias de manejo capazes de otimizar a mitigação climática e a conservação dos ecossistemas. Com foco nas savanas do Cerrado brasileiro e nas florestas de dipterocarpos de Bornéu, e utilizando dados de monitoramento de longo prazo, esta tese investiga como a PPL responde aos eventos climáticos extremos e a mudanças na frequência de queimas. Também analisamos como essas respostas são influenciadas pelos traços funcionais das plantas. Esse objetivo foi abordado em três capítulos. No **Capítulo 3 (Artigo 1)**, investigamos como queimas anuais, bienais e trienais influenciam diferentes fluxos de produtividade e respiração nas savanas do Cerrado. Esses fluxos foram então utilizados para calcular impactos ao nível do ecossistema. A ocorrência repetida de fogo limita a expansão de espécies lenhosas e reduz a PPL total, a respiração, e a eficiência do uso do carbono. Queimas mais intensas apresentaram impactos mais fortes sobre a dinâmica de produtividade. No **Capítulo 4 (Artigo 2)**, aprofundamos na análise da PPL lenhosa de árvores do Cerrado, utilizando dados de inventário florestal e traços funcionais. Os resultados mostram que espécies generalistas dominam a PPL do ecossistema sob supressão do fogo, mas são substituídas por espécies de savana após as queimas. Após fogos mais intensos, uma maior proteção de casca e uma fotossíntese adaptada à grande luminosidade ajudam a manter a produtividade arbórea. No **Capítulo 5 (Artigo 3)**, investigamos se as interações entre produtividade e traços funcionais são comparáveis em diferentes ecossistemas, analisando como a PPL lenhosa em florestas de dipterocarpos responde a mudanças no clima. Extremos de temperatura e seca limitaram a produtividade em florestas primárias. Em florestas exploradas, maiores taxas fotossintéticas e maiores concentrações de nitrogênio foliar estiveram associadas a espécies mais produtivas, porém mais sensíveis a extremos de calor e seca. Esta tese demonstra que a produtividade de florestas e savanas tropicais é fortemente influenciada por mudanças climáticas e regimes de fogo. Em ambos os ecossistemas, traços associados à tolerância ao estresse e à aquisição de recursos desempenham um papel importante na sustentação da PPL, sendo as taxas fotossintéticas preditoras da PPL em diferentes contextos ambientais. Em suma, o uso controlado do fogo e o plantio de mudas são apontados como estratégias eficazes para restaurar o ciclo do carbono e o funcionamento dos ecossistemas em savanas e florestas, respectivamente.

Abstrak

Hutan tropika dan ekosistem savana memainkan peranan asas dalam mengekalkan dan menyokong kepelbagaian biologi serta perkhidmatan ekosistem. Ekosistem tropika mengawal proses iklim dengan menyerap karbon atmosfera ke dalam struktur tumbuhan secara aktif, suatu proses yang dikenali sebagai produktiviti primer bersih (NPP). Walau bagaimanapun, impak antropogenik semakin mengancam kestabilan karbon jangka panjang di kawasan tropika. Dalam konteks ini, pemahaman perubahan iklim dan rejim kebakaran mempengaruhi dinamik produktiviti akan membolehkan strategi pengurusan yang lebih baik untuk mitigasi iklim dan pemuliharaan ekosistem yang optimal untuk menghadapi ancaman perubahan iklim. Dengan memberi tumpuan kepada savana Cerrado di Brazil dan hutan hujan dipterokarpa di Borneo, serta mengguna data pemantauan jangka panjang, tesis ini mengkaji tindak balas NPP terhadap kejadian iklim ekstrem dan perubahan rejim kebakaran, serta meneliti bagaimana perubahan ini dipengaruhi oleh ciri-ciri fungsi tumbuhan. Objektif ini dicapai melalui tiga bab berasaskan data. Dalam **Bab 3 (Kertas Penyelidikan 1)**, saya mengkaji bagaimana kebakaran tahunan, dwitahunan dan tiga tahunan mempengaruhi pelbagai aliran produktiviti dan respirasi dalam savana Cerrado. Aliran individu ini kemudiannya diskala kepada peringkat ekosistem untuk mengkaji kesan terhadap produktiviti dan perbelanjaan karbon tumbuhan. Pembakaran berulang terhadap vegetasi Cerrado mengehadkan pencerobohan tumbuhan berkayu serta mengurangkan NPP, kecekapan penggunaan karbon dan penyerapan karbon. Secara keseluruhan, kebakaran yang lebih intensif memberi kesan yang lebih tinggi terhadap dinamik produktiviti. Dalam **Bab 4 (Kertas Penyelidikan 2)**, saya memberi tumpuan terperinci kepada dinamik produktiviti batang berkayu dalam vegetasi Cerrado, dengan menggunakan data inventori pokok dan ciri fungsi tumbuhan. Hasilnya menunjukkan bahawa spesies generalis mendominasi NPP ekosistem apabila kebakaran dihadkan, tetapi digantikan oleh spesies khusus savana selepas pembakaran. Selepas kebakaran yang intensif, perlindungan kulit batang dan fotosintesis yang disesuaikan dengan cahaya membantu mengekalkan produktiviti batang berkayu. Dalam **Bab 5 (Kertas Penyelidikan 3),** saya meneroka sama ada interaksi antara produktiviti, tekanan persekitaran dan ciri tumbuhan adalah konsisten merentasi ekosistem dan pemacu perubahan, dengan mengkaji tindak balas NPP terhadap variasi iklim jangka panjang dalam hutan dipterokarpa tanah rendah. Suhu ekstrem dan kemarau mengehadkan produktiviti di hutan tua. Dalam hutan yang telah dibalak, kadar fotosintesis yang lebih tinggi dan kepekatan nitrogen daun yang lebih tinggi dikaitkan dengan spesies yang lebih produktif tetapi lebih sensitif terhadap tekanan haba dan kemarau. Tesis ini menunjukkan bahawa produktiviti hutan hujan dipterokarpa tanah rendah dan savana Cerrado sangat dipengaruhi oleh perubahan iklim dan rejim kebakaran. Dalam kedua-dua ekosistem, ciri-ciri yang berkaitan dengan toleransi tekanan dan pemerolehan sumber memainkan peranan penting dalam menyokong dinamik NPP dalam konteks perubahan global. Kadar fotosintesis dikenal pasti sebagai peramal berguna bagi NPP merentasi pelbagai konteks persekitaran, manakala pembakaran berkala dan penanaman pengayaan dikenal pasti sebagai strategi yang berkesan untuk memulihkan kitaran karbon dan fungsi ekosistem masing-masing di savana dan hutan.

Acknowledgements

First and foremost, I would like to thank my supervisors, Andy Hector and Imma Oliveras Menor. Andy, thank you for being so open and enthusiastic about working together, for sharing all your ecological and statistical expertise, and for always being willing to go through my endless email requests and field risk assessments. Imma, thank you so much for supervising and supporting my work from afar, for all the priceless opportunities you have offered me, and for always encouraging me to become a better researcher and ecologist; working with you has been truly life-changing.

I am deeply grateful to my postdoc colleagues Wesley Jonatar Alves da Cruz, Manoela Machado and Eleanor Jackson, for their support in navigating (and surviving) fieldwork and academia. I could not have asked for better role models. This thesis would not have been possible without the rigorous and constant work of Prof. Maria Antonia Carniello, curator of the Herbário do Pantanal, and Flavio de Campos Oliveira, technician of the CERFogo project. I am incredibly grateful to the many students, interns and rangers from UNEMAT and ICMBio who have contributed to the project over the years. Similarly, I thank Mikey O'Brien, Chris Philipson and all the staff from the South East Asia Rainforest Research Partnership for their continued commitment and effort.

Thank you to the members of the DISCOLab research group, and to Carlota Segura-García, Gian Luca Spadoni and Tash Lutz for their friendship. And thank you to the AMAP Research Unit for their hospitality during my time in Montpellier. I am grateful to Yadvinder Malhi for welcoming me to the Ecosystems Lab; and thank you to Nikki, Erika, Jesus, Felipe, Viviane, Milton, Renata, André, Sruthi, Megha, Huanyuan, Xiongjie, Kerry and Kendall for making it such a fascinating and stimulating group. Thank you to the Plant-Ecology/Nature-Based-Solutions gals: Emily, Eleanor, Emma, Elvie, Lila and Aline for making these last months so much more enjoyable.

I would also like to thank my friends from Wolfson College and beyond, Madhu and Christine, Freddie and Sekoah, Cristina and James, Oisin and Nanuk, Laura, Estelle, Theodor, Shreya, Celia and Csabi, Tejo, Sam, Joel, Ivan and Clara for all the good moments during this journey. Thank you to Katie, Suzanne and Harry for reminding me about the wonders of nature conservation.

I am immensely grateful to my parents and my family for their constant care and support despite sacrifices and difficult choices, and for raising me to love nature and learning. Finally, I would like to thank my partner, Bruno, for his wonderful restlessness and loving encouragement, for inspiring me to protect the world around me, and for helping me give my best always.

To you all, truly, thank you!

Funding

This thesis has been funded by the Rafael del Pino Postgraduate Excellence Scholarship (2022). I thank the selection committee and the trustees of the Rafael del Pino Foundation for their trust and support in backing this doctoral research project. This work was also supported by an academic exchange to Montpellier, France, funded by the France Excellence Eiffel Scholarship Programme (2024) from the French Ministry for Europe and Foreign Affairs (Campus France), and by the University of Oxford through the Scatcherd European Scholarship (2024). I also thank Wolfson College, the University of Oxford Department of Biology, the Society of Experimental Biology and The Company of Biologists, the Royal Society of Biology, the Eurofins Foundation, and the British Ecological Society for their support in funding travel and matriculation costs for fieldwork, training courses, and research conferences in the context of this thesis. I am extremely grateful to my supervisor Andy Hector for personally funding my field research trip to Borneo.

The experimental fire and ecosystem monitoring project at Serra das Araras, Mato Grosso, Brazil, was funded by the University of Oxford (John Fell Fund 163/03), the UKRI Natural Environment Research Council (Standard Grant NE/W00058X/1), and the EU Marie Skłodowska-Curie Action awarded to FIRE-ADAPT (project no. 101086416), and logistically supported by the Universidade do Estado de Mato Grosso, the Instituto Chico Mendes de Conservação da Biodiversidade and the Herbário do Pantanal Vali Joana Pott. The Sabah Biodiversity Experiment is part of the Royal Society South East Asia Rainforest Research Programme (Project No. RS243), and was funded by the University of Zurich, The Natural Environment Research Council Centre for Population Biology, the Swiss National Science Foundation SNSF (grant 31003A-125461/1), the DEFRA Darwin Initiative (grant 16011), the Natural Environment Research Council (grant numbers NE/K016253/1 and NE/X000281/1), the Comunidad de Madrid (Atracción de Talento Investigador Fellowship 2018-T1/AMB-11095), and the Agencia Estatal de Investigación de España (Ramón y Cajal Fellowship RYC2021-032049-I); and has been logistically supported by the South East Asian Rainforest Research Partnership and the Sabah Forestry Department.

Copyright

© 2026 Francisco Navarro Rosales. No part of this thesis may be reproduced without proper acknowledgement. This thesis contains third-party material reproduced with permission from the original copyright holders, which may not be reused without permission from those holders.

Table of Contents

Abstract . . . . . **i**

Resumo . . . . . **ii**

Abstrak . . . . . **iii**

Acknowledgements . . . . . **iv**

Funding . . . . . **v**

Copyright . . . . . **v**

Table of Contents . . . . . **vii**

List of Abbreviations . . . . . **xii**

Chapter 1: Introduction **1**

1.1. Thesis rationale **1**

1.1.1. Tropical forests and savannas in a changing world **1**

1.1.2. Impacts of climate change and altered fire regimes on tropical forests and savannas: a key research priority **5**

1.2. Thesis aims and research framework **10**

1.3. Thesis structure **12**

1.4. References **15**

Chapter 2: Research Background **25**

2.1. On the impacts of extreme climate on tropical ecosystems **25**

2.2. On tropical ecosystem responses to altered fire regimes **30**

2.3. On productivity as a key indicator of ecosystem function **33**

2.4. On functional traits as a tool to assess productivity responses **38**

2.5. On Cerrado savannas and lowland dipterocarp rainforests **45**

2.6. References **51**

Chapter 3: Research Paper 1 . . . . . **71**

3.1. Graphical abstract **72**

3.2. Highlights **72**

3.3. Abstract **73**

3.4. Introduction **74**

3.5. Materials and methods **77**

3.5.1. Study site and experimental design **78**

3.5.2. Estimation of carbon fluxes **80**

3.5.3. Error analysis and propagation **84**

3.5.4. Statistical modelling and analysis **85**

3.6. Results **92**

3.6.1. Carbon flux changes over time and fire regime effects **92**

3.6.2. Importance of initial vegetation density **94**

3.6.3. Total net primary productivity, respiration, plant carbon expenditure and carbon use efficiency **94**

3.7. Discussion **95**

3.7.1. Fire reduces the strength of arboreal carbon fluxes **100**

3.7.2. Fire regime properties affect ecosystem components differently, warranting long-term monitoring **102**

3.7.3. Fire influences on carbon flux allocation, carbon use efficiency and ecosystem disequilibria **105**

3.8. Conclusions **107**

3.9. Acknowledgements **108**

3.10. Funding **109**

3.11. Data availability **109**

3.12. References **110**

3.13. Supplementary material **119**

3.13.1. Estimating leaf area index from fisheye lens canopy images **119**

3.13.2. Plot characterisation **121**

3.13.3. Statistical model outputs and pairwise comparisons **123**

3.13.4. Summaries of carbon fluxes and related variables **131**

Chapter 4: Research Paper 2 . . . . . **135**

4.1. Graphical abstract **136**

4.2. Abstract **137**

4.3. Background and aims **138**

4.4. Materials and methods **143**

4.4.1. Study site and experimental design **143**

4.4.2. Productivity, survival and mortality data **145**

4.4.3. Plant functional traits data **147**

4.4.4. Data analysis and statistical modelling **148**

4.4.4.1. Species contribution to plot-level productivity and mortality across fire regimes **148**

4.4.4.2. Changes in species-level stem productivity and survival rates across fire regimes **148**

4.4.4.3. Explaining species-level stem productivity and survival through functional traits **152**

4.5. Results **154**

4.5.1. Species contribution to plot-level productivity and mortality **154**

4.5.2. Fire regime changes in species-level stem productivity and survival **157**

4.5.3. Relating species stem productivity and survival to functional traits **161**

4.6. Discussion **163**

4.6.1. Contributions to NPP_{stem} and $C_{mortality}$ reveal hyperdominance of *Tachigali vulgaris* and reflect trends of encroachment vs openness **164**

4.6.2. Fire-driven changes in species-level NPP_{stem} reveal a trade-off between productivity and fire tolerance **167**

4.6.3. Thick bark and light-adapted photosynthesis maintain NPP_{stem} at triennial fire frequencies **170**

4.7. Conclusions **173**

4.8. Acknowledgements and funding **175**

4.9. Data availability **175**

4.10. References **176**

4.11. Supplementary material **188**

Chapter 5: Research Paper 3 . . . . . **211**

5.1. Abstract **212**

5.2. Introduction **213**

5.3. Materials and methods **217**

5.3.1. Study site and experimental design **217**

5.3.2. Seedling productivity and survival data **221**

5.3.3. Extreme climate data **223**

5.3.4. Functional traits data **226**

5.3.5. Data analysis and statistical modelling **227**

5.3.5.1. Examining seedling productivity and survival in old-growth and logged forest **227**

5.3.5.2. Investigating the effect of extreme climate on seedling productivity and survival **229**

5.3.5.3. Explaining vulnerability of productivity and survival through functional traits **230**

5.4. Results **231**

5.4.1. Productivity and survival in old-growth versus logged forest **232**

5.4.2. The effect of extreme climate on seedling productivity and survival **233**

5.4.3. Exploring climate vulnerability through functional traits **234**

5.5. Discussion **235**

5.5.1. Small seedlings were more productive in the old-growth forest; large seedlings in the logged forest **241**

5.5.2. Extreme heat and drought consistently constrain seedling stem productivity within the old-growth forest **243**

5.5.3. Resource-acquisitive species appear to be more sensitive to climate extremes in the logged forest **246**

5.6. Conclusions **249**

5.7. Acknowledgements **250**

5.8. Funding **250**

5.9. Data availability **250**

5.10. References **251**

5.11. Supplementary material **264**

5.11.1. Species list with updated nomenclature and available trait data **264**

5.11.2. Dealing with tree inventory data **265**

5.11.3. Exploring the effects of liana cutting on NPP_{stem} and survival **267**

5.11.4. Exploring trends in climate data **271**

5.11.5. Models examining NPP_{stem} and survival across forest types **275**

5.11.6. Models investigating the effect of climate on $Pr(NPP_{stem} > 0)$ **280**

5.11.7. Models investigating the effect of climate on $\log_{10}(NPP_{stem})$ **284**

5.11.8. Models investigating the effect of climate on Pr(survival > 0) **288**

5.11.9. Correlations between species random effects for Pr(NPPstem > 0) models and plant functional traits **292**

Chapter 6: Conclusions **293**

6.1. Results synthesis **293**

6.2. Research significance **295**

6.3. General discussion **297**

6.3.1. Productivity of Cerrado savannas versus dipterocarp forests **297**

6.3.2. Comparing NPP responses to changing climate and fire regimes **299**

6.3.3. The fast-slow spectrum as a major driver of stem productivity **303**

6.4. Outstanding questions and future research directions **306**

6.5. References **310**

List of Abbreviations

13C . . . . . foliar carbon-13 isotope concentration
AGB . . . . . aboveground biomass
AIC . . . . . Akaike Information Criterion
Amax . . . . . maximum leaf carbon assimilation rate
ANOVA . . . . . Analysis of Variance
Asat . . . . . light-saturated leaf carbon assimilation rate
BACI . . . . . before-after control-impact
BD . . . . . bark density
BWC . . . . . bark water content
C . . . . . carbon
CI . . . . . control-impact
CUE . . . . . carbon use efficiency
CWD . . . . . cumulative water deficit
D_{base} . . . . . basal diameter
DBH . . . . . diameter at breast height
Dresp . . . . . leaf dark respiration
DRYFLOR . . . . . Dry Tropical Forest Floristic Network
EGM . . . . . electronic gas analyser
EMBRAPA . . . . . Empresa Brasileira de Pesquisa Agropecuária
ENSO . . . . . El Niño Southern Oscillation
ESA . . . . . Estação Ecológica da Serra das Araras
ET . . . . . evapotranspiration
ForestGEO . . . . . Forest Global Earth Observatory Network
GEM . . . . . Global Ecosystems Monitoring Network
GLMMs . . . . . generalised linear mixed-effects models
GPP . . . . . gross primary productivity
H . . . . . tree height
HPAN . . . . . Herbário do Pantanal
IBGE . . . . . Instituto Brasileiro de Geografia e Estatística
IBT . . . . . inner bark thickness
ICMBio . . . . . Instituto Chico Mendes de Conservação da Biodiversidade
IPCC . . . . . Intergovernmental Panel on Climate Change
IRGA . . . . . infrared gas analyser
IUCN . . . . . International Union for Conservation of Nature

IUSS . . . . . International Union of Soil Sciences
LA . . . . . leaf area
LAI . . . . . leaf area index
LDMC . . . . . leaf dry matter content
LMA . . . . . leaf mass per area
LMMs . . . . . linear mixed-effects models
LT . . . . . leaf thickness
NEE . . . . . net ecosystem exchange
NEP . . . . . net ecosystem production
NERC . . . . . Natural Environment Research Council
Nperc . . . . . foliar nitrogen concentration
NPP . . . . . net primary productivity
OBT . . . . . outer bark thickness
P_{05} . . . . . 5^{th} percentile
P_{50} . . . . . 50^{th} percentile
P_{95} . . . . . 95^{th} percentile
PAI . . . . . plant area index
PCA . . . . . principal component analysis
PCE . . . . . plant carbon expenditure
PPT . . . . . precipitation
R . . . . . respiration
RAINFOR . . . . . Rede Amazônica de Inventários Florestais
rBT . . . . . relative bark thickness
RH_{14} . . . . . relative humidity at 14:00
SAI . . . . . stem area index
SEARRP . . . . . Southeast Asia Rainforest Research Partnership
SEOSAW . . . . . Socio-Ecological Observatory for the Southern African Woodlands
SLA . . . . . specific leaf area
SRC . . . . . soil respiration chamber
STol . . . . . photosynthetic shade tolerance
SVP . . . . . saturation vapour pressure
T_{max} . . . . . maximum daily temperature
UKRI . . . . . United Kingdom Research and Innovation
UNEMAT . . . . . Universidade do Estado de Mato Grosso
VPD . . . . . vapour pressure deficit
WD . . . . . wood density
WRB . . . . . World Reference Base for Soil Resources

Chapter 1: Introduction

1.1. Thesis rationale

1.1.1. Tropical forests and savannas in a changing world

Tropical forests and savanna ecosystems play a fundamental role in the functioning of the Earth system. They are reservoirs of huge biological diversity, containing more than 75% of taxa such as terrestrial birds and mammals, amphibians, freshwater fish and flowering plants (Barlow *et al*., 2018). Beyond taxonomic richness, tropical ecosystems hold extensive functional and phylogenetic diversity which supports ecosystem processes and contributes to the maintenance of ecological functioning under environmental change (Silver *et al*., 1996; Aguirre-Gutiérrez *et al*., 2022). The tropics are also important with regard to human habitation, since approximately 40% of the world's population is located in tropical areas (Marcotullio *et al*., 2021). In terms of Nature's contribution to people, tropical systems can be framed as sources of key ecosystem services, not just for tropical communities and nations – which are disproportionately vulnerable in socioeconomic terms – but also for the entire global population (van der Hoff *et al*., 2022; Aguirre-Gutiérrez *et al*., 2023). Tropical ecosystems support livelihoods by providing food and marketable products (Woollen *et al*., 2016; Cuni-Sanchez *et al*., 2019) and by sustaining agriculture, fisheries, and nature-based markets, as well as holding cultural, spiritual, and relational significance for indigenous and local communities (Ryan *et al*., 2016; Reed *et al*., 2017). In addition, tropical ecosystems deliver key regulating services – such as pollination, water cycling and soil stabilisation – that underpin food security and maintain regional and global economies (Hipólito *et al*., 2019; Rodrigues *et al*., 2021; Borma *et al*., 2022).

Tropical forests and savannas also have a central role in the global carbon cycle. By actively sequestering atmospheric carbon dioxide, these ecosystems control atmospheric concentrations of greenhouse gases and regulate global circulation and climatic processes (Pan *et al*., 2011). Together, tropical forests and savannas account for ~60% of global gross primary productivity (GPP), that is, the total rate at which ecosystems sequester carbon via photosynthesis (Beer *et al*., 2010). Tropical forests and savannas each contribute to about one-third of terrestrial net primary productivity (NPP), describing the net rate of ecosystem carbon gain after discounting for losses via respiration (Malhi, 2012; Parr *et al*., 2014). Tropical forests store ~25% of the carbon in the terrestrial biosphere (Bonan, 2008; Baccini *et al*., 2012), whilst savannas maintain ~15% of biospheric carbon (Grace *et al*., 2006; Parr *et al*., 2014). Despite broad similarities, important differences in carbon cycling distinguish tropical forests and savannas. In savannas, frequent fire constitutes a major pathway of carbon release to the atmosphere, reducing the overall carbon sink strength (Grace *et al*., 2006; van der Werf *et al*., 2017). Whereas carbon in tropical forests is predominantly found in aboveground biomass, savanna carbon stocks are disproportionately allocated to belowground pools, particularly soils (Malhi, 2012; Zhou *et al*., 2023). These patterns reflect differences in the ecological processes and functional mechanisms that structure carbon allocation and turnover in forests and savannas, shaping how carbon is stored, cycled, and retained within each system (Oliveras & Malhi, 2016).

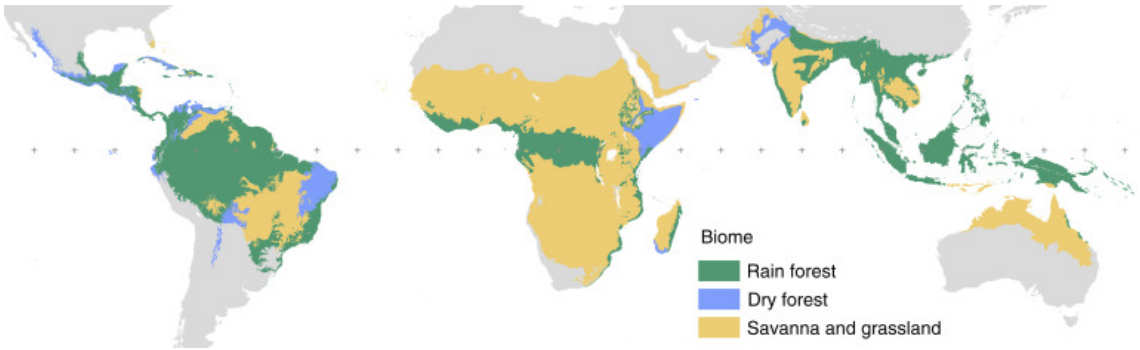


Figure 1.1, global map of tropical wet forests, savannas and dry forests. Reprinted from Current Biology, Vol. 28, Pennington RT, Lehmann CER, Rowland LM, Tropical savannas and dry forests, pp. R541–R545 (https://doi.org/10.1016/j.cub.2018.03.014), Copyright (2018) with permission from Elsevier.

Tropical forests and savannas differ fundamentally in terms of structure, disturbance regimes and plant functional strategies. Tropical forests can be classified into wet and dry forest types. Tropical wet forests generally occur where precipitation is greater than ~2000 mm annually, with little to moderate dry seasons, and are characterised by tall, closed evergreen canopies (Guan *et al*., 2015). Canopy structure in wet forests is typically complex and multi-layered, with emergent trees, a continuous upper canopy, sub-canopy layers, and a shaded understory (Gallery, 2014). Productivity is high, and ecological dynamics are driven by competition for light and nutrient resources, as well as biotic interactions such as herbivory and predation (Gallery, 2014). In contrast, tropical dry forests occur in regions with lower annual precipitation (typically 500-2000 mm) and pronounced dry seasons lasting several months (Pennington *et al*., 2018). These systems are characterised by shorter, sparser canopies and a high proportion of deciduous species that shed leaves during the dry season (Pennington *et al*., 2009). Water availability is the primary limiting factor, strongly constraining tree growth and shaping plant functional strategies (Murphy & Lugo, 1986). Tropical forests are structured by patch-scale disruptions (e.g., treefall gaps) and infrequent disturbances such as storms, and drought-induced mortality (Hunter *et al*., 2015; Siyum, 2020). Because closed canopies in wet and dry forests suppress grass growth, fire is typically rare, meaning wet and dry forests are considered to be sensitive to burning (Dexter *et al*., 2018).

Savannas, by comparison, are defined by a continuous C4 grass layer combined with a discontinuous tree layer, with tree densities ranging from fully open landscapes with sparse individuals to relatively dense woodlands (Lehmann & Parr, 2016). They support high diversity in the herbaceous layer, which often dominates ecosystem productivity and drives seasonal changes (Ratnam *et al*., 2011). Savannas are strongly influenced by frequent disturbances, particularly fire and/or herbivory, which limit tree cover and maintain an open landscape structure (Bond, 2021; Hoffmann *et al*., 2003). Ecological dynamics are characterised by strong grass-tree interactions and functional trade-offs, where allocation to growth, defence, and resprouting capacity determines persistence (Sankaran *et al*., 2005; Bond, 2008; Simon & Pennington, 2012). Fires in savannas are frequent and burnt area is extensive (Parr *et al*., 2014). Although biomass

burning in savannas accounts for a substantial proportion of fire-derived carbon emissions (above 60% globally according to van der Werf *et al*., 2017), rapid post-fire regrowth sustains carbon uptake and allows for a quick recovery of ecosystem productivity (Grace *et al*., 2006). In recent years, however, global patterns of burnt area are becoming increasingly variable, with extreme periods of flammability and emission anomalies across savanna regions (Kelley *et al*., 2025).

Broadly, tropical forests and savannas are distinguished at the (sub)continental scale as distinct biomes (**Figure 1.1**), that is, major vegetation formations with characteristic physical forms and ecological processes (Prentice *et al*., 1992). Historically, climate has been used to delimit biomes usually in terms of mean annual precipitation, seasonality and temperature (e.g., Holdridge, 1947; Whittaker, 1970). However, biomes are now understood as large-scale ecological units emerging from the interaction of climate, disturbance regimes, evolutionary history and biotic feedbacks (Mucina, 2019). In regions where climatic conditions allow for the existence of both forest and savanna ecosystems, factors such as fire regimes and soil properties play a critical role in shaping ecological filtering and vegetation structure (Pausas & Bond, 2020). Extensive areas of humid C4 savannas in South America and Africa have the climate potential to support closed-canopy forests, but are maintained as open systems by recurrent fire (Lehmann *et al*., 2014). Soil fertility may also determine the distribution of dry forests, typically found on less acidic soils than savannas, where higher nutrient availability supports tree growth and canopy closure, suppressing grasses and fire occurrence (Pennington *et al*., 2018). Together, these patterns highlight the critical role of ecosystem processes and vegetation feedbacks in maintaining structure and function in tropical ecosystems (Zuidema *et al*., 2013). However, environmental change is altering key ecological mechanisms and interactions, having far-reaching consequences for the stability, resilience, and long-term persistence of both forests and savannas (Edwards *et al*., 2019; Williams *et al*., 2022).

Anthropogenic impacts on tropical ecosystems are now pervasive and widespread at many scales, caused by a multitude of interacting drivers ranging from direct processes such as land clearance or timber harvesting to indirect ones like climatic changes and altered fire regimes (Malhi *et al*.,

2014; França *et al*., 2020). The dynamics of deforestation and land conversion have been an important research focus given the critical importance of maintaining tropical ecosystem function. Amazonian annual deforestation rates have remained above 5,000 km^2 over the last decade and annual degradation rates from fire, fragmentation and timber extraction have been estimated to reach even higher levels (Lapola *et al*., 2023). In Borneo, an estimated 18.7 million hectares (34%) of rainforest cover have been cleared between 1973 and 2015 (Gaveau *et al*., 2016); whilst native vegetation clearance of the Brazilian Cerrado has accelerated to alarming rates and accounts for more than 46% of the region (Bispo *et al*., 2024). It is important to highlight the multifaceted consequences of land conversion and degradation, leading not just to direct impacts in terms of carbon and biodiversity but also having the potential to reinforce change through climatic and fire feedbacks (**Figure 1.2**). For example, the pronounced (8-11%) reductions in annual precipitation in the southern Amazon basin can be primarily attributed to widespread deforestation over South America (Cui *et al*., 2026). Similarly, Chapman *et al*. (2020) showed conversion of Bornean forests to oil palm and plantations would result in a drier, warmer climate (4.6% less dry season rainfall, 0.39ºC temperature increase), exacerbating fire risk and El Niño intensity. In the Cerrado, temperatures have increased by 2-4ºC between the 1960s and the 2020s, and annual rainfall in some regions has decreased by 50% (Hofmann *et al*., 2021; Hofmann *et al*., 2023), with recent drought and fire seasons being unprecedented in the last 700 years (Stríkis et al., 2024). Shifts in climatic conditions and associated fire regimes are reshaping tropical forest and savanna systems, amplifying vulnerability and threatening long-term function and stability (França *et al*., 2020; Hantson *et al*., 2024).

1.1.2. Impacts of climate change and altered fire regimes on tropical forests and savannas: a key research priority

Tropical ecosystems globally are already facing altered climate and fire regime patterns; and extreme temperatures, droughts and fire events are expected to become more intense and

increasingly common (Deb *et al*., 2018; **Figure 1.2**). For example, Kahana *et al*. (2024) predicted precipitation will decline over most parts of Brazil by 2100, with a drier Amazonia experiencing less frequent but higher intensity rainfall events. In Malaysia, Loh *et al*. (2016) projected temperature increments of about 2-4ºC for different development scenarios, with increasing rainfall variability and a 20-40% decrease of rainfall during the dry season. Singo *et al*. (2023) predicted widespread temperature rises (between 4.5°C and 6°C) and monthly rainfall reductions (-20 mm) across South African savannas, whilst vapour pressure deficit (VPD) in the Cerrado is projected to surge by 30% and 60% under low and high emissions scenarios respectively by the end of the century (Cattelan *et al*., 2024). Under high-emission scenarios, large areas of tropical ecosystems are expected to shift to hot 'hypertropical' climates, that is, beyond temperature and humidity conditions currently recognised as equatorial climate (Chambers *et al*., 2026).

Climate change is also associated with critical shifts in fire regimes (Burton *et al*., 2024). Longer dry seasons and more extreme droughts and heatwaves are contributing to increasing fire size, intensity and frequency across tropical regions (Flannigan *et al*., 2013; Jolly *et al*., 2015). Human activities are similarly linked with increases in the flammability and number of ignitions, but also with landscape fragmentation, fuel discontinuity and fire suppression (Andela & van der Werf, 2014; Archibald, 2016). Brando *et al*. (2020) showed Amazonian fire regimes will intensify under low- and high-emission scenarios, and revealed climate change will double the area burned by wildfires by 2050. González *et al*. (2025) forecasted fire risks in Orinoco savannas could increase by 40% under low-mitigation scenarios. Fire events are predicted to become more frequent, severe and extensive in all biomes globally (except in grassland ecosystems) and the likelihood of fire regime change will increase with higher warming scenarios, leading to reductions in biodiversity, carbon storage, and other ecosystem services (Sayedi *et al*., 2024). Savanna regions worldwide are expected to continue experiencing widespread fire suppression (Moura *et al*., 2019). Because savannas are open ecosystems structured by frequent disturbance, altered fire regimes in the form of fire absence are also disrupting ecological processes and degrading savanna structure and function (Stevens *et al*., 2017).

Climate change and altered fire regimes are already affecting plant performance worldwide, primarily by constraining survival and regeneration (McDowell *et al*., 2018). Hotter conditions and more frequent droughts limit the resources and conditions needed for sustained functioning and biomass accumulation (Rifai *et al*., 2018). Low water availability and heat stress restrict photosynthetic activity, impair canopy development, shorten growing periods and reduce overall growth rates, and can ultimately lead to tissue dieback, topkill and plant death (Teskey *et al*., 2015). Fire also impacts plant growth and survival through direct combustion and heat damage to tissues, as well as increasing post-fire stress and vulnerability to drought, pests, and other disturbances (Brando *et al*., 2012; for more details on the impacts of extreme climate and fire on ecosystems see **Chapter 2**). It is important to note that although heat, drought, and fire stress are in principle harmful to plant tissue and functioning, they are integral parts of all ecosystems to varying degrees (Bond & Keeley, 2005; Allen *et al*., 2010). This means that ecosystems are generally adapted to extreme weather and fire events within their typical frequency, intensity, and extent (Seidl *et al*., 2017; Grau-Andrés *et al*., 2024). It is when climate and fire regime conditions deviate from these historical patterns that vegetation is driven beyond its natural capacity for recovery and resilience (Moss *et al*., 2024; Lindenmayer *et al*., 2025).

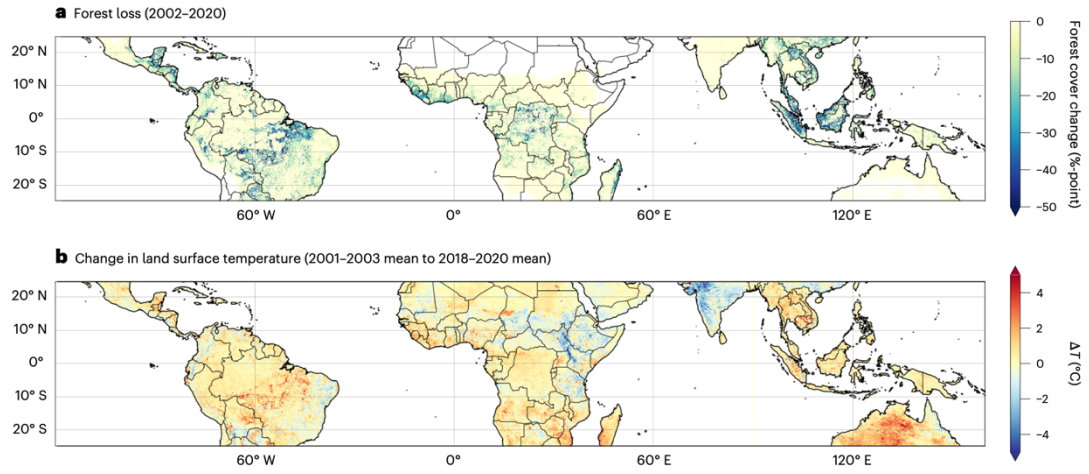


Figure 1.2, deforestation and surface warming across the tropics. **A**) percentage-point change in forest cover from 2001 to 2020. **B**) absolute change in annual mean land surface temperature (ΔT ºC) between the 2001–2003 mean and the 2018–2020 mean. Reproduced from Reddington *et al*., 2025, Tropical deforestation is associated with considerable heat-related mortality, Nature Climate Change, Vol. 15, pp. 992–999 (https://doi.org/10.1038/s41558-025-02411-0), under a Creative Commons Attribution 4.0 International License (http://creativecommons.org/licenses/by/4.0/). Please note panel C from the original image was cropped out of the figure.

As a result, lower rates of growth and survival reduce net primary productivity, thereby decreasing biomass accumulation (Bonal *et al*., 2016). At larger scales, this diminishes carbon uptake and storage in vegetation and soils (Anderegg *et al*., 2012). Reduced productivity, combined with increases in carbon emissions from fire and decomposition from dead stems, can shift ecosystems from functioning as carbon sinks to becoming intermittent or persistent carbon sources (Bonal *et al*., 2016). More intense warming, drying, and burning could therefore further reduce productivity and carbon storage in tropical forests and savannas through a self-reinforcing carbon feedback (Flores & Staal, 2022).

The impacts of climate and fire regime changes on the carbon dynamics and storage capacity of forest and savanna ecosystems are thus critically important, but still poorly understood (Hantson *et al*., 2024). Major uncertainties concern how repeated droughts, heatwaves, and altered fire regimes reshape productivity over the long term through their effects on vegetation structure and recovery dynamics (Grau-Andrés *et al*., 2024; Moss *et al*., 2024). While individual climate events or fires can cause immediate reductions in growth and survival, it remains unclear whether these impacts are transient or instead lead to persistent declines in productivity by altering vegetation structure and shifting species composition (Ohlert *et al*., 2025; Sanchez-Martinez *et al*., 2025; Singh *et al*., 2023). At the same time, productivity responses are spatially heterogeneous and strongly context dependent, varying with local climate, ecosystem organisation, and disturbance history, making it difficult to scale plot-level observations to landscape, regional, or pan-tropical estimates (Rodal *et al*., 2025). Although forests and savannas differ in terms of ecological dynamics and trait adaptations, both biomes exhibit productivity changes mediated by plant strategies and shifts in functional composition, raising questions about the extent to which similar mechanisms govern resilience and long-term carbon balance across these systems (Aleixo *et al*., 2019; Paudel *et al*., 2025).

Climate- and fire-related impacts on tropical forests and savannas should also be considered alongside other drivers of ecosystem functioning and environmental change. Soil nutrient

availability, land-use history and rising atmospheric CO_2 all influence ecosystem productivity and mediate the ability of ecosystems to resist and recover from the impacts of drought, heat, and fire in complex ways (Malhi *et al*., 2014). Although these factors are not directly analysed in this thesis, they provide important context for interpreting variation in ecosystem responses to fire and extreme climate. It is therefore important to recognise that altered climate and fire regimes represent only part of a broader set of drivers of long-term productivity dynamics.

For example, soil characteristics are one of the main drivers influencing the distribution, structure and productivity of forests and savannas worldwide (Pennington *et al*., 2018; Cunha *et al*., 2022), playing a key role in complex feedback processes (e.g., as a result of herbivory, Staver *et al*., 2017; and across vegetation types, Lacerda *et al*., 2025) that determine vegetation growth responses to fire and extreme climate (da Silva & Batalha, 2008; Manu *et al*., 2024; Coetsee *et al*., 2010). Logging, grazing, land abandonment and devegetation also impact tropical forests and savannas by degrading biodiversity, altering ecosystem structure and reinforcing climate, fire and nutrient changes (Gaveau *et al*., 2014; Yusuf *et al*., 2015; Segura-García *et al*., 2025). In turn, increasing atmospheric levels of CO_2 may enhance plant water-use efficiency, potentially allowing for faster biomass growth and resistance to drought in tropical forests (Fleischer *et al*., 2019), whilst encouraging C3 tree growth and encroachment over C4 vegetation across savanna regions (Bond & Midgley, 2012). However, these ecological effects are interactive and complex, shaping biomass carbon growth through ecological processes and limitations (van der Sleen *et al*., 2015). Responses in productivity and biomass are further influenced by the biogeographical contexts of forests and savannas. For example, Bornean forests differ from other rainforest sites in being dominated by large dipterocarp trees, which are sensitive to disturbance and regenerate poorly (Slik *et al*., 2008). In comparison, productivity and recovery in Cerrado savannas are strongly shaped by bark protection and belowground persistence traits (Dantas & Pausas, 2013).

Together, these uncertainties limit our ability to determine whether climate and fire regime changes will result in temporary fluctuations in productivity or sustained reductions in ecosystem

carbon uptake (Grau-Andrés *et al*., 2024; Moss *et al*., 2024). Addressing climate- and fire-related impacts on forests and savannas will improve our interpretation of plot- and landscape-scale observations of growth, mortality, and recovery, and will help clarify how patterns in vegetation structure and functional composition translate to changes in productivity (Clark, 2007). At broader scales, it will enable more robust regional and biome-wide estimates of biomass growth and carbon storage, contributing to climate budgets and Earth-system model predictions (Bonan & Doney, 2018). Understanding productivity responses to altered climate and fire regimes will also help inform effective climate adaptation and mitigation strategies in tropical regions, where carbon sequestration and storage are central to climate regulation efforts (Anderegg *et al*., 2020).

1.2. Thesis aims and research framework

The overarching aim of this thesis is to ***identify and compare productivity responses to altered climate and fire regimes, and investigate how these changes are influenced by plant strategies and functional traits***. This thesis aims to separately investigate the impact of altered climate and fire regimes on tropical ecosystem productivity by focusing on two ecosystem case studies: Cerrado savannas and lowland dipterocarp rainforests. The research presented here is thus integrated within larger scientific projects, which provide the opportunity to take advantage of long-term experimental datasets and collaborative networks to assess productivity responses across tropical systems. In the three data analysis chapters (**Research Papers 1 to 3**), I combine existing datasets on carbon fluxes and tree inventories with newly collected measurements to quantify changes in net primary productivity at ecosystem and stem levels (**Figure 1.3**). I investigate the effects of fire regime shifts on Cerrado savannas and extreme climate on lowland dipterocarp rainforests, and evaluate how functional traits shape productivity and survival responses across tree species. I use a similar analysis approach that accommodates different methodologies and dataset structures to identify mechanisms explaining impacts of disturbance. Specifically, within each of my data analysis chapters, I focus on the following research aims:

1. The main aim of **Chapter 3 (Research Paper 1)** is to ***investigate carbon flux dynamics of Cerrado savannas within experimental fire regimes of different burning frequencies***, and was addressed through the following objectives:

    1.1. To quantify the main carbon fluxes within Cerrado savanna, illustrating flux seasonal changes and trends over time where sampling intensity and temporal replication allow.

    1.2. To determine how the cumulative effects of annual, biennial, and triennial experimental fire frequencies have influenced the main carbon fluxes of Cerrado savanna by comparing estimates in burnt plots against estimates in fire exclusion plots.

    1.3. To provide estimates of ecosystem total carbon budget metrics for Cerrado savanna that has been subjected to fire suppression and compare them to metrics for plots that have experienced annual, biennial, and triennial burns.

2. The main aim of **Chapter 4 (Research Paper 2)** is to ***assess the impacts of changing fire regimes on woody productivity and survival of Cerrado savanna trees – both the continued exclusion of fire and the reintroduction of periodic burning at different frequencies***, and was addressed through the following objectives:

    2.1. To evaluate differences in species contributions to total stem productivity and mortality at the plot scale, comparing patterns across fire regimes of different frequencies.

    2.2. To assess if experimental fire regimes influenced the average stem productivity and survival rates, focusing on patterns of temporal change across 16 dominant tree species.

    2.3. To investigate if variations in leaf, bark, wood and photosynthetic plant functional traits explain patterns in species-level stem productivity and survival of dominant tree species.

3. The main aim of **Chapter 5 (Research Paper 3)** is to ***investigate if extreme climate has consistently influenced stem productivity and survival of seedlings planted in lowland dipterocarp rainforests, comparing productivity and survival dynamics in an old-growth and a logged forest site***, and was addressed through the following objectives:

   3.1. To compare stem productivity and survival dynamics of seedlings planted at old-growth and logged forest sites, considering the potential effects of logging on forest regeneration.

   3.2. To investigate how extreme climate associated with heat and drought stress affects the stem productivity and survival of seedlings planted at old-growth and logged forest sites.

   3.3. To explore whether plant functional traits explain patterns of vulnerability in seedling stem productivity and survival to extreme climate at both forest sites.

1.3. Thesis structure

This thesis is presented in accordance with the requirements for the degree of Doctor of Philosophy in Biology at the University of Oxford, and follows the integrated, article-based format. The thesis is organised into 6 chapters. This chapter (**Chapter 1**) introduces the thesis rationale and sets out the overarching research aim, as well as the specific objectives formulated within each of the data analysis chapters. **Chapter 2** contextualises this thesis by providing background knowledge and identifying the research gaps that motivate the research questions that are addressed. It reviews the impacts of climate change and altered fire regimes on plants and ecosystems, introduces Cerrado savannas and lowland dipterocarp rainforests as study systems, and outlines how plant strategies can be used to identify common productivity responses across locations and stressors.

The main body of the thesis (**Chapters 3 to 5**) consists of three data chapters corresponding to original scientific articles published in or submitted to peer-reviewed journals:

- **Chapter 3 (Research Paper 1)** is titled '***The effect of fire on the carbon fluxes and productivity of Brazilian woodland savannas***'. In this paper, I investigate carbon flux dynamics within woodland Cerrado savannas making use of a prescribed fire experiment at Serra das Araras, Brazil. I present estimates of ecosystem-level carbon budgets, and reveal how annual, biennial and triennial fires influence productivity and respiration fluxes corresponding to different ecosystem components (stems, leaves, roots, herbs and soil). This chapter provides a broader overview of the impacts of different fire frequencies on individual fluxes, which are then scaled up to estimate ecosystem-level impacts on plant carbon expenditure and carbon-use efficiency. This chapter has been published as an original research article in the journal Science of the Total Environment: https://doi.org/10.1016/j.scitotenv.2025.179626.

- **Chapter 4 (Research Paper 2)** is titled '***Bark protection and light-adapted photosynthesis influence woody productivity of Cerrado trees in changing fire regimes***'. Varying trends of change across different ecosystem-level carbon fluxes reveal the need for in-depth analyses of fine-scale patterns behind long-term flux changes. For that reason, in this second paper, I investigate woody stem productivity dynamics of Cerrado vegetation in more detail, aiming to understand the mechanisms behind long-term changes across different fire frequencies. I used tree inventory and functional traits data from Serra das Araras to determine i) how different species contribute to community-scale stem productivity and how this changes with fire; ii) how different fire frequencies affect the average stem productivity and survival of dominant species; and iii) how changes in average stem productivity and survival are influenced by functional traits. This chapter has been published as an original research article in the journal Annals of Botany: https://doi.org/10.1093/aob/mcag115.

- **Chapter 5 (Research Paper 3)** is titled '***Extreme heat and drought influence seedling productivity in tropical forests: insights from two decades of intensive growth and survival monitoring***'. Building on my previous chapters, I sought to explore whether productivity-stressor-trait interactions remain comparable across other ecosystems and drivers of change. I continue focusing on stem productivity and survival responses, but my work shifts to study the effects of long-term climate variation on tree dynamics in lowland dipterocarp forests in Borneo, comparing old-growth and logged forests. I assess if extremes in temperature, precipitation, vapour pressure deficit, and cumulative water deficit affected productivity and survival over a period of over two decades, and then explore if species-level responses are associated with key functional traits. This chapter will be submitted to the journal Global Change Biology after submission of the thesis.

Chapter 6 concludes this thesis by presenting a synthesis of the results and discussing the implications of the research findings. It addresses common patterns in productivity responses across the case study ecosystems and outlines key divergences, limitations and complementarities. Finally, it points to future research avenues and outstanding questions identified by the thesis.

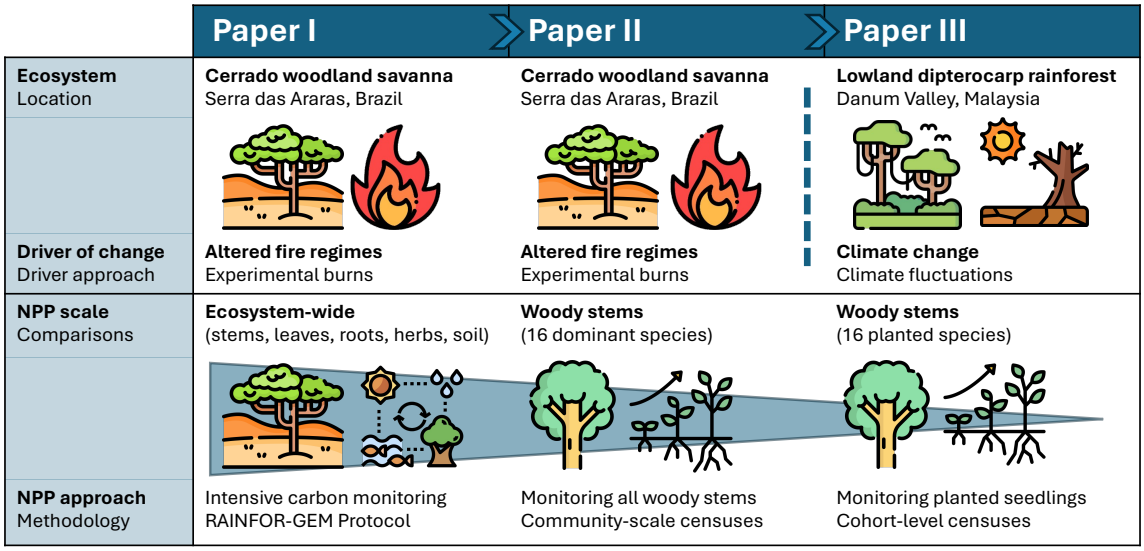


Figure 1.3, schematic diagram describing each of the data analysis chapters integrated in this thesis (**Research Papers 1 to 3**) and their respective case study ecosystem, location, stressor and methodological approach.

1.4. References

Aguirre-Gutiérrez, J., Berenguer, E., Oliveras Menor, I., Bauman, D., Corral-Rivas, J. J., Nava-Miranda, M. G., Both, S., Ndong, J. E., Ondo, F. E., Bengone, N. N., Mihinhou, V., Dalling, J. W., Heineman, K., Figueiredo, A., González-M, R., Norden, N., Hurtado-M, A. B., González, D., Salgado-Negret, B., … Malhi, Y. (2022). Functional susceptibility of tropical forests to climate change. *Nature Ecology & Evolution*, *6*(7), 878–889. https://doi.org/10.1038/s41559-022-01747-6

Aguirre-Gutiérrez, J., Stevens, N., & Berenguer, E. (2023). Valuing the functionality of tropical ecosystems beyond carbon. *Trends in Ecology & Evolution*, *0*(0). https://doi.org/10.1016/j.tree.2023.08.012

Aleixo, I., Norris, D., Hemerik, L., Barbosa, A., Prata, E., Costa, F., & Poorter, L. (2019). Amazonian rainforest tree mortality driven by climate and functional traits. *Nature Climate Change*, *9*(5), 384–388. https://doi.org/10.1038/s41558-019-0458-0

Allen, C. D., Macalady, A. K., Chenchouni, H., Bachelet, D., McDowell, N., Vennetier, M., Kitzberger, T., Rigling, A., Breshears, D. D., Hogg, E. H., Gonzalez, P., Fensham, R., Zhang, Z., Castro, J., Demidova, N., Lim, J.-H., Allard, G., Running, S. W., Semerci, A., & Cobb, N. (2010). A global overview of drought and heat-induced tree mortality reveals emerging climate change risks for forests. *Forest Ecology and Management, Adaptation of Forests and Forest Management to Changing Climate*, *259*(4), 660–684. https://doi.org/10.1016/j.foreco.2009.09.001

Andela, N., & van der Werf, G. R. (2014). Recent trends in African fires driven by cropland expansion and El Niño to La Niña transition. *Nature Climate Change*, *4*(9), 791–795. https://doi.org/10.1038/nclimate2313

Anderegg, W. R. L., Berry, J. A., & Field, C. B. (2012). Linking definitions, mechanisms, and modeling of drought-induced tree death. *Trends in Plant Science*, *17*(12), 693–700. https://doi.org/10.1016/j.tplants.2012.09.006

Anderegg, W. R. L., Trugman, A. T., Badgley, G., Anderson, C. M., Bartuska, A., Ciais, P., Cullenward, D., Field, C. B., Freeman, J., Goetz, S. J., Hicke, J. A., Huntzinger, D., Jackson, R. B., Nickerson, J., Pacala, S., & Randerson, J. T. (2020). Climate-driven risks to the climate mitigation potential of forests. *Science*, *368*(6497), eaaz7005. https://doi.org/10.1126/science.aaz7005

Archibald, S. (2016). Managing the human component of fire regimes: Lessons from Africa. *Philosophical Transactions of the Royal Society B: Biological Sciences*. https://doi.org/10.1098/rstb.2015.0346

Baccini, A., Goetz, S. J., Walker, W. S., Laporte, N. T., Sun, M., Sulla-Menashe, D., Hackler, J., Beck, P. S. A., Dubayah, R., Friedl, M. A., Samanta, S., & Houghton, R. A. (2012). Estimated carbon dioxide emissions from tropical deforestation improved by carbon-density maps. *Nature Climate Change*, *2*(3), 182–185. https://doi.org/10.1038/nclimate1354

Barlow, J., França, F., Gardner, T. A., Hicks, C. C., Lennox, G. D., Berenguer, E., Castello, L., Economo, E. P., Ferreira, J., Guénard, B., Gontijo Leal, C., Isaac, V., Lees, A. C., Parr, C. L., Wilson, S. K., Young, P. J., & Graham, N. A. J. (2018). The future of hyperdiverse tropical ecosystems. *Nature*, *559*(7715), 517–526. https://doi.org/10.1038/s41586-018-0301-1

Beer, C., Reichstein, M., Tomelleri, E., Ciais, P., Jung, M., Carvalhais, N., Rödenbeck, C., Arain, M. A., Baldocchi, D., Bonan, G. B., Bondeau, A., Cescatti, A., Lasslop, G., Lindroth, A., Lomas, M., Luyssaert, S., Margolis, H., Oleson, K. W., Roupsard, O., … Papale, D. (2010). Terrestrial gross carbon dioxide uptake: Global distribution and covariation with climate. *Science*, *329*(5993), 834–838. https://doi.org/10.1126/science.1184984

Bispo, P. C., Picoli, M. C. A., Marimon, B. S., Marimon Junior, B. H., Peres, C. A., Menor, I. O., Silva, D. E., de Figueiredo Machado, F., Alencar, A. A. C., de Almeida, C. A., Anderson, L. O., Aragão, L. E. O. C., Breunig, F. M., Bustamante, M., Dalagnol, R., Diniz-Filho, J. A. F., Ferreira, L. G., Ferreira, M. E., Fisch, G., … Silva-Junior, C. H. L. (2024). Overlooking vegetation loss outside forests imperils the Brazilian Cerrado and other non-forest biomes. *Nature Ecology & Evolution*, *8*(1), 12–13. https://doi.org/10.1038/s41559-023-02256-w

Bonal, D., Burban, B., Stahl, C., Wagner, F., & Hérault, B. (2016). The response of tropical rainforests to drought—Lessons from recent research and future prospects. *Annals of Forest Science*, *73*(1), 27–44. https://doi.org/10.1007/s13595-015-0522-5

Bonan, G. B. (2008). Forests and climate change: Forcings, feedbacks, and the climate benefits of forests. *Science*, *320*(5882), 1444–1449. https://doi.org/10.1126/science.1155121

Bonan, G. B., & Doney, S. C. (2018). Climate, ecosystems, and planetary futures: The challenge to predict life in Earth system models. *Science*, *359*(6375), eaam8328. https://doi.org/10.1126/science.aam8328

Bond, W. J., & Midgley, G. F. (2012). Carbon dioxide and the uneasy interactions of trees and savannah grasses. *Philosophical Transactions of the Royal Society B: Biological Sciences*, *367*(1588), 601–612. https://doi.org/10.1098/rstb.2011.0182

Bond, W. J. (2008). What limits trees in C4 grasslands and savannas? *Annual Review of Ecology, Evolution, and Systematics*, *39*, 641–659. https://doi.org/10.1146/annurev.ecolsys.39.110707.173411

Bond, W. J. (2021). Out of the shadows: Ecology of open ecosystems. *Plant Ecology & Diversity*, *14*(5–6), 205–222. https://doi.org/10.1080/17550874.2022.2034065

Bond, W. J., & Keeley, J. E. (2005). Fire as a global 'herbivore': The ecology and evolution of flammable ecosystems. *Trends in Ecology & Evolution*, *20*(7), 387–394. https://doi.org/10.1016/j.tree.2005.04.025

Borma, L. S., Costa, M. H., da Rocha, H. R., Arieira, J., Nascimento, N. C. C., Jaramillo-Giraldo, C., Ambrosio, G., Carneiro, R. G., Venzon, M., Neto, A. F., van der Hoff, R., Oliveira, B. F. A., Rajão, R., & Nobre, C. A. (2022). Beyond carbon: The contributions of South American tropical humid and subhumid forests to ecosystem services. *Reviews of Geophysics*, *60*(4), e2021RG000766. https://doi.org/10.1029/2021RG000766

Brando, P. M., Nepstad, D. C., Balch, J. K., Bolker, B., Christman, M. C., Coe, M., & Putz, F. E. (2012). Fire-induced tree mortality in a neotropical forest: The roles of bark traits, tree size, wood density and fire behavior. *Global Change Biology*, *18*(2), 630–641. https://doi.org/10.1111/j.1365-2486.2011.02533.x

Brando, P. M., Soares-Filho, B., Rodrigues, L., Assunção, A., Morton, D., Tuchschneider, D., Fernandes, E. C. M., Macedo, M. N., Oliveira, U., & Coe, M. T. (2020). The gathering firestorm in southern Amazonia. *Science Advances*, *6*(2), eaay1632. https://doi.org/10.1126/sciadv.aay1632

Burton, C., Lampe, S., Kelley, D. I., Thiery, W., Hantson, S., Christidis, N., Gudmundsson, L., Forrest, M., Burke, E., Chang, J., Huang, H., Ito, A., Kou-Giesbrecht, S., Lasslop, G., Li, W., Nieradzik, L., Li, F., Chen, Y., Randerson, J., … Mengel, M. (2024). Global burned area increasingly explained by climate change. *Nature Climate Change*, *14*(11), 1186–1192. https://doi.org/10.1038/s41558-024-02140-w

Cattelan, L. G., Mattos, C. R. C., Pamplona, M. B., & Hirota, M. (2024). Mapping climatic regions of the Cerrado: General patterns and future change. *International Journal of Climatology*, *44*(16), 5857–5872. https://doi.org/10.1002/joc.8670

Chambers, J. Q., Nogueira Lima, A. J., Pastorello, G., Gimenez, B. O., Meng, L., Dyer, L. A., Feng, Y., Santos da Silva, C., Costa de Oliveira, R., Weber, A., Koven, C., Negrón-Juárez, R., Spanner, G. C., Gaui, T. D., Fontes, C. G., de Araújo, A. C., McDowell, N., Leung, R., Marra, D. M., … Higuchi, N. (2026). Hot droughts in the Amazon provide a window to a future hypertropical climate. *Nature*, *649*(8099), 1190–1196. https://doi.org/10.1038/s41586-025-09728-y

Chapman, S., Syktus, J., Trancoso, R., Salazar, A., Thatcher, M., Watson, J. E. M., Meijaard, E., Sheil, D., Dargusch, P., & McAlpine, C. A. (2020). Compounding impact of deforestation on Borneo's climate during El Niño events. *Environmental Research Letters*, *15*(8), 084006. https://doi.org/10.1088/1748-9326/ab86f5

Clark, D. A. (2007). Detecting tropical forests' responses to global climatic and atmospheric change: Current challenges and a way forward. *Biotropica*, *39*(1), 4–19. https://doi.org/10.1111/j.1744-7429.2006.00227.x

Coetsee, C., Bond, W. J., & February, E. C. (2010). Frequent fire affects soil nitrogen and carbon in an African savanna by changing woody cover. *Oecologia*, *162*(4), 1027–1034. https://doi.org/10.1007/s00442-009-1490-y

Cui, J., Piao, S., Huntingford, C., Wang, T., & Spracklen, D. V. (2026). Historical deforestation drives strong rainfall decline across the southern Amazon basin. *Nature Communications*, *17*(1), 1642. https://doi.org/10.1038/s41467-026-68361-z

Cunha, H. F. V., Andersen, K. M., Lugli, L. F., Santana, F. D., Aleixo, I. F., Moraes, A. M., Garcia, S., Di Ponzio, R., Mendoza, E. O., Brum, B., Rosa, J. S., Cordeiro, A. L., Portela, B. T. T., Ribeiro, G., Coelho, S. D., de Souza, S. T., Silva, L. S., Antonieto, F., Pires, M., … Quesada, C. A. (2022). Direct evidence for phosphorus limitation on Amazon forest productivity. *Nature*, *608*(7923), 558–562. https://doi.org/10.1038/s41586-022-05085-2

Cuni-Sanchez, A., Imani, G., Bulonvu, F., Batumike, R., Baruka, G., Burgess, N. D., Klein, J. A., & Marchant, R. (2019). Social perceptions of forest ecosystem services in the Democratic Republic of Congo. *Human Ecology*, *47*(6), 839–853. https://doi.org/10.1007/s10745-019-00115-6

da Silva, D. M., & Batalha, M. A. (2008). Soil–vegetation relationships in cerrados under different fire frequencies. *Plant and Soil*, *311*(1), 87–96. https://doi.org/10.1007/s11104-008-9660-y

Dantas, V. L., & Pausas, J. G. (2013). The lanky and the corky: Fire-escape strategies in savanna woody species. *Journal of Ecology*, *101*(5), 1265–1272. https://doi.org/10.1111/1365-2745.12118

Deb, J., Phinn, S., Butt, N., & McAlpine, C. (2018). Climate change impacts on tropical forests: Identifying risks for tropical Asia. *Journal of Tropical Forest Science*, *30*(2), 182–194. https://doi.org/10.26525/jtfs2018.30.2.182194

Dexter, K. G., Pennington, R. T., Oliveira-Filho, A. T., Bueno, M. L., Silva de Miranda, P. L., & Neves, D. M. (2018). Inserting tropical dry forests into the discussion on biome transitions in the tropics. *Frontiers in Ecology and Evolution*, *6*. https://doi.org/10.3389/fevo.2018.00104

Edwards, D. P., Socolar, J. B., Mills, S. C., Burivalova, Z., Koh, L. P., & Wilcove, D. S. (2019). Conservation of tropical forests in the Anthropocene. *Current Biology*, *29*(19), R1008–R1020. https://doi.org/10.1016/j.cub.2019.08.026

Flannigan, M., Cantin, A. S., Groot, W. J. de, Wotton, M., Newbery, A., & Gowman, L. M. (2013). Global wildland fire season severity in the 21st century. *Forest Ecology and Management, The Mega-Fire Reality*, *294*, 54–61. https://doi.org/10.1016/j.foreco.2012.10.022

Fleischer, K., Rammig, A., De Kauwe, M. G., Walker, A. P., Domingues, T. F., Fuchslueger, L., Garcia, S., Goll, D. S., Grandis, A., Jiang, M., Haverd, V., Hofhansl, F., Holm, J. A., Kruijt, B., Leung, F., Medlyn, B. E., Mercado, L. M., Norby, R. J., Pak, B., … Lapola, D. M. (2019). Amazon forest response to CO_2 fertilization dependent on plant phosphorus acquisition. *Nature Geoscience*, *12*(9), 736–741. https://doi.org/10.1038/s41561-019-0404-9

Flores, B. M., & Staal, A. (2022). Feedback in tropical forests of the Anthropocene. *Global Change Biology*, *28*(17), 5041–5061. https://doi.org/10.1111/gcb.16293

França, F. M., Benkwitt, C. E., Peralta, G., Robinson, J. P. W., Graham, N. A. J., Tylianakis, J. M., Berenguer, E., Lees, A. C., Ferreira, J., Louzada, J., & Barlow, J. (2020). Climatic and local stressor interactions threaten tropical forests and coral reefs. *Philosophical Transactions of the Royal Society B: Biological Sciences*, *375*(1794), 20190116. https://doi.org/10.1098/rstb.2019.0116

Gallery, R. E. (2014). Ecology of Tropical Rain Forests. In *Ecology and the Environment* (pp. 247–272). Springer, New York, NY. https://doi.org/10.1007/978-1-4614-7501-9_4

Gaveau, D. L. A., Sheil, D., Husnayaen, Salim, M. A., Arjasakusuma, S., Ancrenaz, M., Pacheco, P., & Meijaard, E. (2016). Rapid conversions and avoided deforestation: Examining four decades of industrial plantation expansion in Borneo. *Scientific Reports*, *6*(1), 32017. https://doi.org/10.1038/srep32017

Gaveau, D. L. A., Sloan, S., Molidena, E., Yaen, H., Sheil, D., Abram, N. K., Ancrenaz, M., Nasi, R., Quinones, M., Wielaard, N., & Meijaard, E. (2014). Four decades of forest persistence, clearance and logging on Borneo. *PLOS ONE*, *9*(7), e101654. https://doi.org/10.1371/journal.pone.0101654

González, T. M., González-Trujillo, J. D., Elizalde, M. M., & Armenteras, D. (2025). Predicting fire risk in Colombia tropical savannas: A multi-scenario approach. *Agricultural and Forest Meteorology*, *369*, 110566. https://doi.org/10.1016/j.agrformet.2025.110566

Grace, J., José, J. S., Meir, P., Miranda, H. S., & Montes, R. A. (2006). Productivity and carbon fluxes of tropical savannas. *Journal of Biogeography*, *33*(3), 387–400. https://doi.org/10.1111/j.1365-2699.2005.01448.x

Grau-Andrés, R., Moreira, B., & Pausas, J. G. (2024). Global plant responses to intensified fire regimes. *Global Ecology and Biogeography*, *33*(8), e13858. https://doi.org/10.1111/geb.13858

Guan, K., Pan, M., Li, H., Wolf, A., Wu, J., Medvigy, D., Caylor, K. K., Sheffield, J., Wood, E. F., Malhi, Y., Liang, M., Kimball, J. S., Saleska, S. R., Berry, J., Joiner, J., & Lyapustin, A. I. (2015). Photosynthetic seasonality of global tropical forests constrained by hydroclimate. *Nature Geoscience*, *8*(4), 284–289. https://doi.org/10.1038/ngeo2382

Hantson, S., Hamilton, D. S., & Burton, C. (2024). Changing fire regimes: Ecosystem impacts in a shifting climate. *One Earth*, *7*(6), 942–945. https://doi.org/10.1016/j.oneear.2024.05.021

Hipólito, J., Sousa, B. dos S. B., Borges, R. C., Brito, R. M. de, Jaffé, R., Dias, S., Imperatriz Fonseca, V. L., & Giannini, T. C. (2019). Valuing nature's contribution to people: The pollination services provided by two protected areas in Brazil. *Global Ecology and Conservation*, *20*, e00782. https://doi.org/10.1016/j.gecco.2019.e00782

Hoffmann, W. A., Orthen, B., & Nascimento, P. K. V. do. (2003). Comparative fire ecology of tropical savanna and forest trees. *Functional Ecology*, *17*(6), 720–726. https://doi.org/10.1111/j.1365-2435.2003.00796.x

Hofmann, G. S., Cardoso, M. F., Alves, R. J. V., Weber, E. J., Barbosa, A. A., de Toledo, P. M., Pontual, F. B., Salles, L. de O., Hasenack, H., Cordeiro, J. L. P., Aquino, F. E., & de Oliveira, L. F. B. (2021). The Brazilian Cerrado is becoming hotter and drier. *Global Change Biology*, *27*(17), 4060–4073. https://doi.org/10.1111/gcb.15712

Hofmann, G. S., Silva, R. C., Weber, E. J., Barbosa, A. A., Oliveira, L. F. B., Alves, R. J. V., Hasenack, H., Schossler, V., Aquino, F. E., & Cardoso, M. F. (2023). Changes in atmospheric circulation and evapotranspiration are reducing rainfall in the Brazilian Cerrado. *Scientific Reports*, *13*(1), 11236. https://doi.org/10.1038/s41598-023-38174-x

Holdridge, L. R. (1947). Determination of World plant formations from simple climatic data. *Science*, *105*(2727), 367–368. https://doi.org/10.1126/science.105.2727.367

Hunter, M. O., Keller, M., Morton, D., Cook, B., Lefsky, M., Ducey, M., Saleska, S., Jr, R. C. de O., & Schietti, J. (2015). Structural dynamics of tropical moist forest gaps. *PLOS ONE*, *10*(7), e0132144. https://doi.org/10.1371/journal.pone.0132144

Jolly, W. M., Cochrane, M. A., Freeborn, P. H., Holden, Z. A., Brown, T. J., Williamson, G. J., & Bowman, D. M. J. S. (2015). Climate-induced variations in global wildfire danger from 1979 to 2013. *Nature Communications*, *6*(1), 7537. https://doi.org/10.1038/ncomms8537

Kahana, R., Halladay, K., Alves, L. M., Chadwick, R., & Hartley, A. J. (2024). Future precipitation projections for Brazil and tropical South America from a convection-permitting climate simulation. *Frontiers in Climate*, *6*. https://doi.org/10.3389/fclim.2024.1419704

Kelley, D. I., Burton, C., Di Giuseppe, F., Jones, M. W., Barbosa, M. L. F., Brambleby, E., McNorton, J. R., Liu, Z., Bradley, A. S. I., Blackford, K., Burke, E., Ciavarella, A., Di Tomaso, E., Eden, J., Ferreira, I. J. M., Fiedler, L., Hartley, A. J., Keeping, T. R., Lampe, S., … Kolden, C. A. (2025). State of wildfires 2024–2025. *Earth System Science Data*, *17*(10), 5377–5488. https://doi.org/10.5194/essd-17-5377-2025

Lacerda, F. da C. B., Mota, N. M., Coelho, A. J. P., Lima, T. T. S., Durán, J., Rodríguez, A., & Alves Meira-Neto, J. A. (2025). Different physiognomies of the Brazilian savanna determine changes in soil C, N and P pools. *Plant Ecology*, *226*(7), 855–866. https://doi.org/10.1007/s11258-025-01535-9

Lapola, D. M., Pinho, P., Barlow, J., Aragão, L. E. O. C., Berenguer, E., Carmenta, R., Liddy, H. M., Seixas, H., Silva, C. V. J., Silva-Junior, C. H. L., Alencar, A. A. C., Anderson, L. O., Armenteras, D., Brovkin, V., Calders, K., Chambers, J., Chini, L., Costa, M. H., Faria, B. L., … Walker, W. S. (2023). The drivers and impacts of Amazon forest degradation. *Science*, *379*(6630), eabp8622. https://doi.org/10.1126/science.abp8622

Lehmann, C. E. R., & Parr, C. L. (2016). Tropical grassy biomes: Linking ecology, human use and conservation. *Philosophical Transactions of the Royal Society B: Biological Sciences*, *371*(1703), 20160329. https://doi.org/10.1098/rstb.2016.0329

Lehmann, C. E. R., Anderson, T. M., Sankaran, M., Higgins, S. I., Archibald, S., Hoffmann, W. A., Hanan, N. P., Williams, R. J., Fensham, R. J., Felfili, J., Hutley, L. B., Ratnam, J., San Jose, J., Montes, R., Franklin, D., Russell-Smith, J., Ryan, C. M., Durigan, G., Hiernaux, P., … Bond, W. J. (2014). Savanna vegetation-fire-climate relationships differ among continents. *Science*, *343*(6170), 548–552. https://doi.org/10.1126/science.1247355

Lindenmayer, D., Zylstra, P., DellaSala, D. A., Taylor, C., & Legge, S. (2025). The response and management of species sensitive to altered fire regimes. *Nature Reviews Biodiversity*, *1*(11), 733–744. https://doi.org/10.1038/s44358-025-00086-1

Loh, J. L., Tangang, F., Juneng, L., Hein, D., & Lee, D.-I. (2016). Projected rainfall and temperature changes over Malaysia at the end of the 21st century based on PRECIS modelling system. *Asia-Pacific Journal of Atmospheric Sciences*, *52*(2), 191–208. https://doi.org/10.1007/s13143-016-0019-7

Malhi, Y. (2012). The productivity, metabolism and carbon cycle of tropical forest vegetation. *Journal of Ecology*, *100*(1), 65–75. https://doi.org/10.1111/j.1365-2745.2011.01916.x

Malhi, Y., Gardner, T. A., Goldsmith, G. R., Silman, M. R., & Zelazowski, P. (2014). Tropical Forests in the Anthropocene. *Annual Review of Environment and Resources*, *39*(Volume 39, 2014), 125–159. https://doi.org/10.1146/annurev-environ-030713-155141

Manu, R., Iddris, N. A.-A., Corre, M. D., Aleeje, A., Mwanjalolo, M. J. G., van Straaten, O., & Veldkamp, E. (2024). Response of tropical forest productivity to seasonal drought mediated by potassium and phosphorus availability. *Nature Geoscience*, *17*(6), 524–531. https://doi.org/10.1038/s41561-024-01448-8

Marcotullio, P. J., Keßler, C., Quintero Gonzalez, R., & Schmeltz, M. (2021). Urban growth and heat in tropical climates. *Frontiers in Ecology and Evolution*, *9*. https://doi.org/10.3389/fevo.2021.616626

McDowell, N., Allen, C. D., Anderson-Teixeira, K., Brando, P., Brienen, R., Chambers, J., Christoffersen, B., Davies, S., Doughty, C., Duque, A., Espirito-Santo, F., Fisher, R., Fontes, C. G., Galbraith, D., Goodsman, D., Grossiord, C., Hartmann, H., Holm, J., Johnson, D. J., … Xu, X. (2018). Drivers and mechanisms of tree mortality in moist tropical forests. *New Phytologist*, *219*(3), 851–869. https://doi.org/10.1111/nph.15027

Moss, W. E., Crausbay, S. D., Rangwala, I., Wason, J. W., Trauernicht, C., Stevens-Rumann, C. S., Sala, A., Rottler, C. M., Pederson, G. T., Miller, B. W., Magness, D. R., Littell, J. S., Frelich, L. E., Frazier, A. G., Davis, K. T., Coop, J. D., Cartwright, J. M., & Booth, R. K. (2024). Drought as an emergent driver of ecological transformation in the twenty-first century. *BioScience*, *74*(8), 524–538. https://doi.org/10.1093/biosci/biae050

Moura, L. C., Scariot, A. O., Schmidt, I. B., Beatty, R., & Russell-Smith, J. (2019). The legacy of colonial fire management policies on traditional livelihoods and ecological sustainability in savannas: Impacts, consequences, new directions. *Journal of Environmental Management*, *232*, 600–606. https://doi.org/10.1016/j.jenvman.2018.11.057

Mucina, L. (2019). Biome: Evolution of a crucial ecological and biogeographical concept. *New Phytologist*, *222*(1), 97–114. https://doi.org/10.1111/nph.15609

Murphy, P. G., & Lugo, A. E. (1986). Ecology of tropical dry forest. *Annual Review of Ecology, Evolution, and Systematics*, *17*(Volume 17, 1986), 67–88. https://doi.org/10.1146/annurev.es.17.110186.000435

Ohlert, T., Smith, M. D., Collins, S. L., Knapp, A. K., Dukes, J. S., Sala, O., Wilkins, K. D., Munson, S. M., Anderson, M. I., Avolio, M. L., Chen, A., Hayden, M. T., Holdrege, M. C., Slette, I. J., Wilfahrt, P., Beier, C., Fraser, L. H., Jentsch, A., Loik, M. E., … Zuo, X. (2025). Drought intensity and duration interact to magnify losses in primary productivity. *Science*, *390*(6770), 284–289. https://doi.org/10.1126/science.ads8144

Oliveras, I., & Malhi, Y. (2016). Many shades of green: The dynamic tropical forest–savannah transition zones. *Philosophical Transactions of the Royal Society B: Biological Sciences*, *371*(1703), 20150308. https://doi.org/10.1098/rstb.2015.0308

Pan, Y., Birdsey, R. A., Fang, J., Houghton, R., Kauppi, P. E., Kurz, W. A., Phillips, O. L., Shvidenko, A., Lewis, S. L., Canadell, J. G., Ciais, P., Jackson, R. B., Pacala, S. W., McGuire, A. D., Piao, S., Rautiainen, A., Sitch, S., & Hayes, D. (2011). A large and persistent carbon sink in the World's forests. *Science*, *333*(6045), 988–993. https://doi.org/10.1126/science.1201609

Parr, C. L., Lehmann, C. E. R., Bond, W. J., Hoffmann, W. A., & Andersen, A. N. (2014). Tropical grassy biomes: Misunderstood, neglected, and under threat. *Trends in Ecology & Evolution*, *29*(4), 205–213. https://doi.org/10.1016/j.tree.2014.02.004

Paudel, P., Olin, S., Tjoelker, M., Pontarp, M., Metcalfe, D., & Smith, B. (2025). Savanna ecosystem structure and productivity along a rainfall gradient: The role of competition and stress tolerance mediated by plant functional traits. *Biogeosciences*, *22*(20), 6153–6171. https://doi.org/10.5194/bg-22-6153-2025

Pausas, J. G., & Bond, W. J. (2020). Alternative Biome States in Terrestrial Ecosystems. *Trends in Plant Science*, *25*(3), 250–263. https://doi.org/10.1016/j.tplants.2019.11.003

Pennington, R. T., Lehmann, C. E. R., & Rowland, L. M. (2018). Tropical savannas and dry forests. *Current Biology*, *28*(9), R541–R545. https://doi.org/10.1016/j.cub.2018.03.014

Prentice, I. C., Cramer, W., Harrison, S. P., Leemans, R., Monserud, R. A., & Solomon, A. M. (1992). A global biome model based on plant physiology and dominance, soil properties and climate. *Journal of Biogeography*, *19*(2), 117–134. https://doi.org/10.2307/2845499

Ratnam, J., Bond, W. J., Fensham, R. J., Hoffmann, W. A., Archibald, S., Lehmann, C. E. R., Anderson, M. T., Higgins, S. I., & Sankaran, M. (2011). When is a 'forest' a savanna, and why does it matter? *Global Ecology and Biogeography*, *20*(5), 653–660. https://doi.org/10.1111/j.1466-8238.2010.00634.x

Reddington, C. L., Smith, C., Butt, E. W., Baker, J. C. A., Oliveira, B. F. A., Yamba, E. I., & Spracklen, D. V. (2025). Tropical deforestation is associated with considerable heat-related mortality. *Nature Climate Change*, *15*(9), 992–999. https://doi.org/10.1038/s41558-025-02411-0

Reed, J., van Vianen, J., Foli, S., Clendenning, J., Yang, K., MacDonald, M., Petrokofsky, G., Padoch, C., & Sunderland, T. (2017). Trees for life: The ecosystem service contribution of trees to food production and livelihoods in the tropics. *Forest Policy and Economics, Forest, Food, and Livelihoods*, *84*, 62–71. https://doi.org/10.1016/j.forpol.2017.01.012

Rifai, S. W., Girardin, C. A. J., Berenguer, E., del Aguila-Pasquel, J., Dahlsjö, C. A. L., Doughty, C. E., Jeffery, K. J., Moore, S., Oliveras, I., Riutta, T., Rowland, L. M., Murakami, A. A., Addo-Danso, S. D., Brando, P., Burton, C., Ondo, F. E., Duah-Gyamfi, A., Amézquita, F. F., Freitag, R., … Malhi, Y. (2018). ENSO Drives interannual variation of forest woody growth across the tropics. *Philosophical Transactions of the Royal Society B: Biological Sciences*, *373*(1760), 20170410. https://doi.org/10.1098/rstb.2017.0410

Rodal, M., Luyssaert, S., Balzarolo, M., & Campioli, M. (2025). A global database of net primary production of terrestrial ecosystems. *Scientific Data*, *12*(1), 1534. https://doi.org/10.1038/s41597-025-05773-4

Rodrigues, A. F., Latawiec, A. E., Reid, B. J., Solórzano, A., Schuler, A. E., Lacerda, C., Fidalgo, E. C. C., Scarano, F. R., Tubenchlak, F., Pena, I., Vicente-Vicente, J. L., Korys, K. A., Cooper, M., Fernandes, N. F., Prado, R. B., Maioli, V., Dib, V., & Teixeira, W. G. (2021). Systematic review of soil ecosystem services in tropical regions. *Royal Society Open Science*, *8*(3), 201584. https://doi.org/10.1098/rsos.201584

Ryan, C. M., Pritchard, R., McNicol, I., Owen, M., Fisher, J. A., & Lehmann, C. (2016). Ecosystem services from southern African woodlands and their future under global change. *Philosophical Transactions of the Royal Society B: Biological Sciences*, *371*(1703), 20150312. https://doi.org/10.1098/rstb.2015.0312

Sanchez-Martinez, P., Martius, L. R., Bittencourt, P., Silva, M., Binks, O., Coughlin, I., Negrão-Rodrigues, V., Athaydes Silva, J., Da Costa, A. C. L., Selman, R., Rifai, S., Rowland, L., Mencuccini, M., & Meir, P. (2025). Amazon rainforest adjusts to long-term experimental drought. *Nature Ecology & Evolution*, *9*(6), 970–979. https://doi.org/10.1038/s41559-025-02702-x

Sankaran, M., Hanan, N. P., Scholes, R. J., Ratnam, J., Augustine, D. J., Cade, B. S., Gignoux, J., Higgins, S. I., Le Roux, X., Ludwig, F., Ardo, J., Banyikwa, F., Bronn, A., Bucini, G., Caylor, K. K., Coughenour, M. B., Diouf, A., Ekaya, W., Feral, C. J., … Zambatis, N. (2005). Determinants of woody cover in African savannas. *Nature*, *438*(7069), 846–849. https://doi.org/10.1038/nature04070

Sayedi, S. S., Abbott, B. W., Vannière, B., Leys, B., Colombaroli, D., Romera, G. G., Słowiński, M., Aleman, J. C., Blarquez, O., Feurdean, A., Brown, K., Aakala, T., Alenius, T., Allen, K., Andric, M., Bergeron, Y., Biagioni, S., Bradshaw, R., Bremond, L., … Daniau, A.-L. (2024). Assessing changes in global fire regimes. *Fire Ecology*, *20*(1), 18. https://doi.org/10.1186/s42408-023-00237-9

Segura-Garcia, C., Alencar, A., S. Arruda, V. L., Bauman, D., Silva, W., Conciani, D. E., & Oliveras Menor, I. (2025). The fire regimes of the Cerrado and their changes through time. *Philosophical Transactions of the Royal Society B: Biological Sciences*, *380*(1924), 20230460. https://doi.org/10.1098/rstb.2023.0460

Seidl, R., Thom, D., Kautz, M., Martin-Benito, D., Peltoniemi, M., Vacchiano, G., Wild, J., Ascoli, D., Petr, M., Honkaniemi, J., Lexer, M. J., Trotsiuk, V., Mairota, P., Svoboda, M., Fabrika, M., Nagel, T. A., & Reyer, C. P. O. (2017). Forest disturbances under climate change. *Nature Climate Change*, *7*(6), 395–402. https://doi.org/10.1038/nclimate3303

Silver, W. L., Brown, S., & Lugo, A. E. (1996). Effects of changes in biodiversity on ecosystem function in tropical forests. *Conservation Biology*, *10*(1), 17–24. https://doi.org/10.1046/j.1523-1739.1996.10010017.x

Simon, M., & Pennington, T. (2012). Evidence for adaptation to fire regimes in the tropical savannas of the Brazilian Cerrado. *International Journal of Plant Sciences*, *173*, 711–723. https://doi.org/10.1086/665973

Singh, J., Boucher, P. B., Hockridge, E. G., & Davies, A. B. (2023). Effects of long-term fixed fire regimes on African savanna vegetation biomass, vertical structure and tree stem density. *Journal of Applied Ecology*, *60*(7), 1223–1238. https://doi.org/10.1111/1365-2664.14435

Singo, M. V., Chikoore, H., Engelbrecht, F. A., Ndarana, T., Muofhe, T. P., Mbokodo, I. L., Murungweni, F. M., & Bopape, M.-J. M. (2023). Projections of future fire risk under climate change over the South African savanna. *Stochastic Environmental Research and Risk Assessment*, *37*(7), 2677–2691. https://doi.org/10.1007/s00477-023-02412-5

Siyum, Z. G. (2020). Tropical dry forest dynamics in the context of climate change: Syntheses of drivers, gaps, and management perspectives. *Ecological Processes*, *9*(1), 25. https://doi.org/10.1186/s13717-020-00229-6

Slik, J. W. F., Bernard, C. S., Van Beek, M., Breman, F. C., & Eichhorn, K. A. O. (2008). Tree diversity, composition, forest structure and aboveground biomass dynamics after single and repeated fire in a Bornean rain forest. *Oecologia*, *158*(3), 579–588. https://doi.org/10.1007/s00442-008-1163-2

Staver, A. C., Botha, J., & Hedin, L. (2017). Soils and fire jointly determine vegetation structure in an African savanna. *New Phytologist*, *216*(4), 1151–1160. https://doi.org/10.1111/nph.14738

Stevens, N., Lehmann, C. E. R., Murphy, B. P., & Durigan, G. (2017). Savanna woody encroachment is widespread across three continents. *Global Change Biology*, *23*(1), 235–244. https://doi.org/10.1111/gcb.13409

Stríkis, N. M., Buarque, P. F. S. M., Cruz, F. W., Bernal, J. P., Vuille, M., Tejedor, E., Santos, M. S., Shimizu, M. H., Ampuero, A., Du, W., Sampaio, G., Sales, H. dos R., Campos, J. L., Kayano, M. T., Apaèstegui, J., Fu, R. R., Cheng, H., Edwards, R. L., Mayta, V. C., … Novello, V. F. (2024). Modern anthropogenic drought in Central Brazil unprecedented during last 700 years. *Nature Communications*, *15*(1), 1728. https://doi.org/10.1038/s41467-024-45469-8

Teskey, R., Wertin, T., Bauweraerts, I., Ameye, M., McGuire, M. A., & Steppe, K. (2015). Responses of tree species to heat waves and extreme heat events. *Plant, Cell & Environment*, *38*(9), 1699–1712. https://doi.org/10.1111/pce.12417

van der Hoff, R., Nascimento, N., Fabrício-Neto, A., Jaramillo-Giraldo, C., Ambrosio, G., Arieira, J., Afonso Nobre, C., & Rajão, R. (2022). Policy-oriented ecosystem services research on tropical forests in South America: A systematic literature review. *Ecosystem Services*, *56*, 101437. https://doi.org/10.1016/j.ecoser.2022.101437

van der Sleen, P., Groenendijk, P., Vlam, M., Anten, N. P. R., Boom, A., Bongers, F., Pons, T. L., Terburg, G., & Zuidema, P. A. (2015). No growth stimulation of tropical trees by 150 years of CO_2 fertilization but water-use efficiency increased. *Nature Geoscience*, *8*(1), 24–28. https://doi.org/10.1038/ngeo2313

van der Werf, G. R., Randerson, J. T., Giglio, L., van Leeuwen, T. T., Chen, Y., Rogers, B. M., Mu, M., van Marle, M. J. E., Morton, D. C., Collatz, G. J., Yokelson, R. J., & Kasibhatla, P. S. (2017). Global fire emissions estimates during 1997–2016. *Earth System Science Data*, *9*(2), 697–720. https://doi.org/10.5194/essd-9-697-2017

Whittaker, R. H. (1970). Communities and Ecosystems. Macmillan, New York.

Williams, B. A., Watson, J. E. M., Beyer, H. L., Grantham, H. S., Simmonds, J. S., Alvarez, S. J., Venter, O., Strassburg, B. B. N., & Runting, R. K. (2022). Global drivers of change across tropical savannah ecosystems and insights into their management and conservation. *Biological Conservation*, *276*, 109786. https://doi.org/10.1016/j.biocon.2022.109786

Woollen, E., Ryan, C. M., Baumert, S., Vollmer, F., Grundy, I., Fisher, J., Fernando, J., Luz, A., Ribeiro, N., & Lisboa, S. N. (2016). Charcoal production in the Mopane woodlands of Mozambique: What are the trade-offs with other ecosystem services? *Philosophical Transactions of the Royal Society B: Biological Sciences*, *371*(1703), 20150315. https://doi.org/10.1098/rstb.2015.0315

Yusuf, H. M., Treydte, A. C., & Sauerborn, J. (2015). Managing semi-arid rangelands for carbon storage: Grazing and woody encroachment effects on soil carbon and nitrogen. *PLOS ONE*, *10*(10), e0109063. https://doi.org/10.1371/journal.pone.0109063

Zhou, Y., Bomfim, B., Bond, W. J., Boutton, T. W., Case, M. F., Coetsee, C., Davies, A. B., February, E. C., Gray, E. F., Silva, L. C. R., Wright, J. L., & Staver, A. C. (2023). Soil carbon in tropical savannas mostly derived from grasses. *Nature Geoscience*, 1–7. https://doi.org/10.1038/s41561-023-01232-0

Zuidema, P. A., Baker, P. J., Groenendijk, P., Schippers, P., van der Sleen, P., Vlam, M., & Sterck, F. (2013). Tropical forests and global change: Filling knowledge gaps. *Trends in Plant Science*, *18*(8), 413–419. https://doi.org/10.1016/j.tplants.2013.05.006

Chapter 2: Research Background

In this chapter, I review key scientific topics and ecological themes providing information and context to support the research undertaken as part of this thesis. I elaborate on the state of knowledge concerning ecosystem responses to altered fire regimes and climate change. I give a brief overview of the importance of investigating responses in terms of primary productivity, and outline the main methodologies used to quantify NPP. I describe the concept of plant strategies and plant functional traits, and propose ways in which they can help us understand responses to altered climate and fire regimes in a more mechanistic way. Finally, I introduce Cerrado savannas and lowland dipterocarp rainforests, describe the ecological characteristics and conservation status of these regions, and briefly describe the relevance of the locations of study.

2.1. On the impacts of extreme climate on tropical ecosystems

The frequency and intensity of heatwaves and droughts are increasing across tropical regions, with potential for profound consequences for plant demography and ecosystem productivity (Xu *et al*., 2019). Drought and heat are biological stressors that impose critical physiological limits on plant function (Burgess, 2024). At the leaf scale, high temperatures disrupt leaf physiology by impairing metabolic stability and altering water balances, whilst drought conditions reduce leaf water availability leading to turgor loss, limited plant water transport and reduced photosynthesis (Sato *et al*., 2024). Balancing leaf and photosynthetic function in the face of dehydration and heat is therefore a fundamental trade-off allowing for continued carbon uptake. Temperature and water stress reduce carbon gain, meaning that continued exposure to heat and drought can limit plant fitness and growth (Corlett, 2016). Plant biomass is built primarily from assimilated carbon, and declines in carbon gain directly constrain the supply of carbohydrates available for growth and maintenance (Bonal *et al*., 2016). As carbon assimilation approaches respiratory demand, a greater proportion of fixed carbon may be used to sustain basic metabolism rather than to support

new tissue production (Crous *et al*., 2022). Over time, this shift reduces stem and root growth, canopy development, and energy storage reserves, limiting overall biomass accumulation and diminishing the capacity of plants to compete and recover from stress (Teskey *et al*., 2015).

Extreme climate events are already affecting tropical forest net primary production and woody growth (**Figure 2.1**). Using dendrometer growth measurements from across the tropics, Rifai *et al*. (2018) found that changes in forest woody growth are best predicted by anomalies in vapour pressure deficit, water deficit and shortwave radiation, and that El Niño events caused pronounced declines in global tropical forest stem growth (-8.3% in 1997/1998, and -9% in 2015/2016), with particularly large impacts in Amazonia. This pattern is consistent with long-term changes in forest biomass. For example, Bauman, Fortunel, Cernusak *et al*. (2022) used 50 years of plot survey data to show that increases in atmospheric evaporative demand and solar radiation consistently reduced tree growth across the Australian wet tropics. In terms of the geographical distribution of climate impacts, Zuidema *et al*. (2022) describe how pantropical dry-season growth responses are amplified in regions that are drier, hotter and more climatically variable, indicating that global warming will aggravate drought-induced declines in tropical vegetation productivity. Although in a more recent publication, Zuidema *et al*. (2025) reveal that drought currently exerts moderate effects on tree growth, they also confirm climate impacts are expected to become progressively more severe under increasing aridity, diminishing the strength of the terrestrial carbon sink.

Persistent reductions in carbon gain due to heat and drought can eventually lead to plant death through carbon starvation (McDowell *et al*., 2008). Another mechanism explaining tree mortality under extreme climate is the hydraulic-failure hypothesis, describing how reduced water availability leads to cavitation in xylem conduits, reducing water transport and causing cell desiccation and tissue death (Martínez-Vilalta *et al*., 2002). Empirical studies have demonstrated that vulnerability to embolism strongly predicts mortality of tropical trees in the face of climatic stress, revealing hydraulic safety as the dominant mechanism influencing survival and biomass dynamics in tropical forests (Anderegg *et al*., 2016; Tavares *et al*., 2023; Tavares *et al*., 2026).

Intense droughts and heatwaves have therefore become key drivers of tree mortality across tropical forest ecosystems (Powers *et al*., 2020). In Sabah, Malaysian Borneo, extreme climate associated with El Niño events has been shown to impair tree growth and survival across elevations and vegetation types, increasing seedling mortality rates by more than three times (Nakagawa *et al*., 2000; Bebber *et al*., 2004; Miyamoto *et al*., 2021). In tropical moist forests in Panama, community-wide seedling mortality increased by 11% during the extreme 2015-2016 El Niño (Browne *et al*., 2021). Seven years of long-term throughfall exclusion at Caxiuanã, Amazonia, doubled mortality rates compared to the control plots (da Costa *et al*., 2010), although after 20 years, mortality and plant biomass stabilised, demonstrating forest resilience through ecosystem reorganisation (Sanchez-Martinez *et al*., 2025). Using almost 50 years of growth data, Bauman, Fortunel, Delhaye *et al*. (2022) showed that higher atmospheric water stress consistently increased tree mortality rates in Australian rainforests. After collating tree survey data from more than 100 monitoring plots across Southeast Asia and the Americas, Phillips *et al*. (2010) showed that stem mortality of trees increased with the intensity of moisture stress during drought intervals, indicating forest biomass sensitivity to drying climate may be widespread across tropical regions.

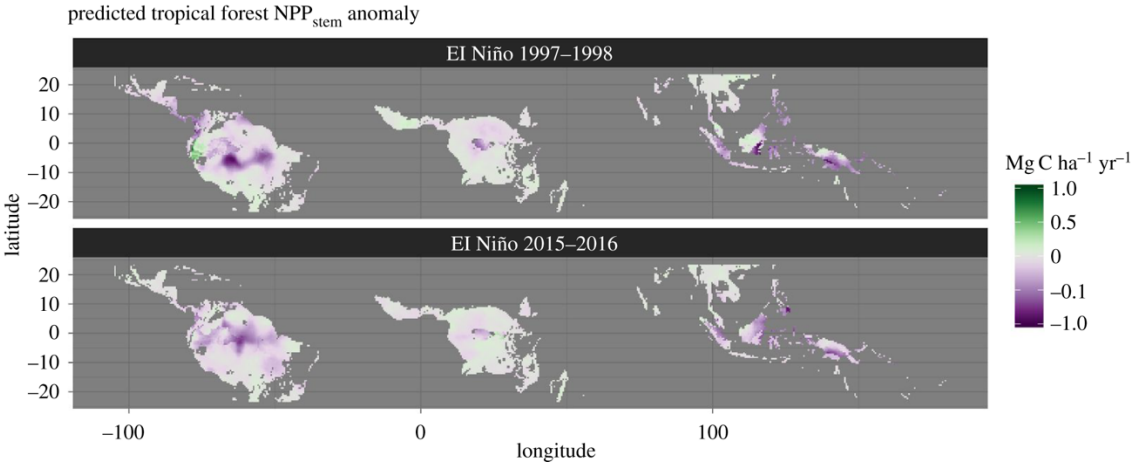


Figure 2.1, pantropical forest maps of predicted woody stem productivity (NPP_{stem}) anomalies during the extreme El Niño events of 1997-1998 and 2015-2016. Units are expressed in MgC ha^{-1} year^{-1}. Reproduced from Rifai *et al*. (2018), ENSO Drives interannual variation of forest woody growth across the tropics, Philosophical Transactions of the Royal Society B, Vol. 373(1760), 20170410 (https://doi.org/10.1098/rstb.2017.0410), with permission from The Royal Society.

Altered climatic conditions drive changes in growth and mortality that scale up to influence ecosystem biomass accumulation. Extreme episodes of combined heat and drought in tropical forests are thus particularly concerning due to significant impacts on carbon storage and greenhouse gas emissions (Barlow *et al*., 2020; Berenguer *et al*., 2021). In Southeast Asia, biomass accumulation and carbon sequestration are periodically suppressed by extreme drought during ENSO events (Qie *et al*., 2017; Kondo *et al*., 2018). Furthermore, during the 2015/2016 El Niño, unprecedented temperatures and rainfall deficits caused a 36% reduction in net carbon uptake within African forests (Bennett *et al*., 2021), and reversed the carbon sink capacity of the Amazon forest region (Bennett *et al*., 2023).

More extreme climates are also expected to substantially alter plant demography and ecosystem productivity in tropical savannas (Sankaran, 2019). For example, Pillay & Ward (2022) found that water availability limited grass production and savanna sapling growth. Fensham *et al*. (2009) describe how an overall increase in tree cover over five decades of above-average rainfall in Australian savannas was offset by sudden tree death after an extreme drought. Gnanamoorthy *et al*. (2026) demonstrated that woody savanna vegetation in Yunnan, China, declined for 3 years after a period of extreme heat and water stress, with disproportionate decreases in shrub abundance. Structural changes caused sustained reductions in evapotranspiration, although gross primary production recovered in the years after drought. Zanella de Arruda *et al*. (2016) reveal that net ecosystem exchange in *campo sujo* savannas in Brazil responded rapidly to temporal variations in soil water availability, becoming a net source of CO_2 during dry periods.

However, in tropical savannas, drought and heatwave impacts on plant performance are not only predicted by tolerance to heat and water stress. Drought-temperature dynamics in open landscape vegetation are instead influenced by many factors including tolerance-avoidance trade-offs, neighbourhood effects, herbivory and competition (Sankaran, 2019). Carbon depletion is thought to play a more prominent role in driving mortality risk in savannas compared to tropical forests, because savanna plants depend heavily on stored carbon reserves to support recovery following

fire, herbivory and seasonal drought (Case *et al*., 2019). Global change impacts in savannas are also difficult to monitor and measure. Although structure is considered a reliable indicator of forest ecosystem decline (Gao *et al*., 2020), savannas differ from forests in that structural loss does not necessarily imply functional or compositional degradation (Veldman, 2016).

Ecosystem responses in tropical savannas are further complicated by complex interactions between the two main vegetation layers – trees and grasses – which respond differently to environmental and biotic changes (Sankaran, 2019). For example, Wigley *et al*. (2024) found that although rising CO_2 concentrations may favour trees, increasing variability in dry season length could give grasses a greater relative advantage, as they are able to exploit moisture availability more efficiently. In turn, Pillay & Ward (2022) demonstrated that experimental warming had a positive effect on tree sapling growth but not on grass biomass. Furthermore, in savanna systems, vegetation dynamics are shaped by fire regimes, which are inherently linked to heat and drought through the dependence of fire behaviour on weather conditions. In the long term, climate conditions influence fuel loads, whilst shorter-term variations in temperature and moisture determine flammability and fire severity (Alvarado *et al*., 2020). Fire intensity and spread are strongly mediated by heat and drought, making it extremely challenging to isolate the independent effects of fire from those of climate extremes (Cardoso *et al*., 2022).

Understanding how climate influences fire regime attributes and coexistence between trees and grasses will be essential for accurately predicting and scaling savanna carbon responses to global change (Accatino *et al*., 2010; Staver, 2018). Across the entire tropics, current knowledge of long-term productivity responses to climatic changes is limited because studies investigating the impacts of droughts and heatwaves have largely focused on single events or on relatively short-term treatments (Bonal *et al*., 2016). In the current context, studies that evaluate the consistency of responses to repeated droughts and heatwaves, or the cumulative effects of long-term interventions, could provide valuable insight on the interactive mechanisms structuring ecosystem responses to altered climate (Metcalfe *et al*., 2010; Müller & Bahn, 2022; Cera *et al*., 2025).

2.2. On tropical ecosystem responses to altered fire regimes

Fire is also considered to be another major driver of ecological degradation in tropical ecosystems, particularly in tropical forests (Malhi *et al*., 2014). Tropical forest systems have evolved in the context of relative fire absence, and are therefore fire vulnerable (**Figure 2.2**), as species have few adaptations to resist burning (Brando *et al*., 2012). Fire can cause extreme tree mortality affecting forest structure and composition (Barlow *et al*., 2003; Armenteras *et al*., 2021). Even low-intensity understory fires can kill a high proportion of the tree community (Slik, Breman *et al*., 2010; Balch *et al*., 2015). Barlow & Peres (2006) found that post-fire mortality of small trees reached 42% in Amazonian forests, and Barlow *et al*. (2003) demonstrated that 3 years after fire, live stem density and biomass were 52% and 49% of those found in the unburnt forest respectively. In rainforests in Indonesian Borneo, Slik *et al*. (2008) found that aboveground biomass decreased between 40 and 92% 1.5 years after fire, with highest relative biomass losses in small diameter classes. Across tropical forests, fires can contribute to similar rates of biodiversity loss as deforestation, and significantly compromise key biophysical processes including evapotranspiration and biomass accumulation (Lapola *et al*., 2023).

Impacts of fire on tropical forests are further amplified by changing climate, as heat and drought associated with extreme weather events increase fire severity and impair plant recovery (McDowell *et al*., 2018). Extreme weather increases forest flammability due to reduced air and vegetation moisture (Ray *et al*., 2010) and increased fuel accumulation from litterfall and mortality (Ray *et al*., 2005), meaning that fires occurring during drought years tend to be larger and more intense, with a disproportionate effect on mortality (Alencar *et al*., 2015). For example, Brando *et al*. (2014) revealed that experimental burning in Southern Amazonian forests during drought years abruptly increased fire-induced tree mortality by 226% and 462%. After a drought

in East Kalimantan, Borneo, van Nieuwstadt & Sheil (2005) found that stem mortality in burnt dipterocarp forests reached ~80%, compared to ~26% in the unburnt forest.

However, fire can also play an important role in maintaining plant function and ecosystem dynamics in fire-adapted systems such as savannas (Higgins *et al*., 2000; **Figure 2.2**). Fire-tolerant plant species possess trait adaptations that allow rapid resprouting following fire, and are able to take advantage of increased light availability and reduced competition (Gomes *et al*., 2021). Fire can also trigger reproductive responses such as germination and flowering, aligning recruitment with periods of favourable resource availability (Fidelis & Zirondi, 2021). In the context of fire-dependent ecosystems, it is changes in fire regime attributes that drive plants beyond ecophysiological and performance thresholds. For example, more frequent fires shorten the interval available for recovery between disturbance events, depleting carbohydrate reserves, limiting resprouting capacity and reducing stem growth and canopy development over time (Fairman *et al*., 2019; Mndela *et al*., 2023). Frequent fire may also prevent individuals from reaching reproductive maturity, lowering propagule production and recruitment (Plumanns-Pouton *et al*., 2024). Conversely, extended intervals without fire can promote canopy closure and fuel accumulation, limiting photosynthesis, growth and recruitment, as well as increasing the likelihood of more intense fires (Chiminazzo *et al*., 2025). More intense fires – often associated with increasingly extreme climatic conditions – have greater impacts on plant structure, increasing the extent of scorching, combustion, and heat injury (Grau-Andrés *et al*., 2024).

Many studies have used distinct seasonal burns as experimental proxies to approximate variation in temperature, fuel moisture, and fire intensity, in an attempt to understand climate and fire behaviour influences on vegetation (Rissi *et al*., 2017). For example, in Guinean savannas, spread and intensity of mid-season and late-season fires were significantly greater than those of early-season burns (N'Dri *et al*., 2018). In Kruger National Park, South Africa, fire season had a significant effect on fire intensity, with very intense winter fires being associated with reductions in grass fuel moisture (Govender *et al*., 2006). Savannas may face increasingly severe ecological

impacts as climate change and human ignitions shift fire occurrence towards periods of extreme heat and drought, with important impacts on vegetation dynamics (Croker *et al*., 2023).

Longer dry seasons and more extreme climates are indeed contributing to an increase in wildfire intensity and frequency across savannas worldwide (Jones *et al*., 2022). Additionally, human activities promote flammability and increase the number of ignitions (Flannigan *et al*., 2013; Jolly *et al*., 2015). Changing fire regimes can profoundly affect the fitness and persistence of savanna plant species and communities by influencing population dynamics and vital rates (Hoffmann *et al*., 2002; **Section 2.1**), which in turn shape ecosystem-level responses in terms of structure and function (Le Stradic *et al*., 2018). Previous studies have shown that burning savannas at different frequencies and intensities significantly affects plant growth and survival (e.g., Rodrigues & Fidelis, 2022; Fontenele & Miranda, 2024) as well as primary production and carbon cycling (e.g., Teixeira *et al*., 2025). Scaling up individual- and species-level responses to understand and predict shifts in ecosystem structure and function remains one of the key challenges in deciphering the consequences of changing fire regimes in tropical savannas (Grau-Andrés *et al*., 2024).

Fire regimes in savannas are also changing as a result of landscape fragmentation, fuel discontinuity and fire suppression (Archibald, 2016), and the burnt area of savannas globally has actually declined over the last decades (Andela *et al*., 2017; Jones *et al*., 2022). Because fire is a crucial factor maintaining open canopies and preventing tree growth (Oliveras & Malhi, 2016; Pausas & Bond, 2020), reduced burnt area and fire occurrence have contributed to extensive woody encroachment and fuel buildup (Stevens *et al*., 2017). Unlike forests, tropical savannas are functionally maintained by fire regimes, where natural or traditional burns are required to promote vegetation regeneration, sustain nutrient cycles, support biodiversity and maintain ecosystem structure (Pivello, 2011; Staver *et al*., 2011; **Figure 2.2**). Decreasing fire frequency and occurrence allows for increased tree establishment and the eventual shift towards higher-biomass woody vegetation, which can be associated with acute losses in savanna species richness and ecosystem services (Abreu *et al*., 2017; Skhosana *et al*., 2025).

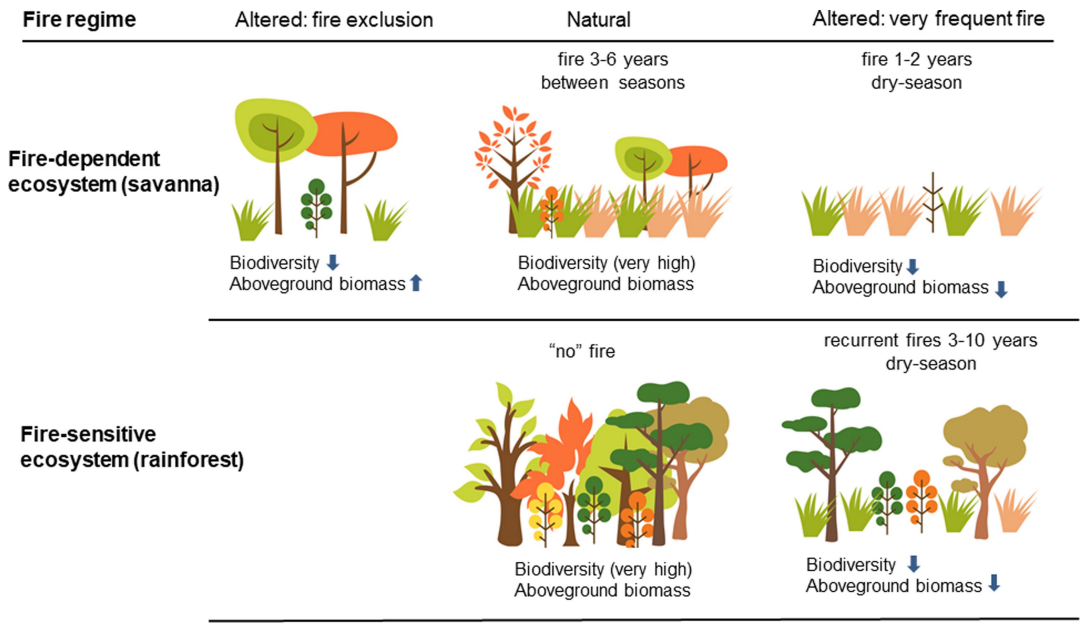


Figure 2.2, comparison of fire regime changes in tropical forests and savannas. In savannas, periodic fires maintain biodiversity and ecological processes, but anthropogenic burning increases fire frequency and intensity, killing young trees and reducing aboveground biomass. Fire exclusion also leads to degradation via tree encroachment, impacting biodiversity and ecosystem processes. In wet forests, natural fires are almost absent, but recurrent fires open up and degrade the forest, reducing biomass, biodiversity and ecosystem function. Reproduced with permission from Pivello *et al.* (2021). This article (https://doi.org/10.1016/j.pecon.2021.06.005) was published in Perspectives in Ecology and Conservation, Volume 19, Issue 3, pages 233-255. Copyright Elsevier (Associação Brasileira de Ciência Ecológica e Conservação) 2021.

2.3. On productivity as a key indicator of ecosystem function

Changes in growth and mortality as a result of altered climate and fire regimes scale up to impact the functioning of tropical forests and savannas at the ecosystem scale (Anderegg *et al.*, 2016). Plant growth rates determine biomass accumulation in plant structures. Consequently, extreme climate or fire events that reduce photosynthesis, increase autotrophic respiration and limit plant performance can have a strong impact on ecosystem carbon (Corlett, 2016). Additionally, tree mortality leads to reduced biomass due to the loss of growing stems; given that carbon accumulation in tropical forests is closely linked to tree basal area (Brienen *et al.*, 2015). Mortality also reduces biomass accumulation as carbon in dead stems is lost to soils and atmosphere via plant matter decomposition (Anderegg *et al.*, 2016). In this context, quantifying growth and

mortality as carbon fluxes allows us to investigate vegetation dynamics within a common currency of energy flow and ecosystem function. Characterising ecosystem carbon fluxes also provides a clearer framework for understanding interactions among vegetation, soils, and the atmosphere, and for interpreting the processes that regulate carbon storage within the broader carbon cycle (Malhi, 2012).

In the broadest of terms, ecosystem carbon fluxes include gross primary productivity (GPP) and net primary productivity (NPP). GPP is the total uptake of carbon by an ecosystem through photosynthesis (Malhi *et al*., 2009). It is an important metric that accounts for the total carbon allocation of ecosystems into growth or metabolic activities (Litton *et al*., 2007). Overall, plant carbon uptake (GPP) can be allocated into tissue growth and metabolism. NPP describes the net ecosystem carbon gained by plants and accrued into vegetation (Girardin *et al*., 2010). In other words, NPP represents plant growth in terms of biomass. Photosynthetic carbon (GPP) is invested into biomass (NPP) but is also allocated to plant metabolism for growth and maintenance, and lost to the atmosphere in terms of autotrophic respiration ($R_{autotrophic}$; Malhi *et al*., 2021). The ratio of net primary productivity (NPP) to gross primary productivity (GPP) is defined as carbon use efficiency (CUE) and describes how efficiently organisms or ecosystems convert assimilated carbon into biomass rather than respiring it back to the atmosphere (Doughty *et al*., 2018). Biomass storage in plant structures is not indefinite, however, and structural carbon is transformed into atmospheric CO_2 by organisms that consume organic tissues ($R_{heterotrophic}$, Malhi, 2012). In terrestrial ecosystems, $R_{heterotrophic}$ is dominated by microbial decomposition of dead plant material, leaf litter, dead roots and soil organic matter (Malhi & Grace, 2000). The difference between GPP and total ecosystem respiration ($R_{autotrophic} + R_{heterotrophic}$) is defined as net ecosystem production (NEP), and represents the net rate of carbon accumulation in an ecosystem (Malhi *et al*., 2015). Positive NEP indicates the ecosystem is storing carbon and functioning as a carbon sink, whilst negative NEP means the ecosystem is acting as a source of atmospheric carbon (Malhi *et al*., 2009). These processes are all expressed as rates of carbon flux per unit land area over time, typically in units of megagrams of carbon per hectare per year (MgC ha^{-1} $year^{-1}$; **Figure 2.3**).

Ecosystem carbon fluxes can be measured using the eddy covariance method, which quantifies the movement of carbon dioxide between an ecosystem and the atmosphere (Malhi *et al*., 1998). Eddy covariance provides continuous measurements of net ecosystem exchange (NEE) and allows ecosystems to be assessed as carbon sinks or sources over time. Gross primary productivity (GPP) and total ecosystem respiration (R_{eco}) can then be derived from NEE measured by eddy covariance (Campioli *et al*., 2016). In theory, NEP should be equivalent to the net ecosystem exchange, where negative NEE indicates net carbon uptake (Clark *et al*., 2001). However, eddy covariance is costly, and only provides a top-down measure of ecosystem carbon fluxes (Malhi *et al*., 2021). Instead, productivity and respiration fluxes can be estimated using a bottom-up approach, in this case, by measuring the carbon fluxes associated with individual ecosystem components: canopy and leaves, stems or wood, roots, and soils (Moore *et al*., 2018). Carbon flux measurements from different ecosystem components can then be summed up to estimate total ecosystem productivity, respiration, and carbon balance (Malhi, 2012). Because ecosystem components are linked to different physiological processes, environmental variables and ecological constraints, quantifying carbon fluxes also helps us identify how altered climate and fire regimes are driving changes in tropical carbon cycling (Poorter *et al*., 2012).

Changes in climate and fire regime conditions have complex effects on NPP across ecosystem components. For example, over the first 4 years of the Caxiuanã Amazon drought experiment, reduced soil moisture led to a small decline in total litterfall (12%), but a very strong decline in reproductive litterfall (54%), as litterfall patterns de-coupled from seasonal climate variables (Rowland *et al*., 2018). However, after 10 years of drought treatment, flowering, fruiting and litterfall-climate relationships re-stabilised. At the ecosystem scale, rainfall exclusion slightly reduced total NPP, but increased autotrophic respiration despite recovery of tree growth (da Costa *et al*., 2010). Alternatively, 21-year monitoring of aboveground NPP within a Costa Rican rainforest revealed that woody production declined in years with warmer nights and hotter dry seasons, but $NPP_{litterfall}$ was related with CO_2 and radiation (Clark *et al*., 2021). Similarly, Hofhansl

et al. (2014) found that NPP_{stem} decreased significantly in response to increasing temperatures during El Niño, reducing ecosystem carbon uptake, but subsequently recovering during La Niña. In Xishuangbanna, Southwest China, precipitation had a positive influence on NPP of both stems and leaves, and periods of low rainfall strongly regulated the productivity of tropical seasonal rainforests (Linger *et al*., 2020). In savannas, previous studies have demonstrated that fire impacts ecosystem carbon uptake through direct emissions, as well as via reduced productivity of stems and canopies (Beringer *et al*., 2007). Murphy *et al*. (2010) estimated that post-fire reductions in tree growth across North Australian savannas reduce woody NPP by 0.19 MgC ha^{-1} $year^{-1}$ (0.51 MgC ha^{-1} $year^{-1}$ in the case of severe fires) compared to overall NPP of 1 to 2 MgC ha^{-1} $year^{-1}$.

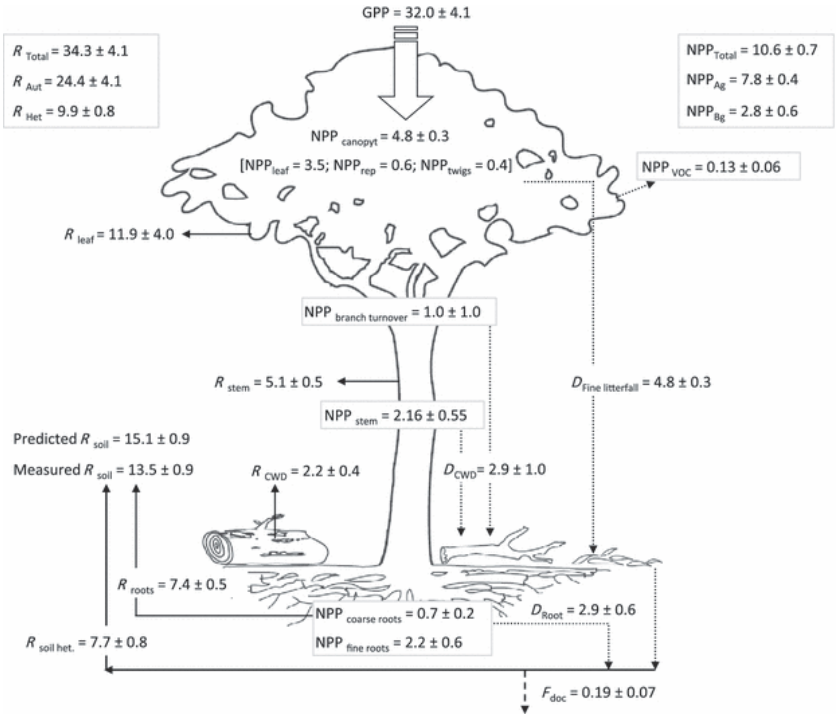


Figure 2.3, example of the full carbon cycle for a tropical forest in Caxiuanã, Brazil. GPP, gross primary productivity; R_{total}, total ecosystem respiration; R_{Aut}, autotrophic respiration; R_{Het}, heterotrophic respiration; NPP_{Total}, total net primary productivity; NPP_{Ag}, above-ground NPP; NPP_{Bg}, below-ground NPP; NPP_{canopy}, canopy NPP; NPP_{leaf}, leaf NPP; NPP_{rep}, reproductive NPP; NPP_{twigs}, twig NPP; NPP_{VOC}, volatile organic compound NPP; $NPP_{branch\ turnover}$, branch turnover NPP; NPP_{stem}, above-ground stem wood NPP; $NPP_{coarse\ roots}$, coarse root NPP; $NPP_{fine\ roots}$, fine root NPP; $D_{fine\ litterfall}$, canopy litterfall; D_{CWD}, woody mortality; D_{Root}, fine root detritus; F_{DOC}, outflow of dissolved organic carbon; $R_{soil\ het}$, soil heterotrophic respiration; R_{roots}, root respiration; R_{CWD}, coarse woody debris respiration; R_{soil}, soil respiration; R_{stem}, above-ground woody respiration; R_{leaf}, leaf dark respiration. All fluxes are in MgC ha^{-1} $year^{-1}$. Reproduced from Malhi Y (2012), The productivity, metabolism and carbon cycle of tropical forest vegetation, Journal of Ecology, Vol. 100(1), pp. 65-75 (https://doi.org/10.1111/j.1365-2745.2011.01916.x), with permission from John Wiley & Sons (on behalf of the British Ecological Society).

Patterns of NPP allocation can also shift in response to environmental conditions, resource availability and plant stress (Girardin *et al*., 2010). For example, across tropical regions, logging and forest disturbance have been shown to shift NPP patterns towards increased allocation into stem biomass development, although responses in net ecosystem balances vary depending on respiration and mortality changes (Riutta *et al*., 2018; Mills *et al*., 2023; Makelele *et al*., 2026). Plants can also use a greater proportion of NPP in growing fine roots to increase access to soil resources, whilst allocating more carbon to leaf production and canopy expansion for improved light capture (Malhi *et al*., 2011). To cope with drought conditions, plants can allocate a greater proportion of NPP to root systems to enhance water uptake, while reducing investment in leaves to limit water loss through transpiration (Yaffar *et al*., 2024). Fire disturbances also alter allocation patterns, for example, in terms of rapid resprouting and regrowth, which allows for a quicker recovery of photosynthetic capacity after fire (Pausas *et al*., 2016). In ecosystems with frequent fires, plants can also invest in belowground productivity, allowing for structures such as roots or storage organs to support post-fire regeneration (Zhou, 2023).

Our understanding of primary productivity in tropical forests has improved over recent decades thanks to the development of monitoring networks and standard measurement approaches (Phillips, 2023). Plot inventory networks such as ForestGEO, RAINFOR and Forestplots.net continue to provide new insights into the variability of forest structure and plant communities, making use of repeated records of tree size and mortality to reveal changes in productivity and carbon balances (Peacock *et al*., 2007; Lopez-Gonzalez *et al*., 2011; Davies *et al*., 2021). Monitoring networks in dry tropical forests and savannas (DRYFLOR, SEOSAW, SECO) have also been consolidated, but important research gaps remain due to the lack of long-term datasets and uneven spatial coverage (The SEOSAW partnership, 2021; Moonlight *et al*., 2021). However, most of these efforts largely focus on woody stem dynamics, overlooking important contributions from other ecosystem components. To complement these large-scale tree monitoring efforts and provide a more comprehensive understanding of ecosystem carbon dynamics, the Global

Ecosystems Monitoring (GEM) network was developed, aiming to describe the productivity and carbon cycling of tropical forests and savannas in greater detail (Malhi *et al*., 2021). It relies on intensive measurements of multiple ecosystem components, including tree growth, litterfall, root production, stem respiration, soil respiration, and leaf gas exchange.

Taken together, tree surveys and carbon flux measurements can provide deeper insight into the integrated responses of ecosystems to changing climates and altered fire regimes. For example, Rocha *et al*. (2014) investigated the effect of annual burns on carbon cycling within the southern limit of the Amazon rainforest in Mato Grosso, Brazil, and found a 15% reduction in total NPP as a result of fire treatment. Although all individual components of NPP declined after fire, losses in productivity were driven by fine root NPP and litterfall NPP, which accounted for 91% of the overall reduction. The authors conclude that the strong decrease in $NPP_{\text{fine roots}}$ was probably caused by the destruction of surface root mats due to fire. Reis *et al*. (2025) investigated 5 years of productivity dynamics in typical Cerrado savanna and transitional forest-savanna vegetation (*cerradão*), and demonstrated that *cerradão* productivity declined by 29% during the 2015/2016 El Niño event, while savanna NPP remained constant over the years. In the *cerradão*, stem productivity was reduced by 58%, and was attributed to the decline of two dominant species. In the savanna, the most affected component was fine roots, which declined by 38%, and could be linked to a more conservative water use strategy of savanna species. Productivity is thus a useful indicator of ecosystem function because it integrates the effects of underlying ecological processes and environmental controls with ecosystem-level changes in carbon and energy flows. Because productivity underpins plant strategies and ecosystem carbon balances, it provides an important basis for climate budgeting and helps inform our understanding of ecosystem responses in the face of global change (Davidson *et al*., 2022).

2.4. On functional traits as a tool to assess productivity responses

Plant functional strategies can help explain patterns in ecosystem productivity, as they underpin plant performance and shape responses to environmental stress (Mauki *et al*., 2025). Plant functional strategies describe the ways in which plants allocate resources and express traits in order to maintain fitness, allowing for survival, growth, and reproduction under particular environmental conditions (Zhou *et al*., 2022). Plant functional strategies reflect evolutionary adaptations to environmental pressures and resource limitations, including nutrient availability, water supply, temperature, and disturbance (Volaire, 2018). By examining how plants balance trade-offs between growth, survival, and reproduction, one can better understand how vegetation communities are structured, and predict how plants respond to environmental changes (Dalle Fratte *et al*., 2025). A major way of understanding plant functional strategies is through the study of plant functional traits (Laughlin, 2023).

Functional traits are mensurable morphological, physiological and phenological characteristics that impact fitness via their effects on growth, reproduction, and survival (Violle *et al*., 2007). Traits can be measured at the individual level, and connect organismal performance to environmental responses and ecosystem processes, acting as key indicators of functional strategies (Diaz *et al*., 2004). Plant traits are also linked with species distribution patterns and community assembly processes, and trait-based approaches allow researchers to predict how plant communities may respond to disturbances and climate variability (Shipley *et al*., 2006). Traits indicate species' capacity to maintain function and ensure survival under environmental stress (Violle *et al*., 2007). Because carbon accumulation depends on sustained plant survival, trait adaptations that enhance species persistence help maintain plant populations and ecosystem productivity (Lavorel & Garnier, 2002). Plant strategies could also help explain patterns in ecosystem productivity by linking functional traits with rates of carbon assimilation and growth (Falster *et al*., 2018). However, mechanistically integrating plant traits to predict ecosystem primary productivity remains one of the key challenges in functional and community ecology (Yan *et al*., 2023).

A wide range of functional traits are thought to be important in determining plant growth and survival in the face of extreme climate. In tropical forests and savannas, functional strategies that allow for growth and survival under drought conditions involve maintaining hydrological balances and physiological function despite water deficits (O'Brien *et al*., 2017). Plants can avoid water stress by accessing deeper soil layers via increased root depth, whilst reduced leaf area, bark protection and waxy cuticles help limit transpiration (Fensham & Fairfax, 2007; Duursma *et al*., 2018; Wolfe, 2020). Drought-tolerant species may also allow for tight stomatal regulation and osmotic adjustments, which help reduce water loss and maintain turgor pressure (He *et al*., 2024). Plants can also adjust their life histories and phenological traits to escape drought altogether, for example, by shedding leaves during dry periods to reduce transpiration (Vico *et al*., 2017). Xylem anatomy traits such as vessel diameter, density and maximum length are also important in determining plant resistance to embolism and are good predictors of drought tolerance across ecosystems (Markesteijn *et al*., 2011). Species with denser wood tend to have higher density of smaller xylem tissues, allowing for increased structural integrity, resistance to cavitation and hydraulic safety margins (Anderegg *et al*., 2016). Consequently, wood density emerges as a key indicator of tree drought tolerance across tropical biomes (O'Brien *et al*., 2017). Non-structural carbohydrates also act as critical energy reserves that buffer against carbon imbalances during drought, maintaining metabolic activity and allowing for rapid recovery (O'Brien *et al*., 2020). However, their precise role in mediating responses to extreme climate across different ecosystems remains unresolved (Piper & Paula, 2020).

Extreme heat also constrains plant function, primarily through interactions with water availability and drought (Sato *et al*., 2024). Plants regulate leaf temperatures through evaporative cooling, but this increases transpiration and may intensify water stress (Evans *et al*., 2025). As a result, drought and heat tolerance strategies are often physiologically and functionally coordinated (Wang *et al*., 2026). In this context, traits that reduce water loss, increase hydraulic safety, or enable seasonal deciduousness also contribute to growth and survival during periods of high temperatures (Zhou *et al*., 2023). Structural traits that help maintain growth and survival under heat stress include

reflective leaf surfaces, waxy cuticles and leaf pubescence, which reduce the amount of solar radiation absorbed by leaves, lowering leaf temperatures (Holmes & Keiller, 2002). Leaf angle also plays an important role in limiting light interception and potential heating (Ishida *et al*., 1999). In turn, smaller leaf sizes and increased leaf thickness and leaf mass per area provide greater structural buffering against high temperatures and allow leaves to dissipate heat more efficiently (Slot *et al*., 2021; Pedraza, 2024). At the cellular level, biochemical traits that allow for continued carbon assimilation under extreme heat include the production of protective molecules and the stabilisation of photosynthetic machinery (Hasanuzzaman *et al*., 2013).

Functional traits are also important in allowing for plant growth and survival within fire regimes (**Figure 2.4**). Plant species can persist after fire by having traits that promote the survival of established individuals through protection and regeneration, or that allow for populations to be maintained through reproductive traits (Clarke *et al*., 2013; Pausas & Keeley, 2014). Traits that enhance post-fire survival include thick bark and leaf bundles that thermally protect vital tissues such as tree cambium and meristems (Pausas, 2015). Protected bud banks beneath the bark or below ground – coupled with energy storage – allow plants to recover rapidly after fire by resprouting (Pausas *et al*., 2016). Plant size, architectural traits and leaf flammability also influence plant exposure to flames and can constrain or promote fire damage (Vesk, 2006; Schwilk, 2015). Reproductive traits that allow populations to be maintained even if some adult plants are killed by fire include post-fire flowering to take advantage of reduced competition (Zirondi *et al*., 2021); serotiny, where seeds are stored in the canopy and released in response to fire (Lamont *et al*., 2020); and persistent soil seed banks that survive heating and germinate after fire (Pausas & Lamont, 2022).

Fire-adapted plants are often classified into broad functional types such as ‘obligate seeders’, ‘facultative seeders/resprouters’, and ‘obligate resprouters’ based on post-fire recovery traits, although life-history strategies and competitive processes should be better integrated into these classifications (Plumanns-Pouton *et al*., 2024). Trait syndromes that allow for persistence can

also be classified according to the fitness advantage they confer to plants (Archibald *et al*., 2019). For example, by minimising fire damage through bark protection ('resistance'), by avoiding exposure to fire through deciduousness or belowground life forms ('avoidance'), or by allowing recovery through resprouting or recruitment ('tolerance'; Pausas, 2019; Chiminazzo *et al*., 2023). In ecosystems where fire-related traits enable regeneration, vegetation productivity and survival are closely linked with fire regimes (Pausas & Ribeiro, 2013; McLeod *et al*., 2025). However, it is important to note that functional trade-offs between fire resilience strategies, resource acquisition, and resistance to heat and drought also have important implications for plant survival and ecosystem productivity (Clarke & Knox, 2009; Post-Leon & Anderegg, 2026).

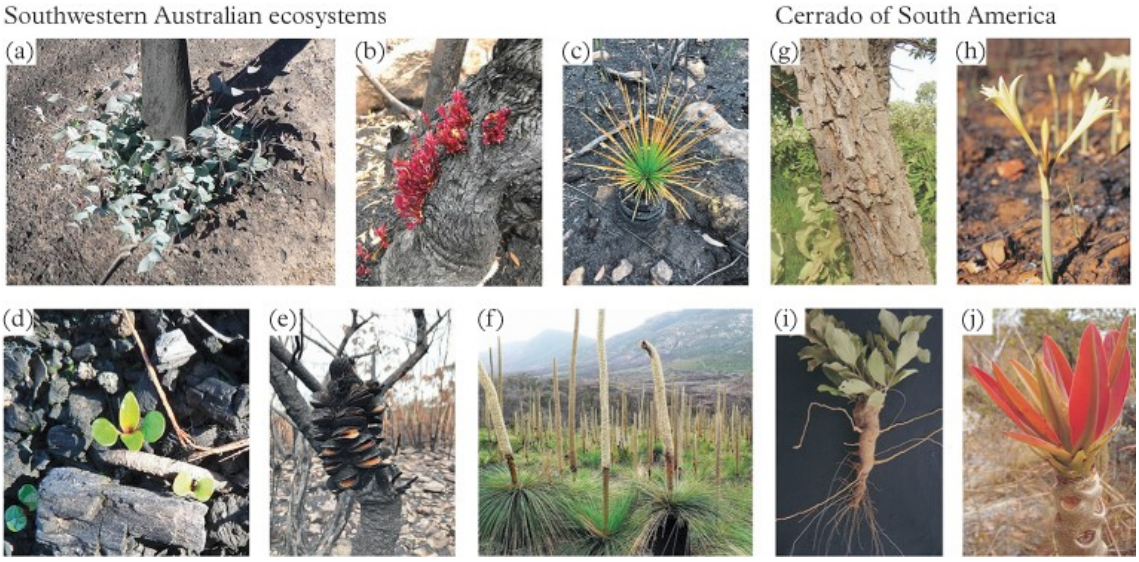


Figure 2.4, functional trait adaptations allowing for plant growth, survival and reproduction in fire-prone ecosystems: **A-F**) southeastern Australia, **G-J**) Cerrado savannas of South America. Traits include **A**) basal sprouting in *Eucalyptus sp*., **B**) epicormic resprouting in *Angophora sp*., **C**) aboveground resprouting in *Xanthorrhoea sp*., **D**) post-fire seed germination in *Eucalyptus sp*., **E**) serotinous cone in *Banksia sp*., **F**) post-fire flowering in *Xanthorrhoea sp*., **G**) thick and corky bark in *Machaerium opacum*, **H**) post-fire flowering in *Hippeastrum goianum*, **I**) xylopodium in *Anemopaegma sp*. which enables resprouting after fire, **J**) thick, fire-resistant terminal branches in *Kielmeyera coriacea*. Reproduced from Laughlin DC (2023), Plant Strategies: The Demographic Consequences of Functional Traits in Changing Environments, Figure 7.11, Copyright © 2023, Oxford Publishing Limited (https://doi.org/10.1093/oso/9780192867940.003.0007). Reproduced with permission of the Licensor through PLSclear. Image material was originally sourced from Nolan RH *et al*. (2021), Limits to post-fire vegetation recovery under climate change, Plant, Cell & Environment, Vol. 44(11), pp. 3471-3489 (https://doi.org/10.1111/pce.14176), Figure 3, reproduced with permission from John Wiley & Sons; and from Simon MF and Pennington T (2012), Evidence for adaptation to fire regimes in the tropical savannas of the Brazilian Cerrado, International Journal of Plant Sciences, 173(6), pp. 711-723 (https://doi.org/10.1086/665973), Figure 1, reproduced with permission from University of Chicago Press.

Functional traits also reflect different ways in which plants allocate resources to growth, survival, and reproduction, as individuals are unable to optimise all functions simultaneously under variable environmental constraints and biotic conditions (Violle *et al*., 2007). Economics spectra describe these fundamental trade-offs in plant strategies between fast resource acquisition and slow resource conservation (Reich, 2014). Although the most well-known example is the leaf economics spectrum (**Figure 2.5**; Wright *et al*., 2004), these trade-offs can be conceptualised in terms of other components (wood, bark, roots) or integrated into a whole-plant spectrum (Li *et al*., 2021). One end of the plant economics spectra is defined by "fast" or acquisitive strategies, where plants invest in traits that maximise resource capture and growth under favourable conditions (Donovan *et al*., 2011). Resource acquisitive plants tend to have high specific leaf area, high leaf nutrient concentrations, and fast assimilation rates, but lower leaf thickness and wood density, allowing for quick returns on investment at the cost of durability and resistance to stress (Chave *et al*., 2009). At the other end are "slow" or conservative plant strategies. In this case, plants exhibit traits that promote longevity and resource retention, such as thicker leaves, denser wood, and high leaf mass per area and structural investment (Gorné *et al*., 2022). Conservative strategies allow species to better cope with resource limitations or stressful environments, increasing survival rates and maintaining growth long-term (Onoda *et al*., 2017). Plant economic spectra also provide a mechanistic justification for the growth-survival trade-off observed in many tropical ecosystems (Meira-Neto *et al*., 2019). This principle highlights that organisms cannot simultaneously maximise fast growth and high survival, and must allocate limited resources to one or the other, meaning that fast-growing species often have low survival rates, whereas slow-growing, conservative species tend to live longer and tolerate stress (Wright *et al*., 2010).

Stress tolerance traits, and traits that inform about potential resource acquisition trade-offs, offer the potential to explain patterns in tree growth and survival as a result of altered climate and fire regimes (Gignoux *et al*., 1997; Wright *et al*., 2010). For example, Berenguer *et al*. (2018) discovered that wood density was a significant factor that helped explain the difference in growth

between trees in burned and unburned forests in eastern Amazonia, with low wood-density trees growing significantly faster in burned sites. Nottingham *et al*. (2023) found that artificial warming in a tropical forest caused relative growth declines in nitrogen-fixing seedlings, suggesting increased nutrient acquisition may be linked with increased vulnerability. In southern African savannas, Wargowsky *et al*. (2023) found that traits describing root vascular anatomy predicted relative growth rates in both trees and grasses. A functional trait framework can therefore help us understand how plants will respond to changes in climate and fire regimes acting as shifting environmental filters (Enright *et al*., 2014). However, key uncertainties remain in predicting how interacting functional traits underpin different facets of plant function, and in integrating trait-response relationships across ecosystem types and under novel environmental conditions (Liu *et al*., 2021). Better understanding the role of plant strategies in species responses to altered climate and fire regimes will enhance our ability to predict ecosystem responses to change, linking plant characteristics with ecosystem function and anticipating impacts on productivity and carbon balances within tropical forests and savannas (Mauki *et al*., 2025).

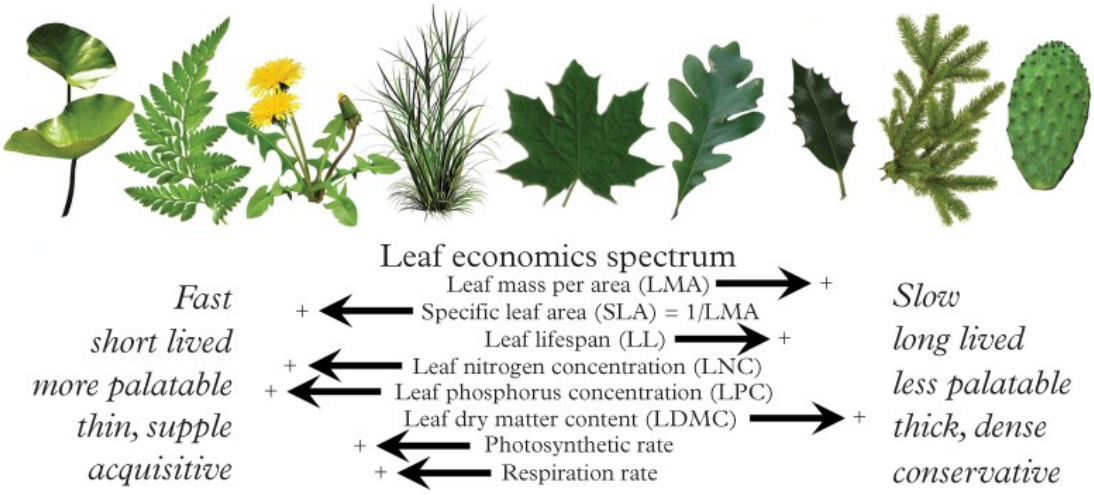


Figure 2.5, schematic representation of the leaf economics spectrum, illustrating coordinated variation in leaf functional traits along a continuum from "fast" to "slow" ecological strategies. Reproduced from Laughlin DC (2023), Plant Strategies: The Demographic Consequences of Functional Traits in Changing Environments, Figure 6.15, Copyright © 2023, Oxford Publishing Limited (https://doi.org/10.1093/oso/9780192867940.003.0007). Reproduced with permission of the Licensor through PLSclear.

2.5. On Cerrado savannas and lowland dipterocarp rainforests

Chapters 3 and 4 of this thesis focus on investigating productivity dynamics within Cerrado savannas (**Figure 2.6**). Cerrado, originally referring to "dense" or "closed" vegetation, is the name given to a South American region dominated by savanna formations (Gottsberger & Silberbauer-Gottsberger, 2006). Occupying 22 million km^2 and spanning a latitudinal gradient of 20º, it is the largest savanna region in the tropical Americas (Sano *et al*., 2019). Most of the Cerrado is found in Brazil, southeast of Amazonia, with a very small proportion also found in Paraguay and Bolivia (Ratter *et al*., 1997). It supports a population of more than 20 million people, and contains several major cities, including the capital, Brasilia (Pereira *et al*., 1997). The Cerrado also extends over the headwaters of important river basins (the Araguaia-Tocantins, the Paraguay-Paraná, and the São Francisco), providing key resources for major aquifers and catchment areas (Oliveira *et al*., 2014). The Cerrado is characterised by strongly seasonal tropical climates, with a wet season during the austral summer, and a dry season during the austral winter (Cattelan *et al*., 2024).

The Cerrado is also critically important in terms of agriculture and economic activities. It is Brazil's primary agricultural region, accounting for 60% of the country's agricultural production (World Economic Forum, 2024). Large-scale levels of land conversion into croplands and pasture have taken place over the last decades (Espírito-Santo *et al*., 2016), meaning there is now less than 50% of the natural land cover remaining (Souza *et al*., 2020). Due to low levels of protection facilitating agricultural expansion, rates of land conversion within the Cerrado have been faster than those in the Amazon (Machado *et al*., 2024). In the Cerrado, landowners are only legally required to preserve 20% of the native Cerrado vegetation within private land (Klink *et al*., 2005), and the Soy Moratorium approved for the Amazon has not been extended to the Cerrado (Soterroni *et al*., 2019). Large-scale land conversion is therefore threatening Cerrado biodiversity, which is characterised by floristic richness and high levels of endemism (Lahsen *et al*., 2016).

The Cerrado region supports more than 10,000 native plant species, of which 30% are thought to be endemic (Giles *et al*., 2026). Cerrado ecosystems are highly heterogeneous, and constitute a mosaic of diverse vegetation formations including grasslands, savannas and forests (Durigan & Ratter, 2016). Cerrado vegetation types can be classified into distinct physiognomies, which include a gradient of savanna vegetation structures ranging from *campo limpo* (open grassland savanna) to *cerradão* (forest-savanna transition woodland), as well as rocky formations, gallery and riparian forests, dry seasonal forests and *vereda* palm fields (Ribeiro & Walter, 2008). This thesis focuses on the typical *cerrado sensu stricto* savanna formation, described as woodland savanna or dense savanna and characterised by small (>6 m) trees and 10% to 60% tree cover (Felfili & da Silva Junior, 1993). In *cerrado sensu stricto* savannas, typical fire intervals range between 2-6 years (Pivello *et al*., 2021), with fires every 3-4 years optimising ecosystem functioning and recovery (Pivello & Coutinho, 1992; Pivello *et al*., 2010; Oliveras *et al*., 2012).

The Cerrado is facing increased ignitions for agricultural conversion purposes, which are shifting fire season towards the peak of the dry season and exposing species to new fire regime conditions (Segura-García *et al*., 2025; Spadoni *et al*., 2025). Geospatial analyses have revealed that fire activity levels in the central and northern Cerrado have increased due to the expansion of the new agricultural frontier, whilst fire activity and frequency have decreased in the South because of land clearance and fragmentation (da Silva Arruda *et al*., 2024). In many areas of natural vegetation, fire exclusion policies have reduced fire frequency and promoted woody encroachment (Rosan *et al*., 2019), having important consequences towards diversity and ecological functioning, and increasing the likelihood of more intense fires (Durigan & Ratter, 2016). Fire exclusion is particularly problematic within protected areas, including Serra das Araras, where two of the thesis' studies (**Chapter 3 and 4**) are located (de Souza *et al*., 2025).

Serra das Araras Ecological Station is an IUCN Category 1A protected area contained within the municipalities of Porto Estrela and Cáceres, in Mato Grosso, central-western Brazil (ICMBio, 2016). The site is situated within the Paraguay River basin and is an ecologically important

reservoir of biological diversity at the intersection of the Amazon, Cerrado and Pantanal regions (Vitorino *et al*., 2018). Over 460 species of plants have been officially recorded (ICMBio, 2016), including critically endangered taxa (Destacio, 2021). Serra das Araras supports a variety of savanna, forest and grassland formations. The studies in **Chapters 3 and 4** were conducted within the central area of the reserve, in the Salobra River Valley, which is made up of *cerrado sensu stricto* vegetation with a well-defined grass layer and small- to medium-sized trees (Goodland, 1971). Research efforts at Serra das Araras are led by academic groups within local universities, and this thesis has been undertaken in close partnership with the State University of Mato Grosso (UNEMAT) and the Chico Mendes Institute for Biodiversity Conservation (ICMBio). Management at Serra das Araras is characterised by strong collaboration with local landowners and traditional *quilombola* communities (ICMBio, 2016). The reserve has recently adopted an integrated fire management strategy and has become an important training hub for fire brigades (ICMBio, 2022).

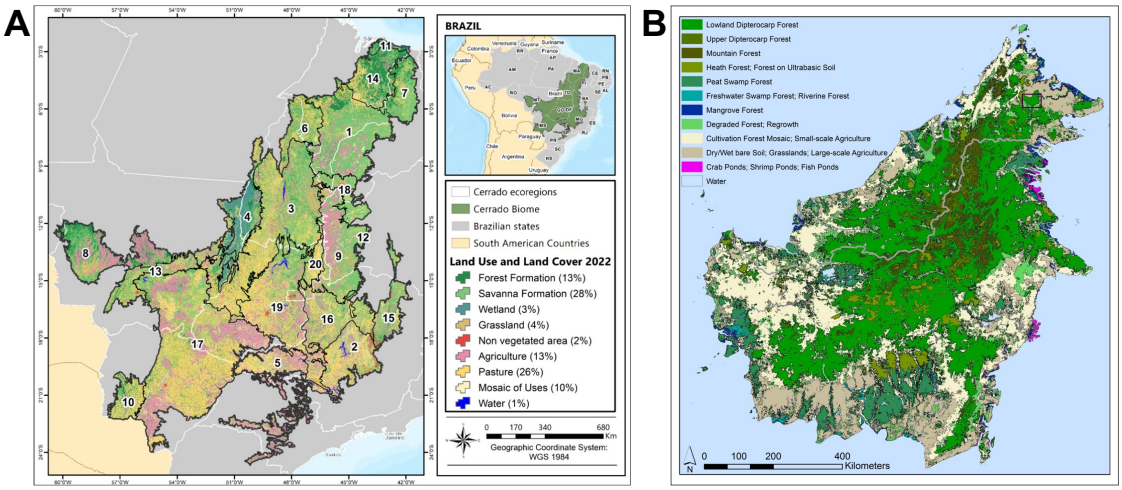


Figure 2.6, map of the ecological regions and the distribution of the ecosystems studied in this thesis. **A**) the Cerrado savanna region in Brazil, including land use and land cover classes based on the MapBiomas Collection 8. Numbers and black lines refer to the different ecoregions identified by Sano *et al*. (2019). Reproduced from da Silva Arruda *et al*., (2024), Assessing four decades of fire behavior dynamics in the Cerrado biome (1985 to 2022), Fire Ecology, Vol. 20(64), (https://doi.org/10.1186/s42408-024-00298-4), under a Creative Commons Attribution 4.0 International License (http://creativecommons.org/licenses/by/4.0/). **B**) map of land use cover across Borneo in 2008. Country borders between Malaysia, Indonesia and Brunei are shown in grey. Please note that many of the forested vegetation types include areas that have already been degraded. Reproduced from Langner *et al*., 2015, Assessment of above-ground biomass of Borneo forests through a new data-fusion approach combining two pan-tropical biomass maps, Land, Vol. 4 (3), land4030656 (https://doi.org/10.3390/land4030656), under a Creative Commons Attribution 4.0 International License (http://creativecommons.org/licenses/by/4.0/). The black rectangle indicates the location of the Langner *et al*. (2015) study area.

Chapter 5 of this thesis is instead focused on lowland dipterocarp rainforest ecosystems within Malaysian Borneo (**Figure 2.6**). Lowland dipterocarp forests are the dominant tropical rainforest type in the island of Borneo and across Southeast Asia (Newbery *et al*., 1996). In Borneo, lowland rainforests cover an area of more than 200,000 km^2, corresponding to about 74% of forest cover and 42% of total land area (Langner *et al*., 2007). They are characterised by having hot and humid climates, with relatively constant precipitation throughout the year (Prohaska *et al*., 2023). They are typically found in elevations below 300 meters, and are dominated by tall hardwood trees from the Dipterocarpaceae family (Shenkin *et al*., 2019; Ashton *et al*., 2021). Dipterocarps (referring to their characteristic 'two-winged fruits') are a pantropical family of fast-growing, mast-fruiting trees that commonly reach heights of 40 to 70 metres (Slik *et al*., 2003). In climax forests, dipterocarps account for 20% of trees (Slik, Aiba *et al*., 2010), and contribute to over 50% of basal area and to more than 60% of standing biomass volume (Sist & Saridan, 1999). Therefore, dipterocarp forests are among the tallest in the world and have an average aboveground biomass that is approximately 60% higher than Amazonian forests (Slik, Aiba *et al*., 2010). As such, they make a significant contribution to global carbon storage and are an important source of timber resources (Saner *et al*., 2012). Lowland dipterocarp forests also support high levels of biodiversity, for example, harbouring most of the 15,000 plant species found across Borneo (Slik *et al*., 2003).

Lowland dipterocarp forests are increasingly threatened by logging and deforestation, which are largely driven by the high economic value of dipterocarp timber and the demand of lowland areas for agriculture (Chen *et al*., 2026). Commercial logging involves the selective removal of large and valuable trees, which disrupts forest structure, reduces biodiversity, and damages surrounding vegetation (Reynolds *et al*., 2011). Timber extraction has been particularly important in Malaysian Borneo, for example, in the 1970s and 1980s, over 50% of the revenue for Sabah State originated in the timber industry (McMorrow & Talip, 2001). From 1979 to 1988, Sabah produced an average of 9 million m^3 of timber per year, and annual production levels now sit around 1 million m^3 (Dauvergne, 1998; Sabah Forestry Department, 2024). Large forest areas are being logged

repeatedly in rotations of less than 60 years, meaning that more than 60% of the remaining forest area in Malaysian Borneo is currently degraded (Bryan *et al*., 2013). Deforestation rates in Borneo have also been especially high. Between 1973 and 2015, about 18.7 million hectares of old-growth forests were cleared, and 7.0 million hectares of forest were replaced by plantations (Gaveau *et al*., 2016). The combined area of industrial oil palm and timber plantations in 2010 occupied 10% of Borneo (Gaveau *et al*., 2014), and across Southeast Asia lowland tropical forests now cover only 30% of their original area (Prohaska *et al*., 2023). Dipterocarp forest regeneration is slow because dipterocarp trees are not pioneer species, and produce limited seedbanks (Chong *et al*., 2016). This means that scaling up active restoration is increasingly important for maintaining dipterocarp forest biodiversity and accelerating recovery (Philipson *et al*., 2020).

The study in **Chapter 5** is placed in the context of the Yayasan Sabah Forest Management Area in Sabah, northern Malaysian Borneo. The Yayasan Sabah Forest Management Area is a publicly-owned large forest reserve of approximately one million hectares, comprised of a mosaic of protected areas, commercial logging concessions and oil palm plantations (Reynolds *et al*., 2011). Most of the area was logged from the 1960s to the 1990s, but many concessions have now been gazetted for conservation and restoration. **Chapter 5** makes use of tree survey data collected at the Sabah Biodiversity Experiment, a large-scale restoration project set up in the Malua Forest Reserve, which was logged in the 1980s (Veryard, 2023). Malua Forest Reserve was heavily degraded by commercial exploitation, resulting in a fragmented ecosystem with some patches of undisturbed forest (Tuck *et al*., 2016). **Chapter 5** compares productivity dynamics in the logged forest with those at a nearby old-growth forest site, in the Danum Valley Conservation Area. The Danum Valley Conservation Area is a 43,800-hectare reserve of old-growth dipterocarp forest that has never been commercially logged. The area was formally designated in 1980, and it is one of the few remaining tracts of old-growth lowland dipterocarp forest in Southeast Asia (Marsh & Greer, 1992). Since the establishment of the Danum Valley Field Centre in 1986, Danum Valley has become an important research hub, contributing significantly to the ecological understanding of tropical forests (Walsh *et al*., 2011). The Danum Valley Field Centre and the Sabah Biodiversity

Experiment are both managed by the Southeast Asia Rainforest Research Partnership (SEARRP), a long-term research and conservation programme that continues to play an important role in capacity building and training for local scientists and forestry professionals (Veryard, 2023).

Despite their contrasting ecological and environmental contexts, Cerrado savannas and lowland dipterocarp forests provide useful case studies for examining and comparing impacts of global change on ecosystem function. This thesis aims to quantify the productivity effects of altered climate on dipterocarp forests, and of fire regimes on Cerrado savanna, comparing and contrasting ecosystem responses across both tropical locations in response to different stressors. Changes in primary productivity as a result of extreme climate and fire regimes can be understood as emerging from impacts on plant performance, which determines survival and growth. In both cases, growth and survival rates will be used to better understand how trade-offs and adaptations to different stressors scale up to determine ecosystem carbon balances. Building on long-term ecological experiments, I aim to explore whether productivity-stressor-trait interactions remain comparable across Cerrado savannas and lowland dipterocarp forests, identifying common functional mechanisms underpinning carbon uptake across ecosystems and drivers of change.

2.6. References

Abreu, R. C. R., Hoffmann, W. A., Vasconcelos, H. L., Pilon, N. A., Rossatto, D. R., & Durigan, G. (2017). The biodiversity cost of carbon sequestration in tropical savanna. *Science Advances*, *3*(8), e1701284. https://doi.org/10.1126/sciadv.1701284

Accatino, F., De Michele, C., Vezzoli, R., Donzelli, D., & Scholes, R. J. (2010). Tree–grass co-existence in savanna: Interactions of rain and fire. *Journal of Theoretical Biology*, *267*(2), 235–242. https://doi.org/10.1016/j.jtbi.2010.08.012

Alencar, A. A., Brando, P. M., Asner, G. P., & Putz, F. E. (2015). Landscape fragmentation, severe drought, and the new Amazon forest fire regime. *Ecological Applications*, *25*(6), 1493–1505. https://doi.org/10.1890/14-1528.1

Alvarado, S. T., Andela, N., Silva, T. S. F., & Archibald, S. (2020). Thresholds of fire response to moisture and fuel load differ between tropical savannas and grasslands across continents. *Global Ecology and Biogeography*, *29*(2), 331–344. https://doi.org/10.1111/geb.13034

Andela, N., Morton, D. C., Giglio, L., Chen, Y., van der Werf, G. R., Kasibhatla, P. S., DeFries, R. S., Collatz, G. J., Hantson, S., Kloster, S., Bachelet, D., Forrest, M., Lasslop, G., Li, F., Mangeon, S., Melton, J. R., Yue, C., & Randerson, J. T. (2017). A human-driven decline in global burned area. *Science*, *356*(6345), 1356–1362. https://doi.org/10.1126/science.aal4108

Anderegg, W. R. L., Klein, T., Bartlett, M., Sack, L., Pellegrini, A. F. A., Choat, B., & Jansen, S. (2016). Meta-analysis reveals that hydraulic traits explain cross-species patterns of drought-induced tree mortality across the globe. *Proceedings of the National Academy of Sciences*, *113*(18), 5024–5029. https://doi.org/10.1073/pnas.1525678113

Archibald, S. (2016). Managing the human component of fire regimes: Lessons from Africa. *Philosophical Transactions of the Royal Society B: Biological Sciences*. *371*(1696): 20150346. https://doi.org/10.1098/rstb.2015.0346

Archibald, S., Hempson, G. P., & Lehmann, C. (2019). A unified framework for plant life-history strategies shaped by fire and herbivory. *New Phytologist*, *224*(4), 1490–1503. https://doi.org/10.1111/nph.15986

Armenteras, D., Meza, M. C., González, T. M., Oliveras, I., Balch, J. K., & Retana, J. (2021). Fire threatens the diversity and structure of tropical gallery forests. *Ecosphere*, *12*(1), e03347. https://doi.org/10.1002/ecs2.3347

Ashton, P. S., Morley, R. J., Heckenhauer, J., & Prasad, V. (2021). The magnificent Dipterocarps: Précis for an Epitaph? *Kew Bulletin*, *76*(2), 87–125. https://doi.org/10.1007/s12225-021-09934-7

Balch, J. K., Brando, P. M., Nepstad, D. C., Coe, M. T., Silvério, D., Massad, T. J., Davidson, E. A., Lefebvre, P., Oliveira-Santos, C., Rocha, W., Cury, R. T. S., Parsons, A., & Carvalho, K. S. (2015). The susceptibility of southeastern Amazon forests to fire: Insights from a large-scale burn experiment. *BioScience*, *65*(9), 893–905. https://doi.org/10.1093/biosci/biv106

Barlow, J., Berenguer, E., Carmenta, R., & França, F. (2020). Clarifying Amazonia's burning crisis. *Global Change Biology*, *26*(2), 319–321. https://doi.org/10.1111/gcb.14872

Barlow, J., & Peres, C. A. (2006). Effects of single and recurrent wildfires on fruit production and large vertebrate abundance in a Central Amazonian forest. *Biodiversity & Conservation*, *15*(3), 985–1012. https://doi.org/10.1007/s10531-004-3952-1

Barlow, J., Peres, C. A., Lagan, B. O., & Haugaasen, T. (2003). Large tree mortality and the decline of forest biomass following Amazonian wildfires. *Ecology Letters*, *6*(1), 6–8. https://doi.org/10.1046/j.1461-0248.2003.00394.x

Bauman, D., Fortunel, C., Cernusak, L. A., Bentley, L. P., McMahon, S. M., Rifai, S. W., Aguirre-Gutiérrez, J., Oliveras, I., Bradford, M., Laurance, S. G. W., Delhaye, G., Hutchinson, M. F., Dempsey, R., McNellis, B. E., Santos-Andrade, P. E., Ninantay-Rivera, H. R., Chambi Paucar, J. R., Phillips, O. L., & Malhi, Y. (2022). Tropical tree growth sensitivity to climate is driven by species intrinsic growth rate and leaf traits. *Global Change Biology*, *28*(4), 1414–1432. https://doi.org/10.1111/gcb.15982

Bauman, D., Fortunel, C., Delhaye, G., Malhi, Y., Cernusak, L. A., Bentley, L. P., Rifai, S. W., Aguirre-Gutiérrez, J., Menor, I. O., Phillips, O. L., McNellis, B. E., Bradford, M., Laurance, S. G. W., Hutchinson, M. F., Dempsey, R., Santos-Andrade, P. E., Ninantay-Rivera, H. R., Chambi Paucar, J. R., & McMahon, S. M. (2022). Tropical tree mortality has increased with rising atmospheric water stress. *Nature*, *608*(7923), 528–533. https://doi.org/10.1038/s41586-022-04737-7

Bebber, D. P., Brown, N. P., & Speight, M. R. (2004). Dipterocarp seedling population dynamics in Bornean primary lowland forest during the 1997-8 El Niño-Southern Oscillation. *Journal of Tropical Ecology*, *20*(1), 11–19. https://doi.org/10.1017/S0266467404006133

Bennett, A. C., Dargie, G. C., Cuni-Sanchez, A., Tshibamba Mukendi, J., Hubau, W., Mukinzi, J. M., Phillips, O. L., Malhi, Y., Sullivan, M. J. P., Cooper, D. L. M., Adu-Bredu, S., Affum-Baffoe, K., Amani, C. A., Banin, L. F., Beeckman, H., Begne, S. K., Bocko, Y. E., Boeckx, P., Bogaert, J., … Lewis, S. L. (2021). Resistance of African tropical forests to an extreme climate anomaly. *Proceedings of the National Academy of Sciences*, *118*(21), e2003169118. https://doi.org/10.1073/pnas.2003169118

Bennett, A. C., Rodrigues de Sousa, T., Monteagudo-Mendoza, A., Esquivel-Muelbert, A., Morandi, P. S., Coelho de Souza, F., Castro, W., Duque, L. F., Flores Llampazo, G., Manoel dos Santos, R., Ramos, E., Vilanova Torre, E., Alvarez-Davila, E., Baker, T. R., Costa, F. R. C., Lewis, S. L., Marimon, B. S., Schietti, J., Burban, B., … Phillips, O. L. (2023). Sensitivity of South American tropical forests to an extreme climate anomaly. *Nature Climate Change*, 1–8. https://doi.org/10.1038/s41558-023-01776-4

Berenguer, E., Lennox, G. D., Ferreira, J., Malhi, Y., Aragão, L. E. O. C., Barreto, J. R., Del Bon Espírito-Santo, F., Figueiredo, A. E. S., França, F., Gardner, T. A., Joly, C. A., Palmeira, A. F., Quesada, C. A., Rossi, L. C., de Seixas, M. M. M., Smith, C. C., Withey, K., & Barlow, J. (2021). Tracking the impacts of El Niño drought and fire in human-modified Amazonian forests. *Proceedings of the National Academy of Sciences*, *118*(30), e2019377118. https://doi.org/10.1073/pnas.2019377118

Berenguer, E., Malhi, Y., Brando, P., Cardoso Nunes Cordeiro, A., Ferreira, J., França, F., Chesini Rossi, L., Maria Moraes de Seixas, M., & Barlow, J. (2018). Tree growth and stem carbon accumulation in human-modified Amazonian forests following drought and fire. *Philosophical Transactions of the Royal Society B: Biological Sciences*, *373*(1760), 20170308. https://doi.org/10.1098/rstb.2017.0308

Beringer, J., Hutley, L. B., Tapper, N. J., & Cernusak, L. A. (2007). Savanna fires and their impact on net ecosystem productivity in North Australia. *Global Change Biology*, *13*(5), 990–1004. https://doi.org/10.1111/j.1365-2486.2007.01334.x

Bonal, D., Burban, B., Stahl, C., Wagner, F., & Hérault, B. (2016). The response of tropical rainforests to drought—Lessons from recent research and future prospects. *Annals of Forest Science*, *73*(1), 27–44. https://doi.org/10.1007/s13595-015-0522-5

Brando, P. M., Balch, J. K., Nepstad, D. C., Morton, D. C., Putz, F. E., Coe, M. T., Silvério, D., Macedo, M. N., Davidson, E. A., Nóbrega, C. C., Alencar, A., & Soares-Filho, B. S. (2014). Abrupt increases in Amazonian tree mortality due to drought–fire interactions. *Proceedings of the National Academy of Sciences*, *111*(17), 6347–6352. https://doi.org/10.1073/pnas.1305499111

Brando, P. M., Nepstad, D. C., Balch, J. K., Bolker, B., Christman, M. C., Coe, M., & Putz, F. E. (2012). Fire-induced tree mortality in a neotropical forest: The roles of bark traits, tree size, wood density and fire behavior. *Global Change Biology*, *18*(2), 630–641. https://doi.org/10.1111/j.1365-2486.2011.02533.x

Brienen, R. J. W., Phillips, O. L., Feldpausch, T. R., Gloor, E., Baker, T. R., Lloyd, J., Lopez-Gonzalez, G., Monteagudo-Mendoza, A., Malhi, Y., Lewis, S. L., Vásquez Martinez, R., Alexiades, M., Álvarez Dávila, E., Alvarez-Loayza, P., Andrade, A., Aragão, L. E. O. C., Araujo-Murakami, A., Arets, E. J. M. M., Arroyo, L., … Zagt, R. J. (2015). Long-term decline of the Amazon carbon sink. *Nature*, *519*(7543), 344–348. https://doi.org/10.1038/nature14283

Browne, L., Markesteijn, L., Engelbrecht, B. M. J., Jones, F. A., Lewis, O. T., Manzané-Pinzón, E., Wright, S. J., & Comita, L. S. (2021). Increased mortality of tropical tree seedlings during the extreme 2015–16 El Niño. *Global Change Biology*, *27*(20), 5043–5053. https://doi.org/10.1111/gcb.15809

Bryan, J. E., Shearman, P. L., Asner, G. P., Knapp, D. E., Aoro, G., & Lokes, B. (2013). Extreme differences in forest degradation in Borneo: Comparing practices in Sarawak, Sabah, and Brunei. *PLOS ONE*, *8*(7), e69679. https://doi.org/10.1371/journal.pone.0069679

Buckley, T. N. (2019). How do stomata respond to water status? *New Phytologist*, *224*(1), 21–36. https://doi.org/10.1111/nph.15899

Burgess, A. J. (2024). Double trouble: Compound effects of heat and drought stress on carbon assimilation. *Plant Physiology*, *194*(3), 1255–1256. https://doi.org/10.1093/plphys/kiad647

Calow, P. (1987). Towards a definition of functional ecology. *Functional Ecology*, *1*(1), 57–61. https://doi.org/10.2307/2389358

Campioli, M., Malhi, Y., Vicca, S., Luyssaert, S., Papale, D., Peñuelas, J., Reichstein, M., Migliavacca, M., Arain, M. A., & Janssens, I. A. (2016). Evaluating the convergence between eddy-covariance and biometric methods for assessing carbon budgets of forests. *Nature Communications*, *7*(1), 13717. https://doi.org/10.1038/ncomms13717

Cardoso, A. W., Archibald, S., Bond, W. J., Coetsee, C., Forrest, M., Govender, N., Lehmann, D., Makaga, L., Mpanza, N., Ndong, J. E., Koumba Pambo, A. F., Strydom, T., Tilman, D., Wragg, P. D., & Staver, A. C. (2022). Quantifying the environmental limits to fire spread in grassy ecosystems. *Proceedings of the National Academy of Sciences*, *119*(26), e2110364119. https://doi.org/10.1073/pnas.2110364119

Case, M. F., Wigley-Coetsee, C., Nzima, N., Scogings, P. F., & Staver, A. C. (2019). Severe drought limits trees in a semi-arid savanna. *Ecology*, *100*(11), e02842. https://doi.org/10.1002/ecy.2842

Cattelan, L. G., Mattos, C. R. C., Pamplona, M. B., & Hirota, M. (2024). Mapping climatic regions of the Cerrado: General patterns and future change. *International Journal of Climatology*, *44*(16), 5857–5872. https://doi.org/10.1002/joc.8670

Cera, A., Brunel-Muguet, S., & Lemauviel-Lavenant, S. (2025). Responses of temperate grassland plants to recurrent heatwaves. *Grass and Forage Science*, *80*(4), e70018. https://doi.org/10.1111/gfs.70018

Chave, J., Coomes, D., Jansen, S., Lewis, S. L., Swenson, N. G., & Zanne, A. E. (2009). Towards a worldwide wood economics spectrum. *Ecology Letters*, *12*(4), 351–366. https://doi.org/10.1111/j.1461-0248.2009.01285.x

Chen, S., Woodcock, C. E., Gu, H., Dong, L., Tang, X., & Olofsson, P. (2026). Drivers of forest disturbance in Southeast Asia. *International Journal of Applied Earth Observation and Geoinformation*, *148*, 105220. https://doi.org/10.1016/j.jag.2026.105220

Chiminazzo, M. A., Bombo, A. B., Charles-Dominique, T., & Fidelis, A. (2023). To protect or to hide: Why not both? An investigation of fire-related strategies in Cerrado woody species. *Flora*, *306*, 152350. https://doi.org/10.1016/j.flora.2023.152350

Chiminazzo, M. A., Charles-Dominique, T., Andrade, R. S., Bombo, A. B., & Fidelis, A. (2025). How do plants survive in the starving, burning, and hiding vegetation realms generated by novel fire regimes? *Perspectives in Plant Ecology, Evolution and Systematics*, *68*, 125885. https://doi.org/10.1016/j.ppees.2025.125885

Chong, K. Y., Chong, R., Tan, L. W. A., Yee, A. T. K., Chua, M. A. H., Wong, K. M., & Tan, H. T. W. (2016). Seed production and survival of four dipterocarp species in degraded forests in Singapore. *Plant Ecology & Diversity*, *9*(5–6), 483–490. https://doi.org/10.1080/17550874.2016.1266404

Clark, D. A., Brown, S., Kicklighter, D. W., Chambers, J. Q., Thomlinson, J. R., Ni, J., & Holland, E. A. (2001). Net primary production in tropical forests: An evaluation and synthesis of existing field data. *Ecological Applications*, *11*(2), 371–384. https://doi.org/10.1890/1051-0761(2001)011%255B0371:NPPITF%255D2.0.CO;2

Clark, D. A., Clark, D. B., & Oberbauer, S. F. (2021). Annual tropical-rainforest productivity through two decades: Complex responses to climatic factors, CO_2 and storm damage. *Journal of Geophysical Research: Biogeosciences*, *126*(12), e2021JG006557. https://doi.org/10.1029/2021JG006557

Clarke, P. J., & Knox, K. J. E. (2009). Trade-offs in resource allocation that favour resprouting affect the competitive ability of woody seedlings in grassy communities. *Journal of Ecology*, *97*(6), 1374–1382. https://doi.org/10.1111/j.1365-2745.2009.01556.x

Clarke, P. J., Lawes, M. J., Midgley, J. J., Lamont, B. B., Ojeda, F., Burrows, G. E., Enright, N. J., & Knox, K. J. E. (2013). Resprouting as a key functional trait: How buds, protection and resources drive persistence after fire. *New Phytologist*, *197*(1), 19–35. https://doi.org/10.1111/nph.12001

Corlett, R. T. (2016). The impacts of droughts in tropical forests. *Trends in Plant Science*, *21*(7), 584–593. https://doi.org/10.1016/j.tplants.2016.02.003

Croker, A. R., Woods, J., & Kountouris, Y. (2023). Changing fire regimes in East and Southern Africa's savanna-protected areas: Opportunities and challenges for indigenous-led savanna burning emissions abatement schemes. *Fire Ecology*, *19*(1), 63. https://doi.org/10.1186/s42408-023-00215-1

Crous, K. Y., Uddling, J., & De Kauwe, M. G. (2022). Temperature responses of photosynthesis and respiration in evergreen trees from boreal to tropical latitudes. *New Phytologist*, *234*(2), 353–374. https://doi.org/10.1111/nph.17951

da Costa, A. C. L., Galbraith, D., Almeida, S., Portela, B. T. T., da Costa, M., de Athaydes Silva Junior, J., Braga, A. P., de Gonçalves, P. H. L., de Oliveira, A. A., Fisher, R., Phillips, O. L., Metcalfe, D. B., Levy, P., & Meir, P. (2010). Effect of 7 yr of experimental drought on vegetation dynamics and biomass storage of an eastern Amazonian rainforest. *New Phytologist*, *187*(3), 579–591. https://doi.org/10.1111/j.1469-8137.2010.03309.x

da Silva Arruda, V. L., Alencar, A. A. C., de Carvalho Júnior, O. A., de Figueiredo Ribeiro, F., de Arruda, F. V., Conciani, D. E., da Silva, W. V., & Shimbo, J. Z. (2024). Assessing four decades of fire behavior dynamics in the Cerrado biome (1985 to 2022). *Fire Ecology*, *20*(1), 1–20. https://doi.org/10.1186/s42408-024-00298-4

Dalle Fratte, M., Bolpagni, R., Pierce, S., & Cerabolini, B. E. L. (2025). Functional ecology of plant communities as a guide for vegetation management. *Flora*, *323*, 152627. https://doi.org/10.1016/j.flora.2024.152627

Dauvergne, P. (1998). Globalisation and deforestation in the Asia-Pacific. *Environmental Politics*, *7*(4), 114–135. https://doi.org/10.1080/09644019808414425

Davidson, S. J., Dazé, E., Byun, E., Hiler, D., Kangur, M., Talbot, J., Finkelstein, S. A., & Strack, M. (2022). The unrecognized importance of carbon stocks and fluxes from swamps in Canada and the USA. *Environmental Research Letters*, *17*(5), 053003. https://doi.org/10.1088/1748-9326/ac63d5

Davies, S. J., Abiem, I., Abu Salim, K., Aguilar, S., Allen, D., Alonso, A., Anderson-Teixeira, K., Andrade, A., Arellano, G., Ashton, P. S., Baker, P. J., Baker, M. E., Baltzer, J. L., Basset, Y., Bissiengou, P., Bohlman, S., Bourg, N. A., Brockelman, W. Y., Bunyavejchewin, S., … Zuleta, D. (2021). ForestGEO: Understanding forest diversity and dynamics through a global observatory network. *Biological Conservation*, *253*, 108907. https://doi.org/10.1016/j.biocon.2020.108907

de Souza, M. R., Filho, M. dos S., Guilherme, M. B. de F., & Bogoni, J. A. (2025). The long-term absence of natural fires restructures the small-bodied mammal assemblages across a Protected Area of Brazilian Cerrado. *Perspectives in Ecology and Conservation*, *23*(3), 165–173. https://doi.org/10.1016/j.pecon.2025.05.003

Destacio, J.C. (2021). *Flora herbácea da Estação Ecológica da Serra das Araras, Mato Grosso, Brasil: uma sinopse*. BSc Dissertation. Universidade do Estado de Mato Grosso.

Diaz, S., Hodgson, J. G., Thompson, K., Cabido, M., Cornelissen, J. H. C., Jalili, A., Montserrat-Martí, G., Grime, J. P., Zarrinkamar, F., Asri, Y., Band, S. R., Basconcelo, S., Castro-Díez, P., Funes, G., Hamzehee, B., Khoshnevi, M., Pérez-Harguindeguy, N., Pérez-Rontomé, M. C., Shirvany, F. A., … Zak, M. R. (2004). The plant traits that drive ecosystems: Evidence from three continents. *Journal of Vegetation Science*, *15*(3), 295–304. https://doi.org/10.1111/j.1654-1103.2004.tb02266.x

Donovan, L. A., Maherali, H., Caruso, C. M., Huber, H., & de Kroon, H. (2011). The evolution of the worldwide leaf economics spectrum. *Trends in Ecology & Evolution*, *26*(2), 88–95. https://doi.org/10.1016/j.tree.2010.11.011

Doughty, C. E., Goldsmith, G. R., Raab, N., Girardin, C. A. J., Farfan-Amezquita, F., Huaraca-Huasco, W., Silva-Espejo, J. E., Araujo-Murakami, A., da Costa, A. C. L., Rocha, W., Galbraith, D., Meir, P., Metcalfe, D. B., & Malhi, Y. (2018). What controls variation in carbon use efficiency among Amazonian tropical forests? *Biotropica*, *50*(1), 16–25. https://doi.org/10.1111/btp.12504

Durigan, G., & Ratter, J. A. (2016). The need for a consistent fire policy for Cerrado conservation. *Journal of Applied Ecology*, *53*(1), 11–15. https://doi.org/10.1111/1365-2664.12559

Duursma, R. A., Blackman, C. J., López, R., Martin-StPaul, N. K., Cochard, H., & Medlyn, B. E. (2019). On the minimum leaf conductance: Its role in models of plant water use, and ecological and environmental controls. *New Phytologist*, *221*(2), 693–705. https://doi.org/10.1111/nph.15395

Enright, N. J., Fontaine, J. B., Lamont, B. B., Miller, B. P., & Westcott, V. C. (2014). Resistance and resilience to changing climate and fire regime depend on plant functional traits. *Journal of Ecology*, *102*(6), 1572–1581. https://doi.org/10.1111/1365-2745.12306

Espírito-Santo, M. M., Leite, M. E., Silva, J. O., Barbosa, R. S., Rocha, A. M., Anaya, F. C., & Dupin, M. G. V. (2016). Understanding patterns of land-cover change in the Brazilian Cerrado from 2000 to 2015. *Philosophical Transactions of the Royal Society B: Biological Sciences*, *371*(1703), 20150435. https://doi.org/10.1098/rstb.2015.0435

Evans, M. E. K., Hu, J., & Michaletz, S. T. (2025). Scaling plant responses to heat: From molecules to the biosphere. *Science*, *388*(6752), 1167–1173. https://doi.org/10.1126/science.adv7597

Fairman, T. A., Bennett, L. T., & Nitschke, C. R. (2019). Short-interval wildfires increase likelihood of resprouting failure in fire-tolerant trees. *Journal of Environmental Management*, *231*, 59–65. https://doi.org/10.1016/j.jenvman.2018.10.021

Falster, D. S., Duursma, R. A., & FitzJohn, R. G. (2018). How functional traits influence plant growth and shade tolerance across the life cycle. *Proceedings of the National Academy of Sciences of the United States of America*, *115*(29), E6789–E6798. https://doi.org/10.1073/pnas.1714044115

Felfili, J. M., & da Silva Junior, M. C. da S. (1993). A comparative study of cerrado (*sensu stricto*) vegetation in Central Brazil. *Journal of Tropical Ecology*, *9*(3), 277–289. https://doi.org/10.1017/S0266467400007306

Fensham, R. J., & Fairfax, R. J. (2007). Drought-related tree death of savanna eucalypts: Species susceptibility, soil conditions and root architecture. *Journal of Vegetation Science*, *18*(1), 71–80. https://doi.org/10.1111/j.1654-1103.2007.tb02517.x

Fensham, R. J., Fairfax, R. J., & Ward, D. P. (2009). Drought-induced tree death in savanna. *Global Change Biology*, *15*(2), 380–387. https://doi.org/10.1111/j.1365-2486.2008.01718.x

Fidelis, A., & Zirondi, H. L. (2021). And after fire, the Cerrado flowers: A review of post-fire flowering in a tropical savanna. *Flora*, *280*, 151849. https://doi.org/10.1016/j.flora.2021.151849

Flannigan, M., Cantin, A. S., Groot, W. J. de, Wotton, M., Newbery, A., & Gowman, L. M. (2013). Global wildland fire season severity in the 21st century. *Forest Ecology and Management, The Mega-Fire Reality*, *294*, 54–61. https://doi.org/10.1016/j.foreco.2012.10.022

Fontenele, H. G. V., & Miranda, H. S. (2024). Fire has contrasting effects on the survival, growth, and reproduction of Cerrado grasses with differing regenerative strategies. *Applied Vegetation Science*, *27*(2), e12775. https://doi.org/10.1111/avsc.12775

Gao, Y., Skutsch, M., Paneque-Gálvez, J., & Ghilardi, A. (2020). Remote sensing of forest degradation: A review. *Environmental Research Letters*, *15*(10), 103001. https://doi.org/10.1088/1748-9326/abaad7

Gaveau, D. L. A., Sheil, D., Husnayaen, Salim, M. A., Arjasakusuma, S., Ancrenaz, M., Pacheco, P., & Meijaard, E. (2016). Rapid conversions and avoided deforestation: Examining four decades of industrial plantation expansion in Borneo. *Scientific Reports*, *6*(1), 32017. https://doi.org/10.1038/srep32017

Gaveau, D. L. A., Sloan, S., Molidena, E., Yaen, H., Sheil, D., Abram, N. K., Ancrenaz, M., Nasi, R., Quinones, M., Wielaard, N., & Meijaard, E. (2014). Four Decades of Forest Persistence, Clearance and Logging on Borneo. *PLOS ONE*, *9*(7), e101654. https://doi.org/10.1371/journal.pone.0101654

Gignoux, J., Clobert, J., & Menaut, J.-C. (1997). Alternative fire resistance strategies in savanna trees. *Oecologia*, *110*(4), 576–583. https://doi.org/10.1007/s004420050198

Giles, A. L., Faria, L. D. B., Souza, H. J. de, Rodrigues, S. B., Munari, L. C., Silva Ribeiro, R. da, Pinho, G. S. C. de, Del Rei Texeira, M., Dianese, É., Grillo, B., Carvalho, R., Leão, R. Á., Trindade, A. L., Junior, C. R. A., Andrade, D. F. C. de, & Françoso, R. (2026). Mapping and revealing the tree biodiversity of the Brazilian Cerrado through biome-wide sampling efforts. *Npj Biodiversity*, *5*(1), 9. https://doi.org/10.1038/s44185-026-00122-z

Girardin, C. A. J., Malhi, Y., Aragão, L. E. O. C., Mamani, M., Huaraca Huasco, W., Durand, L., Feeley, K. J., Rapp, J., Silva-Espejo, J. E., Silman, M., Salinas, N., & Whittaker, R. J. (2010). Net primary productivity allocation and cycling of carbon along a tropical forest elevational transect in the Peruvian Andes: Net primary productivity from Andes to Amazon. *Global Change Biology*, *16*(12), 3176–3192. https://doi.org/10.1111/j.1365-2486.2010.02235.x

Gnanamoorthy, P., Zhao, J., Chen, Y., Jiao, L., Sawasdchai, B., Jing, Z., Chakraborty, A., Burman, P. K. D., Lee, S.-C., Pugh, T. A. M., Zhang, Y., & Song, Q. (2026). Post-drought vegetation shifts lead to divergent carbon, water and energy responses in a savanna ecosystem of southwest China. *Ecology Letters*, *29*(1), e70321. https://doi.org/10.1111/ele.70321

Gomes, L., Lenza, E., Souchie, F. F., Pinto, J. R. R., Maracahipes-Santos, L., Furtado, M. T., Maracahipes, L., & Silvério, D. (2021). Long-term post-fire resprouting dynamics and reproduction of woody species in a Brazilian savanna. *Basic and Applied Ecology*, *56*, 58–71. https://doi.org/10.1016/j.baae.2021.06.005

Goodland, R. (1971). A physiognomic analysis of the `Cerrado' vegetation of Central Brasil. *The Journal of Ecology*, *59*(2), 411. https://doi.org/10.2307/2258321

Gorné, L. D., Díaz, S., Minden, V., Onoda, Y., Kramer, K., Muir, C., Michaletz, S. T., Lavorel, S., Sharpe, J., Jansen, S., Slot, M., Chacon, E., & Boenisch, G. (2022). The acquisitive–conservative axis of leaf trait variation emerges even in homogeneous environments. *Annals of Botany*, *129*(6), 709–722. https://doi.org/10.1093/aob/mcaa198

Gottsberger, G. & Silberbauer-Gottsberger, I. (2006). *Life in the Cerrado - a South American Tropical Seasonal Ecosystem, Volume 1: Origin, Structure, Dynamics and Plant Use*. Reta Verlag.

Govender, N., Trollope, W. S. W., & Van Wilgen, B. W. (2006). The effect of fire season, fire frequency, rainfall and management on fire intensity in savanna vegetation in South Africa. *Journal of Applied Ecology*, *43*(4), 748–758. https://doi.org/10.1111/j.1365-2664.2006.01184.x

Grau-Andrés, R., Moreira, B., & Pausas, J. G. (2024). Global plant responses to intensified fire regimes. *Global Ecology and Biogeography*, *33*(8), e13858. https://doi.org/10.1111/geb.13858

Hasanuzzaman, M., Nahar, K., Alam, M. M., Roychowdhury, R., & Fujita, M. (2013). Physiological, biochemical, and molecular mechanisms of heat stress tolerance in plants. *International Journal of Molecular Sciences*, *14*(5), 9643–9684. https://doi.org/10.3390/ijms14059643

He, J., Ng, K., Qin, L., Shen, Y., Rahardjo, H., Wang, C. L., Kew, H., Chua, Y. C., Poh, C. H., & Ghosh, S. (2024). Photosynthetic gas exchange, plant water relations and osmotic adjustment of three tropical perennials during drought stress and re-watering. *PLOS ONE*, *19*(2), e0298908. https://doi.org/10.1371/journal.pone.0298908

Higgins, S. I., Bond, W. J., & Trollope, W. S. W. (2000). Fire, resprouting and variability: A recipe for grass–tree coexistence in savanna. *Journal of Ecology*, *88*(2), 213–229. https://doi.org/10.1046/j.1365-2745.2000.00435.x

Hoffmann, W. A., Schroeder, W., & Jackson, R. B. (2002). Positive feedbacks of fire, climate, and vegetation and the conversion of tropical savanna. *Geophysical Research Letters*, *29*(22), 9-1. https://doi.org/10.1029/2002GL015424

Hofhansl, F., Kobler, J., Ofner, J., Drage, S., Pölz, E.-M., & Wanek, W. (2014). Sensitivity of tropical forest aboveground productivity to climate anomalies in SW Costa Rica. *Global Biogeochemical Cycles*, *28*(12), 1437–1454. https://doi.org/10.1002/2014GB004934

Holmes, M. G., & Keiller, D. R. (2002). Effects of pubescence and waxes on the reflectance of leaves in the ultraviolet and photosynthetic wavebands: A comparison of a range of species. *Plant, Cell & Environment*, *25*(1), 85–93. https://doi.org/10.1046/j.1365-3040.2002.00779.x

ICMBio – Instituto Chico Mendes de Conservação da Biodiversidade (2016). *Plano de manejo da Estação Ecológica Serra das Araras*. https://www.gov.br/icmbio/pt-br/assuntos/biodiversidade/unidade-de-conservacao/unidades-de-biomas/cerrado/lista-de-ucs/esec-da-serra-das-araras/arquivos/dcom_plano_de_manejo_esec_serra_das_araras planodemanejo.pdf

ICMBio – Instituto Chico Mendes de Conservação da Biodiversidade (2022). *Plano de Manejo Integrado do Fogo da Estação Ecológica da Serra das Araras*. https://www.gov.br/icmbio/pt-br/centrais-de-conteudo/publicacoes/planos-de-manejo-integrado-do-fogo/Plano_de_Manejo_Integrado_do_Fogo_da_Estacao_Ecologica_da_Serra_das_Araras.pdf

Ishida, A., Toma, T., & Marjenah. (1999). Leaf gas exchange and chlorophyll fluorescence in relation to leaf angle, azimuth, and canopy position in the tropical pioneer tree, *Macaranga conifera*. *Tree Physiology*, *19*(2), 117–124. https://doi.org/10.1093/treephys/19.2.117

Jolly, W. M., Cochrane, M. A., Freeborn, P. H., Holden, Z. A., Brown, T. J., Williamson, G. J., & Bowman, D. M. J. S. (2015). Climate-induced variations in global wildfire danger from 1979 to 2013. *Nature Communications*, *6*(1), 7537. https://doi.org/10.1038/ncomms8537

Jones, M. W., Abatzoglou, J. T., Veraverbeke, S., Andela, N., Lasslop, G., Forkel, M., Smith, A. J. P., Burton, C., Betts, R. A., van der Werf, G. R., Sitch, S., Canadell, J. G., Santín, C., Kolden, C., Doerr, S. H., & Le Quéré, C. (2022). Global and regional trends and drivers of fire under climate change. *Reviews of Geophysics*, *60*(3), e2020RG000726. https://doi.org/10.1029/2020RG000726

Klink, C. A., & Machado, R. B. (2005). Conservation of the Brazilian Cerrado. *Conservation Biology*, *19*(3), 707–713. https://doi.org/10.1111/j.1523-1739.2005.00702.x

Kondo, M., Ichii, K., Patra, P. K., Canadell, J. G., Poulter, B., Sitch, S., Calle, L., Liu, Y. Y., van Dijk, A. I. J. M., Saeki, T., Saigusa, N., Friedlingstein, P., Arneth, A., Harper, A., Jain, A. K., Kato, E., Koven, C., Li, F., Pugh, T. A. M., … Rödenbeck, C. (2018). Land use change and El Niño-Southern Oscillation drive decadal carbon balance shifts in Southeast Asia. *Nature Communications*, *9*(1), 1154. https://doi.org/10.1038/s41467-018-03374-x

Lahsen, M., Bustamante, M. M. C., & Dalla-Nora, E. L. (2016). Undervaluing and overexploiting the Brazilian Cerrado at our peril. *Environment: Science and Policy for Sustainable Development*, *58*(6), 4–15. https://doi.org/10.1080/00139157.2016.1229537

Lamont, B. B., Pausas, J. G., He, T., Witkowski, E. T. F., & Hanley, M. E. (2020). Fire as a selective agent for both serotiny and nonserotiny over space and time. *Critical Reviews in Plant Sciences*, *39*(2), 140–172. https://doi.org/10.1080/07352689.2020.1768465

Langner, A., Achard, F., Vancutsem, C., Pekel, J.-F., Simonetti, D., Grassi, G., Kitayama, K., & Nakayama, M. (2015). Assessment of above-ground biomass of Borneo forests through a new data-fusion approach combining two Pan-tropical biomass maps. *Land*, *4*(3), 656–669. https://doi.org/10.3390/land4030656

Langner, A., Miettinen, J., & Siegert, F. (2007). Land cover change 2002–2005 in Borneo and the role of fire derived from MODIS imagery. *Global Change Biology*, *13*(11), 2329–2340. https://doi.org/10.1111/j.1365-2486.2007.01442.x

Lapola, D. M., Pinho, P., Barlow, J., Aragão, L. E. O. C., Berenguer, E., Carmenta, R., Liddy, H. M., Seixas, H., Silva, C. V. J., Silva-Junior, C. H. L., Alencar, A. A. C., Anderson, L. O., Armenteras, D., Brovkin, V., Calders, K., Chambers, J., Chini, L., Costa, M. H., Faria, B. L., … Walker, W. S. (2023). The drivers and impacts of Amazon forest degradation. *Science*, *379*(6630), eabp8622. https://doi.org/10.1126/science.abp8622

Laughlin, D. C. (2023). *Plant Strategies: The Demographic Consequences of Functional Traits in Changing Environments*. Oxford University Press.

Lavorel, S., & Garnier, E. (2002). Predicting changes in community composition and ecosystem functioning from plant traits: Revisiting the Holy Grail: Plant response and effect groups. *Functional Ecology*, *16*(5), 545–556. https://doi.org/10.1046/j.1365-2435.2002.00664.x

Le Stradic, S., Hernandez, P., Fernandes, G. W., & Buisson, E. (2018). Regeneration after fire in *campo rupestre*: Short- and long-term vegetation dynamics. *Flora, Plant Life on Campo Rupestre, a Megadiverse Neotropical Old-Growth Grassland*, *238*, 191–200. https://doi.org/10.1016/j.flora.2016.12.001

Li, J., Chen, X., Niklas, K. J., Sun, J., Wang, Z., Zhong, Q., Hu, D., & Cheng, D. (2022). A whole-plant economics spectrum including bark functional traits for 59 subtropical woody plant species. *Journal of Ecology*, *110*(1), 248–261. https://doi.org/10.1111/1365-2745.13800

Linger, E., Hogan, J. A., Cao, M., Zhang, W.-F., Yang, X.-F., & Hu, Y.-H. (2020). Precipitation influences on the net primary productivity of a tropical seasonal rainforest in Southwest China: A 9-year case study. *Forest Ecology and Management*, *467*, 118153. https://doi.org/10.1016/j.foreco.2020.118153

Litton, C. M., Raich, J. W., & Ryan, M. G. (2007). Carbon allocation in forest ecosystems. *Global Change Biology*, *13*(10), 2089–2109. https://doi.org/10.1111/j.1365-2486.2007.01420.x

Liu, C., Li, Y., Yan, P., & He, N. (2021). How to improve the predictions of plant functional traits on ecosystem functioning? *Frontiers in Plant Science*, *12*. https://doi.org/10.3389/fpls.2021.622260

Lopez-Gonzalez, G., Lewis, S. L., Burkitt, M., & Phillips, O. L. (2011). ForestPlots.net: A web application and research tool to manage and analyse tropical forest plot data. *Journal of Vegetation Science*, *22*(4), 610–613. https://doi.org/10.1111/j.1654-1103.2011.01312.x

Machado, R. B., Aguiar, L. M., & Bustamante, M. M. (2024). Why is it so easy to undergo devegetation in the Brazilian Cerrado? *Perspectives in Ecology and Conservation*, *22*(3), 209–212. https://doi.org/10.1016/j.pecon.2024.08.003

Makelele, I. A., Verheyen, K., Boeckx, P., Van de Velde, V., Ntaboba, L. C., Mujinya Bazirake, B., Boyemba Bosela, F., Kimbesa, F., Bachiseze Magala, J., Lokana Mande, J., Landuyt, D., Ewango, C., & Bauters, M. (2026). Net primary productivity and carbon allocation along secondary succession in a central African tropical forest. *New Phytologist*, *249*(6), 2852–2865. https://doi.org/10.1111/nph.70888

Malhi, Y. (2012). The productivity, metabolism and carbon cycle of tropical forest vegetation: Carbon cycle of tropical forests. *Journal of Ecology*, *100*(1), 65–75. https://doi.org/10.1111/j.1365-2745.2011.01916.x

Malhi, Y., Doughty, C. E., Goldsmith, G. R., Metcalfe, D. B., Girardin, C. A. J., Marthews, T. R., del Aguila-Pasquel, J., Aragão, L. E. O. C., Araujo-Murakami, A., Brando, P., da Costa, A. C. L., Silva-Espejo, J. E., Farfán Amézquita, F., Galbraith, D. R., Quesada, C. A., Rocha, W., Salinas-Revilla, N., Silvério, D., Meir, P., & Phillips, O. L. (2015). The linkages between photosynthesis, productivity, growth and biomass in lowland Amazonian forests. *Global Change Biology*, *21*(6), 2283–2295. https://doi.org/10.1111/gcb.12859

Malhi, Y., Doughty, C., & Galbraith, D. (2011). The allocation of ecosystem net primary productivity in tropical forests. *Philosophical Transactions of the Royal Society B: Biological Sciences*, *366*(1582), 3225–3245. https://doi.org/10.1098/rstb.2011.0062

Malhi, Y., Gardner, T. A., Goldsmith, G. R., Silman, M. R., & Zelazowski, P. (2014). Tropical Forests in the Anthropocene. *Annual Review of Environment and Resources*, *39*(Volume 39, 2014), 125–159. https://doi.org/10.1146/annurev-environ-030713-155141

Malhi, Y., Girardin, C., Metcalfe, D. B., Doughty, C. E., Aragão, L. E. O. C., Rifai, S. W., Oliveras, I., Shenkin, A., Aguirre-Gutiérrez, J., Dahlsjö, C. A. L., Riutta, T., Berenguer, E., Moore, S., Huasco, W. H., Salinas, N., da Costa, A. C. L., Bentley, L. P., Adu-Bredu, S., Marthews, T. R., … Phillips, O. L. (2021). The Global Ecosystems Monitoring network: Monitoring ecosystem productivity and carbon cycling across the tropics. *Biological Conservation*, *253*, 108889. https://doi.org/10.1016/j.biocon.2020.108889

Malhi, Y., & Grace, J. (2000). Tropical forests and atmospheric carbon dioxide. *Trends in Ecology & Evolution*, *15*(8), 332–337. https://doi.org/10.1016/s0169-5347(00)01906-6

Malhi, Y., Nobre, A. D., Grace, J., Kruijt, B., Pereira, M. G. P., Culf, A., & Scott, S. (1998). Carbon dioxide transfer over a Central Amazonian rain forest. *Journal of Geophysical Research: Atmospheres*, *103*(D24), 31593–31612. https://doi.org/10.1029/98JD02647

Malhi, Y., Saatchi, S., Girardin, C., & AragãO, L. E. O. C. (2009). The Production, Storage, and Flow of Carbon in Amazonian Forests. In *Amazonia and Global Change* (pp. 355–372). American Geophysical Union (AGU). https://doi.org/10.1029/2008GM000733

Markesteijn, L., Poorter, L., Bongers, F., Paz, H., & Sack, L. (2011). Hydraulics and life history of tropical dry forest tree species: Coordination of species' drought and shade tolerance. *New Phytologist*, *191*(2), 480–495. https://doi.org/10.1111/j.1469-8137.2011.03708.x

Marsh, C. W., & Greer, A. G. (1992). Forest land-use in Sabah, Malaysia: An introduction to Danum Valley. *Philosophical Transactions of the Royal Society B: Biological Sciences*, *335*(1275), 331–339. https://doi.org/10.1098/rstb.1992.0025

Martínez-Vilalta, J., Piñol, J., & Beven, K. (2002). A hydraulic model to predict drought-induced mortality in woody plants: An application to climate change in the Mediterranean. *Ecological Modelling*, *155*(2), 127–147. https://doi.org/10.1016/S0304-3800(02)00025-X

Mauki, D. G., Manning, P., Schleuning, M., Hemp, A., Schellenberger Costa, D., Sierra Cornejo, N., Becker, J. N., Ensslin, A., Rutten, G., Appelhans, T., & Neyret, M. (2025). Community-level plant functional strategies explain ecosystem carbon storage across a tropical elevational gradient. *Journal of Ecology*, *113*(11), 3328–3344. https://doi.org/10.1111/1365-2745.70162

McDowell, N., Allen, C. D., Anderson-Teixeira, K., Brando, P., Brienen, R., Chambers, J., Christoffersen, B., Davies, S., Doughty, C., Duque, A., Espírito-Santo, F., Fisher, R., Fontes, C. G., Galbraith, D., Goodsman, D., Grossiord, C., Hartmann, H., Holm, J., Johnson, D. J., … Xu, X. (2018). Drivers and mechanisms of tree mortality in moist tropical forests. *New Phytologist*, *219*(3), 851–869. https://doi.org/10.1111/nph.15027

McDowell, N., Pockman, W. T., Allen, C. D., Breshears, D. D., Cobb, N., Kolb, T., Plaut, J., Sperry, J., West, A., Williams, D. G., & Yepez, E. A. (2008). Mechanisms of plant survival and mortality during drought: Why do some plants survive while others succumb to drought? *New Phytologist*, *178*(4), 719–739. https://doi.org/10.1111/j.1469-8137.2008.02436.x

McLeod, G., Tupaj, M., Gann, D., Ross, M., & Malone, S. L. (2025). Fires enhanced productivity in fire-adapted subtropical pinelands of the Florida Everglades. *Science of The Total Environment*, *1003*, 180602. https://doi.org/10.1016/j.scitotenv.2025.180602

McMorrow, J., & Talip, M. A. (2001). Decline of forest area in Sabah, Malaysia: Relationship to state policies, land code and land capability. *Global Environmental Change*, *11*(3), 217–230. https://doi.org/10.1016/S0959-3780(00)00059-5

Meira-Neto, J. A. A., Nunes Cândido, H. M., Miazaki, Â., Pontara, V., Bueno, M. L., Solar, R., & Gastauer, M. (2019). Drivers of the growth–survival trade-off in a tropical forest. *Journal of Vegetation Science*, *30*(6), 1184–1194. https://doi.org/10.1111/jvs.12810

Metcalfe, D. B., Anders, E., Axén, H., Petter Axelsson, E., Bermudez, A. E., Bartholomew, D. C., Butt, N., Cadillo-Quiroz, H., Chaudhary, N., Callebaut, T., Dahlsjö, C. A. L., Dusenge, M. E., Feeley, K. J., Wanger, T. C., Hwang, B. C., Hermans, T. D. G., Jonsson, M., Kardol, P., Lindh, A., … Virkkala, A.-M. (2025). Gaps in tropical science from unrepresentative distribution of sampling and citation across natural terrestrial environments. *Nature Communications*, *16*(1), 11378. https://doi.org/10.1038/s41467-025-67617-4

Metcalfe, D. B., Meir, P., Aragão, L. E. O. C., Lobo-do-Vale, R., Galbraith, D., Fisher, R. A., Chaves, M. M., Maroco, J. P., da Costa, A. C. L., de Almeida, S. S., Braga, A. P., Gonçalves, P. H. L., de Athaydes, J., da Costa, M., Portela, T. T. B., de Oliveira, A. A. R., Malhi, Y., & Williams, M. (2010). Shifts in plant respiration and carbon use efficiency at a large-scale drought experiment in the eastern Amazon. *New Phytologist*, *187*(3), 608–621. https://doi.org/10.1111/j.1469-8137.2010.03319.x

Mills, M. B., Malhi, Y., Ewers, R. M., Kho, L. K., Teh, Y. A., Both, S., Burslem, D. F. R. P., Majalap, N., Nilus, R., Huaraca Huasco, W., Cruz, R., Pillco, M. M., Turner, E. C., Reynolds, G., & Riutta, T. (2023). Tropical forests post-logging are a persistent net carbon source to the atmosphere. *Proceedings of the National Academy of Sciences*, *120*(3), e2214462120. https://doi.org/10.1073/pnas.2214462120

Miyamoto, K., Aiba, S., Aoyagi, R., & Nilus, R. (2021). Effects of El Niño drought on tree mortality and growth across forest types at different elevations in Borneo. *Forest Ecology and Management*, *490*, 119096. https://doi.org/10.1016/j.foreco.2021.119096

Mndela, M., Moss, S., Gusha, B., Thamaga, K. H., Afuye, G. A., Abdo, H. G., & Almohamad, H. (2023). Functional trait responses of C4 bunchgrasses to fire return intervals in the semi-arid savanna of South Africa. *Diversity*, *15*(12). https://doi.org/10.3390/d15121201

Moonlight, P. W., Banda-R, K., Phillips, O. L., Dexter, K. G., Pennington, R. T., Baker, T. R., C. de Lima, H., Fajardo, L., González-M., R., Linares-Palomino, R., Lloyd, J., Nascimento, M., Prado, D., Quintana, C., Riina, R., Rodríguez M., G. M., Maria Villela, D., Aquino, A. C. M. M., Arroyo, L., … Veenendaal, E. (2021). Expanding tropical forest monitoring into Dry Forests: The DRYFLOR protocol for permanent plots. *Plants, People, Planet*, *3*(3), 295–300. https://doi.org/10.1002/ppp3.10112

Moore, S., Adu-Bredu, S., Duah-Gyamfi, A., Addo-Danso, S. D., Ibrahim, F., Mbou, A. T., Grandcourt, A., Valentini, R., Nicolini, G., Djagbletey, G., Owusu-Afriyie, K., Gvozdevaite, A., Oliveras, I., Ruiz-Jaen, M. C., & Malhi, Y. (2018). Forest biomass, productivity and carbon cycling along a rainfall gradient in West Africa. *Global Change Biology*, *24*(2), e496–e510. https://doi.org/10.1111/gcb.13907

Müller, L. M., & Bahn, M. (2022). Drought legacies and ecosystem responses to subsequent drought. *Global Change Biology*, *28*(17), 5086–5103. https://doi.org/10.1111/gcb.16270

Murphy, B. P., Russell-Smith, J., & Prior, L. D. (2010). Frequent fires reduce tree growth in northern Australian savannas: Implications for tree demography and carbon sequestration. *Global Change Biology*, *16*(1), 331–343. https://doi.org/10.1111/j.1365-2486.2009.01933.x

Nakagawa, M., Tanaka, K., Nakashizuka, T., Ohkubo, T., Kato, T., Maeda, T., Sato, K., Miguchi, H., Nagamasu, H., Ogino, K., Teo, S., Hamid, A. A., & Seng, L. H. (2000). Impact of severe drought associated with the 1997–1998 El Niño in a tropical forest in Sarawak. *Journal of Tropical Ecology*, *16*(3), 355–367. https://doi.org/10.1017/S0266467400001450

N'Dri, A. B., Soro, T. D., Gignoux, J., Dosso, K., Koné, M., N'Dri, J. K., Koné, N. A., & Barot, S. (2018). Season affects fire behavior in annually burned humid savanna of West Africa. *Fire Ecology*, *14*(2), 5. https://doi.org/10.1186/s42408-018-0005-9

Newbery, D. McC., Campbell, E. J. F., Proctor, J., & Still, M. J. (1996). Primary lowland dipterocarp forest at Danum Valley, Sabah, Malaysia. Species composition and patterns in the understorey. *Vegetatio*, *122*(2), 193–220. https://doi.org/10.1007/BF00044700

Nottingham, A. T., Montero-Sanchez, M., Slot, M., Szczygieł, H. A., Velasquez, E., & Meir, P. (2023). Seedling growth declines in warmed tropical forest soils. *Biotropica*, btp.13238. https://doi.org/10.1111/btp.13238

O'Brien, M. J., Engelbrecht, B. M. J., Joswig, J., Pereyra, G., Schuldt, B., Jansen, S., Kattge, J., Landhäusser, S. M., Levick, S. R., Preisler, Y., Väänänen, P., & Macinnis-Ng, C. (2017). A synthesis of tree functional traits related to drought-induced mortality in forests across climatic zones. *Journal of Applied Ecology*, *54*(6), 1669–1686. https://doi.org/10.1111/1365-2664.12874

O'Brien, M. J., Valtat, A., Abiven, S., Studer, M. S., Ong, R., & Schmid, B. (2020). The role of soluble sugars during drought in tropical tree seedlings with contrasting tolerances. *Journal of Plant Ecology*, *13*(4), 389–397. https://doi.org/10.1093/jpe/rtaa017

Oliveira, P. T. S., Nearing, M. A., Moran, M. S., Goodrich, D. C., Wendland, E., & Gupta, H. V. (2014). Trends in water balance components across the Brazilian Cerrado. *Water Resources Research*, *50*(9), 7100–7114. https://doi.org/10.1002/2013WR015202

Oliveras, I., & Malhi, Y. (2016). Many shades of green: The dynamic tropical forest–savannah transition zones. *Philosophical Transactions of the Royal Society B: Biological Sciences*, *371*(1703), 20150308. https://doi.org/10.1098/rstb.2015.0308

Oliveras, I., Meirelles, S. T., Hirakuri, V. L., Freitas, C. R., Miranda, H. S., & Pivello, V. R. (2012). Effects of fire regimes on herbaceous biomass and nutrient dynamics in the Brazilian savanna. *International Journal of Wildland Fire*, *22*(3), 368–380. https://doi.org/10.1071/WF10136

Onoda, Y., Wright, I. J., Evans, J. R., Hikosaka, K., Kitajima, K., Niinemets, Ü., Poorter, H., Tosens, T., & Westoby, M. (2017). Physiological and structural tradeoffs underlying the leaf economics spectrum. *New Phytologist*, *214*(4), 1447–1463. https://doi.org/10.1111/nph.14496

Pausas, J. G. (2015). Bark thickness and fire regime. *Functional Ecology*, *29*(3), 315–327. https://doi.org/10.1111/1365-2435.12372

Pausas, J. G. (2019). Generalized fire response strategies in plants and animals. *Oikos*, *128*(2), 147–153. https://doi.org/10.1111/oik.05907

Pausas, J. G., & Bond, W. J. (2020). Alternative biome states in terrestrial ecosystems. *Trends in Plant Science*, *25*(3), 250–263. https://doi.org/10.1016/j.tplants.2019.11.003

Pausas, J. G., & Keeley, J. E. (2014). Evolutionary ecology of resprouting and seeding in fire-prone ecosystems. *The New Phytologist*, *204*(1), 55–65. https://doi.org/10.1111/nph.12921

Pausas, J. G., & Lamont, B. B. (2022). Fire-released seed dormancy—A global synthesis. *Biological Reviews*, *97*(4), 1612–1639. https://doi.org/10.1111/brv.12855

Pausas, J. G., Pratt, R. B., Keeley, J. E., Jacobsen, A. L., Ramirez, A. R., Vilagrosa, A., Paula, S., Kaneakua-Pia, I. N., & Davis, S. D. (2016). Towards understanding resprouting at the global scale. *New Phytologist*, *209*(3), 945–954. https://doi.org/10.1111/nph.13644

Pausas, J. G., & Ribeiro, E. (2013). The global fire–productivity relationship. *Global Ecology and Biogeography*, *22*(6), 728–736. https://doi.org/10.1111/geb.12043

Peacock, J., Baker, T. R., Lewis, S. L., Lopez-Gonzalez, G., & Phillips, O. L. (2007). The RAINFOR database: Monitoring forest biomass and dynamics. *Journal of Vegetation Science*, *18*(4), 535–542. https://doi.org/10.1111/j.1654-1103.2007.tb02568.x

Pedraza, S. (2024). Leaf traits and leaf-to-air temperature differences in tropical plants suggest variability in thermoregulatory capacities across elevations. *Biotropica*, *56*(4), e13332. https://doi.org/10.1111/btp.13332

Pereira, G., Aguiar, J. L. P. de, Moreira, L., & Bezerra, H. da S. (1997). Área e população do cerrado. *Pesquisa Agropecuaria Brasileira*, 759–763. https://doi.org/10.1590/S1678-3921.pab1997.v32.4698

Philipson, C. D., Cutler, M. E. J., Brodrick, P. G., Asner, G. P., Boyd, D. S., Moura Costa, P., Fiddes, J., Foody, G. M., van der Heijden, G. M. F., Ledo, A., Lincoln, P. R., Margrove, J. A., Martin, R. E., Milne, S., Pinard, M. A., Reynolds, G., Snoep, M., Tangki, H., Sau Wai, Y., … Burslem, D. F. R. P. (2020). Active restoration accelerates the carbon recovery of human-modified tropical forests. *Science*, *369*(6505), 838–841. https://doi.org/10.1126/science.aay4490

Phillips, O. L. (2023). Sensing forests directly: The power of permanent plots. *Plants*, *12*(21). https://doi.org/10.3390/plants12213710

Phillips, O. L., van der Heijden, G., Lewis, S. L., López-González, G., Aragão, L. E. O. C., Lloyd, J., Malhi, Y., Monteagudo, A., Almeida, S., Dávila, E. A., Amaral, I., Andelman, S., Andrade, A., Arroyo, L., Aymard, G., Baker, T. R., Blanc, L., Bonal, D., de Oliveira, Á. C. A., … Vilanova, E. (2010). Drought-mortality relationships for tropical forests. *New Phytologist*, *187*(3), 631–646. https://doi.org/10.1111/j.1469-8137.2010.03359.x

Pillay, T., & Ward, D. (2022). Experimental drought suppresses grass productivity and passive warming promotes tree sapling performance: Insights from African savanna species. *Acta Oecologica*, *114*, 103813. https://doi.org/10.1016/j.actao.2022.103813

Pivello, V. R. (2011). The use of fire in the Cerrado and Amazonian rainforests of Brazil: Past and present. *Fire Ecology*, *7*(1), 24–39. https://doi.org/10.4996/fireecology.0701024

Pivello, V. R., & Coutinho, L. M. (1992). Transfer of macro-nutrients to the atmosphere during experimental burnings in an open cerrado (Brazilian savanna). *Journal of Tropical Ecology*, *8*(4), 487–497. https://doi.org/10.1017/S0266467400006829

Pivello, V. R., Oliveras, I., Miranda, H. S., Haridasan, M., Sato, M. N., & Meirelles, S. T. (2010). Effect of fires on soil nutrient availability in an open savanna in Central Brazil. *Plant and Soil*, *337*(1), 111–123. https://doi.org/10.1007/s11104-010-0508-x

Pivello, V. R., Vieira, I., Christianini, A. V., Ribeiro, D. B., da Silva Menezes, L., Berlinck, C. N., Melo, F. P. L., Marengo, J. A., Tornquist, C. G., Tomas, W. M., & Overbeck, G. E. (2021). Understanding Brazil's catastrophic fires: Causes, consequences and policy needed to prevent future tragedies. *Perspectives in Ecology and Conservation*, *19*(3), 233–255. https://doi.org/10.1016/j.pecon.2021.06.005

Plumanns-Pouton, E., Swan, M., Penman, T., & Kelly, L. T. (2024). Using plant functional types to predict the influence of fire on species relative abundance. *Biological Conservation*, *292*, 110555. https://doi.org/10.1016/j.biocon.2024.110555

Poorter, H., Niklas, K. J., Reich, P. B., Oleksyn, J., Poot, P., & Mommer, L. (2012). Biomass allocation to leaves, stems and roots: Meta-analyses of interspecific variation and environmental control. *New Phytologist*, *193*(1), 30–50. https://doi.org/10.1111/j.1469-8137.2011.03952.x

Post-Leon, A. C., & Anderegg, W. R. L. (2026). Divergent shifts in hydraulic versus carbon acquisition functional traits after wildfire in four Rocky Mountain tree species. *Functional Ecology*, *Early View*(n/a). https://doi.org/10.1111/1365-2435.70282

Powers, J. S., Vargas G., G., Brodribb, T. J., Schwartz, N. B., Pérez-Aviles, D., Smith-Martin, C. M., Becknell, J. M., Aureli, F., Blanco, R., Calderón-Morales, E., Calvo-Alvarado, J. C., Calvo-Obando, A. J., Chavarría, M. M., Carvajal-Vanegas, D., Jiménez-Rodríguez, C. D., Murillo Chacon, E., Schaffner, C. M., Werden, L. K., Xu, X., & Medvigy, D. (2020). A catastrophic tropical drought kills hydraulically vulnerable tree species. *Global Change Biology*, *26*(5), 3122–3133. https://doi.org/10.1111/gcb.15037

Prohaska, A., Seddon, A. W. R., Rach, O., Smith, A., Sachse, D., & Willis, K. J. (2023). Long-term ecological responses of a lowland dipterocarp forest to climate changes and nutrient availability. *New Phytologist*, *240*(6), 2513–2529. https://doi.org/10.1111/nph.19169

Qie, L., Lewis, S. L., Sullivan, M. J. P., Lopez-Gonzalez, G., Pickavance, G. C., Sunderland, T., Ashton, P., Hubau, W., Abu Salim, K., Aiba, S.-I., Banin, L. F., Berry, N., Brearley, F. Q., Burslem, D. F. R. P., Dančák, M., Davies, S. J., Fredriksson, G., Hamer, K. C., Hédl, R., … Phillips, O. L. (2017). Long-term carbon sink in Borneo's forests halted by drought and vulnerable to edge effects. *Nature Communications*, *8*(1), 1966. https://doi.org/10.1038/s41467-017-01997-0

Ratter, J. A., Ribeiro, J. F., & Bridgewater, S. (1997). The Brazilian Cerrado vegetation and threats to its biodiversity. *Annals of Botany*, *80*(3), 223–230. https://doi.org/10.1006/anbo.1997.0469

Ray, D., Nepstad, D., & Brando, P. (2010). Predicting moisture dynamics of fine understory fuels in a moist tropical rainforest system: Results of a pilot study undertaken to identify proxy variables useful for rating fire danger. *New Phytologist*, *187*(3), 720–732. https://doi.org/10.1111/j.1469-8137.2010.03358.x

Ray, D., Nepstad, D., & Moutinho, P. (2005). Micrometeorological and canopy controls of fire susceptibility in a forested Amazon landscape. *Ecological Applications*, *15*(5), 1664–1678. https://doi.org/10.1890/05-0404

Reich, P. B. (2014). The world-wide 'fast–slow' plant economics spectrum: A traits manifesto. *Journal of Ecology*, *102*(2), 275–301. https://doi.org/10.1111/1365-2745.12211

Reis, S.M., Malhi, Y., Marimon Junior, B. H., Schwantes Marimon, B., Zhang-Zheng, H., Araújo, I., Freitag, R., Almeida de Oliveira, E., da Silva Peixoto, K., Januário de Souza, L., Souza da Silva, E. L., Bernardes Santos, E., Parreira da Silva, K., Alves Gonçalves, M. D., Girardin, C., Dahlsjö, C., L. Phillips, O., & Oliveras Menor, I. (2025). Sensitivity of tropical woodland savannas to El Niño droughts. *Biogeosciences*, *22*(15), 3949–3964. https://doi.org/10.5194/bg-22-3949-2025

Reynolds, G., Payne, J., Sinun, W., Mosigil, G., & Walsh, R. P. D. (2011). Changes in forest land use and management in Sabah, Malaysian Borneo, 1990–2010, with a focus on the Danum Valley region. *Philosophical Transactions of the Royal Society B: Biological Sciences*, *366*(1582), 3168–3176. https://doi.org/10.1098/rstb.2011.0154

Ribeiro, J.F. & Walter, B.M.T. (2008). As principais fitofisionomias do Bioma Cerrado. In *Cerrado Ecologia e Flora* (pp. 152–212) Planaltina.

Rifai, S. W., Girardin, C. A. J., Berenguer, E., del Aguila-Pasquel, J., Dahlsjö, C. A. L., Doughty, C. E., Jeffery, K. J., Moore, S., Oliveras, I., Riutta, T., Rowland, L. M., Murakami, A. A., Addo-Danso, S. D., Brando, P., Burton, C., Ondo, F. E., Duah-Gyamfi, A., Amézquita, F. F., Freitag, R., … Malhi, Y. (2018). ENSO Drives interannual variation of forest woody growth across the tropics. *Philosophical Transactions of the Royal Society B: Biological Sciences*, *373*(1760), 20170410. https://doi.org/10.1098/rstb.2017.0410

Rissi, M., Baeza, M., Gorgone-Barbosa, E., Zupo, T., & Fidelis, A. (2017). Does season affect fire behaviour in the Cerrado? *International Journal of Wildland Fire*, *26*, 427–433. https://doi.org/10.1071/WF14210

Riutta, T., Malhi, Y., Kho, L. K., Marthews, T. R., Huaraca Huasco, W., Khoo, M., Tan, S., Turner, E., Reynolds, G., Both, S., Burslem, D. F. R. P., Teh, Y. A., Vairappan, C. S., Majalap, N., & Ewers, R. M. (2018). Logging disturbance shifts net primary productivity and its allocation in Bornean tropical forests. *Global Change Biology*, *24*(7), 2913–2928. https://doi.org/10.1111/gcb.14068

Rocha, W., Metcalfe, D. B., Doughty, C. E., Brando, P., Silvério, D., Halladay, K., Nepstad, D. C., Balch, J. K., & Malhi, Y. (2014). Ecosystem productivity and carbon cycling in intact and annually burnt forest at the dry southern limit of the Amazon rainforest (Mato Grosso, Brazil). *Plant Ecology & Diversity*, *7*(1–2), 25–40. https://doi.org/10.1080/17550874.2013.798368

Rodrigues, C. A., & Fidelis, A. (2022). Should we burn the Cerrado? Effects of fire frequency on open savanna plant communities. *Journal of Vegetation Science*, *33*(6), e13159. https://doi.org/10.1111/jvs.13159

Rosan, T. M., Aragão, L. E. O. C., Oliveras, I., Phillips, O. L., Malhi, Y., Gloor, E., & Wagner, F. H. (2019). Extensive 21st-Century Woody Encroachment in South America's Savanna. *Geophysical Research Letters*, *46*(12), 6594–6603. https://doi.org/10.1029/2019GL082327

Rowland, L., da Costa, A. C. L., Galbraith, D. R., Oliveira, R. S., Binks, O. J., Oliveira, A. A. R., Pullen, A. M., Doughty, C. E., Metcalfe, D. B., Vasconcelos, S. S., Ferreira, L. V., Malhi, Y., Grace, J., Mencuccini, M., & Meir, P. (2015). Death from drought in tropical forests is triggered by hydraulics not carbon starvation. *Nature*, *528*(7580), 119–122. https://doi.org/10.1038/nature15539

Rowland, L., da Costa, A. C. L., Oliveira, A. A. R., Oliveira, R. S., Bittencourt, P. L., Costa, P. B., Giles, A. L., Sosa, A. I., Coughlin, I., Godlee, J. L., Vasconcelos, S. S., Junior, J. A. S., Ferreira, L. V., Mencuccini, M., & Meir, P. (2018). Drought stress and tree size determine stem CO_2 efflux in a tropical forest. *New Phytologist*, *218*(4), 1393–1405. https://doi.org/10.1111/nph.15024

Sabah Forestry Department (2024). *Annual report*. https://forest.sabah.gov.my/annual-report/

Sanchez-Martinez, P., Martius, L. R., Bittencourt, P., Silva, M., Binks, O., Coughlin, I., Negrão-Rodrigues, V., Athaydes Silva, J., da Costa, A. C. L., Selman, R., Rifai, S., Rowland, L., Mencuccini, M., & Meir, P. (2025). Amazon rainforest adjusts to long-term experimental drought. *Nature Ecology & Evolution*, *9*(6), 970–979. https://doi.org/10.1038/s41559-025-02702-x

Saner, P., Loh, Y. Y., Ong, R. C., & Hector, A. (2012). Carbon stocks and fluxes in tropical lowland dipterocarp rainforests in Sabah, Malaysian Borneo. *PLOS ONE*, *7*(1), e29642. https://doi.org/10.1371/journal.pone.0029642

Sankaran, M. (2019). Droughts and the ecological future of tropical savanna vegetation. *Journal of Ecology*, *107*(4), 1531–1549. https://doi.org/10.1111/1365-2745.13195

Sano, E. E., Rodrigues, A. A., Martins, E. S., Bettiol, G. M., Bustamante, M. M. C., Bezerra, A. S., Couto, A. F., Vasconcelos, V., Schüler, J., & Bolfe, E. L. (2019). Cerrado ecoregions: A spatial framework to assess and prioritize Brazilian savanna environmental diversity for conservation. *Journal of Environmental Management*, *232*, 818–828. https://doi.org/10.1016/j.jenvman.2018.11.108

Schwilk, D. W. (2015). Dimensions of plant flammability. *New Phytologist*, *206*(2), 486–488. https://doi.org/10.1111/nph.13372

Segura-García, C., Alencar, A., S. Arruda, V. L., Bauman, D., Silva, W., Conciani, D. E., & Oliveras Menor, I. (2025). The fire regimes of the Cerrado and their changes through time. *Philosophical Transactions of the Royal Society B: Biological Sciences*, *380*(1924), 20230460. https://doi.org/10.1098/rstb.2023.0460

Shenkin, A., Chandler, C. J., Boyd, D. S., Jackson, T., Disney, M., Majalap, N., Nilus, R., Foody, G., bin Jami, J., Reynolds, G., Wilkes, P., Cutler, M. E. J., van der Heijden, G. M. F., Burslem, D. F. R. P., Coomes, D. A., Bentley, L. P., & Malhi, Y. (2019). The World's tallest tropical tree in three dimensions. *Frontiers in Forests and Global Change*, *2*. https://doi.org/10.3389/ffgc.2019.00032

Shipley, B., Vile, D., & Garnier, E. (2006). From plant traits to plant communities: A statistical mechanistic approach to biodiversity. *Science*, *314*(5800), 812–814. https://doi.org/10.1126/science.1131344

Skhosana, F. V., Stevens, N., Maoela, M. A., Archibald, S., & Midgley, G. F. (2025). The impacts of woody encroachment on nature's contributions to people in North America and Africa: A systematic review. *People and Nature*, *7*(11), 2585–2601. https://doi.org/10.1002/pan3.70134

Slik, J. W. F., Aiba, S.-I., Brearley, F. Q., Cannon, C. H., Forshed, O., Kitayama, K., Nagamasu, H., Nilus, R., Payne, J., Paoli, G., Poulsen, A. D., Raes, N., Sheil, D., Sidiyasa, K., Suzuki, E., & van Valkenburg, J. L. C. H. (2010). Environmental correlates of tree biomass, basal area, wood specific gravity and stem density gradients in Borneo's tropical forests. *Global Ecology and Biogeography*, *19*(1), 50–60. https://doi.org/10.1111/j.1466-8238.2009.00489.x

Slik, J. W. F., Bernard, C. S., Van Beek, M., Breman, F. C., & Eichhorn, K. A. O. (2008). Tree diversity, composition, forest structure and aboveground biomass dynamics after single and repeated fire in a Bornean rain forest. *Oecologia*, *158*(3), 579–588. https://doi.org/10.1007/s00442-008-1163-2

Slik, J. W. F., Breman, F. C., Bernard, C., van Beek, M., Cannon, C. H., Eichhorn, K. A. O., & Sidiyasa, K. (2010). Fire as a selective force in a Bornean tropical everwet forest. *Oecologia*, *164*(3), 841–849. https://doi.org/10.1007/s00442-010-1764-4

Slik, J. W. F., Poulsen, A. D., Ashton, P. S., Cannon, C. H., Eichhorn, K. A. O., Kartawinata, K., Lanniari, I., Nagamasu, H., Nakagawa, M., van Nieuwstadt, M. G. L., Payne, J., and Saridan, A., Sidiyasa, K., Verburg, R. W., Webb, C. O., & Wilkie, P. (2003). A floristic analysis of the lowland dipterocarp forests of Borneo. *Journal of Biogeography*, *30*(10), 1517–1531. https://doi.org/10.1046/j.1365-2699.2003.00967.x

Slot, M., Nardwattanawong, T., Hernández, G. G., Bueno, A., Riederer, M., & Winter, K. (2021). Large differences in leaf cuticle conductance and its temperature response among 24 tropical tree species from across a rainfall gradient. *New Phytologist*, *232*(4), 1618–1631. https://doi.org/10.1111/nph.17626

Soterroni, A. C., Ramos, F. M., Mosnier, A., Fargione, J., Andrade, P. R., Baumgarten, L., Pirker, J., Obersteiner, M., Kraxner, F., Câmara, G., Carvalho, A. X. Y., & Polasky, S. (2019). Expanding the Soy Moratorium to Brazil's Cerrado. *Science Advances*, *5*(7), eaav7336. https://doi.org/10.1126/sciadv.aav7336

Souza, J. C. de, Martins, P. T. de A., & Druciaki, V. P. (2020). Uso e cobertura do solo no Cerrado: Panorama do período de 1985 a 2018: Soil use and coverage in Cerrado: period overview from 1985 to 2018. *Élisée - Revista de Geografia da UEG*, *9*(2), e922020–e922020.

Spadoni, G. L., Moris, J. V., Segura-García, C., Pessoa, A. C., Jones, M. W., Machado, M. S., Motta, R., Auxiliadora Costa Alencar, A., Ascoli, D., & Menor, I. O. (2025). Devegetation is a widespread driver of fire in the Brazilian Cerrado. *Journal of Environmental Management*, *385*, 125637. https://doi.org/10.1016/j.jenvman.2025.125637

Staver, A. C. (2018). Prediction and scale in savanna ecosystems. *New Phytologist*, *219*(1), 52–57. https://doi.org/10.1111/nph.14829

Staver, A. C., Archibald, S., & Levin, S. A. (2011). The global extent and determinants of savanna and forest as alternative biome states. *Science*, *334*(6053), 230–232. https://doi.org/10.1126/science.1210465

Stevens, N., Lehmann, C. E. R., Murphy, B. P., & Durigan, G. (2017). Savanna woody encroachment is widespread across three continents. *Global Change Biology*, *23*(1), 235–244. https://doi.org/10.1111/gcb.13409

Tavares, J. V., Gloor, E., Silva, T. S. F., Oliveira, R. S., Coelho de Souza, F., Signori-Müller, C., Diniz, F. C., Pereira, L., Acosta, M., Gilpin, M., Marca Zevallos, M. J., Salas Yupayccana, C. A., Perez-Mullisaca, F. M., Jancoski, H., Scalon, M. C., Schwantes Marimon, B., Marimon Junior, B. H., Malhi, Y., Oliveras Menor, I., … Galbraith, D. (2026). Family imprint reveals basin-wide patterns of Amazon forest embolism resistance. *Nature Communications*, *17*(1), 2073. https://doi.org/10.1038/s41467-026-69892-1

Tavares, J. V., Oliveira, R. S., Mencuccini, M., Signori-Müller, C., Pereira, L., Diniz, F. C., Gilpin, M., Marca Zevallos, M. J., Salas Yupayccana, C. A., Acosta, M., Pérez Mullisaca, F. M., Barros, F. de V., Bittencourt, P., Jancoski, H., Scalon, M. C., Marimon, B. S., Oliveras Menor, I., Marimon, B. H., Fancourt, M., … Galbraith, D. R. (2023). Basin-wide variation in tree hydraulic safety margins predicts the carbon balance of Amazon forests. *Nature*, *617*(7959), 111–117. https://doi.org/10.1038/s41586-023-05971-3

Teixeira, J., Souza, L., Bombo, A., & Le Stradic, S. (2025). How does fire exclusion affect the belowground biomass of tropical open ecosystems? *Journal of Vegetation Science*, *36*(2), e70027. https://doi.org/10.1111/jvs.70027

Teskey, R., Wertin, T., Bauweraerts, I., Ameye, M., Mcguire, M. A., & Steppe, K. (2015). Responses of tree species to heat waves and extreme heat events. *Plant, Cell & Environment*, *38*(9), 1699–1712. https://doi.org/10.1111/pce.12417

The SEOSAW Partnership. (2021). A network to understand the changing socio-ecology of the southern African woodlands (SEOSAW): Challenges, benefits, and methods. *Plants, People, Planet*, *3*(3), 249–267. https://doi.org/10.1002/ppp3.10168

Tuck, S. L., O'Brien, M. J., Philipson, C. D., Saner, P., Tanadini, M., Dzulkifli, D., Godfray, H. C. J., Godoong, E., Nilus, R., Ong, R. C., Schmid, B., Sinun, W., Snaddon, J. L., Snoep, M., Tangki, H., Tay, J., Ulok, P., Wai, Y. S., Weilenmann, M., … Hector, A. (2016). The value of biodiversity for the functioning of tropical forests: Insurance effects during the first decade of the Sabah biodiversity experiment. *Proceedings of the Royal Society B: Biological Sciences*, *283*(1844), 20161451. https://doi.org/10.1098/rspb.2016.1451

van Nieuwstadt, M. G. L., & Sheil, D. (2005). Drought, fire and tree survival in a Borneo rain forest, East Kalimantan, Indonesia. *Journal of Ecology*, *93*(1), 191–201. https://doi.org/10.1111/j.1365-2745.2004.00954.x

Veldman, J. W. (2016). Clarifying the confusion: Old-growth savannahs and tropical ecosystem degradation. *Philosophical Transactions of the Royal Society B: Biological Sciences*, *371*(1703), 20150306. https://doi.org/10.1098/rstb.2015.0306

Veryard, R. (2023). *The role of biodiversity in Southeast Asian tropical forest restoration*. PhD Thesis. University of Oxford.

Vesk, P. A. (2006). Plant size and resprouting ability: Trading tolerance and avoidance of damage? *Journal of Ecology*, *94*(5), 1027–1034. https://doi.org/10.1111/j.1365-2745.2006.01154.x

Vico, G., Dralle, D., Feng, X., Thompson, S., & Manzoni, S. (2017). How competitive is drought deciduousness in tropical forests? A combined eco-hydrological and eco-evolutionary approach. *Environmental Research Letters*, *12*(6), 065006. https://doi.org/10.1088/1748-9326/aa6f1b

Violle, C., Navas, M.-L., Vile, D., Kazakou, E., Fortunel, C., Hummel, I., & Garnier, E. (2007). Let the concept of trait be functional! *Oikos*, *116*(5), 882–892. https://doi.org/10.1111/j.0030-1299.2007.15559.x

Vitorino, B. D., Frota, A. V. B. da, Castrillon, S. K. I., & Nunes, J. R. da S. (2018). Birds of Estação Ecológica da Serra das Araras, state of Mato Grosso, Brazil: Additions and review. *Check List*, *14*(5), 893–922. https://doi.org/10.15560/14.5.893

Volaire, F. (2018). A unified framework of plant adaptive strategies to drought: Crossing scales and disciplines. *Global Change Biology*, *24*(7), 2929–2938. https://doi.org/10.1111/gcb.14062

Walsh, R. P. D., Nussbaum, R., Fowler, D., Weilenmann, M., & Hector, A. (2011). Conclusion: Applying South East Asia Rainforest Research Programme science to land-use management policy and practice in a changing landscape and climate. *Philosophical Transactions of the Royal Society B: Biological Sciences*, *366*(1582), 3354–3358. https://doi.org/10.1098/rstb.2011.0179

Wang, Y.-S.-D., Zhang, J.-L., Chen, Y.-J., Posch, B. C., Yang, D., He, P.-C., Zhu, S.-D., Ning, Q.-R., Lu, L.-X., Zhang, H.-P., Wang, Z., Liu, M.-Y., Chen, H., Ye, Q., & Liu, H. (2026). Leaf economic traits link drought and heat tolerance of woody species in two contrasting hydrothermal habitats. *New Phytologist*, *249*(6), 2808–2820. https://doi.org/10.1111/nph.70841

Wargowsky, I. K., NeSmith, J. E., Gajjar, N., & Holdo, R. M. (2023). Root vascular anatomy predicts maximum growth rates in savanna trees and grasses. *Biotropica*, *55*(6), 1159–1164. https://doi.org/10.1111/btp.13262

Wigley, B. J., Coetsee, C., February, E. C., Dobelmann, S., & Higgins, S. I. (2024). Will trees or grasses profit from changing rainfall regimes in savannas? *New Phytologist*, *241*(6), 2379–2394. https://doi.org/10.1111/nph.19538

Wolfe, B. T. (2020). Bark water vapour conductance is associated with drought performance in tropical trees. *Biology Letters*, *16*(8), 20200263. https://doi.org/10.1098/rsbl.2020.0263

World Economic Forum (2024). *The Cerrado: Production and Protection*. White Paper https://www3.weforum.org/docs/WEF_Sustainable_Transition_Cerrado_2024.pdf

Wright, I. J., Reich, P. B., Westoby, M., Ackerly, D. D., Baruch, Z., Bongers, F., Cavender-Bares, J., Chapin, T., Cornelissen, J. H. C., Diemer, M., Flexas, J., Garnier, E., Groom, P. K., Gulias, J., Hikosaka, K., Lamont, B. B., Lee, T., Lee, W., Lusk, C., … Villar, R. (2004). The worldwide leaf economics spectrum. *Nature*, *428*(6985), 821–827. https://doi.org/10.1038/nature02403

Wright, S. J., Kitajima, K., Kraft, N. J. B., Reich, P. B., Wright, I. J., Bunker, D. E., Condit, R., Dalling, J. W., Davies, S. J., Díaz, S., Engelbrecht, B. M. J., Harms, K. E., Hubbell, S. P., Marks, C. O., Ruiz-Jaen, M. C., Salvador, C. M., & Zanne, A. E. (2010). Functional traits and the growth–mortality trade-off in tropical trees. *Ecology*, *91*(12), 3664–3674. https://doi.org/10.1890/09-2335.1

Xu, C., McDowell, N. G., Fisher, R. A., Wei, L., Sevanto, S., Christoffersen, B. O., Weng, E., & Middleton, R. S. (2019). Increasing impacts of extreme droughts on vegetation productivity under climate change. *Nature Climate Change*, *9*(12), 948–953. https://doi.org/10.1038/s41558-019-0630-6

Yaffar, D., Lugli, L. F., Wong, M. Y., Norby, R. J., Addo-Danso, S. D., Arnaud, M., Cordeiro, A. L., Dietterich, L. H., Diaz-Toribio, M. H., Lee, M. Y., Ghimire, O. P., Smith-Martin, C. M., Toro, L., Andersen, K., McCulloch, L. A., Meier, I. C., Powers, J. S., Sanchez-Julia, M., Soper, F. M., & Cusack, D. F. (2024). Tropical root responses to global changes: A synthesis. *Global Change Biology*, *30*(7), e17420. https://doi.org/10.1111/gcb.17420

Yan, P., He, N., Yu, K., Xu, L., & Van Meerbeek, K. (2023). Integrating multiple plant functional traits to predict ecosystem productivity. *Communications Biology*, *6*(1), 239. https://doi.org/10.1038/s42003-023-04626-3

Zanella de Arruda, P. H., Vourlitis, G. L., Santanna, F. B., Pinto Jr., O. B., De Almeida Lobo, F., & de Souza Nogueira, J. (2016). Large net CO_2 loss from a grass-dominated tropical savanna in south-central Brazil in response to seasonal and interannual drought. *Journal of Geophysical Research: Biogeosciences*, *121*(8), 2110–2124. https://doi.org/10.1002/2016JG003404

Zhou, J., Cieraad, E., & van Bodegom, P. M. (2022). Global analysis of trait–trait relationships within and between species. *New Phytologist*, *233*(4), 1643–1656. https://doi.org/10.1111/nph.17879

Zhou, Y. (2023). Root traits in response to frequent fires: Implications for belowground carbon dynamics in fire-prone savannas. *Frontiers in Plant Science*, *14*. https://doi.org/10.3389/fpls.2023.1106531

Zhou, Y., Kitudom, N., Fauset, S., Slot, M., Fan, Z., Wang, J., Liu, W., & Lin, H. (2023). Leaf thermal regulation strategies of canopy species across four vegetation types along a temperature and precipitation gradient. *Agricultural and Forest Meteorology*, *343*, 109766. https://doi.org/10.1016/j.agrformet.2023.109766

Zirondi, H. L., Ooi, M. K. J., & Fidelis, A. (2021). Fire-triggered flowering is the dominant post-fire strategy in a tropical savanna. *Journal of Vegetation Science*, *32*(2), e12995. https://doi.org/10.1111/jvs.12995

Zuidema, P. A., Groenendijk, P., Rahman, M., Trouet, V., Abiyu, A., Acuña-Soto, R., Adenesky-Filho, E., Alfaro-Sánchez, R., Anholetto, C. R., Aragão, J. R. V., Assis-Pereira, G., Astudillo-Sánchez, C. C., Barbosa, A. C., Battipaglia, G., Beeckman, H., Botosso, P. C., Bourland, N., Bräuning, A., Brienen, R., … Babst, F. (2025). Pantropical tree rings show small effects of drought on stem growth. *Science*, *389*(6759), 532–538. https://doi.org/10.1126/science.adq660

Chapter 3: Research Paper 1

The effect of fire on the carbon fluxes and productivity of Brazilian woodland savannas.

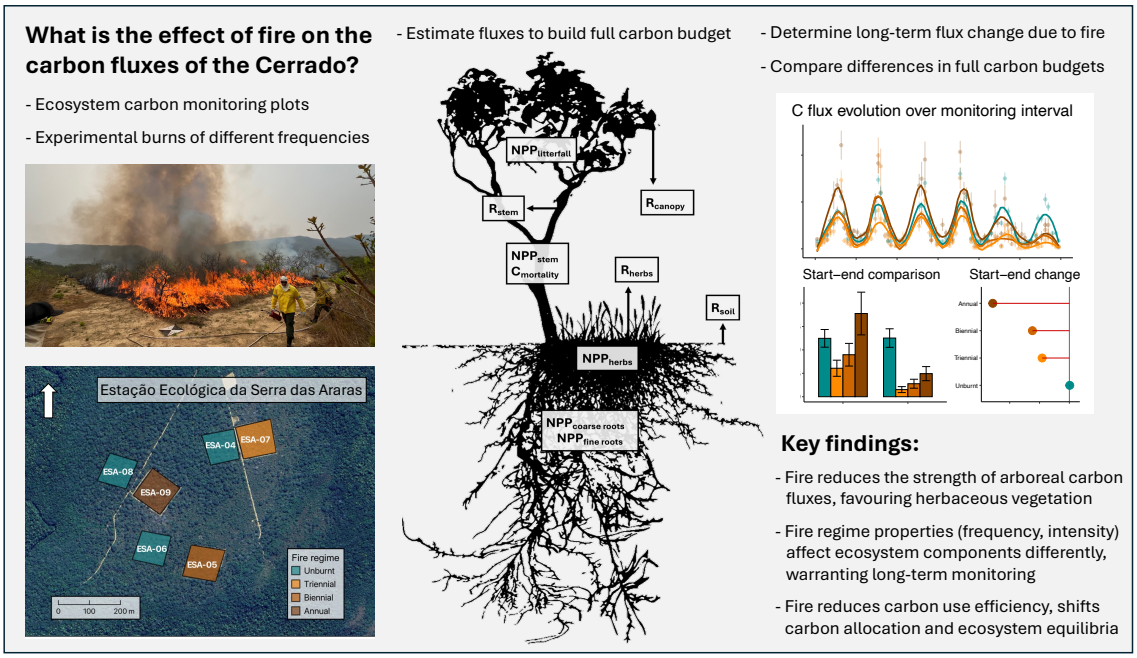
By Francisco Navarro-Rosales, Maria Antonia Carniello, Wesley Jonatar Alves da Cruz, Flavio de Campos Oliveira, Huanyuan Zhang-Zheng, Valéria Lucélia de Oliveira Corrêa, Marcelo Leandro Feitosa de Andrade, Yadvinder Malhi, Andy Hector and Imma Oliveras Menor.

Linking statement: This first chapter was motivated by the need to better understand carbon cycling in Brazilian savannas, and how carbon fluxes may be affected by changing fire regimes. Previous studies have provided estimates of productivity and respiration fluxes for the Cerrado, but have mostly focused on short-term responses and individual ecosystem components. Studies across tropical savannas indicate that burning reduces tree biomass and survival, but also reveal that fire drives productivity through vegetation recovery. Therefore, this chapter examines long-term changes in net primary productivity across experimental fire regimes, using the Global Ecosystems Monitoring protocol to quantify and scale up ecosystem-level carbon balances.

Status: This chapter was published on the 25th of July 2025 in *Science of the Total Environment* (https://doi.org/10.1016/j.scitotenv.2025.179626). A corrigendum was published on the 25th of February 2026 to inform that the species identification of *Tachigali paniculata* Aubl. had been updated to *Tachigali vulgaris* L.G. Silva & H.C. Lima. This work was presented at the 74th Brazilian Congress of Botany and at the 2024 Annual Meeting of the British Ecological Society.

Contributions: I, Francisco Navarro-Rosales, contributed to field data collection at Serra das Araras, cleaned and managed the data, adapted methodological protocols, performed statistical analyses, produced figures and tables, and wrote and reviewed the manuscript. Imma Oliveras Menor and Maria Antonia Carniello conceptualised and designed the study, and secured funding. Marcelo Leandro Feitosa de Andrade led the controlled burning interventions. Maria Antonia Carniello, Wesley Jonatar Alves da Cruz and Flavio de Campos Oliveira led field data collection campaigns. Imma Oliveras Menor, Maria Antonia Carniello, Wesley Jonatar Alves da Cruz, Flavio de Campos Oliveira and Valéria Lucélia de Oliveira Corrêa collated and reviewed carbon flux datasets. Imma Oliveras Menor, Huanyuan Zhang-Zheng, Yadvinder Malhi and Andy Hector supervised and contributed to carbon flux estimation and statistical analyses. Imma Oliveras Menor supervised this research and was involved in all steps of this work.

3.1. Graphical abstract



3.2. Highlights

- Estimated ecosystem carbon budget and fluxes in unburnt and periodically burnt plots
- Fire reduced the strength of arboreal carbon fluxes favouring herbaceous vegetation
- Specific carbon fluxes are diversely related to either fire frequency or intensity
- Fire reduces carbon use efficiency, shifts carbon allocation and ecosystem balances
- Active burning management of altered fire regimes can improve savanna conservation

3.3. Abstract

The effects of altered fire regimes within open ecosystems are poorly understood and can have serious consequences on functioning and conservation across savanna ecoregions worldwide. In South American savannas like the Cerrado, there is a gap of knowledge relating to carbon cycling in the presence of fire, meaning the impacts of altered fire regimes on the carbon fluxes and budgets are virtually unknown. We thus investigate vegetation carbon flux dynamics within the Cerrado, making use of an experimental fire and carbon monitoring research project at the Estação Ecológica da Serra das Araras, Brazil. We present a thorough carbon budget of woodland-type savannas (*cerrado sensu stricto*), and investigate how annual (every year), biennial (every two years), and triennial (every three years) controlled fire frequencies have influenced net primary productivity and respiration fluxes. Six years of experimental fire had noticeable effects on the vegetation structure and carbon dynamics, reducing woody cover and productivity in favour of grass-dominated carbon balances. Woody NPP increased by 35% in the unburnt plots from 2017-2019 to 2021-2023, but decreased by 75%, 33% and 20% in the triennial, biennial and annual fire frequencies. By 2023, burnt plots revealed around three times higher herbaceous NPP than unburnt plots. Fluxes corresponding to different ecosystem components (canopy, stems, roots, herbs) showed varying patterns of change across the gradient of experimental fire frequencies, indicating other fire regime properties distinctively affect each vegetation segment. Fire intensity and severity appear to be linked with patterns in woody stems and the herbaceous layer. Our results indicate periodically burnt *cerrado sensu stricto* vegetation experiences different carbon dynamics than unburnt vegetation. Burning is revealed as a strategy that can successfully limit woody encroachment and help conserve open ecosystem structure in the Cerrado. Our study highlights the importance of long-term monitoring efforts in investigating the effects of management interventions and environmental shifts on ecosystem functioning.

3.4. Introduction

Fire regimes across tropical ecosystems are being shifted by different drivers of global change, altering ecosystem productivity, carbon sequestration and biogeochemical processes (Bowman *et al.*, 2013; Rocha *et al.*, 2014; Zheng *et al.*, 2021; Friedlingstein *et al.*, 2022). Major shifts in tropical fire regimes could alter the Earth system functioning, as fire emission sources are disproportionately tropical – with tropical savannas contributing to approximately 62% of total global fire emissions – and are expected to increase in the face of global change (van der Werf *et al.*, 2003; Krawchuk *et al.*, 2009; van der Werf *et al.*, 2017; Zheng *et al.*, 2021). Increases in the number, intensity, severity and recurrence of fire events can be linked to extreme weather events and climate change (Westerling *et al.*, 2006; Prichard *et al.*, 2017; Diffenbaugh *et al.*, 2021), as well as socioecological factors such as land abandonment or the encroachment of agricultural and urban land uses into natural areas (Prichard *et al.*, 2017; Conciani *et al.*, 2021; Pivello *et al.*, 2021). Extensive burning can also affect water balances, heat fluxes and surface climate in tropical forests and savannas, promoting warmer and drier weather conditions that support more extreme fires, reinforcing global warming impacts (de Sales *et al.*, 2023). Changing fire regimes can thus exacerbate biodiversity loss and climate change and have the potential to compromise key ecosystem services – such as nutrient cycling, water provisioning, habitat protection and carbon storage – and to permanently shift landscapes into alternative stable states (Bowman *et al.*, 2009; Gomes *et al.*, 2020; McLauchlan *et al.*, 2020). However, fire is also a key natural disturbance in many open ecosystems such as woodlands, grasslands, and savannas, allowing structure, biodiversity and functioning to be maintained (Pivello, 2011; Staver *et al.*, 2011).

Tropical savannas are important in terms of biodiversity and global functioning, covering approximately 20% of the Earth's surface and accounting for 30% of the total productivity of terrestrial vegetation (Dexter *et al.*, 2015; Grace *et al.*, 2006). Savannas play an essential role in terms of delivering ecosystem services, providing >1 billion people with food, materials, and

pollinators as well as regulating flows of air, energy and water (Marchant, 2010; Stevens *et al.*, 2022). Savanna ecosystems are maintained by fire regimes; where natural or traditional human-induced burns are required to promote vegetation regeneration, maintain adequate nutrient cycles and control the degree of ecosystem change via woody encroachment (Miller *et al.*, 2017; Kelly *et al.*, 2020), which can cause significant loss of ecological functioning and diversity (Durigan & Ratter, 2016; Rosan *et al.*, 2019; Wieczorkowski & Lehmann, 2022). Consequently, the preservation or restoration of natural fire disturbances or – where the former is not feasible – the implementation of prescribed fire regimes are emerging as potential land management strategies that could help maintain savanna biodiversity and functioning (Durigan & Ratter, 2016).

Improving fire management for ecosystem health and biodiversity conservation has been highlighted as one of the key milestones required for adequate management of the Cerrado, Brazil's savanna ecoregion (Françoso *et al.*, 2015; Prichard *et al.*, 2017). The Cerrado is a 2-million-km^2 biodiversity hotspot (e.g., supporting >10,000 native plant species of which about 40% are endemic – Giles *et al*., 2026) that is also extremely threatened. Higher land clearance rates than the Amazon have led to about 50% of the natural area disappearing already (Françoso *et al.*, 2015). In terms of fire, Brazilian savannas are experiencing higher pressures and impacts from anthropogenic burning as well as ongoing ecosystem degradation from lack of prescribed fire management (Pivello *et al.*, 2021). Burning continues to play a role as an important environmental factor influencing processes like phenology and nutrient stoichiometry (Silva & Batalha, 2008; Oliveras *et al.*, 2012) and many Cerrado plants have successful adaptations that allow them to cope with the interacting impacts of fire and drought (Franco *et al.*, 2008). Thus, the restoration of frequent surface fires in areas of fire suppression could represent a feasible conservation strategy for the Cerrado by reducing wildfire severity and extensive woody encroachment (Durigan *et al.*, 2020). Yet, the effects of prescribed fires on Brazilian savannas are still poorly understood and could lead to unintended effects on ecosystem functioning and vegetation (Hoffmann, 2002; Bustamante *et al.*, 2012; Gomes *et al.*, 2018). Therefore,

investigating the effect of altered fire regimes on ecosystem dynamics is becoming an increasingly key research priority.

Despite the importance of determining and quantifying the impacts of fire on Cerrado ecosystem dynamics, there are disproportionately few experimental studies on controlled burning across such a large and heterogeneous area, and they are mainly focused on open vegetation and grass-dominated dynamics within a handful of locations in the central and south-eastern Cerrado (see Rissi *et al.*, 2017; Durigan *et al.*, 2020; Zupo *et al.*, 2021; Rodrigues *et al.*, 2021; Teixeira *et al.*, 2022; Fontenele and Miranda, 2024). There is a gap of knowledge surrounding key ecosystem metrics relating to carbon cycling in terms of carbon fluxes, both in the presence or absence of fire. Vourlitis *et al.* (2022) have been able to provide a detailed estimate of the main carbon fluxes within a mixed-grassland site in Mato Grosso, Brazil, using field methods from different sources to reconstruct a relatively complete carbon cycle. Additionally, Scalon *et al.* (2022) estimated net primary productivity partitioning for woodland savanna (*cerrado sensu stricto*) and forest-savanna transition woodland (*cerradão*) plots also in Mato Grosso, Brazil. Still, there is no available data linking detailed carbon flux dynamics to the effects of fire. This means the impacts of altered fire regimes on the carbon balance of the Cerrado are virtually unknown. Thus, the aim of this study is to investigate carbon flux dynamics within experimental fire regimes of different burning frequencies, in order to inform about the potential consequences of altered fire regimes within the Cerrado. Overall, we specifically aim to address the following objectives:

1. Quantify the main carbon fluxes within Cerrado woodland savanna, illustrating – where sampling intensity and temporal replication allow – flux seasonal changes and trends over time.

2. Determine how the cumulative effects of the annual, biennial, and triennial experimental fire frequencies have influenced the main carbon fluxes of Cerrado woodland savanna by comparing estimates in burnt plots against estimates in fire exclusion plots.

3. Provide estimates of ecosystem total carbon budget metrics for Cerrado woodland savanna that has been subjected to fire suppression and compare them to metrics for plots that have experienced annual, biennial, and triennial burns.

We expect to find similar carbon flux patterns as those recorded in other Cerrado sites (Scalon *et al.*, 2022; Vourlitis *et al.*, 2022), with comparable distribution across ecosystem components and strong seasonal fluctuations related to water availability (Araujo-Murakami *et al.*, 2014; Rocha *et al.*, 2014). In terms of our hypotheses regarding the long-term effect of fire on the carbon fluxes of savannas, we expect to i) observe a reduction in the intensity of fluxes relating to the arboreal component of the ecosystem within the experimental burning plots. Reduced carbon allocation into arboreal fluxes should correspond to decreases in the survival and growth of trees with recurrent burning (Rodrigues & Fidelis, 2022), and would be consistent with carbon flux patterns observed in burnt vs unburnt plots in Amazonian transitional forests in Mato Grosso (Rocha *et al.*, 2014). We also predict that ii) experimental burns will alter the way in which carbon is allocated into different fluxes, increasing the proportion of productivity distributed into aboveground components due to post-fire recovery and regrowth (Zupo *et al.*, 2021); as well as the proportion of respiration from heterotrophic sources, given fire will transform part of the live biomass stock into decomposable dead matter (Brando *et al.*, 2014). Finally, we expect iii) individual carbon fluxes to potentially show varying patterns of change across the gradient of fire frequencies, since different effects of the fire regime – such as decreased fuel load and fire intensity, or higher proportion of bare ground in more frequently burnt plots – could either exacerbate or compensate the effect of cumulative burns on the different carbon fluxes (Rodrigues *et al.*, 2021; Chiminazzo *et al.*, 2023).

3.5. Materials and methods

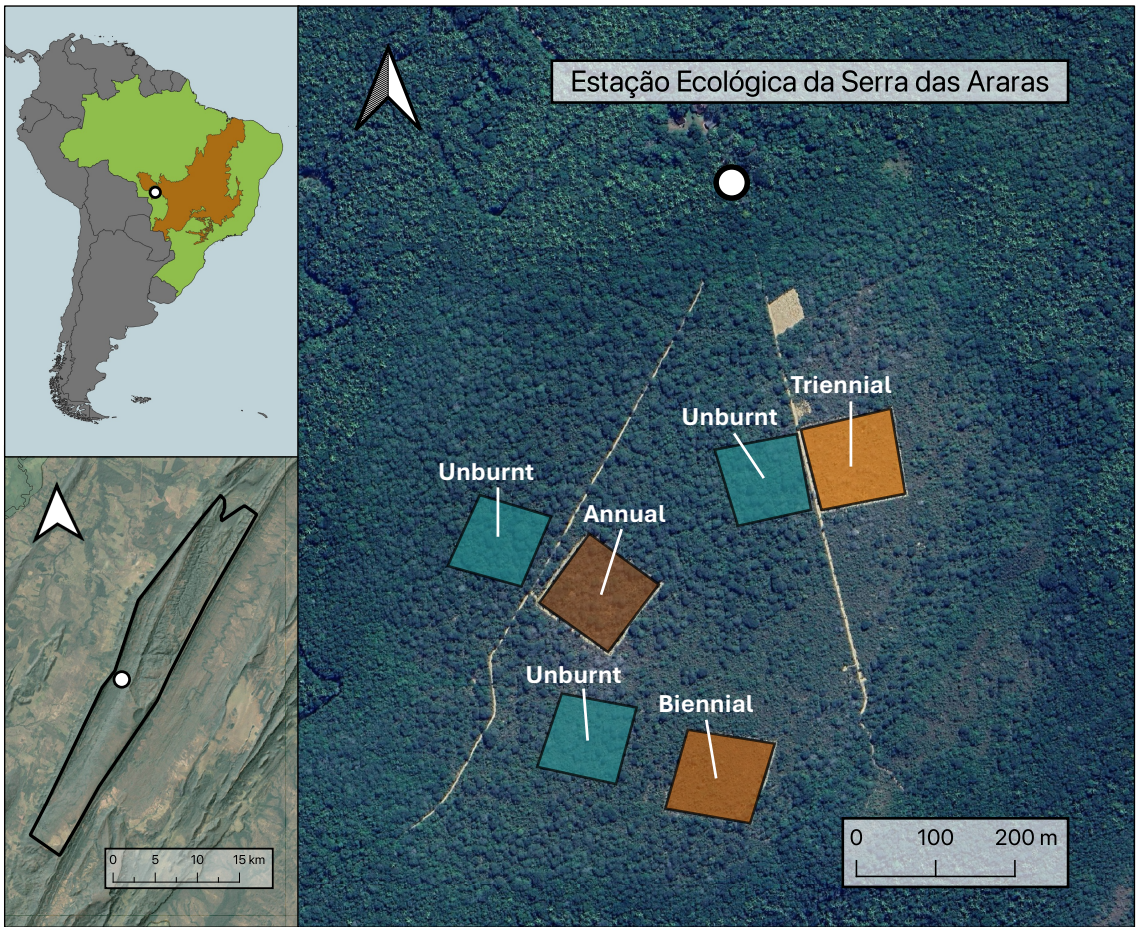


Figure 3.1, location of the monitoring plots. **Top left**) location of the Estação Ecológica da Serra das Araras within South America (Brazil is highlighted in light green, the Cerrado ecoregion in orange). **Bottom left**) position of the *cerrado sensu stricto* study site within the Estação Ecológica da Serra das Araras. **Right**) distribution of the six monitoring plots subjected to experimental burns and fire exclusion.

3.5.1. Study site and experimental design

Our study was located within an area of woodland savanna at the Estação Ecológica da Serra das Araras (Serra das Araras Ecological Station, **Figure 3.1**), in Southwestern Mato Grosso, Brazil (15°39′10.96″S, 057°12′52.54″W, ~320 m above sea level). Serra das Araras is a 27,000-ha IUCN category 1A conservation unit mostly contained within the municipality of Porto Estrela (ICMBio, 2016). The unit is managed by the Instituto Chico Mendes de Conservação da Biodiversidade (ICMBio) and placed in a strategic location near the ecotone between the Cerrado, Pantanal and Amazonian ecoregions, playing a key role in biodiversity conservation. The area has tropical savanna climate with dry winter characteristics, having distinct dry (June-September)

and rainy (November-March) seasons (Kottek *et al*., 2006; Pizzato *et al*., 2012). Mean annual temperature and rainfall for the 1979-2010 period were around 25-26°C and 1268.4 mm respectively (Pizzato *et al*., 2012; Santos *et al*., 2017). The site was historically settled by traditional *quilombola* communities but was transformed into a protected area in 1982. No fires have been recorded within our monitoring area since 1992.

Our monitoring efforts consist of six 1-ha (100×100 m) plots (named ESA-04 to ESA-09) that have been set up and maintained since 2017. Plots are grouped in three burnt/unburnt pairs, and divided into 25 subplots (20×20 m) to provide spatial replication within the plot unit. Most carbon fluxes have been intensively monitored up to the end of 2023 – with the exception of the 2020/2021 COVID-19 lockdowns – based on the methods provided by the RAINFOR-GEM Field Manual for Intensive Census Plots (Marthews *et al*., 2014). The monitoring plots have also been subjected to experimental fire, with three regularly burnt plots and three unburnt ones where all fire is excluded. Each burnt plot has been burnt at different frequencies (annual, biennial and triennial burns) to better determine the effects of different fire regimes on Cerrado vegetation. This means that by December 2023, the annual plot had burnt six times (2018, 2019, 2020, 2021, 2022, 2023), the biennial plot three times (2019, 2021, 2023) and the triennial plot had burnt twice (2018, 2021). We conceptualise each experimental regime as incorporating different fire frequencies, as well as recognising the unique return interval, behaviour, intensity and severity of each set of fires. Controlled burns were undertaken at the peak of the dry season (July – September) to take advantage of good burning conditions – low ambient moisture and high accumulation of dry fuel – and to simulate seasonality of fire within the Cerrado (Pivello, 2011). Upon plot establishment, all six plots shared similar vegetation architecture and composition, although there was variable vegetation density due to the strong heterogeneity characteristic of Cerrado ecosystems (see **Table S3.1** for details). Vegetation was classified as *cerrado sensu stricto* (typical woodland savanna) in transition towards *cerradão* (forest-savanna transition woodland), consisting of small and medium tree species, shrubs and a relatively sparse herbaceous layer. Dominant tree species include *Curatella americana* L., *Kielmeyera grandiflora*

(Wawra) Saddi, Tachigali vulgaris L.G. Silva & H.C. Lima, *Vochysia haenkeana* Mart., *Myrcia bella* Cambess., and *Pouteria ramiflora* (Mart.) Radlk. All plots are characterised by a generally flat topography and share underlying soils formally classified as dystrophic latosols under the Brazilian soil classification system (EMBRAPA, 2018) – largely equivalent to dystric ferralsols under the World Reference Base soil classification system (IUSS Working Group WRB, 2022).

3.5.2. Estimation of carbon fluxes

We make use of an experimental fire and carbon monitoring research project at Serra das Araras, Mato Grosso, Brazil, to track and estimate the area's main carbon fluxes over a period of six years. These include net primary productivity – NPP, defined as the rate at which carbon is incorporated into the biomass of an ecosystem via plant growth, discounting carbon loss through respiration – and respiration – R, describing the rate at which carbon is released by plants or soil as a result of metabolic processes or microbial decomposition (Girardin *et al*., 2010; Moore *et al*., 2018). NPP and R are typically measured in the field based on rates of production and gas exchange of leaves, stems, roots, etc. (Araujo-Murakami *et al*., 2014). The study of the productivity and respiration fluxes of these different ecosystem components gives insight into ecological performance and functioning as they relate to specific biological processes such as stem growth, leaf phenology and plant physiology (Girardin *et al*., 2010). In the wider ecosystem scale, productivity and respiration dynamics are used to estimate ecosystem carbon balance metrics such as plant carbon expenditure (PCE), gross primary productivity (GPP) and carbon use efficiency (CUE) which provide useful information with regard to ecosystem carbon balances and stability, as well as climate budgeting (Metcalfe *et al*., 2010; Malhi, 2012).

We therefore present the first detailed picture of these carbon fluxes within Brazilian woodland-type savannas (*cerrado sensu stricto*; Miranda *et al*., 2014). Since 2016, we collected long-term ecosystem monitoring data from three woodland plots subjected to different fire regimes: annual (every year), biennial (every two years), and triennial (every three years) burns, as well as three

unburnt – fire exclusion plots. We used ecosystem monitoring data to estimate the main carbon fluxes within Cerrado woodland savanna: 1) litterfall NPP, 2) woody stem NPP, 3) herbaceous NPP, 4) coarse root NPP, 5) fine root NPP, 6) canopy R, 7) woody stem R, 8) herbaceous R, and 9) soil R, as well as 10) carbon accumulated in dead stems. We then compare flux estimates between burnt and unburnt plots, which allows us to study the long-term effect of the different experimental fire regimes on the carbon cycling of Cerrado woodland savanna.

The main carbon fluxes of the monitoring plots were estimated from a set of field inventory data based on the RAINFOR-GEM protocol (Marthews *et al*., 2014; Malhi *et al*., 2021). Summaries of the field methods and data processing techniques used to estimate each flux are presented in **Table 3.1** and **Table 3.2**, respectively. In broad terms, carbon fluxes can be estimated from a) census inventory data of all trees within the plots, b) spatially replicated samples taken at monthly or trimestral intervals, or c) a combination of variables derived from both types of data. Because our objectives are to estimate the main carbon fluxes and investigate the long-term effects of fire, we attempted to compare flux estimates using a BACI-based framework (before-after control-impact approach; Christie *et al*., 2019) which allowed us to study the effect of fire by comparing flux change in burnt vs unburnt plots. Thus, we aimed to compare estimates for each carbon flux covering the first and last complete year of data within the experiment, allowing for sufficient data to produce adequate, representative yearly estimates. It is important to note that since the experimental fire regimes were initiated during the first year of data collection, we were unable to implement a fully typical BACI approach for some fluxes, instead comparing 'start' and 'end' flux estimates. Incorporating more reliable full-year start estimates is thus justified because short-term flux changes are negligible in comparison to estimate uncertainty and seasonal variation.

In the case of variables derived from temporally and spatially replicated samples, we compared fluxes using statistical models to account for groupings within the data and extract flux estimate coefficients. In the case of carbon fluxes partially or entirely derived from sums of plot-level inventory allometries, estimates were compared descriptively. Please note that for certain

variables, data collection was only possible at the final stages of the monitoring period. For these fluxes, we used a control-impact (CI) or space-for-time substitution approach (Christie *et al.*, 2019) to compare flux estimates – statistically and descriptively – and evaluate the effect of fire across regimes (**Table 3.2**, **Table 3.3**).

Due to the lack of some initial data, we were only able to parametrise the full carbon cycle for the 2023/2024 focal period, around six years after the start of the experimental fires. This allowed us to calculate ecosystem carbon budget metrics, also comparing them via the CI framework. We integrated carbon fluxes to calculate ecosystem net primary productivity (NPP_{total}) and its aboveground/belowground partition using the following equations:

$$NPP_{aboveground} = NPP_{litterfall} + NPP_{stem} + NPP_{herbs} \quad (3.1)$$

$$NPP_{belowground} = NPP_{coarse\,roots} + NPP_{fine\,roots} \quad (3.2)$$

$$NPP_{total} = NPP_{litterfall} + NPP_{stem} + NPP_{herbs} + NPP_{coarse\,roots} + NPP_{fine\,roots} \quad (3.3)$$

We estimated ecosystem respiration (R_{eco}) by summing all respiration fluxes. In order to estimate total autotrophic respiration ($R_{autotrophic}$) we partitioned R_{soil} into $R_{rhizosphere}$ (autotrophic respiration from the rhizosphere) and $R_{heterotrophic}$ (heterotrophic microbial decomposition, see **Table 3.2** for details).

$$R_{eco} = R_{canopy} + R_{stem} + R_{herbs} + R_{soil} \quad (3.4)$$

$$R_{autotrophic} = R_{canopy} + R_{stem} + R_{herbs} + R_{rhizosphere} \quad (3.5)$$

Obtaining estimates of total autotrophic respiration allowed us to complete our carbon balances by approximately isolating plant-mediated fluxes. We were thus able to derive plant carbon expenditure (PCE), the total amount of carbon expended by trees.

$$(3.6) \quad PCE = NPP_{total} + R_{autotrophic}$$

Under steady-state conditions, the total rate of carbon utilisation by respiration and growth (PCE) should be equal to the photosynthetic carbon inputs into (and respiratory outputs from) the ecosystem (Jones *et al*., 2020).

$$(3.7) \quad GPP \approx PCE \approx R_{eco}$$

Where GPP (gross primary productivity) is the total amount of carbon entering the system via photosynthesis, usually estimated through ecosystem-level gas exchange measurements. Because gas exchange measurements are complex and costly, studies assuming steady-state conditions are able to approximate GPP as PCE, which is derived from field sampling methods. However, in non-stable or perturbed systems such as ours – where burnt plots are subjected to periodic fire and unburnt plots are experiencing woody encroachment – ecosystem-level steady-state conditions should not apply as carbon is expected to be lost or accumulated.

$$(3.8) \quad GPP \approx PCE \approx R_{eco}$$

In our case, because we cannot derive GPP from PCE, we estimated the ecosystem's carbon use efficiency (CUE) of both burnt and unburnt plots as the proportion of total carbon expenditure (PCE) that is invested in total NPP (rather than estimating it as the proportion of GPP invested in NPP, as traditionally reported):

$$(3.9) \quad CUE = NPP_{total}/PCE$$

We acknowledge that our estimation of total productivity and carbon expenditure does neglect some smaller carbon flux terms. These are relatively minor flows of carbon involved in processes like leaf herbivory, decomposition of litter (in the canopy or from below litterfall traps) and wood

(via termites), root exudates and volatile organic compounds (Rocha *et al*., 2014). We excluded these because they represent mostly negligible aspects of carbon expenditure but do recognise that they are still minor missing terms (Scalon *et al*., 2022). We also recognise that the carbon balances presented in this paper do not represent fully complete carbon budgets for Cerrado ecosystems subjected to fire regimes. Firstly, because we only estimate vegetation biomass carbon in terms of fluxes, that is, the transfer of carbon from one ecosystem component to another, and do not quantify corresponding carbon pools, that is, stocks of carbon stored in vegetation, soil and litter. Although estimates of ecosystem biomass are missing, we are still able to approximate the carbon sink (or source) capacity of *cerrado* savannas by scaling up carbon fluxes to find total carbon gains and losses (Malhi *et al*., 2009). Second, due to logistical and sampling difficulties, our study also neglects flows of carbon arising from the direct effects of fire, such as fire emissions from the consumption of biomass in vegetation, soil and leaflitter, as well as the deposition of carbon into soil during fire as charcoal and ash (Pivello & Coutinho, 1992). Indeed, we should clarify that the scope of our analysis was conceptually and temporally constrained to studying the main flows of carbon of *cerrado* savannas in a 'post-fire' state, rather than investigating the entire ecosystem carbon cycle prior to, during, and after burning.

3.5.3. Error analysis and propagation

Many of the carbon fluxes we estimated are calculated from multiple variables or derived from a combination of the more basic fluxes, all of which incorporate error/uncertainties. Systematic and sampling uncertainties of our carbon flux estimates were thus taken into consideration following the methodological uncertainty analysis provided by Malhi *et al*. (2009). Systematic uncertainties of key variables – associated with unknown biases in measurements or scaling methods – were assigned a conservative error estimate based on similar studies or on reported error values of allometric equations and ratios (**Table 3.2**). Sampling uncertainties arising from heterogeneity and random variation in spatially replicated samples were derived using linear mixed models and marginal means. Using marginal means (and their standard errors) derived from mixed models

provided better estimates than those provided through arithmetic means (and their standard errors) because these variables were sampled repeatedly and in groups (see **Section 3.5.4**, **Table 3.2**).

Errors were then propagated by taking the square root of the sum of squared absolute errors for addition and subtraction, and relative errors for division and multiplication (Taylor, 1997), assuming independence and normal distribution of uncertainties (where A and B are example variables, and δ represents their associated uncertainty):

$$(3.10) \quad \delta(A+B) \ \textbf{\textit{or}} \ \delta(A-B) = \sqrt{(\delta A)^2 + (\delta B)^2}$$

$$(3.11) \quad \delta(AB) \ \textbf{\textit{or}} \ \delta(A/B) = \sqrt{(\delta A/A)^2 + (\delta B/B)^2}$$

3.5.4. Statistical modelling and analysis

Statistical models were used to investigate the long-term effect of fire on carbon fluxes ($NPP_{litterfall}$, NPP_{herbs}, $NPP_{fine\ roots}$ and R_{soil}) and flux-related variables (stem DBH growth, stem CO_2 efflux, live herb biomass, and leaf area index) that were spatially and temporally replicated within the monitoring plots (see **Table 3.2**). We preferentially used the stronger BACI approach to compare data encompassing the start and end years of the burning experiment, allowing us to extract the fire regime effects as the changes in flux intensity for $NPP_{litterfall}$, stem DBH growth, $NPP_{fine\ roots}$, stem CO_2 efflux, and R_{soil}. We could statistically model the interaction between start-end change and fire regime using linear mixed models (LMMs), which allowed us to account for groups in the data. We also used a binomial generalised linear mixed model to examine changes in the percentage of growing stems to better fit proportional data. For fluxes and variables whose data only covered the end phases of the experiment (NPP_{herbs}, live herb biomass, and LAI), we used the CI or space-for-time substitution framework enabling us to examine spatial differences between fire regimes without being able to isolate the specific fire-regime effect. In this case, we investigated differences between experimental fire regimes by using one-way LMMs (**Table 3.3**).

Table 3.1, sampling methodologies used for the study of carbon flux dynamics at the Estação Ecológica da Serra das Araras (adapted from the RAINFOR-GEM protocol). Includes period of measurement and sampling interval. Multiple variables were collected for some fluxes; these are indicated as separate paragraphs within a cell.

Flux	Description	Period	Interval
$\mathbf{NPP_{litterfall}}$	Litterfall production of dead organic material was estimated by collecting litterfall at nine litter traps (each 0.25 m^2) per plot (N = 9), each of them placed 1 m above ground level at the centre of the nine central subplots. We did not distinguish between coarse and fine litterfall components, but classified litterfall into types: leaves, twigs, flowers, fruits, seeds, and other objects. All components were oven dried at 80°C to constant mass and weighed.	2018 to 2023	15 days/1 month
$\mathbf{NPP_{stem}}$	**Forest inventory**: All trees ≥5 cm in diameter at breast height (DBH) and ≥3 m in height were tagged and identified to species level where possible. DBH and height of each tree were measured and re-censused every two years to describe vegetation structure and determine growth rate of existing surviving trees. Census data was also used to calculate rates of tree mortality ($C_{mortality}$).	2017 to 2023	2 years
	Seasonal growth: dendrometer bands were installed on a subset of trees at each plot (N = 100 at the unburnt plots, N = 25 at the biennial and triennial plots, N = 50 at the annual plot) to determine the seasonal variation in stem growth.	2019 to 2023	3 months
$\mathbf{NPP_{herbs}}$	Production of herbaceous biomass was measured at permanent quadrats set in the corners of even-numbered subplots (N = 12) within all plots. All herbaceous growth (2 cm above the surface) within the quadrats was harvested monthly. Herbaceous biomass was classified into live and dead matter, oven-dried at 80°C to constant mass and weighed.	Nov 2023 to Oct 2024	1 month
$\mathbf{NPP_{coarse\ roots}}$	Productivity of coarse roots was not measured directly but derived from estimates of aboveground woody productivity calculated from inventory data (see **Table 3.2** for details on analysis).	2017 to 2023	2 years
$\mathbf{NPP_{fine\ roots}}$	Nine ingrowth cores (mesh cages of 14 cm in diameter, mesh size 1.5 cm) were installed in every plot (N = 9). They were placed in each of the central subplots to 30 cm soil depth. Cores were extracted every 3 months and roots were manually removed from the soil samples in four 10-min time steps. Root-free soil was then re-inserted into the ingrowth core, which was placed back into the soil. Collected roots were cleaned, oven-dried at 80°C and weighed. Ingrowth cores were gradually relocated within subplots in 2022 to avoid any potential loss of productivity and fertility within the core.	2018 to 2023	3 months

R_{canopy}	**Leaf area index**: canopy images were recorded with a digital camera and fish-eye lens at the centre of each of the 25 sub-plots in each plot, at a height of 1 m, and during overcast weather or indirect sunlight conditions. The camera was horizontally- and north-aligned.	Dec 2022 to Nov 2023	1 month
	Leaf dark respiration: dark respiration was not measured at the Estação Ecológica da Serra das Araras. We used mean respiration values of Cerrado trees (10 species) measured at the Reserva Ecológica do IBGE near Brasília in February 2009 (Rossatto and Franco, 2017).	n/a	n/a
R_{stem}	**Stem CO_2 efflux**: was measured at 15 trees in each plot (N = 15), using the closed dynamic chamber method. CO_2 concentration and accumulation were measured with an infra-red gas analyser (IRGA EGM-4 and EGM-5, PP Systems) and soil respiration chamber (SRC-1, PP Systems) connected to a permanent collar sealed to the bole surface.	Sep 2018 to Dec 2023	1 month
	Stem surface area: surface area data was derived from the forest inventory data of each plot (see above).	2017 to 2023	2 years
R_{herbs}	**Live herbaceous biomass**: the standing stock of herbaceous biomass at each plot was sampled during the set-up of the 12 permanent herbaceous quadrats per plot (N = 12). All herbaceous material (2 cm above the surface) was harvested, classified into live and dead matter, oven-dried at 80°C until constant mass and weighed. An approximate proportion of forb and grass cover was noted.	Oct 2023	n/a
	Herbaceous dark respiration: dark respiration was not measured at the Estação Ecológica da Serra das Araras. Instead, we use dark respiration and specific leaf area (SLA) values of native Cerrado forbs (10 species) and grasses (10 species) measured at the Reserva Ecológica do IBGE near Brasília in February 2009 (Rossatto and Franco, 2017).	n/a	n/a
R_{soil}	Total soil CO_2 efflux was measured at the centre of the nine central subplots in each plot (N = 9 per plot), using the closed dynamic chamber method. CO_2 concentration and accumulation were measured with an infra-red gas analyser (IRGA EGM-4 and EGM-5, PP Systems) and soil respiration chamber (SRC-1, PP Systems) sealed to a permanent collar in the soil.	Sep 2018 to Dec 2023	1 month
	Soil moisture: was measured monthly at the nine central subplots in each plot alongside soil CO_2 efflux (IRGA EGM-5, PP Systems).	Nov 2023 to Oct 2024	1 month

Table 3.2, summary of the analysis techniques used for the study of carbon dynamics at the Estação Ecológica da Serra das Araras experimental fire and ecosystem monitoring project, Brazil. Numerical transformations and statistical analyses were performed in R (version 4.3.3) via RStudio (version 2023.12.1 + 402).

Component	Description
$\mathbf{NPP_{litterfall}}$	Dry litterfall biomass values were converted into carbon content by multiplying by the 0.49 biomass-to-carbon ratio (IPCC, 2006). Carbon accumulation was then standardised by interval length and scaled up to obtain estimates per hectare per year. Since litterfall data was spatially and temporally replicated (N = 9 subplots per plot per month/fortnight), we obtained annual $NPP_{litterfall}$ estimates at each fire regime for the earliest (2018) and latest (2023) years with complete data using a linear mixed model (**Section 3.5.4**, **Table 3.3**, model 1). The standard error of the regime-level marginal means of the mixed model was taken to represent sampling uncertainty. No further value of systematic uncertainty was assigned (Girardin *et al*., 2014).
$\mathbf{NPP_{stem}}$	**Forest inventory**: aboveground woody carbon stocks were estimated using the Rezende *et al.* (2006) allometric equation for *cerrado sensu stricto*: $C = 0.24564 + 0.01456 \cdot H \cdot D^2$, where C is aboveground carbon (kg), H is tree height (m) and D is DBH (cm). NPP_{stem} for each tree was calculated as the difference in aboveground woody carbon stock between a census and the previous one, standardised by the interval length between measurements. Total plot NPP_{stem} for a given interval was calculated as the sum of individual-level, positive NPP_{stem} values for stems present at both censuses. Mortality carbon was described as the sum of carbon stock of trees that died by the following census date, as a per-year rate. We compared the earliest (2017-2019) and latest (2021-2023) estimates of NPP_{stem} and $C_{mortality}$ for all experimental fire regimes (using a mean for the unburnt plots). Since these are calculated as a plot-level sum, we did not perform any statistical test as there is no within-plot replication. Following Girardin *et al*. (2014), we assigned a systematic uncertainty value to our final NPP_{stem} estimates; in our case, 26% error based on the allometric model error reported by Rezende *et al*. (2006). Since NPP_{stem} is derived from complete plot inventories, it was not assigned sampling uncertainties. **Seasonal growth**: growth increment values obtained from dendrometer bands were used as a proxy variable to gain insight on seasonal variation in NPP_{stem}. Circumference increments were converted to diameter (DBH) increments and standardised by interval length. Because dendrometer measurements were spatially and temporally replicated (N = 25 to 100 stems per plot per trimester, see **Table 3.1**), we analysed them statistically. Since dendrometer data is zero-inflated, we undertook two separate statistical analyses, one using binary data to study the proportion of growing trees, another with positive non-zero data to investigate variation in the magnitude of growth rate of growing trees. We thus obtained model estimates for 1) the proportion of growing trees and 2) growth rates of growing trees at each fire regime during the earliest (2019) and latest (2023) years with complete data using mixed-effects models (**Section 3.5.4**, **Table 3.3**, models 2 and 3). The standard errors of the regime-level marginal means of the mixed models were taken to represent sampling uncertainty. No further value of systematic uncertainty was assigned (Girardin *et al*., 2014).
$\mathbf{NPP_{herbs}}$	Total dry herbaceous biomass values were converted into carbon content by multiplying by the 0.49 biomass-to-carbon ratio (IPCC, 2006). Herbaceous carbon production was standardised by interval length and scaled up to obtain monthly estimates in relevant units (per hectare per year). Since herbaceous biomass data was spatially and temporally replicated (N = 12 quadrats per plot per month) but was only measured at the end of the experiment (from November 2023) we used a linear mixed model to obtain and compare annual estimates of NPP_{herbs} at each fire regime (**Section 3.5.4**, **Table 3.3**, model 7). The standard errors of the regime-level marginal means of the model were taken to represent sampling uncertainty. No further value of systematic uncertainty was assigned.

$NPP_{coarse\ roots}$	Estimated by assuming that coarse root biomass and productivity was 1.37 ± 0.93 times larger than above-ground woody stems. This root-to-shoot ratio was based on a review of coarse root and above-ground biomass studies from the Cerrado (Miranda *et al*., 2014). We assigned this root-to-shoot ratio a systematic uncertainty value of ± 0.93 (calculated by propagating the standard errors of mean root and shoot biomass estimates presented by Miranda *et al*., 2014). Total plot $NPP_{coarse\ roots}$ was calculated by multiplying total NPP_{stem} by the root-to-shoot ratio and propagating their uncertainties (this is equivalent to estimating the tree-level coarse root biomass by multiplying individual stem biomass by 1.37, then calculating the standardised interval difference and summing $NPP_{coarse\ roots}$ across the entire plot). We then compared the earliest (2017-2019) and latest (2021-2023) $NPP_{coarse\ roots}$ estimates for all regimes, avoiding statistical tests due to the lack of within-plot replication. Because they are derived from complete plot inventories, our estimates of $NPP_{coarse\ roots}$ were not assigned sampling uncertainties.
$NPP_{fine\ roots}$	Values of root biomass over the four 10-min time steps were used to model the pattern of cumulative extraction for each ingrowth core sample, using logarithmic regression. Total root biomass in each core was then estimated by solving to 120 min (approximate amount of time required to remove all of the fine roots from a core; see Metcalfe, Meir *et al*., 2007; Metcalfe, Williams *et al*., 2007). Estimated biomass was converted into carbon content by multiplying by the 0.45 biomass-to-carbon ratio for tropical fine roots (Huaraca Huasco *et al*., 2021), standardised by interval length and scaled up to obtain productivity estimates per hectare. We applied a depth-correction proportion of 1.125 to account for additional root growth beyond 30 cm depth based on Yoda (1983) and Kho *et al*. (2013). Since fine root data was spatially and temporally replicated (N = 9 subplots per plot per trimester), we obtained annual $NPP_{fine\ roots}$ estimates at the earliest (2018) and latest (2023) years with complete data using a linear model (**Section 3.5.4**, **Table 3.3**, model 4). The standard errors of the regime-level marginal means of the mixed model were taken to represent sampling uncertainty. No further value of systematic uncertainty was assigned (Girardin *et al*., 2014).
R_{canopy}	**Leaf area index**: LAI of each plot was estimated from fisheye lens images using 'ilastik' (Berg *et al*., 2019), MATLAB and 'CANEYE' (Weiss & Baret, 2017) software for pixel classification, image cropping and LAI calculations respectively (see **Section 3.13** for details). Annual LAI estimates (alongside standard error) for each regime were obtained through linear mixed models (**Section 3.5.4**). Since plot-level LAI data was temporally replicated but was only measured at the end of the experiment (from December 2022) we used a linear mixed model to obtain and compare annual LAI estimates at each fire regime (**Section 3.5.4**, **Table 3.3**, model 9). The standard errors of the regime-level marginal means of the mixed model were taken to represent sampling uncertainty. **Leaf dark respiration**: mean leaf dark respiration (1.34 ± 0.30 μmol m^{-2} s^{-1}) was transformed and multiplied by LAI estimates to obtain canopy respiration for each regime (Girardin *et al*., 2014). The standard error of the mean of respiration values provided by Rossatto & Franco (2017) was used as an estimate of systematic uncertainty, and propagated with LAI sampling uncertainty. We then applied the inhibition factor from Malhi *et al.* (2009) to account for daytime light inhibition of leaf dark respiration: 67% of daytime dark respiration, 34% of total dark respiration. Dry season respiration values were linearly scaled by soil moisture to allow for drought inhibition and continuous variation in respiration (in dry season months, respiration was scaled down by multiplying it by the proportion of that month's moisture with regard to the average wet season soil moisture).
R_{stem}	**Stem CO_2 efflux**: For each EGM sample, the rate of stem CO_2 efflux (μmol m^{-2} s^{-1}) was calculated from the linear rate of increase in CO_2 concentration within the chamber (Metcalfe, Meir *et al*., 2007; Metcalfe, Williams *et al*., 2007). Since stem CO_2 efflux data was spatially and temporally replicated (N = 15 stems per plot per month), we obtained annual estimates at each fire regime for the earliest (Sep 2018 to Aug 2019 for plots ESA-04, ESA-07, ESA-08 and ESA-09, and Sep 2019 to Mar 2020 for ESA-05 and ESA-06) and latest (2023) years with complete data using a linear mixed model (**Section 3.5.4**, **Table 3.3**, model 5). The standard errors of the regime-level marginal means of the mixed model were taken to represent sampling uncertainty.

	Stem surface area: Surface area (SA) of every stem was estimated with the Chambers *et al*. (2004) equation: $\log(SA) = -0.105 - 0.686 \cdot \log(D) + 2.208 \cdot \log(D)^2 - 0.627 \cdot \log(D)^3$, where D is DBH in cm. Individual surface area was then summed to calculate regime tree surface area per hectare. Surface area estimates were assigned a systematic error of 10% based on similar studies (Girardin *et al*., 2014). R_{stem} was estimated by scaling up start and end stem CO_2 efflux estimates with total tree surface area in 2019 and 2023 respectively. We compared the earliest and latest R_{stem} estimates for all regimes, propagating stem CO_2 efflux sampling uncertainty and surface area systematic uncertainty. Since R_{stem} was calculated from a plot-level sum, we did not perform any statistical analysis.
R_{herbs}	**Live herbaceous biomass**: dried live herbaceous biomass values were converted into carbon content by multiplying by the 0.49 biomass-to-carbon ratio (IPCC, 2006). Since herbaceous biomass data was temporally replicated (N = 12 quadrats) but was only measured once at the end of the experiment (October 2023) we used a linear mixed model to obtain and compare estimates at each fire regime (**Section 3.5.4**, **Table 3.3**, model 8). The standard errors of the regime-level marginal means of the mixed model were taken to represent sampling uncertainty. **Herbaceous dark respiration**: leaf dark respiration of each species was multiplied by SLA to obtain dark respiration values in terms of dry biomass. We obtained a weighted mean of dark respiration (0.031 μmol g^{-1} s^{-1}) where grasses were assigned a total weight of 0.8 and forbs 0.2 based on the approximate proportion of biomass, and multiplied it by the herbaceous live biomass estimates for each regime to obtain R_{herbs} (based on the canopy respiration methodology included in Girardin *et al*., 2014). The standard error of this weighted mean of grass and forb respiration values provided by Rossatto & Franco (2017) was used as an estimate of systematic uncertainty (± 0.003 μmol g^{-1} s^{-1}), and propagated with live herbaceous biomass sampling uncertainty. We also applied the inhibition factor from Malhi *et al.* (2009) to account for daytime light inhibition of leaf dark respiration: 67% of daytime leaf dark respiration. Dry season respiration was linearly scaled by soil moisture to account for drought inhibition and allow for continuous variation of leaf respiration (in dry season months, respiration was scaled down by multiplying it by the proportion of that month's moisture with regard to the average wet season soil moisture).
R_{soil}	For each EGM sample, soil CO_2 efflux rates were calculated from the linear rate of increase in CO_2 concentration within the chamber (Metcalfe, Meir *et al*., 2007; Metcalfe, Williams *et al*., 2007). CO_2 efflux rates were then scaled up to R_{soil} at the hectare level. Since R_{soil} data was spatially and temporally replicated (N = 9 subplots per plot per month), we obtained annual estimates at each fire regime for the earliest (Sep 2018 to Aug 2019) and latest (2023) years with complete data using a linear mixed model (**Section 3.5.4**, **Table 3.3**, model 6). The standard errors of the regime-level marginal means of the mixed model were taken to represent sampling uncertainty. No further value of systematic uncertainty was assigned to R_{soil}. We estimated the partition of total R_{soil} into $R_{rhizosphere}$ (autotrophic respiration from plant roots) and $R_{heterotrophic}$ (heterotrophic respiration from microbes) using a ratio of R_{soil} to $R_{heterotrophic}$ based on the values reported by Butler *et al*. (2012) at another *cerrado sensu stricto* site in Mato Grosso. To calculate the systematic uncertainty associated with this ratio, we extracted the standard errors of the mean for R_{soil} (17.41 ± 1.47) and $R_{heterotrophic}$ (6.49 ± 0.87) reported by Butler *et al.* (2012), and propagated them accordingly (R_{soil}:$R_{heterotrophic}$ = 0.37 ± 0.06). We then applied this ratio and its complement ratio to our estimate of R_{soil}, propagating their respective systematic and sampling uncertainties to obtain our own estimates of $R_{rhizosphere}$ and $R_{heterotrophic}$.

Table 3.3, description of the mixed-effects models used to examine differences in fluxes and related variables across experimental fire regimes and start-end monitoring periods at the Estação Ecológica da Serra das Araras. All ecologically justified random effects are listed, however, those that did not explain enough variation or increased model complexity beyond convergence were discarded, and have been shown as deleted: ~~(1|factor)~~. Random effects represented groupings within the data and included: plot pair (since plots were set up in pairs), plot (since unburnt plots were grouped within the unburnt fire regime), subplot (for measurements sampled in different subplots over time), stem (for measurements sampled in different tree stems over time) and species (to account for functional/phylogenetic similarities between stems).

	family	response variable	fixed effects	random effects
1	gaussian	$\log_{10}(NPP_{litterfall} + 0.1)$	regime * period	~~(1|plot pair)~~ + (1|plot) + (1|subplot)
2	binomial	binary DBH growth	regime * period	~~(1|plot pair)~~ + ~~(1|plot)~~ + ~~(1|subplot)~~ + ~~(1|species)~~ + (1|stem)
3	gaussian	$\log_{10}$(positive DBH growth)	regime * period	~~(1|plot pair)~~ + (1|plot) + ~~(1|subplot)~~ + (1|species) + (1|stem)
4	gaussian	$\log_{10}(NPP_{fine\ roots} + 0.2)$	regime * period	~~(1|plot pair)~~ + ~~(1|plot)~~ + ~~(1|subplot)~~
5	gaussian	stem CO_2 efflux	regime * period	~~(1|plot pair)~~ + (1|plot) + ~~(1|subplot)~~ + (1|species) + (1|stem)
6	gaussian	R_{soil}	regime * period	~~(1|plot pair)~~ + (1|plot) + (1|subplot)
7	gaussian	$\log_{10}(NPP_{herbs} + 0.05)$	regime	~~(1|plot pair)~~ + (1|plot) + (1|subplot)
8	gaussian	$\log_{10}$(live herb biomass + 1)	regime	~~(1|plot pair)~~ + (1|plot)
9	gaussian	LAI	regime	~~(1|plot pair)~~ + (1|plot)

Mixed-effects models were implemented using the lme4 (version 1.1-35.1) and lmerTest (version 3.1-3) packages in R (Bates *et al*., 2015; Kuznetsova *et al*., 2017). The random effects included within the LMMs, and the transformations used to achieve acceptable homoskedasticity and residual normality were specific to each variable being tested (see **Table 3.3**). For models using untransformed response variables, we extracted marginal means and their standard error using the emmeans package (version 1.10.0, Lenth, 2024). If response variables were transformed, we extracted back-transformed marginal means and approximate standard errors via the delta method using the car package (version 3.1-2, Fox & Weisberg, 2019). We also used the emmeans package to determine if the carbon flux or variable change at each experimental fire regime is significant by obtaining marginal contrasts for the start/end periods at the regime level.

We decided to undertake an additional analysis to complement our BACI and CI frameworks by accounting for the potentially confounding effect of ecosystem heterogeneity between the monitoring plots, as initial differences in vegetation structure could have influenced the intensity

of carbon fluxes and the way in which different variables are affected by fire. We therefore calculated the total basal area – standard indicator of vegetation structure – for each plot using census data from 2017 and included it as an additional additive fixed effect in duplicate versions of models 1 to 9. We then compared models with and without this 'initial basal area' effect using the Akaike information criterion (AIC; Akaike, 1974). Indistinguishable models (difference in AIC is smaller than 2) were discarded, whilst distinct ones (ΔAIC >2) were run and interpreted.

3.6. Results

Overall, we measured a total of 4623 different stems, belonging to 71 species and 33 botanical families (**Table S3.1**). At the first census (2017) the monitoring plots supported 39 species, stem density of 627 stems ha^{-1} and aboveground stem carbon stocks of 3.86 MgC ha^{-1} on average. There was substantial heterogeneity between plots despite proximity – with plot ESA-04 (unburnt) having highest carbon density (5.78 MgC ha^{-1}) in contrast to the least dense (triennially burnt) ESA-07 plot (2.16 MgC ha^{-1}, see **Table S3.1**). Fire had noticeable effects on the vegetation structure by 2023, reducing stem density by 113 stems ha^{-1} in the triennial plot, 119 stems ha^{-1} in the biennial plot, and 119 stems ha^{-1} in the annual plot (corresponding to decreases of 0.16 and 0.49 MgC ha^{-1} in the triennially and biennially burnt plots, but an increase of 1.15 MgC ha^{-1} in the annual burns regime, **Table S3.1**). We also obtained long-term datasets of different intensively sampled variables (e.g., 5895 datapoints for $NPP_{litterfall}$ or 3312 for stem CO_2 efflux) which allowed us to examine trends and fire-related changes in carbon fluxes.

3.6.1. Carbon flux changes over time and fire regime effects

Upon observation of trends in **Figure 3.2**, repeatedly sampled variables showed seasonal fluctuations, with peaks corresponding to the dry ($NPP_{litterfall}$) or wet (stem DBH growth, $NPP_{fine\ roots}$, stem CO_2 efflux and R_{soil}) seasons. Comparison of estimates at the start and end of the

experiment allowed us to determine if changes in key variables are different in burnt vs unburnt plots, and thus attributable to the fire effect. $NPP_{litterfall}$ within unburnt plots remained constant from 2018 to 2023, but decreased within the burn plots (**Figure 3.2**, **Table S3.2**, **Table S3.3**). Stem growth in the unburnt plots – only including positive growth – decreased by 0.09 cm/year between 2019 and 2023 (**Figure 3.2**, **Table S3.4**, **Table S3.5**) but stayed constant in the burnt plots. The proportion of growing stems was statistically similar in all regimes, in 2019 and 2023 (**Table S3.6**, **Table S3.7**). $NPP_{fine\ roots}$ decreased from 2018 to 2023 in all fire regimes (**Figure 3.2**, **Table S3.8**, **Table S3.9**), with a stronger change in the triennial and annual burns plots (-1.41 and -1.46 MgC ha^{-1} $year^{-1}$) compared to the unburnt plots (-1.04 MgC ha^{-1} $year^{-1}$). Stem CO_2 efflux decreased only within the biennially burnt regime (**Figure 3.2**, **Table S3.10**, **Table S3.11**). R_{soil} was reduced in all but the biennial burns plot (**Figure 3.2**, **Table S3.12**, **Table S3.13**).

Fluxes derived from census inventory data also showed different rates of change as a result of fire frequency. Total woody productivity (the sum of NPP_{stem} and $NPP_{coarse\ roots}$) increased by 35% in the unburnt plots from 2017-2019 to 2021-2023, but decreased by 75%, 33% and 20% in the triennial, biennial and annual fire regimes (**Figure 3.3**). $C_{mortality}$ remained constant in the unburnt plots but increased by 0.69, 0.76 and 1.19 MgC ha^{-1} $year^{-1}$ in plots with triennial, biennial and annual burns. Stem respiration increased by 0.48 MgC ha^{-1} $year^{-1}$ in unburnt plots but decreased by 0.59, 0.73 and 0.29 MgC ha^{-1} $year^{-1}$ in the triennial, biennial and annual plots as a result of the reduction in plot-level woody stem surface area (-34% on average from 2019 to 2023).

Variables measured at the later phases of the fire experiment showed seasonal variation peaking in the wet season (NPP_{herbs}, LAI) and revealed consistent patterns across fire frequencies (**Figure 3.4**). Linear mixed models testing for regime differences in log-transformed NPP_{herbs} and live herbaceous biomass stock did not reveal any significant fire regime effect (**Table S3.14**, **Table S3.15**). However, despite being statistically indistinguishable, burnt plots showed higher NPP_{herbs} and live herbaceous stock values, with those corresponding to the triennially burnt plot being 3.6 and 9.4 times larger than the unburnt plots (**Figure 3.4**). LAI estimates displayed the reverse

trend, as LAI in the unburnt plots was approximately 10, 4 and 2 times larger than in the triennial, biennial and annual fire regimes; though only the biennial and triennial regime coefficients were significant (**Table S3.16**, **Figure 3.4**). As a result, R_{canopy} in the unburnt plots was 3.91 MgC ha^{-1} $year^{-1}$ higher than in the triennially burnt regime, whereas R_{herbs} in the triennially burnt plots was 4.70 MgC ha^{-1} $year^{-1}$ higher than in the unburnt plots. Mean tree, forb and grass dark respiration values obtained from Rossatto & Franco (2017) were 1.34 ± 0.30, 2.25 ± 0.49 and 3.08 ± 0.37 μmol m^{-2} s^{-1} (± standard error). Estimates of the plots' carbon fluxes at the end of the experimental period are visually represented in **Figure 3.5**. Estimates of carbon fluxes and key variables both at the start and end of the experiment (where relevant) are found in **Tables S3.20** to **S3.23**.

3.6.2. Importance of initial vegetation density

We then compared the fit of our mixed-effect models with and without initial basal area as a fixed effect. Models incorporating initial basal area were all indistinguishable (ΔAIC <2, **Table S3.17**), except for models estimating NPP_{herbs} and live herbaceous biomass. Mixed models studying the regime-level differences in log-transformed NPP_{herbs} and live herbaceous biomass revealed the distribution of stocks and productivity could be explained by a gradient in initial basal area, with triennially and annually burnt plots presenting significantly higher estimates than those just predicted by initial basal area (**Table S3.18**, **Table S3.19**).

3.6.3. Total net primary productivity, respiration, plant carbon expenditure and carbon use efficiency

The individual components of NPP were added to give an estimate of $NPP_{aboveground}$, $NPP_{belowground}$ and NPP_{total} (**Figure 3.5**). NPP_{total} for the unburnt plots was 3.72 ± 0.71 MgC ha^{-1} $year^{-1}$, 0.92 ± 0.15 MgC ha^{-1} $year^{-1}$ for the triennial plot, 1.31 ± 0.22 MgC ha^{-1} $year^{-1}$ for the biennial plot and 2.40 ± 0.63 MgC ha^{-1} $year^{-1}$ for the annually burnt plots. The proportion of $NPP_{aboveground}$ within

NPP_{total} was 0.53 ± 0.12 in the unburnt plots, 0.43 ± 0.11 in the triennial burns plot, 0.42 ± 0.11 in the biennial burns plot, and 0.48 ± 0.16 in the annual burns plot. We partitioned total R_{soil} using the proportion of $R_{rhizosphere}$ and $R_{heterotrophic}$ where $R_{heterotrophic}$ represents 0.37 ± 0.06 of R_{soil}. Subsequently, the components of R were also summed to give estimates of R_{eco} and $R_{autotrophic}$. R_{eco} in the unburnt plots was 14.57 ± 1.21 MgC ha^{-1} $year^{-1}$, and 13.74 ± 3.43, 11.55 ± 1.32 and 12.72 ± 1.12 MgC ha^{-1} $year^{-1}$ for the triennially, biennially and annually burnt plots. The proportion of $R_{autotrophic}$ within R_{eco} was 0.81 ± 0.11 in the unburnt plots, 0.80 ± 0.32 in the triennial burns plot, 0.73 ± 0.14 in the biennial burns plot, and 0.77 ± 0.11 in the annual burns plot. The sum of NPP_{total} and $R_{autotrophic}$ yielded an estimated PCE of 15.58 ± 1.44 MgC ha^{-1} $year^{-1}$ for the unburnt plots, and 11.96 ± 3.42, 9.79 ± 1.33 and 12.18 ± 1.28 for the triennially, biennially and annually burnt plots respectively. The ratio of NPP_{total} to PCE gave an estimated CUE of 0.24 ± 0.05 in the unburnt plots, 0.08 ± 0.03 in the triennial burns plot, 0.13 ± 0.03 in the biennial burns plot, and 0.20 ± 0.06 in the annual burns plot (**Figure 3.5**).

3.7. Discussion

This study provides the most detailed carbon flux dataset within South American savannas and represents one of the few tropical studies to thoroughly examine the effect of fire on net primary productivity and respiration dynamics using field-based ecosystem monitoring – similar studies exploring fire responses in NPP, R, and GPP have been undertaken in fire-sensitive tropical forests in Amazonia (Rocha *et al*., 2014; Berenguer *et al*., 2021). Until now, findings from the Cerrado have either focused on quantifying natural ecosystem nutrient and carbon balances (Scalon *et al*., 2022; Vourlitis *et al*., 2022) or investigating the effect of fire on individual fluxes and vegetation components (e.g., Meirelles & Henriques, 1992; Le Stradic *et al*., 2021). We thus focus our discussion on the main insights that our experimental burning and monitoring project brings to the understanding of how carbon fluxes are affected by altered fire regimes in Brazilian woodland savannas.

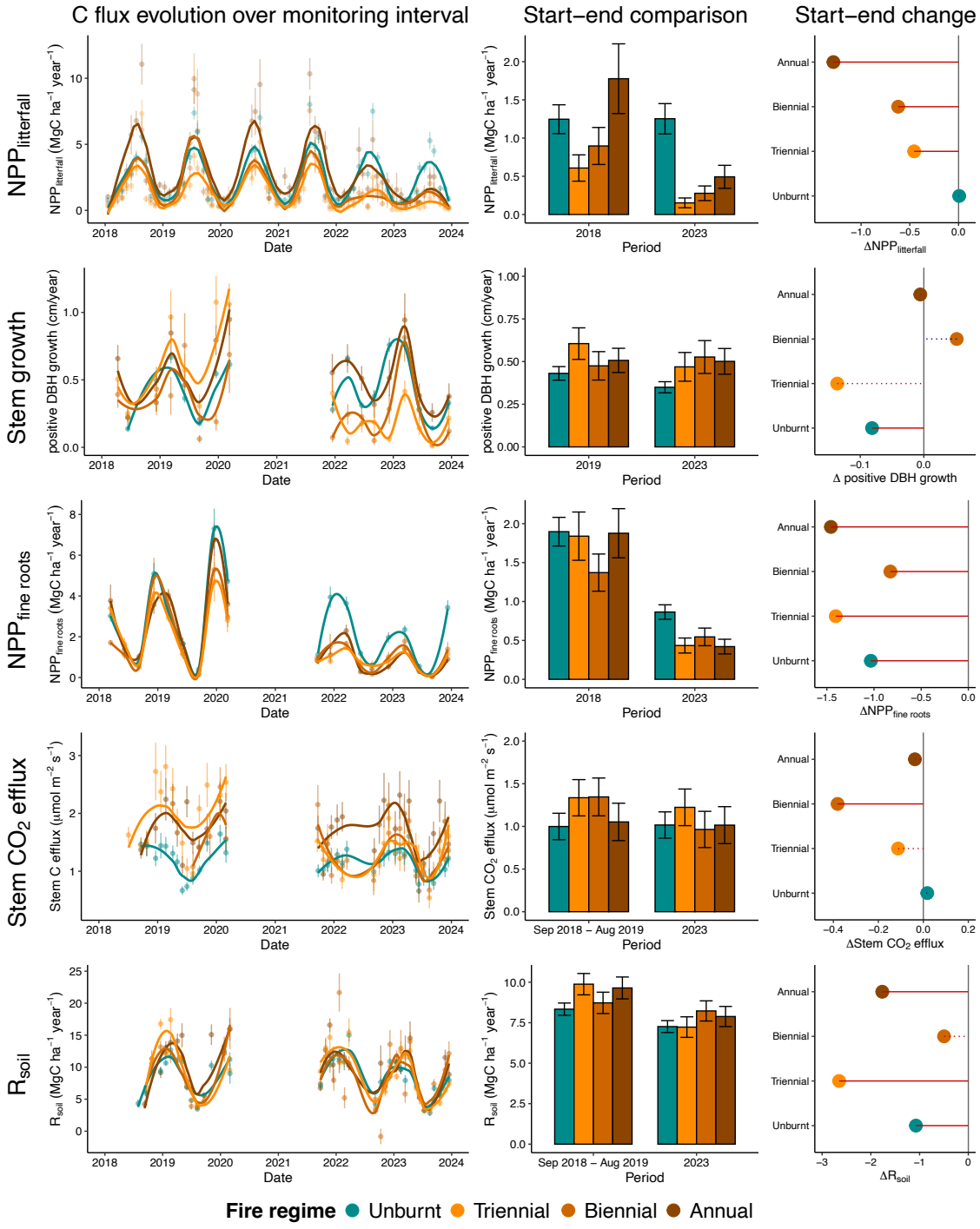


Figure 3.2, influence of experimental fire regimes on variables that were intensively sampled throughout the duration of the experiment at the Estação Ecológica da Serra das Araras. Plots on the left present the trends over time using monthly averages and loess smoothers (error bars represent arithmetic standard error values per fire regime per sampling date, see **Table 3.1** for sample size details). Plots in the centre show the estimates, in absolute terms, for each regime at the start and end periods (error bars represent marginal mean standard error derived from the linear mixed models; please see **Tables S3.2** to **S3.13** for model output details). Plots on the right illustrate the start-end change in variables (represented by delta Δ, same units as absolute values), with solid lines indicating statistically significant contrasts between periods.

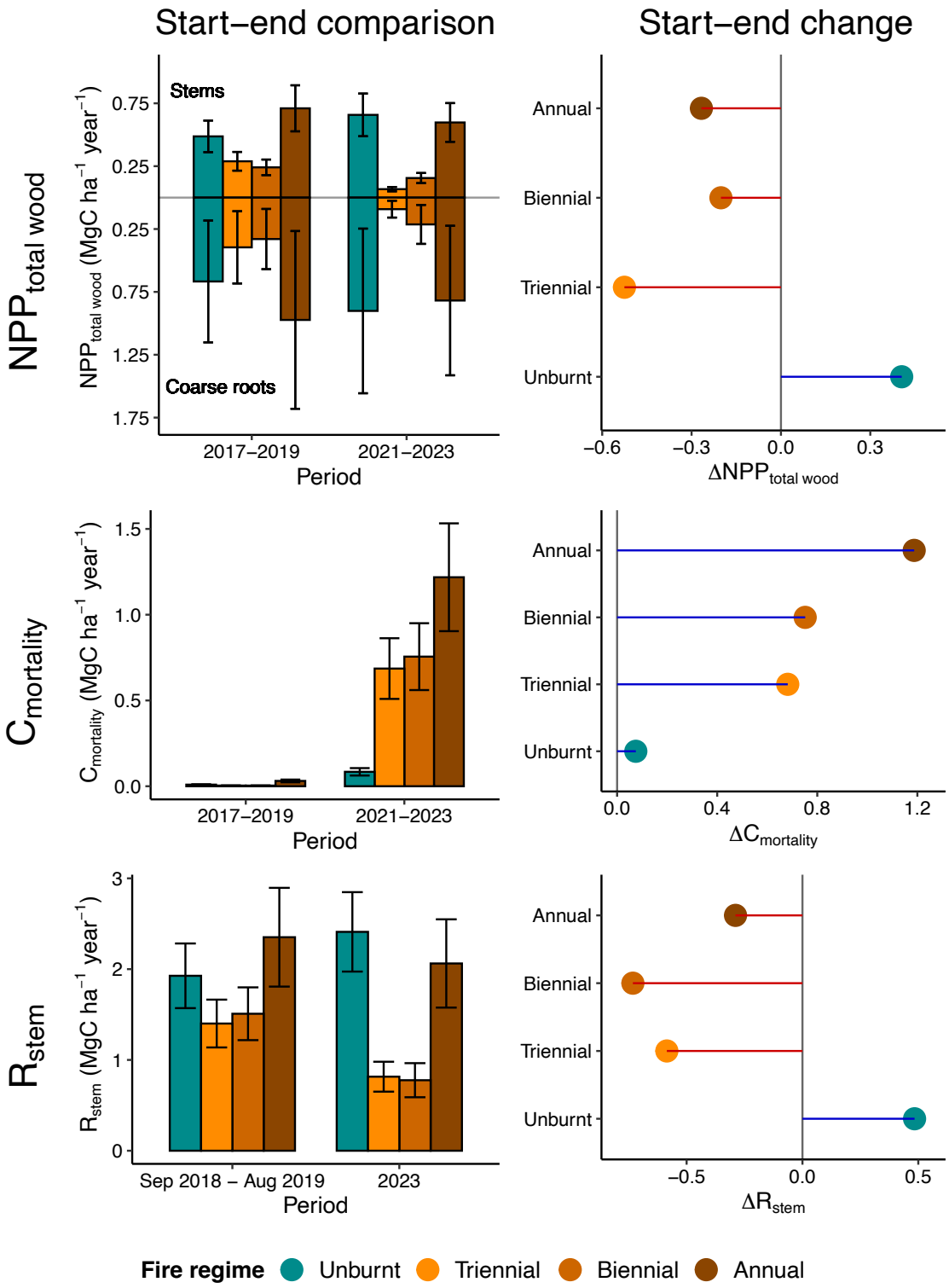


Figure 3.3, influence of fire regimes on carbon fluxes (MgC ha^{-1} $year^{-1}$) that were derived from tree inventory data. Plots on the left show the regime-level comparison of each variable at the start and end of the experiment in terms of absolute values. Plots on the right reveal the degree of change in fluxes over time (represented by the delta symbol Δ, same units as absolute values). Error bars indicate systematic uncertainty in the case of NPP_{stem} and $C_{mortality}$, and propagated error including systematic uncertainty and sampling error for $NPP_{coarse\ roots}$ and R_{stem} (see **Table 3.2** for details).

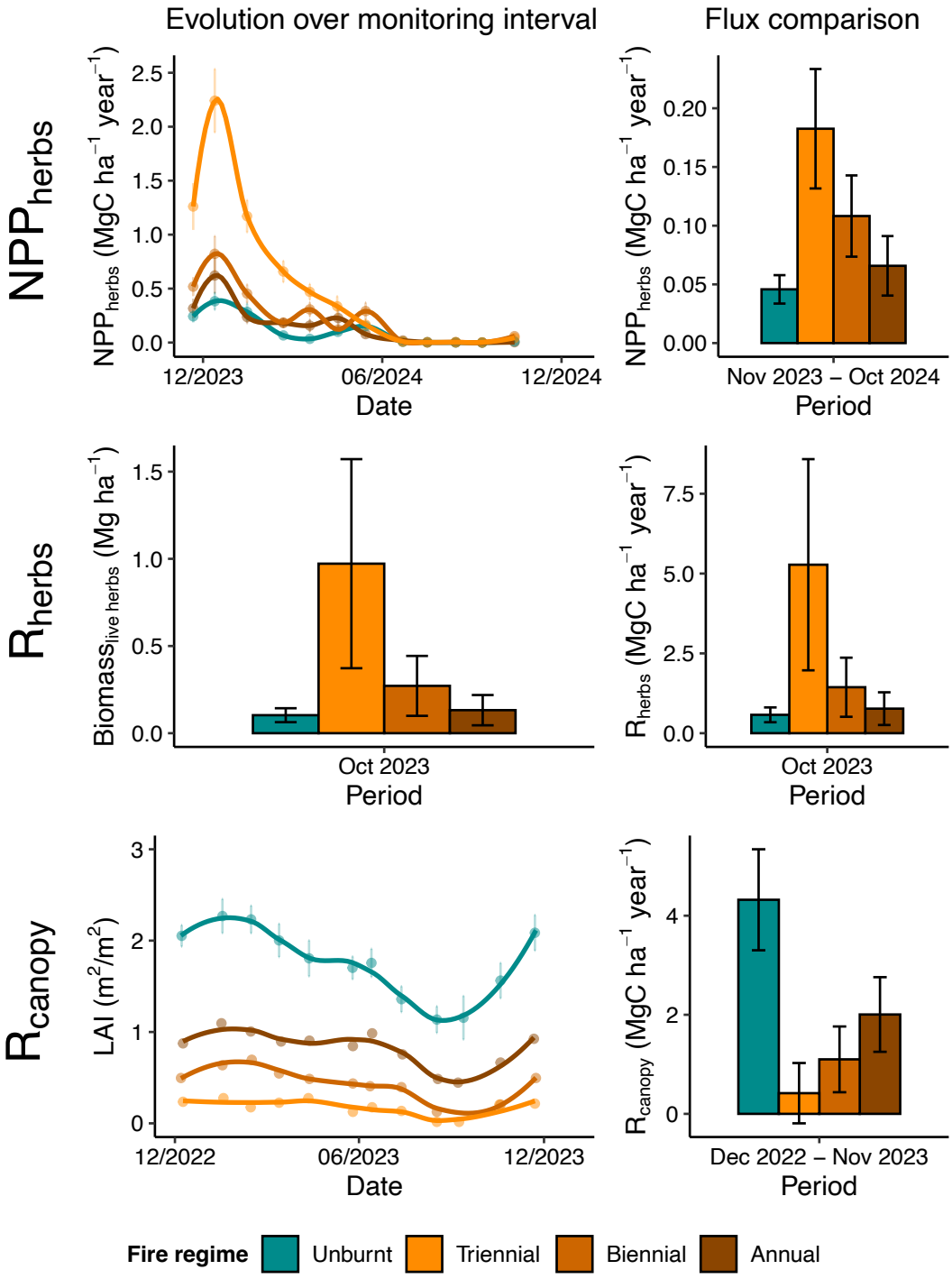


Figure 3.4, regime-level comparison of carbon fluxes and related variables that were sampled at the end of the experimental fire project at the Estação Ecológica da Serra das Araras. Plots on the left represent the evolution of sampled variables over time using monthly averages and loess smoothers (error bars represent arithmetic standard error values per fire regime per sampling date, see **Table 3.1** for sample size details). Please note R_{herbs} and R_{canopy} were not measured directly; biomass of live herbs and LAI were respectively measured as proxy variables, then scaled up to plot-level using dark respiration values. Also note the biomass of live herbs was measured once; error bars instead represent marginal mean standard error derived from the linear mixed model (model 8). Plots on the right include the regime-level comparison of the scaled-up fluxes (error bars represent sampling error as marginal mean standard error derived from the linear mixed model in the case of NPP_{herbs}, and propagated error including sampling and systematic uncertainty for R_{canopy} and R_{herbs}; see **Table 3.2** and **Tables S3.12** to **S3.16** for details).

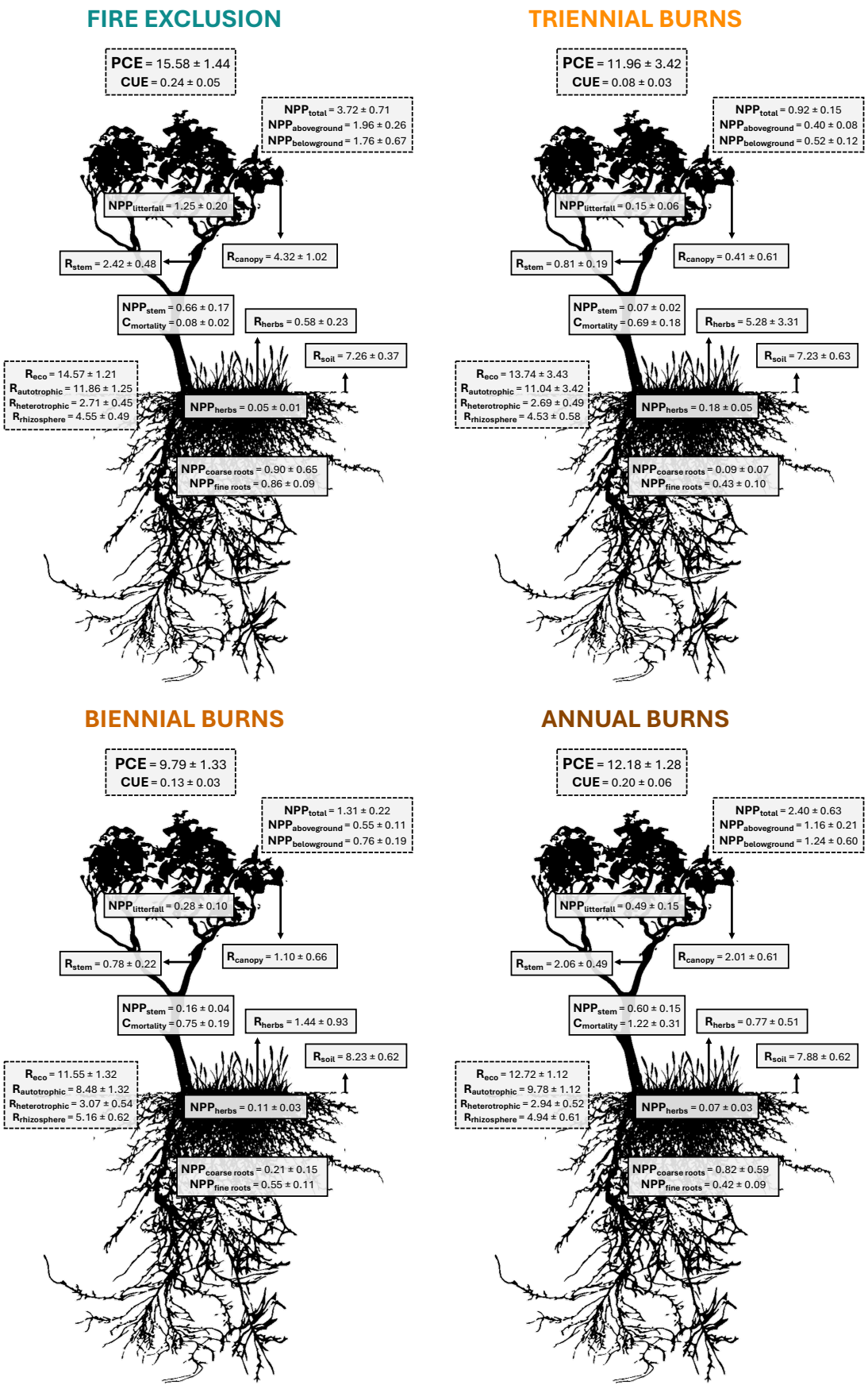


Figure 3.5, main carbon fluxes (MgC ha^{-1} $year^{-1}$) and associated uncertainties within the experimental burning plots at the Estação Ecológica da Serra das Araras. Fluxes were estimated approximately six years into the experimental fire regimes.

3.7.1. Fire reduces the strength of arboreal carbon fluxes

The results presented in this study provide useful insight into the dynamics of arboreal carbon fluxes ($NPP_{litterfall}$, NPP_{stem}, $NPP_{coarse\ roots}$, R_{canopy} and R_{stem}) in the Cerrado, both in the presence and absence of fire. NPP_{stem} is notably lower than the estimate of 2.79 ± 0.45 MgC ha^{-1} $year^{-1}$ provided by Scalon *et al*. (2022), giving the first insight into the potential range of values of NPP_{stem} within Cerrado woodland savannas. In comparison to other vegetation types, our unburnt plot estimates show lower stem productivity than more forested formations like *cerradão* (2.77 ± 0.58 MgC ha^{-1} $year^{-1}$; Scalon *et al*., 2022) and gallery forests (1.67 MgC ha^{-1} $year^{-1}$; Vourlitis *et al*., 2022), but higher estimates than those with more open structures like *campo sujo* (0.345 MgC ha^{-1} $year^{-1}$; Vourlitis *et al*., 2022). Our results also reveal that in unburnt plots, NPP_{stem} is not constrained by competition arising from denser vegetation structure (Falster *et al*., 2011; Ma *et al*., 2020), but that NPP_{stem} appears to increase with basal area and stem density (**Figure S3.2**). Values of litterfall productivity fit those previously estimated by Peres *et al*. (1983), Wilcke & Lilienfein (2002), Nardoto *et al*. (2006) and Kozovits *et al*. (2007) who all reported total annual $NPP_{litterfall}$ for *cerrado sensu stricto* within the 1.5 MgC ha-^{1} $year^{-1}$ range. We present one of the first estimates of $NPP_{coarse\ roots}$, R_{canopy} and R_{stem} within South American savannas. We recognise that the $NPP_{coarse\ roots}$ results here presented are broad estimates derived from a proportion of NPP_{stem} that might hide important dynamics across time and fire regimes. Coarse root harvests could reveal distinct patterns in root productivity arising as a result of the variation in R:S across environmental gradients within the Cerrado (Terra *et al*., 2023) or due to changes in belowground carbon allocation after frequent fires (Zhou *et al*., 2022).

Our findings are consistent with our initial hypothesis, confirming the fact that recurrent burning within *cerrado sensu stricto* vegetation causes a reduction in vegetation density, number of trees and live biomass, and limits the strength of tree-mediated fluxes. These patterns are linked to the increases in stem mortality rates within the experimentally burnt plots and reveal that the growth and performance of surviving trees are also affected by fire (Reis *et al*., 2015; Rodrigues &

Fidelis, 2022). Experimental burning also appears to have led to higher herbaceous biomass and productivity. This is consistent with patterns presented by Meirelles & Henriques (1992), Gomes *et al*. (2020) and Teixeira *et al*. (2022), and provides supporting evidence towards the use of controlled burning as a management strategy against woody encroachment (Pivello *et al*., 2021).

We recognise that our experimental design had important limitations, principally because our fire regimes were not fully replicated, since regimes of different fire frequencies were undertaken within single plots (in addition to three unburnt plots). Replicating fire regimes would have been unfeasible due to the high logistical costs of burning and monitoring further plots, and because the management plan of the conservation unit limits interventions in natural areas (ICMBio, 2016). Furthermore, there were substantial differences in initial vegetation densities across the plots; for example, the unburnt plot ESA-04 had more than double the basal area as the triennially burnt plot. We acknowledge these limitations placed important constraints on our statistical analyses, limiting our ability to attribute observed effects to the different fire regimes through causal inference. This is a particularly important issue for the carbon fluxes that were measured as plot-scale estimates ($NPP_{stem,}$ $NPP_{coarse\ roots}$, R_{stem} and $C_{mortality}$) or only at the end of the experimental period (NPP_{herbs}, R_{herbs}, R_{canopy}), given we lack repeated samples and/or baseline values to determine how much variation could have arisen due to pre-existing plot differences. Our investigation of ecosystem-level carbon fluxes at the end of the experiment (e.g., NPP_{total}, R_{eco}, PCE) is therefore limited to descriptive comparisons of plot-level estimates incorporating indistinguishable effects of both plot differences and fire regimes.

We are confident, however, that our comparison of spatially and temporally replicated estimates at the start and end of the experiment – following a BACI-type approach – allowed us to better isolate the ecological effect of our experimental fire regimes by acknowledging the background variation in flux patterns due to stochasticity – that is, the degree of change in the unburnt plots. Because our analyses investigate the effect of fire only across a specific period, and capture the ecological effect of somewhat different aspects of each regime (different starting points, number

of fire events, and times since last fire), future research should focus on better predicting the gradual dynamics of fire regime impacts using improved analytical frameworks such as the BACI paired-series or progressive-change BACI approaches (Thiault *et al*., 2017), although the integration of strong seasonal fluctuations and uneven sampling intervals remains challenging.

Despite this, extracting accurate fire regime effects was further difficulted by differences in arboreal vegetation density across plots. Spatial replicates within our monitoring plots allowed us to account for substantial within-plot heterogeneity for some fluxes, although, as a form of pseudoreplication, we cannot reliably conclude fire regime impacts will exhibit similar dynamics across areas of vegetation with different composition and structure. Still, in most cases, incorporating an initial structural indicator variable such as basal area did not improve model fit, confirming patterns of flux change appear unaffected by vegetation structure. The distribution of herbaceous biomass and productivity could be partially explained by a gradient in initial basal area, as the weaker space-for-time substitution analysis used for these variables does not incorporate before-impact spatial differences, although the presence of significant fire regime coefficients in the basal area models confirms strong experimental fire effects on herbaceous fluxes. For plot-level estimates of carbon fluxes and ecosystem-level balances, a decomposition assessment of carbon allocation patterns in relation to basal area (*sensu* Riutta *et al*., 2018) would provide a more robust framework for disentangling the impacts of fire versus vegetation density.

3.7.2. Fire regime properties affect ecosystem components differently, warranting long-term monitoring

Our second main finding is that fluxes corresponding to the different ecosystem components (canopy, stems, roots, herbs and soil) showed varying distributions and patterns of change across the gradient of experimental fire frequencies, meeting our expectations and indicating different fire regime properties distinctively affect each part of the vegetation. By definition, each fire

regime incorporates a range of patterns including the timing, duration, seasonality, behaviour, distribution, intensity and severity of the fire events (Kelly *et al*., 2023). Our experimental fire regimes also encompassed the particular characteristics of each fire event, as experimental burns are unique, non-replicable disturbances with singular temporal and energetic dynamics that limit the applicability of the traditional treatment-control experimental design. In our experiment, controlled fire events exhibited substantial differences between fire regimes, where smaller intervals between fires in the annually burnt plot led to patchy, low-intensity surface fires due to lower accumulation of fuel and higher proportion of bare soil (Rodrigues & Fidelis, 2022). Alternatively, fires in the biennially and triennially burnt plots were quicker, more severe and homogeneous, and affected the canopy to a greater extent (Rissi *et al*., 2017). The trade-off between fire frequency and intensity allowed us to determine which fluxes are primarily influenced by these broad fire regime axes. Fire intensity and severity seem to be more strongly linked with patterns in fluxes of woody stems and herbs, the two vegetation components that are most affected by burning under the low-intensity fire regimes of the Cerrado (Chiminazzo *et al*., 2023). In contrast, long-term changes in $NPP_{litterfall}$ and mortality carbon appear to be more strongly related to fire frequency rather than fire intensity. Reduced litterfall productivity and higher mortality in the annually burnt plot could be explained by the negligible impact of short-term leaf charring and consumption on overall leaf production, by more cumulative burns with short recovery interval having stronger tree-wide impacts on fitness, or by an interactive effect between fire impacts and stem density. The mismatch between trends in mortality and NPP_{stem} – where a stronger decline in the triennial plot reveals more intense fires disproportionately reduce aboveground growth in surviving trees – warrants a more detailed analysis on tree vulnerability across species and functional strategies.

It is important to note that the herbaceous layer exhibits short-term responses and recovery after fire (Fontenele & Miranda, 2024). This explains why the biennial plot exhibits lower herbaceous biomass and productivity, as it was burnt shortly before herbaceous monitoring was implemented. On the contrary, fire had a more delayed effect on tree fluxes. Despite burning in 2018, the annual

and triennial plots showed negligible mortality rates along the 2017-2019 interval, and supported relatively constant stem respiration rates 6 years into burning, indicating lags in fire mortality and physiological resilience of surviving trees (Berenguer *et al*., 2021). Overall, in the long term, we observe the most dramatic differences in herbaceous vs arboreal dominance within the triennially burnt plot, as indicated by the fire regime 'control-impact' comparisons of herbaceous biomass and LAI. However, the lack of data at the start of the experiment prevents us from determining the degree of change of these variables as a result of fire, meaning we are unable to synthetically address the overall trade-off between fire intensity and frequency effects in terms of rate of change. Still, LAI distribution is consistent with end-period $NPP_{litterfall}$ values across regimes, and inversely related with both herbaceous biomass and productivity values. Patterns of herbaceous vegetation and LAI also suggest the implementation of controlled fire could have further influenced carbon fluxes and ecosystem processes in indirect ways, as a more open canopy could have increased temperature and water deficits (de Sales *et al*., 2023), whilst grass dominance could have increased competition against seedling establishment and resprouting (Sankaran *et al*., 2004). We therefore conclude that less frequent but more severe fires, coupled with a smaller proportion of surviving stems in the plots, could be providing a positive feedback dynamic that leads to more drastic changes in vegetation structure towards grass-dominated savanna systems in the Cerrado. However, less clear patterns of change in several other carbon fluxes could also indicate that ecosystem shifts might not be consistent and unidirectional across different ecological processes.

Analysing positive stem growth values revealed diameter growth significantly decreased within the unburnt plots, which seems to contradict our plot-level NPP_{stem} results. We recognise that dendrometer bands focus only on diameter growth, and were only installed within larger individuals, therefore capturing only part of the woody productivity dynamics. Dendrometer measurements would have also incorporated water swelling and shrinking, as well as bark loss to fire, limiting the adequacy of data as a proxy for seasonal stem productivity. Similarly, smaller

sample sizes in the burnt plots, alongside high tree mortality, could have restricted the representativeness of our data.

Lower stem CO_2 efflux could have arisen as a result of compromised plant metabolism after the intense 2023 fire in the biennially burnt plot (Cernusak *et al*., 2006), although true patterns could have been masked by large variation in efflux values as a result of confounding variables relating to time of day, temperature, species composition, hydrology and metabolism (Rowland *et al*., 2018), supporting the need for more detailed investigation into stem respiration patterns. More detailed, long-term research into soil respiration and fine root productivity will also help us determine why the intensity of these two fluxes decreases regardless of fire regime. High dynamism in soil ecosystem processes (Nottingham *et al*., 2015) and the onset of warmer and drier El Niño conditions at the end of 2023 could have explained this trend. We therefore highlight the importance of continuing long-term studies in order to disentangle the ecological effects of fire, as well as the interactions between burning and other pressures.

3.7.3. Fire influences on carbon flux allocation, carbon use efficiency and ecosystem disequilibria

Long-term monitoring of the main ecosystem components allowed us to study if experimental burns have influenced the way in which carbon is allocated into different fluxes, partially supporting our expectations and hypotheses. Comparison of NPP components across the fire regimes revealed burning appears to have reduced the proportion of productivity distributed into aboveground fluxes. This pattern was not consistent with our expectation of higher aboveground productivity due to post-fire resprouting and regrowth (Le Stradic *et al*., 2018), as increasing herbaceous productivity has not yet compensated for reduced arboreal growth. Carbon allocation into total heterotrophic respiration appears to have increased within the burnt plots – despite estimate uncertainty – supporting our hypothesis of stronger influence of microbial metabolism

as live biomass stock is replaced by decomposable dead matter (Brando *et al*., 2014). The use of a respiration partition ratio derived from data from a nearby site allowed us to construct a full carbon balance but might not adequality represent the real ecological dynamics in our plots. The implementation of root exclusion methods in situ would enable us to provide better estimates of $R_{heterotrophic}$ and $R_{autotrophic}$. More accurate soil respiration partitioning between rhizosphere and microbial sources would account for temporal variations and changes in the soil environment across fire regimes (Butler *et al*., 2012). Similarly, measuring site-specific dark respiration values across local species of trees and herbs would provide more reliable estimates of R_{herbs} and R_{canopy}, helping tackle the critical lack of information on plant respiration rates across South American savannas. We acknowledge that using dark respiration measurements from another site measured in the wet season and in the absence of fire only lets us produce a very rough estimate of annual respiration fluxes, and this is reflected in the disproportionately large uncertainty of R_{herbs} and R_{canopy} estimates. Still, the use of LAI and herbaceous biomass to scale up leaf respiration – adapting a well-established methodology (Malhi *et al*., 2009) – allows us to bring forth a first approximation of respiratory dynamics and quantify the ecosystem-level carbon balance of mixed tree-grassland ecosystems despite carrying significant uncertainty at this stage.

The ecosystem-level carbon fluxes presented in this study seem to fit within the aridity and vegetation cover gradients observed in South American ecosystem monitoring plots (Zhang-Zheng *et al*., 2024), where values for NPP_{total}, GPP or PCE, and CUE are lower than those reported for seasonally dry forests in the margins of Amazonia in Bolivia (Araujo-Murakami *et al*., 2014) and Mato Grosso (Rocha *et al*., 2014). Total NPP was also substantially smaller than the sum of $NPP_{litterfall}$, NPP_{stem} and $NPP_{fine\ roots}$ presented by Scalon *et al*. (2022), for both *cerrado sensu stricto* and *cerradão*. Plot-specific results within the fire exclusion regime also suggest more efficient use of carbon is dependent on higher woody vegetation density at the local scale as a result of woody encroachment. Our values for the carbon use efficiency of the burnt plots fall closer to some of the estimates provided by Vourlitis *et al*. (2022) for grassland savannas near Cuiabá, Mato Grosso (0.16 and 0.29 using inventory-based estimates, and 0.08 and 0.15 from eddy

covariance methods). Although substantial interannual variation, mismatch between eddy covariance and inventory methods, and differences in sampling methodology imply any comparison should be taken with caution, lower CUE estimates could indicate our experimental fire regimes are shifting ecosystem-wide balances towards those of grass-dominated savannas.

Experimental burning also appears to be switching ecosystem equilibrium dynamics from carbon accumulation to carbon losses, as illustrated by the comparison of $R_{heterotrophic}$ and NPP_{total}, which represent the overall inputs and outputs of carbon into the soil, approximately matching one another in steady-state conditions (Raich & Nadelhoffer, 1989). Within the unburnt plots, NPP_{total} exceeds $R_{heterotrophic}$ by >1 MgC ha^{-1} $year^{-1}$, yet $R_{heterotrophic}$ is larger than total productivity in all burnt plots. We recognise, however, that this exercise simplifies complex ecosystem dynamics by assuming no lags in the dynamics of carbon inputs and outputs, and ignores heterotrophic respiration arising from other ecosystem components. Several unknowns remain regarding the role of dead wood and charcoal in the carbon balance of burnt plots, given the high proportion of standing dead stems and the amount of partially combusted wood that is inputted into the soil (Gomes *et al*., 2020; Teixeira *et al*., 2022). Further study of the dynamics of the deadwood and soil carbon pools, as well as quantification of the direct carbon emissions through fire combustion, would allow for a better evaluation of the carbon impacts of altered fire regimes in the face of intensifying global change (Terra *et al*., 2023).

3.8. Conclusions

The findings presented by this study have provided useful insight into the net primary productivity and carbon flux dynamics within the Cerrado biodiversity hotspot. It represents an initial step towards the understanding of how altered fire regimes are influencing its ecosystem functioning and carbon budgeting. Experimental burning regimes affected the vegetation structure and carbon dynamics by reducing woody cover and arboreal productivity, leading to a shift towards more

open, grass-dominated vegetation. Our findings indicate periodically burnt *cerrado sensu stricto* would experience overall carbon losses, although the different patterns of change across ecosystem components reveal shifts are not consistent across ecological processes as a result of interactions between fire regime variables and other environmental factors. Our work complements previous studies revealing the variability of productivity and respiration of South American savanna vegetation, emphasising the diversity of ecological processes and responses to pressure between ecosystems. Long-term research on the effect of fire on carbon should therefore be extended into different locations and vegetation types incorporating a diverse range of geographies, vegetation characteristics, and experimental burning strategies, and be integrated across regional and biome scales with the help of technological advances in automation and remote sensing. Our results can aid and inform fire management programmes that prioritise biodiversity and landscape conservation. In that respect, controlled burning strategies within savannas and other open ecosystems should adjust fire frequencies depending on the reduction on woody cover and arboreal productivity that is desired. Nonetheless, fire management programs must also account for the effect of fire on species performance, biodiversity and ecosystem services, as well as social considerations and political constraints. Only then will we obtain a coherent and improved understanding of fire management for the conservation of fire-mediated ecosystems worldwide.

3.9. Acknowledgements

We thank Davi Rodrigo Rossatto and Augusto César Franco for sharing their data; and Simone Matias Reis, Carlota Segura-García, Manoela Machado and Cecilia Dahlsjö, for support in fieldwork and writing. We are grateful to ICMBio professionals assisting in site conservation and controlled burns, and to the many interns and volunteers associated with UNEMAT and the HPAN (Herbário do PANtanal) who contributed to botanical and data collection activities. We

are thankful to our institutions and colleagues for their continued support, highlighting the transport and logistical assistance provided by UNEMAT and ICMBio.

3.10. Funding

This work was supported by the University of Oxford (John Fell Fund 163/03), the UKRI Natural Environment Research Council (Standard Grant NE/W00058X/1), the Fundación Rafael del Pino, Madrid, Spain (Postgraduate Excellence Scholarship to Francisco Navarro-Rosales), and the EU Marie Skłodowska-Curie Action awarded to FIRE-ADAPT (project no. 101086416).

3.11. Data availability

Carbon flux and related variable data is available within the supplementary material. Raw data will be available upon request to the authors. Tree inventory data is available through Forestplots.net.

3.12. References

Akaike, H. (1974). A new look at the statistical model identification. *IEEE Trans. Autom. Control*, 19(6), 716–723. https://doi.org/10.1109/TAC.1974.1100705

Araujo-Murakami, A., Doughty, C.E., Metcalfe, D.B., Silva-Espejo, J.E., Arroyo, L., Heredia, J.P., Flores, M., Sibler, R., Mendizabal, L.M., Pardo-Toledo, E., Vega, M., Moreno, L., Rojas-Landivar, V.D., Halladay, K., Girardin, C.A.J., Killeen, T.J. & Malhi, Y. (2014). The productivity, allocation and cycling of carbon in forests at the dry margin of the Amazon forest in Bolivia. *Plant Ecol. Divers.*, 7(1–2), 55–69. https://doi.org/10.1080/17550874.2013.798364

Bates, D., Mächler, M., Bolker, B. & Walker, S. (2015). Fitting linear mixed-effects models using lme4. *J. Stat. Softw.*, 67, 1–48. https://doi.org/10.18637/jss.v067.i01

Berenguer, E., Lennox, G.D., Ferreira, J., Malhi, Y., Aragão, L.E.O.C., Barreto, J.R., Del Bon Espírito-Santo, F., Figueiredo, A.E.S., França, F., Gardner, T.A., Joly, C.A., Palmeira, A.F., Quesada, C.A., Rossi, L.C., de Seixas, M.M.M., Smith, C.C., Withey, K. & Barlow, J. (2021). Tracking the impacts of El Niño drought and fire in human-modified Amazonian forests. *Proc. Natl. Acad. Sci. USA*, 118(30), e2019377118. https://doi.org/10.1073/pnas.2019377118

Berg, S., Kutra, D., Kroeger, T., Straehle, C.N., Kausler, B.X., Haubold, C., Schiegg, M., Ales, J., Beier, T., Rudy, M., Eren, K., Cervantes, J.I., Xu, B., Beuttenmueller, F., Wolny, A., Zhang, C., Koethe, U., Hamprecht, F.A. & Kreshuk, A. (2019). ilastik: Interactive machine learning for (bio)image analysis. *Nat. Methods*, 16(12), 1226–1232. https://doi.org/10.1038/s41592-019-0582-9

Bowman, D.M.J.S., Balch, J.K., Artaxo, P., Bond, W.J., Carlson, J.M., Cochrane, M.A., D'Antonio, C.M., DeFries, R.S., Doyle, J.C., Harrison, S.P., Johnston, F.H., Keeley, J.E., Krawchuk, M.A., Kull, C.A., Marston, J.B., Moritz, M.A., Prentice, I.C., Roos, C.I., Scott, A.C., Swetnam, T.W., van der Werf, G. & Pyne, S.J. (2009). Fire in the Earth System. *Science*, 324(5926), 481–484. https://doi.org/10.1126/science.1163886

Bowman, D.M.J.S., O'Brien, J.A. & Goldammer, J.G. (2013). Pyrogeography and the global quest for sustainable mire management. *Annu. Rev. Environ. Resour.*, 38(1), 57–80. https://doi.org/10.1146/annurev-environ-082212-134049

Brando, P.M., Balch, J.K., Nepstad, D.C., Morton, D.C., Putz, F.E., Coe, M.T., Silvério, D., Macedo, M.N., Davidson, E.A., Nóbrega, C.C., Alencar, A. & Soares-Filho, B.S. (2014). Abrupt increases in Amazonian tree mortality due to drought–fire interactions. *Proc. Natl. Acad. Sci. USA*, 111(17), 6347–6352. https://doi.org/10.1073/pnas.1305499111

Bustamante, M., Nardoto, G., Pinto, A.S., Resende, J.C.F., Takahashi, F.S.C. & Vieira, L.C.G. (2012). Potential impacts of climate change on biogeochemical functioning of Cerrado ecosystems. *Braz. J. Biol.*, 72(3 suppl), 655–671. https://doi.org/10.1590/S1519-69842012000400005

Butler, A., Meir, P., Saiz, G., Maracahipes, L., Marimon, B.S. & Grace, J. (2012). Annual variation in soil respiration and its component parts in two structurally contrasting woody savannas in Central Brazil. *Plant Soil*, 352(1), 129–142. https://doi.org/10.1007/s11104-011-0984-7

Cernusak, L.A., Hutley, L.B., Beringer, J. & Tapper, N.J. (2006). Stem and leaf gas exchange and their responses to fire in a north Australian tropical savanna. *Plant Cell Environ.*, 29(4), 632–646. https://doi.org/10.1111/j.1365-3040.2005.01442.x

Chiminazzo, M.A., Charles-Dominique, T., Rossatto, D.R., Bombo, A.B. & Fidelis, A. (2023). Why woody plant modularity through time and space must be integrated in fire research? *AoB Plants*, 15(3), plad029. https://doi.org/10.1093/aobpla/plad029

Christie, A.P., Amano, T., Martin, P.A., Shackelford, G.E., Simmons, B.I. & Sutherland, W.J. (2019). Simple study designs in ecology produce inaccurate estimates of biodiversity responses. *J. Appl. Ecol.*, 56(12), 2742–2754. https://doi.org/10.1111/1365-2664.13499

Conciani, D.E., Santos, L.P. dos, Silva, T.S.F., Durigan, G. & Alvarado, S.T. (2021). Human-climate interactions shape fire regimes in the Cerrado of São Paulo state, Brazil. *J. Nat. Conserv.*, 61, 126006. https://doi.org/10.1016/j.jnc.2021.126006

da Silva, D.M. & Batalha, M.A. (2008). Soil–vegetation relationships in cerrados under different fire frequencies. *Plant Soil*, 311(1), 87–96. https://doi.org/10.1007/s11104-008-9660-y

de Miranda, S. do C., Bustamante, M., Palace, M., Hagen, S., Keller, M. & Ferreira, L.G. (2014). Regional variations in biomass distribution in Brazilian savanna woodland. *Biotropica*, 46(2), 125–138. https://doi.org/10.1111/btp.12095

De Sales, F., Werner, Z. & de Souza Ribeiro, J.G. (2023). Quantifying fire-induced surface climate changes in the savanna and rainforest biomes of Brazil. *Fire*, 6(8), Article 8. https://doi.org/10.3390/fire6080311

Dexter, K.G., Smart, B., Baldauf, C., Baker, T.R., Balinga, M.P., Brienen, R.J.W., Fauset, S., Feldpausch, T.R., Silva, L. Ferreira-Da, Muledi, J. Ilunga, Lewis, S.L., Lopez-Gonzalez, G., Marimon-Junior, B.H., Marimon, B.S., Meerts, P., Page, N., Parthasarathy, N., Phillips, O.L., Sunderland, T.C.H., Theilade, I., Weintritt, J., Affum-Baffoe, K., Araujo, A., Arroyo, L., Begne, S.K., Neves, E. Carvalho-Das, Collins, M., Cuni-Sanchez, A., Djuikouo, M.N.K., Elias, F., Foli, E.G., Jeffery, K.J., Killeen, T.J., Malhi, Y., Maracahipes, L., Mendoza, C., Monteagudo-Mendoza, A., Morandi, P., Santos, C. Oliveira-Dos, Parada, A.G., Pardo, G., Peh, K.S.H., Salomão, R.P., Silveira, M., Sinatora–Miranda, H., Slik, J.W.F., Sonke, B., Taedoumg, H.E., Toledo, M., Umetsu, R.K., Villaroel, R.G., Vos, V.A., White, L.J.T. & Pennington, R.T. (2015). Floristics and biogeography of vegetation in seasonally dry tropical regions. *Int. For. Rev.*, 17(S2), 10–32. https://doi.org/10.1505/146554815815834859

Diffenbaugh, N.S., Konings, A.G. & Field, C.B. (2021). Atmospheric variability contributes to increasing wildfire weather but not as much as global warming. *Proc. Natl. Acad. Sci. USA*, 118(46), e2117876118. https://doi.org/10.1073/pnas.2117876118

Durigan, G., Pilon, N.A.L., Abreu, R.C.R., Hoffmann, W.A., Martins, M., Fiorillo, B.F., Antunes, A.Z., Carmignotto, A.P., Maravalhas, J.B., Vieira, J. & Vasconcelos, H.L. (2020). No net loss of species diversity after prescribed fires in the Brazilian savanna. *Front. For. Glob. Change*, 3. https://doi.org/10.3389/ffgc.2020.00013

Durigan, G. & Ratter, J.A. (2016). The need for a consistent fire policy for Cerrado conservation. *J. Appl. Ecol.*, 53(1), 11–15. https://doi.org/10.1111/1365-2664.12559

Empresa Brasileira de Pesquisa Agropecuária – EMBRAPA (2018). Sistema Brasileiro de Classificação de Solos, 5ª Edição. Centro Nacional de Pesquisa de Solos, Brasília.

Falster, D.S., Brännström, Å., Dieckmann, U. & Westoby, M. (2011). Influence of four major plant traits on average height, leaf-area cover, net primary productivity, and biomass density in single-species forests: A theoretical investigation. *J. Ecol.*, 99(1), 148–164. https://doi.org/10.1111/j.1365-2745.2010.01735.x

Fontenele, H.G.V. & Miranda, H.S. (2024). Fire has contrasting effects on the survival, growth, and reproduction of Cerrado grasses with differing regenerative strategies. *Appl. Veg. Sci.*, 27(2), e12775. https://doi.org/10.1111/avsc.12775

Fox, J. & Weisberg, S. (2019). Nonlinear regression, nonlinear least squares, and nonlinear mixed models in R. *Popul.*, 150.

Franco, A.C., Haridasan, M. & Ferreira, C. da S. (2008). Physiological ecology of cerrado plants: New insights and new approaches. *Braz. J. Plant Physiol.*, 20, 165–166. https://doi.org/10.1590/S1677-04202008000300001

Françoso, R.D., Brandão, R., Nogueira, C.C., Salmona, Y.B., Machado, R.B. & Colli, G.R. (2015). Habitat loss and the effectiveness of protected areas in the Cerrado Biodiversity Hotspot. *Nat. Conserv.*, 13(1), 35–40. https://doi.org/10.1016/j.ncon.2015.04.001

Friedlingstein, P., Jones, M.W., O'Sullivan, M., Andrew, R.M., Bakker, D.C.E., Hauck, J., Le Quéré, C., Peters, G.P., Peters, W., Pongratz, J., Sitch, S., Canadell, J.G., Ciais, P., Jackson, R.B., Alin, S.R., Anthoni, P., Bates, N.R., Becker, M., Bellouin, N., Bopp, L., Chau, T.T.T., Chevallier, F., Chini, L.P., Cronin, M., Currie, K.I., Decharme, B., Djeutchouang, L.M., Dou, X., Evans, W., Feely, R.A., Feng, L., Gasser, T., Gilfillan, D., Gkritzalis, T., Grassi, G., Gregor, L., Gruber, N., Gürses, Ö., Harris, I., Houghton, R.A., Hurtt, G.C., Iida, Y., Ilyina, T., Luijkx, I.T., Jain, A., Jones, S.D., Kato, E., Kennedy, D., Klein Goldewijk, K., Knauer, J., Korsbakken, J.I., Körtzinger, A., Landschützer, P., Lauvset, S.K., Lefèvre, N., Lienert, S., Liu, J., Marland, G., McGuire, P.C., Melton, J.R., Munro, D.R., Nabel, J.E.M.S., Nakaoka, S.I., Niwa, Y., Ono, T., Pierrot, D., Poulter, B., Rehder, G., Resplandy, L., Robertson, E., Rödenbeck, C., Rosan, T.M., Schwinger, J., Schwingshackl, C., Séférian, R., Sutton, A.J., Sweeney, C., Tanhua, T., Tans, P.P., Tian, H., Tilbrook, B., Tubiello, F., van der Werf, G.R., Vuichard, N., Wada, C., Wanninkhof, R., Watson, A.J., Willis, D., Wiltshire, A.J., Yuan, W., Yue, C., Yue, X., Zaehle, S. & Zeng, J. (2022). Global Carbon Budget 2021. *Earth Syst. Sci. Data*, 14(4), 1917–2005. https://doi.org/10.5194/essd-14-1917-2022

Giles, A.L., Faria, L.D.B., Souza, H J. de, Rodrigues, S.B., Munari, L.C., Silva Ribeiro, R. da, Pinho, G.S.C. de, del Rei Texeira, M., Dianese, É., Grillo, B., Carvalho, R., Leão, R.Á., Trindade, A.L., Junior, C.R.A., Andrade, D.F.C. de, & Françoso, R. (2026). Mapping and revealing the tree biodiversity of the Brazilian Cerrado through biome-wide sampling efforts. *Npj Biodiversity*, 5(1), 9. https://doi.org/10.1038/s44185-026-00122-z

Girardin, C.A.J., Espejo, J.E.S., Doughty, C.E., Huasco, W.H., Metcalfe, D.B., Durand-Baca, L., Marthews, T.R., Aragao, L.E.O.C., Farfán-Rios, W., García-Cabrera, K., Halladay, K., Fisher, J.B., Galiano-Cabrera, D.F., Huaraca-Quispe, L.P., Alzamora-Taype, I., Eguiluz-Mora, L., Revilla, N.S., Silman, M.R., Meir, P. & Malhi, Y. (2014). Productivity and carbon allocation in a tropical montane cloud forest in the Peruvian Andes. *Plant Ecol. Divers.*, 7(1–2), 107–123. https://doi.org/10.1080/17550874.2013.820222

Girardin, C.A.J., Malhi, Y., Aragão, L.E.O.C., Mamani, M., Huaraca Huasco, W., Durand, L., Feeley, K.J., Rapp, J., Silva-Espejo, J.E., Silman, M., Salinas, N. & Whittaker, R.J. (2010). Net primary productivity allocation and cycling of carbon along a tropical forest elevational transect in the Peruvian Andes: Net primary productivity from Andes to Amazon. *Glob. Change Biol.*, 16(12), 3176–3192. https://doi.org/10.1111/j.1365-2486.2010.02235.x

Gomes, L., Miranda, H.S. & Bustamante, M.M.da C. (2018). How can we advance the knowledge on the behavior and effects of fire in the Cerrado biome? *For. Ecol. Manag.*, 417, 281–290. https://doi.org/10.1016/j.foreco.2018.02.032

Gomes, L., Miranda, H.S., Soares-Filho, B., Rodrigues, L., Oliveira, U. & Bustamante, M. M. C. (2020). Responses of plant biomass in the Brazilian savanna to frequent fires. *Front. For. Glob. Change*, 3, 507710. https://doi.org/10.3389/ffgc.2020.507710

Grace, J., José, J.S., Meir, P., Miranda, H.S. & Montes, R.A. (2006). Productivity and carbon fluxes of tropical savannas. *J. Biogeogr.*, 33(3), 387–400. https://doi.org/10.1111/j.1365-2699.2005.01448.x

Hoffmann, W.A. (2002). Direct and indirect effects of fire on radial growth of cerrado savanna trees. *J. Trop. Ecol.*, 18(1), 137–142. https://doi.org/10.1017/S0266467402002080

Hoffmann, W.A., Da Silva, E.R., Machado, G.C., Bucci, S.J., Scholz, F.G., Goldstein, G. & Meinzer, F.C. (2005). Seasonal leaf dynamics across a tree density gradient in a Brazilian savanna. *Oecologia*, *145*, 306–315. https://doi.org/10.1007/s00442-005-0129-x

Huaraca Huasco, W., Riutta, T., Girardin, C.A.J., Hancco Pacha, F., Puma Vilca, B.L., Moore, S., Rifai, S.W., del Aguila-Pasquel, J., Araujo Murakami, A., Freitag, R., Morel, A.C., Demissie, S., Doughty, C.E., Oliveras, I., Galiano Cabrera, D.F., Durand Baca, L., Farfán Amézquita, F., Silva Espejo, J.E., da Costa, A.C.L., Mendoza, E.O., Quesada, C.A., Ondo, F.E., Ndong, J.E., Jeffery, K.J., Mihindou, V., White, L.T.J., Bengone, N.N., Ibrahim, F., Addo-Danso, S.D., Duah-Gyamfi, A., Djagbletey, G.D., Owusu-Afriyie, K., Amissah, L., Mbou, A.T., Marthews, T.R., Metcalfe, D.B., Aragão, L.E.O., Marimon-Junior, B.H., Marimon, B.S., Majalap, N., Adu-Bredu, S., Abernethy, K.A., Silman, M., Ewers, R.M., Meir, P. & Malhi, Y. (2021). Fine root dynamics across pantropical rainforest ecosystems. *Glob. Change Biol.*, 27(15), 3657–3680. https://doi.org/10.1111/gcb.15677

ICMBio (2016) Plano de Manejo. Estação Ecológica da Serra das Araras. ICMBio, Brasília.

IPCC. (2006). Chapter 4: Forest Land. In S. Eggleston, L. Buendia, K. Miwa, T. Ngara & K. Tanabe (Eds.), 2006 *IPCC Guidelines for National Greenhouse Gas Inventories* (Vol. 4): Agriculture, Forestry and Other Land Use. Hayama: IPCC/IGES.

IUSS Working Group WRB (2022). World Reference Base for Soil Resources. International soil classification system for naming soils and creating legends for soil maps, Fourth Edition. International Union of Soil Sciences (IUSS), Vienna, Austria.

Jones, S., Rowland, L., Cox, P., Hemming, D., Wiltshire, A., Williams, K., Parazoo, N.C., Liu, J., Costa, A.C.L., Meir, P., Mencuccini, M., Harper, A.B. (2020). The impact of a simple representation of non-structural carbohydrates on the simulated response of tropical forests to drought. *Biogeosciences* 17 (13), 3589–3612. https://doi.org/10.5194/bg-17-3589-2020

Kelly, L.T., Fletcher, M.S., Menor, I.O., Pellegrini, A.F.A., Plumanns-Pouton, E.S., Pons, P., Williamson, G.J. & Bowman, D.M.J.S. (2023). Understanding fire regimes for a better Anthropocene. *Annu. Rev. Environ. Resour.*, 48(48), 207–235. https://doi.org/10.1146/annurev-environ-120220-055357

Kelly, L.T., Giljohann, K.M., Duane, A., Aquilué, N., Archibald, S., Batllori, E., Bennett, A.F., Buckland, S.T., Canelles, Q., Clarke, M.F., Fortin, M.J., Hermoso, V., Herrando, S., Keane, R.E., Lake, F.K., McCarthy, M.A., Morán-Ordóñez, A., Parr, C.L., Pausas, J.G., Penman, T.D., Regos, A., Rumpff, L., Santos, J.L., Smith, A.L., Syphard, A.D., Tingley, M.W. & Brotons, L. (2020). Fire and biodiversity in the Anthropocene. *Science*, 370(6519), eabb0355. https://doi.org/10.1126/science.abb0355

Kho, L.K., Malhi, Y. & Tan, S.K.S. (2013). Annual budget and seasonal variation of aboveground and belowground net primary productivity in a lowland dipterocarp forest in Borneo. *J. Geophys. Res. Biogeosci.*, 118(3), 1282–1296. https://doi.org/10.1002/jgrg.20109

Kottek, M., Grieser, J., Beck, C., Rudolf, B. & Rubel, F. (2006). World Map of the Köppen-Geiger climate classification updated. *Meteorol. Z.*, 259–263. https://doi.org/10.1127/0941-2948/2006/0130

Kozovits, A.R., Bustamante, M.M.C., Garofalo, C.R., Bucci, S., Franco, A.C., Goldstein, G. & Meinzer, F.C. (2007). Nutrient resorption and patterns of litter production and decomposition in a Neotropical Savanna. *Funct. Ecol.*, 21(6), 1034–1043. https://doi.org/10.1111/j.1365-2435.2007.01325.x

Krawchuk, M.A., Moritz, M.A., Parisien, M.A., Van Dorn, J. & Hayhoe, K. (2009). Global pyrogeography: The current and future Distribution of wildfire. *PLoS ONE*, 4(4), e5102. https://doi.org/10.1371/journal.pone.0005102

Kuznetsova, A., Brockhoff, P.B. & Christensen, R.H.B. (2017). lmerTest Package: Tests in linear mixed effects models. *J. Stat. Softw.*, 82, 1–26. https://doi.org/10.18637/jss.v082.i13

Le Stradic, S., Hernandez, P., Fernandes, G.W. & Buisson, E. (2018). Regeneration after fire in *campo rupestre*: Short- and long-term vegetation dynamics. *Flora*, 238, 191–200. https://doi.org/10.1016/j.flora.2016.12.001

Le Stradic, S., Roumet, C., Durigan, G., Cancian, L. & Fidelis, A. (2021). Variation in biomass allocation and root functional parameters in response to fire history in Brazilian savannas. *J. Ecol.*, 109(12), 4143–4157. https://doi.org/10.1111/1365-2745.13786

Lenth, R. (2024). emmeans: Estimated Marginal Means, aka Least-Squares Means. Available at: https://CRAN.R-project.org/package=emmeans.

Ma, F., Song, B., Quan, Q., Zhang, F., Wang, J., Zhou, Q. & Niu, S. (2020). Light competition and biodiversity loss cause saturation response of aboveground net primary productivity to nitrogen enrichment. *J. Geophys. Res. Biogeosci.*, 125(3), e2019JG005556. https://doi.org/10.1029/2019JG005556

Malhi, Y. (2012). The productivity, metabolism and carbon cycle of tropical forest vegetation. *J. Ecol.*, 100(1), 65–75. https://doi.org/10.1111/j.1365-2745.2011.01916.x

Malhi, Y., Aragão, L.E.O.C., Metcalfe, D.B., Paiva, R., Quesada, C.A., Almeida, S., Anderson, L., Brando, P., Chambers, J.Q., da Costa, A.C.L., Hutyra, L.R., Oliveira, P., Patiño, S., Pyle, E.H., Robertson, A.L. & Teixeira, L.M. (2009). Comprehensive assessment of carbon productivity, allocation and storage in three Amazonian forests. *Glob. Change Biol.*, 15(5), 1255–1274. https://doi.org/10.1111/j.1365-2486.2008.01780.x

Malhi, Y., Girardin, C., Metcalfe, D.B., Doughty, C.E., Aragão, L.E.O.C., Rifai, S.W., Oliveras, I., Shenkin, A., Aguirre-Gutiérrez, J., Dahlsjö, C.A.L., Riutta, T., Berenguer, E., Moore, S., Huasco, W.H., Salinas, N., da Costa, A.C.L., Bentley, L.P., Adu-Bredu, S., Marthews, T.R., ... Phillips, O.L. (2021). The Global Ecosystems Monitoring network: Monitoring ecosystem productivity and carbon cycling across the tropics. *Biol. Conserv.*, 253, 108889. https://doi.org/10.1016/j.biocon.2020.108889

Marchant, R. (2010). Understanding complexity in savannas: Climate, biodiversity and people. *Curr. Opin. Environ. Sustain.*, 2(1), 101–108. https://doi.org/10.1016/j.cosust.2010.03.001

Marthews, T.R., Riutta, T., Oliveras Menor, I., Urrutia, R., Moore, S., Metcalfe, D., Malhi, Y., Phillips, O., Huaraca Huasco, W., Ruiz Jaén, M., Girardin, C., Butt, N., Cain, R. & colleagues from the RAINFOR and GEM networks (2014). Measuring Tropical Forest Carbon Allocation and Cycling: A RAINFOR-GEM Field Manual for Intensive Census Plots (v3.0). Manual, Global Ecosystems Monitoring network.

McLauchlan, K.K., Higuera, P.E., Miesel, J., Rogers, B.M., Schweitzer, J., Shuman, J.K., Tepley, A.J., Varner, J.M., Veblen, T.T., Adalsteinsson, S.A., Balch, J.K., Baker, P., Batllori, E., Bigio, E., Brando, P., Cattau, M., Chipman, M.L., Coen, J., Crandall, R., Daniels, L., Enright, N., Gross, W.S., Harvey, B.J., Hatten, J.A., Hermann, S., Hewitt, R.E., Kobziar, L.N., Landesmann, J.B., Loranty, M.M., Maezumi, S.Y., Mearns, L., Moritz, M., Myers, J.A., Pausas, J.G., Pellegrini, A.F.A., Platt, W.J., Roozeboom, J., Safford, H., Santos, F., Scheller, R.M., Sherriff, R.L., Smith, K.G., Smith, M.D., Watts, A.C. (2020). Fire as a fundamental ecological process: Research advances and frontiers. *J. Ecol.*, 108(5), 2047-2069. https://doi.org/10.1111/1365-2745.13403

Meirelles, M.L. & Henriques, R.P. (1992). Produção primária líquida em área queimada e não queimada de campo sujo de cerrado (Planaltina—DF). *Acta Bot. Bras.*, 6, 3–14. https://doi.org/10.1590/S0102-33061992000200001

Metcalfe, D.B., Meir, P., Aragão, L.E.O.C., Lobo-do-Vale, R., Galbraith, D., Fisher, R.A., Chaves, M.M., Maroco, J.P., da Costa, A.C.L., de Almeida, S.S., Braga, A.P., Gonçalves, P.H.L., de Athaydes, J., da Costa, M., Portela, T.T.B., de Oliveira, A.A.R., Malhi, Y. & Williams, M. (2010). Shifts in plant respiration and carbon use efficiency at a large-scale drought experiment in the eastern Amazon. *New Phytol.*, 187(3), 608–621. https://doi.org/10.1111/j.1469-8137.2010.03319.x

Metcalfe, D.B., Meir, P., Aragão, L.E.O.C., Malhi, Y., da Costa, A.C.L., Braga, A., Gonçalves, P.H.L., de Athaydes, J., de Almeida, S.S. & Williams, M. (2007). Factors controlling spatio-temporal variation in carbon dioxide efflux from surface litter, roots, and soil organic matter at four rain forest sites in the eastern Amazon. *J. Geophys. Res. Biogeosci.*, 112(G4). https://doi.org/10.1029/2007JG000443

Metcalfe, D.B., Williams, M., Aragão, L.E.O.C., Da Costa, A.C.L., de Almeida, S.S., Braga, A.P., Gonçalves, P.H.L., de Athaydes Silva Junior, J., Malhi, Y. & Meir, P. (2007). A method for extracting plant roots from soil which facilitates rapid sample processing without compromising measurement accuracy. *New Phytol.*, 174(3), 697-703. https://doi.org/10.1111/j.1469-8137.2007.02032.x

Miller, J.E.D., Damschen, E.I., Ratajczak, Z. & Özdoğan, M. (2017). Holding the line: Three decades of prescribed fires halt but do not reverse woody encroachment in grasslands. *Landsc. Ecol.*, 32(12), 2297–2310. https://doi.org/10.1007/s10980-017-0569-9

Moore, S., Adu-Bredu, S., Duah-Gyamfi, A., Addo-Danso, S.D., Ibrahim, F., Mbou, A.T., Grandcourt, A., Valentini, R., Nicolini, G., Djagbletey, G., Owusu-Afriyie, K., Gvozdevaite, A., Oliveras, I., Ruiz-Jaen, M.C. & Malhi, Y. (2018). Forest biomass, productivity and carbon cycling along a rainfall gradient in West Africa. *Glob. Change Biol.*, 24(2), e496–e510. https://doi.org/10.1111/gcb.13907

Nardoto, G.B., Bustamante, M.M.C., Pinto, A.S. & Klink, C.A. (2006). Nutrient use efficiency at ecosystem and species level in savanna areas of Central Brazil and impacts of fire. *J. Trop. Ecol.*, 22(2), 191–201. https://doi.org/10.1017/S0266467405002865

Nottingham, A.T., Whitaker, J., Turner, B.L., Salinas, N., Zimmermann, M., Malhi, Y. & Meir, P. (2015). Climate warming and soil carbon in tropical forests: Insights from an elevation gradient in the Peruvian Andes. *BioScience*, 65(9), 906–921. https://doi.org/10.1093/biosci/biv109

Oliveras, I., Meirelles, S.T., Hirakuri, V.L., Freitas, C.R., Miranda, H.S. & Pivello, V.R. (2012). Effects of fire regimes on herbaceous biomass and nutrient dynamics in the Brazilian savanna. *Int. J. Wildland Fire*, 22(3), 368–380. https://doi.org/10.1071/WF10136

Peres, J.R.R., Suher, A.R., Vargas, M.A.T. & Drozdowicz, A. (1983). Litter production in areas of Brazilian "cerrados." *Pesqui. Agropecu. Bras.*, 18(9), 1037–1043.

Pivello, V.R. (2011). The use of fire in the Cerrado and Amazonian rainforests of Brazil: Past and present. *Fire Ecol.*, 7(1), 24–39. https://doi.org/10.4996/fireecology.0701024

Pivello, V.R. & Coutinho, L.M. (1992). Transfer of macro-nutrients to the atmosphere during experimental burnings in an open *cerrado* (Brazilian savanna). *J. Trop. Ecol.*, 8(4), 487-497. https://doi.org/10.1017/S0266467400006829

Pivello, V.R., Vieira, I., Christianini, A.V., Ribeiro, D.B., da Silva Menezes, L., Berlinck, C.N., Melo, F.P.L., Marengo, J.A., Tornquist, C.G., Tomas, W.M. & Overbeck, G.E. (2021). Understanding Brazil's catastrophic fires: Causes, consequences and policy needed to prevent future tragedies. *Perspect. Ecol. Conserv.*, 19(3), 233–255. https://doi.org/10.1016/j.pecon.2021.06.005

Pizzato, J.A., Dallacort, R., Tieppo, R.C., Modolo, A.J., Cremon, C. & Moreira, P.S.P. (2012). Distribuição e probabilidade de ocorrência de precipitação em Cáceres (MT). *Pesqui. Agropecu. Trop.*, 42, 137–142. https://doi.org/10.1590/S1983-40632012000200006

Prichard, S.J., Stevens-Rumann, C.S. & Hessburg, P.F. (2017). Tamm Review: Shifting global fire regimes: Lessons from reburns and research needs. *For. Ecol. Manag.*, 396, 217–233. https://doi.org/10.1016/j.foreco.2017.03.035

Raich, J.W. & Nadelhoffer, K.J. (1989). Belowground Carbon Allocation in Forest Ecosystems: Global Trends. *Ecology*, 70(5), 1346–1354. https://doi.org/10.2307/1938194

Reis, S.M., Lenza, E., Marimon, B.S., Gomes, L., Forsthofer, M., Morandi, P.S., Marimon-Junior, B.H., Feldpausch, T.R. & Elias, F. (2015). Post-fire dynamics of the woody vegetation of a savanna forest (*cerradão*) in the Cerrado-Amazon transition zone. *Acta Bot. Bras.*, 29, 408–416. https://doi.org/10.1590/0102-33062015abb0009

Rezende, A.V., Sanquetta, C.R., Filho, A.F. & Felfili, J.M. (2006). Comparação de modelos matemáticos para estimativa do volume, biomassa e estoque de carbono da vegetação lenhosa de um cerrado *sensu stricto* em Brasília, DF. *Sci. For.*, 71, 65–76.

Rissi, M.N., Baeza, M.J., Gorgone-Barbosa, E., Zupo, T. & Fidelis, A. (2017). Does season affect fire behaviour in the Cerrado? *Int. J. Wildland Fire*, 26(5), 427–433. https://doi.org/10.1071/WF14210

Riutta, T., Malhi, Y., Kho, L.K., Marthews, T.R., Huaraca Huasco, W., Khoo, M., Tan, S., Turner, E., Reynolds, G., Both, S., Burslem, D.F.R.P., Teh, Y.A., Vairappan, C.S., Majalap, N. & Ewers, R.M. (2018). Logging disturbance shifts net primary productivity and its allocation in Bornean tropical forests. *Glob. Change Biol.*, *24*(7), 2913–2928. https://doi.org/10.1111/gcb.14068

Rocha, W., Metcalfe, D.B., Doughty, C.E., Brando, P., Silvério, D., Halladay, K., Nepstad, D.C., Balch, J.K. & Malhi, Y. (2014). Ecosystem productivity and carbon cycling in intact and annually burnt forest at the dry southern limit of the Amazon rainforest (Mato Grosso, Brazil). *Plant Ecol. Divers.*, 7(1–2), 25–40. https://doi.org/10.1080/17550874.2013.798368

Rodrigues, C.A. & Fidelis, A. (2022). Should we burn the Cerrado? Effects of fire frequency on open savanna plant communities. *J. Veg. Sci.*, 33(6), e13159. https://doi.org/10.1111/jvs.13159

Rodrigues, C.A., Zirondi, H.L. & Fidelis, A. (2021). Fire frequency affects fire behavior in open savannas of the Cerrado. *For. Ecol. Manag.*, 482, 118850. https://doi.org/10.1016/j.foreco.2020.118850

Rosan, T.M., Aragao, L.E., Oliveras, I., Phillips, O.L., Malhi, Y., Gloor, E. & Wagner, F.H. (2019). Extensive 21st century woody encroachment in South America's savanna. *Geophys. Res. Lett.*, 46(12), 6594–6603. https://doi.org/10.1029/2019GL082327

Rossatto, D.R. & Franco, A.C. (2017). Expanding our understanding of leaf functional syndromes in savanna systems: The role of plant growth form. *Oecologia*, 183(4), 953–962. https://doi.org/10.1007/s00442-017-3815-6

Rowland, L., da Costa, A.C.L., Oliveira, A.A.R., Oliveira, R.S., Bittencourt, P.L., Costa, P.B., Giles, A.L., Sosa, A.I., Coughlin, I., Godlee, J.L., Vasconcelos, S.S., Junior, J.A.S., Ferreira, L.V., Mencuccini, M. & Meir, P. (2018). Drought stress and tree size determine stem CO_2 efflux in a tropical forest. *New Phytol.*, 218(4), 1393–1405. https://doi.org/10.1111/nph.15024

Sankaran, M., Ratnam, J. & Hanan, N.P. (2004). Tree–grass coexistence in savannas revisited – insights from an examination of assumptions and mechanisms invoked in existing models. *Ecol. Lett.*, 7(6), 480–490. https://doi.org/10.1111/j.1461-0248.2004.00596.x

Santos, L. dos, Zamparoni, C.A.G.P. & Soares, J.C. de Oliveira. (2017). A variabilidade pluviométrica na região de Cáceres-MT entre 1971 e 2010. *Formação (Online)*, 24(43), Article 43. https://doi.org/10.33081/formacao.v24i43.4746

Scalon, M.C., Oliveras Menor, I., Freitag, R., Peixoto, K.S., Rifai, S.W., Marimon, B.S., Marimon-Junior, B.H. & Malhi, Y. (2022). Contrasting strategies of nutrient demand and use between savanna and forest ecosystems in a Neotropical transition zone. *Biogeosciences*, 19(15), 3649–3661. https://doi.org/10.5194/bg-19-3649-2022

Staver, A.C., Archibald, S. & Levin, S. (2011). Tree cover in sub-Saharan Africa: Rainfall and fire constrain forest and savanna as alternative stable states. *Ecology*, 92(5), 1063–1072. https://doi.org/10.1890/10-1684.1

Stevens, N., Bond, W., Feurdean, A. & Lehmann, C.E.R. (2022). Grassy ecosystems in the Anthropocene. *Annu. Rev. Environ. Resour.*, 47(1), 261–289. https://doi.org/10.1146/annurev-environ-112420-015211

Taylor, J.R (1997). *Error analysis*, 2nd edition. University Science Books: Sausalito, California.

Teixeira, J., Souza, L., Le Stradic, S. & Fidelis, A. (2022). Fire promotes functional plant diversity and modifies soil carbon dynamics in tropical savanna. *Sci. Total Environ.*, 812, 152317. https://doi.org/10.1016/j.scitotenv.2021.152317

Terra, M.C.N.S., Nunes, M.H., Souza, C.R., Ferreira, G.W.D., Prado-Junior, J.A. do, Rezende, V.L., Maciel, R., Mantovani, V., Rodrigues, A., Morais, V.A., Scolforo, J.R.S. & Mello, J.M. de. (2023). The inverted forest: Aboveground and notably large belowground carbon stocks and their drivers in Brazilian savannas. *Sci. Total Environ.*, 867, 161320. https://doi.org/10.1016/j.scitotenv.2022.161320

Thiault, L., Kernaléguen, L., Osenberg, C.W. & Claudet, J. (2017). Progressive-change BACIPS: A flexible approach for environmental impact assessment. *Methods Ecol. Evol.*, 8(3), 288–296. https://doi.org/10.1111/2041-210X.12655

van Der Werf, G.R., Randerson, J.T., Collatz, G.J. & Giglio, L. (2003). Carbon emissions from fires in tropical and subtropical ecosystems. *Glob. Change Biol.*, 9(4), 547–562. https://doi.org/10.1046/j.1365-2486.2003.00604.x

van der Werf, G.R., Randerson, J.T., Giglio, L., van Leeuwen, T.T., Chen, Y., Rogers, B.M., Mu, M., van Marle, M.J.E., Morton, D.C., Collatz, G.J., Yokelson, R.J. & Kasibhatla, P.S. (2017). Global fire emissions estimates during 1997–2016. *Earth Syst. Sci. Data*, 9(2), 697–720. https://doi.org/10.5194/essd-9-697-2017

Vourlitis, G.L., Pinto, O.B., Dalmagro, H.J., Enrique Zanella de Arruda, P., de Almeida Lobo, F. & de Souza Nogueira, J. (2022). Net primary production and ecosystem carbon flux of Brazilian tropical savanna ecosystems from eddy covariance and inventory methods. *J. Geophys. Res. Biogeosci.*, 127(8), 006780. https://doi.org/10.1029/2021JG006780

Weiss, M. & Baret, F. (2017). CAN_EYE V6. 4.91 user manual.

Westerling, A.L., Hidalgo, H.G., Cayan, D.R. & Swetnam, T.W. (2006). Warming and earlier spring increase Western U.S. forest wildfire activity. *Science*, 313(5789), 940–943. https://doi.org/10.1126/science.1128834

Wieczorkowski, J.D. & Lehmann, C.E.R. (2022). Encroachment diminishes herbaceous plant diversity in grassy ecosystems worldwide. *Glob. Change Biol.*, 28(18), 5532–5546. https://doi.org/10.1111/gcb.16300

Wilcke, W. & Lilienfein, J. (2002). Biogeochemical consequences of the transformation of native Cerrado into *Pinus caribaea* plantations in Brazil. *Plant Soil*, 238(2), 175–189. https://doi.org/10.1023/A:1014421305608

Yoda, K. (1983). Community respiration in a lowland rainforest in Pasoh, Peninsular Malaysia. *Jpn. J. Ecol.*, 33(2), 183–197. https://doi.org/10.18960/seitai.33.2_183

Zhang-Zheng, H., Adu-Bredu, S., Duah-Gyamfi, A., Moore, S., Addo-Danso, S.D., Amissah, L., Valentini, R., Djagbletey, G., Anim-Adjei, K., Quansah, J., Sarpong, B., Owusu-Afriyie, K., Gvozdevaite, A., Tang, M., Ruiz-Jaen, M.C., Ibrahim, F., Girardin, C.A.J., Rifai, S., Dahlsjö, C.A.L., Riutta, T., Deng, X., Sun, Y., Prentice, I.C., Oliveras Menor, I. & Malhi, Y. (2024). Contrasting carbon cycle along tropical forest aridity gradients in West Africa and Amazonia. *Nat. Commun.*, 15(1), 3158. https://doi.org/10.1038/s41467-024-47202-x

Zheng, B., Ciais, P., Chevallier, F., Chuvieco, E., Chen, Y. & Yang, H. (2021). Increasing forest fire emissions despite the decline in global burned area. *Sci. Adv.*, 7(39), eabh2646. https://doi.org/10.1126/sciadv.abh2646

Zhou, Y., Singh, J., Butnor, J.R., Coetsee, C., Boucher, P.B., Case, M.F., Hockridge, E.G., Davies, A.B. & Staver, A.C. (2022). Limited increases in savanna carbon stocks over decades of fire suppression. *Nature*, 603(7901), 445–449. https://doi.org/10.1038/s41586-022-04438-1

Zupo, T., Daibes, L.F., Pausas, J.G. & Fidelis, A. (2021). Post-fire regeneration strategies in a frequently burned Cerrado community. *J. Veg. Sci.*, 32(1), e12968. https://doi.org/10.1111/jvs.12968

Zuur, A.F., Ieno, E.N., Walker, N.J., Saveliev, A.A. & Smith, G.M. (2009). *Mixed effects models and extensions in ecology with R* (Vol. 574, p. 574). New York: Springer.

3.13. Supplementary material

3.13.1. Estimating leaf area index from fisheye lens canopy images

Leaf area index (LAI) of each plot was estimated from fisheye lens images of the canopy collected every month from December 2022 to November 2023. Images were taken with a Nikon D3200 camera and Samyang 8mm F3.5 UMC CS II Fisheye lens. Images were then processed using 'ilastik' (Berg *et al*., 2019), MATLAB and 'CANEYE' (Weiss & Baret, 2017) software for pixel classification, image cropping and LAI calculations respectively. Ilastik was used to segment images into vegetation and sky pixels. Ilastik assigns labels to pixels using a Random Forest classifier based on pixel labels and features (intensity, edge filters and textures) interactively set to enhance classification quality. Training was performed on a set of 10 images, indicating areas of sky and vegetation. All images were then processed and visually inspected. Inadequately segmented images were subsequently re-processed using a different training dataset and feature selection, and this process was repeated until all images were adequately segmented. Segmented images were then transformed to .tif format in MATLAB by changing pixel class values and applying a mask to pixels outside a 47º angle of view.

CANEYE was then used to obtain PAI (plant area index) estimates from segmented images. The software provides an estimate of PAI based on gap fraction and considering leaf distribution, inclination, and image projection function (Weiss & Baret, 2017). CANEYE reported one PAI value per plot per month, as a synthesis of the images of the 25 subplots. We used the 'CE V5.1 True PAI' method of PAI calculation, as our limited angle of view is not suitable for more recent calculation versions (requiring more than 60º angle of view). The following parameters were supplied to CANEYE based on image and camera characteristics:

1) CALIBRATION PARAMETERS

image size: dimensions of the image (in landscape orientation) in terms of rows and columns of pixels (ROW: 4000, COLUMN: 6016, meaning 6016 x 4000 pixels).
angle of view: 47º, where the vertical edge of the photo is the horizon, and the centroid is the zenith.
COI: 45 degrees, defining the area of radius to be analysed, and incorporating a 2-degree buffer to account for edge imperfections.
Sub Sample Factor: 1, using default value as reducing computational memory is not required.

We created a projection function and inputted the optical centre characteristics:

- Optical Centre: the central pixel of the image defined as the midpoint pixel in the x and y direction (LINE: 2000, COLUMN 3008).
- Polynomial order: 1, as the projection is assumed to be equidistant/polar.
- P1: 0.013, representing the angle of view of the fisheye lens divided by the number of pixels from the centroid of the fisheye image to the image horizon.

2) ANGULAR RESOLUTION

Angular Resolution: 2.5º in the zenith (θ) and azimuth (ϕ) directions, determining the angles for which the gap fraction is computed. It is set to the lowest value (highest resolution) for both angles.

FCover: 20 degrees, used to calculate the percentage of black pixels within central 20-degree ring, not relevant to LAI.

3) CLUMPING PARAMETER

PAIsat: 8, used to address the issue of mathematically calculated PAI being infinite in completely black pixels. To address this, we used a value of 8 in such cases. This value is the intermediate default value provided and based on the guess that the densest point in the sampled plots would have a PAI of 8.

4) FAPAR COMPUTATION

Latitude: 15 degrees, based on the location of the plots.

Day of Year: 150, in this case it represents a random number as variations in radiation is not expected to be large in tropical areas, and because it is not relevant to the calculation of PAI.

Finally, we derived the true LAI values from the PAI estimates obtained from CANEYE by accounting for the percentage of PAI attributable to stems (stem area index – SAI). First, we used the percentage of PAI associated with stems and leaves of Cerrado trees provided by Hoffmann *et al*. (2005) – where SAI and LAI account for 13.9% and 86.1% of PAI respectively – to calculate SAI and LAI proportions of PAI in each of the plots during the month with highest canopy cover. We also accounted for dead standing trees in each plot, by scaling the proportion of SAI in accordance with the proportion of standing dead trees (100% live trees means SAI = 0.139*PAI, and 100% dead standing trees means SAI = 1.000*PAI). We thus obtained the value of SAI for each plot, and since we assume that SAI does not vary seasonally, we subtracted SAI from all other PAI values to account for the stem fraction of the canopy cover in all other months, obtaining true green leaf LAI.

3.13.2. Plot characterisation

Table S3.1, description of the initial (2017 plot census) ecosystem characteristics of each monitoring plot at the Estação Ecológica da Serra das Araras fire experiment. Aboveground dry biomass and aboveground carbon stocks were calculated using the equations provided by Rezende *et al*. (2006).

Plot	**ESA-04**	**ESA-05**	**ESA-06**	**ESA-07**	**ESA-08**	**ESA-09**
Fire regime	Unburnt	Biennial burns	Unburnt	Triennial burns	Unburnt	Annual burns
Number of stems (ha^{-1})	831	426	625	362	687	770
Basal area (m^2 ha^{-1})	5.45	2.50	3.83	2.32	4.43	5.47
Aboveground biomass (Mg ha^{-1})	11.55	4.41	6.68	4.31	8.55	10.85
Aboveground C stock (MgC ha^{-1})	5.78	2.21	3.34	2.16	4.27	5.43
Tree species richness	49	35	36	28	40	43
Most common species	*Curatella americana*	*Tachigali vulgaris*	*Kielmeyera grandiflora*	*Pouteria ramiflora*	*Tachigali vulgaris*	*Kielmeyera grandiflora*
	Pouteria ramiflora	*Curatella americana*	*Curatella americana*	*Tachigali vulgaris*	*Pouteria ramiflora*	*Pouteria ramiflora*
	Myrcia bella	*Kielmeyera grandiflora*	*Tachigali vulgaris*	*Curatella americana*	*Kielmeyera grandiflora*	*Tachigali vulgaris*
	Tachigali vulgaris	*Myrcia bella*	*Pouteria ramiflora*	*Kielmeyera grandiflora*	*Curatella americana*	*Vochysia haenkeana*
	Hancornia speciosa	*Pouteria ramiflora*	*Myrcia bella*	*Vochysia haenkeana*	*Myrcia bella*	*Curatella americana*
	Kielmeyera grandiflora	*Vochysia haenkeana*	*Hancornia speciosa*	*Byrsonima coccolobifolia*	*Qualea grandiflora*	*Dimorphandra mollis*
	Qualea grandiflora	*Byrsonima coccolobifolia*	*Vochysia haenkeana*	*Hymenaea stigonocarpa*	*Xylopia aromatica*	*Hancornia speciosa*
	Vochysia haenkeana	*Qualea multiflora*	*Byrsonima coccolobifolia*	*Hancornia speciosa*	*Byrsonima coccolobifolia*	*Byrsonima coccolobifolia*
	Qualea parviflora	*Himatanthus obovatus*	*Qualea grandiflora*	*Myrcia bella*	*Byrsonima verbascifolia*	*Byrsonima verbascifolia*
	Eriotheca gracilipes	*Hymenaea stigonocarpa*	*Xylopia aromatica*	*Xylopia aromatica*	*Vochysia haenkeana*	*Qualea grandiflora*

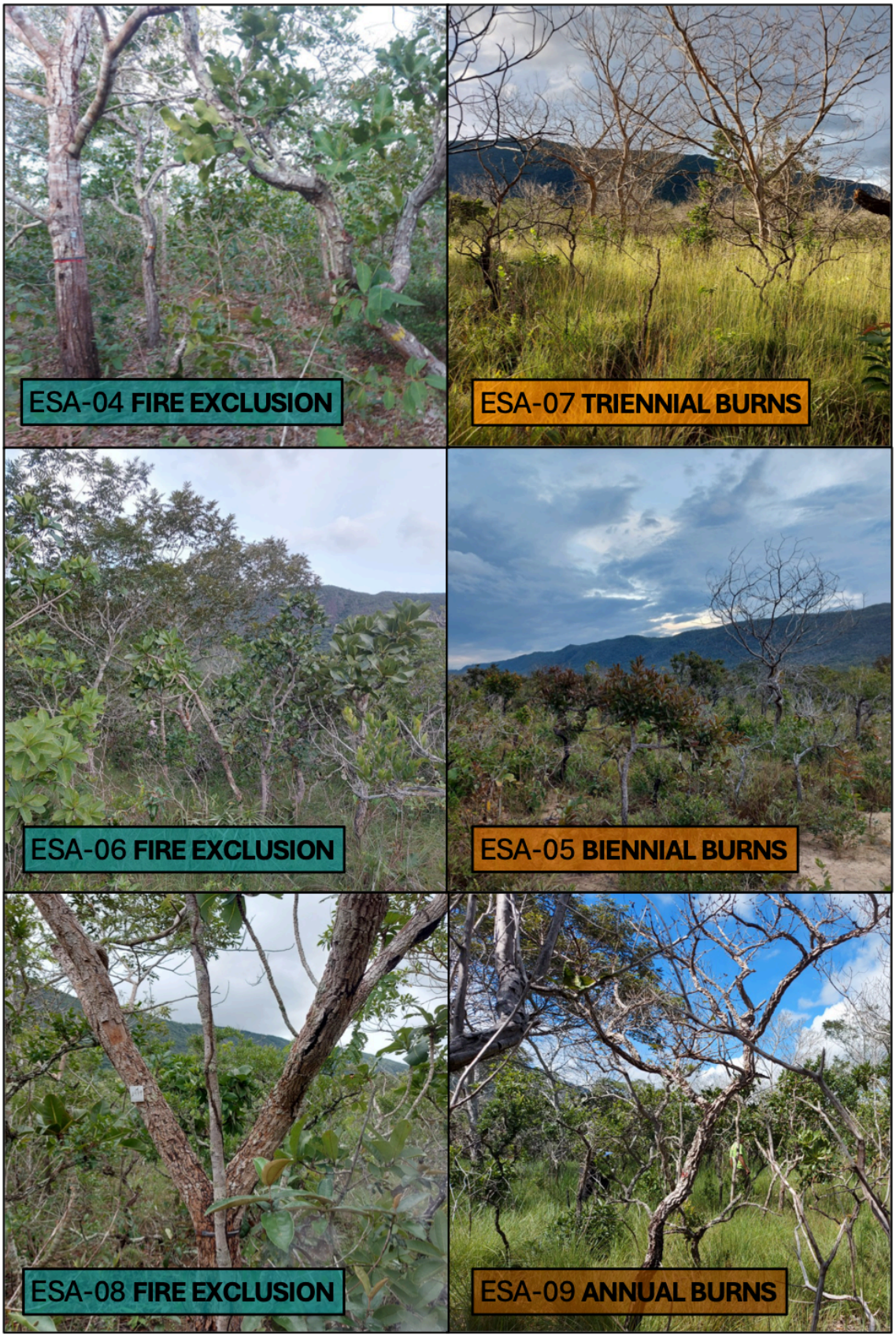


Figure S3.1, images of the woodland savanna (*cerrado sensu stricto*) vegetation within the monitoring plots at the Estação Ecológica da Serra das Araras fire experiment, taken March to April 2023.

3.13.3. Statistical model outputs and pairwise comparisons

Table S3.2, summary statistics for the linear mixed model testing if litterfall net primary productivity ($NPP_{litterfall}$) varies between fire regimes at the start (2018) and end (2023) monitoring periods. The model includes an interaction between fire regime and period. The response variable was transformed to meet statistical assumptions. The table includes fixed effect coefficients (in the transformed scale) and random effect variances. Plot and subplot identity were used as random effects to account for non-independence.

Formula: $\log_{10}(NPP_{litterfall} + 0.1) \sim$ regime * year + (1|plot) + (1|subplot)				
Fixed effects	**Estimate**	**Std. Error**	**t-value**	**Pr(>|t|)**
(Intercept)	0.12930	0.06095	2.121	0.162
regimeTriennial	-0.27915	0.12190	-2.290	0.143
regimeBiennial	-0.13072	0.12190	-1.072	0.391
regimeAnnual	0.14416	0.12190	1.183	0.354
period2023	0.00196	0.02992	0.065	0.948
regimeTriennial:period2023	**-0.45068**	**0.05980**	**-7.537**	**7.26e-14**
regimeBiennial:period2023	**-0.42377**	**0.06009**	**-7.052**	**2.42e-12**
regimeAnnual:period2023	**-0.50232**	**0.05980**	**-8.401**	**< 2e-16**

Random effects	**Variance**	**Groups**
subplot	0.049904	54
plot	0.004753	6
residual	0.198053	2049

Table S3.3, summary of the regime-level contrasts extracted from the linear mixed model testing if $NPP_{litterfall}$ varies between the start (2018) and end (2023) monitoring periods at each of the fire regimes (**Table S3.2**). The estimate values presented below represent the difference between the overall regime marginal mean, and 2018 and 2023 marginal means within that regime. Thus, contrast estimates are symmetrically opposite and correspond to half of the period2023 model coefficients. P-values under 0.05 indicate significant differences (Šídák method).

regime = Unburnt					
contrast	**estimate**	**SE**	**df**	**t.ratio**	**p.value**
period2018 effect	-0.00098	0.0150	1991	-0.065	0.9973
period2023 effect	0.00098	0.0150	1991	0.065	0.9973
regime = Triennial					
contrast	**estimate**	**SE**	**df**	**t.ratio**	**p.value**
period2018 effect	**0.22436**	0.0259	1991	8.667	**<.0001**
period2023 effect	**-0.22436**	0.0259	1991	-8.667	**<.0001**
regime = Biennial					
contrast	**estimate**	**SE**	**df**	**t.ratio**	**p.value**
period2018 effect	**0.21091**	0.0261	1991	8.095	**<.0001**
period2023 effect	**-0.21091**	0.0261	1991	-8.095	**<.0001**
regime = Annual					
contrast	**estimate**	**SE**	**df**	**t.ratio**	**p.value**
period2018 effect	**0.25018**	0.0259	1991	9.665	**<.0001**
period2023 effect	**-0.25018**	0.0259	1991	-9.665	**<.0001**

Table S3.4, summary statistics for the linear mixed model testing if positive values of stem DBH growth (from dendrometer data) vary between experimental fire regimes and at the start (2019) and end (2023) monitoring periods. The model includes an interaction between fire regime and period. Note the response variable was transformed to meet statistical assumptions. The table includes transformed-scale fixed effect coefficients and random effect variances. Plot, species and stem were used as random effects to account for non-independence.

Formula: $\log_{10}$(positive stem DBH growth) ~ regime * year + (1|plot) + (1|stem) + (1|species)				
Fixed effects	**Estimate**	**Std. Error**	**t-value**	**Pr(>|t|)**
(Intercept)	**-0.36561**	**0.04002**	**-9.136**	**2.01e-06**
regimeTriennial	0.14759	0.06383	2.312	0.0677
regimeBiennial	0.04234	0.07618	0.556	0.5902
regimeAnnual	0.07052	0.05850	1.205	0.3012
period2023	**-0.09093**	**0.01820**	**-4.997**	**6.50e-07**
regimeTriennial:period2023	-0.01979	0.07622	-0.260	0.7952
regimeBiennial:period2023	0.13584	0.08627	1.575	0.1156
regimeAnnual:period2023	0.08615	0.05537	1.556	0.1199

Random effects	**Variance**	**Groups**
stem	0.008108	349
species	0.011200	28
plot	0.001499	6
residual	0.103973	1656

Table S3.5, summary of the regime-level contrasts of marginal means extracted from the linear mixed model testing if positive values of stem DBH growth (from dendrometer data) vary between fire regimes and at the start (2019) and end (2023) monitoring periods (**Table S3.4**). The estimate values presented below represent the difference between the overall fire regime marginal mean, and the period-specific marginal mean within the fire regime. P-values below 0.05 indicate significant differences according to the Šídák method.

regime = Unburnt					
contrast	**estimate**	**SE**	**df**	**t.ratio**	**p.value**
period2019 effect	**0.04547**	0.00911	1529	4.992	**<.0001**
period2023 effect	**-0.04547**	0.00911	1529	-4.992	**<.0001**
regime = Triennial					
contrast	**estimate**	**SE**	**df**	**t.ratio**	**p.value**
period2019 effect	0.05536	0.03712	961	1.492	0.2538
period2023 effect	-0.05536	0.03712	961	-1.492	0.2538
regime = Biennial					
contrast	**estimate**	**SE**	**df**	**t.ratio**	**p.value**
period2019 effect	-0.02246	0.04228	1460	-0.531	0.8363
period2023 effect	0.02246	0.04228	1460	0.531	0.8363
regime = Annual					
contrast	**estimate**	**SE**	**df**	**t.ratio**	**p.value**
period2019 effect	0.00239	0.02617	1607	0.091	0.9947
period2023 effect	-0.00239	0.02617	1607	-0.091	0.9947

Table S3.6, summary statistics for the generalised linear mixed model testing if the proportion of stems sampled with dendrometer bands showing positive DBH growth varies between experimental fire regimes at the start (2019) and end (2023) monitoring periods. The model includes an interaction between fire regime and period. The table includes fixed effect coefficients (in the logit scale) and random effect variances. Stem identity was used as a random effect to account for non-independence.

Formula: binary stem DBH growth ~ regime * year + (1|stem)				
Family: binomial (logit)				
logLik:1632.2 **deviance:** 3264.3 **df.resid:** 3236 **observations:** 3245				
Fixed effects	**Estimate**	**Std. Error**	**t-value**	**Pr(>|z|)**
(Intercept)	0.26288	0.17330	1.517	0.1293
regimeTriennial	-0.23115	0.52532	-0.440	0.6599
regimeBiennial	-0.92338	0.58663	-1.574	0.1155
regimeAnnual	0.31482	0.45026	0.699	0.4844
period2023	-0.06727	0.10920	-0.616	0.5378
regimeTriennial:period2023	0.19244	0.43994	0.437	0.6618
regimeBiennial:period2023	0.76883	0.45625	1.685	0.0920
regimeAnnual:period2023	-0.56550	0.33957	-1.685	0.0958

Random effects	**Variance**	**Groups**
stem	6.901	435

Table S3.7, summary of the regime-level contrasts of marginal means extracted from the generalised linear mixed model testing if the proportion of dendrometer stems with positive DBH growth varies between fire regimes at the start (2019) and end (2023) monitoring periods (**Table S3.6**). The estimate values presented below represent the difference between the overall fire regime marginal mean, and the period-specific marginal mean within the fire regime. P-values below 0.05 indicate significant differences according to the Šídák method.

regime = Unburnt					
contrast	**estimate**	**SE**	**df**	**z.ratio**	**p.value**
period2019 effect	0.0336	0.0546	Inf	0.616	0.7864
period2023 effect	-0.0336	0.0546	Inf	-0.616	0.7864
regime = Triennial					
contrast	**estimate**	**SE**	**df**	**t.ratio**	**p.value**
period2019 effect	-0.0626	0.2215	Inf	-1.584	0.2136
period2023 effect	0.0626	0.2215	Inf	1.584	0.2136
regime = Biennial					
contrast	**estimate**	**SE**	**df**	**t.ratio**	**p.value**
period2019 effect	-0.3508	0.2215	Inf	-1.584	0.2136
period2023 effect	0.3508	0.2215	Inf	1.584	0.2136
regime = Annual					
contrast	**estimate**	**SE**	**df**	**t.ratio**	**p.value**
period2019 effect	0.3164	0.1608	Inf	1.968	0.0958
period2023 effect	-0.3164	0.1608	Inf	-1.968	0.0958

Table S3.8, summary statistics for the linear model testing if fine root net primary productivity ($NPP_{fine\ roots}$) varies between fire regimes at the start (2018) and end (2023) monitoring periods. The model includes an interaction between fire regime and period. Note the response variable was transformed to meet statistical assumptions. The table includes fixed effect coefficients (in the transformed scale). Please note no random effects were used to avoid model overcomplexity.

Formula: $\log_{10}(NPP_{fine\ roots} + 0.2) \sim$ regime * year				
Adjusted R-squared: 0.1987 **F-statistic:** 16.3 **DF:** 7,425 **p-value:** < 2.2e-16				
Fixed effects	**Estimate**	**Std. Error**	**t-value**	**Pr(>|t|)**
(Intercept)	**0.321710**	**0.038113**	**8.441**	**5.01e-16**
regimeTriennial	-0.012090	0.076227	-0.159	0.8741
regimeBiennial	-0.125426	0.076227	-1.645	0.1006
regimeAnnual	-0.004198	0.076227	-0.055	0.9561
period2023	**-0.294563**	**0.053777**	**-5.478**	**7.40e-08**
regimeTriennial:period2023	**-0.212798**	**0.107739**	**-1.975**	**0.0489**
regimeBiennial:period2023	-0.029413	0.107739	-0.273	0.7850
regimeAnnual:period2023	**-0.230118**	**0.107739**	**-2.136**	**0.0333**

Table S3.9, summary of the regime-level contrasts of marginal means extracted from the linear model testing if fine root net primary productivity ($NPP_{fine\ roots}$) varies between experimental fire regimes and between the start (2018) and end (2023) monitoring periods (**Table S3.8**). The estimate values presented below represent the difference between the overall fire regime marginal mean, and the period-specific marginal mean within the fire regime. P-values below 0.05 indicate significant differences according to the Šídák method.

regime = Unburnt					
contrast	**estimate**	**SE**	**df**	**t.ratio**	**p.value**
period2019 effect	**0.147**	0.0269	425	5.478	**<.0001**
period2023 effect	**-0.147**	0.0269	425	-5.478	**<.0001**
regime = Triennial					
contrast	**estimate**	**SE**	**df**	**t.ratio**	**p.value**
period2019 effect	**0.254**	0.0467	425	5.435	**<.0001**
period2023 effect	**-0.254**	0.0467	425	-5.435	**<.0001**
regime = Biennial					
contrast	**estimate**	**SE**	**df**	**t.ratio**	**p.value**
period2019 effect	**0.162**	0.0467	425	-3.470	**0.0011**
period2023 effect	**-0.162**	0.0467	425	3.470	**0.0011**
regime = Annual					
contrast	**estimate**	**SE**	**df**	**t.ratio**	**p.value**
period2019 effect	**-0.262**	0.0467	425	5.620	**<.0001**
period2023 effect	**0.262**	0.0467	425	-5.620	**<.0001**

Table S3.10, summary statistics for the linear mixed model testing if stem CO_2 efflux varies between fire regimes at the start (Sep 2018 to Aug 2019) and end (2023) monitoring periods. The model includes an interaction between fire regime and period. The table includes fixed effect coefficients and random effect variances. Plot, species and stem identity were used as random effects to account for non-independence. Please note that the start period data for plots ESA-05 and ESA-06 was taken from September 2019 to March 2020.

Formula: stem CO_2 efflux ~ regime * year + (1|plot) + (1|species) + (1|stem)				
Fixed effects	**Estimate**	**Std. Error**	**t-value**	**Pr(>|t|)**
(Intercept)	**0.97911**	**0.15874**	**6.168**	**0.000410**
regimeTriennial	0.35463	0.21532	1.647	0.257029
regimeBiennial	0.36415	0.23451	1.553	0.236216
regimeAnnual	0.07337	0.22109	0.332	0.771980
period2023	0.03564	0.05820	0.612	0.540294
regimeTriennial:period2023	-0.14840	0.12685	-1.170	0.242218
regimeBiennial:period2023	**-0.41677**	**0.12595**	**-3.309**	**0.000954**
regimeAnnual:period2023	-0.07310	0.10906	-0.670	0.502746

Random effects	**Variance**	**Groups**
stem	0.14859	100
species	0.21570	21
plot	0.02089	6
residual	0.69510	1828

Table S3.11, summary of the regime-level contrasts of marginal means extracted from the linear mixed model testing if stem CO_2 efflux varies between fire regimes at the start (Sep 2018 to Aug 2019) and end (2023) monitoring periods (**Table S3.10**). The estimate values presented below represent the difference between the overall fire regime marginal mean, and the period-specific marginal mean within the fire regime. P-values below 0.05 indicate significant differences according to the Šídák method.

regime = Unburnt					
contrast	**estimate**	**SE**	**df**	**t.ratio**	**p.value**
period(Sep 2018 - Aug 2019) effect	-0.0178	0.0292	1743	-0.611	0.7894
period2023 effect	0.0178	0.0292	1743	0.611	0.7894
regime = Triennial					
contrast	**estimate**	**SE**	**df**	**t.ratio**	**p.value**
period(Sep 2018 - Aug 2019) effect	0.0564	0.0566	1432	0.996	0.5369
period2023 effect	-0.0564	0.0566	1432	-0.996	0.5369
regime = Biennial					
contrast	**estimate**	**SE**	**df**	**t.ratio**	**p.value**
period(Sep 2018 - Aug 2019) effect	**0.1906**	0.0559	1800	3.409	**0.0013**
period2023 effect	**-0.1906**	0.0559	1800	-3.409	**0.0013**
regime = Annual					
contrast	**estimate**	**SE**	**df**	**t.ratio**	**p.value**
period(Sep 2018 - Aug 2019) effect	0.0187	0.0461	1725	0.406	0.9006
period2023 effect	-0.0187	0.0461	1725	-0.406	0.9006

Table S3.12, summary statistics for the linear mixed model testing if soil respiration (R_{soil}) varies between fire regimes at the start (Sep 2018 to Aug 2019) and end (2023) monitoring periods. The model includes an interaction between fire regime and period. The table includes fixed effect coefficients and random effect variances. Plot and subplot identity were used as random effects to account for non-independence.

Formula: R_{soil} ~ regime * year + (1|plot) + (1|subplot)				
Fixed effects	**Estimate**	**Std. Error**	**t-value**	**Pr(>|t|)**
(Intercept)	**8.3362**	**0.3791**	**21.989**	**7.82e-05**
regimeTriennial	1.5443	0.7610	2.029	0.12221
regimeBiennial	0.3896	0.7610	0.512	0.63918
regimeAnnual	1.3116	0.7757	1.691	0.17023
period2023	**-1.0747**	**0.3527**	**-3.047**	**0.00236**
regimeTriennial:period2023	**-1.5766**	**0.7057**	**-1.170**	**0.02566**
regimeBiennial:period2023	0.6952	0.6952	2.234	0.40690
regimeAnnual:period2023	-0.6904	0.7114	-0.971	0.33197

Random effects	**Variance**	**Groups**
subplot	1.1366	54
plot	0.1062	6
residual	18.2605	1194

Table S3.13, summary of the regime-level contrasts of marginal means extracted from the linear mixed model testing if soil respiration (R_{soil}) varies between fire regimes at the start (Sep 2018 to Aug 2019) and end (2023) monitoring periods (**Table S3.12**). The estimate values presented below represent the difference between the overall fire regime marginal mean, and the period-specific marginal mean within the fire regime. P-values below 0.05 indicate significant differences according to the Šídák method.

regime = Unburnt					
contrast	**estimate**	**SE**	**df**	**t.ratio**	**p.value**
period(Sep 2018 - Aug 2019) effect	**0.537**	0.176	1143	3.046	**0.0047**
period2023 effect	**-0.537**	0.176	1143	-3.046	**0.0047**
regime = Triennial					
contrast	**estimate**	**SE**	**df**	**t.ratio**	**p.value**
period(Sep 2018 - Aug 2019) effect	**1.326**	0.306	1136	4.338	**<.0001**
period2023 effect	**-1.326**	0.306	1136	-4.338	**<.0001**
regime = Biennial					
contrast	**estimate**	**SE**	**df**	**t.ratio**	**p.value**
period(Sep 2018 - Aug 2019) effect	0.249	0.300	1136	0.831	0.6474
period2023 effect	-0.249	0.300	1136	-0.831	0.6474
regime = Annual					
contrast	**estimate**	**SE**	**df**	**t.ratio**	**p.value**
period(Sep 2018 - Aug 2019) effect	**0.883**	0.309	1137	2.857	**0.0087**
period2023 effect	**-0.883**	0.309	1137	-2.857	**0.0087**

Table S3.14, summary statistics for the linear mixed model testing if herbaceous net primary productivity (NPP_{herbs}) varies between fire regimes. The table includes transformed fixed effect coefficients and random effect variances. Plot and subplot were used as random effects to account for non-independence.

Formula: $\log_{10}(NPP_{herbs} + 0.05) \sim$ regime + (1|plot) + (1|subplot)					
Fixed effects			**Estimate**	**Std. Error**	**t-value**	**Pr(>|t|)**
(Intercept)			**-1.01880**	**0.05485**	**-18.574**	**0.0029**
regimeTriennial			0.38534	0.10970	3.513	0.0724
regimeBiennial			0.21803	0.10970	1.987	0.1852
regimeAnnual			0.08250	0.10970	0.752	0.5305
Random effects	**Variance**	**Groups**				
subplot	0.004291	72				
plot	0.007381	6				
residual	0.185449	864				

Table S3.15, summary statistics for the linear mixed model testing if live herbaceous biomass varies between fire regimes. The table includes transformed fixed effect coefficients and random effect variances. Plot was used as a random effect to account for non-independence.

Formula: $\log_{10}$(live herbaceous biomass + 1) ~ regime + (1|plot)					
Fixed effects			**Estimate**	**Std. Error**	**t-value**	**Pr(>|t|)**
(Intercept)			**1.05406**	**0.15306**	**6.887**	**0.0204**
regimeTriennial			0.93808	0.30612	3.064	0.0920
regimeBiennial			0.39530	0.30612	1.291	0.3257
regimeAnnual			0.09873	0.30612	0.323	0.7777
Random effects	**Variance**	**Groups**				
plot	0.05759	6				
residual	0.15227	72				

Table S3.16, summary statistics for the linear mixed model testing if leaf area index (LAI) varies between fire regimes. The table includes fixed effect coefficients and random effect variances. LAI was calculated as a single value per plot and month, so plot was used as a random effect to account for non-independence.

Formula: LAI ~ regime + (1 | plot)					
Fixed effects			**Estimate**	**Std. Error**	**t-value**	**Pr(>|t|)**
(Intercept)			**1.7600**	**0.1444**	**12.192**	**0.00666**
regimeTriennial			**-1.5866**	**0.2887**	**-5.495**	**0.03156**
regimeBiennial			**-1.3121**	**0.2900**	**-4.524**	**0.04403**
regimeAnnual			-0.9362	0.2887	-3.242	0.08339
Random effects	**Variance**	**Groups**				
plot	0.05416	6				
residual	0.10035	71				

Table S3.17, comparison of AIC (Akaike's information criterion) values for models comparing variables at different fire regimes and monitoring periods with and without an additional fixed effect for basal area in 2017. Linear mixed models were fit using ML estimation rather than REML for adequate comparisons between different sets of fixed effects (Zuur *et al*., 2009).

Variable	**AIC(df) –** without initial basal area	**AIC(df) –** with initial basal area	**ΔAIC**
$NPP_{litterfall}$	2639.80 (11)	2640.46 (11)	0.66
positive DBH growth	1098.72 (12)	1099.45 (13)	0.73
binary DBH growth	3282.31 (9)	3282.29 (10)	-0.02
$NPP_{fine\ roots}$	436.70 (9)	436.92 (10)	0.22
Stem CO_2 efflux	4727.53 (12)	4725.60 (13)	-1.93
R_{soil}	6918.26 (11)	6919.35 (12)	1.09
NPP_{herbs}	1031.37 (7)	1024.18 (8)	**-7.19**
live herb biomass	84.49 (7)	77.64 (8)	**-6.85**
LAI	55.68 (6)	56.22 (7)	-0.46

Table S3.18, summary statistics for the linear mixed model testing if herbaceous net primary productivity (NPP_{herbs}) varies between fire regimes, including an additional fixed effect for plot-level basal area in 2017. Plot and subplot were used as random effects in order to maintain model structure (**Table S3.15**).

Formula: $\log_{10}(\mathbf{NPP_{herbs}} + 0.05) \sim$ regime + initial_basal_area + (1|plot) + (1|subplot)					
Fixed effects			**Estimate**	**Std. Error**	**t-value**	**Pr(>|t|)**
(Intercept)			**-0.50434**	**0.16134**	**-3.126**	**0.00262**
initial_basal_area			**-0.11260**	**0.03494**	**-3.223**	**0.00196**
regimeTriennial			0.13209	0.09142	1.445	0.15318
regimeBiennial			-0.01456	0.08597	-0.169	0.86599
regimeAnnual			**0.18383**	**0.05631**	**3.265**	**0.00173**
Random effects	**Variance**	**Groups**				
subplot	0.0042	72				
plot	0.0000	6				
residual	0.1854	504				

Table S3.19, summary statistics for the linear mixed model testing if live herbaceous biomass varies between fire regimes, including an additional fixed effect for plot-level basal area in 2017. Plot was used as a random effect in order to maintain model structure (**Table S3.16**).

Formula: $\log_{10}$(live herbaceous biomass + 1) ~ regime + (1|plot)					
Fixed effects			**Estimate**	**Std. Error**	**t-value**	**Pr(>|t|)**
(Intercept)			**2.46461**	**0.43340**	**5.687**	**2.59e-07**
initial_basal_area			**-0.30872**	**0.09386**	**-3.289**	**0.00156**
regimeTriennial			0.24371	0.24558	0.992	0.32434
regimeBiennial			-0.24242	0.23094	-1.050	0.29737
regimeAnnual			**0.37656**	**0.15126**	**2.489**	**0.01510**
Random effects	**Variance**	**Groups**				
plot	0.0000	6				
residual	0.1417	72				

Table S3.20, summary of initial and final carbon flux estimates within the experimental fire regimes at the Estação Ecológica da Serra das Araras (MgC ha^{-1} year^{-1}).

START

Flux	**$NPP_{litterfall}$**	**NPP_{stem}**	**NPP_{herbs}**	**$NPP_{coarse\ roots}$**	**$NPP_{fine\ roots}$**	**R_{canopy}**	**R_{stem}**	**R_{herbs}**	**R_{soil}**	**$C_{mortality}$**
Period	Jan 2018 - Dec 2018	Jul 2017 - Sep 2019	-	Jul 2017 - Sep 2019	Jan 2018 - Dec 2018	-	Sep 2018 - Aug 2019	-	Sep 2018 - Aug 2019	Jul 2017 - Sep 2019
Unburnt	1.25 ± 0.19	0.49 ± 0.13	-	0.67 ± 0.48	1.90 ± 0.18	-	1.93 ± 0.36	-	8.34 ± 0.38	0.01 ± 0.00
Triennial	0.61± 0.17	0.29 ± 0.07	-	0.39 ± 0.29	1.84 ± 0.31	-	1.41 ± 0.26	-	9.88 ± 0.66	0.00 ± 0.00
Biennial	0.90 ± 0.24	0.24 ± 0.06	-	0.33 ± 0.24	1.37 ± 0.24	-	1.51 ± 0.29	-	8.73 ± 0.66	0.00 ± 0.00
Annual	1.78 ± 0.46	0.71 ± 0.18	-	0.97 ± 0.71	1.88 ± 0.32	-	2.35 ± 0.54	-	9.65 ± 0.68	0.03 ± 0.01

END

Flux	**$NPP_{litterfall}$**	**NPP_{stem}**	**NPP_{herbs}**	**$NPP_{coarse\ roots}$**	**$NPP_{fine\ roots}$**	**R_{canopy}**	**R_{stem}**	**R_{herbs}**	**R_{soil}**	**$C_{mortality}$**
Period	Jan 2023 - Dec 2023	Sep 2021 - Sep 2023	Nov 2023 - Oct 2024	Sep 2021 - Sep 2023	Jan 2023 - Dec 2023	Dec 2022 - Nov 2023	Jan 2023 - Dec 2023	Oct 2023	Jan 2023 - Dec 2023	Sep 2021 - Sep 2023
Unburnt	1.25 ± 0.20	0.66 ± 0.17	0.05 ± 0.01	0.90 ± 0.65	0.86 ± 0.09	4.32 ± 1.02	2.41 ± 0.48	0.58 ± 0.23	7.26 ± 0.37	0.08 ± 0.02
Triennial	0.15 ± 0.06	0.07 ± 0.02	0.18 ± 0.05	0.09 ± 0.07	0.43 ± 0.10	0.41 ± 0.61	0.82 ± 0.19	5.28 ± 3.31	7.23 ± 0.63	0.69 ± 0.18
Biennial	0.28 ± 0.10	0.16 ± 0.04	0.11 ± 0.03	0.21 ± 0.15	0.55 ± 0.11	1.10 ± 0.66	0.78 ± 0.22	1.44 ± 0.93	8.23 ± 0.62	0.76 ± 0.19
Annual	0.49 ± 0.15	0.60 ± 0.15	0.07 ± 0.03	0.82 ± 0.59	0.42 ± 0.09	2.01 ± 0.61	2.06 ± 0.49	0.77 ± 0.51	7.88 ± 0.62	1.22 ± 0.31

Table S3.21, summary of initial and final carbon fluxes within the experimental fire project at the Estação Ecológica da Serra das Araras (MgC ha^{-1} year^{-1}), separated by individual plot. Where flux estimates were derived from statistical models, plot was used as fixed effect instead of regime, and removed as a random effect.

START

Flux	**$NPP_{litterfall}$**	**NPP_{stem}**	**NPP_{herbs}**	**$NPP_{coarse\ roots}$**	**$NPP_{fine\ roots}$**	**R_{canopy}**	**R_{stem}**	**R_{herbs}**	**R_{soil}**	**$C_{mortality}$**
Period	Jan 2018 - Dec 2018	Jul 2017 - Sep 2019	-	Jul 2017 - Sep 2019	Jan 2018 - Dec 2018	-	Sep 2018 - Aug 2019	-	Sep 2018 - Aug 2019	Jul 2017 - Sep 2019
ESA-04	1.36 ± 0.27	0.62 ± 0.16	-	0.84 ± 0.61	2.33 ± 0.38	-	2.38 ± 0.46	-	8.82 ± 0.56	0.02 ± 0.01
ESA-05	0.90 ± 0.18	0.24 ± 0.06	-	0.33 ± 0.24	1.37 ± 0.24	-	1.51 ± 0.25	-	8.73 ± 0.57	0.00 ± 0.00
ESA-06	0.99 ± 0.20	0.33 ± 0.09	-	0.45 ± 0.33	1.61 ± 0.27	-	1.67 ± 0.35	-	7.47 ± 0.58	0.01 ± 0.00
ESA-07	0.61± 0.13	0.29 ± 0.07	-	0.39 ± 0.29	1.84 ± 0.31	-	1.39 ± 0.22	-	9.88 ± 0.57	0.00 ± 0.00
ESA-08	1.43 ± 0.28	0.51± 0.13	-	0.70 ± 0.51	1.82 ± 0.31	-	1.86 ± 0.37	-	8.68 ± 0.57	0.00 ± 0.00
ESA-09	1.78 ± 0.35	0.71 ± 0.18	-	0.97 ± 0.71	1.88 ± 0.32	-	2.33 ± 0.45	-	9.65 ± 0.59	0.23 ± 0.05

END

Flux	**$NPP_{litterfall}$**	**NPP_{stem}**	**NPP_{herbs}**	**$NPP_{coarse\ roots}$**	**$NPP_{fine\ roots}$**	**R_{canopy}**	**R_{stem}**	**R_{herbs}**	**R_{soil}**	**$C_{mortality}$**
Period	Jan 2023 - Dec 2023	Sep 2021 - Sep 2023	Nov 2023 - Oct 2024	Sep 2021 - Sep 2023	Jan 2023 - Dec 2023	Dec 2022 - Nov 2023	Jan 2023 - Dec 2023	Oct 2023	Jan 2023 - Dec 2023	Sep 2021 - Sep 2023
ESA-04	1.34 ± 0.28	0.94 ± 0.24	0.03 ± 0.01	1.29 ± 0.94	0.88 ± 0.16	4.60 ± 1.04	4.04 ± 0.64	0.37 ± 0.11	7.08 ± 0.54	0.06 ± 0.02
ESA-05	0.28 ± 0.07	0.16 ± 0.04	0.11 ± 0.03	0.21 ± 0.15	0.55 ± 0.11	1.10 ± 0.34	0.77 ± 0.15	1.49 ± 0.42	8.23 ± 0.53	0.76 ± 0.19
ESA-06	0.81 ± 0.18	0.38 ± 0.10	0.07 ± 0.01	0.52 ± 0.38	0.81 ± 0.15	3.60 ± 0.83	1.56 ± 0.37	1.15 ± 0.32	6.84 ± 0.56	0.15 ± 0.04
ESA-07	0.15 ± 0.05	0.07 ± 0.02	0.18 ± 0.02	0.09 ± 0.07	0.43 ± 0.10	0.42 ± 0.24	0.81 ± 0.14	5.33 ± 1.50	7.23 ± 0.54	0.69 ± 0.18
ESA-08	1.80 ± 0.38	0.65 ± 0.17	0.04 ± 0.01	0.87 ± 0.65	0.90 ± 0.17	4.77 ± 1.08	1.88 ± 0.43	0.57 ± 0.16	7.87 ± 0.54	0.04 ± 0.01
ESA-09	0.49 ± 0.12	0.60 ± 0.15	0.07 ± 0.01	0.82 ± 0.59	0.42 ± 0.09	2.01 ± 0.50	2.04 ± 0.40	0.82 ± 0.23	7.88 ± 0.53	1.22 ± 0.31

Table S3.22, summary of initial and final estimates of flux-related variables within the experimental burning regimes at the Estação Ecológica da Serra das Araras.

START

Variable	**positive DBH growth**	**proportion of growing stems**	**leaf area index**	**Stem CO_2 efflux**	**stem surface area**	**live herbaceous biomass**
Units	cm $year^{-1}$	-	m^2m^{-2}	µmol m^{-2} s^{-1}	m^2 ha^{-1}	g m^{-2}
Period	Jan 2019 - Dec 2019	Jan 2019 - Dec 2019	-	Sep 2018 - Aug 2019	Jan 2018 - Dec 2018	-
Unburnt	0.43 ± 0.04	0.54 ± 0.02	-	1.00 ± 0.16	5096.38 ± 509.64	-
Triennial	0.61 ± 0.09	0.51 ± 0.07	-	1.34 ± 0.21	2770.75 ± 277.08	-
Biennial	0.48 ± 0.07	0.41 ± 0.07	-	1.35 ± 0.22	2962.50 ± 296.25	-
Annual	0.51 ± 0.07	0.58 ± 0.05	-	1.05 ± 0.22	5904.41 ± 590.44	-

END

Variable	**positive DBH growth**	**proportion of growing stems**	**leaf area index**	**Stem CO_2 efflux**	**stem surface area**	**live herbaceous biomass**
Units	cm $year^{-1}$	-	m^2m^{-2}	µmol m^{-2} s^{-1}	m^2 ha^{-1}	g m^{-2}
Period	Jan 2023 - Dec 2023	Jan 2023 - Dec 2023	Dec 2022 - Nov 2023	Jan 2023 - Dec 2023	Sep 2023	Oct 2023
Unburnt	0.35 ± 0.03	0.53 ± 0.03	1.76 ± 0.14	1.02 ± 0.15	6267.44 ± 626.74	10.33 ± 3.99
Triennial	0.47 ± 0.08	0.52 ± 0.07	0.17 ± 0.25	1.22 ± 0.21	1761.10 ± 176.11	97.21 ± 59.95
Biennial	0.53 ± 0.10	0.51 ± 0.07	0.45 ± 0.25	0.96 ± 0.21	2128.08 ± 212.81	27.14 ± 17.18
Annual	0.50 ± 0.08	0.50 ± 0.06	0.82 ± 0.25	1.01 ± 0.22	5370.34 ± 537.03	13.22 ± 8.68

Table S3.23, summary of initial and final estimates of flux-related variables within the experimental fire project at the Estação Ecológica da Serra das Araras separated by individual plot. Where flux estimates were derived from statistical models, plot was used as fixed effect instead of regime, and removed as a random effect.

START

Variable	**positive DBH growth**	**proportion of growing stems**	**leaf area index**	**Stem CO_2 efflux**	**stem surface area**	**live herbaceous biomass**
Units	cm $year^{-1}$	-	m^2m^{-2}	µmol m^{-2} s^{-1}	m^2 ha^{-1}	g m^{-2}
Period	Jan 2019 - Dec 2019	Jan 2019 - Dec 2019	-	Sep 2018 - Aug 2019	Jan 2018 - Dec 2018	-
ESA-04	0.46 ± 0.04	0.60 ± 0.04	-	1.03 ± 0.17	6138.72 ± 613.87	-
ESA-05	0.47 ± 0.07	0.41 ± 0.07	-	1.34 ± 0.18	2962.50 ± 296.25	-
ESA-06	0.46 ± 0.04	0.51 ± 0.04	-	1.05 ± 0.19	4200.30 ± 420.03	-
ESA-07	0.60 ± 0.07	0.51 ± 0.07	-	1.33 ± 0.17	2770.75 ± 277.08	-
ESA-08	0.37 ± 0.03	0.49 ± 0.04	-	0.99 ± 0.17	4950.11 ± 485.01	-
ESA-09	0.50 ± 0.05	0.58 ± 0.05	-	1.04 ± 0.17	5904.41 ± 590.44	-

END

Variable	**positive DBH growth**	**proportion of growing stems**	**leaf area index**	**Stem CO_2 efflux**	**stem surface area**	**live herbaceous biomass**
Units	cm $year^{-1}$	-	m^2m^{-2}	µmol m^{-2} s^{-1}	m^2 ha^{-1}	g m^{-2}
Period	Jan 2023 - Dec 2023	Jan 2023 - Dec 2023	Dec 2022 - Nov 2023	Jan 2023 - Dec 2023	Sep 2023	Oct 2023
ESA-04	0.39 ± 0.03	0.56 ± 0.08	1.83 ± 0.09	1.40 ± 0.17	7648.15 ± 764.82	6.43 ± 1.69
ESA-05	0.53 ± 0.08	0.51 ± 0.08	0.45 ± 0.10	0.96 ± 0.17	2128.08 ± 212.81	28.04 ± 7.30
ESA-06	0.33 ± 0.03	0.51 ± 0.04	1.48 ± 0.09	0.82 ± 0.18	5020.68 ± 502.07	21.73 ± 5.66
ESA-07	0.47 ± 0.07	0.52 ± 0.07	0.17 ± 0.09	1.22 ± 0.17	1761.10 ± 176.11	98.11 ± 25.47
ESA-08	0.33 ± 0.03	0.52 ± 0.04	1.97 ± 0.09	0.81 ± 0.17	6133.49 ± 613.35	10.09 ± 2.64
ESA-09	0.50 ± 0.06	0.50 ± 0.06	0.82 ± 0.09	1.01 ± 0.17	5370.34 ± 537.03	14.12 ± 3.69

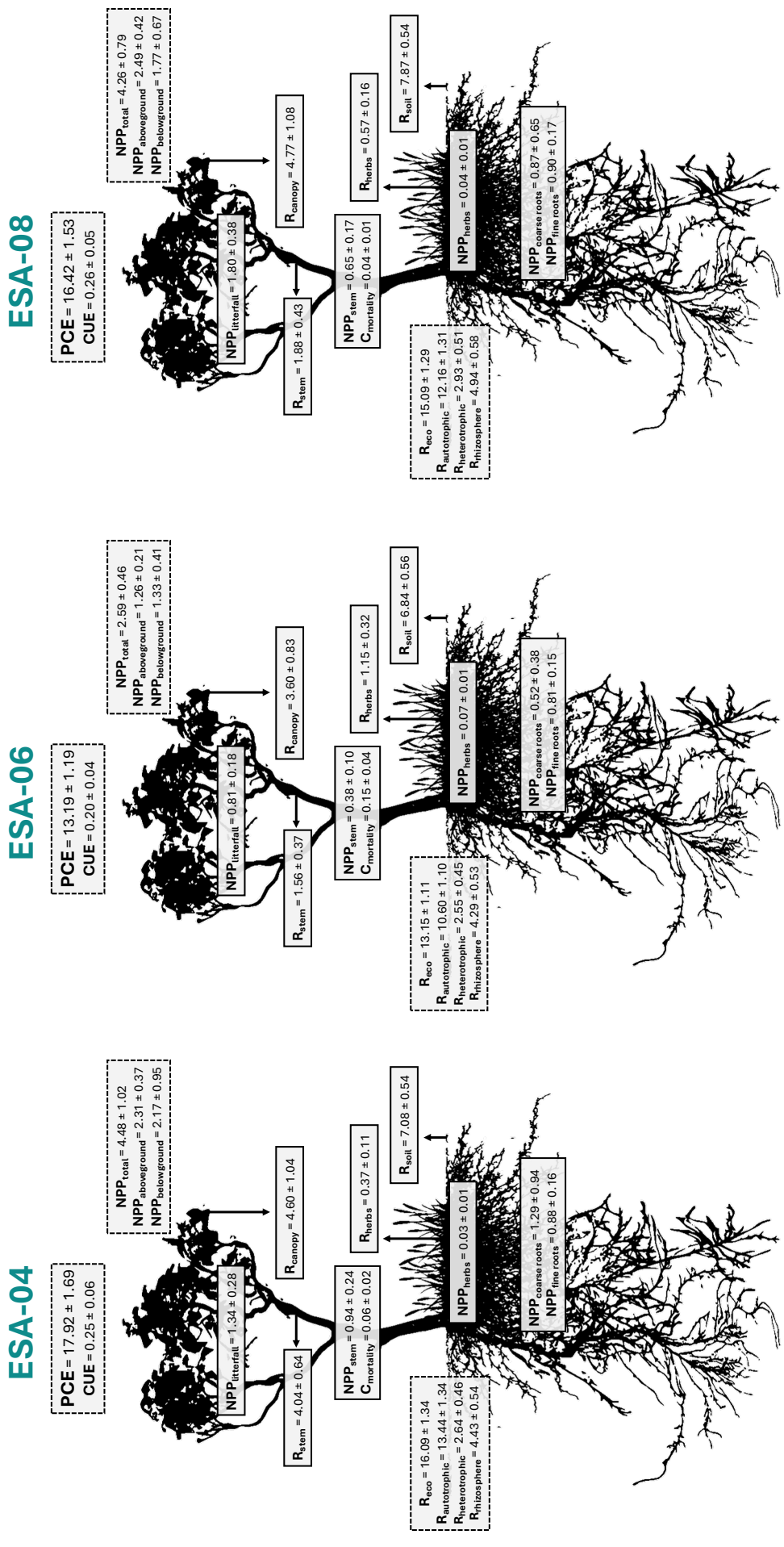


Figure S3.2, main carbon fluxes (MgC ha^{-1} year^{-1}) within the unburnt fire regime at the Estação Ecológica da Serra das Araras, separated by plot. Fluxes were estimated approximately six years into the experimental fire regimes. Where flux estimates were derived from statistical models, plot was used as fixed effect instead of regime.

Chapter 4: Research Paper 2

Bark protection and light-adapted photosynthesis influence woody productivity of Cerrado trees in changing fire regimes.

By Francisco Navarro-Rosales, Wesley Jonatar Alves da Cruz, Edouard Philippe Distin-Carvalho, Manoela Machado, Flavio de Campos Oliveira, Marcelo Leandro Feitosa de Andrade, Maria Antonia Carniello and Imma Oliveras Menor.

Linking statement: This chapter expands on **Chapter 3 (Research Paper 1)** by investigating woody stem productivity dynamics in more detail, focusing on patterns of productivity across tree species. This chapter was motivated by the need to functionally understand why savanna woody productivity declined after repeated burning despite evolutionary adaptations to fire. This chapter uses tree inventory data to identify how fast-growing generalist species dominate productivity in the absence of fire, but become compromised after burning. Then, it explores how long-term fire regimes affect rates of productivity and survival, and describes how leaf, bark, photosynthetic and wood functional traits underpin these long-term changes across the different fire regimes.

Status: This chapter was published on the 29th of April 2026 in the journal Annals of Botany (https://doi.org/10.1093/aob/mcag115). The chapter was originally submitted to the special issue *State of the Global Flora (Cerrado/Tropical Grasslands)*. This work was presented at the 65th Annual Meeting of the Association of Tropical Biology and Conservation in Oaxaca, México, and at the 27th Congress of the "01" Regional Council of Biologists (Cáceres, Brazil).

Contributions: I, Francisco Navarro-Rosales, developed the research questions, contributed to field data collection at Serra das Araras, collated and cleaned the data, performed statistical analyses, produced figures and tables, and wrote and reviewed the manuscript. Imma Oliveras Menor and Maria Antonia Carniello secured funding and designed and coordinated the prescribed burning and monitoring study. Marcelo Leandro Feitosa de Andrade led the controlled burning interventions. Maria Antonia Carniello, Wesley Jonatar Alves da Cruz and Flavio de Campos Oliveira led tree survey campaigns. Wesley Jonatar Alves da Cruz, Manoela Machado, Imma Oliveras Menor, and I collected functional traits data, with contributions from Flavio de Campos Oliveira and Edouard Philippe Distin-Carvalho. Imma Oliveras Menor, Wesley Jonatar Alves da Cruz and Manoela Machado contributed to research hypotheses, analyses, and text editing. Imma Oliveras Menor supervised this research and was involved in all steps of this work.

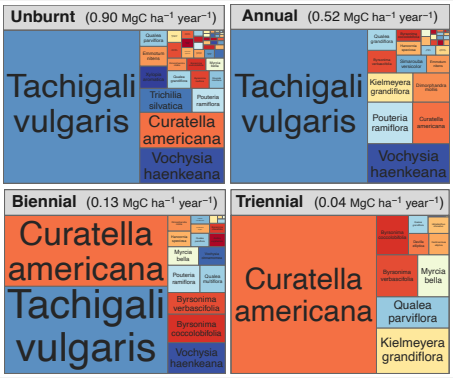
4.1. Graphical abstract

How does the stem productivity of Cerrado trees respond to fire regimes, and can these responses be explained by leaf, bark, wood and photosynthetic functional traits?

Research aims & key findings:

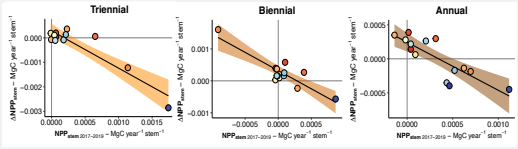
1) Determine species contributions to stem productivity at the community level across fire regimes

Generalist species are hyperdominant under fire exclusion, but contributions to productivity shift with increasing fire intensity

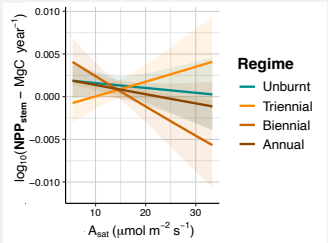


2) Investigate how fire regimes affect stem productivity at the dominant species level (focusing on long-term change)

Trade-off between NPP and fire tolerance (*excluding T. vulgaris*)



3) Explore if traits explain patterns in species-level NPP_{stem}



In the triennially burnt plot (high fire intensity) NPP is maintained by:

bark protection
+
light-adapted photosynthesis

Structure-acquisition dimensionality of traits

4.2. Abstract

Background and Aims: Changes in fire regimes within open ecosystems have important impacts on plant vulnerability, carbon cycling and ecosystem functioning. Thus, in this study, we investigate stem net primary productivity (NPP) dynamics of savanna vegetation in the Amazon-Cerrado transition, making use of an experimental fire and ecosystem monitoring project. We aimed to determine i) how different species contribute to plot-level stem NPP and how this changes with fire frequency; ii) how different fire frequencies affect the average stem NPP and survival of dominant species; and iii) if fire-induced changes in species-level stem NPP and survival are influenced by functional traits.

Methods: We use tree inventory data (height and diameter of stems) to quantify plot- and tree-level stem NPP across unburnt, annual, biennial and triennial fire frequencies. We compare before and after estimates of average stem NPP and survival of dominant species using mixed-effects models, and identify key traits linked with changes in productivity and survival via principal component and regime-interval-trait interaction analyses.

Key Results: Generalist species dominate stem NPP in unburnt conditions (*Tachigali vulgaris* accounts for 72% of NPP), but become less dominant within our less frequent fire regimes (biennially and triennially burnt plots), which favour more sclerophyllous savanna trees. There is a trade-off between plant productivity and tolerance to fire, influenced by functional traits. In less frequent fire conditions (within the triennially burnt plot), tree growth and productivity are determined by bark protection, high photosynthetic rates and photosynthetic shade intolerance.

Conclusions: These findings allow us to better predict how fire regimes of varying frequencies will filter the communities of Cerrado trees, and which set of species will confer greater resilience to landscapes across this threatened region. The diverse productivity strategies of Cerrado vegetation are determined by the interaction between fire regimes and functional traits. Burning can successfully limit woody encroachment and help conserve open ecosystem diversity and functioning in the Cerrado.

4.3. Background and aims

Open ecosystems worldwide are experiencing substantial changes in fire regimes (Goldammer, 2013; Jones *et al*., 2022; Sayedi *et al*., 2024). In savannas, longer dry seasons and more extreme droughts and heatwaves are contributing to an increase in wildfire intensity and frequency (Flannigan *et al*., 2013; Jolly *et al*., 2015), with human activities being linked to increases in flammability and number of ignitions, but also to landscape fragmentation, fuel discontinuity, fire suppression and overall reductions in burnt area (Andela & van der Werf, 2014; Archibald, 2016; Andela *et al*., 2017; Jones *et al*., 2022). The Cerrado – Brazil's savanna region covering more than 2 million km^2 and supporting more than 10,000 native plant species (Giles *et al*., 2026) – is currently threatened by alarming rates of land clearance and increased ignitions for agricultural conversion purposes, which are shifting fire seasons, driving landscape change, and exposing species lacking the ecological adaptations needed to survive new fire regime conditions (Françoso *et al*., 2015; Schmidt & Eloy, 2020; Segura-García *et al*., 2025; Spadoni *et al*., 2025). Cerrado savannas are characterised by relatively frequent fire regimes consisting of low-intensity surface burns, with typical fire intervals ranging between 2-6 years (Eiten, 1972; Pereira *et al.*, 2014; Pivello *et al*., 2021), with fire intervals of 3-4 years appearing to optimise ecosystem functioning and recovery (Pivello & Coutinho, 1992; Kauffman *et al*., 1994; Pivello *et al*., 2010; Oliveras *et al*., 2012). Recent geospatial analyses have revealed that fire activity levels in the central and northern Cerrado have increased over the last four decades due to the expansion of the new agricultural frontier, whilst fire activity and frequency decreased in the South as a result of sweeping clearance and fragmentation (da Silva Arruda *et al*., 2024; Segura-García *et al*., 2025). In the remaining areas of natural vegetation, fire exclusion policies have reduced fire frequency and promoted landscape change via woody encroachment (Rosan *et al*., 2019) which can increase the likelihood of intense fires and have important consequences towards diversity and ecological functioning (Durigan & Ratter, 2016; Kelly *et al*., 2020).

Changing fire regimes can profoundly affect the fitness and persistence of savanna plant species and communities by influencing vital rates, population dynamics and reproduction success (Hoffmann, 2002; Pilon *et al*., 2021; Zirondi *et al*., 2021), which in turn shape ecosystem-level responses in terms of structure and function (Le Stradic *et al*., 2018). Although fire-induced effects on savanna vegetation are highly contextual, frequent fire regimes tend to promote more open landscapes and grass-dominated systems by constraining juvenile trees and promoting the rapid recovery of the herbaceous layer (Higgins *et al*., 2024; Singh *et al*., 2023). In contrast, decreasing fire frequency and occurrence allows for increased tree establishment and the eventual shift towards higher-biomass woody vegetation (Hoffmann *et al*., 2020), which can be associated with acute losses in savanna species richness and ecosystem services (Abreu *et al*., 2017; Skhosana *et al*., 2025). Tropical savannas are thus functionally maintained by fire regimes, where natural or traditional burns are required to promote vegetation regeneration, sustain nutrient cycles, support biodiversity and maintain ecosystem structure (Pivello, 2011; Staver *et al*., 2011).

One of the most informative indicators describing ecosystem functioning is net primary productivity (NPP), defined as the net rate at which ecosystems accrue carbon into organic plant structures (Malhi *et al*., 2011). Studying woody NPP – essentially growth in terms of woody biomass accumulation (Hilty *et al*., 2021) – provides insight into plant performance, ecophysiological processes, climate budgeting, and ecosystem services (Girardin *et al*., 2010; Malhi, 2012). Previous studies in the Cerrado have shown that, for example, burning at different fire frequencies and intensities can significantly affect plant growth and survival (e.g., Rodrigues *et al*., 2021; Rodrigues & Fidelis, 2022; Fontenele & Miranda, 2024) as well as primary production and carbon cycling (e.g., Teixeira *et al*., 2022; Navarro-Rosales *et al*., 2025; Teixeira *et al*., 2025). Despite these findings, scaling up individual- and species-level responses to understand and predict shifts in ecosystem structure and function remains one of the key challenges in deciphering the consequences of changing fire regimes (Grau-Andrés *et al*., 2024).

Using trait-based approaches to investigate functional responses to fire offers a valuable framework for elucidating the mechanistic underpinnings of fire response strategies and their relationship with plant fitness (Clarke *et al*., 2013; Rosell *et al*., 2014). A functional trait framework can help predict how plants in fire-prone ecosystems respond to changes in fire regimes, as traits that confer tolerance and resistance to environmental pressures will shape the fitness and persistence of species and individuals in the face of shifting ecological filters (Plumanns-Pouton *et al*., 2024). Functional traits can thus be used to track community-level responses to changing environmental conditions (Aguirre-Gutiérrez *et al*., 2025) and to distil complex species-environment relationships into generalisable patterns that remain valid across scales and locations (Sommer *et al*., 2014). In areas like the Cerrado, where fire-prone savannas and fire-vulnerable forests are able to coexist as alternative 'stable' states (Staver *et al*., 2011), community composition, vegetation structure and ecosystem function are likely governed by an interplay between fire regimes and plant strategies (Dantas *et al*., 2013). Fire-related traits such as thick bark insulation, bud protection, bud placement, resource storage, and rapid resprouting are common in species subjected to frequent low-intensity fires and are key determinants of woody plant survival and productivity in fire-prone ecosystems (Charles-Dominique *et al*., 2015; Pilon *et al*., 2021). In contrast, resource-acquisition traits, such as lower structural investment, higher photosynthetic capacity and rapid growth rates, allow for increased survival and faster biomass accumulation under fire suppression (Flake *et al*., 2021).

Despite the importance of predicting changes in survival and growth under altered fire regimes – and of understanding the role of functional traits in shaping these responses – few studies have examined how woody productivity changes in relation to both fire regimes and functional traits in the Cerrado (e.g., Terra *et al*., 2021). Thus, the overall aim of our study was to investigate productivity and survival responses of Cerrado savanna trees to changing fire regimes using a functional traits perspective. We make use of a long-term experimental fire project at Serra das Araras, Mato Grosso, Brazil, where, since 2016, we have monitored carbon fluxes and tree size in six permanent plots exposed to different fire frequencies: fire exclusion and annual, biennial,

and triennial burns. In a recent publication (Navarro-Rosales *et al*., 2025), we explored how the reintroduction of fire after 30 years of fire exclusion reduced arboreal carbon fluxes, reflecting a shift in community composition due to the decline of generalist tree species associated with forest-savanna transitions (de Souza *et al*., 2025). Building upon this earlier work, and taking advantage of tree inventory datasets collected every 2 years, we aimed to comprehensively assess the impacts of changing fire regimes – both the continued exclusion of fire and the reintroduction of periodical burning at different frequencies – on woody productivity and survival.

Our overarching hypothesis is that without the effect of fire and other notable disturbances, generalist species relying on fast-growth, resource acquisitive strategies will have a growth and survival competitive advantage over conservative, slow-growing savanna species investing in structural integrity and bark protection (Gignoux *et al*., 2016; Chiminazzo *et al*., 2025). In burnt plots, however, woody productivity and survival will be primarily determined by fire protection and resprouting traits allowing for tissue integrity and regrowth (Scalon *et al*., 2020; Flake *et al*., 2021). We expect fire protection and resprouting traits to have a stronger influence on productivity and survival within the triennially and biennially burnt plots reflecting how these fire regimes supported more intense fire events (Navarro-Rosales *et al*., 2025). We predict the annually burnt plot will show similar patterns to our fire exclusion plots given Cerrado plants have developed strategies allowing for success under both high fire frequencies and fire absence (Chiminazzo *et al*., 2025). To adequately evaluate the validity of these hypotheses, we specifically aim to address the following research objectives:

1. First, we **evaluate differences in species contributions to total stem productivity and mortality at the plot scale, comparing patterns across fire regimes of different frequencies**. In unburnt plots, we expect a higher contribution to NPP from larger, fast-growing generalist species, while in the burnt plots we expect fire-tolerant, conservative savanna trees to contribute most to NPP (as the abundance and growth of fire-vulnerable generalist species are compromised, reducing overall NPP; de Miranda Santos *et al*.,

2024; Navarro-Rosales *et al*., 2025). We expect to observe greater shifts towards savanna-species dominance of NPP_{stem} in our less frequent fire regimes (biennially and triennially burnt plots). We also expect a complementary shift in species contributions to mortality, with generalist species exhibiting higher mortality rates after less frequent, more intense fires (biennially and triennially burnt plots).

2. To understand trends in productivity and mortality at the species level and to evaluate whether there is a trade-off between productivity and fire tolerance, we also aim to **assess if experimental fire regimes influenced average stem productivity and survival rates, focusing on patterns of temporal change across 16 dominant tree species**. We expect fire to have a strongly negative effect on the survival and productivity of fast-growing generalist species, but a more moderate – or even positive – effect on the productivity and survival of conservative savanna trees (Hoffmann & Solbrig, 2003). We predict patterns of change in both survival and productivity will be more pronounced in plots where less frequent fires have likely allowed for increased fire intensity (biennially and triennially burnt plots). Patterns of change should also reflect an underlying trade-off whereby species with the potential for higher vital rates (in the absence of disturbance) will be increasingly fire-vulnerable (Russo *et al*., 2020).

3. Finally, we **investigate whether variations in leaf, bark, wood and photosynthetic plant functional traits explain patterns in the species-level stem productivity and survival rates of dominant tree species.** We hypothesise that average productivity and survival rates in the unburnt plots will be linked with traits reflecting low structural investment and minimal bark protection, coupled with high carbon assimilation and fast resource capture (Flake *et al*., 2021). In the burnt plots, we expect a shift toward trait-performance relationships favouring thicker bark, greater structural investment, and more conservative resource-use strategies (Pausas, 2015; Chiminazzo *et al*., 2023). We expect

shifts in trait-performance relationships to be stronger within the less frequently burnt plots (biennially and triennially burnt plots) as a result of increased fire impacts.

4.4. Materials and methods

4.4.1. Study site and experimental design

Our study was conducted within an area of Cerrado savanna at the Estação Ecológica da Serra das Araras (Serra das Araras Ecological Station) in Porto Estrela municipality, Mato Grosso, Brazil (15º39'10.96"S, 057º12'52.54"W, ~320 m above sea level). Serra das Araras is a 27,000-ha IUCN Category 1A strict conservation unit managed by the Instituto Chico Mendes de Conservação da Biodiversidade (ICMBio). The area plays a key role in biodiversity conservation, placed in a strategic location near the ecotone between the Cerrado, Pantanal and Amazonian ecoregions (ICMBio, 2016). The climate is classified as tropical savanna with dry winter characteristics, having distinct dry (June–September) and rainy (November–March) seasons (Kottek *et al*., 2006; Pizzato *et al*., 2012). Mean annual temperature for the 1979-2010 period was around 25-26ºC, with mean annual rainfall of approximately 1300 mm (Pizzato *et al*., 2012; Santos *et al*., 2018). The site was historically settled by traditional *quilombola* communities and designated a protected area in 1982.

Our experimental design consists of six 1-ha (100×100 m^2) permanent vegetation plots (named ESA-04 to ESA-09), which have been established and monitored since 2017. These plots are part of the ForestPlots Network (Forestplots.net) and are divided into 25 subplots (20×20 m^2) to provide spatial replication/information within the plot unit. The plots have been experimentally subjected to fire, with three regularly burnt plots and three unburnt ones where all fire is excluded. Burnt plots have been burnt at different frequencies: annually (every year), biennially (every two years), and triennially (every three years) to better determine the effects of fire regimes with

different frequencies and intensities on Cerrado vegetation. As of September 2023, the annual plot had been burnt five times (2018, 2019, 2020, 2021, 2022), and the biennial and triennial plots had been burnt twice (2019, 2021 and 2018, 2021 respectively). Experimental burns were undertaken during the peak of the dry season (July – September) to take advantage of good burning conditions and reflecting the altered fire seasonality currently dominating most fire events in the Cerrado (Pivello, 2011). Because the experiment was designed in line with the management plan of the conservation unit – which limits operational resource use and interventions in natural areas – replication of experimental fire regimes was unfeasible. Furthermore, each fire is inherently unique in its behaviour and spread, making it impossible to replicate and randomise distinct disturbance events into consistent and fully replicable fire treatments (van Mantgem *et al*., 2001). We also acknowledge that our fire experiment has had limited time to fully represent well-established altered fire regimes. Consequently, we recognise that our experimental interventions capture the early ecological effects of changing fire regimes involving very few recurrent burns, and that these effects are expected to evolve as fire impacts accumulate and ecosystem processes stabilise over time.

Despite these constraints, the implemented fire regimes exhibited a trade-off between fire frequency and intensity: our more frequent fires (annually burnt plot) led to patchy low-intensity surface burns, and our less frequent fires (biennially and triennially burnt plots) were quicker, homogeneous and more severe (Navarro-Rosales *et al*., 2025).

Upon plot establishment, all six plots shared similar vegetation architecture and composition, although vegetation density varied due to the inherent heterogeneity typical within Cerrado ecosystems. Before the plots were set up, fire had been completely excluded from the monitoring area since 1992. As a result, vegetation was officially classified as *cerrado sensu stricto* (typical woodland savanna) in transition towards *cerradão* (forest-savanna transition woodland), consisting of a mix of small and medium tree species, shrubs and a relatively sparse herbaceous layer (ICMBio, 2016). The transition from open *cerrado* savanna to closed *cerradão* woodland

has resulted from the colonisation of savanna areas by some forest transition species (*Tachigali vulgaris* L.G. Silva & H.C. Lima, *Trichilia silvatica* C.DC, *Vochysia haenkeana* Mart. and *Xylopia aromatica* (Lam.) Mart.). These species are henceforth referred to as 'generalist species' because they are able to occur in both forests and savannas, in contrast with specialist species that are only present in either habitat (Flake *et al*., 2021). Being already found in many savanna areas, they are key to the dynamics of forest development because they able to colonise open sites rapidly after fire is suppressed (Geiger *et al*., 2011). Generalist species are thought to exhibit trait distributions intermediate to those of savanna and forest species, although their functional strategies are still poorly characterised (Chiminazzo *et al*., 2023).

Since 1992, vegetation density has continued increasing in the unburnt plots, while the reintroduction of fire in the burnt plots has reversed the encroachment trend by reducing woody biomass and promoting grass cover (Navarro-Rosales *et al*., 2025). All plots are situated on a relatively flat topography, and underlying soils are classified as dystrophic latosols under the Brazilian soil classification system (EMBRAPA, 2018).

4.4.2. Productivity, survival and mortality data

Ecosystem processes and carbon fluxes have been monitored across the study plots since 2017 (see Navarro-Rosales *et al*., 2025) following the protocols outlined in the RAINFOR-GEM Field Manual for Intensive Census Plots (Marthews *et al*., 2014). A complete vegetation census is conducted at two-year intervals, during which all tree stems with a diameter at breast height (DBH) ≥5 cm and a height ≥3 m are tagged, identified to species level where possible, and measured in terms of DBH and height. Species were identified by experts in local flora (identification was revised by taxonomic specialists where possible) with voucher samples deposited at the Herbário do Pantanal Vali Joana Pott in Cáceres, Mato Grosso. To maximise accuracy and consistency, height measurements were taken using a laser tape, following protocol instructions to determine the measuring point for each stem. Census data (from 2017, 2019, 2021

and 2023) was used to calculate the aboveground woody carbon stock of each individual stem using the Rezende *et al.* (2006) allometric equation for *cerrado sensu stricto*:

$$C = 0.24564 + 0.01456 \cdot H \cdot D^2 \quad (4.1)$$

Where C is aboveground woody carbon (kg), H is tree height (m) and D is diameter (cm). Using this general allometry allowed us to estimate woody carbon for all species whilst maintaining consistency with previous findings (Scalon *et al*., 2022; Navarro-Rosales *et al*., 2025; Reis *et al*., 2025). Aboveground woody stem productivity (NPP_{stem}) for each stem during a given census interval was calculated as the difference in aboveground woody carbon stock between a census and the previous one, standardised by the interval length between measurements (Girardin *et al*., 2010). Thus, NPP_{stem} was individually calculated for stems present at the start and end of each interval (2017-2019, 2019-2021 and 2021-2023). Following the definition of productivity as a measure of biomass increment, NPP_{stem} is typically assumed to be equal to or larger than zero, meaning negative NPP_{stem} values are usually equated to zero or excluded from analysis (Clark *et al*., 2001; Roxburgh *et al*., 2005). However, excluding negative productivity values in our context would have artificially skewed our dataset and removed important information relating to fire effects across species and traits, so we decided to maintain negative NPP_{stem} datapoints. We therefore recognise that our conceptualisation of NPP_{stem} reflects a net carbon balance dominated by biomass increments that also incorporates biomass loss due to branchfall and reduced water storage (Girardin *et al*., 2010; Lim *et al*., 2024) as well as fire consumption and post-fire die-back (Pereira *et al*., 2025).

Two different types of data were used to characterise mortality and survival patterns. To address our first research aim, we quantified mortality as a flow of carbon ($C_{mortality}$). This metric represents the total amount of woody stem carbon lost from the ecosystem carbon pool as a result of tree death, and allows for a direct comparison with carbon gained through NPP_{stem} (both in $MgC\ ha^{-1}\ year^{-1}$). Mortality carbon was defined as the carbon stock of living stems alive in a given

census that died by the following census date, also standardised as an annual rate (Silva *et al*., 2018). For our second and third research aims, we focused on survival as a binary variable (opposite to mortality) where 1 and 0 respectively indicate a stem survived or died during a census interval. We investigated species-level patterns of survival instead of mortality because survival provides a more ecologically meaningful representation of species' responses to environmental conditions and allows for more straightforward analytical interpretation.

4.4.3. Plant functional traits data

To explain patterns in productivity and survival, we investigated the influence of different plant functional traits on both variables. To this end, we measured key leaf, bark, wood and photosynthetic traits of dominant tree species (across all fire regime frequencies) in March 2025 following a standardised trait collection protocol and pipeline (based on Pérez-Harguindeguy *et al*., 2013; Oliveras *et al*., 2020; Wigley *et al*., 2021; and Cruz *et al*., 2025, **Table 4.1**). Dominant species were selected in terms of basal area, and were defined as those contributing the most to up to 80% of the basal area within each plot (Oliveras *et al*., 2020). Dominant species were determined using the data from the most recent census (2023), 4-5 years after the experimental fire regimes were implemented. Thus, 7 dominant species were selected in the annually burnt plot, 9 species in the biennially burnt plot, 8 in the triennially burnt plot, and 10, 6 and 7 species in the unburnt plots (ESA-04, ESA-06 and ESA-08 respectively, see **Table S4.1**). Because the dominant species found in the ESA-06 and ESA-08 unburnt plots overlapped with those in the ESA-04 unburnt plot, trait sampling within the fire exclusion regime was conducted at ESA-04 only to avoid redundancy. This means that we sampled 16 species overall, comprising of 34 species-regime combinations.

For each dominant species specific to each regime (**Table S4.1**), we selected 3-5 surviving individuals adding up to a total of 167 trees. Bark samples were collected across all 167 individuals. Wood density was measured across 102 of these individuals (three individuals per

species per regime), giving preference to stems with the largest DBH to obtain sufficiently large wood cores for analysis while minimising damage (Chave, 2005). Leaf and photosynthetic traits were measured on a separate subset of 102 trees (three individuals per species per regime), selected based on canopy health and the availability of branches large enough (50-100 cm) to maintain leaf hydration post-harvest (Missik *et al*., 2021). For each of these trees, we removed a single branch to sample photosynthetic and leaf traits, using three leaves per tree/branch. Branches were re-cut underwater to prevent xylem embolism, and leaves exhibiting fewer signs of herbivory, senescence, or disease were selected (Busch *et al*., 2024). The full list of sampled traits, along with detailed field methods and data processing techniques used to measure them are presented in **Table 4.1**.

4.4.4. Data analysis and statistical modelling

4.4.4.1. Species contribution to plot-level productivity and mortality across fire regimes

All data processing and statistical analyses were performed in R (version 4.4.2) via R Studio (version 2024.12.0+467). To characterise the contribution of different species towards plot-level NPP_{stem} within each fire regime and census interval, we calculated the total plot/species NPP_{stem} as a sum of all individual NPP_{stem} estimates for each plot/species in each census interval. Similarly, we calculated the total plot and species $C_{mortality}$ as a sum of all individual $C_{mortality}$ estimates for each plot and species in each census interval. We numerically explored and compared differences in contributions to NPP_{stem} and $C_{mortality}$ across plots and intervals. Please note we calculated NPP_{stem} and $C_{mortality}$ separately for our three unburnt plots. Combining data from multiple plots would have distorted patterns of species richness and composition compared to single-plot regimes.

4.4.4.2. Changes in species-level stem productivity and survival rates across fire regimes

Table 4.1, sampling and processing methods used to measure leaf, bark, wood and photosynthetic traits of dominant tree species at the Estação Ecológica da Serra das Araras.

Trait	Units	Methods
Leaf traits		
Leaf area (LA)	cm^2	Fresh leaf projected area was measured using a scaled flatbed colour scanner and the ImageJ image processing software (Schneider *et al*., 2012), avoiding leaf curling or overlapping as much as possible (Perez-Harguindeguy *et al*., 2013). To ensure that leaf area values captured the full extent of the leaf structure, we included the area of the petiole in the case of simple leaves, as well as the area of the rachis and all leaflets in the case of compound leaves (Garnier *et al*., 2017). LA is related to abiotic gradients, phylogeny and ecological strategies.
Leaf dry-matter content (LDMC)	$mg\ g^{-1}$	Leaves were hydrated for 24 hours to measure water-saturated mass (g) then oven-dried at 60ºC for 48 hours to obtain leaf dry mass (mg). LDMC was calculated as leaf dry mass divided by water-saturated mass (Perez-Harguindeguy *et al*., 2013). For compound leaves with leaflets large enough to fill the Li-6800 chamber, we calculated LDMC for the measured leaflet only, to better reflect the leaf traits influencing gas exchange measurements (dos Anjos *et al*., 2014). LDMC is a structural functional trait related with toughness and physical hazards, but inversely correlating with growth (Oliveras *et al*., 2020).
Specific leaf area (SLA)	$mm^2\ mg^{-1}$	SLA was calculated by dividing leaf area by leaf dry mass (see above; Perez-Harguindeguy *et al*., 2013). For compound leaves with leaflets large enough to fill the Li-6800 chamber, we calculated SLA for the measured leaflet only (including leaflet blade and petiolule), to better reflect the leaf traits influencing gas exchange measurements (dos Anjos *et al*., 2014). As one of the components of the leaf economic spectrum, SLA is a key indicator of resource use strategies (Wright *et al*., 2004).
Leaf thickness (LT)	mm	Thickness of re-hydrated leaves was measured using a digital micrometre at three random points along the leaf blade, avoiding the midrib and important secondary veins (Perez-Harguindeguy *et al*., 2013). LT plays a key role in determining the physical strength of leaves, and is an indicator of resource acquisition and physiological adaptations (Araújo *et al*., 2021).
Bark traits		
Outer bark thickness (OBT)	mm	Bark samples (2 x 2 cm) were removed from the stem using a chisel, approximately at 50 cm height (representing the height at which fire usually affects stems during surface fires, Poorter *et al*., 2014). The inner bark (secondary phloem produced by the vascular cambium) and outer bark (corky dead material produced by the cork cambium) layers were carefully separated, and their thickness measured separately at three points with a calliper. Inner bark thickness is related with nutrient transport and water storage, whilst OBT is linked with water retention, pathogen protection and fire insulation (Pausas, 2015).
Inner bark thickness (IBT)	mm	
Relative bark thickness (rBT)	%	rBT was defined as total bark thickness (the sum of OBT and IBT) expressed as a percentage of stem diameter at 50 cm height (Perez-Harguindeguy *et al*., 2013). It is a standard metric of investment into bark protection across stem sizes (Midgley & Lawes, 2016).

Bark density (BD)	g cm^{-3}	The total fresh volume (cm^{-3}) of the (outer and inner) bark samples was determined via the water displacement method (Perez-Harguindeguy *et al*., 2013). Outer and inner bark samples were oven dried at 72ºC for 48 hours until constant weight (Loram-Lourenço *et al*., 2022) to determine total dry mass (g), which was then divided by fresh volume to obtain BD. BD is a key factor in determining bark insulation capacity and flammability (Brando *et al*., 2012).
Bark water content (BWC)	%	BWC represents the mass of water stored in the bark (fresh minus dry mass) expressed as a percentage of dry mass (Loram-Lourenço *et al*., 2022). BWC is linked with drought tolerance and thermal conductivity (Brando *et al*., 2012).
Wood traits		
Wood density (WD)	g cm^{-3}	Wood cores (~5 cm deep) were taken from trees using an increment borer at 50 cm height (Chave, 2005). The total fresh volume (cm^{-3}) of the wood core samples was determined via the water displacement method. Wood core samples were then oven dried at 105ºC for 48 hours until constant weight to determine total dry mass (g), which was then divided by fresh volume to obtain WD (Perez-Harguindeguy *et al*., 2013). WD is a key wood economic spectrum functional trait underpinning plant stability, hydraulics, biomass and growth-survival trade-offs (Chave *et al*., 2009)
Photosynthetic traits		
Shade tolerance (STol)	-	Leaf carbon assimilation at light intensities of 500 and 1500 µmol m^{-2} s^{-1} (A_{500} and A_{1500}) were measured with the LI-6800 portable photosynthesis system (LI-COR biosciences, USA) under standard conditions (temperature at 30ºC, relative humidity at 60% and CO_2 at 420 ppm). STol was calculated as the ratio of A_{500} and A_{1500} (dimensionless). STol values close to 1 and 0.5 respectively indicate shade tolerance (no response to low light levels) vs light demand (negative response to low light levels; Wigley *et al*., 2021).
Light-saturated assimilation (Asat)	µmol m^{-2} s^{-1}	Asat was measured as leaf carbon assimilation at saturating light intensity (2000 µmol m^{-2} s^{-1}) under standard conditions (temperature at 30ºC, relative humidity at 60%, CO_2 at 420 ppm) using the LI-6800 portable photosynthesis system. Asat is a key component of the leaf economic spectrum determining carbon uptake and metabolic capacity (Oliveras *et al*., 2020).
Maximum assimilation (Amax)	µmol m^{-2} s^{-1}	Amax was measured as leaf carbon assimilation at saturating light intensity (2000 µmol m^{-2} s^{-1}) and CO_2 concentration (2000 ppm) under standard temperature (30ºC) and relative humidity (60%) using the LI-6800 portable photosynthesis system. Amax is a valuable metric linked to physiological constraints and indicating metabolic and primary productivity potential (Perez-Harguindeguy *et al*., 2013).
Leaf dark respiration (Dresp)	µmol m^{-2} s^{-1}	Dresp was measured as leaf carbon efflux in dark conditions under standard environments (temperature at 30ºC, relative humidity at 60%, CO_2 at 420 ppm) using the LI-6800 portable photosynthesis system. Leaves remained in the dark for at least 30 minutes before measurement to allow for dark-acclimation. Dresp is a major determinant of leaf/plant metabolic capacity, growth rate and carbon balances, as well as ecosystem carbon cycling (Chambers *et al*., 2004)

We then sought to assess if experimental fire regimes have influenced the stem productivity and survival of the dominant tree species, and to evaluate whether there is a trade-off between productivity and fire tolerance. To this end, we focused on patterns of temporal change across dominant tree species. Our analysis consisted of a series of two-way ANOVAs allowing for an interaction between census interval and fire regime. This way, we estimated average NPP_{stem} and survival rates for each species across each fire regime and census interval. We investigated stem NPP and survival for the pool of 16 dominant species identified across all plots (**Table S4.1**), and species were analysed individually. Building a single model for all species was not ideal because unequal sample size, variance and separation difficulted model convergence and masked coefficient significance.

To estimate NPP_{stem} across regimes and census intervals, we implemented a series of linear mixed-effect models with fire regime and census interval as interactive fixed effects (eq. 4.2) using R packages lme4 (version 1.1–36, Bates *et al*., 2015) and lmerTest (version 3.1–3, Kuznetsova *et al*., 2017). Where model convergence and singular fit allowed, we also included random effects to account for plot and subplot groupings, as well as repeated measures. To model survival probabilities, we built a series of Firth's bias-reduced logistic regressions interacting regime and interval (eq. 4.3) using the logistf package (version 1.26.0, Heinze & Schemper, 2002). Although this approach prevented us from incorporating random effects accounting for spatial groupings (repeated measures of survival are considered independent), it allowed us to better account for poor separation in survival data and provide more robust and reliable estimates of standard errors and p-values.

$$(4.2) \quad \text{lmer}(\log_{10}(NPP_{stem} + 0.1) \sim regime * interval + (1|\, plot) + (1|\, subplot) + (1|\, tree\ tag))$$

$$(4.3) \quad \text{logistf}(survival \sim regime * interval)$$

Because model coefficients are provided in the transformed scale and relative to the reference value, we then used the emmeans package (version 1.10.0, Lenth, 2024) to extract NPP_{stem} and

survival marginal means for each regime-interval combination. We then contrasted these marginal means at the regime level to determine significant differences in NPP_{stem} and survival across intervals within each fire regime, focusing on the differences between the first (2017-2019) and last (2021-2023) census intervals. This way, we were able to statistically test if experimental fire regimes influenced the average stem productivity and survival rates, and to then explore if there is a link between productivity and vulnerability to fire.

To evaluate whether there is a trade-off between productivity and fire tolerance, we investigated if there is an overall relationship between initial productivity under unburnt conditions and resistance to fire in terms of productivity and survival change. Using the marginal means derived from our species-specific models, we extracted estimates of initial NPP_{stem} for each fire regime and species, and used the contrasts between the first (2017-2019) and last (2021-2023) interval to obtain values for change in NPP_{stem} (ΔNPP_{stem}) and survival (Δsurvival) at the regime-species level. We then described the relationship between species-level initial NPP_{stem} and ΔNPP_{stem} (eq. 4.4), and initial NPP_{stem} and Δsurvival (eq. 4.5) using linear models (Δsurvival estimates were kept in the logit scale to maintain model linearity). Because NPP_{stem} dynamics were dominated by *Tachigali vulgaris* L.G. Silva & H.C. Lima, we ran these linear models twice, with and without data for this species, to account for any potential outlier effect.

$$(4.4) \quad \mathrm{lm}(initial\ NPP_{stem} \sim \Delta NPP_{stem})$$

$$(4.5) \quad \mathrm{lm}(initial\ NPP_{stem} \sim \mathrm{logit}(\Delta survival))$$

4.4.4.3. Explaining species-level stem productivity and survival through functional traits

To understand how functional traits influence productivity and survival through contrasting plant strategies, we first explored the relationships and covariation among leaf, bark, wood and photosynthetic traits. To do this, we carried out a principal component analysis (PCA) of standardised traits for individuals from across all fire regimes to determine how traits covary in

multidimensional trait space. Due to incomplete overlap between individuals sampled for wood traits versus leaf and photosynthetic traits, incorporating WD data meant a reduced sample size obscuring patterns in our PCA analysis. To address this, we performed the PCA analysis twice, with and without wood density data. We first used individuals with data for bark, leaf, and photosynthetic traits, excluding wood traits (N = 115), and then used individuals with complete trait data including wood density (N = 71).

Finally, we determined if functional traits influenced the effect of experimental fire regimes on NPP_{stem} and survival across dominant species using a series of linear mixed models fitted with the glmmTMB package (McGillycuddy *et al*., 2025), which allowed us to incorporate a more complex model structure without compromising model convergence. For productivity, we matched individual-scale trait and productivity data from the set of 167 trees sampled in 2025. We modelled log-transformed NPP_{stem} as a function of a triple interaction between fire regime, interval and trait; repeating the analysis for each trait and including random effects for species and tree tag where possible (eq. 4.6). In this case, the models' outputs revealed if NPP_{stem} differs across the regime, interval and trait-gradient combinations. Inspecting the significance of the regime:interval:trait interaction coefficients allowed us to determine if the influence of a given trait on NPP_{stem} differs from one regime to another due to the cumulative, long-term effects of burning. For survival, a slightly different approach was used due to the constraint presented by all trees sampled in 2025 having remained alive throughout the monitoring period. In this instance, we calculated an average trait value for each of the dominant species in each regime. We matched individual-scale survival data from across the six plots to their corresponding trait average, and investigated how survival varied across a triple interaction between regime, interval and trait using a generalised linear mixed model with binomial distribution (eq. 4.7). We also inspected the regime:interval:trait interaction coefficients to discern if the relationship between trait and survival is influenced by the effects of the different fire regimes.

$$\text{(4.6)}\quad \text{glmmTMB}(log_{10}(NPP_{stem} + 0.1) \sim regime * interval * \boldsymbol{trait} + (1|\, species) + (1|\, tree\ tag), \text{family} = \text{gaussian})$$

$$(4.7) \quad \text{glmmTMB}(survival \sim regime * interval * \boldsymbol{trait} + (1|\, plot) + (1|\, species), \text{family} = \text{binomial})$$

We also included tree size data from the last (2023) census into our functional traits analyses, treating DBH and H as additional functional traits. This allowed us to determine if productivity and survival size-dependency vary across fire regimes, accounting for the physical dimension component of plant strategies (Chiminazzo *et al*., 2025).

4.5. Results

Across the four censuses, we identified and measured a total of 4,623 living stems, representing 69 species from 33 botanical families. At the first census (2017), the plots collectively supported 62 species: 28, 34 and 42 species in the triennially, biennially and annually burnt plots, respectively, and an average of 41 species across the unburnt plots. Between the first (2017-2019) and last (2021-2023) interval, average total NPP_{stem} in the burnt plots declined by 0.16 MgC ha^{-1} $year^{-1}$, while $C_{mortality}$ increased by 0.87 MgC ha^{-1} $year^{-1}$. In contrast, unburnt plots showed increases in average NPP_{stem} (0.19 MgC ha^{-1} $year^{-1}$), and $C_{mortality}$ (0.07 MgC ha^{-1} $year^{-1}$), over the same period.

4.5.1. Species contribution to plot-level productivity and mortality

During the initial census interval (2017-2019), the contributions to stem woody productivity were overwhelmingly dominated by *Tachigali vulgaris* L.G. Silva & H.C. Lima, both in the burnt and unburnt plots (please refer to **Figure S4.1**). On average, initial NPP_{stem} of *T. vulgaris* was 0.29 MgC ha^{-1} $year^{-1}$ across all six plots, representing approximately 70% of the total plot NPP_{stem}. Overall, the population of *T. vulgaris* was about eight times more productive than the species with second-highest NPP_{stem}. From 2017 to 2019 *Vochysia haenkeana* Mart. was the second most productive species in all plots except for the ESA-08 unburnt plot, where *Curatella americana* L.

came second whilst *V. haenkeana* ranked fourth. *V. haenkeana* and *C. americana* respectively supported an average of 11.5% and 7.5% of total plot NPP_{stem}. Other species repeatedly appearing in the top 5 most productive were *Xylopia aromatica* (Lam.) Mart. (in the ESA-04 and ESA-08 unburnt plots and in the triennial plot) and *Dimorphandra mollis* Benth. (in the ESA-06 and ESA-08 unburnt plots and in the annual plot). Other top-ranking species in terms of abundance included *Pouteria ramiflora* (Mart.) Radlk., *Myrcia bella* Cambess. and *Kielmeyera grandiflora* (Wawra) Saddi, respectively accounting for 0.0015, -0.0014 and -0.0012 MgC ha^{-1} $year^{-1}$ of NPP_{stem} on average from 2017 to 2019, where negative values for *M. bella* and *K. grandiflora* indicate a net loss of biomass.

In the burnt plots, fire reduced total NPP_{stem} and shifted the way species contributed to it, limiting the hyperdominance of *T. vulgaris* and other generalist species. In the long term, between 2017-2019 and 2021-2023, the stem productivity of *T. vulgaris* decreased by 0.159, 0.098, and 0.153 MgC ha^{-1} $year^{-1}$ in the triennial, biennial and annual plots (accounting for -7%, 41% and 63% of total plot NPP_{stem} during 2021-2023), but increased by an average of 0.13 MgC ha^{-1} $year^{-1}$ in the unburnt regime. Remarkably, *T. vulgaris* becomes even more dominant in unburnt plot ESA-08, providing 91% of total stem productivity during the last interval (**Figure 4.1**). Total NPP_{stem} for *V. haenkeana* and *X. aromatica* also decreased consistently across all burnt plots, unlike *C. americana*, *M. bella* and *K. grandiflora*, which consistently increased in NPP_{stem}. *C. americana* became the most productive species in the triennially burnt plot, accounting for 83% of NPP_{stem} (0.031 MgC ha^{-1} $year^{-1}$), with *Qualea parviflora* Mart., *Byrsonima verbascifolia* (L.) DC. and *Byrsonima coccolobifolia* Kunth appearing as new top-ranking species in terms of NPP_{stem}.

Fire also increased and shifted species' contributions towards $C_{mortality}$ across the monitoring plots. Mortality rates were minimal during the first interval (2017-2019): only 4 stems died on average across the burnt plots (0.023 MgC ha^{-1} $year^{-1}$) compared to 3.7 stems across the unburnt ones (0.014 MgC ha^{-1} $year^{-1}$). During the last interval (2021-2023) mortality increased to 12 stems per hectare in the unburnt plots (0.088 MgC ha^{-1} $year^{-1}$), compared to an average of 25 stems (0.891

MgC ha^{-1} $year^{-1}$) in the burnt plots (**Figure 4.1**). *T. vulgaris* accounted for most $C_{mortality}$ in the triennial (42%), biennial (65%), annual (68%) and ESA-06 unburnt (62%) plots; *V. haenkeana* ranked second in the triennial (24%), biennial (8%), annual (13%) plots. *M. bella*, *K. grandiflora* and *Hancornia speciosa* Gomes consistently reappeared as top-ranking species in terms of $C_{mortality}$ in unburnt conditions.

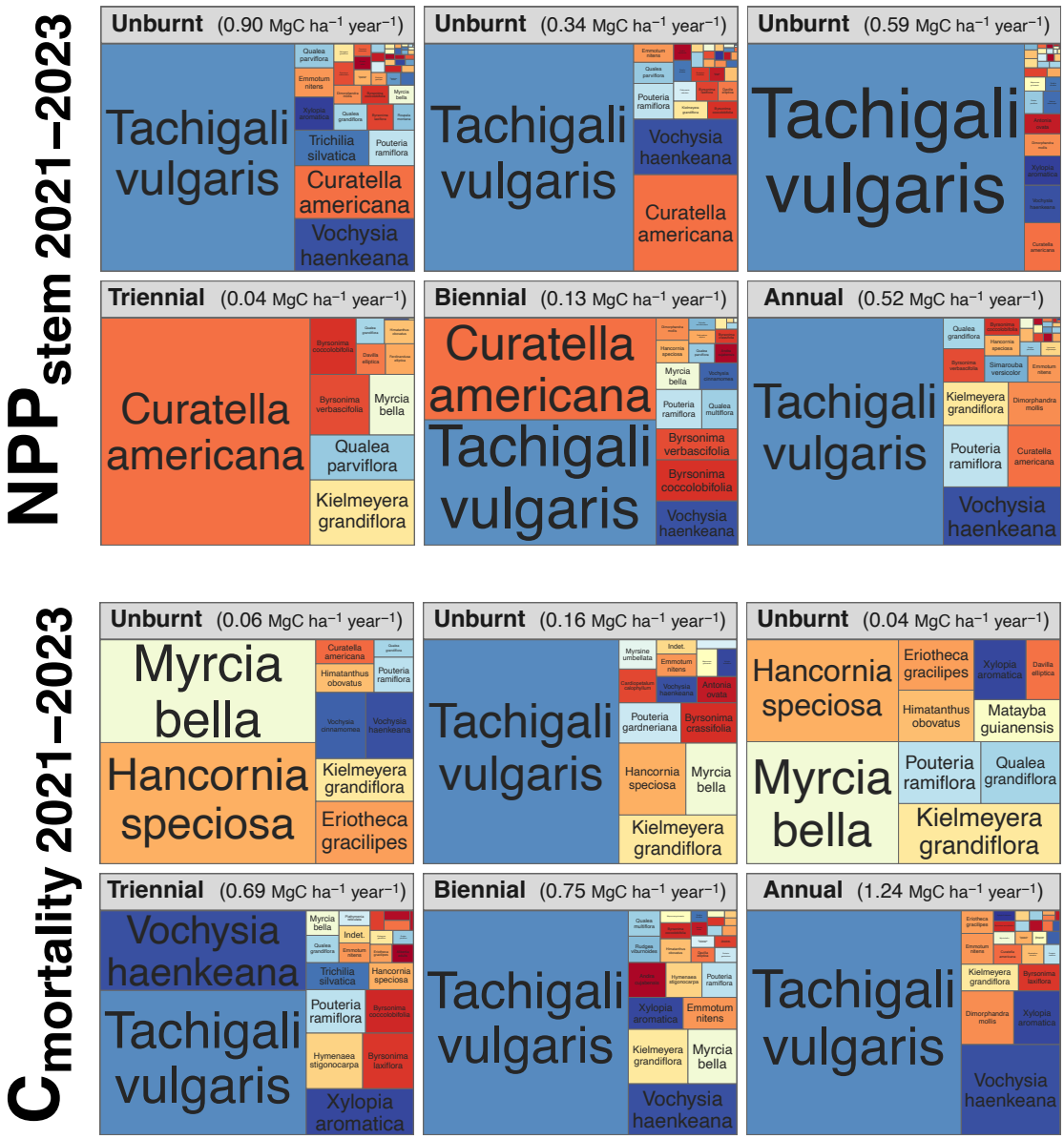


Figure 4.1, species contributions towards plot-level aboveground woody stem net primary productivity (NPP_{stem}) and mortality carbon ($C_{mortality}$) across the experimental fire monitoring plots at Serra das Araras, Brazil, during the 2021 to 2023 census interval. Within each facet, the area occupied by any given species represents its proportion of total plot NPP_{stem} and $C_{mortality}$ (total plot values are included above each facet). Please note this figure illustrates differences in community NPP_{stem} and $C_{mortality}$ at the plot-level.

4.5.2. Fire regime changes in species-level stem productivity and survival

We investigated fire-driven changes in average productivity at the species level using linear mixed-effects models. Model marginal means (please refer to **Figure S4.3** and **Table S4.2**) indicated species NPP_{stem} estimates before and after the long-term effects of our fire regimes. These revealed *T. vulgaris* also supported the highest rates of NPP_{stem} at the species level. During the first interval (2017-2019), estimated NPP_{stem} for *T. vulgaris* was 0.00308 ± 0.00117, 0.00213 ± 0.00113, 0.00577 ± 0.00116, and 0.00339 ± 0.00065 MgC $year^{-1}$ in the triennial, biennial, annual and unburnt fire regimes respectively. After *T. vulgaris*; *V. haenkeana*, *Trichilia silvatica* C.DC, and *C. americana* were most productive species, respectively showing NPP_{stem} rates of 0.00120, 0.000676 and 0.000419 MgC $year^{-1}$ on average across all regimes during this first interval. Two species, *K. grandiflora* and *M. bella*, revealed slightly negative NPP_{stem} rates in unburnt conditions during the first interval (respectively -0.0000629 ± 0.0000125 and -0.0000461 ± 0.0000195 MgC $year^{-1}$).

Marginal mean contrasts allowed us to test if the implementation of experimental fire regimes significantly affected NPP_{stem} for each of the dominant species between the first (2017-2019) and last (2021-2023) intervals (lmer emmeans contrasts, $p < 0.05$, see **Figure 4.2**). In the unburnt plot, the average NPP_{stem} of *K. grandiflora*, *M. bella*, *P. ramiflora*, and *T. vulgaris* increased, but that of *X. aromatica* decreased. The average NPP_{stem} of *B. verbascifolia*, *P. ramiflora*, and *T. vulgaris* increased significantly in the annually burnt plot, whilst individuals of *B. coccolobifolia*, *B. verbascifolia* and *T. vulgaris* became more productive in the biennially burnt plot. In the triennially burnt plot, the average NPP_{stem} of *K. grandiflora* increased, but that of *T. vulgaris* and *V. haenkeana* decreased. *T. vulgaris* showed the strongest long-term reduction in average NPP_{stem} (-0.036476 ± 0.01450 MgC $year^{-1}$) within the triennially burnt plot.

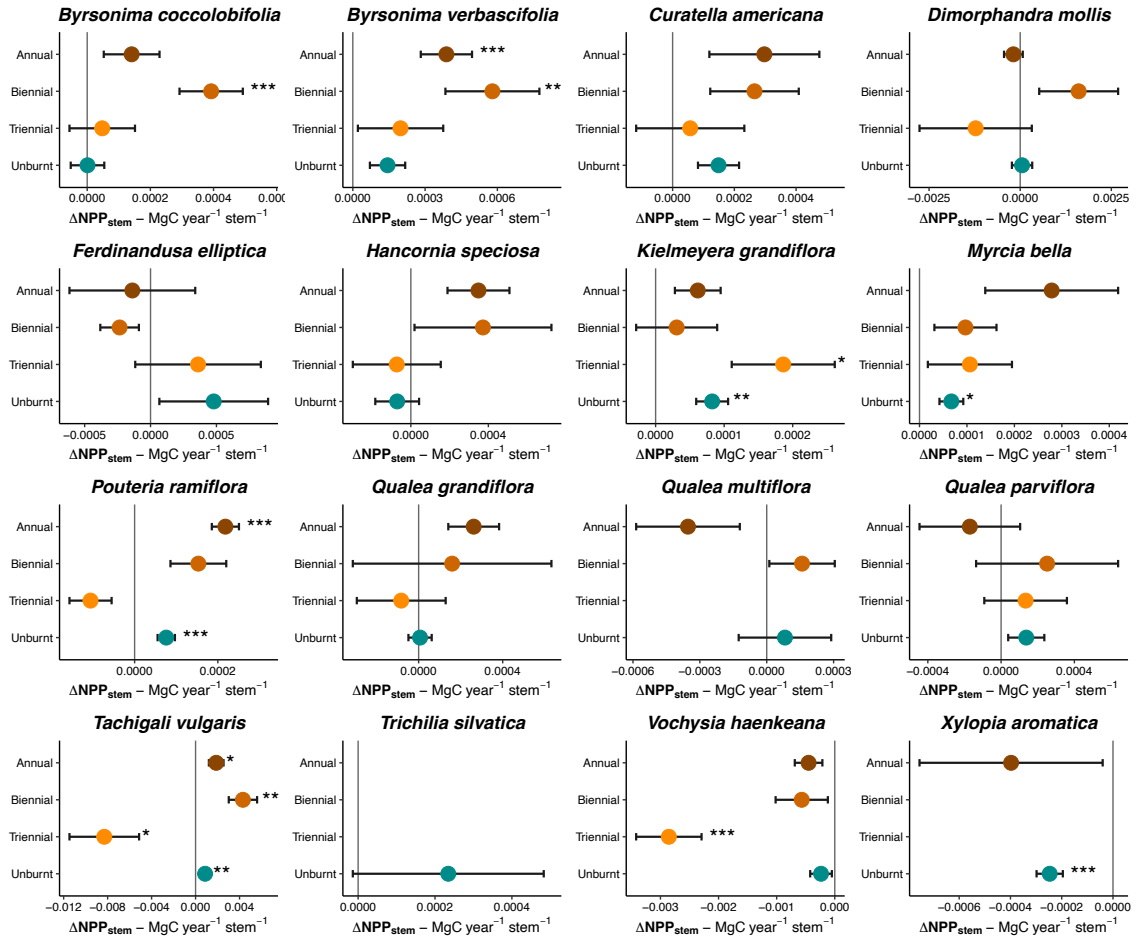


Figure 4.2, change in species-level NPP_{stem} (MgC ha^{-1} $year^{-1}$) for each of the 16 dominant species across the experimental fire regimes at Serra das Araras, Brazil. Points illustrate differences between NPP_{stem} estimates for the first (2017-2019) and last (2021-2023) census intervals (represented by ΔNPP_{stem}, alongside standard error). These NPP_{stem} estimates represent marginal means derived from mixed-effect models specific to each species (see **Table S4.2** and **Figure S4.3**). Statistical contrasts between marginal means were undertaken in the log-transformed scale to determine if triennial, biennial and annual burns, as well as fire exclusion, had a long-term effect on NPP_{stem}. Asterisks indicate statistically significant contrasts between intervals (* $p < 0.05$, ** $p < 0.01$, *** $p < 0.001$) within each fire regime. The vertical grey line for each graph indicates zero ΔNPP_{stem}. Axis ranges were allowed to vary to facilitate visual interpretation. Empty spaces indicate we were unable to calculate ΔNPP_{stem} because marginal mean estimates were not available.

We investigated fire-driven changes in survival rate at the species level using bias-reduced logistic regression models. Contrasts between model marginal means indicating survival for our first and last intervals (logistf emmeans contrasts, $p < 0.05$, **Figure S4.4**, **Table S4.3**) revealed significant changes in survival due to the long-term effects of our fire regimes (**Figure 4.3**). For example, survival of *B. coccolobifolia* and *P. ramiflora* declined in the triennial plot, whilst that of *M. bella*, *P. ramiflora* and *K. grandiflora*, decreased in the biennial plot. The latter also showed

reduced survival in the annual plot. Survival rates of *T. vulgaris*, *T. silvatica*, *V. haenkeana* and *X. aromatica* fell drastically across all the burnt plots. For these species, rates of survival were lowest in the triennially burnt plot (respectively: 0.088 ± 0.069, 0.083 ± 0.113, 0.236 ± 0.071, 0.019 ± 0.026) followed by the biennially (respectively: 0.147 ± 0.046, 0.250 ± 0.306, 0.403 ± 0.081, 0.063 ± 0.086) and annually (respectively: 0.426 ± 0.053, NA, 0.534 ± 0.046, 0.078 ± 0.062) burnt plots. *H. speciosa* and *M. bella* were the only two species whose survival decreased in the unburnt fire regime.

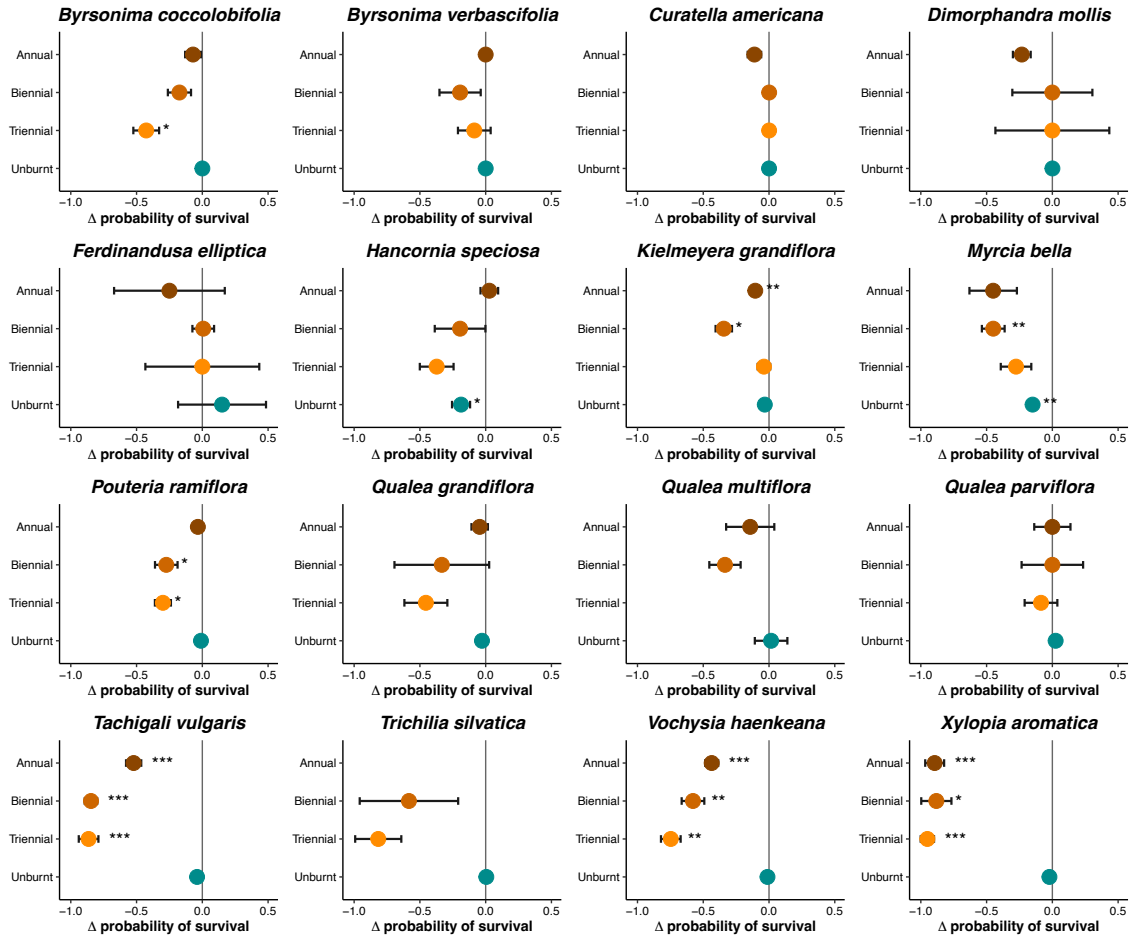


Figure 4.3, change in species-level survival for each of the 16 dominant species across the experimental fire regimes at Serra das Araras, Brazil. Points illustrate differences between probability of survival for the first (2017-2019) and last (2021-2023) census intervals (represented by Δsurvival, alongside standard error). These survival estimates represent marginal means derived from logistic regression models specific to each species (see **Table S4.3** and **Figure S4.4**). Statistical contrasts between marginal means were undertaken in the logit scale to determine if triennial, biennial and annual burns, as well as fire exclusion, had a long-term effect on survival. Asterisks indicate statistically significant contrasts between intervals (* $p < 0.05$, ** $p < 0.01$, *** $p < 0.001$) within each fire regime. The vertical grey line for each graph indicates zero Δsurvival. Empty spaces indicate we were unable to calculate Δsurvival because marginal mean estimates were not available.

After extracting the species level NPP_{stem} marginal means and calculating the degree of change between 2017-2019 and 2021-2023, we used linear models to compare the relationship between initial productivity and ΔNPP_{stem}. We identified a negative relationship between initial NPP_{stem} and ΔNPP_{stem} in the triennial plot, but a positive one within the biennial, annual and control plots (please refer to model parameters in **Table S4.4**). However, once data from *T. vulgaris* was excluded, we observed a consistently negative relationship between initial productivity and ΔNPP_{stem} across all burnt plots (**Figure 4.4**, **Table S4.5**). We found a negative relationship between initial NPP_{stem} and Δsurvival of all 16 species within the biennially burnt plot. Although not statistically significant, Δsurvival also appears to be negatively related to initial NPP_{stem} within the unburnt and triennially and annually burnt plots (**Table S4.6**). When *T. vulgaris* was excluded, there also appeared to be negative non-significant relationships between initial NPP_{stem} and Δsurvival across the burnt plots (**Table S4.7**).

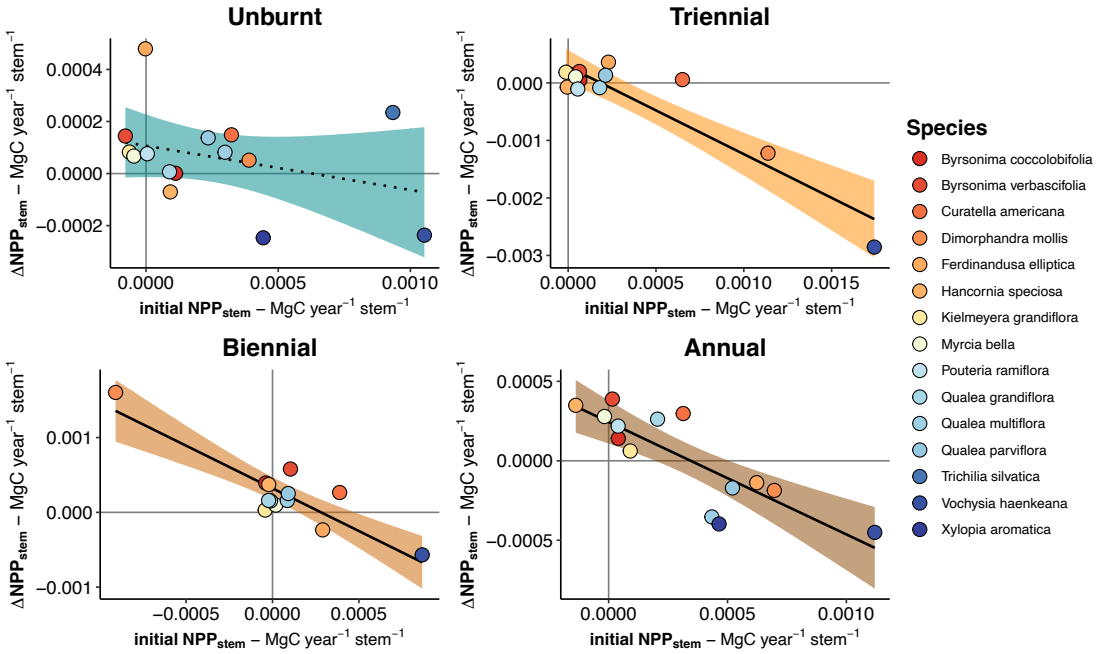


Figure 4.4, trade-off between initial NPP_{stem} (marginal means for the 2017-2019 interval) and NPP_{stem} change (ΔNPP_{stem}, contrasts between 2017-2019 and 2021-2023 marginal means) for the dominant species across the experimental fire regimes in Serra das Araras (excluding *Tachigali vulgaris*). Solid lines represent significant relationships. Please note axis ranges were specific to each plot, and allowed to vary to facilitate visual understanding. Vertical and horizontal grey lines at zero initial NPP_{stem} and zero ΔNPP_{stem} were also included to facilitate interpretation.

4.5.3. Relating species stem productivity and survival to functional traits

PCA analyses were conducted on standardised bark, leaf and photosynthetic trait data to identify major axes of variation in the species trait space. The first principal component of this PCA (PC1) explained 25.2% of the total variance and primarily captured variation along a gradient of diverging structural investment strategies (**Figure 4.5**, please refer to PC loadings in **Table S4.8**). PC1 was positively associated with H, BD, DBH, SLA, LDMC and BWC, and negatively with rBT, LT and OBT. The second principal component (PC2) accounted for 16.8% of the variation, representing variation along a photosynthetic and metabolic gradient. PC2 was positively associated with STol and Dresp, but negatively with Amax, Asat and LA. Together, PC1 and PC2 explained 42% of the total trait variation.

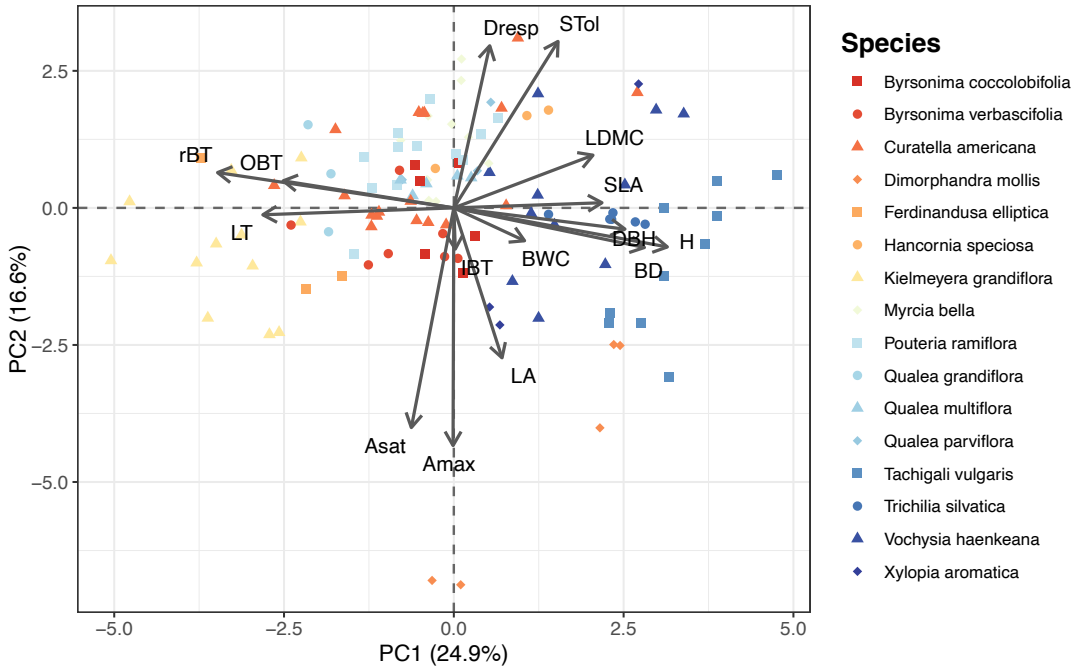


Figure 4.5, principal component analysis (PCA) for standardised bark, leaf and photosynthetic traits of dominant tree species across the experimental fire regimes in Serra das Araras. Amax = maximum photosynthetic rate, Asat = light-saturated photosynthetic rate, BD = bark density, BWC = bark water content, DBH = diameter at breast height, Dresp = leaf dark respiration, H = height, IBT = inner bark thickness, LA = leaf area, LDMC = leaf dry-matter content, LT = leaf thickness, OBT = outer bark thickness, rBT = relative bark thickness, SLA = specific leaf area, STol = photosynthetic shade tolerance.

Dominant species clustered along both axes of variation indicating different strategies. Cerrado species investing in bark and leaf protection such as *K. grandiflora* were positioned in the negative regions of PC1, in contrast with large, fast-growing species such as *T. vulgaris*. Species with large leaf areas and high photosynthetic rates such as *D. mollis*, clustered in the negative region of PC2, unlike those with smaller leaves and slower carbon assimilation (e.g., *M. bella*). Performing a PCA with individuals with complete trait data (including WD) revealed similar results, again showing two axes of variation associated with structural investment (25.2% of variance) and photosynthetic (13.7% of variance) strategies (**Figure S4.5**). Although smaller sample size makes patterns less clear, WD remains positively associated with PC1 (**Table S4.9**).

Finally, we determined if functional traits influenced the effect of experimental fire regimes on NPP_{stem} using mixed models incorporating a triple interaction between fire regime, interval and trait. Our findings revealed that in unburnt conditions during the first interval, NPP_{stem} appeared to be positively associated with LA, LDMC, OBT, BD, WD, Asat, Amax, DBH and H; but negatively linked with LT, SLA, IBT, rBT, BWC, STol and Dresp; although only DBH and H showed significant coefficients (gaussian glmmTMB, $p < 0.05$). Inspecting the interaction coefficients between trait, regime, and the 2021-2023 period allowed us to determine if the influence of a given trait on NPP_{stem} differs from that within unburnt conditions due to the long-term effects of burning (**Figure 4.6**). Our models for SLA and WD revealed a stronger association between traits and NPP_{stem} in the biennial regime (see **Table S4.10** and **Table S4.11**), but not across the other burnt plots. In the triennial plot, OBT (see **Table S4.12**) rBT (see **Table S4.13**) and Asat (see **Table S4.14**) were more positively associated with NPP_{stem}, whilst STol showed a significantly more negative relationship with NPP_{stem} (see **Table S4.15**). DBH and H were linked to higher NPP_{stem} values in the biennial fire regime compared to the unburnt plots, but lower NPP_{stem} in the triennially and annually burnt plots (see **Table S4.16** and **Table S4.17**). Our models interacting survival with species-level traits across fire regimes and intervals revealed survival is positively linked with LDMC and BWC in unburnt conditions, but negatively with rBT (binomial

glmmTMB, $p < 0.05$). In the 2021-2023 interval, survival was more negatively associated with IBT (see **Table S4.18**) and Amax (see **Table S4.19**) in the biennially burnt plot.

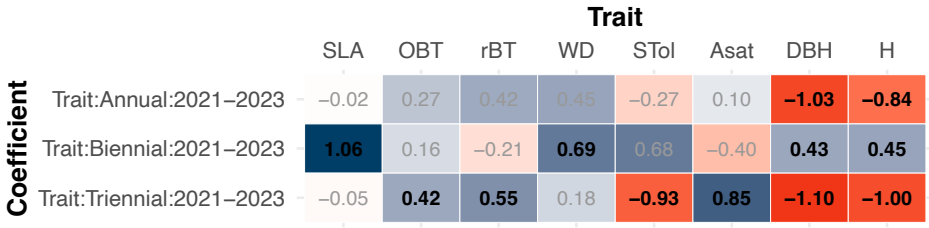


Figure 4.6, model coefficients for the interaction between traits, regimes, and the 2021-2023 census interval. Significant effects indicate the relationship between a given trait and NPP_{stem} differs from that within unburnt conditions due to the long-term effects of burning. The displayed effect sizes are standardised to allow for cross-trait comparisons, where an effect of 1 means a 1 standard deviation increase in traits is associated with a 1 standard deviation increase in NPP_{stem}. Bold numbers indicate statistically significant effects ($p < 0.05$). Traits include light-saturated photosynthetic rate (Asat), diameter at breast height (DBH), height (H), outer bark thickness (OBT), relative bark thickness (rBT), specific leaf area (SLA), photosynthetic shade tolerance (STol), and wood density (WD).

4.6. Discussion

Although previous studies have examined the effects of fire on community composition and growth (e.g., Reis *et al*., 2015; Montenegro *et al*., 2025), explored the relationship between productivity and community composition and diversity (e.g., Vourlitis *et al*., 2024), or investigated the role of functional traits in shaping growth and survival (e.g., Rossatto & Franco, 2017; Cruz *et al*., 2025), our study is among the first to integrate woody productivity contribution dynamics in relation to fire regimes and functional traits within the Cerrado. We found that generalist species disproportionately dominate stem NPP in fire exclusion plots, with *T. vulgaris* alone accounting for over 70% of NPP_{stem}. Generalist species become less dominant after fire, especially in our less frequent fire regimes (biennially and triennially burnt plots), which favours more typical savanna trees. With regards to species-level NPP_{stem}, we identified a trade-off between plant productivity and tolerance to fire in terms of ΔNPP_{stem} across all burnt regimes. More productive species (in conditions without fire) showed a greater long-term reduction in

NPP_{stem} after the introduction of experimental burns. However, this trade-off was only apparent, when estimates for *T. vulgaris* are removed, indicating its strong influence on plot-level patterns. Furthermore, we found that functional traits strongly influence species-level NPP_{stem} responses under our less frequent fire regimes (biennially and triennially burnt plots), likely as a result of increased fire intensity. Productivity was positively associated with bark protection, and photosynthetic rates, but negatively linked to photosynthetic shade intolerance. In the following sections, we interpret and synthesise the significance of these results, discussing the ecological implications of our findings.

4.6.1. Contributions to NPP_{stem} and $C_{mortality}$ reveal hyperdominance of *Tachigali vulgaris* and reflect trends of encroachment vs openness

Previous studies have demonstrated that a restricted number of species often contributes disproportionately to plant abundance and biomass in tropical ecosystems, a pattern observed at local, regional and continental scales (e.g., Macía & Svenning, 2005; Damasco *et al*., 2021). Although most research into hyperdominant species has focused on tropical forests (ter Steege *et al*., 2013; Fauset *et al*., 2015), species hyperdominance can also be found across savannas worldwide (Shirima *et al*., 2011; Amara *et al*., 2023), being an important characteristic of savanna formations such as the Miombo woodlands of Southern Africa (Ribeiro *et al*., 2013) and the Eucalypt rangelands of Northern Australia (Chen *et al*., 2003). Hyperdominance is also typical of Cerrado vegetation, where low soil fertility, toxic aluminium concentrations, and fire are key filters shaping species distributions (Solórzano *et al*., 2012; Terra *et al*., 2021; de Souza *et al*., 2022; Alvarez *et al*., 2025). The dominant species assemblage at Serra das Araras matches biogeographic patterns of diversity and commonness identity for Cerrado vegetation (Bridgewater *et al*., 2004; Machado *et al*., 2019), reflecting advantageous strategies that allow dominant species to, for example, fix nitrogen (Fabaceae; Faria *et al*., 1989) or tolerate high aluminium concentrations (Vochysiaceae; Haridasan, 2008). Our results corroborate previous

findings, revealing that at the start of our experiment, the monitoring plots at Serra das Araras were functionally dominated by a few generalist species: *V. haenkeana*, *X. aromatica*, *T. silvatica* and, above all, *T. vulgaris*, which single-handedly accounted for over 70% of woody productivity.

T. vulgaris belongs to a taxonomically complex and unresolved genus (*Tachigali* Aubl., partially synonymous to *Sclerolobium* Vogel) of leguminous trees widely distributed throughout the Neotropics (Deccache *et al*., 2024). Although accurate *Tachigali* identification remains challenging within plot-based inventories – warranting caution in species-level interpretations and emphasising the need for continued taxonomic revision and phylogenetic studies (Silva & Lima, 2007), Cerrado-based studies consistently document patterns of hyperdominance and habitat generalism across the genus (Solorzano *et al*., 2012; da Silva *et al.*, 2016; Silva Neto *et al*., 2016; Aguiar *et al.*, 2019; Alvarez *et al.*, 2025). The literature also supports the characterisation of *Tachigali* as disturbance-resistant, fast-growing trees driving forest expansion in Cerrado savannas (do Vale & Felfili, 2005; Aquino *et al*., 2007; Pellizzaro *et al*., 2017; Oliveira *et al*., 2021; Neri *et al*., 2023). At the Parque Municipal do Bacaba in Nova Xavantina, Mato Grosso, multiple studies have reported a growing dominance of *T. vulgaris* (Franczak *et al*., 2011; Morandi *et al*., 2016; Oliveira *et al*., 2017; Peixoto *et al*., 2017; Elias *et al*., 2019) and revealed a substantial increase in its post-fire basal area due to the growth of surviving individuals (Reis *et al*., 2015; Reis *et al*., 2017). Our results also suggest that the growth of *T. vulgaris* may be stimulated by fire, as evidenced by disproportionately high NPP_{stem} rates among surviving individuals in the annually and biennially burnt plots. In comparison to other generalist species, increased growth after more frequent, less intense fires (annually and biennially burnt plots) could be explained by traits promoting bark insulation and efficient carbon fixation (Coneglian *et al*., 2022; de Souza Reis *et al*., 2023), phenotypic plasticity (Felfili, 1995; Felfili *et al*., 1999), nitrogen fixing ability (Faria *et al*., 1989; Silva *et al*., 2013) and reduced competition (Reis *et al*., 2017). Nonetheless, productivity decreased drastically within the triennial plot, suggesting there is a fire frequency/intensity threshold beyond which the ability of *T. vulgaris* to rebound after burning becomes compromised (Kelly *et al*., 2025). Given the species' hyperdominance, fire regime

thresholds may play a key role in shaping ecosystem-level dynamics and regulating alternative states in forest-savanna ecotones (Dantas *et al*., 2013).

Long-term ecological monitoring projects and fire manipulation experiments have indeed shown that fire suppression in open ecosystems is a key facilitator of the progressive replacement of savanna by forest vegetation, both within the Cerrado (e.g., Durigan & Ratter, 2006; Geiger *et al*., 2011) and across other savanna systems worldwide (e.g., Australia, Lehmann *et al*., 2009; North America, Capozzelli *et al*., 2020; Southern Africa, Case & Staver, 2017; and South Asia, Kumar *et al*., 2020). Individuals of forest species capable of tolerating abiotic stresses of open environments can trigger forest expansion, setting in motion biogeochemical feedback cycles that increase soil fertility and alter floristic structure and composition (Silva *et al*., 2013; Abreu *et al*., 2021; Oliveira *et al*., 2021). Our results confirm that, under fire suppression, *cerrado sensu stricto* areas are experiencing self-reinforcing woody encroachment driven by the continued increase in NPP_{stem} of fast-growing, resource-acquisitive, generalist species (Navarro-Rosales *et al*., 2025). In our experimentally burnt plots, however, woody encroachment trends are reduced, or even reversed, as vegetation density falls and contributions towards plot-scale NPP_{stem} become dominated by fire-tolerant, conservative savanna trees. We observed that, as fire frequency decreases across our burnt plots, contributions to NPP_{stem} reflected a stronger shift in functional composition toward a more open savanna assemblage (Ribeiro & Tabarelli, 2002; Machida *et al*., 2021). These changes suggest that our less frequent fire regimes (biennially and triennially burnt plots) exert a stronger influence on community composition of Cerrado plants, and this pattern could be explained by the broad trade-off between fire frequency and intensity generally describing fire regimes worldwide (Chiminazzo *et al*., 2025). Although detailed fire behaviour data for Serra das Araras is not yet available (Oliveras Menor *et al*., in preparation), field observations suggest our less frequent fires in the biennially and triennially burnt plots were faster-moving, more severe and homogeneous (Rissi *et al*., 2017). More intense fires have previously been shown to cause increased damage, topkill and mortality of woody vegetation (Kauffman *et al*., 1994; Hoffmann & Solbrig, 2003; Montenegro *et al*., 2025).

Patterns in the contributions to $C_{mortality}$ following fire – where the mortality carbon flux is dominated by *T. vulgaris*, *V. haenkeana* and *X. aromatica* – closely align with our NPP_{stem} findings. The species exhibiting the greatest reductions in total NPP_{stem} also dominated plot mortality, indicating vulnerability to fire. However, the death of these larger trees might have further skewed the contributions to $C_{mortality}$ due to their disproportionate biomass contribution (Gora & Esquivel-Muelbert, 2021). Using a community-wide allometry to calculate carbon stocks in woody stems could have introduced additional bias, particularly because our larger-sized species also exhibited higher levels of wood density. To better understand the structural and demographic mechanisms driving shifts in woody productivity across fire regimes, more accurate allometric equations reflecting species-specific variations in wood density and plant architecture should be formulated, and future research efforts should increasingly focus on tracking changes in mortality, recruitment, abundance and species size distributions over time.

4.6.2. Fire-driven changes in species-level NPP_{stem} reveal a trade-off between productivity and fire tolerance

Fire appears to have stimulated woody productivity in 5 out of 16 dominant Cerrado tree species (*B. coccolobifolia, B. verbascifolia*, *K. grandiflora, P. ramiflora*, and *T. vulgaris*) under at least one fire regime, consistent with the notion that fire-adapted species invest in rapid resprouting and growth after burning (Zupo *et al*., 2021; Cruz *et al*., 2025). Our results reveal that in the triennially burnt plot, where fires are potentially more intense, average woody productivity declined for the two most common generalist species*, T. vulgaris* and *V. haenkeana*. This likely reflects the negative impact of more severe burns on growth and biomass accumulation in surviving individuals (Hoffmann & Solbrig, 2003). In the unburnt plot, however, average NPP_{stem} of *P. ramiflora*, and *T. vulgaris* increased, indicating that denser vegetation structure enhances productivity (Franczak *et al*., 2011), thereby reinforcing woody encroachment processes (Peixoto

et al., 2017). An unexpected reduction in average NPP_{stem} of *X. aromatica* in the unburnt plots can be explained by the inclusion of smaller (DBH ≥ 5 cm) individuals, warranting further research into size class dynamics (e.g., Oliveira *et al.*, 2021). Substantial variation in NPP_{stem} data, combined with small population sizes in some plots, likely limited our ability to detect detailed fitness responses to periodic burning (Newbery & Lingenfelder, 2017). Limited NPP_{stem} responses to fire could also be explained by our experimental fire regimes being implemented for a restricted amount of time, reflecting an insufficient period to characterise well-established fire regimes. Our biennial and triennial regimes consisted of a very limited number of fire intervals. Rather than representing typical fire regimes that have been stable during a long period of time, our experimental interventions captured the initial effect of fire reintroductions into a previously unburnt landscape, warranting further study into the longer-term fire ecological effects of our fire interventions.

Nevertheless, we are confident that our analysis captured the overall effects of the first 5 years of our experimental fire regimes on NPP_{stem}, especially after accounting for the outlier influence of *T. vulgaris*. Our comparison of NPP_{stem} marginal means revealed a consistent negative association between initial productivity estimates and subsequent ΔNPP_{stem}. In other words, more productive species show smaller increases – or greater reductions – in productivity following exposure to fire. The consistency of this pattern across fire frequencies, combined with strong model fit, suggest that these patterns are unlikely to have arisen by chance but reflect an underlying trade-off between fire tolerance and productivity/growth. Trade-offs between tree fire tolerance and growth rates have been outlined across savannas in Africa (Gignoux *et al*., 2009) and Australia (Lawes *et al*., 2011), although increased growth and height are also important strategies allowing for resistance to fire in those regions (Lehmann *et al*., 2009). In Cerrado savannas, where fire tolerance strategies primarily rely on bark growth (Dantas & Pausas, 2013), fire exclusion of faster growing forest species is relatively well documented (Hoffmann *et al*., 2003; Hoffmann *et al*., 2009). Precisely, Scalon *et al.* (2020) discovered a trade-off between fast growth and traits associated with fire resistance, such as bud protection and bark thickness, representing strategies

to escape or withstand fire (Hoffmann *et al*., 2012). More broadly, this trade-off reflects contrasting ecological strategies: species optimised for light competition and fast growth in forest assemblages versus those adapted to persist in fire-prone savanna systems through structural defence against fire, resprouting capacity, and conservative resource use (Gignoux *et al*., 2016; Charles-Dominique *et al*., 2018; Bernardino *et al*., 2022). This fundamental trade-off between fire resistance and productivity plays a central role in maintaining the savanna-forest mosaic as a system of alternative stable states, having important implications for species demography and ecosystem dynamics under changing fire regimes (Gignoux *et al*., 1997; Silva *et al*., 2013).

Indeed, survival of some of our savanna species (*B. coccolobifolia*, *K. grandiflora*, *M. bella* and *P. ramiflora*) decreased under certain fire frequencies. Varying patterns of Δsurvival across species indicate that different mechanisms, potentially linked to differences in fire intensity and severity, may govern post-fire survival in ways not fully captured in our current dataset (Cruz *et al*., 2025). In contrast, generalist species (*T. vulgaris*, *T. silvatica*, *V. haenkeana* and *X. aromatica*) consistently showed reduced survival within our fire regimes, supporting the interpretation that these species are investing in fast growth and light resource competition at the expense of fire resistance (Hoffmann *et al*., 2012). Interestingly, some typical Cerrado species experienced reduced survival in the unburnt plots (*H. speciosa* and *K. grandiflora*). This may reflect an inability to maintain fitness under intense shade and competition in the absence of fire (Oliveira & Silva, 1993). Despite these patterns, we found limited evidence for a consistent trade-off between productivity (or growth) and survival across the different fire regimes. Only in the biennially burnt plot – and only when *T. vulgaris* estimates were included – was higher initial NPP_{stem} significantly associated with lower survival. Weaker patterns could be explained by high rates of survival within fire exclusion plots, which restricted statistical power due to data separation (Heinze & Schemper, 2002). Survival patterns might have also been underestimated by the challenge of distinguishing stem topkill from true individual mortality. Monitoring underground dynamics and belowground resprouting would therefore provide a more accurate estimate of survival rates (Hoffmann *et al*., 2009).

4.6.3. Thick bark and light-adapted photosynthesis maintain NPP_{stem} at triennial fire frequencies

With the aim of understanding if plant strategies can explain the observed patterns in survival and NPP_{stem}, we investigated how functional traits influence productivity and survival of dominant Cerrado trees at Serra das Araras. We explored the relationships and covariation between leaf, bark, wood and photosynthetic traits using a principal component analysis, which revealed there are two main axis of trait variation across dominant species, each reflecting distinct ecological trade-offs. The first principal component captured a trade-off in structural investment strategies: species investing in lower-cost foliage, increased size and higher wood density; vs species investing in bark protection and leaf resistance. Rather than reflecting a clear resource acquisition gradient, this first axis of variation hints at the interplay between different structural investment strategies across forest-savanna transitions (Dantas *et al*., 2024). The choice between investing in building a tall canopy vs investing in thick insulating bark is a well explored trade-off across savanna ecosystems worldwide (e.g., Gignoux *et al*., 1997; Hoffmann *et al*., 2009) allowing for more efficient growth and resource acquisition in forest assemblages compared to higher fire resistance and conservativeness in fire-prone systems (Gignoux *et al*., 2016; Charles-Dominique *et al*., 2018; Bernardino *et al*., 2022). We expected sclerophyllous savanna tree species to exhibit consistent trait syndromes reflecting conservative acquisition strategies. Although wood density can be linked to drought resistance, slower tree growth and reduced wood decay after fire (Chave *et al*., 2009; Brando *et al*., 2012), we observed higher wood densities were actually associated with faster-growing, fire-vulnerable species. Trade-offs between bark and woody investment have been previously reported in Cerrado savanna and other environments (Loram-Lourenço *et al*., 2020; Dantas *et al*., 2024), as wood density appears to be positively associated with inner and outer bark densities, but negatively related to bark thickness (Rosell *et al*., 2014; Scalon *et al*., 2020). These patterns are consistent with our earlier findings from a smaller-scale fire experiment

at Serra das Araras (Cruz *et al*., 2025), where species that increased in abundance after fire had thicker bark and lower wood density. Wood density was a poor predictor of mortality and topkill, suggesting that bark traits play a more direct role in conferring fire tolerance within fire-prone savanna ecosystems (Rosell *et al*., 2014).

Our second axis of variation also incorporates traits associated with plant economic spectra, revealing a gradient from broader leaves and fast gas exchange rates in comparison to smaller leaf size and photosynthetic shade tolerance (Poorter, 2009; Niinemets, 2023). Although photosynthetic rates do not directly reflect the amount of carbon used invested on stem biomass growth (Trugman & Anderegg, 2025), photosynthetic strategies are important determinants of Cerrado plant persistence after fire (Scalon & Rossatto, 2021) and under woody encroachment conditions (Rossatto *et al*., 2018; da Cruz Junior *et al*., 2025), yet appear to vary independently from structural investment trade-offs.

When examining the relationship between NPP_{stem} and functional traits across fire regimes and census intervals, we found that only size-related variables (height and DBH) showed a (positive) statistically significant relationship with woody productivity in the unburnt plots. This pattern can be explained by metabolic scaling theory, which describes how larger trees sequester carbon at higher rates than smaller trees (Šímová *et al*., 2019), and reflects the growth-rate advantage of generalist species in the absence of fire or other major disturbances (Rossatto *et al*., 2009). Weak relationships between NPP_{stem} and functional traits could be explained by the substantial variation characteristic of vegetation dynamics (Reis *et al*., 2025), but could also suggest that under fire exclusion, filtering pressures resulting from woody encroachment in Cerrado savanna are not yet strong enough to affect fitness in a detectable way (de Miranda Santos *et al*., 2024). Similarly, the trait-regime-interval interaction coefficients revealed there was no significant change in the relationship between traits and NPP_{stem} after the long-term implementation of annual burns. Given that high-intensity, low-frequency fire regimes exert a stronger filtering pressure on plant function and plant communities (Chiminazzo *et al*., 2025; Montenegro *et al*., 2025), it is not surprising

that NPP_{stem} remains unrelated to functional traits in the annually burned plot. Interestingly, the absence of a relationship between productivity and functional traits occurs in the two plots that most strongly deviate from the typical 3-4 years fire intervals of the Cerrado, potentially indicating how altered fire regimes might compromise functional strategies allowing species to persist in relation to fire (Kelly *et al*., 2025).

In the biennially burnt plot, however, woody productivity during the last interval showed significantly stronger relationships with wood density, specific leaf area and tree size, driven by the extreme recovery of surviving *T. vulgaris*. This provides further evidence that *T. vulgaris* – one of the species with the highest wood density and specific leaf area at Serra das Araras (also see de Souza Reis *et al*., 2023) – disproportionately dominates functional responses to fire under certain regime conditions. In the triennial plot, which comparatively has less frequent fires (associated with higher fire intensity), NPP_{stem} is more strongly associated with increased bark protection (outer and relative bark thickness), light-adapted photosynthesis (higher rates of light-saturated carbon assimilation and lower photosynthetic tolerance to shade) and smaller tree size (as growth of larger-sized generalist species is compromised). The mechanism by which bark thickness confers resistance and contributes to tolerance of fire regimes has been extensively described in the global savanna literature (e.g., Lawes *et al*., 2013; Pausas, 2015; Chiminazzo *et al*., 2023), and these findings directly imply that bark protection acts as a trait mediating impacts on growth and fitness of Cerrado trees under higher burning intensity. Overall, these results provide empirical evidence towards the existence of different plant strategies in response to altered fire regimes in the Cerrado. In the triennially burnt plot, species capable of shielding themselves from flames and investing in aboveground protection have an advantage over species with higher capacity to explore vertical space and maintain competition for light (Chiminazzo *et al*., 2025). Nonetheless, our results also confirm productivity after our less frequent fires (biennially and triennially burnt plots) is still linked with acquisitive, shade-sensitive photosynthetic strategies, indicating fire acts as an important driver of maximum photosynthetic

rates, allowing for optimised carbon capture in open environments with higher levels of irradiance (Rossatto *et al*., 2018; Scalon & Rossatto, 2021).

We therefore propose woody productivity under triennial fire regimes is mediated by a structure-acquisition dimensionality of trait syndromes. If productivity is strongly influenced by economic spectra, intense fires requiring increased bark investment could constrain a species' ability to maximise resource acquisition via structural traits (Scalon *et al*., 2020), but not via photosynthetic rates (Paula *et al*., 2015). Our findings suggest there is no simple trade-off between resource acquisition and fire protection traits across a gradient of fire regimes, but that both are important phenotypic strategies contributing to fitness, warranting further research into trait coordination in relation to direct and indirect impacts of fire (Díaz, 2025). More detailed research into trait syndromes could also help us determine if functional traits are actually impacting species persistence across our monitoring plots. When relating survival to functional traits across regimes and intervals, we only found that inner bark thickness and maximum photosynthetic rates showed significantly more negative relationships with survival at the biennially burnt plot. This could be driven by high values of inner bark thickness and photosynthetic rates in susceptible *T. vulgaris*, but interpretation should be taken with care due to very large error margins. The absence of further relationships could be attributed to our necessarily weaker analytical choice, given that we analysed the relationship between population-wide survival and species-specific trait averages (from surviving trees). Tracking the survival, productivity, and trait values of the selected trees over the coming years – as the ecological effects of better-established fire regimes stabilise – could provide a more reliable picture of the trait-mediated responses to fire at Serra das Araras, helping us better understand how multiple facets of plant fitness are shaped by functional strategies across changing fire regimes.

4.7. Conclusions

This study demonstrates how experimental burning regimes affect the vegetation structure and carbon dynamics of Cerrado vegetation through a complex interplay between average biomass accumulation and survival rates mediated by patterns of dominance, functional traits and plant strategies. Our results reveal that both fire exclusion and fire reintroduction alter patterns of woody productivity, reflecting broader ecological processes of woody encroachment and savanna restoration. Changes in species-level NPP_{stem} and survival indicate there is a trade-off between plant productivity and vulnerability to fire across all burning regimes in terms of NPP_{stem} change, but not in terms of survival change. These findings point to the existence of distinct strategies allowing Cerrado trees to better respond to different fire regimes, although in fire exclusion conditions and at very high (annual) fire frequencies, the functionally-mediated persistence of generalist and typical savanna species is not strongly compromised. Our results provide useful insights towards fire management of the Cerrado, revealing comparatively less frequent but potentially more intense burning regimes in the biennial and triennial plots have a stronger effect on arboreal communities, with important consequences towards the permanence of important tree species. The significance of tree hyperdominance across savanna communities towards resilience and vulnerability should be further investigated, given ecosystem function and services might disproportionately rely on the maintenance of species such as *Tachigali vulgaris*.

We experimentally reveal how bark protection and light-adapted photosynthesis maintain productivity at triennial frequencies, meaning carbon balance responses to changing fire regimes could be better predicted across species assemblages and locations. Nonetheless, it is important to acknowledge that these results represent patterns in aboveground woody dynamics, and that understanding the effects of altered fire regimes on herbaceous vegetation, underground organs and carbon pools is still a research priority of key importance. Although the aim of this study has been to characterise biomass gain in tree species, it is worth noting that woody stem productivity is only one of the multiple components of savanna plant performance. Other strategies maximising plant fitness and species/individual persistence through belowground allocation, resprouting and reproduction may be equally, if not more, important within fire-prone systems, especially for the

smaller shrub and herbaceous species making up the bulk of Cerrado plant diversity. In the face of increasingly extreme climate events and continued land conversion, future studies should therefore focus on investigating how assemblages of other functional types of Cerrado plants mechanistically respond to the interactive effect of combined disturbances through trait coordination into successful plant strategies that underline ecological resilience.

4.8. Acknowledgements and funding

We thank David Bauman and Andy Hector for their support and advice. We are grateful to ICMBio professionals assisting in site conservation and controlled burns, and to the interns at UNEMAT and the Herbário do PANtanal who contributed to botanical and data collection. We thank UNEMAT and ICMBio for the transport and logistical assistance. This work was supported by the University of Oxford (John Fell Fund 163/03), the UKRI Natural Environment Research Council (Standard Grant NE/W00058X/1), and the EU Marie Skłodowska-Curie Action awarded to FIRE-ADAPT (project no. 101086416), as well as the Fundación Rafael del Pino Excellence Scholarship and the Campus France Bourse Excellence Eiffel to Francisco Navarro-Rosales.

4.9. Data availability

Tree inventory data is available at Forestplots.net. Functional trait data is available upon request.

4.10. References

Abreu RCR, Durigan G, Melo ACG, Pilon NAL, Hoffmann WA. 2021. Facilitation by isolated trees triggers woody encroachment and a biome shift at the savanna–forest transition. *Journal of Applied Ecology* 58: 2650–2660. DOI: 10.1111/1365-2664.13994.

Abreu RCR, Hoffmann WA, Vasconcelos HL, Pilon NA, Rossatto DR, Durigan G. 2017. The biodiversity cost of carbon sequestration in tropical savanna. *Science Advances* 3: e1701284. DOI: 10.1126/sciadv.1701284.

Aguiar BAC, Epifânio MLG, Souza PB de. 2019. Fitossociologia de uma área de cerrado *sensu stricto* e do sub-bosque de clones de *Eucalyptus*, Aliança, Tocantins, Brasil. *Élisée - Revista de Geografia da UEG* 8: e82197–e82197.

Aguirre-Gutiérrez J, Díaz S, Rifai SW, *et al.* 2025. Tropical forests in the Americas are changing too slowly to track climate change. *Science* 387: eadl5414. DOI: 10.1126/science.adl5414.

Amara E, Adhikari H, Mwamodenyi JM, Pellikka PKE, Heiskanen J. 2023. Contribution of Tree Size and Species on Aboveground Biomass across Land Cover Types in the Taita Hills, Southern Kenya. *Forests* 14: 642. DOI: 10.3390/f14030642.

Andela N, Morton DC, Giglio L, *et al.* 2017. A human-driven decline in global burned area. *Science* 356: 1356–1362. DOI: 10.1126/science.aal4108.

Andela N, van der Werf GR. 2014. Recent trends in African fires driven by cropland expansion and El Niño to La Niña transition. *Nature Climate Change* 4: 791–795.
DOI: 10.1038/nclimate2313.

dos Anjos L, Oliva MA, Kuki KN, *et al.* 2015. Key leaf traits indicative of photosynthetic plasticity in tropical tree species. *Trees* 29: 247–258. DOI: 10.1007/s00468-014-1110-2.

Aquino F de G, Walter BMT, Ribeiro JF. 2007. Woody community dynamics in two fragments of "cerrado" *stricto sensu* over a seven-year period (1995-2002), MA, Brazil. *Brazilian Journal of Botany* 30: 113–121. DOI: 10.1590/S0100-84042007000100011.

Araújo I, Marimon BS, Scalon MC, *et al.* 2021. Intraspecific variation in leaf traits facilitates the occurrence of trees at the Amazonia–Cerrado transition. *Flora* 279: 151829.
DOI: 10.1016/j.flora.2021.151829.

Archibald S. 2016. Managing the human component of fire regimes: lessons from Africa. *Philosophical Transactions of the Royal Society B: Biological Sciences*.
DOI: 10.1098/rstb.2015.0346.

Bates D, Mächler M, Bolker B, Walker S. 2015. Fitting linear mixed-effects models using lme4. *Journal of Statistical Software* 67: 1–48. DOI: 10.18637/jss.v067.i01.

Bernardino PN, Dantas VL, Hirota M, Pausas JG, Oliveira RS. 2022. Savanna–forest coexistence across a fire gradient. *Ecosystems* 25: 279–290. DOI: 10.1007/s10021-021-00654-4.

Bowman DMJS, O'Brien JA, Goldammer JG. 2013. Pyrogeography and the global quest for sustainable fire management. *Annual Review of Environment and Resources* 38: 57–80. DOI: 10.1146/annurev-environ-082212-134049.

Brando PM, Nepstad DC, Balch JK, *et al.* 2012. Fire-induced tree mortality in a neotropical forest: the roles of bark traits, tree size, wood density and fire behavior. *Global Change Biology* 18: 630–641. DOI: 10.1111/j.1365-2486.2011.02533.x.

Busch FA, Ainsworth EA, Amtmann A, *et al.* 2024. A guide to photosynthetic gas exchange measurements: Fundamental principles, best practice and potential pitfalls. *Plant, Cell & Environment* 47: 3344–3364. DOI: 10.1111/pce.14815.

Capozzelli JF, Miller JR, Debinski DM, Schacht WH. 2020. Restoring the fire–grazing interaction promotes tree–grass coexistence by controlling woody encroachment. *Ecosphere* 11: e02993. DOI: 10.1002/ecs2.2993.

Case MF, Staver AC. 2017. Fire prevents woody encroachment only at higher-than-historical frequencies in a South African savanna. *Journal of Applied Ecology* 54: 955–962. DOI: 10.1111/1365-2664.12805.

Chambers JQ, Tribuzy ES, Toledo LC, *et al.* 2004. Respiration from a tropical forest ecosystem: partitioning of sources and low carbon use efficiency. *Ecological Applications* 14: 72–88. DOI: 10.1890/01-6012.

Charles-Dominique T, Beckett H, Midgley GF, Bond WJ. 2015. Bud protection: a key trait for species sorting in a forest–savanna mosaic. *New Phytologist* 207: 1052–1060. DOI: 10.1111/nph.13406.

Charles-Dominique T, Midgley GF, Tomlinson KW, Bond WJ. 2018. Steal the light: shade vs fire adapted vegetation in forest–savanna mosaics. *New Phytologist* 218: 1419–1429. DOI: 10.1111/nph.15117.

Chave, J. 2005. *Measuring wood density for tropical forest trees: A field manual*. Laboratoire Evolution et Diversité Biologique, Université Paul Sabatier, France

Chave J, Coomes D, Jansen S, Lewis SL, Swenson NG, Zanne AE. 2009. Towards a worldwide wood economics spectrum. *Ecology Letters* 12: 351–366. DOI: 10.1111/j.1461-0248.2009.01285.x.

Chen X, Hutley LB, Eamus D. 2003. Carbon balance of a tropical savanna of northern Australia. *Oecologia* 137: 405–416. DOI: 10.1007/s00442-003-1358-5.

Chiminazzo MA, Bombo AB, Charles-Dominique T, Fidelis A. 2023. Bark production of generalist and specialist species across savannas and forests in the Cerrado. *Annals of Botany* 131: 613–621. DOI: 10.1093/aob/mcad014.

Chiminazzo MA, Charles-Dominique T, Andrade RS, Bombo AB, Fidelis A. 2025. How do plants survive in the starving, burning, and hiding vegetation realms generated by novel fire regimes? *Perspectives in Plant Ecology, Evolution and Systematics* 68: 125885. DOI: 10.1016/j.ppees.2025.125885.

Clark DA, Brown S, Kicklighter DW, *et al.* 2001. Net primary production in tropical forests: an evaluation and synthesis of existing field data. *Ecological Applications* 11: 371–384. DOI: 10.1890/1051-0761(2001)011[0371:NPPITF]2.0.CO;2.

Clarke PJ, Lawes MJ, Midgley JJ, *et al.* 2013. Resprouting as a key functional trait: how buds, protection and resources drive persistence after fire. *New Phytologist* 197: 19–35. DOI: 10.1111/nph.12001.

Coneglian A, Santos BG dos, Costa DB da, Brito SL da L, Cunha SD, Pereira IM. 2022. Tempo de letalidade do câmbio de duas espécies arbóreas do Cerrado a 60ºC. *Revista do Instituto Florestal* 34: 182–187. DOI: 10.24278/2178-5031.202234207.

da Cruz Júnior PF da, Pinheiro LFS, Rossatto DR, Kolb RM. 2025. Woody encroachment and leaf functional traits of ground-layer savanna species. *Flora* 326: 152709. DOI: 10.1016/j.flora.2025.152709.

Cruz WJA, Machado MS, Navarro-Rosales F, *et al.* 2025. Deciphering fire tolerance of trees at the Amazonia–Cerrado transition by trait-based approach: Implications from species to communities. *American Journal of Botany* n/a: e70066. DOI: 10.1002/ajb2.70066.

da Cruz Silva A, Veenendaal E, Van der Plas F, de Oliveira Júnior VD, do Vale VS, Meira-Neto JAA. 2025. Vegetation transition in the central Brazilian Cerrado is better explained by structure than tree composition differences. *Plant Ecology* 226: 563–572. DOI: 10.1007/s11258-025-01500-6.

Damasco G, Baraloto C, Vicentini A, Daly DC, Baldwin BG, Fine PVA. 2021. Revisiting the hyperdominance of Neotropical tree species under a taxonomic, functional and evolutionary perspective. *Scientific Reports* 11: 9585. DOI: 10.1038/s41598-021-88417-y.

Dantas VL, Batalha MA, Pausas JG. 2013. Fire drives functional thresholds on the savanna–forest transition. *Ecology* 94: 2454–2463. DOI: 10.1890/12-1629.1.

Dantas VL, Oliveira LCS, Marcati CR, Sonsin-Oliveira J. 2024. Coordination of bark and wood traits underlies forest-to-savanna evolutionary transitions. *Journal of Biogeography* 51: 1801–1813. DOI: 10.1111/jbi.14850.

Dantas VL, Pausas JG. 2013. The lanky and the corky: fire-escape strategies in savanna woody species. *Journal of Ecology* 101: 1265–1272. DOI: 10.1111/1365-2745.12118.

Deccache LSJ, Lima HC de, Fraga CN de. 2024. Nomenclatural revision and typification of extra-Amazonian *Tachigali* (Leguminosae - Caesalpinioideae). *Plant Ecology and Evolution* 157: 137–148. DOI: 10.5091/plecevo.111072.

Díaz S. 2025. Plant functional traits and the entangled phenotype. *Functional Ecology* n/a. DOI: 10.1111/1365-2435.70017.

Durigan G, Ratter JA. 2016. The need for a consistent fire policy for Cerrado conservation. *Journal of Applied Ecology* 53: 11–15. DOI: 10.1111/1365-2664.12559.

Eiten G. 1972. The Cerrado vegetation of Brazil. *The Botanical Review* 38: 201–341. DOI: 10.1007/BF02859158.

Elias F, Marimon Junior BH, de Oliveira FJM, de Oliveira JCA, Marimon BS. 2019. Soil and topographic variation as a key factor driving the distribution of tree flora in the Amazonia/Cerrado transition. *Acta Oecologica* 100: 103467. DOI: 10.1016/j.actao.2019.103467.

Empresa Brasileira de Pesquisa Agropecuária – EMBRAPA. 2018. *Sistema Brasileiro de Classificação de Solos, 5ª Edição*. Centro Nacional de Pesquisa de Solos, Brasília.

Faria SM, Lewis GP, Sprent JI, Sutherland JM. 1989. Occurrence of nodulation in the Leguminosae. *New Phytologist* 111: 607–619. DOI: 10.1111/j.1469-8137.1989.tb02354.x.

Fauset S, Johnson MO, Gloor M, *et al.* 2015. Hyperdominance in Amazonian forest carbon cycling. *Nature Communications* 6: 6857. DOI: 10.1038/ncomms7857.

Felfili JM. 1995. Diversity, structure and dynamics of a gallery forest in central Brazil. *Vegetatio* 117: 1–15. DOI: 10.1007/BF00033255.

Felfili JM, Hilgbert LF, Franco AC, Sousa-Silva JC, Resende AV, Nogueira MVP. 1999. Comportamento de plântulas de *Sclerolobium paniculatum* Vog. var. *rubiginosum* (Tul.) Benth. sob diferentes níveis de sombreamento, em viveiro. *Brazilian Journal of Botany* 22: 297–301. DOI: 10.1590/S0100-84041999000500011.

Flake SW, Abreu RCR, Durigan G, Hoffmann WA. 2021. Savannas are not old fields: Functional trajectories of forest expansion in a fire-suppressed Brazilian savanna are driven by habitat generalists. *Functional Ecology* 35: 1797–1809. DOI: 10.1111/1365-2435.13818.

Flannigan M, Cantin AS, Groot WJ de, Wotton M, Newbery A, Gowman LM. 2013. Global wildland fire season severity in the 21st century. *Forest Ecology and Management* 294: 54–61. DOI: 10.1016/j.foreco.2012.10.022.

Fontenele HGV, Miranda HS. 2024. Fire has contrasting effects on the survival, growth, and reproduction of Cerrado grasses with differing regenerative strategies. *Applied Vegetation Science* 27: e12775. DOI: 10.1111/avsc.12775.

Françoso RD, Brandão R, Nogueira CC, Salmona YB, Machado RB, Colli GR. 2015. Habitat loss and the effectiveness of protected areas in the Cerrado Biodiversity Hotspot. *Natureza & Conservação* 13: 35–40. DOI: 10.1016/j.ncon.2015.04.001.

Franczak DD, Marimon BS, Marimon-Junior BH, Mews HA, Maracahipes L, Oliveira EA de. 2011. Changes in the structure of a savanna forest over a six-year period in the Amazon-Cerrado transition, Mato Grosso state, Brazil. *Rodriguésia* 62: 425–436.
DOI: 10.1590/2175-7860201162215.

Garnier E, Stahl U, Laporte M-A, *et al.* 2017. Towards a thesaurus of plant characteristics: an ecological contribution. *Journal of Ecology* 105: 298–309. DOI: 10.1111/1365-2745.12698.

Geiger EL, Gotsch SG, Damasco G, Haridasan M, Franco AC, Hoffmann WA. 2011. Distinct roles of savanna and forest tree species in regeneration under fire suppression in a Brazilian savanna. *Journal of Vegetation Science* 22: 312–321. DOI: 10.1111/j.1654-1103.2011.01252.x.

Gignoux J, Clobert J, Menaut J-C. 1997. Alternative fire resistance strategies in savanna trees. *Oecologia* 110: 576–583. DOI: 10.1007/s004420050198.

Gignoux J, Konaté S, Lahoreau G, Le Roux X, Simioni G. 2016. Allocation strategies of savanna and forest tree seedlings in response to fire and shading: outcomes of a field experiment. *Scientific Reports* 6: 38838. DOI: 10.1038/srep38838.

Gignoux J, Lahoreau G, Julliard R, Barot S. 2009. Establishment and early persistence of tree seedlings in an annually burned savanna. *Journal of Ecology* 97: 484–495. DOI: 10.1111/j.1365-2745.2009.01493.x.

Giles AL, Faria LDB, Souza HJ de, *et al.* 2026. Mapping and revealing the tree biodiversity of the Brazilian Cerrado through biome-wide sampling efforts. *npj Biodiversity* 5: 9. DOI: 10.1038/s44185-026-00122-z

Girardin CAJ, Malhi Y, Aragão LEOC, *et al.* 2010. Net primary productivity allocation and cycling of carbon along a tropical forest elevational transect in the Peruvian Andes. *Global Change Biology* 16: 3176–3192. DOI: 10.1111/j.1365-2486.2010.02235.x.

Gora EM, Esquivel-Muelbert A. 2021. Implications of size-dependent tree mortality for tropical forest carbon dynamics. *Nature Plants* 7: 384–391. DOI: 10.1038/s41477-021-00879-0.

Grau-Andrés R, Moreira B, Pausas JG. 2024. Global plant responses to intensified fire regimes. *Global Ecology and Biogeography* n/a: e13858. DOI: 10.1111/geb.13858.

Haridasan M. 2008. Nutritional adaptations of native plants of the cerrado biome in acid soils. *Brazilian Journal of Plant Physiology* 20: 183–195. DOI: 10.1590/S1677-04202008000300003.

Heinze G, Schemper M. 2002. A solution to the problem of separation in logistic regression. *Statistics in Medicine* 21: 2409–2419. DOI: 10.1002/sim.1047.

Higgins SI, Banerjee S, Baudena M, *et al.* 2024. Reassessing the alternative ecosystem states proposition in the African savanna-forest domain. *New Phytologist* 243: 1660–1669. DOI: 10.1111/nph.19911.

Hilty J, Muller B, Pantin F, Leuzinger S. 2021. Plant growth: the What, the How, and the Why. *New Phytologist* 232: 25–41. DOI: 10.1111/nph.17610.

Hoffmann WA. 2002. Direct and indirect effects of fire on radial growth of Cerrado savanna trees. *Journal of Tropical Ecology* 18: 137–142. DOI: 10.1017/S0266467402002080.

Hoffmann WA, Adasme R, Haridasan M, *et al.* 2009. Tree topkill, not mortality, governs the dynamics of savanna–forest boundaries under frequent fire in central Brazil. *Ecology* 90: 1326–1337. DOI: 10.1890/08-0741.1.

Hoffmann WA, Geiger EL, Gotsch SG, *et al.* 2012. Ecological thresholds at the savanna-forest boundary: how plant traits, resources and fire govern the distribution of tropical biomes. *Ecology Letters* 15: 759–768. DOI: 10.1111/j.1461-0248.2012.01789.x.

Hoffmann WA, Orthen B, Nascimento PKV do. 2003. Comparative fire ecology of tropical savanna and forest trees. *Functional Ecology* 17: 720–726. DOI: 10.1111/j.1365-2435.2003.00796.x.

Hoffmann WA, Sanders RW, Just MG, Wall WA, Hohmann MG. 2020. Better lucky than good: How savanna trees escape the fire trap in a variable world. *Ecology* 101: e02895. DOI: 10.1002/ecy.2895.

Hoffmann WA, Solbrig OT. 2003. The role of topkill in the differential response of savanna woody species to fire. *Forest Ecology and Management* 180: 273–286. DOI: 10.1016/S0378-1127(02)00566-2.

ICMBio. 2016. *Plano de Manejo. Estação Ecológica da Serra das Araras*. ICMBio, Brasilia.

Jolly WM, Cochrane MA, Freeborn PH, *et al.* 2015. Climate-induced variations in global wildfire danger from 1979 to 2013. *Nature Communications* 6: 7537. DOI: 10.1038/ncomms8537.

Jones MW, Abatzoglou JT, Veraverbeke S, *et al.* 2022. Global and regional trends and drivers of fire under climate change. *Reviews of Geophysics* 60: e2020RG000726. DOI: 10.1029/2020RG000726.

Kauffman JB, Cummings DL, Ward DE. 1994. Relationships of fire, biomass and nutrient dynamics along a vegetation gradient in the Brazilian Cerrado. *The Journal of Ecology* 82: 519–531. DOI: 10.2307/2261261.

Kelly LT, Giljohann KM, Duane A, *et al.* 2020. Fire and biodiversity in the Anthropocene. *Science* 370: eabb0355. DOI: 10.1126/science.abb0355.

Kelly LT, Hoffmann AA, Nitschke CR, Pausas JG. 2025. Can plants keep up with fire regime changes through evolution? *Trends in Ecology & Evolution*. DOI: 10.1016/j.tree.2025.04.009.

Kottek M, Grieser J, Beck C, Rudolf B, Rubel F. 2006. World Map of the Köppen-Geiger climate classification updated. *Meteorologische Zeitschrift*: 259–263.
DOI: 10.1127/0941-2948/2006/0130.

Kumar D, Pfeiffer M, Gaillard C, Langan L, Martens C, Scheiter S. 2020. Misinterpretation of Asian savannas as degraded forest can mislead management and conservation policy under climate change. *Biological Conservation* 241: 108293. DOI: 10.1016/j.biocon.2019.108293.

Kuznetsova A, Brockhoff PB, Christensen RHB. 2017. lmerTest Package: Tests in Linear Mixed Effects Models. *Journal of Statistical Software* 82: 1–26. DOI: 10.18637/jss.v082.i13.

Lawes MJ, Adie H, Russell-Smith J, Murphy B, Midgley JJ. 2011. How do small savanna trees avoid stem mortality by fire? The roles of stem diameter, height and bark thickness. *Ecosphere* 2: art42. DOI: 10.1890/ES10-00204.1.

Lawes MJ, Midgley JJ, Clarke PJ. 2013. Costs and benefits of relative bark thickness in relation to fire damage: a savanna/forest contrast. *Journal of Ecology* 101: 517–524. DOI: 10.1111/1365-2745.12035.

Le Stradic S, Hernandez P, Fernandes GW, Buisson E. 2018. Regeneration after fire in *campo rupestre*: Short- and long-term vegetation dynamics. *Flora* 238: 191–200.
DOI: 10.1016/j.flora.2016.12.001.

Lehmann CER, Prior LD, Bowman DMJS. 2009. Decadal dynamics of tree cover in an Australian tropical savanna. *Austral Ecology* 34: 601–612. DOI: 10.1111/j.1442-9993.2009.01964.x.

Lenth, R. (2024). *emmeans: Estimated Marginal Means, aka Least-Squares Means*. Available at: https://CRAN.R-project.org/package=emmeans. 23 Jul. 2025

Lim H, Medvigy D, Mäkelä A, *et al.* 2024. Overlooked branch turnover creates a widespread bias in forest carbon accounting. *Proceedings of the National Academy of Sciences* 121: e2401035121. DOI: 10.1073/pnas.2401035121.

Loram-Lourenço L, Farnese FS, Alves RDFB, *et al.* 2022. Variations in bark structural properties affect both water loss and carbon economics in neotropical savanna trees in the Cerrado region of Brazil. *Journal of Ecology* 110: 1826–1843. DOI: 10.1111/1365-2745.13908.

Loram-Lourenço L, Farnese F dos S, Sousa LF de, *et al.* 2020. A structure shaped by fire, but also water: ecological consequences of the variability in bark properties across 31 species from the Brazilian Cerrado. *Frontiers in Plant Science* 10. DOI: 10.3389/fpls.2019.01718.

Machida WS, Gomes L, Moser P, *et al.* 2021. Long term post-fire recovery of woody plants in savannas of central Brazil. *Forest Ecology and Management* 493: 119255.
DOI: 10.1016/j.foreco.2021.119255.

Macía MJ, Svenning J-C. 2005. Oligarchic dominance in western Amazonian plant communities. *Journal of Tropical Ecology* 21: 613–626. DOI: 10.1017/S0266467405002579.

Malhi Y. 2012. The productivity, metabolism and carbon cycle of tropical forest vegetation: Carbon cycle of tropical forests. *Journal of Ecology* 100: 65–75.
DOI: 10.1111/j.1365-2745.2011.01916.x.

Malhi Y, Doughty C, Galbraith D. 2011. The allocation of ecosystem net primary productivity in tropical forests. *Philosophical Transactions of the Royal Society B: Biological Sciences* 366: 3225–3245. DOI: 10.1098/rstb.2011.0062.

Marthews TR, Riutta T, Oliveras Menor I, *et al.* 2014. *Measuring Tropical Forest Carbon Allocation and Cycling: A RAINFOR-GEM Field Manual for Intensive Census Plots (v3.0)*. Global Ecosystems Monitoring Network.

McGillycuddy M, Popovic G, Bolker BM, Warton DI. 2025. Parsimoniously Fitting Large Multivariate Random Effects in glmmTMB. *Journal of Statistical Software* 112: 1–19. DOI: 10.18637/jss.v112.i01.

Midgley JJ, Lawes MJ. 2016. Relative bark thickness: towards standardised measurement and analysis. *Plant Ecology* 217: 677–681. DOI: 10.1007/s11258-016-0587-8.

de Miranda Santos FF, Durigan G, Boschi RS, Ivanauskas N, Rodrigues RR. 2024. Tree community dynamics in the cerradão (2002-2016): A case of biome shift. *Forest Ecology and Management* 555: 121698. DOI: 10.1016/j.foreco.2024.121698.

Missik JEC, Oishi AC, Benson MC, Meretsky VJ, Phillips RP, Novick KA. 2021. Performing gas-exchange measurements on excised branches - evaluation and recommendations. *Photosynthetica* 59: 61–73. DOI: 10.32615/ps.2020.079.

Montenegro S da R, Ferreira MC, Santos AC dos, Fonseca CB, Rodrigues CA, Schmidt IB. 2025. Fire management benefits tree growth and survival in the Brazilian savanna. *Journal of Environmental Management* 380: 125085. DOI: 10.1016/j.jenvman.2025.125085.

Morandi PS, Marimon-Junior BH, Oliveira EA de, *et al.* 2016. Vegetation succession in the Cerrado–Amazonian forest transition zone of Mato Grosso state, Brazil. *Edinburgh Journal of Botany* 73: 83–93. DOI: 10.1017/S096042861500027X.

Navarro-Rosales F, Carniello MA, Cruz WJA da, *et al.* 2025. The effect of fire on the carbon fluxes and productivity of Brazilian woodland savannas. *Science of the Total Environment* 987: 179626. DOI: 10.1016/j.scitotenv.2025.179626.

Neri SCM, Bomfim B, Pereira RS, dos Santos PV, Tetto AF. 2023. Decadal fire effects on the structure, composition, diversity, and aboveground carbon stocks of a neotropical savanna. *Forests* 14: 2294. DOI: 10.3390/f14122294.

Newbery DM, Lingenfelder M. 2022. Stem girth changes in response to soil water potential in lowland dipterocarp forest in Borneo: An individualistic time-series analysis. *PLOS ONE* 17: e0270140. DOI: 10.1371/journal.pone.0270140.

Niinemets Ü. 2023. Variation in leaf photosynthetic capacity within plant canopies: optimization, structural, and physiological constraints and inefficiencies. *Photosynthesis Research* 158: 131–149. DOI: 10.1007/s11120-023-01043-9.

Oliveira B de, Marimon Junior BH, Mews HA, Valadão MBX, Marimon BS. 2017. Unravelling the ecosystem functions in the Amazonia–Cerrado transition: evidence of hyperdynamic nutrient cycling. *Plant Ecology* 218: 225–239. DOI: 10.1007/s11258-016-0681-y.

Oliveira PE, Silva JCS. 1993. Reproductive biology of two species of *Kielmeyera* (Guttiferae) in the cerrados of Central Brazil. *Journal of Tropical Ecology* 9: 67–79. DOI: 10.1017/S0266467400006970.

Oliveira MC de, Silva LAX, Aquino F de G. 2021. Occupation strategy of the arboreal species *Tachigali rubiginosa* (mart. ex tul.) Oliveira-Filho: evidence of forest expansion over grassland areas. *Revista Árvore* 45: e4529. DOI: 10.1590/1806-908820210000029.

Oliveras I, Bentley L, Fyllas NM, *et al.* 2020. The influence of taxonomy and environment on leaf trait variation along tropical abiotic gradients. *Frontiers in Forests and Global Change* 3. DOI: 10.3389/ffgc.2020.00018.

Oliveras I, Meirelles S, Hirakuri V, Freitas C, Miranda H, Pivello V. 2012. Effects of fire regimes on herbaceous biomass and nutrient dynamics in the Brazilian savanna. *International Journal of Wildland Fire* 22: 368–380. DOI: 10.1071/WF10136.

Paula SM, Naves ER, Franco IM, *et al.* 2015. Desempenho fotossintético de folhas jovens e maduras de *Vochysia cinnamomea* (Vochysiaceae) em áreas de cerrado rupestre intactas e pós-queimada. *Bioscience Journal* 31: 591–600. DOI: 10.14393/BJ-v31n2a2015-23474.

Pausas JG. 2015. Bark thickness and fire regime. *Functional Ecology* 29: 315–327. DOI: 10.1111/1365-2435.12372.

Peixoto KS, Marimon-Junior BH, Marimon BS, *et al.* 2017. Unravelling ecosystem functions at the Amazonia-Cerrado transition: II. Carbon stocks and CO_2 soil efflux in cerradão forest undergoing ecological succession. *Acta Oecologica* 82: 23–31. DOI: 10.1016/j.actao.2017.05.005.

Pellizzaro KF, Cordeiro AOO, Alves M, *et al.* 2017. "Cerrado" restoration by direct seeding: field establishment and initial growth of 75 trees, shrubs and grass species. *Brazilian Journal of Botany* 40: 681–693. DOI: 10.1007/s40415-017-0371-6.

Pereira AC, Oliveira SLJ, Pereira JMC, Turkman MAA. 2014. Modelling Fire Frequency in a Cerrado Savanna Protected Area. *PLOS ONE* 9: e102380. DOI: 10.1371/journal.pone.0102380.

Pereira MB, Elias F, Teixeira NDA, Feldpausch TR, Marimon-Junior BH, Marimon BS. 2025. Post-fire changes in tree diversity, composition and carbon in seasonal forests in the Southern Amazonia. *Forest Ecology and Management* 578: 122447. DOI: 10.1016/j.foreco.2024.122447.

Pérez-Harguindeguy N, Díaz S, Garnier E, *et al.* 2013. New handbook for standardised measurement of plant functional traits worldwide. *Australian Journal of Botany* 61: 167–234. DOI: 10.1071/BT12225.

Pilon NAL, Cava MGB, Hoffmann WA, Abreu RCR, Fidelis A, Durigan G. 2021. The diversity of post-fire regeneration strategies in the cerrado ground layer. *Journal of Ecology* 109: 154–166. DOI: 10.1111/1365-2745.13456.

Pivello VR. 2011. The use of fire in the Cerrado and Amazonian rainforests of Brazil: past and present. *Fire Ecology* 7: 24–39. DOI: 10.4996/fireecology.0701024.

Pivello VR, Coutinho LM. 1992. Transfer of macro-nutrients to the atmosphere during experimental burnings in an open cerrado (Brazilian savanna). *Journal of Tropical Ecology* 8: 487–497. DOI: 10.1017/S0266467400006829.

Pivello VR, Oliveras I, Miranda HS, Haridasan M, Sato MN, Meirelles ST. 2010. Effect of fires on soil nutrient availability in an open savanna in Central Brazil. *Plant and Soil* 337: 111–123. DOI: 10.1007/s11104-010-0508-x.

Pivello VR, Vieira I, Christianini AV, *et al.* 2021. Understanding Brazil's catastrophic fires: Causes, consequences and policy needed to prevent future tragedies. *Perspectives in Ecology and Conservation* 19: 233–255. DOI: 10.1016/j.pecon.2021.06.005.

Pizzato JA, Dallacort R, Tieppo RC, Modolo AJ, Cremon C, Moreira PSP. 2012. Distribuição e probabilidade de ocorrência de precipitação em Cáceres (MT). *Pesquisa Agropecuária Tropical* 42: 137–142. DOI: 10.1590/S1983-40632012000200006.

Plumanns-Pouton E, Swan M, Penman T, Kelly LT. 2024. Using plant functional types to predict the influence of fire on species relative abundance. *Biological Conservation* 292: 110555. DOI: 10.1016/j.biocon.2024.110555.

Poorter L. 2009. Leaf traits show different relationships with shade tolerance in moist versus dry tropical forests. *New Phytologist* 181: 890–900. DOI: 10.1111/j.1469-8137.2008.02715.x.

Poorter L, McNeil A, Hurtado V-H, Prins HHT, Putz FE. 2014. Bark traits and life-history strategies of tropical dry- and moist forest trees. *Functional Ecology* 28: 232–242. DOI: 10.1111/1365-2435.12158.

Reis SM, Lenza E, Marimon BS, *et al.* 2015. Post-fire dynamics of the woody vegetation of a savanna forest (Cerradão) in the Cerrado-Amazon transition zone. *Acta Botanica Brasilica* 29: 408–416. DOI: 10.1590/0102-33062015abb0009.

Reis SM, Malhi Y, Marimon Junior BH, *et al.* 2025. Sensitivity of tropical woodland savannas to El Niño droughts. *Biogeosciences* 22: 3949–3964. DOI: 10.5194/bg-22-3949-2025.

Reis SM, de Oliveira EA, Elias F, *et al.* 2017. Resistance to fire and the resilience of the woody vegetation of the "cerradão" in the "Cerrado"–Amazon transition zone. *Brazilian Journal of Botany* 40: 193–201. DOI: 10.1007/s40415-016-0336-1.

Rezende AV, Sanquetta CR, Filho AF, Felfili JM. 2006. Comparação de modelos matemáticos para estimativa do volume, biomassa e estoque de carbono da vegetação lenhosa de um cerrado sensu stricto em Brasília, DF. *Scientia Forestalis*: 65–76.

Ribeiro LF, Tabarelli M. 2002. A structural gradient in cerrado vegetation of Brazil: changes in woody plant density, species richness, life history and plant composition. *Journal of Tropical Ecology* 18: 775–794. DOI: 10.1017/S026646740200250X.

Ribeiro NS, Matos CN, Moura IR, Washington-Allen RA, Ribeiro AI. 2013. Monitoring vegetation dynamics and carbon stock density in miombo woodlands. *Carbon Balance and Management* 8: 11. DOI: 10.1186/1750-0680-8-11.

Rissi MN, Baeza MJ, Gorgone-Barbosa E, Zupo T, Fidelis A. 2017. Does season affect fire behaviour in the Cerrado? *International Journal of Wildland Fire* 26: 427–433. DOI: 10.1071/WF14210.

Rodrigues CA, Fidelis A. 2022. Should we burn the Cerrado? Effects of fire frequency on open savanna plant communities. *Journal of Vegetation Science* 33. DOI: 10.1111/jvs.13159.

Rodrigues CA, Zirondi HL, Fidelis A. 2021. Fire frequency affects fire behavior in open savannas of the Cerrado. *Forest Ecology and Management* 482: 118850. DOI: 10.1016/j.foreco.2020.118850.

Rosan TM, Aragão LEOC, Oliveras I, *et al.* 2019. Extensive 21st-Century Woody Encroachment in South America's Savanna. *Geophysical Research Letters* 46: 6594–6603. DOI: 10.1029/2019GL082327.

Rosell JA, Gleason S, Méndez-Alonzo R, Chang Y, Westoby M. 2014. Bark functional ecology: evidence for tradeoffs, functional coordination, and environment producing bark diversity. *New Phytologist* 201: 486–497. DOI: 10.1111/nph.12541.

Rossatto DR, de Araújo PE, da Silva BHP, Franco AC. 2018. Photosynthetic responses of understory savanna plants: Implications for plant persistence in savannas under tree encroachment. *Flora* 240: 34–39. DOI: 10.1016/j.flora.2017.12.009.

Rossatto DR, Franco AC. 2017. Expanding our understanding of leaf functional syndromes in savanna systems: the role of plant growth form. *Oecologia* 183: 953–962. DOI: 10.1007/s00442-017-3815-6.

Rossatto DR, Hoffmann WA, Franco AC. 2009. Differences in growth patterns between co-occurring forest and savanna trees affect the forest–savanna boundary. *Functional Ecology* 23: 689–698. DOI: 10.1111/j.1365-2435.2009.01568.x.

Roxburgh SH, Berry SL, Buckley TN, Barnes B, Roderick ML. 2005. What is NPP? Inconsistent accounting of respiratory fluxes in the definition of net primary production. *Functional Ecology* 19: 378–382. DOI: 10.1111/j.1365-2435.2005.00983.x.

Russo SE, McMahon SM, Detto M, *et al.* 2021. The interspecific growth–mortality trade-off is not a general framework for tropical forest community structure. *Nature Ecology & Evolution* 5: 174–183. DOI: 10.1038/s41559-020-01340-9.

Santos L dos, Zamparoni CAGP, Soares JC de Oliveira. 2017. A variabilidade pluviométrica na região de Cáceres-MT entre 1971 e 2010. *Formação (Online)* 24.
DOI: 10.33081/formacao.v24i43.4746.

Sayedi SS, Abbott BW, Vannière B, *et al.* 2024. Assessing changes in global fire regimes. *Fire Ecology* 20: 18. DOI: 10.1186/s42408-023-00237-9.

Scalon MC, Maia Chaves Bicalho Domingos F, Jonatar Alves da Cruz W, Marimon Júnior BH, Schwantes Marimon B, Oliveras I. 2020. Diversity of functional trade-offs enhances survival after fire in Neotropical savanna species. *Journal of Vegetation Science* 31: 139–150.
DOI: 10.1111/jvs.12823.

Scalon MC, Rossatto DR. 2021. Ground layer Cerrado plants sustain higher maximum photosynthetic rates after medium-term fire events. *Flora* 285: 151962.
DOI: 10.1016/j.flora.2021.151962.

Schmidt IB, Eloy L. 2020. Fire regime in the Brazilian Savanna: Recent changes, policy and management. *Flora* 268: 151613. DOI: 10.1016/j.flora.2020.151613.

Schneider CA, Rasband WS, Eliceiri KW. 2012. NIH Image to ImageJ: 25 years of image analysis. *Nature Methods* 9: 671–675. DOI: 10.1038/nmeth.2089.

Segura-Garcia C, Alencar A, S. Arruda VL, *et al.* 2025. The fire regimes of the Cerrado and their changes through time. *Philosophical Transactions of the Royal Society B: Biological Sciences* 380: 20230460. DOI: 10.1098/rstb.2023.0460.

Shirima DD, Munishi PKT, Lewis SL, *et al.* 2011. Carbon storage, structure and composition of miombo woodlands in Tanzania's Eastern Arc Mountains. *African Journal of Ecology* 49: 332–342. DOI: 10.1111/j.1365-2028.2011.01269.x.

da Silva Arruda VL, Alencar AAC, de Carvalho Júnior OA, *et al.* 2024. Assessing four decades of fire behavior dynamics in the Cerrado biome (1985 to 2022). *Fire Ecology* 20: 1–20. DOI: 10.1186/s42408-024-00298-4.

Silva CVJ, Aragão LEOC, Barlow J, *et al.* 2018. Drought-induced Amazonian wildfires instigate a decadal-scale disruption of forest carbon dynamics. *Philosophical Transactions of the Royal Society B: Biological Sciences* 373: 20180043. DOI: 10.1098/rstb.2018.0043.

Silva LCR, Hoffmann WA, Rossatto DR, Haridasan M, Franco AC, Horwath WR. 2013. Can savannas become forests? A coupled analysis of nutrient stocks and fire thresholds in central Brazil. *Plant and Soil* 373: 829–842. DOI: 10.1007/s11104-013-1822-x.

da Silva LFG, de Lima HC. 2007. Mudanças nomenclaturais no gênero *Tachigali* Aubl. (Leguminosae - Caesalpinioideae) no Brasil. *Rodriguésia* 58: 397–401. DOI: 10.1590/2175-7860200758214.

Silva Neto VL, Oliveira AL de, Ferreira RQ de S, Souza PB de, Viola MR. 2016. Fitossociologia e distribuição diamétrica de uma área de cerrado sensu stricto, Dueré-TO. *Revista de Ciências Ambientais* 10: 91–106. DOI: 10.18316/1981-8858.16.24.

Šímová I, Sandel B, Enquist BJ, *et al.* 2019. The relationship of woody plant size and leaf nutrient content to large-scale productivity for forests across the Americas. *Journal of Ecology* 107: 2278–2290. DOI: 10.1111/1365-2745.13163.

Singh J, Boucher PB, Hockridge EG, Davies AB. 2023. Effects of long-term fixed fire regimes on African savanna vegetation biomass, vertical structure and tree stem density. *Journal of Applied Ecology* 60: 1223–1238. DOI: 10.1111/1365-2664.14435.

Skhosana FV, Stevens N, Maoela MA, Archibald S, Midgley GF. 2025. The impacts of woody encroachment on nature's contributions to people in North America and Africa: A systematic review. *People and Nature* n/a: pan3.70134. DOI: 10.1002/pan3.70134.

Solórzano A, Pinto JRR, Felfili JM, Hay JDV. 2012. Perfil florístico e estrutural do componente lenhoso em seis áreas de cerradão ao longo do bioma Cerrado. *Acta Botanica Brasilica* 26: 328–341. DOI: 10.1590/S0102-33062012000200009.

Sommer B, Harrison PL, Beger M, Pandolfi JM. 2014. Trait-mediated environmental filtering drives assembly at biogeographic transition zones. *Ecology* 95: 1000–1009. DOI: 10.1890/13-1445.1.

de Souza HJ, Miguel EP, Resende RT, *et al.* 2022. Effects of functional traits on the spatial distribution and hyperdominance of tree species in the Cerrado biome. *iForest - Biogeosciences and Forestry* 15: 339. DOI: 10.3832/ifor3920-015.

de Souza MR, Filho M dos S, Guilherme MB de F, Bogoni JA. 2025. The long-term absence of natural fires restructures the small-bodied mammal assemblages across a Protected Area of Brazilian Cerrado. *Perspectives in Ecology and Conservation* 23: 165–173.
DOI: 10.1016/j.pecon.2025.05.003.

de Souza Reis LB, Miranda S do C de, Machida WS, Gonçalves L de A, De-Carvalho PS. 2023. Aspectos ecológicos, funcionais e anatômicos de três espécies lenhosas de cerradão. *Revista Brasileira de Geografia Física* 16: 968–985. DOI: 10.26848/rbgf.v16.2.p968-985.

Spadoni GL, Moris JV, Segura-Garcia C, *et al.* 2025. Devegetation is a widespread driver of fire in the Brazilian Cerrado. *Journal of Environmental Management* 385: 125637.
DOI: 10.1016/j.jenvman.2025.125637.

Staver AC, Archibald S, Levin S. 2011. Tree cover in sub-Saharan Africa: Rainfall and fire constrain forest and savanna as alternative stable states. *Ecology* 92: 1063–1072. DOI: 10.1890/10-1684.1.

ter Steege H, Pitman NCA, Sabatier D, *et al.* 2013. Hyperdominance in the Amazonian Tree Flora. *Science* 342: 1243092. DOI: 10.1126/science.1243092.

Teixeira J, Souza L, Bombo A, Le Stradic S. 2025. How does fire exclusion affect the belowground biomass of tropical open ecosystems? *Journal of Vegetation Science* 36: e70027. DOI: 10.1111/jvs.70027.

Teixeira J, Souza L, Le Stradic S, Fidelis A. 2022. Fire promotes functional plant diversity and modifies soil carbon dynamics in tropical savanna. *Science of the Total Environment* 812: 152317. DOI: 10.1016/j.scitotenv.2021.152317.

Terra M de CNS, Prado-Júnior JA do, Souza CR de, *et al.* 2021. Tree species dominance in neotropical savanna aboveground biomass and productivity. *Forest Ecology and Management* 496: 119430. DOI: 10.1016/j.foreco.2021.119430.

Trugman AT, Anderegg LDL. 2025. Source vs sink limitations on tree growth: from physiological mechanisms to evolutionary constraints and terrestrial carbon cycle implications. *New Phytologist* 245: 966–981. DOI: 10.1111/nph.20294.

do Vale AT, Felfili JM. 2005. Dry biomass distribution in a cerrado sensu stricto site in Brazil central. *Revista Árvore* 29: 661–669. DOI: 10.1590/S0100-67622005000500001.

van Mantgem PJ, Schwartz MW, Keifer M. 2001. Monitoring wildfire effects: Coming to terms with pseudoreplication. *Natural Areas Journal* 21: 266–273.

Vourlitis GL, Pinto OB, Dalmagro HJ, Arruda PH, de Almeida Lobo F. 2024. Diversity-productivity relationships of savanna ecosystems in the Cerrado-Pantanal transition of southern Mato Grosso, Brazil. *Frontiers in Forests and Global Change* 7. DOI: 10.3389/ffgc.2024.1380600.

Wigley BJ, Charles-Dominique T, Hempson GP, *et al.* 2020. A handbook for the standardised sampling of plant functional traits in disturbance-prone ecosystems, with a focus on open ecosystems. *Australian Journal of Botany* 68: 473–531. DOI: 10.1071/BT20048.

Wright IJ, Reich PB, Westoby M, *et al.* 2004. The worldwide leaf economics spectrum. *Nature* 428: 821–827. DOI: 10.1038/nature02403.

Zirondi HL, Ooi MKJ, Fidelis A. 2021. Fire-triggered flowering is the dominant post-fire strategy in a tropical savanna. *Journal of Vegetation Science* 32: e12995. DOI: 10.1111/jvs.12995.

Zupo T, Daibes LF, Pausas JG, Fidelis A. 2021. Post-fire regeneration strategies in a frequently burned Cerrado community. *Journal of Vegetation Science* 32: e12968. DOI: 10.1111/jvs.12968.

4.11. Supplementary material

Table S4.1, list of dominant tree species selected for each plot and experimental fire regime. Dominant species were selected in terms of basal area (m^2 ha^{-1}), and were defined as those contributing the most to up to 80% of the basal area within each plot. Dominant species were determined using the data from the most recent census (2023). For each plot, basal area values for each species are reported, as well as the total plot basal area and the total basal area of dominant species.

Unburnt					**Triennial**		**Biennial**		**Annual**	
ESA-04	8.04	**ESA-06**	5.22	**ESA-08**	6.42	**ESA-07**	1.81	**ESA-05**	2.19	**ESA-09**	5.70
dominant species	6.57	**dominant species**	4.34	**dominant species**	5.21	**dominant species**	1.48	**dominant species**	1.79	**dominant species**	4.72
Tachigali vulgaris	2.55	*Tachigali vulgaris*	1.71	*Tachigali vulgaris*	3.18	*Curatella americana*	0.54	*Curatella americana*	0.64	*Tachigali vulgaris*	1.83
Curatella americana	1.49	*Curatella americana*	0.88	*Kielmeyera grandiflora*	0.50	*Pouteria ramiflora*	0.18	*Tachigali vulgaris*	0.28	*Kielmeyera grandiflora*	0.78
Vochysia haenkeana	0.64	*Kielmeyera grandiflora*	0.82	*Curatella americana*	0.45	*Kielmeyera grandiflora*	0.18	*Kielmeyera grandiflora*	0.20	*Pouteria ramiflora*	0.57
Pouteria ramiflora	0.44	*Pouteria ramiflora*	0.33	*Pouteria ramiflora*	0.44	*Vochysia haenkeana*	0.18	*Vochysia haenkeana*	0.16	*Vochysia haenkeana*	0.54
Myrcia bella	0.28	*Vochysia haenkeana*	0.32	*Qualea grandiflora*	0.23	*Myrcia bella*	0.13	*Myrcia bella*	0.15	*Curatella americana*	0.42
Qualea grandiflora	0.25	*Myrcia bella*	0.26	*Xylopia aromatica*	0.22	*Byrsonima coccolobifolia*	0.10	*Pouteria ramiflora*	0.10	*Dimorphandra mollis*	0.38
Kielmeyera grandiflora	0.23			*Vochysia haenkeana*	0.19	*Hancornia speciosa*	0.09	*Byrsonima coccolobifolia*	0.10	*Byrsonima verbascifolia*	0.19
Trichilia silvatica	0.23					*Byrsonima verbascifolia*	0.09	*Ferdinandusa elliptica*	0.09		
Qualea parviflora	0.23							*Qualea multiflora*	0.06		
Xylopia aromatica	0.22										

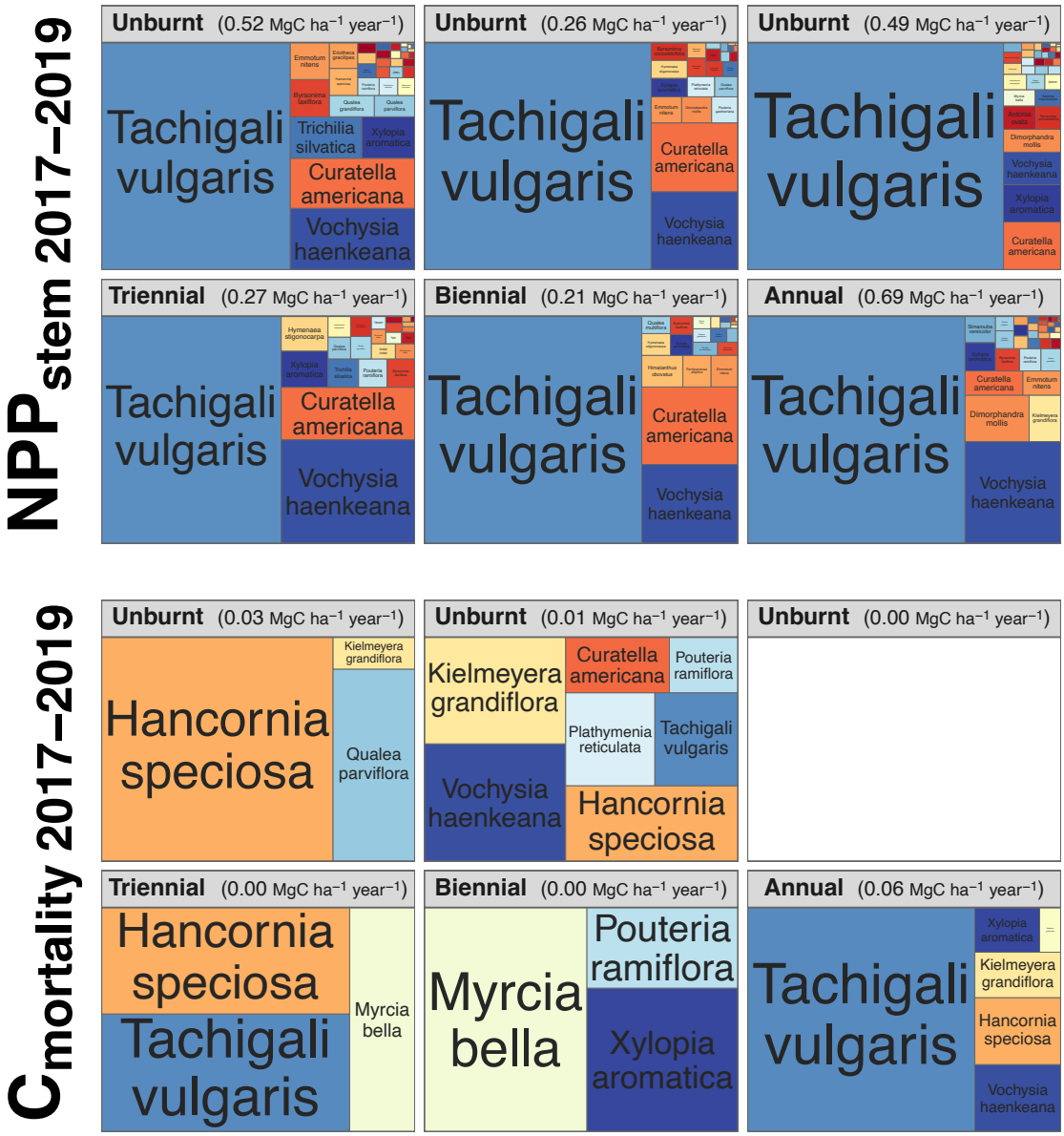


Figure S4.1, species contributions to plot-level aboveground woody stem net primary productivity (NPP_{stem}) and mortality carbon ($C_{mortality}$) across the experimental fire monitoring plots at Serra das Araras, Brazil, during the 2017 to 2019 census interval. Within each facet, the area occupied by any given species represents its proportion of total plot NPP_{stem} and $C_{mortality}$ (total plot values are included above each facet).

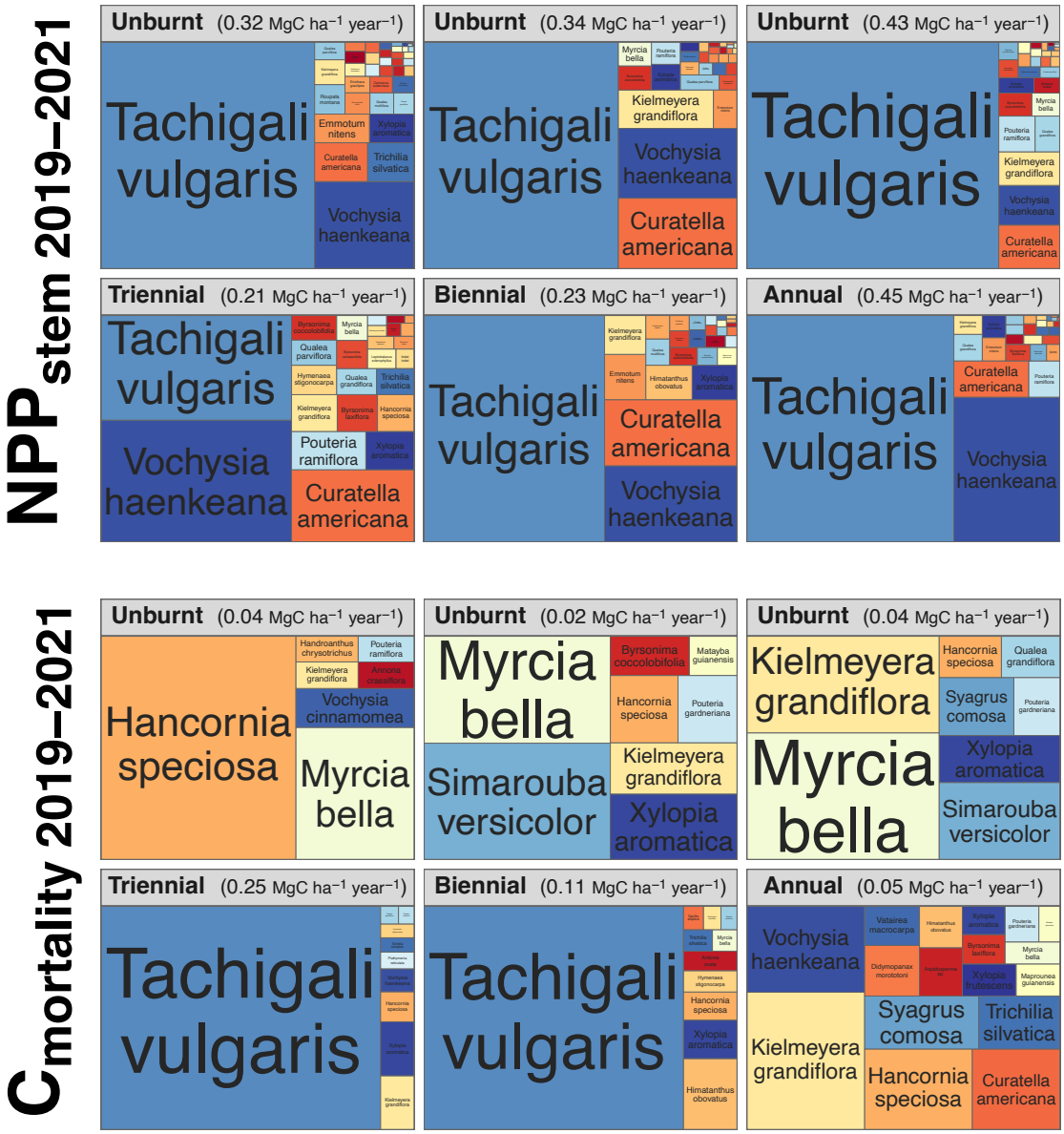


Figure S4.2, species contributions to plot-level aboveground woody stem net primary productivity (NPP_{stem}) and mortality carbon ($C_{mortality}$) across the experimental fire monitoring plots at Serra das Araras, Brazil, during the 2019 to 2021 census interval. Within each facet, the area occupied by any given species represents its proportion of total plot NPP_{stem} and $C_{mortality}$ (total plot values are included above each facet).

Table S4.2, estimates of woody stem productivity (± standard error) for each of the 16 dominant tree species across fire regimes and census intervals. Estimates represent marginal means extracted from species-specific linear mixed models interacting regime and interval.

Species	Regime	$NPP_{stem\ 2017\text{-}2019}$	$NPP_{stem\ 2019\text{-}2021}$	$NPP_{stem\ 2021\text{-}2023}$
Byrsonima coccolobifolia	Unburnt	0.00011181 ± 0.00003985	0.00012781 ± 0.00003944	0.00011280 ± 0.00003909
	Triennial	0.00006633 ± 0.00006669	0.00012447 ± 0.00006319	0.00011396 ± 0.00008328
	Biennial	-0.00003905 ± 0.00006938	0.00007319 ± 0.00006946	0.00035346 ± 0.00007655
	Annual	0.00004065 ± 0.00006425	0.00003402 ± 0.00006313	0.00018139 ± 0.00006551
Byrsonima verbascifolia	Unburnt	-0.00007822 ± 0.00006050	0.00005412 ± 0.00006058	0.00006594 ± 0.00006024
	Triennial	0.00006401 ± 0.00013345	0.00028967 ± 0.00013375	0.00026212 ± 0.00013371
	Biennial	0.00010367 ± 0.00014065	0.00004298 ± 0.00013342	0.00068302 ± 0.00015021
	Annual	0.00001585 ± 0.00008817	0.00004152 ± 0.00008820	0.00040427 ± 0.00008852
Curatella americana	Unburnt	0.00032304 ± 0.00006204	0.00022883 ± 0.00006097	0.00047180 ± 0.00006068
	Triennial	0.00065064 ± 0.00014169	0.00060562 ± 0.00013774	0.00070777 ± 0.00013788
	Biennial	0.00038850 ± 0.00012309	0.00044499 ± 0.00011955	0.00065382 ± 0.00011726
	Annual	0.00031350 ± 0.00013842	0.00040232 ± 0.00013858	0.00061071 ± 0.00014444
Dimorphandra mollis	Unburnt	0.00038954 ± 0.00019858	-0.00005344 ± 0.00019449	0.00044097 ± 0.00019545
	Triennial	0.00113792 ± 0.00109579	-0.00005318 ± 0.00108289	-0.00008372 ± 0.00108255
	Biennial	-0.00090786 ± 0.00075917	-0.00059736 ± 0.00076155	0.00069607 ± 0.00077146
	Annual	0.00069678 ± 0.00017039	-0.00018593 ± 0.00016687	0.00051023 ± 0.00019251
Ferdinandusa elliptica	Unburnt	-0.00000241 ± 0.00039281	0.00017406 ± 0.00023285	0.00047690 ± 0.00020270
	Triennial	0.00022941 ± 0.00040441	0.00053196 ± 0.00040563	0.00058975 ± 0.00040587
	Biennial	0.00029025 ± 0.00012744	0.00018180 ± 0.00012179	0.00005549 ± 0.00011654
	Annual	0.00062268 ± 0.00040422	0.00035367 ± 0.00028632	0.00048471 ± 0.00040367
Hancornia speciosa	Unburnt	0.00009194 ± 0.00006698	-0.00005049 ± 0.00007759	0.00002141 ± 0.00009104
	Triennial	-0.00000545 ± 0.00013568	0.00022267 ± 0.00013599	-0.00007802 ± 0.00018191
	Biennial	-0.00002201 ± 0.00020349	0.00002385 ± 0.00025752	0.00035016 ± 0.00028885
	Annual	-0.00013848 ± 0.00011064	-0.00001070 ± 0.00011289	0.00021052 ± 0.00011538
Kielmeyera grandiflora	Unburnt	-0.00006290 ± 0.00001784	0.00011579 ± 0.00001805	0.00001958 ± 0.00001789
	Triennial	-0.00001248 ± 0.00005062	0.00018704 ± 0.00005516	0.00017373 ± 0.00005619
	Biennial	-0.00004227 ± 0.00003812	0.00009176 ± 0.00003817	-0.00001155 ± 0.00004592
	Annual	0.00009082 ± 0.00002341	0.00002278 ± 0.00002375	0.00015232 ± 0.00002522
Myrcia bella	Unburnt	-0.00004609 ± 0.00001952	0.00004366 ± 0.00002021	0.00002107 ± 0.00002148
	Triennial	0.00004216 ± 0.00006060	0.00013722 ± 0.00005901	0.00014836 ± 0.00006950
	Biennial	0.00001895 ± 0.00004144	-0.00003351 ± 0.00004184	0.00011577 ± 0.00005623
	Annual	-0.00001762 ± 0.00007941	-0.00001290 ± 0.00008401	0.00026098 ± 0.00011830
Pouteria ramiflora	Unburnt	0.00000474 ± 0.00002127	0.00003822 ± 0.00002120	0.00008080 ± 0.00002119
	Triennial	0.00005476 ± 0.00004220	0.00014716 ± 0.00004180	-0.00005115 ± 0.00004662
	Biennial	-0.00001160 ± 0.00005150	-0.00000184 ± 0.00004929	0.00014163 ± 0.00005686
	Annual	0.00003979 ± 0.00003492	0.00006213 ± 0.00003487	0.00025796 ± 0.00003520
Qualea grandiflora	Unburnt	0.00008884 ± 0.00005523	0.00005530 ± 0.00005462	0.00009562 ± 0.00005447
	Triennial	0.00017955 ± 0.00013686	0.00031149 ± 0.00013704	0.00009676 ± 0.00018329
	Biennial	-0.00002266 ± 0.00027945	-0.00004410 ± 0.00027939	0.00013667 ± 0.00039099
	Annual	0.00020570 ± 0.00010450	0.00023183 ± 0.00010453	0.00046770 ± 0.00010646
Qualea multiflora	Unburnt	0.00029864 ± 0.00015681	0.00046947 ± 0.00013603	0.00038039 ± 0.00013591
	Triennial			
	Biennial	0.00008559 ± 0.00009034	0.00012073 ± 0.00009299	0.00024402 ± 0.00011575
	Annual	0.00043414 ± 0.00015702	0.00018746 ± 0.00015663	0.00008090 ± 0.00017140
Qualea parviflora	Unburnt	0.00023506 ± 0.00008585	0.00016491 ± 0.00008349	0.00037239 ± 0.00007739
	Triennial	0.00021289 ± 0.00018271	0.00038424 ± 0.00018302	0.00034668 ± 0.00017884
	Biennial	0.00009090 ± 0.00030882	0.00012394 ± 0.00030892	0.00034209 ± 0.00030959
	Annual	0.00052084 ± 0.00021444	0.00017650 ± 0.00021370	0.00035009 ± 0.00021407
Tachigali vulgaris	Unburnt	0.00338905 ± 0.00064989	0.00268146 ± 0.00064189	0.00425587 ± 0.00065110
	Triennial	0.00308250 ± 0.00117283	0.00336934 ± 0.00138269	-0.00522172 ± 0.00329180
	Biennial	0.00212675 ± 0.00112838	0.00225008 ± 0.00114746	0.00643525 ± 0.00166337
	Annual	0.00576581 ± 0.00115624	0.00355182 ± 0.00113044	0.00764286 ± 0.00125809
Trichilia silvatica	Unburnt	0.00093355 ± 0.00032021	0.00016850 ± 0.00029865	0.00116808 ± 0.00030106
	Triennial	0.00082627 ± 0.00054496	0.00098997 ± 0.00059866	
	Biennial	0.00034620 ± 0.00068791	0.00015383 ± 0.00091002	
	Annual	0.00059622 ± 0.00068962		
Vochysia haenkeana	Unburnt	0.00105292 ± 0.00019523	0.00080352 ± 0.00017951	0.00081624 ± 0.00016852
	Triennial	0.00174295 ± 0.00033603	0.00198946 ± 0.00031419	-0.00111221 ± 0.00054266
	Biennial	0.00086610 ± 0.00034834	0.00102805 ± 0.00031843	0.00029752 ± 0.00043307
	Annual	0.00111938 ± 0.00022931	0.00103082 ± 0.00022005	0.00066879 ± 0.00024651
Xylopia aromatica	Unburnt	0.00044337 ± 0.00007721	0.00010297 ± 0.00007422	0.00019646 ± 0.00007340
	Triennial	0.00043085 ± 0.00014462	0.00024211 ± 0.00013425	
	Biennial	0.00020595 ± 0.00017337	0.00072405 ± 0.00017427	
	Annual	0.00046451 ± 0.00013991	0.00018865 ± 0.00013953	0.00006699 ± 0.00036549

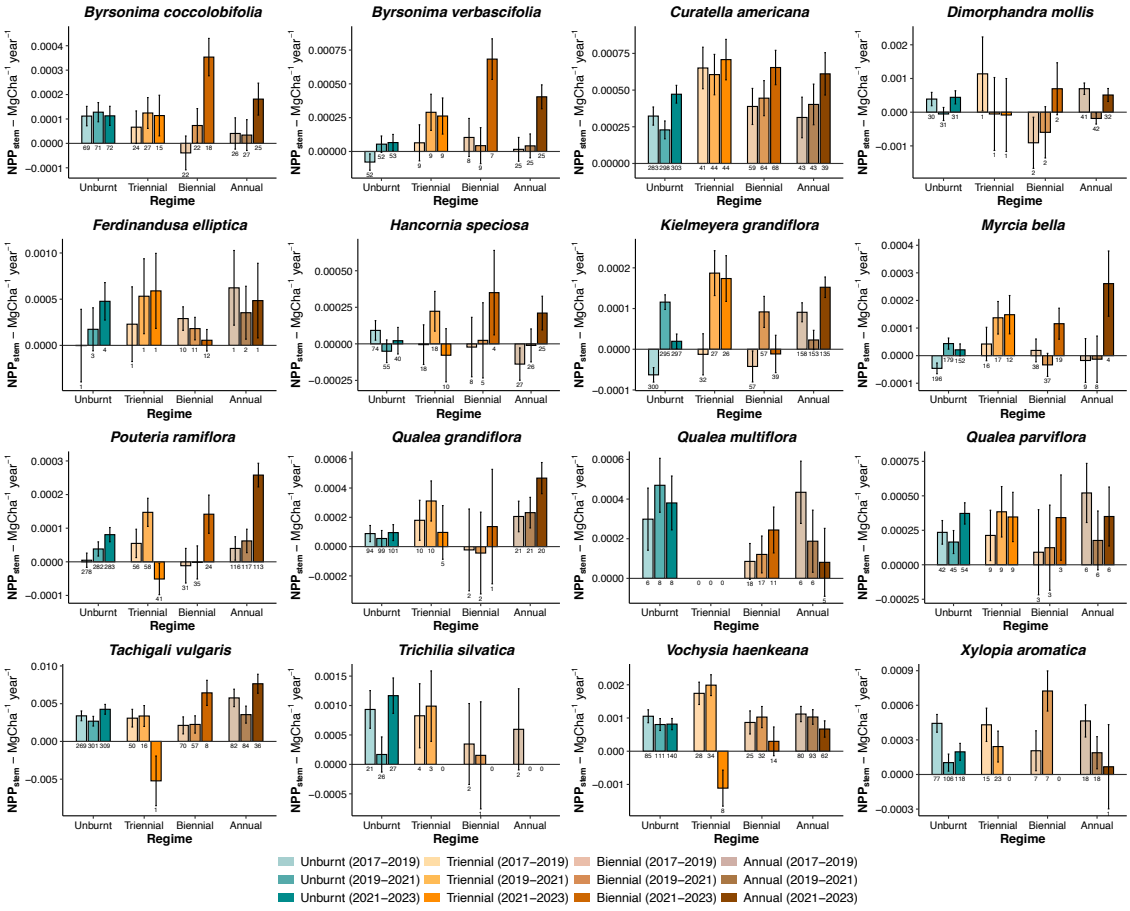


Figure S4.3, NPP_{stem} estimates (MgC ha^{-1} $year^{-1}$) for the 16 dominant species across census intervals and experimental fire regimes at Serra das Araras, Brazil. Estimates were derived from species-specific mixed-effect models, from which marginal means were extracted for each interval-regime combination (alongside their corresponding standard error). Fire regimes include triennially, biennially and annually burnt plots, as well as unburnt plots; and there were three census intervals (2017 to 2019, 2019 to 2021 and 2021 to 2023). Please note axis ranges were specific to each plot, and allowed to vary to facilitate visual understanding. The horizontal grey line for each graph indicates zero NPP_{stem}. Empty spaces indicate we were unable to calculate NPP_{stem} for that species during that particular census interval, as there were no stems present both at the start and end of the interval. Each bar is accompanied by a numeric label indicating the number of stems from which NPP_{stem} was estimated.

Table S4.3, estimates of survival rates (± standard error) for each of the 16 dominant tree species across fire regimes and census intervals. Estimates represent back-transformed marginal means extracted from species-specific binomial mixed models interacting regime and interval.

Species	Regime	survival 2017-2019	survival 2019-2021	survival 2021-2023
Byrsonima coccolobifolia	Unburnt	0.993 ± 0.010	0.979 ± 0.017	0.993 ± 0.010
	Triennial	0.980 ± 0.028	0.982 ± 0.025	0.554 ± 0.094
	Biennial	0.978 ± 0.030	0.978 ± 0.030	0.804 ± 0.083
	Annual	0.981 ± 0.026	0.982 ± 0.025	0.911 ± 0.054
Byrsonima verbascifolia	Unburnt	0.991 ± 0.013	0.991 ± 0.013	0.991 ± 0.013
	Triennial	0.950 ± 0.069	0.950 ± 0.069	0.864 ± 0.103
	Biennial	0.944 ± 0.076	0.950 ± 0.069	0.750 ± 0.137
	Annual	0.981 ± 0.027	0.981 ± 0.027	0.981 ± 0.027
Curatella americana	Unburnt	0.995 ± 0.004	0.998 ± 0.002	0.995 ± 0.004
	Triennial	0.988 ± 0.017	0.989 ± 0.016	0.989 ± 0.016
	Biennial	0.992 ± 0.012	0.992 ± 0.011	0.993 ± 0.010
	Annual	0.989 ± 0.016	0.946 ± 0.033	0.878 ± 0.049
Dimorphandra mollis	Unburnt	0.984 ± 0.023	0.984 ± 0.022	0.984 ± 0.022
	Triennial	0.750 ± 0.306	0.750 ± 0.306	0.750 ± 0.306
	Biennial	0.833 ± 0.215	0.833 ± 0.215	0.833 ± 0.215
	Annual	0.988 ± 0.017	0.988 ± 0.016	0.756 ± 0.066
Ferdinandusa elliptica	Unburnt	0.750 ± 0.306	0.875 ± 0.165	0.900 ± 0.134
	Triennial	0.750 ± 0.306	0.750 ± 0.306	0.750 ± 0.306
	Biennial	0.955 ± 0.063	0.958 ± 0.058	0.962 ± 0.053
	Annual	0.750 ± 0.306	0.833 ± 0.215	0.500 ± 0.289
Hancornia speciosa	Unburnt	0.898 ± 0.033	0.740 ± 0.051	0.711 ± 0.060
	Triennial	0.925 ± 0.059	0.881 ± 0.071	0.553 ± 0.114
	Biennial	0.944 ± 0.076	0.611 ± 0.162	0.750 ± 0.177
	Annual	0.917 ± 0.050	0.883 ± 0.059	0.944 ± 0.044
Kielmeyera grandiflora	Unburnt	0.992 ± 0.005	0.978 ± 0.008	0.960 ± 0.011
	Triennial	0.985 ± 0.021	0.833 ± 0.065	0.946 ± 0.043
	Biennial	0.991 ± 0.012	0.991 ± 0.012	0.648 ± 0.061
	Annual	0.984 ± 0.010	0.930 ± 0.020	0.880 ± 0.026
Myrcia bella	Unburnt	0.997 ± 0.004	0.889 ± 0.022	0.847 ± 0.027
	Triennial	0.971 ± 0.041	0.972 ± 0.039	0.694 ± 0.109
	Biennial	0.962 ± 0.030	0.962 ± 0.031	0.513 ± 0.081
	Annual	0.950 ± 0.069	0.850 ± 0.113	0.500 ± 0.167
Pouteria ramiflora	Unburnt	0.995 ± 0.004	0.995 ± 0.004	0.984 ± 0.007
	Triennial	0.991 ± 0.012	0.975 ± 0.020	0.692 ± 0.060
	Biennial	0.955 ± 0.036	0.986 ± 0.020	0.681 ± 0.078
	Annual	0.996 ± 0.006	0.996 ± 0.006	0.962 ± 0.018
Qualea grandiflora	Unburnt	0.995 ± 0.007	0.985 ± 0.012	0.967 ± 0.018
	Triennial	0.955 ± 0.063	0.955 ± 0.063	0.500 ± 0.151
	Biennial	0.833 ± 0.215	0.833 ± 0.215	0.500 ± 0.289
	Annual	0.977 ± 0.032	0.977 ± 0.032	0.932 ± 0.054
Qualea multiflora	Unburnt	0.929 ± 0.097	0.944 ± 0.076	0.944 ± 0.076
	Triennial	0.974 ± 0.037	0.921 ± 0.062	0.639 ± 0.113
	Biennial	0.929 ± 0.097	0.929 ± 0.097	0.786 ± 0.155
	Annual	0.966 ± 0.027	0.989 ± 0.015	0.991 ± 0.013
Qualea parviflora	Unburnt	0.950 ± 0.069	0.950 ± 0.069	0.864 ± 0.103
	Triennial	0.875 ± 0.165	0.875 ± 0.165	0.875 ± 0.165
	Biennial	0.929 ± 0.097	0.929 ± 0.097	0.929 ± 0.097
	Annual	0.998 ± 0.003	0.998 ± 0.002	0.958 ± 0.011
Tachigali vulgaris	Unburnt	0.953 ± 0.029	0.300 ± 0.062	0.088 ± 0.069
	Triennial	0.993 ± 0.010	0.639 ± 0.051	0.147 ± 0.046
	Biennial	0.948 ± 0.024	0.994 ± 0.008	0.426 ± 0.053
	Annual	0.993 ± 0.010	0.979 ± 0.017	0.993 ± 0.010
Trichilia silvatica	Unburnt	0.977 ± 0.032	0.981 ± 0.026	0.982 ± 0.025
	Triennial	0.900 ± 0.134	0.700 ± 0.205	0.083 ± 0.113
	Biennial	0.833 ± 0.215	0.500 ± 0.289	0.250 ± 0.306
	Annual	0.833 ± 0.215	0.167 ± 0.215	
Vochysia haenkeana	Unburnt	0.994 ± 0.008	0.996 ± 0.006	0.983 ± 0.011
	Triennial	0.983 ± 0.024	0.908 ± 0.047	0.236 ± 0.071
	Biennial	0.981 ± 0.027	0.985 ± 0.021	0.403 ± 0.082
	Annual	0.970 ± 0.019	0.954 ± 0.021	0.534 ± 0.046
Xylopia aromatica	Unburnt	0.994 ± 0.009	0.959 ± 0.019	0.971 ± 0.015
	Triennial	0.969 ± 0.043	0.783 ± 0.075	0.019 ± 0.026
	Biennial	0.944 ± 0.076	0.577 ± 0.137	0.062 ± 0.086
	Annual	0.974 ± 0.037	0.925 ± 0.059	0.079 ± 0.062

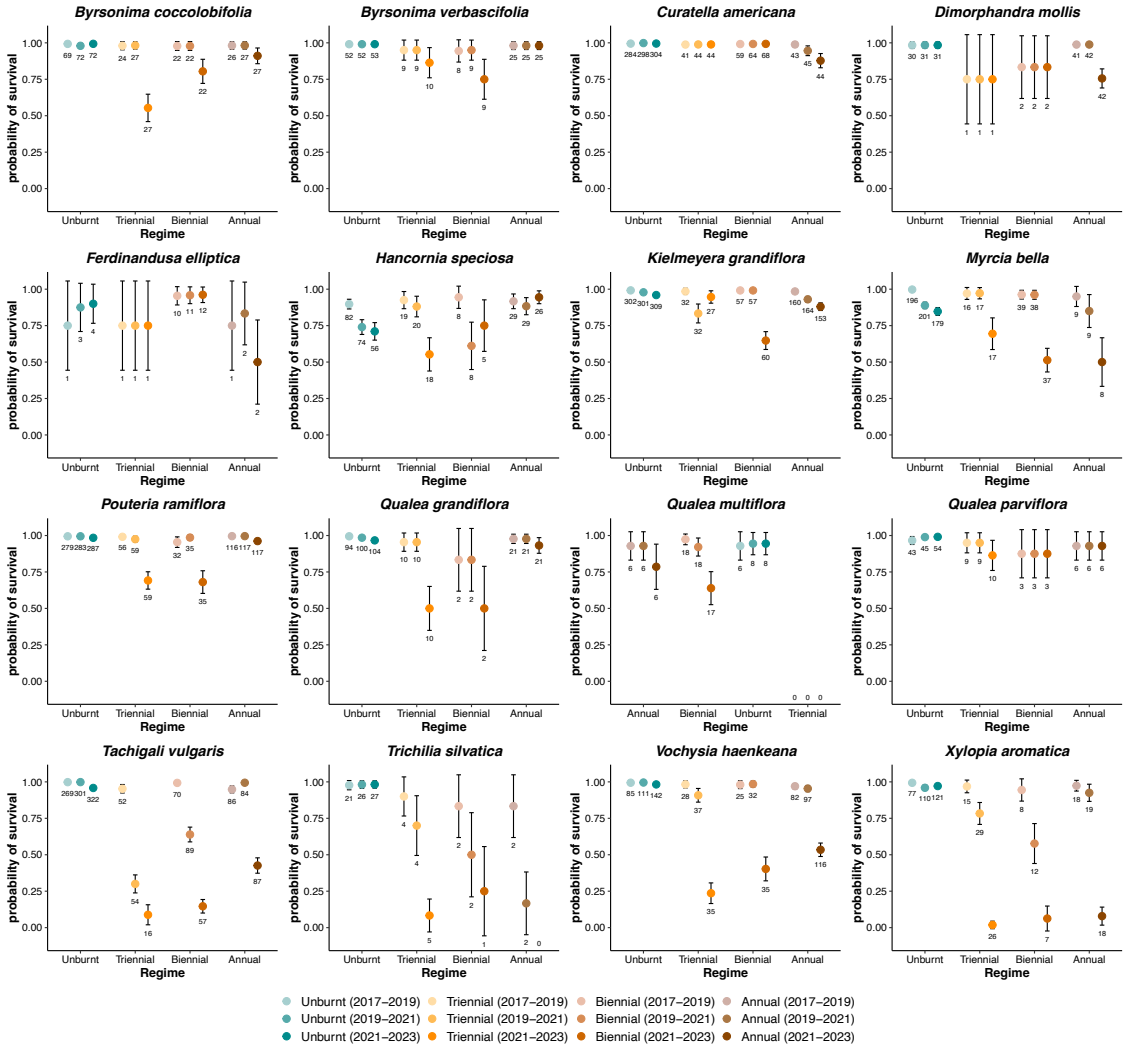


Figure S4.4, survival estimates (describing the probability of stems surviving from one census to the next) for the 16 dominant species across census intervals and experimental fire regimes at Serra das Araras, Brazil. Estimates were derived from species-specific bias-reduced logistic regression models, from which marginal means were extracted for each interval-regime combination (alongside their corresponding standard error). Fire regimes include triennially, biennially and annually burnt plots, as well as unburnt plots; and there were three census intervals (2017 to 2019, 2019 to 2021 and 2021 to 2023). Please note axis ranges were standardised across all plots, reflecting the full range in survival probability (0 = 0% chance of survival, 1 = 100% chance of survival). Empty spaces indicate we were unable to calculate survival for that species during that particular census interval, as there were no stems present at the start of the interval. Each point is accompanied by a numeric label indicating the number of stems from which survival was estimated.

Table S4.4, summary statistics for the linear models testing if species-level estimates of ΔNPP_{stem} vary with estimates of initial NPP_{stem}. Different models were used for each plot, **with data from the 16 dominant species including *Tachigali vulgaris***. Initial NPP_{stem} reflects woody stem, productivity estimates for the 2017-2019 interval, derived from species-specific linear mixed models (**Table S4.2**). ΔNPP_{stem} was calculated as the difference between final (2021-2023) and initial (2017-2019) estimates.

Unburnt: initial NPP_{stem} ~ ΔNPP_{stem}				
Analysis of Variance	**R^2**	**DF**	**F-value**	**Pr(>F)**
	0.364	1,14	8.012	0.013
Coefficients	**Estimate**	**Std. Error**	**t-value**	**Pr(>|t|)**
(Intercept)	0.0002243	0.0001941	1.155	0.267
ΔNPP_{stem}	**2.0200536**	**0.7136698**	**2.831**	**0.013**

Triennial: initial NPP_{stem} ~ ΔNPP_{stem}				
Analysis of Variance	**R^2**	**DF**	**F-value**	**Pr(>F)**
	0.913	1,11	115.9	0.000
Coefficients	**Estimate**	**Std. Error**	**t-value**	**Pr(>|t|)**
(Intercept)	**2.462e-04**	**8.405e-05**	**2.929**	**0.013**
ΔNPP_{stem}	**-3.674e-01**	**3.413e-02**	**-10.766**	**0.000**

Biennial: initial NPP_{stem} ~ ΔNPP_{stem}				
Analysis of Variance	**R^2**	**DF**	**F-value**	**Pr(>F)**
	0.313	1,12	5.474	0.037
Coefficients	**Estimate**	**Std. Error**	**t-value**	**Pr(>|t|)**
(Intercept)	3.917e-05	1.697e-04	0.231	0.821
ΔNPP_{stem}	**3.142e-01**	**1.343e-01**	**2.340**	**0.037**

Annual: initial NPP_{stem} ~ ΔNPP_{stem}				
Analysis of Variance	**R^2**	**DF**	**F-value**	**Pr(>F)**
	0.541	1,13	15.35	0.002
Coefficients	**Estimate**	**Std. Error**	**t-value**	**Pr(>|t|)**
(Intercept)	0.0004014	0.0002720	1.476	0.164
ΔNPP_{stem}	**1.9118513**	**0.4880237**	**3.918**	**0.002**

Table S4.5, summary statistics for the linear models testing if species-level estimates of ΔNPP_{stem} vary with estimates of initial NPP_{stem} (see **Figure 4.4**). Different models were used for each plot, **with data from 15 dominant species but excluding *Tachigali vulgaris***. Initial NPP_{stem} reflects woody stem productivity estimates for the 2017-2019 interval, derived from species-specific linear mixed models (**Table S4.2**). ΔNPP_{stem} was calculated as the difference between final (2021-2023) and initial (2017-2019) estimates.

Unburnt: initial NPP_{stem} ~ ΔNPP_{stem}				
Analysis of Variance	**R^2**	**DF**	**F-value**	**Pr(>F)**
	0.111	1,13	1.614	0.226
Coefficients	**Estimate**	**Std. Error**	**t-value**	**Pr(>|t|)**
(Intercept)	**2.938e-04**	**9.305e-05**	**3.157**	**0.008**
ΔNPP_{stem}	-6.508e-01	5.122e-01	-1.271	0.226

Triennial: initial NPP_{stem} ~ ΔNPP_{stem}				
Analysis of Variance	**R^2**	**DF**	**F-value**	**Pr(>F)**
	0.849	1,10	56.24	0.000
Coefficients	**Estimate**	**Std. Error**	**t-value**	**Pr(>|t|)**
(Intercept)	**2.124e-04**	**6.764e-05**	**3.141**	**0.011**
ΔNPP_{stem}	**-5.583e-01**	**7.444e-02**	**-7.500**	**0.000**

Biennial: initial NPP_{stem} ~ ΔNPP_{stem}				
Analysis of Variance	**R^2**	**DF**	**F-value**	**Pr(>F)**
	0.784	1,11	39.92	0.000
Coefficients	**Estimate**	**Std. Error**	**t-value**	**Pr(>|t|)**
(Intercept)	**2.336e-04**	**5.873e-05**	**3.977**	**0.002**
ΔNPP_{stem}	**-6.866e-01**	**1.087e-01**	**-6.318**	**0.000**

Annual: initial NPP_{stem} ~ ΔNPP_{stem}				
Analysis of Variance	**R^2**	**DF**	**F-value**	**Pr(>F)**
	0.695	1,12	27.38	0.000
Coefficients	**Estimate**	**Std. Error**	**t-value**	**Pr(>|t|)**
(Intercept)	**3.359e-04**	**5.378e-05**	**6.246**	**0.000**
ΔNPP_{stem}	**-9.829e-01**	**1.879e-01**	**-5.233**	**0.000**

Table S4.6, summary statistics for the linear models testing if species-level estimates of Δsurvival vary with estimates of initial NPP_{stem}. Different models were used for each plot, **with data from the 16 dominant species including *Tachigali vulgaris***. Initial NPP_{stem} reflects woody stem productivity estimates for the 2017-2019 interval, derived from species-specific linear mixed models (**Table S4.2**). Δsurvival was calculated as the logit-transformed difference between final (2021-2023) and initial (2017-2019) survival estimates, also derived from species-specific mixed models (**Table S4.3**).

Unburnt: initial NPP_{stem} ~ logit(Δsurvival)				
Analysis of Variance	**R^2**	**DF**	**F-value**	**Pr(>F)**
	0.109	1,14	1.718	0.211
Coefficients	**Estimate**	**Std. Error**	**t-value**	**Pr(>|t|)**
(Intercept)	0.0002945	0.0002406	1.224	0.241
logit(Δsurvival)	-0.0001909	0.0001456	-1.311	0.211

Triennial: initial NPP_{stem} ~ logit(Δsurvival)				
Analysis of Variance	**R^2**	**DF**	**F-value**	**Pr(>F)**
	0.108	1,13	1.574	0.232
Coefficients	**Estimate**	**Std. Error**	**t-value**	**Pr(>|t|)**
(Intercept)	0.0002648	0.0003316	0.798	0.439
logit(Δsurvival)	-0.0001251	0.0000997	-1.254	0.232

Biennial: initial NPP_{stem} ~ logit(Δsurvival)				
Analysis of Variance	**R^2**	**DF**	**F-value**	**Pr(>F)**
	0.341	1,14	7.241	0.018
Coefficients	**Estimate**	**Std. Error**	**t-value**	**Pr(>|t|)**
(Intercept)	-1.832e-04	1.979e-04	-0.926	0.370
logit(Δsurvival)	**-1.733e-04**	**6.442e-05**	**-2.691**	**0.018**

Annual: initial NPP_{stem} ~ logit(Δsurvival)				
Analysis of Variance	**R^2**	**DF**	**F-value**	**Pr(>F)**
	0.076	1,13	1.069	0.320
Coefficients	**Estimate**	**Std. Error**	**t-value**	**Pr(>|t|)**
(Intercept)	0.0001919	0.0006003	0.320	0.754
logit(Δsurvival)	-0.0002397	0.0002318	-1.034	0.320

Table S4.7, summary statistics for the linear models testing if species-level estimates of Δsurvival change vary with estimates of initial NPP_{stem}. Different models were used for each plot, **with data from 15 dominant species but excluding *Tachigali vulgaris*.** Initial NPP_{stem} reflects woody stem productivity estimates for the 2017-2019 interval, derived from species-specific linear mixed models (**Table S4.2**). Δsurvival was calculated as the logit-transformed difference between final (2021-2023) and initial (2017-2019) survival estimates, also derived from species-specific mixed models (**Table S4.3**).

Unburnt: initial NPP_{stem} ~ logit(Δsurvival)				
Analysis of Variance	**R^2**	**DF**	**F-value**	**Pr(>F)**
	0.026	1,13	0.348	0.565
Coefficients	**Estimate**	**Std. Error**	**t-value**	**Pr(>|t|)**
(Intercept)	**2.785e-04**	**1.014e-04**	**2.746**	**0.017**
logit(Δsurvival)	3.992e-05	6.763e-05	0.590	0.565

Triennial: initial NPP_{stem} ~ logit(Δsurvival)				
Analysis of Variance	**R^2**	**DF**	**F-value**	**Pr(>F)**
	0.007	1,12	0.089	0.771
Coefficients	**Estimate**	**Std. Error**	**t-value**	**Pr(>|t|)**
(Intercept)	3.541e-04	2.144e-04	1.652	0.125
logit(Δsurvival)	-2.040e-05	6.843e-05	-0.298	0.771

Biennial: initial NPP_{stem} ~ logit(Δsurvival)				
Analysis of Variance	**R^2**	**DF**	**F-value**	**Pr(>F)**
	0.068	1,13	0.943	0.0349
Coefficients	**Estimate**	**Std. Error**	**t-value**	**Pr(>|t|)**
(Intercept)	-1.746e-05	1.457e-04	-0.120	0.906
logit(Δsurvival)	-5.328e-05	5.484e-05	-0.971	0.349

Annual: initial NPP_{stem} ~ logit(Δsurvival)				
Analysis of Variance	**R^2**	**DF**	**F-value**	**Pr(>F)**
	0.140	1,12	1.96	0.187
Coefficients	**Estimate**	**Std. Error**	**t-value**	**Pr(>|t|)**
(Intercept)	1.647e-04	1.401e-04	1.175	0.263
logit(Δsurvival)	-7.718e-05	5.519e-05	-1.398	0.187

Table S4.8, summary statistics for the principal component analysis (PCA) on standardised functional traits of dominant tree species across the experimental fire regimes in Serra das Araras (includes bark, leaf and photosynthetic traits, without wood density, see **Figure 4.5**). Describes the proportion of variance explained by each principal component as well as the loadings of each trait.

Principal Component Analysis	**PC1**	**PC2**	**PC3**	**PC4**	**PC5**	**PC6**
standard deviation	1.945	1.585	1.322	1.263	1.133	1.035
proportion of variance	0.252	0.168	0.116	0.106	0.086	0.071
cumulative proportion	0.252	0.420	0.536	0.643	0.728	0.800
LA – leaf area	0.088	-0.370	-0.352	0.064	0.285	-0.317
LT – leaf thickness	-0.352	-0.016	0.014	-0.338	0.075	-0.137
LDMC – leaf dry-matter content	0.251	0.131	0.231	0.294	-0.493	0.123
SLA – specific leaf area	0.286	0.001	-0.330	0.188	0.468	0.119
OBT – outer bark thickness	-0.305	0.032	-0.456	-0.111	-0.334	0.012
IBT – inner bark thickness	0.047	-0.142	-0.150	-0.365	0.149	0.706
rBT – relative bark thickness	-0.427	0.078	-0.200	0.065	-0.024	0.138
BD – bark density	0.345	-0.095	-0.179	0.345	0.012	0.060
BWC – bark water content	0.116	-0.048	0.540	-0.270	0.314	0.131
STol – photosynthetic shade tolerance	0.205	0.365	-0.122	-0.186	0.045	-0.361
Asat – light-saturated photosynthetic rate	-0.091	-0.486	0.064	0.259	-0.216	0.203
Amax – maximum photosynthetic rate	-0.014	-0.543	0.028	-0.068	-0.083	-0.121
Dresp – leaf dark respiration	0.088	0.347	-0.226	0.069	-0.009	0.346
DBH – diameter at breast height	0.320	-0.086	-0.212	-0.430	-0.321	0.004
H – tree height	0.392	-0.122	-0.069	-0.349	-0.243	-0.084

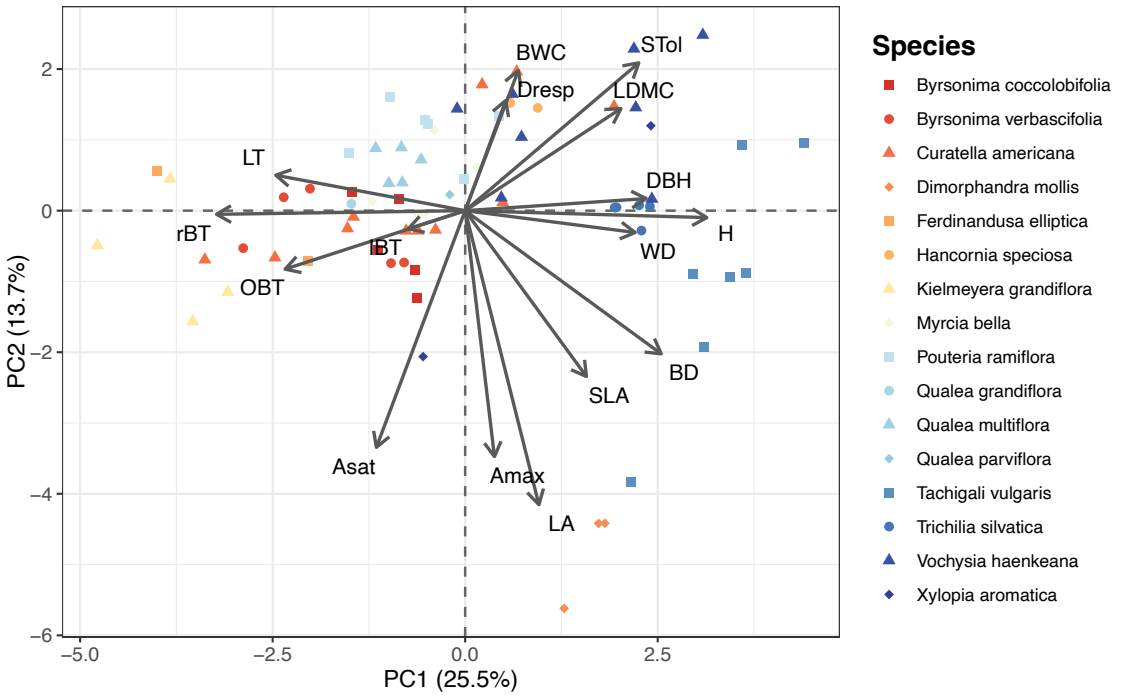


Figure S4.5, principal component analysis (PCA) for standardised functional traits of dominant tree species across the experimental fire regimes in Serra das Araras (includes bark, leaf, wood and photosynthetic traits, see **Table S4.9** for details).

Table S4.9, summary statistics for the principal component analysis (PCA) on standardised functional traits of dominant tree species across the experimental fire regimes in Serra das Araras (includes bark, leaf, photosynthetic and wood traits). Describes the proportion of variance explained by each principal component as well as the loadings of each trait.

Principal Component Analysis	**PC1**	**PC2**	**PC3**	**PC4**	**PC5**	**PC6**
standard deviation	2.010	1.483	1.353	1.324	1.220	1.044
proportion of variance	0.252	0.137	0.114	0.110	0.093	0.068
cumulative proportion	0.252	0.390	0.504	0.614	0.707	0.775
LA – leaf area	0.126	-0.513	-0.032	-0.067	-0.223	-0.154
LT – leaf thickness	-0.322	0.051	0.135	-0.274	0.033	-0.016
LDMC – leaf dry-matter content	0.258	0.183	-0.121	0.404	0.352	0.096
SLA – specific leaf area	0.218	-0.279	-0.127	0.038	-0.538	0.241
OBT – outer bark thickness	-0.278	-0.099	-0.487	-0.213	0.165	-0.064
IBT – inner bark thickness	-0.048	-0.004	-0.103	-0.403	-0.098	0.648
rBT – relative bark thickness	-0.398	-0.007	-0.306	0.014	0.021	0.124
BD – bark density	0.315	-0.264	-0.128	0.192	-0.144	-0.057
BWC – bark water content	0.065	0.249	0.581	-0.045	-0.068	0.270
WD – wood density	0.279	-0.032	-0.187	0.033	0.382	0.083
STol – photosynthetic shade tolerance	0.283	0.271	-0.111	-0.173	-0.168	-0.136
Asat – light-saturated photosynthetic rate	-0.138	-0.422	0.119	0.234	0.352	0.220
Amax – maximum photosynthetic rate	0.045	-0.432	0.300	-0.146	0.280	0.199
Dresp – leaf dark respiration	0.081	0.203	-0.276	0.267	-0.073	0.526
DBH – diameter at breast height	0.292	0.031	-0.163	-0.472	0.212	-0.054
H – tree height	0.392	-0.001	0.007	-0.328	0.217	0.025

Table S4.10, summary statistics for the log-transformed linear mixed model testing if woody stem NPP of dominant Cerrado tree species at Serra das Araras varies across fire regime, census interval, and a gradient in specific leaf area (SLA, mm^2 mg^{-1}). The model includes a triple interaction between regime, interval and SLA; using individually-matched productivity data and trait measurements from the set of 167 trees sampled in 2025. Species identity and tree code were used as random effects to account for non-independence and repeated sampling.

Formula: glmmTMB($log_{10}(NPP_{stem} + 0.1) \sim$ regime*interval*SLA + (1|species) + (1|tree_code))				
Family: gaussian				
Fixed effects	**Estimate**	**Std. Error**	**z-value**	**Pr(>|z|)**
(Intercept)	**-0.9957**	**0.0106**	**-93.5824**	**0.0000**
regimeTriennial	-0.0008	0.0170	-0.0476	0.9621
regimeBiennial	0.0213	0.0174	1.2229	0.2214
regimeAnnual	-0.0085	0.0143	-0.5947	0.5520
interval2019-2021	0.0003	0.0132	0.0264	0.9790
interval2021-2023	0.0120	0.0132	0.9104	0.3626
SLA	-0.0001	0.0014	-0.0626	0.9501
regimeTriennial:interval2019-2021	-0.0058	0.0222	-0.2622	0.7932
regimeBiennial:interval2019-2021	0.0062	0.0224	0.2780	0.7810
regimeAnnual:interval2019-2021	0.0046	0.0183	0.2530	0.8002
regimeTriennial:interval2021-2023	-0.0049	0.0222	-0.2215	0.8247
regimeBiennial:interval2021-2023	**-0.0606**	**0.0224**	**-2.7048**	**0.0068**
regimeAnnual:interval2021-2023	-0.0009	0.0183	-0.0511	0.9592
regimeTriennial:SLA	0.0005	0.0025	0.1974	0.8435
regimeBiennial:SLA	-0.0039	0.0026	-1.5064	0.1320
regimeAnnual:SLA	0.0010	0.0019	0.5066	0.6125
interval2019-2021:SLA	-0.0004	0.0018	-0.2227	0.8238
interval2021-2023:SLA	-0.0010	0.0018	-0.5758	0.5648
regimeTriennial:interval2019-2021:SLA	0.0015	0.0032	0.4589	0.6463
regimeBiennial:interval2019-2021:SLA	-0.0005	0.0034	-0.1528	0.8786
regimeAnnual:interval2019-2021:SLA	-0.0003	0.0024	-0.1363	0.8915
regimeTriennial:interval2021-2023:SLA	-0.0005	0.0032	-0.1480	0.8823
regimeBiennial:interval2021-2023:SLA	**0.0094**	**0.0034**	**2.8075**	**0.0050**
regimeAnnual:interval2021-2023:SLA	-0.0002	0.0024	-0.0755	0.9398

Random effects	**Variance**	**Groups**
species	6.153e-05	16
tree code	6.321e-06	102
residual	9.990e-05	354

Table S4.11, summary statistics for the log-transformed linear mixed model testing if woody stem NPP of dominant Cerrado tree species at Serra das Araras varies across fire regime, census interval, and a gradient in wood density (WD, g cm^{-3}). The model includes a triple interaction between regime, interval and WD; using individually-matched productivity data and trait measurements from the set of 167 trees sampled in 2025. Species identity and tree code were used as random effects to account for non-independence and repeated sampling.

Formula: glmmTMB($log_{10}(NPP_{stem} + 0.1)$ ~ regime*interval*WD + (1|species) + (1|tree code))				
Family: gaussian				
Fixed effects	**Estimate**	**Std. Error**	**z-value**	**Pr(>|z|)**
(Intercept)	**-1.0115**	**0.0149**	**-67.6739**	**0.0000**
regimeTriennial	0.0104	0.0207	0.5040	0.6142
regimeBiennial	0.0246	0.0182	1.3507	0.1768
regimeAnnual	0.0137	0.0200	0.6844	0.4937
interval2019-2021	0.0088	0.0195	0.4500	0.6527
interval2021-2023	0.0085	0.0195	0.4350	0.6636
WD	0.0274	0.0250	1.0983	0.2721
regimeTriennial:interval2019-2021	0.0021	0.0281	0.0736	0.9413
regimeBiennial:interval2019-2021	-0.0127	0.0252	-0.5041	0.6142
regimeAnnual:interval2019-2021	0.0108	0.0276	0.3917	0.6953
regimeTriennial:interval2021-2023	-0.0204	0.0281	-0.7259	0.4679
regimeBiennial:interval2021-2023	**-0.0515**	**0.0252**	**-2.0431**	**0.0410**
regimeAnnual:interval2021-2023	-0.0414	0.0276	-1.4964	0.1345
regimeTriennial:WD	-0.0144	0.0367	-0.3914	0.6955
regimeBiennial:WD	-0.0502	0.0316	-1.5911	0.1116
regimeAnnual:WD	-0.0212	0.0340	-0.6237	0.5328
interval2019-2021:WD	-0.0182	0.0325	-0.5589	0.5762
interval2021-2023:WD	-0.0079	0.0325	-0.2437	0.8074
regimeTriennial:interval2019-2021:WD	0.0007	0.0496	0.0150	0.9881
regimeBiennial:interval2019-2021:WD	0.0270	0.0436	0.6197	0.5354
regimeAnnual:interval2019-2021:WD	-0.0203	0.0469	-0.4332	0.6649
regimeTriennial:interval2021-2023:WD	0.0255	0.0496	0.5139	0.6073
regimeBiennial:interval2021-2023:WD	**0.0963**	**0.0436**	**2.2100**	**0.0271**
regimeAnnual:interval2021-2023:WD	0.0623	0.0469	1.3287	0.1839

Random effects	**Variance**	**Groups**
species	7.727e-13	16
tree code	6.875e-05	101
residual	1.139e-04	362

Table S4.12, summary statistics for the log-transformed linear mixed model testing if woody stem NPP of dominant Cerrado tree species at Serra das Araras varies across fire regime, census interval, and a gradient in outer bark thickness (OBT, mm). The model includes a triple interaction between regime, interval and OBT; using individually-matched productivity data and trait measurements from the set of 167 trees sampled in 2025. Species identity and tree code were used as random effects to account for non-independence and repeated sampling.

Formula: glmmTMB($\log_{10}(NPP_{stem} + 0.1)$ ~ regime*interval*OBT + (1|species) + (1|tree code))				
Family: gaussian				
Fixed effects	**Estimate**	**Std. Error**	**z-value**	**Pr(>|z|)**
(Intercept)	**-0.9971**	**0.0033**	**-303.0549**	**0.0000**
regimeTriennial	0.0048	0.0042	1.1449	0.2522
regimeBiennial	-0.0054	0.0041	-1.3314	0.1831
regimeAnnual	0.0019	0.0045	0.4178	0.6761
interval2019-2021	-0.0022	0.0033	-0.6576	0.5108
interval2021-2023	0.0059	0.0033	1.7864	0.0740
OBT	0.0001	0.0003	0.4402	0.6598
regimeTriennial:interval2019-2021	0.0056	0.0052	1.0764	0.2817
regimeBiennial:interval2019-2021	0.0037	0.0052	0.7096	0.4780
regimeAnnual:interval2019-2021	-0.0001	0.0058	-0.0236	0.9812
regimeTriennial:interval2021-2023	**-0.0127**	**0.0052**	**-2.4171**	**0.0156**
regimeBiennial:interval2021-2023	-0.0020	0.0052	-0.3793	0.7045
regimeAnnual:interval2021-2023	-0.0077	0.0057	-1.3578	0.1745
regimeTriennial:OBT	-0.0003	0.0003	-0.9697	0.3322
regimeBiennial:OBT	0.0003	0.0004	0.7018	0.4828
regimeAnnual:OBT	-0.0002	0.0004	-0.4057	0.6849
interval2019-2021:OBT	0.0000	0.0003	-0.0756	0.9398
interval2021-2023:OBT	-0.0004	0.0003	-1.4193	0.1558
regimeTriennial:interval2019-2021:OBT	-0.0002	0.0005	-0.4353	0.6633
regimeBiennial:interval2019-2021:OBT	-0.0001	0.0005	-0.1371	0.8910
regimeAnnual:interval2019-2021:OBT	0.0001	0.0005	0.1215	0.9033
regimeTriennial:interval2021-2023:OBT	**0.0009**	**0.0005**	**1.9870**	**0.0469**
regimeBiennial:interval2021-2023:OBT	0.0003	0.0005	0.6718	0.5017
regimeAnnual:interval2021-2023:OBT	0.0006	0.0005	1.0950	0.2735

Random effects	**Variance**	**Groups**
species	5.267e-05	16
tree code	3.233e-12	165
residual	8.728e-05	569

Table S4.13, summary statistics for the log-transformed linear mixed model testing if woody stem NPP of dominant Cerrado tree species at Serra das Araras varies across fire regime, census interval, and a gradient in relative bark thickness (rBT, %). The model includes a triple interaction between regime, interval and rBT; using individually-matched productivity data and trait measurements from the set of 167 trees sampled in 2025. Species identity and tree code were used as random effects to account for non-independence and repeated sampling.

Formula: glmmTMB($\log_{10}(NPP_{stem} + 0.1)$ ~ regime*interval*rBT + (1|species) + (1|tree code))				
Family: gaussian				
Fixed effects	**Estimate**	**Std. Error**	**z-value**	**Pr(>|z|)**
(Intercept)	**-0.9915**	**0.0032**	**-306.8765**	**0.0000**
regimeTriennial	0.0066	0.0048	1.3898	0.1646
regimeBiennial	**-0.0104**	**0.0042**	**-2.4992**	**0.0124**
regimeAnnual	0.0040	0.0047	0.8506	0.3950
interval2019-2021	-0.0054	0.0033	-1.6179	0.1057
interval2021-2023	0.0061	0.0033	1.8274	0.0676
rBT	-0.0004	0.0002	-1.8266	0.0678
regimeTriennial:interval2019-2021	0.0094	0.0063	1.4960	0.1346
regimeBiennial:interval2019-2021	0.0069	0.0055	1.2409	0.2146
regimeAnnual:interval2019-2021	0.0000	0.0062	-0.0020	0.9984
regimeTriennial:interval2021-2023	**-0.0186**	**0.0063**	**-2.9619**	**0.0031**
regimeBiennial:interval2021-2023	0.0055	0.0055	0.9949	0.3198
regimeAnnual:interval2021-2023	-0.0123	0.0062	-2.0007	0.0454
regimeTriennial:rBT	-0.0004	0.0003	-1.2056	0.2280
regimeBiennial:rBT	0.0006	0.0003	1.8600	0.0629
regimeAnnual:rBT	-0.0003	0.0003	-0.9367	0.3489
interval2019-2021:rBT	0.0002	0.0002	1.0559	0.2910
interval2021-2023:rBT	-0.0003	0.0002	-1.4565	0.1453
regimeTriennial:interval2019-2021:rBT	-0.0005	0.0004	-1.0802	0.2801
regimeBiennial:interval2019-2021:rBT	-0.0003	0.0004	-0.7706	0.4409
regimeAnnual:interval2019-2021:rBT	0.0001	0.0005	0.1125	0.9104
regimeTriennial:interval2021-2023:rBT	**0.0011**	**0.0004**	**2.5973**	**0.0094**
regimeBiennial:interval2021-2023:rBT	-0.0004	0.0004	-0.9900	0.3222
regimeAnnual:interval2021-2023:rBT	0.0008	0.0005	1.7754	0.0758

Random effects	**Variance**	**Groups**
species	4.355e-05	16
tree code	2.382e-12	165
residual	8.360e-05	569

Table S4.14, summary statistics for the log-transformed linear mixed model testing if woody stem NPP of dominant Cerrado tree species at Serra das Araras varies across fire regime, census interval, and a gradient in light-saturated photosynthetic rate (Asat, μmol m^{-2} s^{-1}). The model includes a triple interaction between regime, interval and Asat; using individually-matched productivity data and trait measurements from the set of 167 trees sampled in 2025. Species identity and tree code were used as random effects to account for non-independence and repeated sampling.

Formula: glmmTMB($\log_{10}(NPP_{stem} + 0.1)$ ~ regime*interval*Asat + (1|species) + (1|tree code))				
Family: gaussian				
Fixed effects	**Estimate**	**Std. Error**	**z-value**	**Pr(>|z|)**
(Intercept)	**-1.0026**	**0.0074**	**-135.9736**	**0.0000**
regimeTriennial	**0.0225**	**0.0103**	**2.1753**	**0.0296**
regimeBiennial	0.0008	0.0114	0.0716	0.9430
regimeAnnual	0.0072	0.0089	0.8047	0.4210
interval2019-2021	0.0119	0.0096	1.2347	0.2170
interval2021-2023	0.0133	0.0096	1.3806	0.1674
Asat	0.0004	0.0005	0.7286	0.4663
regimeTriennial:interval2019-2021	0.0018	0.0139	0.1267	0.8992
regimeBiennial:interval2019-2021	-0.0009	0.0159	-0.0580	0.9537
regimeAnnual:interval2019-2021	-0.0136	0.0122	-1.1154	0.2647
regimeTriennial:interval2021-2023	**-0.0391**	**0.0139**	**-2.8187**	**0.0048**
regimeBiennial:interval2021-2023	0.0155	0.0159	0.9743	0.3299
regimeAnnual:interval2021-2023	-0.0059	0.0122	-0.4881	0.6255
regimeTriennial:Asat	-0.0013	0.0007	-1.8266	0.0678
regimeBiennial:Asat	-0.0002	0.0008	-0.2482	0.8040
regimeAnnual:Asat	-0.0005	0.0006	-0.8305	0.4063
interval2019-2021:Asat	-0.0010	0.0006	-1.4758	0.1400
interval2021-2023:Asat	-0.0006	0.0006	-0.9276	0.3536
regimeTriennial:interval2019-2021:Asat	0.0000	0.0010	0.0443	0.9646
regimeBiennial:interval2019-2021:Asat	0.0002	0.0011	0.2311	0.8172
regimeAnnual:interval2019-2021:Asat	0.0010	0.0008	1.3244	0.1854
regimeTriennial:interval2021-2023:Asat	**0.0023**	**0.0010**	**2.3990**	**0.0164**
regimeBiennial:interval2021-2023:Asat	-0.0011	0.0011	-1.0180	0.3087
regimeAnnual:interval2021-2023:Asat	0.0003	0.0008	0.3388	0.7347

Random effects	**Variance**	**Groups**
species	5.849e-05	16
tree code	1.691e-11	102
residual	9.723e-05	354

Table S4.15, summary statistics for the log-transformed linear mixed model testing if woody stem NPP of dominant Cerrado tree species at Serra das Araras varies across fire regime, census interval, and a gradient in photosynthetic shade tolerance (STol, dimensionless). The model includes a triple interaction between regime, interval and STol; using individually-matched productivity data and trait measurements from the set of 167 trees sampled in 2025. Species identity and tree code were used as random effects to account for non-independence and repeated sampling.

Formula: glmmTMB($log_{10}(NPP_{stem} + 0.1)$ ~ regime*interval* STol + (1|species) + (1|tree code))				
Family: gaussian				
Fixed effects	**Estimate**	**Std. Error**	**z-value**	**Pr(>|z|)**
(Intercept)	**-0.9905**	**0.0239**	**-41.3656**	**0.0000**
regimeTriennial	-0.0716	0.0366	-1.9575	0.0503
regimeBiennial	0.0205	0.0445	0.4604	0.6452
regimeAnnual	-0.0057	0.0307	-0.1854	0.8530
interval2019-2021	-0.0186	0.0328	-0.5674	0.5704
interval2021-2023	-0.0367	0.0328	-1.1213	0.2621
STol	-0.0078	0.0273	-0.2866	0.7744
regimeTriennial:interval2019-2021	-0.0325	0.0503	-0.6462	0.5182
regimeBiennial:interval2019-2021	0.0096	0.0610	0.1578	0.8746
regimeAnnual:interval2019-2021	0.0161	0.0417	0.3871	0.6987
regimeTriennial:interval2021-2023	0.1377	0.0503	2.7355	0.0062
regimeBiennial:interval2021-2023	-0.1064	0.0610	-1.7437	0.0812
regimeAnnual:interval2021-2023	0.0406	0.0417	0.9730	0.3305
regimeTriennial:STol	**0.0878**	**0.0422**	**2.0799**	**0.0375**
regimeBiennial:STol	-0.0265	0.0515	-0.5154	0.6063
regimeAnnual:STol	0.0065	0.0357	0.1827	0.8550
interval2019-2021:STol	0.0191	0.0375	0.5107	0.6096
interval2021-2023:STol	0.0475	0.0375	1.2676	0.2050
regimeTriennial:interval2019-2021:STol	0.0425	0.0582	0.7296	0.4656
regimeBiennial:interval2019-2021:STol	-0.0077	0.0708	-0.1090	0.9132
regimeAnnual:interval2019-2021:STol	-0.0168	0.0485	-0.3462	0.7292
regimeTriennial:interval2021-2023:STol	**-0.1688**	**0.0582**	**-2.9007**	**0.0037**
regimeBiennial:interval2021-2023:STol	0.1247	0.0708	1.7620	0.0781
regimeAnnual:interval2021-2023:STol	-0.0497	0.0485	-1.0244	0.3056

Random effects	**Variance**	**Groups**
species	5.315e-05	16
tree code	3.275e-07	102
residual	9.452e-05	354

Table S4.16, summary statistics for the log-transformed linear mixed model testing if woody stem NPP of dominant Cerrado tree species at Serra das Araras varies across fire regime, census interval, and a gradient in diameter at breast height (DBH, cm). The model includes a triple interaction between regime, interval and DBH; using individually-matched productivity data and size measurements from the set of 167 trees sampled in 2025. Species identity and tree code were used as random effects to account for non-independence and repeated sampling.

Formula: glmmTMB($\log_{10}(NPP_{stem} + 0.1)$ ~ regime*interval*DBH + (1|species) + (1|tree code))				
Family: gaussian				
Fixed effects	**Estimate**	**Std. Error**	**z-value**	**Pr(>|z|)**
(Intercept)	**-1.0079**	**0.0025**	**-396.9156**	**0.0000**
regimeTriennial	-0.0029	0.0040	-0.7184	0.4725
regimeBiennial	**0.0083**	**0.0035**	**2.3763**	**0.0175**
regimeAnnual	-0.0073	0.0038	-1.9288	0.0538
interval2019-2021	0.0024	0.0031	0.7975	0.4251
interval2021-2023	**-0.0070**	**0.0031**	**-2.2934**	**0.0218**
DBH	**0.0011**	**0.0002**	**6.0324**	**0.0000**
regimeTriennial:interval2019-2021	-0.0068	0.0053	-1.2827	0.1996
regimeBiennial:interval2019-2021	-0.0024	0.0046	-0.5194	0.6035
regimeAnnual:interval2019-2021	0.0050	0.0051	0.9764	0.3289
regimeTriennial:interval2021-2023	**0.0213**	**0.0053**	**3.9991**	**0.0001**
regimeBiennial:interval2021-2023	**-0.0094**	**0.0046**	**-2.0168**	**0.0437**
regimeAnnual:interval2021-2023	**0.0237**	**0.0051**	**4.6280**	**0.0000**
regimeTriennial:DBH	0.0003	0.0003	0.9517	0.3413
regimeBiennial:DBH	**-0.0009**	**0.0003**	**-3.6724**	**0.0002**
regimeAnnual:DBH	**0.0006**	**0.0003**	**2.2118**	**0.0270**
interval2019-2021:DBH	-0.0004	0.0002	-1.7054	0.0881
interval2021-2023:DBH	**0.0008**	**0.0002**	**3.6100**	**0.0003**
regimeTriennial:interval2019-2021:DBH	**0.0009**	**0.0004**	**2.0801**	**0.0375**
regimeBiennial:interval2019-2021:DBH	0.0004	0.0004	1.2316	0.2181
regimeAnnual:interval2019-2021:DBH	-0.0003	0.0004	-0.8940	0.3713
regimeTriennial:interval2021-2023:DBH	**-0.0023**	**0.0004**	**-5.3114**	**0.0000**
regimeBiennial:interval2021-2023:DBH	**0.0009**	**0.0004**	**2.4956**	**0.0126**
regimeAnnual:interval2021-2023:DBH	**-0.0021**	**0.0004**	**-5.8067**	**0.0000**

Random effects	**Variance**	**Groups**
species	1.137e-05	16
tree code	1.796e-13	165
residual	6.048e-05	567

Table S4.17, summary statistics for the log-transformed linear mixed model testing if woody stem NPP of dominant Cerrado tree species at Serra das Araras varies across fire regime, census interval, and a gradient in tree height (H, m). The model includes a triple interaction between regime, interval and H; using individually-matched productivity data and size measurements from the set of 167 trees sampled in 2025. Species identity and tree code were used as random effects to account for non-independence and repeated sampling.

Formula: glmmTMB($log_{10}(NPP_{stem} + 0.1)$ ~ regime*interval*H + (1|species) + (1|tree code))				
Family: gaussian				
Fixed effects	**Estimate**	**Std. Error**	**z-value**	**Pr(>|z|)**
(Intercept)	**-1.0162**	**0.0033**	**-310.6718**	**0.0000**
regimeTriennial	-0.0025	0.0048	-0.5143	0.6070
regimeBiennial	**0.0115**	**0.0044**	**2.6473**	**0.0081**
regimeAnnual	-0.0065	0.0048	-1.3451	0.1786
interval2019-2021	0.0042	0.0042	1.0237	0.3060
interval2021-2023	**-0.0097**	**0.0042**	**-2.3294**	**0.0198**
H	**0.0040**	**0.0006**	**7.2487**	**0.0000**
regimeTriennial:interval2019-2021	-0.0077	0.0065	-1.1881	0.2348
regimeBiennial:interval2019-2021	-0.0040	0.0059	-0.6770	0.4984
regimeAnnual:interval2019-2021	0.0011	0.0066	0.1618	0.8714
regimeTriennial:interval2021-2023	**0.0252**	**0.0065**	**3.8946**	**0.0001**
regimeBiennial:interval2021-2023	-0.0096	0.0059	-1.6206	0.1051
regimeAnnual:interval2021-2023	**0.0249**	**0.0066**	**3.7545**	**0.0002**
regimeTriennial:H	0.0010	0.0009	1.0387	0.2989
regimeBiennial:H	**-0.0026**	**0.0008**	**-3.1642**	**0.0016**
regimeAnnual:H	0.0014	0.0008	1.6999	0.0891
interval2019-2021:H	-0.0012	0.0007	-1.6510	0.0987
interval2021-2023:H	**0.0022**	**0.0007**	**3.1451**	**0.0017**
regimeTriennial:interval2019-2021:H	0.0022	0.0013	1.7486	0.0804
regimeBiennial:interval2019-2021:H	0.0013	0.0011	1.1199	0.2628
regimeAnnual:interval2019-2021:H	-0.0002	0.0012	-0.1696	0.8653
regimeTriennial:interval2021-2023:H	**-0.0062**	**0.0013**	**-4.8447**	**0.0000**
regimeBiennial:interval2021-2023:H	**0.0028**	**0.0011**	**2.4507**	**0.0143**
regimeAnnual:interval2021-2023:H	**-0.0052**	**0.0012**	**-4.4947**	**0.0000**

Random effects	**Variance**	**Groups**
species	5.910e-06	16
tree code	3.001e-13	164
residual	6.366e-05	565

Table S4.18, summary statistics for the binomial generalised mixed model testing if survival of dominant Cerrado tree species at Serra das Araras varies across fire regime, census interval, and a gradient in inner bark thickness (IBT, mm). The model includes a triple interaction between regime, interval and IBT; using survival data from census inventories and average trait values for each of the dominant species in each regime – from the set of 167 trees sampled in 2025. Species identity was used as random effects to account for non-independence.

Formula: glmmTMB(survival ~ regime*interval*IBT + (1|species))				
Family: binomial (logit)				
Fixed effects	**Estimate**	**Std. Error**	**z-value**	**Pr(>|z|)**
(Intercept)	7.8714	4.1910	1.8781	0.0604
regimeTriennial	62.5804	10517.9616	0.0059	0.9953
regimeBiennial	-6.1565	5.7429	-1.0720	0.2837
regimeAnnual	-1.4415	4.4719	-0.3223	0.7472
interval2019-2021	**-11.7281**	**4.2122**	**-2.7843**	**0.0054**
interval2021-2023	-9.5317	4.1312	-2.3072	0.0210
IBT	-0.2066	0.6702	-0.3082	0.7579
regimeTriennial:interval2019-2021	-54.7784	10517.9616	-0.0052	0.9958
regimeBiennial:interval2019-2021	**20.0166**	**6.0751**	**3.2949**	**0.0010**
regimeAnnual:interval2019-2021	7.7323	4.6524	1.6620	0.0965
regimeTriennial:interval2021-2023	-63.6526	10517.9511	-0.0061	0.9952
regimeBiennial:interval2021-2023	11.3591	5.7919	1.9612	0.0499
regimeAnnual:interval2021-2023	5.2897	4.4714	1.1830	0.2368
regimeTriennial:IBT	-6.5701	1093.2702	-0.0060	0.9952
regimeBiennial:IBT	0.8734	0.9363	0.9328	0.3509
regimeAnnual:IBT	0.0468	0.6901	0.0679	0.9459
interval2019-2021:IBT	**1.7605**	**0.6835**	**2.5759**	**0.0100**
interval2021-2023:IBT	1.1950	0.6602	1.8100	0.0703
regimeTriennial:interval2019-2021:IBT	5.0125	1093.2692	0.0046	0.9963
regimeBiennial:interval2019-2021:IBT	**-3.2136**	**0.9752**	**-3.2955**	**0.0010**
regimeAnnual:interval2019-2021:IBT	-1.3165	0.7288	-1.8063	0.0709
regimeTriennial:interval2021-2023:IBT	6.1959	1093.2686	0.0057	0.9955
regimeBiennial:interval2021-2023:IBT	**-2.2342**	**0.9448**	**-2.3647**	**0.0180**
regimeAnnual:interval2021-2023:IBT	-1.0601	0.6921	-1.5318	0.1256

Random effects	**Variance**	**Groups**
species	2.091	16
residual	-	8734

Table S4.19, summary statistics for the binomial generalised mixed model testing if survival of dominant Cerrado tree species at Serra das Araras varies across fire regime, census interval, and a gradient in maximum photosynthetic capacity (Amax, μmol m^{-2} s^{-1}). The model includes a triple interaction between regime, interval and Amax; using survival data from census inventories and average trait values for each of the dominant species in each regime – from the set of 167 trees sampled in 2025. Species identity and plot code were used as random effects to account for non-independence.

Formula: glmmTMB(survival ~ regime*interval*Amax + (1|species) + (1|plot code))				
Family: binomial (logit)				
Fixed effects	**Estimate**	**Std. Error**	**z-value**	**Pr(>|z|)**
(Intercept)	**4.6729**	**1.8667**	**2.5032**	**0.0123**
regimeTriennial	-7.5225	10.5950	-0.7100	0.4777
regimeBiennial	-9.9122	6.5764	-1.5072	0.1317
regimeAnnual	3.5156	4.6811	0.7510	0.4526
interval2019-2021	-2.9516	1.8816	-1.5687	0.1167
interval2021-2023	-2.6601	1.8224	-1.4597	0.1444
Amax	0.0996	0.1012	0.9847	0.3248
regimeTriennial:interval2019-2021	16.1812	11.0848	1.4598	0.1444
regimeBiennial:interval2019-2021	**18.4695**	**7.2240**	**2.5567**	**0.0106**
regimeAnnual:interval2019-2021	-2.6192	5.0180	-0.5220	0.6017
regimeTriennial:interval2021-2023	7.5894	10.6997	0.7093	0.4781
regimeBiennial:interval2021-2023	11.4931	6.5731	1.7485	0.0804
regimeAnnual:interval2021-2023	0.2417	4.7522	0.0509	0.9594
regimeTriennial:Amax	0.4083	0.6598	0.6188	0.5360
regimeBiennial:Amax	0.4598	0.3542	1.2983	0.1942
regimeAnnual:Amax	-0.2259	0.1823	-1.2393	0.2152
interval2019-2021:Amax	0.0639	0.1048	0.6094	0.5422
interval2021-2023:Amax	0.0084	0.1005	0.0835	0.9334
regimeTriennial:interval2019-2021:Amax	-0.9330	0.6798	-1.3725	0.1699
regimeBiennial:interval2019-2021:Amax	**-0.9586**	**0.3798**	**-2.5240**	**0.0116**
regimeAnnual:interval2019-2021:Amax	0.1123	0.1967	0.5709	0.5681
regimeTriennial:interval2021-2023:Amax	-0.5767	0.6645	-0.8678	0.3855
regimeBiennial:interval2021-2023:Amax	**-0.7027**	**0.3544**	**-1.9829**	**0.0474**
regimeAnnual:interval2021-2023:Amax	-0.0414	0.1855	-0.2231	0.8234

Random effects	**Variance**	**Groups**
species	1.551e+00	16
plot code	1.977e-06	6
residual	-	8734

Chapter 5: Research Paper 3

Extreme heat and drought influence seedling productivity in tropical forests: insights from two decades of intensive growth and survival monitoring.

By Francisco Navarro-Rosales, Eleanor E. Jackson, Michael O'Brien, Christopher D. Philipson, Ryan Veryard, Imma Oliveras Menor, Maria Christodoulou, Elia Binti Godoong, Sabine Both, David F.R.P. Burslem and Andy Hector.

Linking statement: Building on the findings from **Chapter 4 (Research Paper 2)**, this chapter sought to investigate further effects of global change on stem productivity and survival; in this case, using a different ecosystem, disturbance type, and dataset structure. I used long-term planting experiments and climate monitoring data to determine how changes in climate conditions affect productivity in old-growth vs logged dipterocarp forests in Sabah, Malaysia. I then explored if leaf and branch traits help explain long-term responses to extreme heat and drought. This chapter was motivated by a desire to compare changes in productivity across ecosystems, and to outline potentially common mechanisms allowing for tolerance to environmental stressors.

Status: This chapter will be submitted to Global Change Biology after submission of the thesis.

Contributions: I, Francisco Navarro-Rosales, contributed to collating and cleaning the data, developed the specific research questions, designed and performed statistical analyses, produced figures and tables, and wrote and reviewed the manuscript. Andy Hector secured funding and designed and coordinated the Sabah Biodiversity Experiment and Danum seedling monitoring project, with contributions from David F.R.P. Burslem, Michael O'Brien and Christopher D. Philipson. Michael O'Brien and Christopher D. Philipson secured additional funding and coordinated survey campaigns. Michael O'Brien and Elia Binti Godoong provided resources and logistical support. Sabine Both and David F.R.P. Burslem collected functional traits data. Eleanor E. Jackson, Ryan Veryard and Michael O'Brien collated and managed tree survey data. Michael O'Brien collated and managed daily climate datasets. Andy Hector, Imma Oliveras Menor, Eleanor E. Jackson and Maria Christodoulou contributed to the design of statistical analyses. Eleanor E. Jackson, Michael O'Brien, Christopher D. Philipson, Imma Oliveras Menor, David F.R.P. Burslem and Andy Hector contributed to manuscript editing. Andy Hector conceptualised the main research question, supervised this research and was involved in all steps of this work.

5.1. Abstract

Tropical forests are increasingly exposed to extreme heat and drought, yet the long-term consequences of climate extremes on forest functioning and regeneration remain poorly understood. Here, we examine the effects of long-term climate variation on more than two decades of tree productivity in lowland tropical forests in Borneo, comparing dynamics in old-growth and logged forests. Using daily weather data, we identified extremes in temperature, precipitation, vapour pressure deficit, and cumulative water deficit for each census interval, and assessed their effects on net primary stem productivity and survival with mixed-effects models. Productivity and survival increased with seedling size in both forest types. Productivity of smaller seedlings was higher in the old-growth forest, whereas larger seedlings became more productive in the logged forest, likely reflecting increased resource availability and reduced competition. In the old-growth forest, extreme heat and drought consistently reduced the stem productivity of growing seedlings, with disproportionately strong effects on smaller individuals. In the logged forest, extreme temperatures also reduced productivity, but drier conditions were associated with increased productivity and survival, likely because logging and high local rainfall increased sensitivity to excess moisture. Pairwise correlations between species-level random effects and key functional traits revealed that species with more resource-acquisitive strategies in the logged forest (higher foliar nitrogen and faster carbon assimilation rates) achieved higher productivity under average conditions but were more sensitive to climatic extremes. Our results indicate that dipterocarp seedlings are able to shift growth trajectories and trait-performance relationships following enrichment planting, taking advantage of altered ecological conditions in logged forests. Although further research is needed to disentangle the physiological effects of extreme heat and water shortages, extremes of hot and dry climate emerge as important constraints on tree growth and survival, limiting ecological functioning, carbon storage, and the provision of ecosystem services in tropical forests.

5.2. Introduction

Tropical forests play a fundamental role in the functioning of the Earth's biosphere (Malhi *et al*., 2014), controlling concentrations of greenhouse gases and regulating global atmospheric circulation and climatic processes (Pan *et al*., 2011). They account for one-third of terrestrial productivity (Malhi, 2012) and store 25% of terrestrial carbon (Bonan, 2008; Baccini *et al*., 2012). Tropical forests are major reservoirs of biological diversity and provide direct ecosystem services for the 40% of the global population living in tropical countries (Myers *et al*., 2000; Barlow *et al*., 2018; Díaz *et al*., 2018). However, tropical forest ecosystems are vulnerable to increasingly altered climatic patterns that are already transforming ecosystem processes and ecological dynamics across scales (Phillips, 1996). Unprecedented heat and rainfall deficits during the 2015/2016 El Niño caused a 36% reduction in net carbon uptake within African forests (Bennett *et al*., 2021), and reversed the carbon sink capacity of the Amazon (Phillips *et al*., 2009; Bennett *et al*., 2023). In the dipterocarp forests of Southeast Asia, biomass accumulation and carbon sequestration are periodically suppressed by extreme El Niño events (Qie *et al*., 2017; Kondo *et al*., 2018; Qian *et al*., 2025) and drought intensity and frequency are increasing (Walsh, 1996). Understanding the effects of climate change is particularly urgent because tropical forests are rapidly approaching thermal and hydrological thresholds beyond which tree physiology, photosynthetic activity, and survival are compromised (Doughty *et al*., 2023; Restrepo-Coupe *et al*., 2023; Chambers *et al*., 2026). Although plants can respond to heat and drought extremes through physiological adjustments, changes in biochemical investment, and longer-term acclimation (Sterck *et al*., 2016; Nunes *et al*., 2019; Evans *et al*., 2025; Sanchez-Martinez *et al*., 2025), recent studies have revealed that novel climatic conditions are driving turnover in tree species assemblages, and that functional changes remain too slow to track the pace of climate change (Feeley *et al*., 2023; Aguirre-Gutiérrez *et al*., 2025).

Extreme climate events have been shown to reduce the growth and survival of seedlings and adult trees across tropical forests (Phillips *et al*., 2010; Browne *et al*., 2021). Intense droughts and heatwaves have become key drivers of tree mortality across the tropics (Powers *et al*., 2020; Bauman, Fortunel, Delhaye *et al*., 2022), and are significantly impacting the net primary productivity (NPP, carbon accumulation via plant biomass growth; Malhi, 2012) of surviving trees (Rifai *et al*., 2018). In Sabah, Malaysian Borneo, extreme climate associated with El Niño events has been shown to impair tree growth and survival across elevations and vegetation types, increasing seedling mortality rates by more than three times (Nakagawa *et al*., 2000; Bebber *et al*., 2004; Miyamoto *et al*., 2021). However, responses to heatwaves and drought are strongly influenced by local environmental conditions and biological interactions (Bebber *et al*., 2002; O'Brien, Reynolds *et al*., 2017), as well as plant functional strategies underpinning vulnerability to heat and water deficits (Bauman, Fortunel, Cernusak *et al*., 2022). Balancing carbon uptake in the face of water shortage and heat damage is a fundamental functional trade-off allowing for growth and survival under adverse conditions (Rowland *et al*., 2015). For example, species investing in cavitation-resistant tissues, tough leaves and tight stomatal regulation could maintain function at lower levels of water availability, but this will have consequences on resource acquisition and evaporative cooling during heat extremes (Ichie *et al*., 2023; Ziegler *et al*., 2024; Evans *et al*., 2025).

Mechanistically understanding how plant strategies mediate the impacts of extreme heat and water shortage is central to predicting plant vulnerability to climate change, but remains a key challenge due to difficulties in identifying climate trends and linking them with long-term monitoring data and functional traits (O'Brien, Engelbrecht *et al*., 2017; Evans *et al*., 2025). This challenge is further compounded by the multidimensional nature of drought, as plants may respond differently to soil moisture deficits versus atmospheric water demand, which can operate independently or interactively and impose distinct constraints on plant adaptive strategies (Wang *et al*., 2025). Because studies investigating the impacts of droughts and heatwaves have largely focused on single events (e.g., Bebber *et al*., 2004; Browne *et al*., 2021) or on experimentally

applied treatments (e.g., Burslem *et al*., 1996; Nottingham *et al*., 2023), insight into the potential responses to climate extremes is often limited to short-term responses within specific temporal and spatial contexts. Studies that evaluate the consistency of responses to repeated droughts and heatwaves, or the cumulative effects of extreme climatic conditions, remain scarce (Kupers *et al*., 2019; Bauman, Fortunel, Cernusak *et al*., 2022; Bauman, Fortunel, Delhaye *et al*., 2022; O'Brien *et al*., 2024), limiting our ability to predict climate-driven changes in tree dynamics, ecological functioning and the provision of downstream ecosystem services (Feeley *et al*., 2011; Aguirre-Gutiérrez *et al*., 2019).

Climate change is interacting with human modification, which in concert is exacerbating biodiversity loss and forest sustainability (Hosonuma *et al*., 2012; Malhi *et al*., 2014; Pearson *et al*., 2017; Grantham *et al*., 2020). Logging changes the structure and functioning of forests by reducing tree density, modifying tree species composition, and creating canopy gaps (Fauset *et al*., 2017; Milodowski *et al*., 2021). These processes alter microclimate conditions, increasing temperature and vapour pressure deficit (Ewers & Banks-Leite, 2013; Jucker *et al*., 2018; Santos *et al*., 2024). Southeast Asia, and Borneo in particular, has experienced particularly intense selective logging, largely because of industrial timber extraction focused on high-value dipterocarps, extensively altering forest structure and diversity (Imai *et al*., 2012; Gaveau *et al*., 2014). Although degraded forests retain considerable value for biodiversity and ecosystem functioning (Edwards *et al*., 2014; Malhi *et al*., 2022; Marsh *et al*., 2025), scaling up active restoration is increasingly important for accelerating dipterocarp forest recovery (Hector *et al*., 2011; Yeong *et al*., 2016; Philipson *et al*., 2020). Heat and drought have been identified as some of the most important factors limiting the success potential of active restoration strategies via planting (Banin *et al*., 2022; Puértolas *et al*., 2024). Therefore, functionally understanding responses to climate change in the context of logging and restoration also remains a critical research gap (Qie *et al*., 2019; Veryard *et al*., 2023).

In this study, we examine the effects of long-term climate variations on more than two decades of tree dynamics in lowland tropical forests in Borneo, focusing on survival and net primary stem productivity (NPP_{stem}, describing growth in terms of stem biomass). We build upon earlier work by Jackson *et al*. (in preparation), where we conducted a detailed investigation of growth and survival trajectories for dipterocarp species planted in selectively logged and old-growth forests. In that study, we used flexible, non-linear, size-dependent statistical models to estimate continuous growth and survival probability curves at the level of individual seedlings. We now make use of the same two planting experiments where individual seedlings have been intensively monitored approximately every year (Hector *et al*., 2011; O'Brien *et al*., 2024) to investigate differences in productivity and survival in old-growth versus logged forests with respect to climate. We use daily weather data collected at both forest sites to calculate extremes of heat and drought at every monitoring interval, and determine if extreme climate has consistently influenced tree productivity dynamics. Overall, we aim to address the following objectives:

- First, we begin by examining stem productivity and survival of seedlings in old-growth and logged forest, to establish baseline patterns of seedling dynamics across our study sites.

- Second, we investigate how extreme climate associated with heat and drought affects the stem productivity and survival of seedlings planted at the old-growth versus logged forest.

- Finally, we explore whether plant functional traits could explain patterns of vulnerability in seedling stem productivity and survival to extreme climate at both forest sites.

Our hypothesis was that seedling productivity and survival are reduced within the logged forest as a result of altered conditions following disturbance (Imai *et al*., 2019; O'Brien *et al*., 2019). We expected extreme heat and drought to reduce productivity and survival in both forest types, consistent with patterns previously observed across lowland dipterocarp rainforests (Bebber *et al*., 2004; Miyamoto *et al*., 2021). We also expected climate extremes to have disproportionate

impacts on the productivity and survival of smaller seedlings (due to limited rooting depth and carbon storage; Kitajima, 1996; Engelbrecht *et al*., 2002) and of seedlings planted within the logged forest (where degraded canopies increase exposure to climatic extremes; Qie *et al*., 2019; Santos *et al*., 2024). Finally, we posited species with functional traits related to resource acquisition and carbon assimilation attain faster rates of growth and productivity, whilst traits related to hydraulic safety and conservative resource use would be correlated with increased survival and tolerance to climate extremes (Ziegler *et al*., 2024; Evans *et al*., 2025).

5.3. Materials and methods

5.3.1. Study site and experimental design

Our study compared seedlings planted within two neighbouring areas of lowland tropical forest in Sabah, Malaysian Borneo: the selectively logged Malua Forest Reserve and the old-growth forest of Danum Valley Conservation Area (**Figure 5.1**). In the Malua Forest Reserve, seedlings of 16 species of dipterocarp trees were planted as part of the Sabah Biodiversity Experiment (see below). Subsequently, surplus seedlings of 15 of those species plus seedlings of an additional 10 species from the same nursery collections were planted into paired gap and understory sites within the old-growth forest near the Danum Valley Field Centre. Both sites are located within 23 km of each other and share similar environmental conditions. Climate is equatorial and aseasonal; mean annual rainfall is ~3000 mm, and mean annual temperature is ~27ºC, with an annual range of 1.7ºC (Hanya & Bernard, 2012). Rainfall is distributed evenly across all months, and irregular droughts driven by the El Niño Southern Oscillation lead to dry periods of consecutive days with no rain (Walsh *et al*., 2011; O'Brien *et al*. 2024). Overall, the region is experiencing increasing rainfall variability and daily temperatures (Hamed *et al*., 2024). Soils are classified as orthic acrisol, being acidic (pH 6), highly weathered, and low in available nutrients and organic carbon content; bedrock consists of a mixture of mudstone and sandstone (Hector *et al*., 2011).

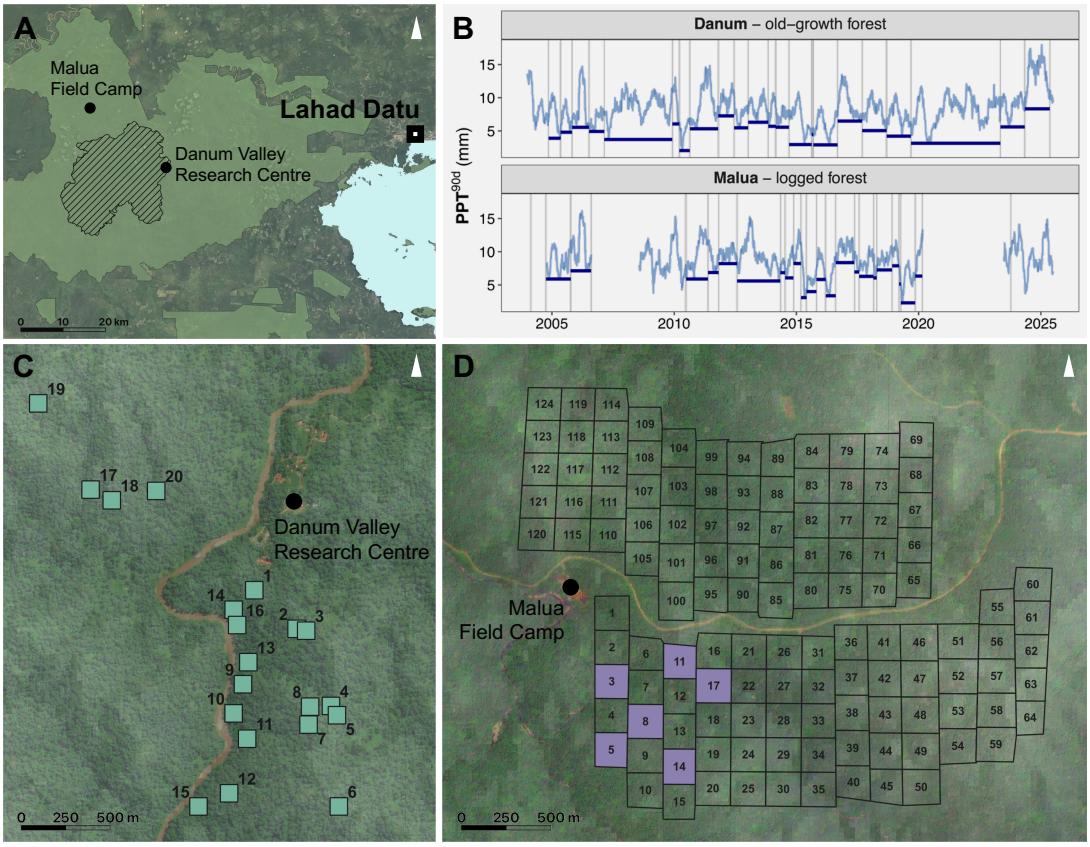


Figure 5.1, geographical context and experimental design of the tree planting and seedling monitoring projects used in this study. **A**) location of the Danum Valley Research Centre (old-growth forest site) and the Malua Field Camp (logged forest site) within the Lahad Datu region in Sabah, Malaysian Borneo. Protected areas are shown in light green, and the Danum Valley Conservation Area is shaded in diagonal black lines. **B**) long-term trends in rainfall (90-day running averages) at both forest sites (see **Figure S5.6** and **Figure S5.7** for trends in maximum daily temperature, vapour pressure deficit and cumulative water deficit). Vertical grey lines indicate median census dates for each forest type. To investigate the effect of extreme climate on seedling productivity and survival, we calculated extremes of heat and drought for every census interval (in this case, minimum 90-day average of daily rainfall, represented by the horizontal blue lines). Please note that climate extremes were calculated independently for each seedling, that is, allowing for variation in census dates. **C**) location of the 20 planting and seedling monitoring plots distributed in canopy gaps within the old-growth forest around the Danum Valley Research Centre (not to scale). **D**) Map of the Sabah Biodiversity Experiment at the Malua Logged Forest Reserve (logged forest), consisting of 124 four-hectare plots. The intensively monitored plots used in this study (plots 3, 5, 8, 11, 14 and 17) are highlighted in purple.

The Sabah Biodiversity Experiment (**Figure 5.1**) adjacent to the Malua Field Camp (05°05'20"N, 117°38'32"E, 102 m above sea level) was established in 2002 in the southern part of the Malua Forest Reserve, a 35,000-hectare concession area used for selective logging (hereafter referred to as logged forest). The reserve was selectively logged in the late 1980s, and re-logged in 2007 (re-logging excluded the Sabah Biodiversity Experiment; Hector *et al.*, 2011). The experiment consists of 124 4-hectare plots (496 hectares total) where seedlings of 16 native dipterocarp

species (**Table S5.1**) were enrichment planted at different diversity levels following a randomised block design. Seedlings were planted along lines cut into the pre-existing logged forest whereby lines were 10 m apart with one seedling planted every 3 m (20 planting lines and up to 1,320 seedlings in each plot). Seedlings were planted in two rounds (July 2002 to September 2003 and January 2009 to October 2010), following standard practice designed to replace seedlings initially dying from transplant shock. Seedlings for the first planting cohort were sourced from nearby nurseries, whilst those corresponding to the second planting round were germinated locally at the field site (Hector *et al*., 2011). In our current study, we use data from the six plots that have been intensively monitored since planting (plots 3, 5, 8, 11, 14 and 17), which contain the full array of 16 seedling species and have been inventoried at least 12 times. Three of these intensively monitored plots (plots 5, 11 and 14) received an additional liana removal treatment where all lianas were cut at the base in 2011 and again in 2014 (O'Brien *et al*., 2019). Since we found no consistent long-term effect of liana cutting on seedling productivity and survival (see **Section 5.11.3**), liana cutting was not considered further in our study.

Danum Valley Conservation Area is a 43,800-hectare protected area (IUCN Class I – full protection) that has never been commercially logged (hereafter referred to as old-growth forest). Using surplus seedlings from the Sabah Biodiversity Experiment (same nursery collections), 40 (paired) seedling monitoring plots were set up in 20 blocks near the Danum Valley Field Centre (04°57'36"N, 117°48'00"E, 180 m above sea level) to monitor gap dynamics in primary forests (**Figure 5.1**). Seedlings were planted in November 2004, and any initial mortalities were replaced after one and three months. Within each site, two plots were established: one in a canopy gap and one in the understory nearby (<30 m distance). In our current study, we only use data from the plots within canopy gaps, to standardise the light effects from the logged forest (**Table 5.1**). Each plot consisted of two replicate subplots, in which 25 seedlings (of 25 native forest species, **Table S5.1**) were planted in a 5 x 5 grid with 0.75 x 0.75 m spacing between them. One of the two subplots at each plot was used for a drought experiment from 2013 to 2014 (O'Brien *et al*., 2024); only unmanipulated subplots are included in this study to account for natural climatic variation.

Table 5.1, summary of ecological and environmental conditions at the old-growth (Danum) and logged (Malua) dipterocarp forest study sites in Sabah, Malaysia. Physical environment variables, timber volumes, basal areas values and aboveground carbon stocks were reproduced from Saner *et al*. (2012), Carbon stocks and fluxes in tropical lowland dipterocarp rainforests in Sabah, Malaysian Borneo, PLoS ONE, 7(1), e29642 (https://doi.org/10.1371/journal.pone.0029642), licensed under open access CC BY 4.0 (http://creativecommons.org/licenses/by/4.0/). Timber volumes estimated in 1983 represent pre-logging conditions at Malua. LiDAR data collected in 2014 and 2020 were used to estimate canopy cover for a raster above each monitoring plot (plus a 30 m radius around the old-growth plots at Danum); canopy cover was defined as the proportion of each raster with vegetation taller than 10 m. Microclimate comparisons between the two sites were performed for the 2008 to 2015 period, the longest continuous interval with full annual data.

Site characteristics	**Danum** – old-growth forest	**Malua** – logged forest
Physical environment		
Elevation (m)	< 250	< 250
Topography	Slopes 15–25º	Slopes 0–20º
Bedrock	Mudstone	Mudstone
Soil type	Orthic acrisol	Orthic acrisol
Microclimate – 2008-2015		
Mean annual rainfall (mm)	3014 ± 161	3271 ± 151
Mean annual maximum daily temperature (ºC)	32.0 ± 0.24	28.8 ± 0.76
Mean annual minimum daily temperature (ºC)	22.5 ± 0.29	23.9 ± 0.18
Vegetation structure		
Timber volume – 1983 (m^3 ha^{-1})	178–230	193–221
Dipterocarp timber volume – 1983 (m^3 ha^{-1})	149–225	180–216
Total basal area – 2008 (m^2 ha^{-1})	29.9 ± 0.7	25.0 ± 0.8
Dipterocarp basal area – 2008 (m^2 ha^{-1})	18.2 ± 0.7	6.9 ± 0.2
Aboveground carbon stock – 2008 (MgC ha^{-1})	128 ± 13.4	91.9 ± 2.9
Canopy cover – 2014 (%)	89.4 ± 2.9	90.3 ± 1.2
Canopy cover – 2020 (%)	93.0 ± 2.9	93.2 ± 2.0
Planting design		
Plot size	0.0009 ha (3 x 3 m)	4 ha (200 x 200 m)
Number of plots	20	6
Seedlings per plot	25	~1320
Planting arrangement	grid planting (5 x 5)	line planting (20 lines)
Spacing	0.75 m x 0.75m	10 m x 3 m

Overall, 500 seedlings were planted within our old-growth forest plots, and 11,118 were planted in our logged forest plots (7,864 in the first planting round and 3,434 in the second one). Old-growth and logged plots share 15 planted seedling species (**Table S5.1**). Similar environmental conditions across both plots allowed for the comparison of ecological dynamics in the face of disturbance and climate extremes (Saner *et al*., 2012). Before the Malua Forest Reserve was logged, forest overstory at both sites was dominated by large lowland dipterocarp trees (family

Dipterocarpaceae), with canopy height of about 50 m and emergent trees >70 m (Newbery *et al*., 1999; **Table 5.1**). During logging, most of the large dipterocarp trees were removed, meaning total basal area is 16% smaller in the logged forest, with Dipterocarp basal area decreasing by 62% (Saner *et al*., 2012). Vegetation height is substantially lower in the logged forest, yet increased dominance of pioneer species means canopy cover values (and therefore light levels) are relatively similar to those of old-growth forest plots located in gaps. Site microclimate appears to be relatively similar, with wetter conditions and a narrower temperature range in the logged forest. It is important to note differences in microclimate across the different plots within each site were not measured. Overall, the most important factor influencing seedling performance is likely to be planting design and tree density. Because line planting could not be implemented in the old-growth forest, seedlings were planted in a smaller grid with higher tree densities (**Table 5.1**). We assumed competition for light and resources to be negligible at these seedling densities (>3 seedlings m^{-2}), at least at lower seedling sizes (Malik *et al*., 2023).

5.3.2. Seedling productivity and survival data

Planted seedlings were repeatedly surveyed within the old-growth and the logged forests following the same methodology, with comparable census intervals and overall survey frequency (23 and 26 surveys in the old-growth and logged forests respectively, details in **Section 5.11.2**). During each census, individual seedlings – identified by unique tag numbers – were recorded as alive or dead. Basal stem diameter (D_{base}) of living seedlings was measured 1-5 cm above the ground surface (unless the stem was damaged or buttressed, in which case diameter was measured at the lowest undisturbed point). D_{base} was measured using diameter tapes or callipers; if callipers were used, two measurements were taken perpendicular to each other and averaged.

D_{base} was used to estimate the aboveground stem productivity of the planted seedlings across the different census intervals. First, we estimated the aboveground stem dry biomass (AGB_{stem}) of

each individual seedling at each census using the basal diameter allometric equation for secondary tropical forests in Sarawak provided by Kenzo *et al*. (2009):

$$(5.1) \quad AGB_{stem} = 0.0238 \cdot (D_{base})^{2.82}$$

Although altered canopy structure and resource conditions between old-growth and logged forests may influence shoot architecture and aboveground-belowground allocation, this approach allowed us to directly estimate AGB_{stem} from available data without introducing additional uncertainty associated with non-regional data, taper equations, height allometries and wood-density averages from external datasets (Carle *et al*., 2025). Specifically, we decided not to use wood density to estimate AGB_{stem} because *in situ* data were not available for either the logged or old-growth forest sites, and because wood density variation across seedling sizes would have introduced additional bias. Furthermore, this method provides a more conservative estimate of AGB_{stem} compared with other regional and pan-tropical allometric models, and it is based on a size range of seedlings comparable to those in our study (Kenzo *et al*., 2009). Stem dry carbon content was assumed to be 50% of total dry biomass (Saner *et al*., 2012), and aboveground stem productivity (NPP_{stem} – KgC $year^{-1}$) for each seedling was calculated as the difference in aboveground stem carbon between a census and the previous one, standardised by the interval length (per year) between measurements (Girardin *et al*., 2010):

$$(5.2) \quad NPP_{stem} = \frac{(0.5 \cdot AGB_{stem})_n - (0.5 \cdot AGB_{stem})_{n-1}}{\text{interval length}}$$

Thus, NPP_{stem} was individually calculated for each seedling at each census interval if it remained alive (and data were available) at the start and end of each interval. Following the definition of productivity as a measure of biomass increment, we assumed NPP_{stem} to be equal to or larger than zero, equating negative values to zero (Clark *et al*., 2001; Roxburgh *et al*., 2005). It is important to note that we only calculated NPP_{stem} for seedlings that were measured in consecutive censuses.

That is, if a seedling was skipped during a given census but measured again at a later census, we did not compute NPP_{stem} across the extended interval, allowing us to maintain sequentially independent intervals for each seedling. It is also important to note that NPP_{stem} estimates from intervals shorter than three months were excluded from our analysis, as biomass change over short periods is more likely to be dominated by measurement uncertainty rather than true growth.

We defined interval survival as the probability of a seedling surviving from one census to the next (interval survival is only computed for seedlings that are alive at the start of the interval, with 1 and 0 respectively indicating a seedling survived or died). By characterising survival as an interval-based variable, we were able to use a consistent analytical framework for both survival and productivity. To maintain consistency, we computed interval survival only for seedlings that were surveyed in consecutive censuses, excluding intervals of less than three months.

5.3.3. Extreme climate data

Weather measurements were taken daily at both the Danum Valley Field Centre (old-growth forest) and the Malua Field Camp (logged forest), including records of maximum daily temperature (T_{max} – ºC), relative humidity at 14:00 (RH_{14} – %), and daily rainfall (PPT – mm). Rainfall has been measured at the old-growth forest site since July 1985, and both T_{max} and RH_{14} have been consistently recorded since January 1988. At the logged forest site, weather variables have been recorded from July 2008 to January 2020 and June 2023 onwards, as a result of the COVID-19 pandemic. Because the logged forest site at Malua is considerably more isolated, keeping a continuous coverage of weather data has been more challenging due to logistical constraints. Upon preliminary screening of weather trends, we discovered unusual periods where the distribution and anomalies of the data could not be readily explained by natural variation (**Figure S5.4**). To maintain consistent quality in climate data, records of T_{max} collected at the old-growth forest from August 2016 to August 2017, and measurements of T_{max} and RH_{14} collected at the logged forest from August 2015 to October 2016 were excluded from the analysis.

Daily values of T_{max} and PPT were used to characterise heat and water availability. Additionally, we also estimated maximum daily vapour pressure deficit (VPD_{max}, atmospheric water demand) and daily cumulative water deficit (CWD) to describe further aspects of atmosphere dryness and water shortage experienced by the seedlings during climate extremes (Rifai *et al*., 2018; Carle *et al*., 2025). These four variables were not strongly correlated to each other except for T_{max} and VPD_{max} (see **Figure S5.5**). Indeed, VPD_{max} was estimated from T_{max} and RH_{14} using an approximation based on the Magnus-Bolton formulation for saturation vapour pressure (Bolton, 1980; Hardwick *et al*., 2015):

$$(5.3) \quad SVP = 6.112 \cdot e^{\frac{17.67 \cdot T_{max}}{T_{max} + 243.5}}$$

Where SVP is saturation vapour pressure (hPa). VPD_{max} (also in hPa) was then computed as the difference between saturation vapour pressure and actual vapour pressure, taking actual vapour pressure as the product of SVP and relative humidity (expressed as a decimal):

$$(5.4) \quad VPD_{max} = SVP - SVP\frac{RH_{14}}{100}$$

Because relative humidity measured in the early afternoon coincides with the hottest and driest time of the day, we assumed combining measurements of T_{max} and RH_{14} provided an accurate estimate of VPD_{max} (Walsh & Newbery, 1999). Cumulative water deficit was calculated on a daily basis, as the cumulative difference between rainfall and evapotranspiration (ET), taking into account water deficit conditions from the previous timestep (Malhi *et al*., 2009):

$$(5.5) \quad CWD_n = |CWD_{n-1} + PPT_n - ET_n|$$

$$\min(CWD_n) = 0$$

CWD was constrained to zero, such that water surpluses were not accumulated. CWD values were reported as absolute positive magnitudes, such that higher values indicate greater water deficit. Because rainfall in the region is particularly frequent (with a maximum of 15 and 22 consecutive days with no rain in the old-growth and logged forest, respectively), there was no need to reset CWD values at fixed intervals (except for gaps of >5 days in rain data, after which the balance was reset to zero when the time series resumed). Evapotranspiration was kept constant (Malhi *et al*., 2009) and assumed to be 4 mm per day (O'Brien *et al*., 2024), following typical values measured across lowland forests in Borneo (e.g., Kumagai *et al*., 2005; Kume *et al*., 2011). Despite being an approximate indicator of soil water deficit and seedling water availability (Malhi *et al*., 2009), CWD still provided an ecologically meaningful metric of water availability, allowing us to better capture the cumulative effects of drought and water balance beyond that of rainfall intensity (Phillips *et al*., 2010).

Our objective was to investigate if extreme climate associated with heat and water limitation affected seedling productivity and survival in a consistent way. Instead of focusing on the effects of specific climate events, we calculated climate extremes for each census interval, and related them to our interval-based estimates of NPP_{stem} and survival as continuous response and explanatory variables. In line with previous studies, we calculated the 90-day rolling average of T_{max}, PPT, VPD_{max} and CWD (**Figure 5.1**, **Figure S5.6**), which helped us describe conditions affecting seedling productivity and survival in a timescale that incorporates short-term and cumulative impacts of climate on plant performance and carbon accumulation (Carle *et al*., 2025). To deal with discontinuous measurements, we only calculated a 90-day rolling average if at least 30 days of data were present within the 3-month cut-off. For each variable, we then extracted the daily rolling average time series corresponding to each seedling record of NPP_{stem} and survival – that is, bounded by the start and end dates for each interval – and identified the most extreme 3-month period indicating highest heat and drought (**Figure S5.7**):

- maximum 90-day rolling average of maximum daily temperature ($\mathbf{maxT_{max}^{90d}}$)
- minimum 90-day rolling average of daily rainfall ($\mathbf{minPPT^{90d}}$)
- maximum 90-day rolling average of maximum daily vapour pressure deficit ($\mathbf{maxVPD_{max}^{90d}}$)
- maximum 90-day rolling average of daily cumulative water deficit ($\mathbf{maxCWD^{90d}}$)

Because climate extremes varied through time, we were able to determine how more intense heat and drought extremes affected seedling performance. Climate extremes were independently calculated for each census interval, and census intervals were specific to each seedling. This means that, where data are available, each NPP_{stem} and survival record is distinctly associated with four separate values of climate extremes. Please note that seedling-climate records do not incorporate differences in microclimate, as weather data were collected at only one station at each location. Instead, seedling-specific records incorporated variations in climate due to different survey dates, which allowed for better model parametrisation. Climate extremes were not computed for intervals with more than 10% missing data points, since they would not give a reliable representation of climate across the interval period.

5.3.4. Functional traits data

Leaf and branch functional traits data were obtained from Both, Burslem *et al*. (2019), who measured at, or close to, our old-growth forest site. From this dataset, we selected the species measured within the undisturbed Danum Valley and Maliau Basin Conservation Areas whose identities overlapped with the planted seedling species used in our study (14 out of the 25 species in the old-growth forest and 12 out of the 16 species in the logged forest; see **Table S5.1**). We calculated species-mean trait values for specific leaf area (SLA – $m^2\ mg^{-1}$), wood density (WD – $g\ cm^{-3}$), light-saturated carbon assimilation rate (Asat – $\mu mol\ s^{-1}\ m^{-2}$), foliar nitrogen concentration (Nperc – %) and foliar 13C isotope concentration (13C – ‰ relative to Vienna Pee Dee Belemnite). These traits were selected to provide insight into the functional mechanisms

underpinning growth and tolerance at our study sites. SLA, Nperc, Asat and WD are key components of plant economic spectra, and important indicators of acquisitive versus resource-conservative strategies influencing tree survival and growth (Wright *et al*., 2004). WD and 13C also reflect differences in hydraulic safety and water use strategies maintaining productivity and survival under drought and heat (Perez-Harguindeguy *et al*., 2013). Trait mean values were obtained from measurements taken from 1 to 9 individuals for each species.

5.3.5. Data analysis and statistical modelling

We obtained a total of 4,982 individual NPP_{stem} records within the old-growth forest (from 478 seedlings and 21 non-nested census intervals), and 10,690 records in the logged forest (from 3,355 seedlings and 20 non-nested census intervals). Survival records totalled 5,794 within the old-growth forest (from 500 seedlings and 21 non-nested census intervals), and 15,393 in the logged forest (from 4,317 seedlings and 20 non-nested census intervals). In the old-growth forest, +4,800 NPP_{stem} records and +5,100 survival records could be matched with climate extreme values, while in the logged forest, +5,600 NPP_{stem} records and +6,500 survival records were matched with climate extremes. All data processing steps and statistical analyses were performed using the R statistical software (version 4.4.2) via RStudio (version 2024.12.0+467).

5.3.5.1. Examining seedling productivity and survival in old-growth and logged forest

To describe interval stem productivity and survival in the old-growth and logged forest, and outline potential differences between forest sites, we fitted mixed-effects models using the glmmTMB package (version 1.1.13; McGillycuddy *et al*., 2025). First, we analysed differences in NPP_{stem} using a two-part hurdle model framework rather than more complex zero-inflated alternatives (Feng, 2021). This approach allowed us to consider the high proportion of zeros within the productivity dataset whilst maintaining adequate model convergence and parametrisation. NPP_{stem} values estimated only from seedling diameter data cannot be attributed

to distinct ecological processes (e.g., biomass loss versus growth). We first considered NPP_{stem} as a binary variable and modelled the probability/proportion of seedlings growing ($Pr(NPP_{stem} > 0)$), that is, the probability/proportion of seedlings attaining positive NPP_{stem}. We used a binomial generalised mixed-effects model (with the default logistic link function) incorporating forest type as a fixed effect, and included log-transformed seedling basal diameter at the start of the interval (D_{base}) as an interactive covariate to account for the positive effect of seedling size on productivity (given larger trees attain higher growth rates due to metabolic scaling; Coomes & Allen, 2009) and to consider the effects of cumulative growth through time (**Figure 5.2**). Census interval, species identity, plot number and seedling cohort were included as random effect intercepts (specific to each forest type) to account for spatial, temporal and taxonomic groupings within the data:

$$\begin{aligned}(5.6)\quad \text{glmmTMB}(\Pr(\text{NPP}_{\text{stem}} > 0) \sim \text{forest\_type} + \log_{10}(\text{D}_{\text{base}}) + \text{forest\_type}{:}\,\log_{10}(\text{D}_{\text{base}}) + \\ (1 \mid \text{forest\_type}{:}\,\text{interval}) + (1 \mid \text{forest\_type}{:}\,\text{cohort}) + (1 \mid \text{forest\_type}{:}\,\text{plot}) + \\ (1 \mid \text{forest\_type}{:}\,\text{species}),\ \text{family} = \text{binomial})\end{aligned}$$

Where the model terms are as defined above, interacting terms are separated by colons, random effects are enclosed in parentheses, and family indicates the type of link function used. We then extracted all records of growing seedlings, that is, records where seedlings showed positive productivity, and modelled the variation of log-transformed NPP_{stem} of growing seedlings ($\log_{10}(NPP_{stem})$) using a gaussian linear mixed-effect model. We included forest type and log-transformed D_{base} (a covariate to control for differences in size at the start of the interval) as interactive fixed effects, and forest-type-specific random intercepts for census interval, species identity, plot number, seedling cohort and seedling identity. Log-transforming NPP_{stem} and D_{base} on base 10 allowed us to maintain interpretability and approximate a linear relationship to meet model assumptions. Seedling random intercepts accounted for variation from repeated measurements through time.

$$(5.7)\quad \text{glmmTMB}(\log_{10}(\text{NPP}_{\text{stem}}) \sim \text{forest\_type} + \log_{10}(\text{D}_{\text{base}}) + \text{forest\_type}{:}\,\log_{10}(\text{D}_{\text{base}}) + (1 \mid \text{forest\_type}{:}\,\text{interval}) + (1 \mid \text{forest\_type}{:}\,\text{cohort}) + (1 \mid \text{forest\_type}{:}\,\text{plot}) + (1 \mid \text{forest\_type}{:}\,\text{species}) + (1 \mid \text{seedling}),\ \text{family} = \text{gaussian})$$

We then modelled differences in the probability of seedling interval survival (Pr(survival > 0)) across the old-growth and logged forest sites using a binomial generalised mixed-effects model, also incorporating forest type and log-transformed D_{base} as fixed effects (accounting for size-dependence in survival likelihood, **Figure 5.2**). Because interval survival does not explicitly account for interval length, we also included log-transformed interval length (in days) as an additional fixed effect. We did not expect the size-effect on survival to vary with interval length; therefore, D_{base} and interval length were allowed to interact with forest type, but not with each other to maintain model convergence and avoid overfitting. Census interval, species identity, plot number and seedling cohort were also included as random effects specific to each forest type.

$$(5.8)\quad \text{glmmTMB}(\text{Pr}(\text{survival} > 0) \sim \text{forest\_type} + \log_{10}(\text{D}_{\text{base}}) + \log_{10}(\text{interval\_length}) + \text{forest\_type}{:}\,\log_{10}(\text{D}_{\text{base}}) + \text{forest\_type}{:}\,\log_{10}(\text{interval\_length}) + (1 \mid \text{forest\_type}{:}\,\text{interval}) + (1 \mid \text{forest\_type}{:}\,\text{cohort}) + (1 \mid \text{forest\_type}{:}\,\text{plot}) + (1 \mid \text{forest\_type}{:}\,\text{species}),\ \text{family} = \text{binomial})$$

To explore if patterns in productivity and survival were consistent across census intervals and species, we extracted random-effect coefficients for census interval and species from each of the three models, and examined their pairwise correlations (**Figure S5.8** to **Figure S5.10**).

5.3.5.2. Investigating the effect of extreme climate on seedling productivity and survival

To investigate how changes in extreme heat and drought across census intervals have affected the stem productivity and survival of seedlings at the old-growth and logged forest sites, we fitted a series of mixed-effects models consistent with the initial analyses described above (again using package glmmTMB). For each response variable (binary NPP_{stem}, continuous non-zero NPP_{stem},

and survival), separate models were fitted with each climate extreme variable included as the focal explanatory variable (maxT^{90d}_{max}, minPPT^{90d}, $\text{maxVPD}^{90d}_{max}$, maxCWD^{90d}). In all cases, we fitted a separate model for each forest site, helping us isolate the site-specific effect of climate extremes whilst maintaining model interpretability. The models also included log-transformed D_{base} (at the start of the interval) as a continuous covariate interacted with the climate extreme variable (and log-transformed interval length as an additive fixed effect within the survival models). Census interval, species identity, plot number, and seedling cohort (for logged-forest models only) were specified as random effect intercepts in all models, with seedling identity incorporated in models using non-zero continuous NPP_{stem} as the response variable. Where model convergence allowed, we also included species-level random slopes for the focal climate extreme variable, allowing for interspecific variation in sensitivity to climate extremes to be explicitly modelled. We were therefore able to fit a total of 24 separate models (x3 response variables x4 climate extreme variables x2 forest sites). See **Table S5.5** to **Table S5.28** for model details.

$$\begin{aligned}(5.9)\quad &\text{glmmTMB}(\Pr(\text{NPP}_{\text{stem}} > 0) \sim \log_{10}(\text{D}_{\text{base}}) + \mathbf{climate\_extreme} + \\ &\log_{10}(\text{D}_{\text{base}}) : \mathbf{climate\_extreme} + (1 \mid \text{interval}) + (1 \mid \text{cohort}) + (1 \mid \text{plot}) + \\ &(1 + \mathbf{climate\_extreme} \mid \text{species}),\ \text{family} = \text{binomial})\end{aligned}$$

$$\begin{aligned}(5.10)\quad &\text{glmmTMB}(\log_{10}(\text{NPP}_{\text{stem}}) \sim \log_{10}(\text{D}_{\text{base}}) + \mathbf{climate\_extreme} + \\ &\log_{10}(\text{D}_{\text{base}}) : \mathbf{climate\_extreme} + (1 \mid \text{interval}) + (1 \mid \text{cohort}) + (1 \mid \text{plot}) + \\ &(1 + \mathbf{climate\_extreme} \mid \text{species}) + (1 \mid \text{seedling}),\ \text{family} = \text{gaussian})\end{aligned}$$

$$\begin{aligned}(5.11)\quad &\text{glmmTMB}(\Pr(\text{survival} > 0) \sim \log_{10}[\text{interval\_length}] + \log_{10}(\text{D}_{\text{base}}) + \\ &\mathbf{climate\_extreme} + \log_{10}(\text{D}_{\text{base}}) : \mathbf{climate\_extreme} + (1 \mid \text{interval}) + (1 \mid \text{cohort}) + \\ &(1 \mid \text{plot}) + (1 + \mathbf{climate\_extreme} \mid \text{species}),\ \text{family} = \text{binomial})\end{aligned}$$

5.3.5.3. Explaining vulnerability of productivity and survival through functional traits

To assess whether functional strategies could explain patterns of vulnerability in seedling productivity and survival, we examined the relationship between species-level responses to climate extremes and functional traits at both forest sites. We approximated species-level responses (in terms of binary NPP_{stem}, continuous non-zero NPP_{stem}, and survival) to the different climate extreme variables ($maxT_{max}^{90d}$, $minPPT^{90d}$, $maxVPD_{max}^{90d}$, $maxCWD^{90d}$) at each forest site (old-growth versus logged) using the models described in **Section 5.3.5.2**. For each of the 24 model combinations, we extracted the random effect coefficients for each species (also known as best linear unbiased predictions or as conditional means; Pinheiro & Bates, 2000). Species-level intercepts indicate differences in productivity/survival relative to the average species baseline. Species-level slopes indicate how much each species' response to climate extremes deviates from the average species-level response to those extremes. Species-level intercepts and slopes from each model were then correlated with the means of the different traits, and we evaluated the consistency and significance of correlation coefficients across model variables and forest sites.

5.4. Results

Mean basal diameter of seedlings planted within canopy gaps at the old-growth forest increased from 4.52 ± 0.07 mm in the first census (November 2004) to 82.4 ± 8.28 mm in the most recent census (May 2025, by which only 44% of seedlings survived). In the logged forest, mean basal diameter increased from 6.55 ± 0.06 mm (February 2004) to 52.5 ± 1.73 mm (October 2023, by which only 25% of seedlings survived). Maximum seedling size reached 564 mm and 556 mm respectively in the most recent censuses of the logged and old-growth forests. Climate conditions were generally comparable at both forest sites, with the logged forest being wetter and showing a narrower temperature range (from July 2008 to July 2015, annual rainfall in the logged forest was 257 mm above that of the old-growth forest; annual maximum and minimum daily temperatures were 3.2°C lower and 1.4°C higher in the logged forest). Despite gaps in weather data, census intervals associated with the most extreme climate conditions coincided with El Niño periods at both forest sites (**Figure S5.6**).

5.4.1. Productivity and survival in old-growth versus logged forest

The probability of seedlings growing ($Pr(NPP_{stem} > 0)$) increased with greater log-transformed basal diameter (D_{base}) at both forest sites (**Figure 5.2**, **Table S5.2**). Logged forest type appears to have a negative main effect on the proportion of growing seedlings, although this effect was not statistically significant. Log-transformed NPP_{stem} among growing seedlings also increased (linearly) with log-transformed basal diameter (**Figure 5.2**, **Table S5.3**). However, there was a significant interaction between basal diameter and forest type. Logged forest type had a significantly negative main effect on $\log_{10}(NPP_{stem})$, and there was also a positive interaction between basal diameter and forest type. Although productivity at smaller seedling sizes was reduced within the logged forest, stronger positive effects of basal diameter on both $Pr(NPP_{stem} > 0)$ and $\log_{10}(NPP_{stem})$ indicated larger seedlings eventually become more productive than those in the old-growth forest. Log-transformed D_{base} also had a positive effect on seedling survival (**Figure 5.2**, **Table S5.4**), whilst longer intervals were associated with reduced survival at both forest types (**Figure 5.2**). Although there was no significant main effect of forest type, the negative interaction between $\log_{10}(D_{base})$ and forest type indicates that the somewhat lower probability of survival in the old-growth forest canopy gaps at small sizes was reversed at larger seedling sizes.

Within each forest type, we found strong correlations between interval and species coefficients from the $Pr(NPP_{stem} > 0)$ and $\log_{10}(NPP_{stem})$ models (**Figure S5.8**, **Figure S5.9**). That is, within each forest type, intervals and species associated with higher probabilities of growth also showed increased rates of NPP_{stem}. Overall, productivity coefficients were generally unrelated to survival coefficients at both the interval and species levels, with the exception of interval effects in the old-growth forest, where higher survival was associated with higher $\log_{10}(NPP_{stem})$ (**Figure S5.8**). When comparing species-level coefficients between old-growth and logged forest types, species showed similar relative responses only in terms of survival (**Figure S5.10**).

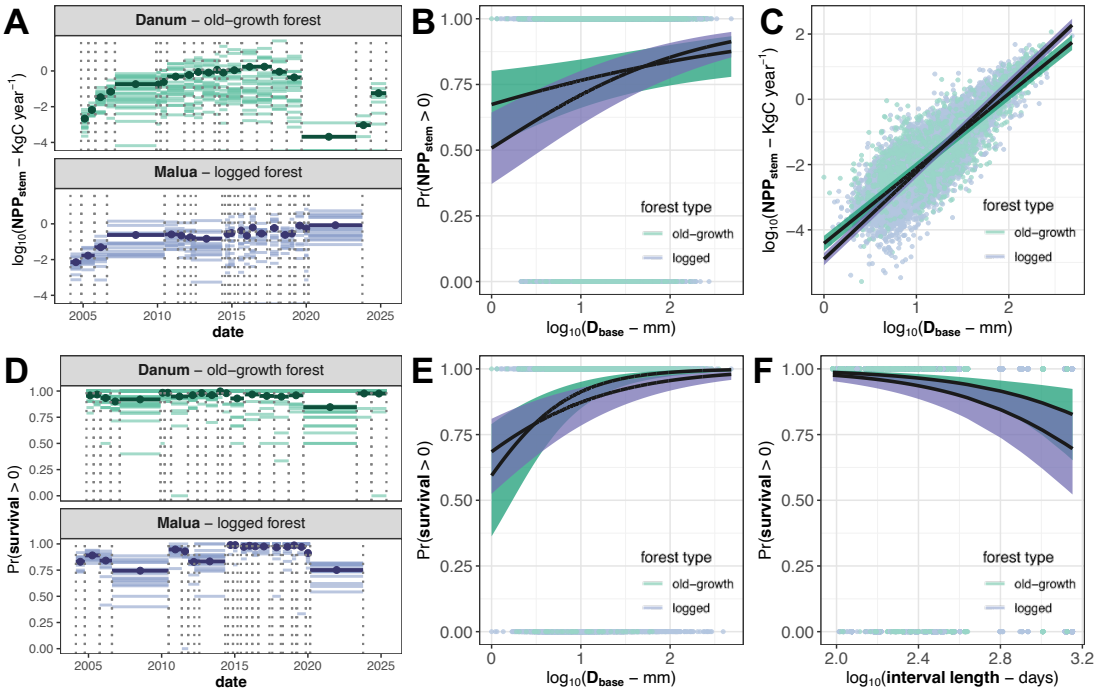


Figure 5.2, stem productivity and survival dynamics of dipterocarp seedlings planted within old-growth and logged tropical forest sites. **A**) raw changes in (log-transformed) seedling NPP_{stem} across the monitoring period. Points and thick lines represent the simple means of log-transformed seedling NPP_{stem} for each census interval (including data from all seedlings). Thin lines indicate average productivity for each species. Vertical dashed lines indicate median census dates for each forest type. **B**) estimated differences in the probability of seedlings attaining positive NPP_{stem} ($Pr(NPP_{stem} > 0)$) across seedling sizes (log-transformed basal diameter) for each forest type (alongside 95% confidence intervals). **C**) estimated differences in the rates of log-transformed NPP_{stem} of growing seedlings ($log_{10}(NPP_{stem})$) across seedling sizes (log-transformed basal diameter) for each forest type (alongside 95% confidence intervals). **D**) raw changes in seedling interval survival across the monitoring period. Points and thick lines represent the simple means of seedling survival (0 = died, 1 = survived) for each census interval. Thin lines indicate average survival for each species. Vertical dashed lines indicate median census dates for each forest type. **E**) estimated differences in the probability of seedling survival ($Pr(survival > 0)$) across seedling sizes (log-transformed basal diameter) for each forest type (alongside 95% confidence intervals). **F**) estimated differences in the probability of seedling survival as a function of (log-transformed) interval length for each forest type (alongside 95% confidence intervals).

5.4.2. The effect of extreme climate on seedling productivity and survival

Models investigating the probability of seedlings growing ($Pr(NPP_{stem} > 0)$) revealed there is no significant effect of climate extremes within the old-growth forest (**Figure 5.3**, **Table S5.5**, **Table S5.7**, **Table S5.9**, **Table S5.11**). In the logged forest, extreme high temperatures ($maxT_{max}^{90d}$) had a negative effect on growth probability ($Pr(NPP_{stem} > 0)$) (**Figure 5.3**, **Table S5.6**). Lower rainfall

(minPPT^{90d}), and higher vapour pressure deficit (maxVPD$^{90d}_{max}$) and greater cumulative water deficit (maxCWD^{90d}) were associated with a higher probability of growth, meaning seedlings are more likely to grow in drier conditions (**Figure 5.3**, **Table S5.8**, **Table S5.10**, **Table S5.12**).

Models investigating the variation in magnitude of productivity (NPP_{stem}) of growing seedlings revealed consistent effects of climate on $\log_{10}(NPP_{stem})$ within the old-growth forest. In this case, $\log_{10}(NPP_{stem})$ was positively related to rainfall (minPPT^{90d}), but negatively associated with maxT$^{90d}_{max}$, maxVPD$^{90d}_{max}$ and maxCWD^{90d} (**Table S5.13**, **Table S5.15**, **Table S5.17**, **Table S5.19**), indicating productivity is reduced in conditions of heat and low water availability (**Figure 5.4**). Old-growth forest models for maxT$^{90d}_{max}$, minPPT^{90d} and maxVPD$^{90d}_{max}$ also showed significant interactions between climate variables and $\log_{10}(D_{base})$, demonstrating that the effect of climate extremes on NPP_{stem} decreases with increasing seedling sizes. In the logged forest, maxT$^{90d}_{max}$ also had a negative effect on $\log_{10}(NPP_{stem})$ (**Figure 5.4**, **Table S5.14**), but productivity appears not to be significantly affected by other climate variables (**Table S5.16**, **Table S5.18**, **Table S5.20**).

None of the climate extreme variables had a significant main effect on survival within the old-growth forest (**Figure 5.5**, **Table S5.21**, **Table S5.23**, **Table S5.25**, **Table S5.27**). In the logged forest, maxT$^{90d}_{max}$ and maxVPD$^{90d}_{max}$ had a positive main effect on interval survival (**Figure 5.5**, **Table S5.22**, **Table S5.26**). We found a positive interaction between $\log_{10}(D_{base})$ and maxVPD$^{90d}_{max}$, and between $\log_{10}(D_{base})$ and minPPT^{90d}, indicating the positive effects of rain and atmosphere dryness on survival diminished with increasing seedling size (**Table S5.24**, **Table S5.26**).

5.4.3. Exploring climate vulnerability through functional traits

None of the species-level random intercepts or random slopes from models describing the probability of seedlings growing showed significant correlations with functional traits (**Figure S5.11**). Random effect intercepts and slopes from our models describing variation in

$\log_{10}(NPP_{stem})$ within the old-growth forest were also unrelated with traits (**Figure 5.6**). In contrast, within the logged forest, Asat and Nperc were positively correlated with species-level random intercepts (from the $maxT_{max}^{90d}$ model for Asat; and from the $maxT_{max}^{90d}$, $minPPT^{90d}$ and $maxCWD^{90d}$ models for Nperc), but negatively correlated with species-level slopes (in terms of $maxT_{max}^{90d}$ and $maxVPD_{max}^{90d}$ for both Asat and Nperc). In other words, species with higher Asat and Nperc showed higher NPP_{stem} under average conditions but were more sensitive to temperature and VPD extremes (despite there being no overall effect of $maxVPD_{max}^{90d}$ on NPP_{stem}). Higher WD appears to be correlated with a lower probability of seedling survival at the species level within the old-growth forest, particularly for species-level random intercepts from the $minPPT^{90d}$ model (**Figure 5.7**). In the logged forest, species-level random slopes with respect to $minPPT^{90d}$ were significantly correlated with Asat and SLA, indicating that species with higher carbon assimilation rates and specific leaf area were more likely to survive with increasing rainfall.

5.5. Discussion

We found that seedling productivity and survival increased with basal diameter across both forest types. Stem NPP – both the probability of growth and the variability in NPP_{stem} among growing seedlings – was higher for smaller seedlings planted within canopy gaps in the old-growth forest, whereas larger seedlings were more productive in the logged forest. Dry and hot climate extremes significantly reduced the productivity of growing seedlings in the old-growth forest, with disproportionately strong effects on smaller individuals. In the logged forest, high temperatures reduced seedling productivity but were associated with increased survival. Periods of reduced rainfall and high vapour pressure deficit increased the probability of positive productivity in the logged forest, with extreme VPD also associated with higher survival rates. Species with faster assimilation rates and higher foliar nitrogen and specific leaf area appear to be more sensitive to extreme climate, but only in the logged forest. In the following sections, we interpret and synthesise the significance of these results, discussing the ecological implications of our findings.

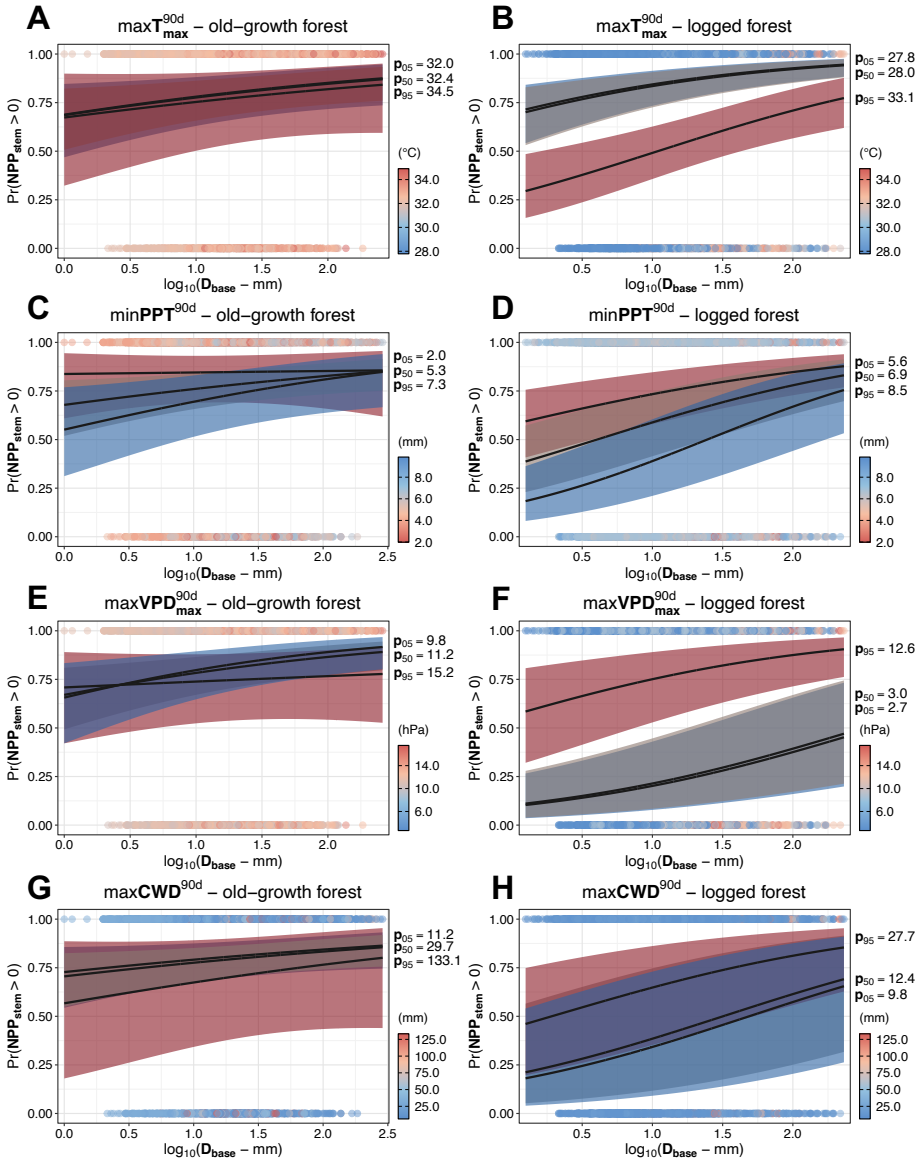


Figure 5.3, graphical representation of the estimated effect of climate extremes on the probability of seedlings attaining positive NPP_{stem} across census intervals – $Pr(NPP_{stem} > 0)$. Models (**Table S5.5** to **Table S5.12**) were specific to each forest type (old-growth forest: plots **A**, **C**, **E** and **G**; logged forest: plots **B**, **D**, **F**, and **H**). $Pr(NPP_{stem} > 0)$ was modelled as a function of $\log_{10}(D_{base})$ interacted with the different climate extremes experienced by each seedling in each census interval: **A-B**), maximum 90-day running average of daily maximum temperature ($maxT^{90d}_{max}$), **C-D**) minimum 90-day running average of daily precipitation ($minPPT^{90d}$), **E-F**) maximum 90-day running average of daily maximum vapour pressure deficit ($maxVPD^{90d}_{max}$), **G-H**) maximum 90-day running average of daily cumulative water deficit ($maxCWD^{90d}$). To represent the co-variation across the two continuous variables, we have included three lines of best fit for each plot, illustrating how the relationship between $Pr(NPP_{stem} > 0)$ and $\log_{10}(D_{base})$ varies at different percentiles of the climate extreme variables (P_{05} = 5th percentile, P_{50} = 50th percentile, P_{95} = 95th percentile). Percentiles are specific to each forest type, and the numerical value of each percentile is indicated to the right of the corresponding line. Each line is accompanied by its estimated 95% confidence interval, with blue shades representing cool/wet conditions, grey representing intermediate conditions and red shades indicating hotter/drier climate averages. $Pr(NPP_{stem} > 0)$ estimates and their corresponding confidence intervals have been back-transformed from the logit scale. We include the raw data points, and an accompanying legend with a common colour gradient for each climate extreme variable across both forest types (blue = cool/wet, red = hot/dry). Colour palettes for raw datapoints and percentile lines are independent of each other.

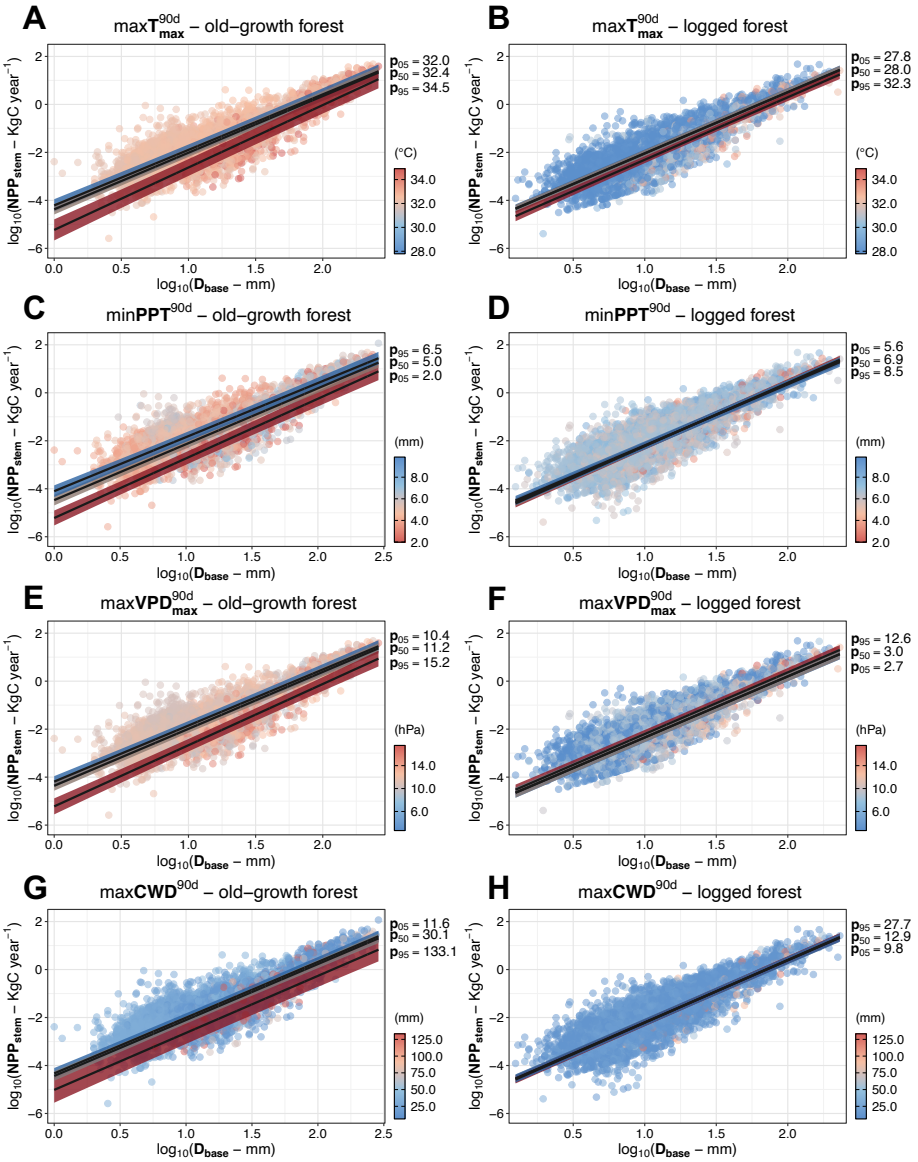


Figure 5.4, graphical representation of the estimated effect of climate extremes on log-transformed NPP_{stem} of growing seedlings across census intervals – $\log_{10}(NPP_{stem})$. Models (**Table S5.13** to **Table S5.20**) were specific to each forest type (old-growth forest: plots **A**, **C**, **E** and **G**; logged forest: plots **B**, **D**, **F**, and **H**). $\log_{10}(NPP_{stem})$ was modelled as a function of $\log_{10}(D_{base})$ interacted with the different climate extremes experienced by each seedling in each census interval: **A-B**), maximum 90-day running average of daily maximum temperature ($maxT^{90d}_{max}$), **C-D**) minimum 90-day running average of daily precipitation ($minPPT^{90d}$), **E-F**) maximum 90-day running average of daily maximum vapour pressure deficit ($maxVPD^{90d}_{max}$), **G-H**) maximum 90-day running average of daily cumulative water deficit ($maxCWD^{90d}$). To represent the co-variation across the two continuous variables, we have included three lines of best fit for each plot, illustrating how the relationship between $\log_{10}(NPP_{stem})$ and $\log_{10}(D_{base})$ varies at different percentiles of the climate extreme variables (P_{05} = 5th percentile, P_{50} = 50th percentile, P_{95} = 95th percentile). Percentiles are specific to each forest type, and the numerical value of each percentile is indicated to the right of the corresponding line. Each line is accompanied by its estimated 95% confidence interval, with blue shades representing cool/wet conditions, grey representing intermediate conditions and red shades indicating hotter/drier climate averages. $\log_{10}(NPP_{stem})$ estimates and their corresponding confidence intervals remain in the logarithmic scale. We include the raw data points, and an accompanying legend with a common colour gradient for each climate extreme variable across both forest types (blue = cool/wet, red = hot/dry). Colour palettes for raw datapoints and percentile lines are independent of each other.

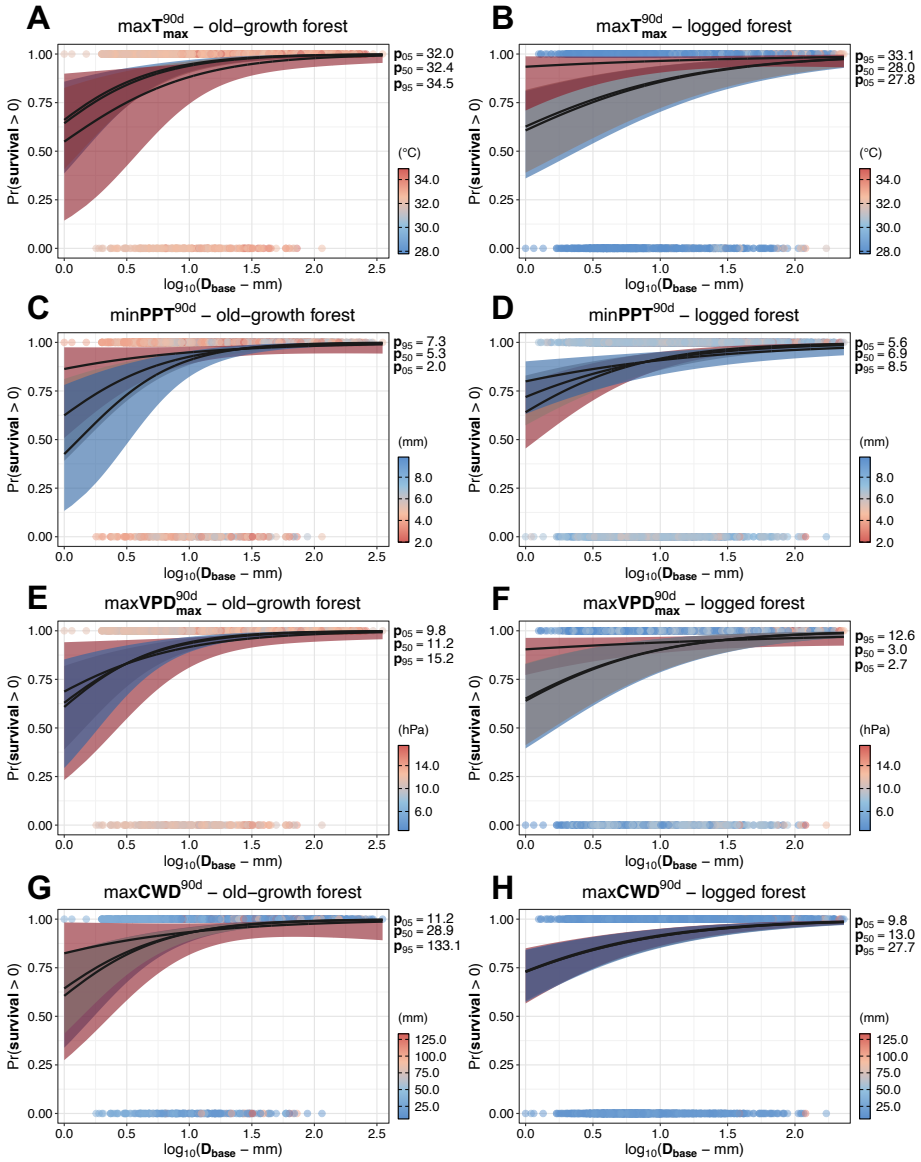


Figure 5.5, graphical representation of the estimated effect of climate extremes on the interval survival rate of seedlings – Pr(survival > 0). Models (**Table S5.21** to **Table S5.28**) were specific to each forest type (old-growth forest: plots **A**, **C**, **E** and **G**; logged forest: plots **B**, **D**, **F**, and **H**). Pr(survival > 0) was modelled as a function of $\log_{10}(D_{base})$ interacted with the different climate extremes experienced by each seedling in each census interval: **A-B**), maximum 90-day running average of daily maximum temperature ($maxT^{90d}_{max}$), **C-D**) minimum 90-day running average of daily precipitation ($minPPT^{90d}$), **E-F**) maximum 90-day running average of daily maximum vapour pressure deficit ($maxVPD^{90d}_{max}$), **G-H**) maximum 90-day running average of daily cumulative water deficit ($maxCWD^{90d}$). To represent the co-variation across the two continuous variables, we have included three lines of best fit for each plot, illustrating how the relationship between Pr(survival > 0) and $\log_{10}(D_{base})$ varies at different percentiles of the climate extreme variables (P_{05} = 5th percentile, P_{50} = 50th percentile, P_{95} = 95th percentile). Percentiles are specific to each forest type, and the numerical value of each percentile is indicated to the right of the corresponding line. Each line is accompanied by its estimated 95% confidence interval, with blue shades representing cool/wet conditions, grey representing intermediate conditions and red shades indicating hotter/drier climate averages. Pr(survival > 0) estimates and their corresponding confidence intervals have been back-transformed from the logit scale. We include the raw data points, and an accompanying legend with a common colour gradient for each climate extreme variable across both forest types (blue = cool/wet, red = hot/dry). Colour palettes for raw datapoints and percentile lines are independent of each other.

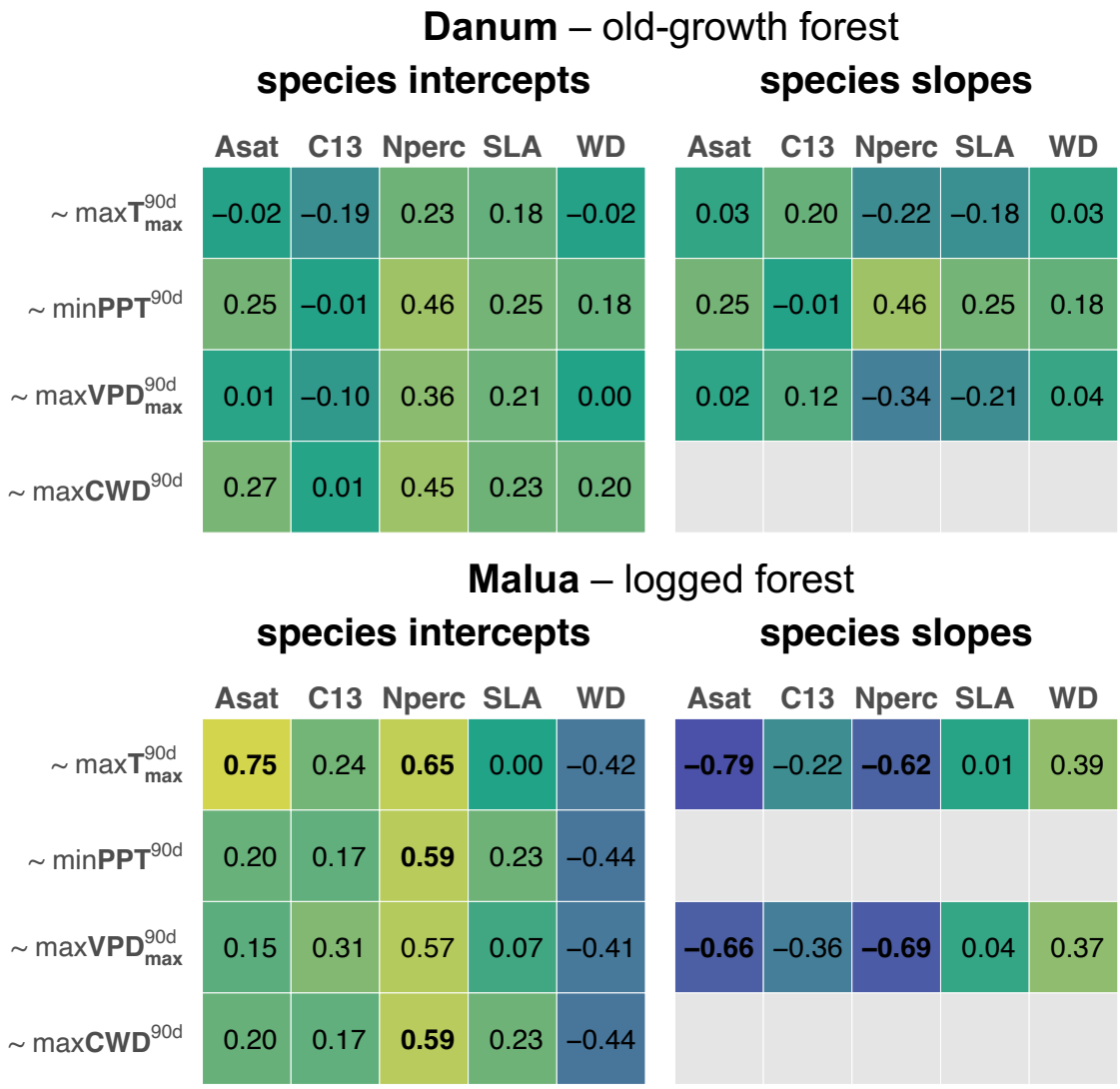


Figure 5.6, correlation matrices illustrating the relationship between species-level random-effect estimates from $\log_{10}(NPP_{stem})$ models and plant functional trait means. Species-level random-effect estimates (both random intercepts and slopes in terms of climate extreme variables) were derived from models investigating how the log-transformed NPP_{stem} of growing seedlings varies as a function of $\log_{10}(D_{base})$ interacted with climate extreme variables (see **Table S5.13** to **Table S5.20**). Random intercepts (left) represent the species-specific deviation from the overall model intercept, reflecting species with proportionally lower/higher $\log_{10}(NPP_{stem})$. Random slopes (right) represent species-specific deviations from the climate extreme variables effect on $\log_{10}(NPP_{stem})$, reflecting species with proportionally lower/higher climate extreme sensitivity. Each row represents the species-level random effects derived from the models including the corresponding climate extreme variable. Columns represent each functional trait. Trait values for each species were obtained as averages from Both, Burslem *et al.* (2019). Models were specific for each forest type: correlations for the old-growth forest are shown on top, logged forest below. Correlation coefficients are indicated within each cell (blue, r = -1; yellow, r = 1). Statistically significant correlation coefficients are shown in bold.

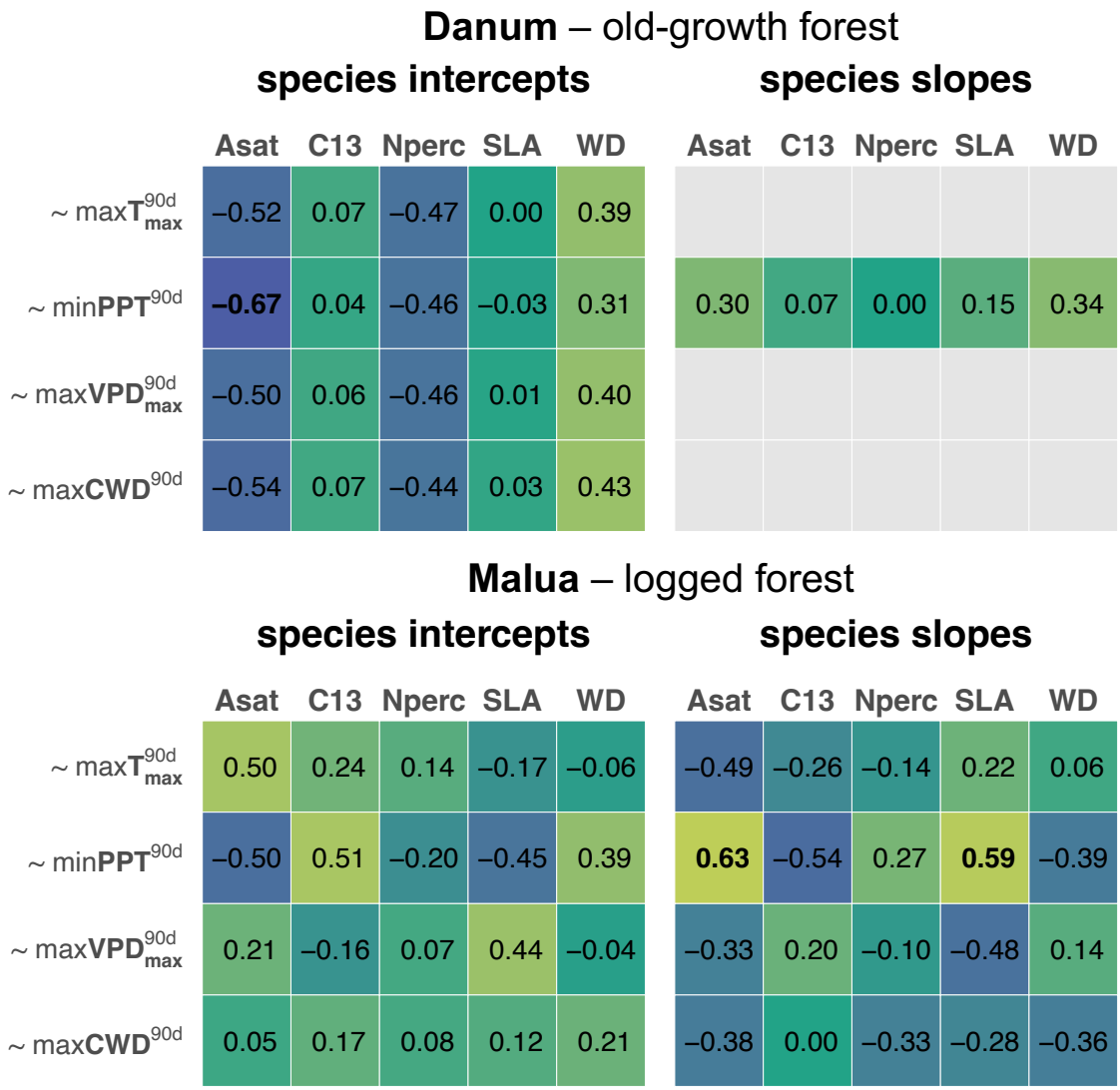


Figure 5.7, correlation matrices illustrating the relationship between species-level random-effect estimates from Pr(survival > 0) models and plant functional trait means. Species-level random-effect estimates (both random intercepts and slopes in terms of climate extreme variables) were derived from models investigating how the probability of seedlings surviving across the different intervals varies as a function of $\log_{10}(D_{base})$ interacted with climate extreme variables (plus an additive effect of interval length; see **Table S5.21** to **Table S5.28**). Random intercepts (left) represent the species-specific deviation from the overall model intercept, reflecting species with proportionally lower/higher Pr(survival > 0). Random slopes (right) represent species-specific deviations from the climate extreme variables effect on Pr(survival > 0), reflecting species with proportionally lower/higher climate extreme sensitivity. Each row represents the species-level random effects derived from the models including the corresponding climate extreme variable. Columns represent each functional trait. Trait values for each species were obtained as averages from Both, Burslem *et al.* (2019). Models were specific for each forest type: correlations for the old-growth forest are shown on top, logged forest below. Correlation coefficients are indicated within each cell (blue, r = -1; yellow, r = 1). Statistically significant correlation coefficients are shown in bold.

5.5.1. Small seedlings were more productive in the old-growth forest; large seedlings in the logged forest

Productivity increased with basal diameter in both forest types, in agreement with plant metabolic scaling theory, which predicts that photosynthetic capacity, carbon sequestration, and resource acquisition scale positively with size (Coomes & Allen, 2009). Because productivity was modelled as a function of $\log_{10}(D_{base})$, we infer that, broadly, NPP_{stem} increased exponentially with basal diameter, consistent with tree life history dynamics at early growth stages (Paine *et al*., 2012). Although declines in relative growth rates of stem and height as trees mature are often assumed, changes in biomass productivity are less certain, with volume and biomass growth potentially increasing throughout a tree's lifespan (Sheil *et al*., 2016). Within canopy gaps in the old-growth forest, small seedlings showed higher productivity than in the logged forest, possibly due to more favourable microclimatic and environmental conditions (Howlett & Davidson, 2003). Contrary to expectations, this growth advantage diminished and even reversed at larger seedling sizes. Even though seedlings were planted within canopy gaps at both forest sites, reduced vegetation cover and disturbed conditions associated with logged forest environments may have inhibited the growth of smaller, more sensitive individuals, but more established trees could have benefited from reduced competition (Chambers *et al*., 2004).

These results align with our previous findings from Jackson *et al*. (in preparation), where detailed analyses of non-linear, size-dependent growth trajectories also revealed growth dynamics differed markedly between forest types. Seedlings in old-growth forest canopy gaps exhibited rapid early growth that peaked quickly and saturated at smaller sizes, whereas seedlings in the logged forest grew more slowly but steadily, ultimately attaining larger sizes. Indeed, increased woody productivity in logged forests relative to old-growth forests has been documented in Sabah and across the tropics (Bischoff *et al*., 2005; Riutta *et al*., 2018; Mills *et al*., 2023). Higher seedling productivity at larger seedling sizes in the logged forest may also reflect differences in planting

design, as cutting lines into the pre-existing logged forest allowed for larger spaces between planted seedlings (Hector *et al*., 2011). Examining variation in NPP_{stem} across plots with differing neighbourhood densities could help disentangle the direct effects of competition on productivity (O'Brien, Reynolds *et al*., 2017). However, because logging can shift allocation toward increased woody stem production at the expense of canopy leaf tissue, other components of productivity would need to be examined to fully understand differences in total NPP (Riutta *et al*., 2018; Mills *et al*., 2023). Measuring wood density across species and seedling class sizes at both forest sites, and incorporating these values into our NPP_{stem} allometry, would also provide a more accurate estimate of productivity dynamics in the face of logging disturbance.

Interval survival rates also increased with seedling diameter, but were statistically indistinguishable between forest sites. A stronger size effect on survival within the old-growth forest could suggest a trade-off between productivity and survival (Philipson *et al*., 2014), but may actually reflect differences in survey history. In the old-growth forest, seedlings were measured shortly after being planted, but in the logged forest seedlings were first surveyed months later, meaning 5,461 seedlings had already died before the first census. Because these early deaths were excluded from the analysis due to missing planting dates and sizes (see **Section 5.11.2**), we presume survival probabilities at smaller sizes in the logged forest were likely overestimated. Cumulative survival was lower within the logged forest, supporting our initial hypothesis.

Responses across seedling sizes and forest types were similar in models analysing both the proportion of growing seedlings and variation in NPP_{stem} rates among growing trees. This consistency supports our use of a hurdle modelling approach to investigate changes in productivity (Feng, 2021). This pattern was further reinforced by strong correlations between interval- and species-level random-effect coefficients from the $Pr(NPP_{stem} > 0)$ and $\log_{10}(NPP_{stem})$ models within each forest type, indicating similar processes govern growth occurrence and growth magnitude (Roxburgh *et al*., 2005). Correlation between random effect intercepts revealed NPP responses across species and census intervals were not generally consistent with patterns in

survival; we hypothesise that seedling survival is disproportionately influenced by thresholds in resource limitations and environmental stochasticity (Alvarez-Clare & Kitajima, 2009; O'Brien, Ong & Reynolds, 2017). Thus, unlike previous studies, we find no direct evidence for a growth-survival trade-off in dipterocarp seedlings (Brown *et al*., 1999; Philipson *et al*., 2014). We acknowledge that unaccounted sources of variation, shrinkage of random-effects, and the exclusion of negative growth values likely constrained our ability to detect robust relationships using this species-level correlation approach.

5.5.2. Extreme heat and drought consistently constrain seedling stem productivity within the old-growth forest

Our analysis also revealed that dry and hot climate extremes significantly reduced the magnitude of productivity of growing seedlings within the old-growth forest. These effects were consistent across all climate variables, supporting our initial hypothesis and highlighting climate extremes as a key driver of primary productivity and carbon uptake in aseasonal old-growth forests. This may be because seedlings planted within undisturbed gaps could be less acclimated to climatic extremes (Blonder *et al*., 2018; Rifai *et al*., 2018). These responses likely arise from physiological constraints imposed by heat and drought, with increased atmospheric dryness and soil water deficits reducing stomatal conductance, carbon assimilation and water transport, and high temperatures impairing photosynthetic efficiency (Kitao *et al*., 2001; Ichie *et al*., 2023; Ziegler *et al*., 2024). Together, these processes limit carbon gain during adverse conditions, although further research is needed to disentangle the effects of different climatic stressors and identify the physiological processes that most strongly constrain seedling performance (Grossiord *et al*., 2020; Sato *et al*., 2024).

Warmer and drier conditions at the old-growth forest site, combined with more intense climate extremes, suggest that seedlings may already be exposed to levels of heat and drought close to

their limits of performance and growth, helping to explain the stronger climate effects on stem NPP. As expected, extremes in temperature, rainfall and VPD had disproportionately strong effects on smaller individuals. In the case of small seedlings, shallower root systems and lower carbon and water reserves probably reduced hydraulic and thermal buffering capacity, limiting their ability to maintain high levels of stomatal conductance and photosynthesis during climatic extremes (Kitajima, 1996; Engelbrecht *et al*., 2002).

Despite having strong effects on the variation in NPP_{stem} among growing seedlings, climate extremes in the old-growth forest did not significantly influence the probability of seedlings growing, nor the probability of seedlings surviving between censuses. Probabilities of both positive NPP_{stem} and survival were already high across most of the study period, and much of the variation in these probabilities was instead captured by seedling diameter (and interval length in the case of survival), leaving limited scope for additional explanatory effects of climate extremes (Lingenfelder & Newbery, 2009). Alternatively, variation in $Pr(NPP_{stem} > 0)$ and $Pr(survival > 0)$ could have also been influenced by unaccounted factors such as light availability and topographic position and biotic interactions (O'Brien, Ong & Reynolds, 2017; O'Brien & Escudero, 2022; O'Brien et al., 2022; O'Brien et al., 2024). These drivers can substantially constrain seedling growth and survival, but may operate independently of short-term climate extremes, obscuring direct climate effects on demographic rates (Uriarte *et al*., 2017).

In the logged forest, extremes of maximum daily temperature reduced both the proportion of growing stems and the magnitude of productivity among growing seedlings. Temperature sensitivity in NPP_{stem} was observed at both forest types, matching temperature-driven reductions in carbon sequestration reported at other locations in Borneo (Fichtbauer, 2022), and indicating that heat may be a limiting factor for seedling performance in dipterocarp forests across environmental conditions (Dongsansuk *et al*., 2020). However, our survival model revealed, despite high uncertainty, that temperature extremes had the opposite effect, appearing to promote seedling survival. This pattern underscores the need for more detailed analyses to clarify if the

links between temperature, productivity and survival are driven by consistent causal mechanisms (Vlam *et al*., 2014; Sato *et al*., 2024). Temperature impacts on tree growth and mortality across Southeast Asia remain understudied, as most research on climate extremes has primarily focused on the effects of drought (e.g., Bebber *et al*., 2004; Lingenfelder & Newbery, 2009; O'Brien, Reynolds *et al*., 2017; Miyamoto *et al*., 2021). As heatwaves and extreme El Niño events are expected to become more frequent and intense in the coming decades, and with forests approaching critical temperature thresholds, we highlight the need for considering temperature effects on tree and carbon dynamics across forests in tropical Asia (Deb *et al*., 2017).

Tree dynamics across the two forest types also differed in their responses to drought extremes. In the logged forest, reduced rainfall and higher VPD increased the probability of seedling growth but had no effect on $\log_{10}(NPP_{stem})$. VPD extremes also had a positive effect on seedling survival. These findings were unexpected (Qie *et al*., 2019), indicating that in the logged forest, drier conditions do not appear to be detrimental to survival and productivity, and suggesting that higher water availability may have actually reduced seedling fitness. Our results could be explained by differences in data availability. Meteorological data coverage at the logged forest site was limited due to logistical constraints, meaning that climate extreme variables were calculated for fewer census intervals. Less variation in climate extremes likely reduced statistical power and constrained our ability to detect clear or consistent relationships between climate, productivity, and survival.

Additionally, productivity and survival patterns may also reflect environmental differences between the two sites. At Malua, logging would have altered soil structure and hydrology, increasing compaction, erosion and runoff (Douglas, 2022). Such changes would have reduced the forest's capacity to buffer extreme rainfall events, resulting in nutrient losses and prolonged soil water saturation (Nainar *et al*., 2018). Despite being located only 23 km apart and experiencing similar regional climates, precipitation was greater at the logged forest site. Greater rainfall, combined with gentler slopes (Saner *et al*., 2012), could have also increased the

likelihood of waterlogging relative to the old-growth forest site. Indeed, waterlogging and extreme rainfall have been identified as important factors constraining tree growth and survival in lowland dipterocarp forests (Born *et al*., 2015; Margrove *et al*., 2015). Water saturation may have increased pathogen loads, restricted root growth as a result of hypoxia, and promoted treefall by reducing soil stability and increasing the likelihood of mechanical failure (Ferry *et al*., 2010; Manghwar *et al*., 2024). O'Brien *et al.* (2024) showed that excess rainfall exerted a stronger influence on tree dynamics compared to drought, with 12 of the planted species at our old-growth forest site exhibiting declines in relative growth rates during periods of high rainfall, and 23 species showing reduced survival. Although understanding NPP_{stem} and survival responses to positive rainfall extremes falls outside the scope of the current study, examining the consequences of water surpluses for tree performance would be an important research priority that would allow us to assess the vulnerability of tropical forests to future climate conditions (Chu *et al*., 2026).

5.5.3. Resource-acquisitive species appear to be more sensitive to climate extremes in the logged forest

We explored if plant functional traits could explain patterns of vulnerability in productivity and survival by extracting model random effects for each species and correlating them with species-level means of key functional traits. We recognise that the inferential power of this approach is limited, and that substantial variation in vital rates, combined with uncertainty of using trait means from other trees and locations, constrained our ability to detect clear links between traits and fitness responses to climate extremes (Sandel *et al*., 2015). Furthermore, shrinkage of random effect predictions towards the fixed-effect mean – particularly for species with limited data – likely prevented us from obtaining clear patterns of correlation with functional traits (Pinheiro & Bates, 2000). These limitations may explain why species-level random effects from models investigating the probability of seedling growth showed no significant associations with functional traits.

Despite this, we were still able to identify patterns that point to key functional mechanisms associated with heat and drought tolerance in productivity and survival (Liu *et al*., 2021).

Species-level random intercepts extracted from our $\log_{10}(NPP_{stem})$ models for the logged forest site were positively correlated with Asat and Nperc. In other words, species with faster assimilation rates and higher foliar nitrogen had higher rates of NPP_{stem} relative to other species. At the same time, strong negative correlations between these traits and random effect slopes reveal these species were more sensitive to climate extremes. This pattern is consistent with plant economic spectra, indicating that species with more acquisitive resource-use strategies – characterised by greater investment in photosynthetic machinery and higher carbon assimilation capacity – were able to maximise productivity under favourable conditions (Wright *et al*., 2014; Reich, 2014). High carbon assimilation and resource acquisition also help explain increased sensitivity to heat and drought, as productive species would be unable to sustain stomatal conductance and high metabolic activity without risking hydraulic failure or photosynthetic damage (Ziegler *et al*., 2024; Evans *et al*., 2025).

Although non-significant, negative correlations between climate sensitivity and 13C might support the idea of acquisitive species responding to climate extremes through isohydric responses, with tight stomatal regulation reducing water loss at the expense of carbon assimilation (Martínez-Vilalta & García-Forner, 2017; Ichie *et al*., 2023). Higher wood density, associated with slower growth rates but greater hydraulic safety also appears to confer tolerance to heat and drought extremes (Chave *et al*., 2009; O'Brien, Engelbrecht *et al*., 2017). Interestingly, correlations between random effects for $\log_{10}(NPP_{stem})$ and functional traits were only observed in the logged forest, suggesting that physiological advantages in carbon assimilation may only translate into higher stem productivity under conditions of reduced competition (Tuomela *et al*., 1996). This highlights how logging disturbance can shift trait-performance relationships, with implications for restoration success and ecosystem functioning, enabling faster regeneration through enhanced resource acquisition while potentially increasing sensitivity to climate

(Carreño-Rocabado *et al*., 2012; Both, Riutta *et al*., 2019; Han *et al*., 2021). In the context of enrichment planting, maintaining sufficient species and functional diversity among planted seedlings would allow for effective forest restoration while enhancing ecosystem resilience to climate change (Veryard *et al*., 2023).

In terms of survival, random effects extracted from our mixed-effects models also revealed patterns consistent with plant functional trade-offs. Within the old-growth forest, species with higher foliar nitrogen concentrations and faster carbon assimilation rates appear to have lower probability of survival, and species with greater wood density appear to show a survival advantage. Acquisitive strategies appear to reduce seedling resilience, while increased structural investment enhances tolerance (Reich, 2014). Unfortunately, high survival rates across some of the census intervals led to data separation, which hindered model convergence and prevented us from incorporating random effect slopes, limiting our ability to assess how functional traits relate to climate sensitivity (Heinze & Schemper, 2002). In the logged forest, species-level random slopes with respect to $\text{minPPT}^{90\text{d}}$ were significantly correlated with Asat and SLA, suggesting that species with higher carbon assimilation rates and specific leaf areas were able to take advantage of increased rainfall to maintain survival (Markesteijn & Poorter, 2009).

Correlations were less consistent across the logged forest models, likely because the exact mechanisms behind the mortality are complex, and may not be directly associated with a single functional trait, with the potential for unmeasured traits to play an important role. In particular, variation in non-structural carbohydrate levels may be a key determinant of species' responses; acting as carbon reserves, they may buffer periods of reduced assimilation and have been shown to be a major factor shaping dipterocarp responses to drought and light intensity (O'Brien *et al*., 2015; Saner *et al*., 2016; O'Brien *et al*., 2020). Monitoring physiological responses to extreme climate events in terms of gas exchange and carbon storage could therefore help us understand the mechanistic causes of mortality and would help clarify how productivity and survival are linked (Philipson *et al*., 2014; Ichie *et al*., 2023). Disentangling the functional constraints imposed

by heat and water deficits is essential for identifying the processes that limit tree performance and improving predictions of forest resilience under climate change (Sato *et al*., 2024; Evans *et al*., 2025).

5.6. Conclusions

Using more than two decades of intensive tree monitoring within two planting experiments, this study demonstrates that extreme heat and drought can strongly constrain seedling productivity in lowland tropical forests, although climate effects may depend on disturbance history, environmental conditions and species functional strategies. Across old-growth and logged forest types, productivity increased with seedling size; larger individuals attained higher productivity in the logged forest, reflecting disturbance-mediated shifts in resource availability and competition. Productivity declined under hot and dry extremes in the old-growth forest, particularly for smaller seedlings, revealing there are strong physiological limitations to carbon gain under adverse climate. In logged forest, temperature extremes also reduced productivity, but growth and survival seem to be positively linked to increased drought and atmospheric water demand, probably because wetter conditions promote waterlogging and constrain tree fitness. Functional trait analyses indicate that resource-acquisitive species can achieve higher productivity under favourable conditions but are more sensitive to climatic extremes, especially in logged forests, whereas more conservative strategies confer greater tolerance to heat and water deficits. Together, these results show that climate extremes are already shaping regeneration and carbon storage dynamics in tropical forests, and reveal that logging can alter both the magnitude and mechanisms of climate vulnerability. Accounting for ecophysiological trade-offs and disturbance-mediated responses will be critical for predicting forest resilience to climate extremes. Restoration strategies should prioritise functional diversity to support effective ecosystem recovery and maintain ecosystem function under intensifying climate change.

5.7. Acknowledgements

We are extremely grateful to all collaborators including SEARRP staff and research assistants for the help in establishing, maintaining and periodically surveying the Sabah Biodiversity Experiment and the Danum plots. We acknowledge assistance and support from Yayasan Sabah and the Sabah Forestry Department.

5.8. Funding

Francisco Navarro-Rosales was supported by the Fundación Rafael del Pino Excellence Scholarship (2022), the France Excellence Eiffel Scholarship (2024) and the Scatcherd European Scholarship from the University of Oxford (2024). Eleanor E. Jackson and Andrew Hector were supported by the Natural Environment Research Council (NERC) [grant number NE/X000281/1]. Michael O'Brien was supported by the Atracción de Talento Investigador Fellowship from the Comunidad de Madrid (2018-T1/AMB-11095) and the Ramón y Cajal Fellowship from the Agencia Estatal de Investigación de España (RYC2021-032049-I). Christopher D. Philipson was supported by the European Space Agency (ESA)'s Business Applications and Space Solutions (BASS) Space Supporting Environmental Claims Kick-Start call for the project Conservation Integrity: Geo-AI powered transparency for Nature-Based Solution to belian.earth.

5.9. Data availability

Plot monitoring data for the Sabah Biodiversity Experiment within the logged forest at Malua can be found at: https://zenodo.org/records/17567533. Survey data for the old-growth forest plots at Danum are available at: https://zenodo.org/records/20065342. Species functional trait data can be found at: https://zenodo.org/records/3247631. Daily climate data for both the old-growth and logged forest sites at Danum and Malua are available at: https://zenodo.org/records/18159592

5.10. References

Aguirre-Gutiérrez, J., Díaz, S., Rifai, S. W., Corral-Rivas, J. J., Nava-Miranda, M. G., González-M, R., Hurtado-M, A. B., Revilla, N. S., Vilanova, E., Almeida, E., de Oliveira, E. A., Alvarez-Davila, E., Alves, L. F., de Andrade, A. C. S., Lola da Costa, A. C., Vieira, S. A., Aragão, L., Arets, E., Aymard C., G. A., … Malhi, Y. (2025). Tropical forests in the Americas are changing too slowly to track climate change. *Science*, *387*(6738), eadl5414. https://doi.org/10.1126/science.adl5414

Aguirre-Gutiérrez, J., Oliveras, I., Rifai, S., Fauset, S., Adu-Bredu, S., Affum-Baffoe, K., Baker, T. R., Feldpausch, T. R., Gvozdevaite, A., Hubau, W., Kraft, N. J. B., Lewis, S. L., Moore, S., Niinemets, Ü., Peprah, T., Phillips, O. L., Ziemińska, K., Enquist, B., & Malhi, Y. (2019). Drier tropical forests are susceptible to functional changes in response to a long-term drought. *Ecology Letters*, *22*(5), 855–865. https://doi.org/10.1111/ele.13243

Alvarez-Clare, S., & Kitajima, K. (2009). Susceptibility of tree seedlings to biotic and abiotic hazards in the understory of a moist tropical forest in Panama. *Biotropica*, *41*(1), 47–56. https://doi.org/10.1111/j.1744-7429.2008.00442.x

Ashton, P. S., & Heckenhauer, J. (2022). Tribe Shoreae (Dipterocarpaceae subfamily Dipterocarpoideae) Finally Dissected. *Kew Bulletin*, *77*(4), 885–903. https://doi.org/10.1007/s12225-022-10057-w

Baccini, A., Goetz, S. J., Walker, W. S., Laporte, N. T., Sun, M., Sulla-Menashe, D., Hackler, J., Beck, P. S. A., Dubayah, R., Friedl, M. A., Samanta, S., & Houghton, R. A. (2012). Estimated carbon dioxide emissions from tropical deforestation improved by carbon-density maps. *Nature Climate Change*, *2*(3), 182–185. https://doi.org/10.1038/nclimate1354

Banin, L. F., Raine, E. H., Rowland, L. M., Chazdon, R. L., Smith, S. W., Rahman, N. E. B., Butler, A., Philipson, C., Applegate, G. G., Axelsson, E. P., Budiharta, S., Chua, S. C., Cutler, M. E. J., Elliott, S., Gemita, E., Godoong, E., Graham, L. L. B., Hayward, R. M., Hector, A., … Burslem, D. F. R. P. (2022). The road to recovery: A synthesis of outcomes from ecosystem restoration in tropical and sub-tropical Asian forests. *Philosophical Transactions of the Royal Society B: Biological Sciences*, *378*(1867), 20210090. https://doi.org/10.1098/rstb.2021.0090

Barlow, J., França, F., Gardner, T. A., Hicks, C. C., Lennox, G. D., Berenguer, E., Castello, L., Economo, E. P., Ferreira, J., Guénard, B., Gontijo Leal, C., Isaac, V., Lees, A. C., Parr, C. L., Wilson, S. K., Young, P. J., & Graham, N. A. J. (2018). The future of hyperdiverse tropical ecosystems. *Nature*, *559*(7715), 517–526. https://doi.org/10.1038/s41586-018-0301-1

Bauman, D., Fortunel, C., Cernusak, L. A., Bentley, L. P., McMahon, S. M., Rifai, S. W., Aguirre-Gutiérrez, J., Oliveras, I., Bradford, M., Laurance, S. G. W., Delhaye, G., Hutchinson, M. F., Dempsey, R., McNellis, B. E., Santos-Andrade, P. E., Ninantay-Rivera, H. R., Chambi Paucar, J. R., Phillips, O. L., & Malhi, Y. (2022). Tropical tree growth sensitivity to climate is driven by species intrinsic growth rate and leaf traits. *Global Change Biology*, *28*(4), 1414–1432. https://doi.org/10.1111/gcb.15982

Bauman, D., Fortunel, C., Delhaye, G., Malhi, Y., Cernusak, L. A., Bentley, L. P., Rifai, S. W., Aguirre-Gutiérrez, J., Menor, I. O., Phillips, O. L., McNellis, B. E., Bradford, M., Laurance, S. G. W., Hutchinson, M. F., Dempsey, R., Santos-Andrade, P. E., Ninantay-Rivera, H. R., Chambi Paucar, J. R., & McMahon, S. M. (2022). Tropical tree mortality has increased with rising atmospheric water stress. *Nature*, *608*(7923), 528–533. https://doi.org/10.1038/s41586-022-04737-7

Bebber, D., Brown, N., & Speight, M. (2002). Drought and root herbivory in understorey *Parashorea* Kurz (Dipterocarpaceae) seedlings in Borneo. *Journal of Tropical Ecology*, *18*(5), 795–804. https://doi.org/10.1017/S0266467402002511

Bebber, D. P., Brown, N. P., & Speight, M. R. (2004). Dipterocarp seedling population dynamics in Bornean primary lowland forest during the 1997-8 El Niño-Southern Oscillation. *Journal of Tropical Ecology*, *20*(1), 11–19. https://doi.org/10.1017/S0266467404006133

Bennett, A. C., Dargie, G. C., Cuni-Sanchez, A., Tshibamba Mukendi, J., Hubau, W., Mukinzi, J. M., Phillips, O. L., Malhi, Y., Sullivan, M. J. P., Cooper, D. L. M., Adu-Bredu, S., Affum-Baffoe, K., Amani, C. A., Banin, L. F., Beeckman, H., Begne, S. K., Bocko, Y. E., Boeckx, P., Bogaert, J., … Lewis, S. L. (2021). Resistance of African tropical forests to an extreme climate anomaly. *Proceedings of the National Academy of Sciences*, *118*(21), e2003169118. https://doi.org/10.1073/pnas.2003169118

Bennett, A. C., Rodrigues de Sousa, T., Monteagudo-Mendoza, A., Esquivel-Muelbert, A., Morandi, P. S., Coelho de Souza, F., Castro, W., Duque, L. F., Flores Llampazo, G., Manoel dos Santos, R., Ramos, E., Vilanova Torre, E., Alvarez-Davila, E., Baker, T. R., Costa, F. R. C., Lewis, S. L., Marimon, B. S., Schietti, J., Burban, B., … Phillips, O. L. (2023). Sensitivity of South American tropical forests to an extreme climate anomaly. *Nature Climate Change*, *13*(9), 967–974. https://doi.org/10.1038/s41558-023-01776-4

Bischoff, W., Newbery, D. M., Lingenfelder, M., Schnaeckel, R., Petol, G. H., Madani, L., & Ridsdale, C. E. (2005). Secondary succession and dipterocarp recruitment in Bornean rain forest after logging. *Forest Ecology and Management*, *218*(1), 174–192. https://doi.org/10.1016/j.foreco.2005.07.009

Blonder, B., Both, S., Coomes, D. A., Elias, D., Jucker, T., Kvasnica, J., Majalap, N., Malhi, Y. S., Milodowski, D., Riutta, T., & Svátek, M. (2018). Extreme and Highly Heterogeneous Microclimates in Selectively Logged Tropical Forests. *Frontiers in Forests and Global Change*, *1*. https://doi.org/10.3389/ffgc.2018.00005

Bolton, D. (1980). The computation of equivalent potential temperature. *Monthly Weather Review*, *108*(7), 1046–1053. https://doi.org/10.1175/1520-0493(1980)108%253C1046:TCOEPT%253E2.0.CO;2

Bonan, G. B. (2008). Forests and climate change: Forcings, feedbacks, and the climate benefits of forests. *Science*, *320*(5882), 1444–1449. https://doi.org/10.1126/science.1155121

Born, J., Bagchi, R., Burslem, D., Nilus, R., Tellenbach, C., Pluess, A. R., & Ghazoul, J. (2015). Differential responses of dipterocarp seedlings to soil moisture and microtopography. *Biotropica*, *47*(1), 49–58. https://doi.org/10.1111/btp.12180

Both, S., Burslem, D. F. R. P., Riutta, T., Malhi, Y., Majalap, N., & Teh, Y. A. (2019). *Functional traits of tree species in old-growth and selectively logged forest* [Dataset]. Zenodo. https://doi.org/10.5281/zenodo.3247631

Both, S., Riutta, T., Paine, C. E. T., Elias, D. M. O., Cruz, R. S., Jain, A., Johnson, D., Kritzler, U. H., Kuntz, M., Majalap-Lee, N., Mielke, N., Montoya Pillco, M. X., Ostle, N. J., Arn Teh, Y., Malhi, Y., & Burslem, D. F. R. P. (2019). Logging and soil nutrients independently explain plant trait expression in tropical forests. *New Phytologist*, *221*(4), 1853–1865. https://doi.org/10.1111/nph.15444

Brown, N., Press, M., & Bebber, D. (1999). Growth and survivorship of dipterocarp seedlings: Differences in shade persistence create a special case of dispersal limitation. *Philosophical Transactions of the Royal Society B: Biological Sciences*, *354*(1391), 1847–1855. https://doi.org/10.1098/rstb.1999.0526

Browne, L., Markesteijn, L., Engelbrecht, B. M. J., Jones, F. A., Lewis, O. T., Manzané-Pinzón, E., Wright, S. J., & Comita, L. S. (2021). Increased mortality of tropical tree seedlings during the extreme 2015–16 El Niño. *Global Change Biology*, *27*(20), 5043–5053. https://doi.org/10.1111/gcb.15809

Burslem, D. F. R. P., Grubb, P. J., & Turner, I. M. (1996). Responses to simulated drought and elevated nutrient supply among shade-tolerant tree seedlings of lowland tropical forest in Singapore. *Biotropica*, *28*(4), 636–648. https://doi.org/10.2307/2389050

Carle, H., Neeman, T., Murphy, H., Bauman, D., Binks, O., Coughlin, I., Ford, A., Nicotra, A., & Meir, P. (2025). Contributions of height allometry and within-species trait variation to uncertainty in estimates of tropical forest carbon stocks. *Forestry: An International Journal of Forest Research*, cpaf084. https://doi.org/10.1093/forestry/cpaf084

Carreño-Rocabado, G., Peña-Claros, M., Bongers, F., Alarcón, A., Licona, J.-C., & Poorter, L. (2012). Effects of disturbance intensity on species and functional diversity in a tropical forest. *Journal of Ecology*, *100*(6), 1453–1463. https://doi.org/10.1111/j.1365-2745.2012.02015.x

Chambers, J. Q., Higuchi, N., Teixeira, L. M., dos Santos, J., Laurance, S. G., & Trumbore, S. E. (2004). Response of tree biomass and wood litter to disturbance in a Central Amazon forest. *Oecologia*, *141*(4), 596–611. https://doi.org/10.1007/s00442-004-1676-2

Chambers, J. Q., Nogueira Lima, A. J., Pastorello, G., Gimenez, B. O., Meng, L., Dyer, L. A., Feng, Y., Santos da Silva, C., Costa de Oliveira, R., Weber, A., Koven, C., Negrón-Juárez, R., Spanner, G. C., Gaui, T. D., Fontes, C. G., de Araújo, A. C., McDowell, N., Leung, R., Marra, D. M., … Higuchi, N. (2026). Hot droughts in the Amazon provide a window to a future hypertropical climate. *Nature*, *649*(8099), 1190–1196. https://doi.org/10.1038/s41586-025-09728-y

Chave, J., Coomes, D., Jansen, S., Lewis, S. L., Swenson, N. G., & Zanne, A. E. (2009). Towards a worldwide wood economics spectrum. *Ecology Letters*, *12*(4), 351–366. https://doi.org/10.1111/j.1461-0248.2009.01285.x

Chu, Y., Guo, L., Yang, G., Xu, H., Li, T., He, X., Zheng, H., Yao, S., Liu, H., & He, B. (2026). Increasing climate variability makes Southeast Asian forests more vulnerable to anthropogenic and environmental stressors. *Global and Planetary Change*, *256*, 105138. https://doi.org/10.1016/j.gloplacha.2025.105138

Clark, D. A., Brown, S., Kicklighter, D. W., Chambers, J. Q., Thomlinson, J. R., Ni, J., & Holland, E. A. (2001). Net primary production in tropical forests: An evaluation and synthesis of existing field data. *Ecological Applications*, *11*(2), 371–384. https://doi.org/10.1890/1051-0761(2001)011%255B0371:NPPITF%255D2.0.CO;2

Coomes, D. A., & Allen, R. B. (2009). Testing the metabolic scaling theory of tree growth. *Journal of Ecology*, *97*(6), 1369–1373. https://doi.org/10.1111/j.1365-2745.2009.01571.x

Deb, J., Phinn, S., Butt, N., & Mcalpine, C. (2018). Climate change impacts on tropical forests: Identifying risks for tropical Asia. *Journal of Tropical Forest Science*, *30*(2), 182–194. https://doi.org/10.26525/jtfs2018.30.2.182194

Díaz, S., Pascual, U., Stenseke, M., Martín-López, B., Watson, R. T., Molnár, Z., Hill, R., Chan, K. M. A., Baste, I. A., Brauman, K. A., Polasky, S., Church, A., Lonsdale, M., Larigauderie, A., Leadley, P. W., van Oudenhoven, A. P. E., van der Plaat, F., Schröter, M., Lavorel, S., … Shirayama, Y. (2018). Assessing nature's contributions to people. *Science*, *359*(6373), 270–272. https://doi.org/10.1126/science.aap8826

Dongsansuk, A., Sumthonglang, N., Kantachot, C., Lontom, W., Theerakulpisut, P., & Kawjumpa, N. (2020). Effect of high temperature and light intensity on physiology and morphology in young *Dipterocarpus alatus* Roxb. Leaf. *Pertanika Journal of Tropical Agricultural Science*, *43*(2), 193–206.

Doughty, C. E., Keany, J. M., Wiebe, B. C., Rey-Sanchez, C., Carter, K. R., Middleby, K. B., Cheesman, A. W., Goulden, M. L., da Rocha, H. R., Miller, S. D., Malhi, Y., Fauset, S., Gloor, E., Slot, M., Oliveras Menor, I., Crous, K. Y., Goldsmith, G. R., & Fisher, J. B. (2023). Tropical forests are approaching critical temperature thresholds. *Nature*, *621*(7977), 105–111. https://doi.org/10.1038/s41586-023-06391-z

Douglas, I. (2022). Impact of Logging on Interception and Soil Water. In I. Douglas (Ed.), *Water and the rainforest in Malaysian Borneo: Hydrological research at the Danum Valley Field Studies Center* (pp. 243–258). Springer International Publishing. https://doi.org/10.1007/978-3-030-91544-5_14

Edwards, F. A., Edwards, D. P., Larsen, T. H., Hsu, W. W., Benedick, S., Chung, A., Vun Khen, C., Wilcove, D. S., & Hamer, K. C. (2014). Does logging and forest conversion to oil palm agriculture alter functional diversity in a biodiversity hotspot? *Animal Conservation*, *17*(2), 163–173. https://doi.org/10.1111/acv.12074

Engelbrecht, B. M. J., Wright, S. J., & Steven, D. D. (2002). Survival and ecophysiology of tree seedlings during El Niño drought in a tropical moist forest in Panama. *Journal of Tropical Ecology*, *18*(4), 569–579. https://doi.org/10.1017/S0266467402002377

Evans, M. E. K., Hu, J., & Michaletz, S. T. (2025). Scaling plant responses to heat: From molecules to the biosphere. *Science*, *388*(6752), 1167–1173. https://doi.org/10.1126/science.adv7597

Ewers, R. M., & Banks-Leite, C. (2013). Fragmentation impairs the microclimate buffering effect of tropical forests. *PLOS ONE*, *8*(3), e58093. https://doi.org/10.1371/journal.pone.0058093

Fauset, S., Gloor, M. U., Aidar, M. P. M., Freitas, H. C., Fyllas, N. M., Marabesi, M. A., Rochelle, A. L. C., Shenkin, A., Vieira, S. A., & Joly, C. A. (2017). Tropical forest light regimes in a human-modified landscape. *Ecosphere*, *8*(11), e02002. https://doi.org/10.1002/ecs2.2002

Feeley, K. J., Bernal-Escobar, M., Fortier, R., & Kullberg, A. T. (2023). Tropical trees will need to acclimate to rising temperatures—but can they? *Plants*, *12*(17), 3142. https://doi.org/10.3390/plants12173142

Feeley, K. J., Davies, S. J., Perez, R., Hubbell, S. P., & Foster, R. B. (2011). Directional changes in the species composition of a tropical forest. *Ecology*, *92*(4), 871–882. https://doi.org/10.1890/10-0724.1

Feng, C. X. (2021). A comparison of zero-inflated and hurdle models for modeling zero-inflated count data. *Journal of Statistical Distributions and Applications*, *8*(1), 8. https://doi.org/10.1186/s40488-021-00121-4

Ferry, B., Morneau, F., Bontemps, J.-D., Blanc, L., & Freycon, V. (2010). Higher treefall rates on slopes and waterlogged soils result in lower stand biomass and productivity in a tropical rain forest. *Journal of Ecology*, *98*(1), 106–116. https://doi.org/10.1111/j.1365-2745.2009.01604.x

Fichtbauer, A. (2022). *Temperature increase explains loss of productivity in Borneo rainforest with largest impact on suppressed trees and logged stands* [Master Thesis, Utretch University]. https://studenttheses.uu.nl/handle/20.500.12932/43214

Gaveau, D. L. A., Sloan, S., Molidena, E., Yaen, H., Sheil, D., Abram, N. K., Ancrenaz, M., Nasi, R., Quinones, M., Wielaard, N., & Meijaard, E. (2014). Four decades of forest persistence, clearance and logging on Borneo. *PLOS ONE*, *9*(7), e101654. https://doi.org/10.1371/journal.pone.0101654

Girardin, C. A. J., Malhi, Y., Aragão, L. E. O. C., Mamani, M., Huaraca Huasco, W., Durand, L., Feeley, K. J., Rapp, J., Silva-Espejo, J. E., Silman, M., Salinas, N., & Whittaker, R. J. (2010). Net primary productivity allocation and cycling of carbon along a tropical forest elevational transect in the Peruvian Andes: Net primary productivity from Andes to Amazon. *Global Change Biology*, *16*(12), 3176–3192. https://doi.org/10.1111/j.1365-2486.2010.02235.x

Grantham, H. S., Duncan, A., Evans, T. D., Jones, K. R., Beyer, H. L., Schuster, R., Walston, J., Ray, J. C., Robinson, J. G., Callow, M., Clements, T., Costa, H. M., DeGemmis, A., Elsen, P. R., Ervin, J., Franco, P., Goldman, E., Goetz, S., Hansen, A., … Watson, J. E. M. (2020). Anthropogenic modification of forests means only 40% of remaining forests have high ecosystem integrity. *Nature Communications*, *11*(1), 5978. https://doi.org/10.1038/s41467-020-19493-3

Grossiord, C., Buckley, T. N., Cernusak, L. A., Novick, K. A., Poulter, B., Siegwolf, R. T. W., Sperry, J. S., & McDowell, N. G. (2020). Plant responses to rising vapor pressure deficit. *New Phytologist*, *226*(6), 1550–1566. https://doi.org/10.1111/nph.16485

Hamed, M. M., Al-Sakkaf, A. S., Rady, M., & Shahid, S. (2024). Temperature and precipitation extremes over Borneo island: An integrated climate risk assessment. *International Journal of Climatology*, *44*(16), 6040–6064. https://doi.org/10.1002/joc.8682

Hammond, W. M., & Adams, H. D. (2019). Dying on time: Traits influencing the dynamics of tree mortality risk from drought. *Tree Physiology*, *39*(6), 906–909. https://doi.org/10.1093/treephys/tpz050

Han, X., Huang, J., Yao, J., Xu, Y., Ding, Y., & Zang, R. (2021). Effects of logging on the ecological strategy spectrum of a tropical montane rain forest. *Ecological Indicators*, *128*, 107812. https://doi.org/10.1016/j.ecolind.2021.107812

Hanya, G., & Bernard, H. (2012). Fallback foods of red leaf monkeys (*Presbytis rubicunda*) in Danum Valley, Borneo. *International Journal of Primatology*, *33*(2), 322–337. https://doi.org/10.1007/s10764-012-9580-9

Hardwick, S. R., Toumi, R., Pfeifer, M., Turner, E. C., Nilus, R., & Ewers, R. M. (2015). The relationship between leaf area index and microclimate in tropical forest and oil palm plantation: Forest disturbance drives changes in microclimate. *Agricultural and Forest Meteorology*, *201*, 187–195. https://doi.org/10.1016/j.agrformet.2014.11.010

Hayward, R. M., Banin, L. F., Burslem, D. F. R. P., Chapman, D. S., Philipson, C. D., Cutler, M. E. J., Reynolds, G., Nilus, R., & Dent, D. H. (2021). Three decades of post-logging tree community recovery in naturally regenerating and actively restored dipterocarp forest in Borneo. *Forest Ecology and Management*, *488*, 119036. https://doi.org/10.1016/j.foreco.2021.119036

Hector, A., Philipson, C., Saner, P., Chamagne, J., Dzulkifli, D., O'Brien, M., Snaddon, J. L., Ulok, P., Weilenmann, M., Reynolds, G., & Godfray, H. C. J. (2011). The Sabah Biodiversity Experiment: A long-term test of the role of tree diversity in restoring tropical forest structure and functioning. *Philosophical Transactions of the Royal Society B: Biological Sciences*, *366*(1582), 3303–3315. https://doi.org/10.1098/rstb.2011.0094

Heinze, G., & Schemper, M. (2002). A solution to the problem of separation in logistic regression. *Statistics in Medicine*, *21*(16), 2409–2419. https://doi.org/10.1002/sim.1047

Hiromi, T., Ichie, T., Kenzo, T., & Ninomiya, I. (2012). Interspecific variation in leaf water use associated with drought tolerance in four emergent dipterocarp species of a tropical rain forest in Borneo. *Journal of Forest Research*, *17*(4), 369–377. https://doi.org/10.1007/s10310-011-0303-4

Hosonuma, N., Herold, M., De Sy, V., De Fries, R. S., Brockhaus, M., Verchot, L., Angelsen, A., & Romijn, E. (2012). An assessment of deforestation and forest degradation drivers in developing countries. *Environmental Research Letters*, *7*(4), 044009. https://doi.org/10.1088/1748-9326/7/4/044009

Howlett, B. E., & Davidson, D. W. (2003). Effects of seed availability, site conditions, and herbivory on pioneer recruitment after logging in Sabah, Malaysia. *Forest Ecology and Management*, *184*(1), 369–383. https://doi.org/10.1016/S0378-1127(03)00161-0

Ichie, T., Igarashi, S., Tanimoto, T., Inoue, Y., Mohizah, M., & Kenzo, T. (2023). Ecophysiological responses of seedlings of six dipterocarp species to short-term drought in Borneo. *Frontiers in Forests and Global Change*, *6*. https://doi.org/10.3389/ffgc.2023.1112852

Imai, N., Seino, T., Aiba, S., Takyu, M., Titin, J., & Kitayama, K. (2012). Effects of selective logging on tree species diversity and composition of Bornean tropical rain forests at different spatial scales. *Plant Ecology*, *213*(9), 1413–1424. https://doi.org/10.1007/s11258-012-0100-y

Imai, N., Sugau, J. B., Pereira, J. T., Titin, J., & Kitayama, K. (2019). Impacts of selective logging on spatial structure of tree species composition in Bornean tropical rain forests. *Journal of Forest Research*, *24*(6), 335–340. https://doi.org/10.1080/13416979.2019.1666958

Jucker, T., Hardwick, S. R., Both, S., Elias, D. M. O., Ewers, R. M., Milodowski, D. T., Swinfield, T., & Coomes, D. A. (2018). Canopy structure and topography jointly constrain the microclimate of human-modified tropical landscapes. *Global Change Biology*, *24*(11), 5243–5258. https://doi.org/10.1111/gcb.14415

Kenzo, T., Ichie, T., Hattori, D., Itioka, T., Handa, C., Ohkubo, T., Kendawang, J., Nakamura, M., Sakaguchi, M., Takahashi, N., Okamoto, M., Tanaka-Oda, A., Sakurai, K., & Ninomiya, I. (2009). Development of allometric relationships for accurate estimation of above- and below-ground biomass in tropical secondary forests in Sarawak, Malaysia. *Journal of Tropical Ecology*, *25*, 371–386. https://doi.org/10.1017/S0266467409006129

Kitajima, K. (1996). Ecophysiology of tropical tree seedlings. In S. S. Mulkey, R. L. Chazdon, & A. P. Smith (Eds.), *Tropical Forest Plant Ecophysiology* (pp. 559–596). Springer US. https://doi.org/10.1007/978-1-4613-1163-8_19

Kitao, M., Lei, T. T., Koike, T., Tobita, H., Maruyama, Y., Matsumoto, Y., & Ang, L.-H. (2000). Temperature response and photoinhibition investigated by chlorophyll fluorescence measurements for four distinct species of dipterocarp trees. *Physiologia Plantarum*, *109*(3), 284–290. https://doi.org/10.1034/j.1399-3054.2000.100309.x

Kondo, M., Ichii, K., Patra, P. K., Canadell, J. G., Poulter, B., Sitch, S., Calle, L., Liu, Y. Y., van Dijk, A. I. J. M., Saeki, T., Saigusa, N., Friedlingstein, P., Arneth, A., Harper, A., Jain, A. K., Kato, E., Koven, C., Li, F., Pugh, T. A. M., … Rödenbeck, C. (2018). Land use change and El Niño-Southern Oscillation drive decadal carbon balance shifts in Southeast Asia. *Nature Communications*, *9*(1), 1154. https://doi.org/10.1038/s41467-018-03374-x

Kumagai, T., Saitoh, T. M., Sato, Y., Takahashi, H., Manfroi, O. J., Morooka, T., Kuraji, K., Suzuki, M., Yasunari, T., & Komatsu, H. (2005). Annual water balance and seasonality of evapotranspiration in a Bornean tropical rainforest. *Agricultural and Forest Meteorology*, *128*(1), 81–92. https://doi.org/10.1016/j.agrformet.2004.08.006

Kume, T., Tanaka, N., Kuraji, K., Komatsu, H., Yoshifuji, N., Saitoh, T. M., Suzuki, M., & Kumagai, T. (2011). Ten-year evapotranspiration estimates in a Bornean tropical rainforest. *Agricultural and Forest Meteorology*, *151*(9), 1183–1192. https://doi.org/10.1016/j.agrformet.2011.04.005

Kupers, S. J., Wirth, C., Engelbrecht, B. M. J., Hernández, A., Condit, R., Wright, S. J., & Rüger, N. (2019). Performance of tropical forest seedlings under shade and drought: An interspecific trade-off in demographic responses. *Scientific Reports*, *9*(1), 18784. https://doi.org/10.1038/s41598-019-55256-x

Lingenfelder, M., & Newbery, D. M. (2009). On the detection of dynamic responses in a drought-perturbed tropical rainforest in Borneo. In A. G. Van der Valk (Ed.), *Forest Ecology: Recent Advances in Plant Ecology* (pp. 267–290). Springer Netherlands. https://doi.org/10.1007/978-90-481-2795-5_21

Liu, C., Li, Y., Yan, P., & He, N. (2021). How to improve the predictions of plant functional traits on ecosystem functioning? *Frontiers in Plant Science*, *12*. https://doi.org/10.3389/fpls.2021.622260

Malik, N., Edwards, D., & Freckleton, R. P. (2023). Distance and density dependence in two native Bornean dipterocarp species. *Ecology and Evolution*, *13*(4), e10004. https://doi.org/10.1002/ece3.10004

Malhi, Y. (2012). The productivity, metabolism and carbon cycle of tropical forest vegetation: Carbon cycle of tropical forests. *Journal of Ecology*, *100*(1), 65–75. https://doi.org/10.1111/j.1365-2745.2011.01916.x

Malhi, Y., Aragão, L. E. O. C., Galbraith, D., Huntingford, C., Fisher, R., Zelazowski, P., Sitch, S., McSweeney, C., & Meir, P. (2009). Exploring the likelihood and mechanism of a climate-change-induced dieback of the Amazon rainforest. *Proceedings of the National Academy of Sciences*, *106*(49), 20610–20615. https://doi.org/10.1073/pnas.0804619106

Malhi, Y., Gardner, T. A., Goldsmith, G. R., Silman, M. R., & Zelazowski, P. (2014). Tropical forests in the Anthropocene. *Annual Review of Environment and Resources*, *39*(Volume 39, 2014), 125–159. https://doi.org/10.1146/annurev-environ-030713-155141

Malhi, Y., Riutta, T., Wearn, O. R., Deere, N. J., Mitchell, S. L., Bernard, H., Majalap, N., Nilus, R., Davies, Z. G., Ewers, R. M., & Struebig, M. J. (2022). Logged tropical forests have amplified and diverse ecosystem energetics. *Nature*, *612*(7941), 707–713. https://doi.org/10.1038/s41586-022-05523-1

Manghwar, H., Hussain, A., Alam, I., Khoso, M. A., Ali, Q., & Liu, F. (2024). Waterlogging stress in plants: Unravelling the mechanisms and impacts on growth, development, and productivity. *Environmental and Experimental Botany*, *224*, 105824. https://doi.org/10.1016/j.envexpbot.2024.105824

Margrove, J. A., Burslem, D. F. R. P., Ghazoul, J., Khoo, E., Kettle, C. J., & Maycock, C. R. (2015). Impacts of an extreme precipitation event on dipterocarp mortality and habitat filtering in a Bornean tropical rain forest. *Biotropica*, *47*(1), 66–76. https://doi.org/10.1111/btp.12189

Markesteijn, L., & Poorter, L. (2009). Seedling root morphology and biomass allocation of 62 tropical tree species in relation to drought- and shade-tolerance. *Journal of Ecology*, *97*(2), 311–325. https://doi.org/10.1111/j.1365-2745.2008.01466.x

Marsh, C. J., Turner, E. C., Blonder, B. W., Bongalov, B., Both, S., Cruz, R. S., Elias, D. M. O., Hemprich-Bennett, D., Jotan, P., Kemp, V., Kritzler, U. H., Milne, S., Milodowski, D. T., Mitchell, S. L., Pillco, M. M., Nunes, M. H., Riutta, T., Robinson, S. J. B., Slade, E. M., … Hector, A. (2025). Tropical forest clearance impacts biodiversity and function, whereas logging changes structure. *Science*, *387*(6730), 171–175. https://doi.org/10.1126/science.adf9856

Martínez-Vilalta, J., & García-Forner, N. (2017). Water potential regulation, stomatal behaviour and hydraulic transport under drought: Deconstructing the iso/anisohydric concept. *Plant, Cell & Environment*, *40*(6), 962–976. https://doi.org/10.1111/pce.12846

McGillycuddy, M., Popovic, G., Bolker, B. M., & Warton, D. I. (2025). Parsimoniously fitting large multivariate random effects in glmmTMB. *Journal of Statistical Software*, *112*, 1–19. https://doi.org/10.18637/jss.v112.i01

Mills, M. B., Malhi, Y., Ewers, R. M., Kho, L. K., Teh, Y. A., Both, S., Burslem, D. F. R. P., Majalap, N., Nilus, R., Huaraca Huasco, W., Cruz, R., Pillco, M. M., Turner, E. C., Reynolds, G., & Riutta, T. (2023). Tropical forests post-logging are a persistent net carbon source to the atmosphere. *Proceedings of the National Academy of Sciences*, *120*(3), e2214462120. https://doi.org/10.1073/pnas.2214462120

Milodowski, D. T., Coomes, D. A., Swinfield, T., Jucker, T., Riutta, T., Malhi, Y., Svátek, M., Kvasnica, J., Burslem, D. F. R. P., Ewers, R. M., Teh, Y. A., & Williams, M. (2021). The impact of logging on vertical canopy structure across a gradient of tropical forest degradation intensity in Borneo. *Journal of Applied Ecology*, *58*(8), 1764–1775. https://doi.org/10.1111/1365-2664.13895

Miyamoto, K., Aiba, S., Aoyagi, R., & Nilus, R. (2021). Effects of El Niño drought on tree mortality and growth across forest types at different elevations in Borneo. *Forest Ecology and Management*, *490*, 119096. https://doi.org/10.1016/j.foreco.2021.119096

Myers, N., Mittermeier, R. A., Mittermeier, C. G., da Fonseca, G. A. B., & Kent, J. (2000). Biodiversity hotspots for conservation priorities. *Nature*, *403*(6772), 853–858. https://doi.org/10.1038/35002501

Nainar, A., Tanaka, N., Bidin, K., Annammala, K. V., Ewers, R. M., Reynolds, G., & Walsh, R. P. D. (2018). Hydrological dynamics of tropical streams on a gradient of land-use disturbance and recovery: A multi-catchment experiment. *Journal of Hydrology*, *566*, 581–594. https://doi.org/10.1016/j.jhydrol.2018.09.022

Nakagawa, M., Tanaka, K., Nakashizuka, T., Ohkubo, T., Kato, T., Maeda, T., Sato, K., Miguchi, H., Nagamasu, H., Ogino, K., Teo, S., Hamid, A. A., & Seng, L. H. (2000). Impact of severe drought associated with the 1997–1998 El Niño in a tropical forest in Sarawak. *Journal of Tropical Ecology*, *16*(3), 355–367. https://doi.org/10.1017/S0266467400001450

Newbery, D. M., Kennedy, D. N., Petol, G. H., Madani, L., & Ridsdale, C. E. (1999). Primary forest dynamics in lowland dipterocarp forest at Danum Valley, Sabah, Malaysia, and the role of the understorey. *Philosophical Transactions of the Royal Society B: Biological Sciences*, *354*(1391), 1763–1782. https://doi.org/10.1098/rstb.1999.0519

Nottingham, A. T., Montero-Sanchez, M., Slot, M., Szczygieł, H. A., Velasquez, E., & Meir, P. (2023). Seedling growth declines in warmed tropical forest soils. *Biotropica*, btp.13238. https://doi.org/10.1111/btp.13238

Nunes, M. H., Both, S., Bongalov, B., Brelsford, C., Khoury, S., Burslem, D. F. R. P., Philipson, C., Majalap, N., Riutta, T., Coomes, D. A., & Cutler, M. E. J. (2019). Changes in leaf functional traits of rainforest canopy trees associated with an El Niño event in Borneo. *Environmental Research Letters*, *14*(8), 085005. https://doi.org/10.1088/1748-9326/ab2eae

O'Brien, M. J., Burslem, D. F. R. P., Caduff, A., Tay, J., & Hector, A. (2015). Contrasting nonstructural carbohydrate dynamics of tropical tree seedlings under water deficit and variability. *New Phytologist*, *205*(3), 1083–1094. https://doi.org/10.1111/nph.13134

O'Brien, M. J., Engelbrecht, B. M. J., Joswig, J., Pereyra, G., Schuldt, B., Jansen, S., Kattge, J., Landhäusser, S. M., Levick, S. R., Preisler, Y., Väänänen, P., & Macinnis-Ng, C. (2017). A synthesis of tree functional traits related to drought-induced mortality in forests across climatic zones. *Journal of Applied Ecology*, *54*(6), 1669–1686. https://doi.org/10.1111/1365-2664.12874

O'Brien, M. J., & Escudero, A. (2022). Topography in tropical forests enhances growth and survival differences within and among species via water availability and biotic interactions. *Functional Ecology*, *36*(3), 686–698. https://doi.org/10.1111/1365-2435.13977

O'Brien, M. J., Hector, A., Kellenberger, R. T., Maycock, C. R., Ong, R., Philipson, C. D., Powers, J. S., Reynolds, G., & Burslem, D. F. R. P. (2022). Demographic consequences of heterogeneity in conspecific density dependence among mast-fruiting tropical trees. *Proceedings of the Royal Society B: Biological Sciences*, *289*(1977), 20220739. https://doi.org/10.1098/rspb.2022.0739

O'Brien, M. J., Hector, A., Ong, R., & Philipson, C. D. (2024). Tree growth and survival are more sensitive to high rainfall than drought in an aseasonal forest in Malaysia. *Communications Earth & Environment*, *5*(1), 179. https://doi.org/10.1038/s43247-024-01335-5

O'Brien, M. J., Ong, R., & Reynolds, G. (2017). Intra-annual plasticity of growth mediates drought resilience over multiple years in tropical seedling communities. *Global Change Biology*, *23*(10), 4235–4244. https://doi.org/10.1111/gcb.13658

O'Brien, M. J., Philipson, C. D., Reynolds, G., Dzulkifli, D., Snaddon, J. L., Ong, R., & Hector, A. (2019). Positive effects of liana cutting on seedlings are reduced during El Niño-induced drought. *Journal of Applied Ecology*, *56*(4), 891–901. https://doi.org/10.1111/1365-2664.13335

O'Brien, M. J., Reynolds, G., Ong, R., & Hector, A. (2017). Resistance of tropical seedlings to drought is mediated by neighbourhood diversity. *Nature Ecology & Evolution*, *1*(11), 1643–1648. https://doi.org/10.1038/s41559-017-0326-0

O'Brien, M. J., Valtat, A., Abiven, S., Studer, M. S., Ong, R., & Schmid, B. (2020). The role of soluble sugars during drought in tropical tree seedlings with contrasting tolerances. *Journal of Plant Ecology*, *13*(4), 389–397. https://doi.org/10.1093/jpe/rtaa017

Paine, C. E. T., Marthews, T. R., Vogt, D. R., Purves, D., Rees, M., Hector, A., & Turnbull, L. A. (2012). How to fit nonlinear plant growth models and calculate growth rates: An update for ecologists. *Methods in Ecology and Evolution*, *3*(2), 245–256. https://doi.org/10.1111/j.2041-210X.2011.00155.x

Pan, Y., Birdsey, R. A., Fang, J., Houghton, R., Kauppi, P. E., Kurz, W. A., Phillips, O. L., Shvidenko, A., Lewis, S. L., Canadell, J. G., Ciais, P., Jackson, R. B., Pacala, S. W., McGuire, A. D., Piao, S., Rautiainen, A., Sitch, S., & Hayes, D. (2011). A large and persistent carbon sink in the World's forests. *Science*, *333*(6045), 988–993. https://doi.org/10.1126/science.1201609

Pearson, T. R. H., Brown, S., Murray, L., & Sidman, G. (2017). Greenhouse gas emissions from tropical forest degradation: An underestimated source. *Carbon Balance and Management*, *12*(1), 3. https://doi.org/10.1186/s13021-017-0072-2

Pérez-Harguindeguy, N., Díaz, S., Garnier, E., Lavorel, S., Poorter, H., Jaureguiberry, P., Bret-Harte, M. S., Cornwell, W. K., Craine, J. M., Gurvich, D. E., Urcelay, C., Veneklaas, E. J., Reich, P. B., Poorter, L., Wright, I. J., Ray, P., Enrico, L., Pausas, J. G., de Vos, A. C., … Cornelissen, J. H. C. (2013). New handbook for standardised measurement of plant functional traits worldwide. *Australian Journal of Botany*, *61*(3), 167–234. https://doi.org/10.1071/BT12225

Philipson, C. D., Cutler, M. E. J., Brodrick, P. G., Asner, G. P., Boyd, D. S., Moura Costa, P., Fiddes, J., Foody, G. M., van der Heijden, G. M. F., Ledo, A., Lincoln, P. R., Margrove, J. A., Martin, R. E., Milne, S., Pinard, M. A., Reynolds, G., Snoep, M., Tangki, H., Sau Wai, Y., … Burslem, D. F. R. P. (2020). Active restoration accelerates the carbon recovery of human-modified tropical forests. *Science*, *369*(6505), 838–841. https://doi.org/10.1126/science.aay4490

Philipson, C. D., Dent, D. H., O'Brien, M. J., Chamagne, J., Dzulkifli, D., Nilus, R., Philips, S., Reynolds, G., Saner, P., & Hector, A. (2014). A trait-based trade-off between growth and mortality: Evidence from 15 tropical tree species using size-specific relative growth rates. *Ecology and Evolution*, *4*(18), 3675–3688. https://doi.org/10.1002/ece3.1186

Phillips, O. L. (1996). Long-term environmental change in tropical forests: Increasing tree turnover. *Environmental Conservation*, *23*(3), 235–248. https://doi.org/10.1017/S0376892900038856

Phillips, O. L., Aragão, L. E. O. C., Lewis, S. L., Fisher, J. B., Lloyd, J., López-González, G., Malhi, Y., Monteagudo, A., Peacock, J., Quesada, C. A., van der Heijden, G., Almeida, S., Amaral, I., Arroyo, L., Aymard, G., Baker, T. R., Bánki, O., Blanc, L., Bonal, D., … Torres-Lezama, A. (2009). Drought sensitivity of the Amazon rainforest. *Science*, *323*(5919), 1344–1347. https://doi.org/10.1126/science.1164033

Phillips, O. L., van der Heijden, G., Lewis, S. L., López-González, G., Aragão, L. E. O. C., Lloyd, J., Malhi, Y., Monteagudo, A., Almeida, S., Dávila, E. A., Amaral, I., Andelman, S., Andrade, A., Arroyo, L., Aymard, G., Baker, T. R., Blanc, L., Bonal, D., de Oliveira, Á. C. A., … Vilanova, E. (2010). Drought-mortality relationships for tropical forests. *New Phytologist*, *187*(3), 631–646. https://doi.org/10.1111/j.1469-8137.2010.03359.x

Pinheiro, J. C., & Bates, D. M. (2000). Mixed-Effects Models in S and S-PLUS. Springer-Verlag. https://doi.org/10.1007/b98882

Powers, J. S., Vargas G., G., Brodribb, T. J., Schwartz, N. B., Pérez-Aviles, D., Smith-Martin, C. M., Becknell, J. M., Aureli, F., Blanco, R., Calderón-Morales, E., Calvo-Alvarado, J. C., Calvo-Obando, A. J., Chavarría, M. M., Carvajal-Vanegas, D., Jiménez-Rodríguez, C. D., Murillo Chacon, E., Schaffner, C. M., Werden, L. K., Xu, X., & Medvigy, D. (2020). A catastrophic tropical drought kills hydraulically vulnerable tree species. *Global Change Biology*, *26*(5), 3122–3133. https://doi.org/10.1111/gcb.15037

Puértolas, J., Villar-Salvador, P., Andivia, E., Ahuja, I., Cocozza, C., Cvjetković, B., Devetaković, J., Diez, J. J., Fløistad, I. S., Ganatsas, P., Mariotti, B., Tsakaldimi, M., Vilagrosa, A., Witzell, J., & Ivetić, V. (2024). Die-hard seedlings. A global meta-analysis on the factors determining the effectiveness of drought hardening on growth and survival of forest plantations. *Forest Ecology and Management*, *572*, 122300. https://doi.org/10.1016/j.foreco.2024.122300

Qian, Z., Chen, S., Li, X., Wang, S., Liu, Z., Chen, X., & Darjee, A. (2025). The response of vegetation productivity to the El Niño-Southern Oscillation in Southeast Asia. *Journal of Geophysical Research: Biogeosciences*, *130*(7), e2024JG008606. https://doi.org/10.1029/2024JG008606

Qie, L., Lewis, S. L., Sullivan, M. J. P., Lopez-Gonzalez, G., Pickavance, G. C., Sunderland, T., Ashton, P., Hubau, W., Abu Salim, K., Aiba, S.-I., Banin, L. F., Berry, N., Brearley, F. Q., Burslem, D. F. R. P., Dančák, M., Davies, S. J., Fredriksson, G., Hamer, K. C., Hédl, R., … Phillips, O. L. (2017). Long-term carbon sink in Borneo's forests halted by drought and vulnerable to edge effects. *Nature Communications*, *8*(1), 1966. https://doi.org/10.1038/s41467-017-01997-0

Qie, L., Telford, E. M., Massam, M. R., Tangki, H., Nilus, R., Hector, A., & Ewers, R. M. (2019). Drought cuts back regeneration in logged tropical forests. *Environmental Research Letters*, *14*(4), 045012. https://doi.org/10.1088/1748-9326/ab0783

Rahman, M., Billah, M., Rahman, M. O., Datta, D., Ahsanuzzaman, M., & Islam, M. (2021). Disentangling the role of competition, light interception, and functional traits in tree growth rate variation in South Asian tropical moist forests. *Forest Ecology and Management*, *483*, 118908. https://doi.org/10.1016/j.foreco.2020.118908

Reich, P. B. (2014). The world-wide 'fast–slow' plant economics spectrum: A traits manifesto. *Journal of Ecology*, *102*(2), 275–301. https://doi.org/10.1111/1365-2745.12211

Restrepo-Coupe, N., O'Donnell Christoffersen, B., Longo, M., Alves, L. F., Campos, K. S., da Araujo, A. C., de Oliveira Jr, R. C., Prohaska, N., da Silva, R., Tapajos, R., Wiedemann, K. T., Wofsy, S. C., & Saleska, S. R. (2023). Asymmetric response of Amazon forest water and energy fluxes to wet and dry hydrological extremes reveals onset of a local drought-induced tipping point. *Global Change Biology*, *29*(21), 6077–6092. https://doi.org/10.1111/gcb.16933

Rifai, S. W., Girardin, C. A. J., Berenguer, E., del Aguila-Pasquel, J., Dahlsjö, C. A. L., Doughty, C. E., Jeffery, K. J., Moore, S., Oliveras, I., Riutta, T., Rowland, L. M., Murakami, A. A., Addo-Danso, S. D., Brando, P., Burton, C., Ondo, F. E., Duah-Gyamfi, A., Amézquita, F. F., Freitag, R., … Malhi, Y. (2018). ENSO Drives interannual variation of forest woody growth across the tropics. *Philosophical Transactions of the Royal Society B: Biological Sciences*, *373*(1760), 20170410. https://doi.org/10.1098/rstb.2017.0410

Riutta, T., Malhi, Y., Kho, L. K., Marthews, T. R., Huaraca Huasco, W., Khoo, M., Tan, S., Turner, E., Reynolds, G., Both, S., Burslem, D. F. R. P., Teh, Y. A., Vairappan, C. S., Majalap, N., & Ewers, R. M. (2018). Logging disturbance shifts net primary productivity and its allocation in Bornean tropical forests. *Global Change Biology*, *24*(7), 2913–2928. https://doi.org/10.1111/gcb.14068

Rowland, L., da Costa, A. C. L., Galbraith, D. R., Oliveira, R. S., Binks, O. J., Oliveira, A. A. R., Pullen, A. M., Doughty, C. E., Metcalfe, D. B., Vasconcelos, S. S., Ferreira, L. V., Malhi, Y., Grace, J., Mencuccini, M., & Meir, P. (2015). Death from drought in tropical forests is triggered by hydraulics not carbon starvation. *Nature*, *528*(7580), 119–122. https://doi.org/10.1038/nature15539

Roxburgh, S. H., Berry, S. L., Buckley, T. N., Barnes, B., & Roderick, M. L. (2005). What is NPP? Inconsistent accounting of respiratory fluxes in the definition of net primary production. *Functional Ecology*, *19*(3), 378–382. https://doi.org/10.1111/j.1365-2435.2005.00983.x

Sanchez-Martinez, P., Mencuccini, M., García-Valdés, R., Hammond, W. M., Serra-Diaz, J. M., Guo, W.-Y., Segovia, R. A., Dexter, K. G., Svenning, J.-C., Allen, C., & Martínez-Vilalta, J. (2023). Increased hydraulic risk in assemblages of woody plant species predicts spatial patterns of drought-induced mortality. *Nature Ecology & Evolution*. https://doi.org/10.1038/s41559-023-02180-z

Sandel, B., Gutiérrez, A. G., Reich, P. B., Schrodt, F., Dickie, J., & Kattge, J. (2015). Estimating the missing species bias in plant trait measurements. *Journal of Vegetation Science*, *26*(5), 828–838. https://doi.org/10.1111/jvs.12292

Saner, P., Loh, Y. Y., Ong, R. C., & Hector, A. (2012). Carbon stocks and fluxes in tropical lowland dipterocarp rainforests in Sabah, Malaysian Borneo. *PLoS ONE*, *7*(1), e29642. https://doi.org/10.1371/journal.pone.0029642

Saner, P., Philipson, C. D., Peters, S., Keller, F., Bigler, L., Turnbull, L. A., & Hector, A. (2016). Growth rates and relative change in non-structural carbohydrates of dipterocarp seedlings in response to light acclimation. *Plant Ecology & Diversity*, *9*(5–6), 491–504. https://doi.org/10.1080/17550874.2016.1227385

Santos, E. G., Svátek, M., Nunes, M. H., Aalto, J., Senior, R. A., Matula, R., Plichta, R., & Maeda, E. E. (2024). Structural changes caused by selective logging undermine the thermal buffering capacity of tropical forests. *Agricultural and Forest Meteorology*, *348*, 109912. https://doi.org/10.1016/j.agrformet.2024.109912

Sato, H., Mizoi, J., Shinozaki, K., & Yamaguchi-Shinozaki, K. (2024). Complex plant responses to drought and heat stress under climate change. *The Plant Journal*, tpj.16612. https://doi.org/10.1111/tpj.16612

Sheil, D., Eastaugh, C. S., Vlam, M., Zuidema, P. A., Groenendijk, P., van der Sleen, P., Jay, A., & Vanclay, J. (2017). Does biomass growth increase in the largest trees? Flaws, fallacies and alternative analyses. *Functional Ecology*, *31*(3), 568–581. https://doi.org/10.1111/1365-2435.12775

Sterck, F., Anten, N. P. R., Schieving, F., & Zuidema, P. A. (2016). Trait acclimation mitigates mortality risks of tropical canopy trees under global warming. *Frontiers in Plant Science*, *7*. https://doi.org/10.3389/fpls.2016.00607

Tuomela, K., Kuusipalo, J., Vesa, L., Nuryanto, K., Sagala, A. P. S., & Ådjers, G. (1996). Growth of dipterocarp seedlings in artificial gaps: An experiment in a logged-over rainforest in South Kalimantan, Indonesia. *Forest Ecology and Management*, *81*(1), 95–100. https://doi.org/10.1016/0378-1127(95)03655-5

Uriarte, M., Muscarella, R., & Zimmerman, J. K. (2018). Environmental heterogeneity and biotic interactions mediate climate impacts on tropical forest regeneration. *Global Change Biology*, *24*(2), e692–e704. https://doi.org/10.1111/gcb.14000

Veryard, R., Wu, J., O'Brien, M. J., Anthony, R., Both, S., Burslem, D. F. R. P., Chen, B., Fernandez-Miranda Cagigal, E., Godfray, H. C. J., Godoong, E., Liang, S., Saner, P., Schmid, B.,

Sau Wai, Y., Xie, J., Reynolds, G., & Hector, A. (2023). Positive effects of tree diversity on tropical forest restoration in a field-scale experiment. *Science Advances*, *9*(37), eadf0938. https://doi.org/10.1126/sciadv.adf0938

Vlam, M., Baker, P. J., Bunyavejchewin, S., & Zuidema, P. A. (2014). Temperature and rainfall strongly drive temporal growth variation in Asian tropical forest trees. *Oecologia*, *174*(4), 1449–1461. https://doi.org/10.1007/s00442-013-2846-x

Walsh, R. P. D. (1996). Drought frequency changes in Sabah and adjacent parts of northern Borneo since the late nineteenth century and possible implications for tropical rain forest dynamics. *Journal of Tropical Ecology*, *12*(3), 385-407. https://doi.org/10.1017/S0266467400009585

Walsh, R. P. D., Bidin, K., Blake, W. H., Chappell, N. A., Clarke, M. A., Douglas, I., Ghazali, R., Sayer, A. M., Suhaimi, J., Tych, W., & Annammala, K. V. (2011). Long-term responses of rainforest erosional systems at different spatial scales to selective logging and climatic change. *Philosophical Transactions of the Royal Society B: Biological Sciences*, *366*(1582), 3340–3353. https://doi.org/10.1098/rstb.2011.0054

Walsh, R. P. D., & Newbery, D. M. (1999). The ecoclimatology of Danum, Sabah, in the context of the World's rainforest regions, with particular reference to dry periods and their impact. *Philosophical Transactions: Biological Sciences*, *354*(1391), 1869–1883. https://doi.org/10.1098/rstb.1999.0528

Wang, X., Jiao, L., Xue, R., Zhang, P., Li, Q., & Yuan, X. (2025). Drought type determines the pattern of ecological response to drought in trees with different sensitivities. *Plant and Soil*, *513*(2), 3027–3039. https://doi.org/10.1007/s11104-025-07365-y

Wright, I. J., Reich, P. B., Westoby, M., Ackerly, D. D., Baruch, Z., Bongers, F., Cavender-Bares, J., Chapin, T., Cornelissen, J. H. C., Diemer, M., Flexas, J., Garnier, E., Groom, P. K., Gulias, J., Hikosaka, K., Lamont, B. B., Lee, T., Lee, W., Lusk, C., … Villar, R. (2004). The worldwide leaf economics spectrum. *Nature*, *428*(6985), 821–827. https://doi.org/10.1038/nature02403

Yeong, K. L., Reynolds, G., & Hill, J. K. (2016). Enrichment planting to improve habitat quality and conservation value of tropical rainforest fragments. *Biodiversity and Conservation*, *25*(5), 957–973. https://doi.org/10.1007/s10531-016-1100-3

Ziegler, C., Cochard, H., Stahl, C., Foltzer, L., Gérard, B., Goret, J.-Y., Heuret, P., Levionnois, S., Maillard, P., Bonal, D., & Coste, S. (2024). Residual water losses mediate the trade-off between growth and drought survival across saplings of 12 tropical rainforest tree species with contrasting hydraulic strategies. *Journal of Experimental Botany*, *75*(13), 4128–4147. https://doi.org/10.1093/jxb/erae159

5.11. Supplementary material

5.11.1. Species list with updated nomenclature and available trait data

Table S5.1, list of the seedling species planted at the old-growth (Danum Valley) and logged (Malua – Sabah Biodiversity Experiment) monitoring plots. The table includes the original species nomenclature and matching updates (see Ashton & Heckenhauer, 2022). † indicates functional trait data from old-growth forest at Danum and Maliau are available from Both, Burslem *et al.* (2019).

ORIGINAL NOMENCLATURE	UPDATED NOMENCLATURE
both old-growth and logged forest	**both old-growth and logged forest**
Dipterocarpus conformis Slooten	*Dipterocarpus conformis* Slooten
Dryobalanops lanceolata Burck†	*Dryobalanops lanceolata* Burck†
Hopea sangal Korth.†	*Hopea sangal* Korth.†
Parashorea malaanonan (Blanco) Merr.†	*Parashorea malaanonan* (Blanco) Merr.†
Parashorea tormentella (Symington) Meijer†	*Parashorea tormentella* (Symington) Meijer†
Shorea argentifolia Symington	*Rubroshorea argentifolia* (Symington) P.S.Ashton & J.Heck.
Shorea beccariana Burck†	*Rubroshorea beccariana* (Burck) P.S.Ashton & J.Heck.†
Shorea faguetiana F.Heim†	*Richetia faguetiana* (F.Heim) P.S.Ashton & J.Heck.†
Shorea gibbosa Brandis†	*Richetia gibbosa* (Brandis) P.S.Ashton & J.Heck.†
Shorea johorensis Foxw.†	*Rubroshorea johorensis* (Foxw.) P.S.Ashton & J.Heck.†
Shorea leprosula Miq.†	*Rubroshorea leprosula* (Miq.) P.S.Ashton & J.Heck.†
Shorea macrophylla de Vriese	*Rubroshorea macrophylla* (de Vriese) P.S.Ashton & J.Heck.
Shorea macroptera Dyer†	*Rubroshorea macroptera* (Dyer) P.S.Ashton & J.Heck.†
Shorea ovalis Korth.†	*Rubroshorea ovalis* (Korth.) P.S.Ashton & J.Heck.†
Shorea parvifolia Dyer†	*Rubroshorea parvifolia* (Dyer) P.S.Ashton & J.Heck.†
old-growth forest only	**old-growth forest only**
Dryobalanops beccarii Dyer	*Dryobalanops beccarii* Dyer
Durio graveolens Becc.†	*Durio graveolens* Becc.†
Shorea acuminatissima Symington	*Richetia acuminatissima* (Symington) P.S.Ashton & J.Heck.
Shorea guiso Blanco	*Shorea guiso* (Blanco) Blume
Shorea mecistopteryx Ridl.	*Rubroshorea mecistopteryx* (Ridl.) P.S.Ashton & J.Heck.
Shorea oleosa Meijer	*Rubroshorea fallax* (Meijer) P.S.Ashton & J.Heck.
Shorea parvistipulata F.Heim	*Rubroshorea parvistipulata* (F.Heim) P.S.Ashton & J.Heck.
Shorea pinanga Scheff.	*Rubroshorea pinanga* (Scheff.) P.S.Ashton & J.Heck.
Shorea smithiana Symington	*Rubroshorea smithiana* (Symington) P.S.Ashton & J.Heck.
Shorea superba Symington†	*Shorea superba* Symington†
logged forest only	**logged forest only**
Hopea ferruginea Parijs	*Hopea ferruginea* Parijs

5.11.2. Dealing with tree inventory data

Available data for the Danum Valley forest gaps and the Sabah Biodiversity Experiment consisted of seedling inventories undertaken at regular intervals. The old-growth forest plots at Danum were first surveyed in late 2004, revisited at approximately six-month intervals from 2004 to 2011 (with a gap between early 2007 and late 2009), and then surveyed annually from late 2014 onward (except for a three-year gap due to the COVID-19 pandemic). Not all plots were surveyed during every census due to logistical constraints, which means the number of census points for a given old-growth forest plot (and seedling) ranged from 13 to 23 surveys. The intensively monitored plots at Malua (logged forest) were fully surveyed 11 times between 2004 and 2023 (three complete censuses of the entire Sabah Biodiversity Experiment in 2004, 2012 and 2023; and eight additional surveys of the intensively monitored plots; Hector *et al*., 2011; Philipson *et al*., 2014). Plots 3, 5 and 8 had an additional census in 2006; and two planting lines from plots 3, 5, 8, 11 and 14 were surveyed an additional 14 times between 2014 and 2019 (O'Brien *et al*., 2019). Because seedlings planted in 2009-2010 to replace initial mortalities missed the first five censuses, the number of census points for an individual seedling in the logged forest at Malua ranged from 6 to 26 surveys.

Seedling inventories for the old-growth and logged forest plots were collated and merged into a single dataset, initially consisting of 52,612 records of 11,618 planted seedlings. To maintain adequate data quality, given that the dataset spans more than two decades and includes tens of thousands of data points, we carried out a preliminary data-cleaning process comprising of six steps:

1. If an individual seedling (identified via unique plant id number) had multiple species identifications (181 seedlings), we assumed the most recent ID was accurate, as older seedlings are easier to identify.

2. If the survey date was missing (107 records), we used the median survey date for that census and plot.

3. Once an individual was recorded as dead, we filled records of "dead" for subsequent censuses in which they were missing. This allowed us to fully backfill the dataset to 135,212 records.

4. If an individual seedling record was noted as dead but recorded as alive in later surveys, we assumed the most recent alive record was correct (1,284 records).

5. If an individual seedling was never recorded as alive (that is, they died in the period between planting and the first census; all of which occurred in the logged forest since diameter measurements were not taken at the time of planting), it was automatically excluded from the analysis because we lack date and diameter information to describe interval survival and productivity (68,771 records of 5,461 seedlings).

6. If an individual seedling record could not be assigned to any given cohort, it was excluded (33 records).

7. If an individual seedling showed annual growth rates of basal diameter (D_{base}) above 40 mm $year^{-1}$ and rates of negative D_{base} change below -30 mm $year^{-1}$ during a given census interval, we manually extracted and examined all of the seedling's datapoints. Obvious typos and misplaced decimal places were corrected, and the remaining anomalous values were removed (95 records of 45 seedlings).

The resulting dataset was thus comprised of 66,408 records from 6,158 seedlings (9,743 records from 500 seedlings in the old-growth forest, and 56,665 records from 5,658 seedlings in the logged forest). Because size of dead trees was not recorded, our dataset included 26,680 records of basal diameter (6,018 for the old-growth forest and 20,662 for the logged forest). It is also important to note that if seedlings were tall enough, stem diameter was also measured at 130 cm height (DBH, diameter at breast height). In some cases, especially in the most recent censuses of the old-growth forest plots at Danum, seedlings were measured at breast height but not at the base, meaning 319 records of D_{base} are missing for 188 seedlings.

5.11.3. Exploring the effects of liana cutting on NPP_{stem} and survival

Three of the intensively monitored plots within the logged forest site at Malua (plots 5, 11 and 14 of the Sabah Biodiversity Experiment) received a complete liana cutting treatment as part of an experimental study testing the effectiveness of liana removal in logged forest restoration (O'Brien *et al*., 2019). In these plots, all lianas ≥ 10 cm in height covering planted seedlings and surrounding trees were cut at the base in 2011 and again in 2014. To explore if liana cutting had a significant long-term effect on NPP_{stem} and survival, we ran preliminary mixed-effects models (using data from the logged forest only) investigating if NPP_{stem} and survival varied as a function of log-transformed diameter, census interval and liana cutting treatment, acknowledging an interaction between all three variables. For NPP_{stem}, we followed a hurdle analysis approach, first modelling the probability of seedlings attaining positive NPP_{stem} using a logistic regression (binomial) model, then modelling (log-transformed) positive NPP_{stem} values using a linear (gaussian) model. Both were fitted with the glmmTMB package (version 1.1.13; McGillycuddy *et al*., 2025) and included random effects for seedling identity (gaussian model only), species, plot, and cohort to account for non-independence. We modelled interval survival using a bias-reduced logistic regression model using the logistf package (version 1.26.0, Heinze & Schemper, 2002), which prevented us from incorporating random effects but allowed for model convergence despite data separation (full survival across certain intervals). We did not include interval length as a predictor because model contrasts were performed within intervals of equal length.

$$\text{(S5.1)} \quad \text{glmmTMB}(\Pr(\text{NPP}_{\text{stem}}) \sim \log_{10}(\text{D}_{\text{base}}) * \text{interval} * \text{treatment} + (1|\text{species}) + (1|\text{plot}) + (1|\text{cohort}),\ \text{family} = \text{binomial})$$

$$\text{(S5.2)} \quad \text{glmmTMB}(\log_{10}(\text{NPP}_{\text{stem}}) \sim \log_{10}(\text{D}_{\text{base}}) * \text{interval} * \text{treatment} + (1|\text{seedling}) + (1|\text{species}) + (1|\text{plot}) + (1|\text{cohort}),\ \text{family} = \text{gaussian})$$

$$\text{(S5.3)} \quad \text{logistf}(\text{survival} \sim \log_{10}(\text{D}_{\text{base}}) * \text{interval} * \text{treatment})$$

For each of the three models, we then extracted the marginal means corresponding to each census interval in both the cut and uncut treatments using the emmeans package (version 1.10.0, Lenth, 2024). We also extracted marginal slopes (with respect to diameter) for each census interval at each treatment to explore if liana cutting altered productivity and survival across size classes. We then performed contrasts of marginal means and marginal slopes at each census interval, comparing cut and uncut treatments. Contrasts revealed no consistent long-term effect of liana cutting on NPP_{stem} and survival (**Figure S5.1** to **Figure S5.3**), warranting further research into growth dynamics but discouraging us from including liana cutting as a predictor in our models.

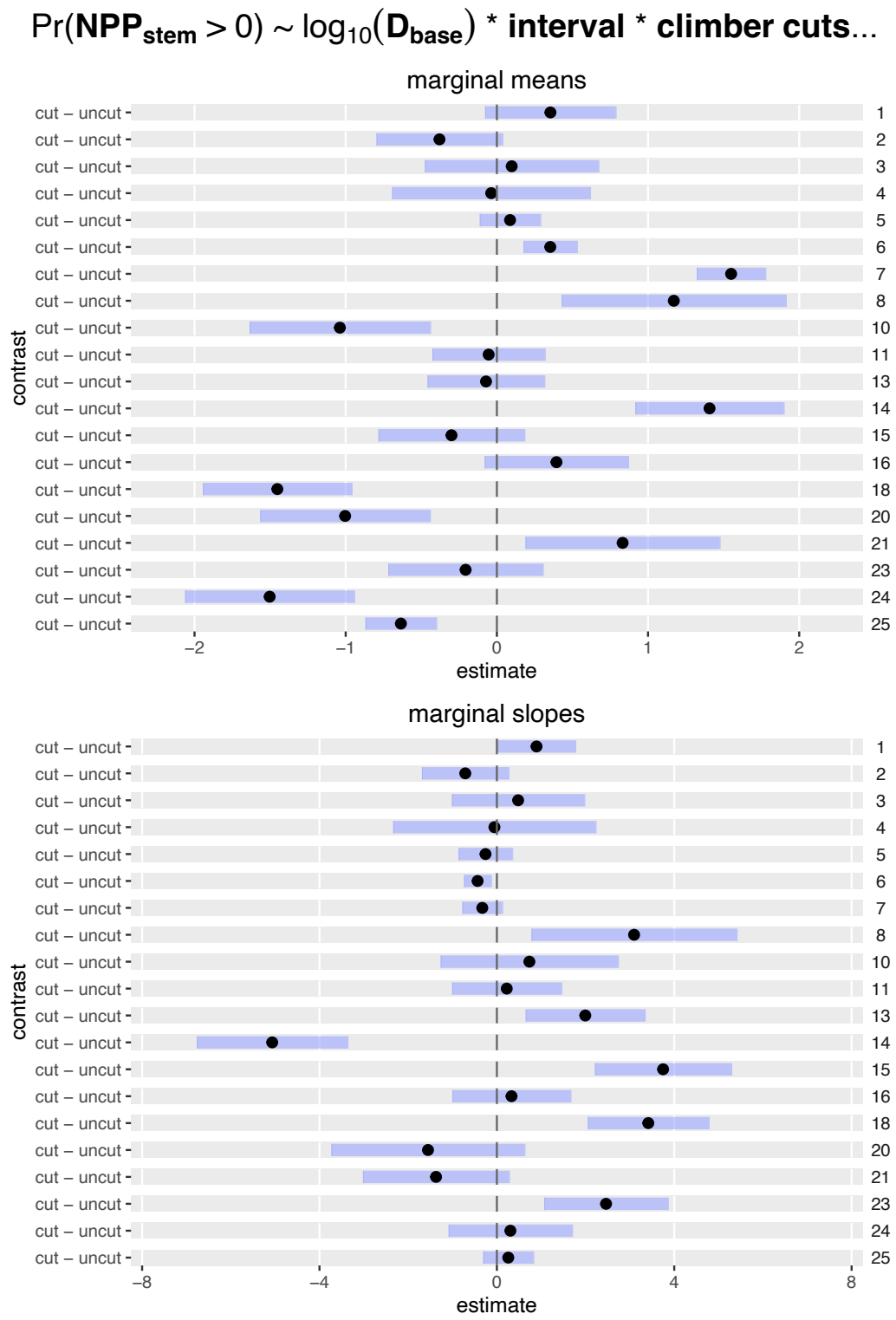


Figure S5.1, contrasts between marginal means and marginal slopes for each census interval reveal there is no consistent, long-term effect of liana cutting on $Pr(NPP_{stem} > 0)$ within the logged forest monitoring plots at Malua. Contrasts represent the difference between marginal means and marginal slopes for the liana-cut compared to the uncut plots (± standard error), still in the logit-transformed scale. Marginal means represent the model-predicted values of $Pr(NPP_{stem} > 0)$ evaluated at $\log_{10}(D_{base}) = 0$ for each treatment at each census interval. Marginal slopes represent the model-predicted effect of $\log_{10}(D_{base})$ on $Pr(NPP_{stem} > 0)$ for each treatment at each census interval. Liana cutting treatments were implemented in 2011 (intervals 5 to 7) and 2014 (interval 9 to 11). Please note intervals of less than 3 months were excluded from the analyses.

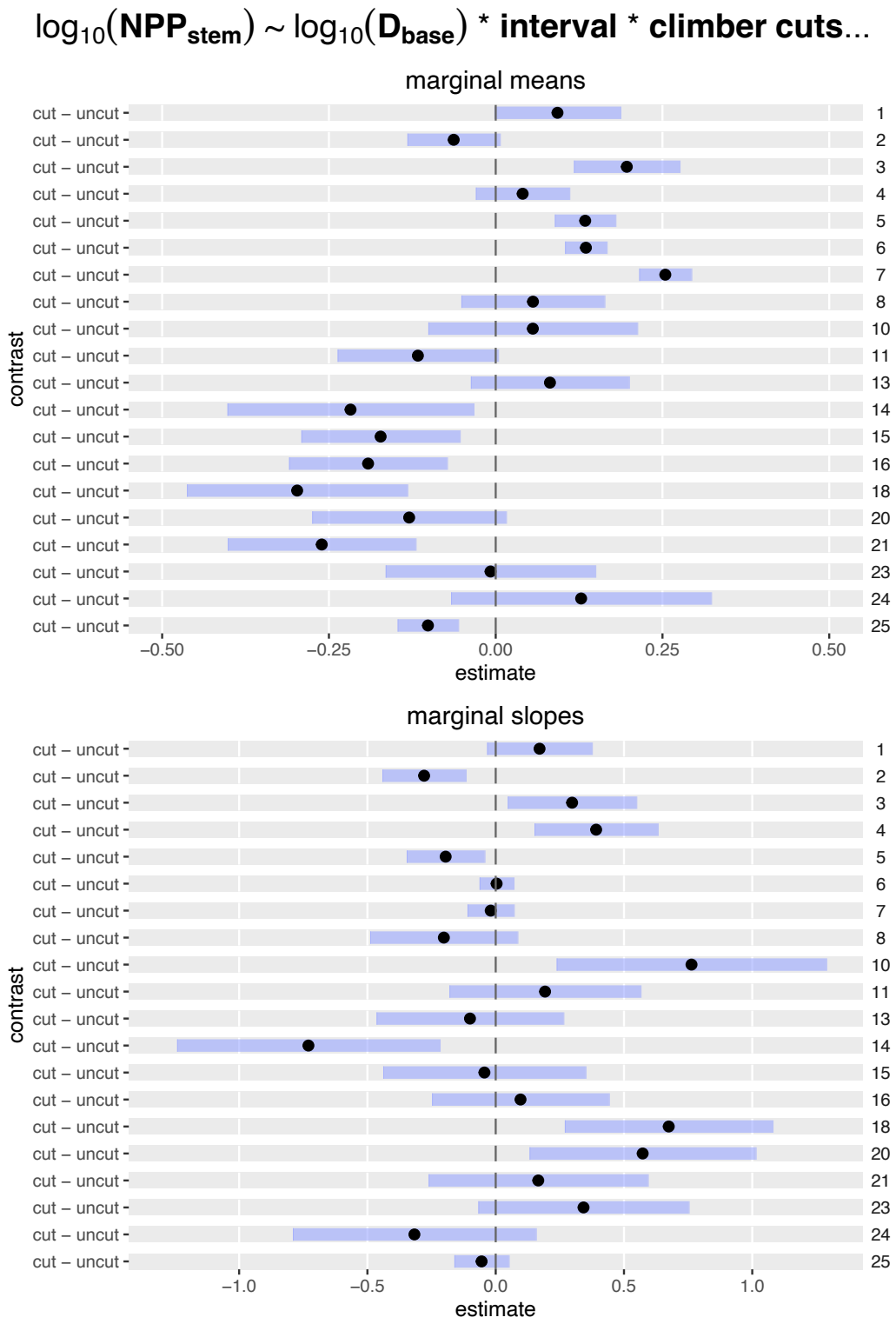


Figure S5.2, contrasts between marginal means and marginal slopes for each census interval reveal there is no consistent, long-term effect of liana cutting on $\log_{10}(NPP_{stem})$ within the logged forest monitoring plots at Malua. Contrasts represent the difference between marginal means and marginal slopes for the liana-cut compared to the uncut plots (± standard error), still in the log-transformed scale. Marginal means represent the model-predicted values of $\log_{10}(NPP_{stem})$ evaluated at $\log_{10}(D_{base}) = 0$ for each treatment at each census interval. Marginal slopes represent the model-predicted effect of $\log_{10}(D_{base})$ on $\log_{10}(NPP_{stem})$ for each treatment at each census interval. Liana cutting treatments were implemented in 2011 (intervals 5 to 7) and 2014 (interval 9 to 11). Please note intervals of less than 3 months were excluded from the analyses.

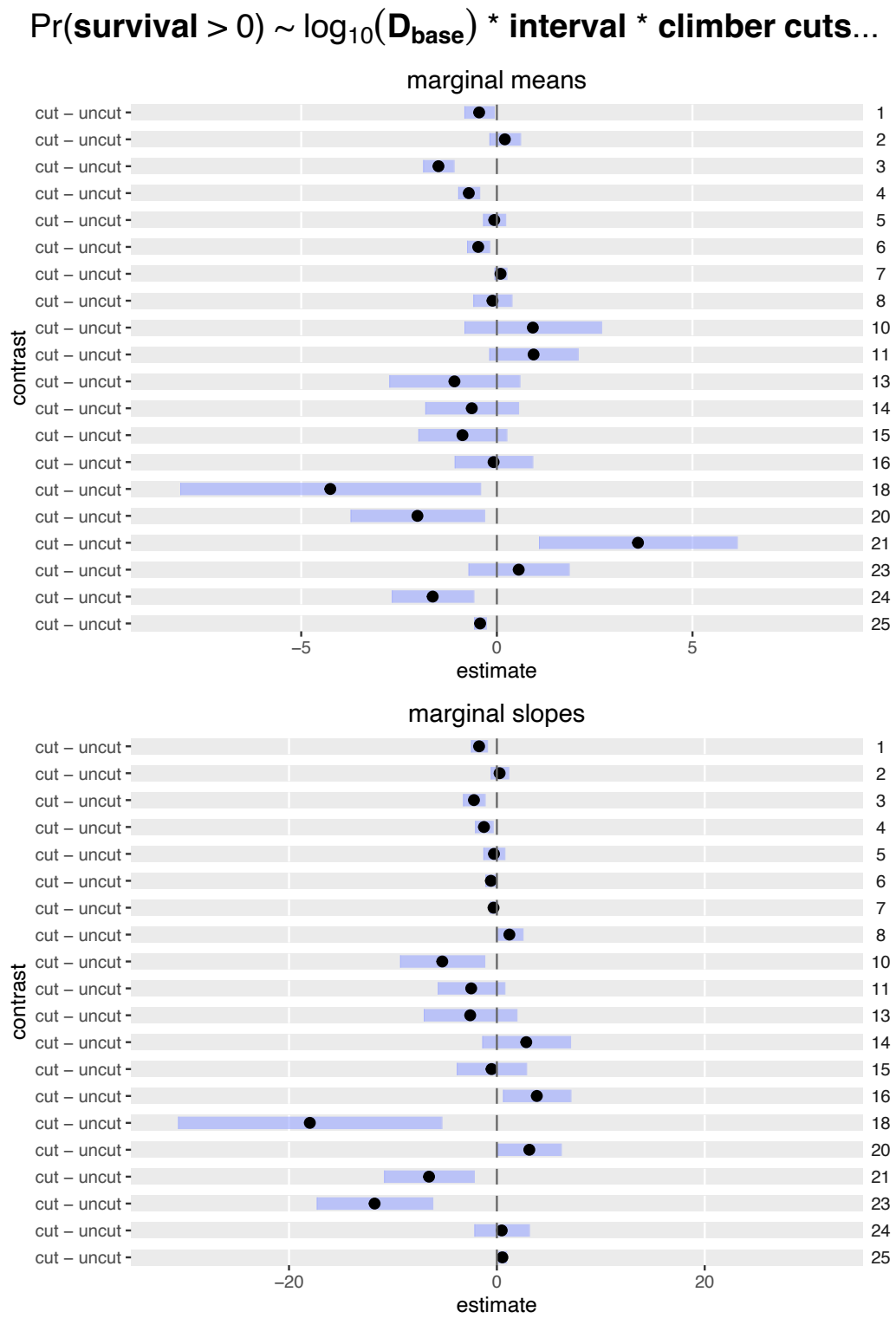


Figure S5.3, contrasts between marginal means and marginal slopes for each census interval reveal there is no consistent, long-term effect of liana cutting on Pr(survival > 0) within the logged forest monitoring plots at Malua. Contrasts represent the difference between marginal means and marginal slopes for the liana-cut compared to the uncut plots (± standard error), still in the logit-transformed scale. Marginal means represent the model-predicted values of Pr(survival > 0) evaluated at $\log_{10}(D_{base}) = 0$ for each treatment at each census interval. Marginal slopes represent the model-predicted effect of $\log_{10}(D_{base})$ on Pr(survival > 0) for each treatment at each census interval. Liana cutting treatments were implemented in 2011 (intervals 5 to 7) and 2014 (interval 9 to 11). Please note intervals of less than 3 months were excluded from the analyses.

5.11.4. Exploring trends in climate data

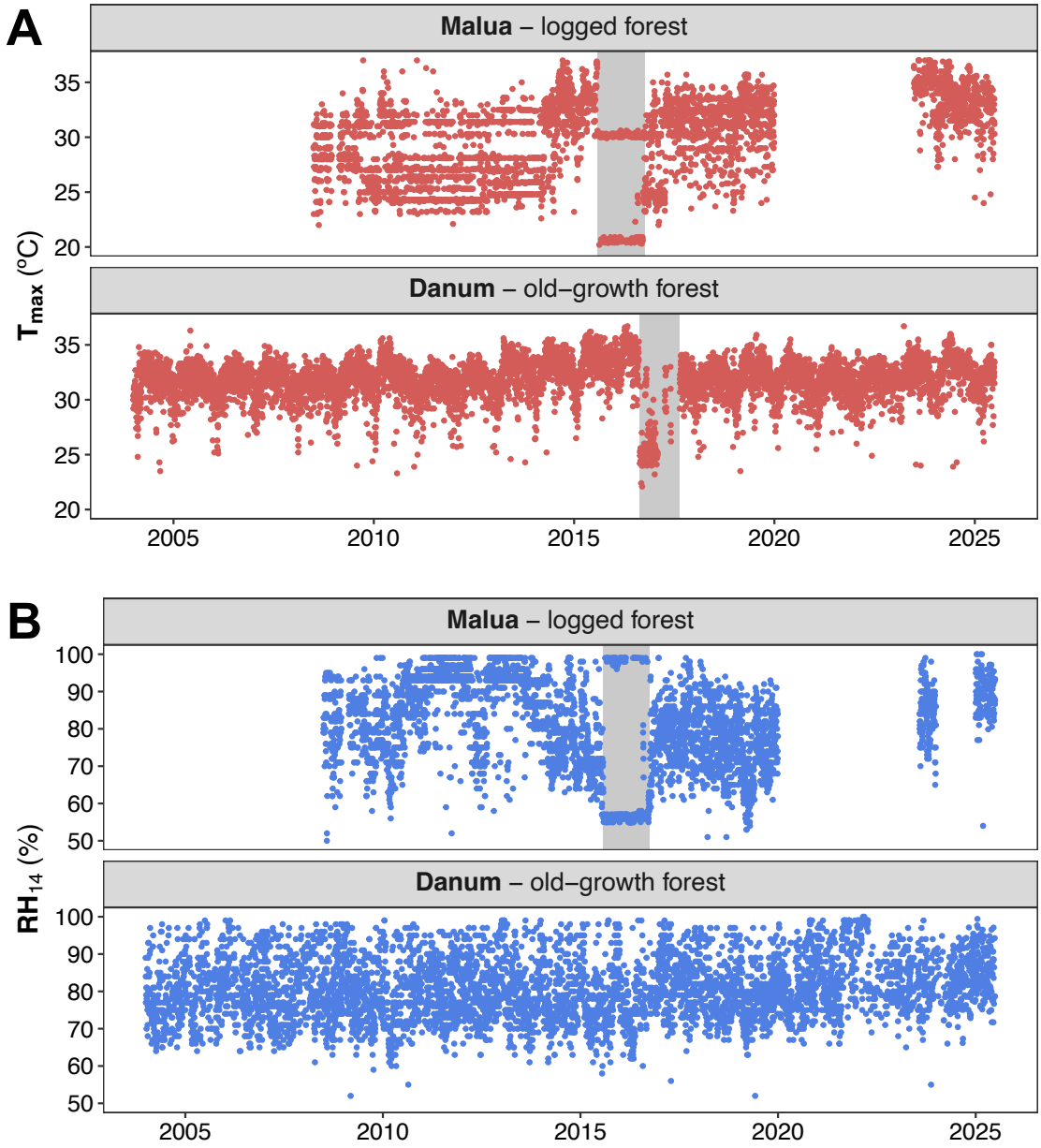


Figure S5.4, variation in daily climate variables at the old-growth (Danum) and logged (Malua) forest sites. **A**) $T_{max,}$ maximum daily temperature (ºC); **B**) RH_{14} relative humidity at 14:00 (%). Intervals shaded in grey represent unusual periods where the distribution of the data could not be readily explained by natural variation (T_{max} collected at the old-growth forest from August 2016 to August 2017, and measurements of T_{max} and RH_{14} collected at the logged forest from August 2015 to October 2016). These records were excluded from the analysis to maintain consistent quality in climate data.

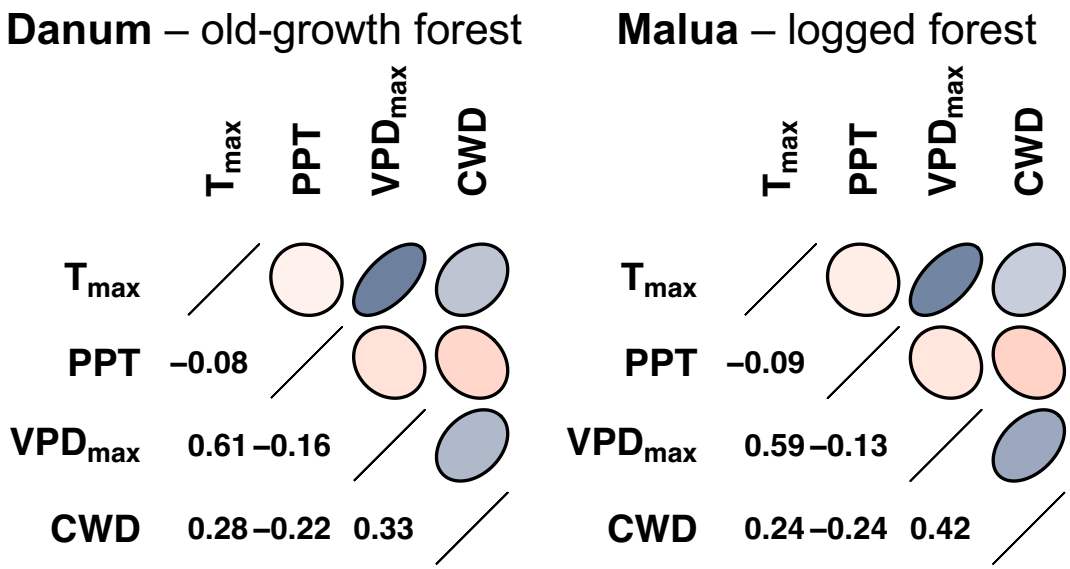


Figure S5.5, matrices of pairwise correlations between daily climate variables at the old-growth (Danum) and logged (Malua) forest sites. $T_{max,}$ maximum daily temperature (ºC); PPT, daily rainfall (mm); VPD_{max}, maximum daily vapour pressure deficit (hPa); CWD, daily cumulative water deficit (mm). Correlation matrices were computed from all available datapoints that have been collected at each forest type. Correlation coefficients are displayed on the left-hand side, with those in bold indicating statistically significant values (all coefficients are bold in this case). Ellipses on the right-hand side visually represent the direction and strength of the correlation (blue and red respectively indicate positive and negative coefficients).

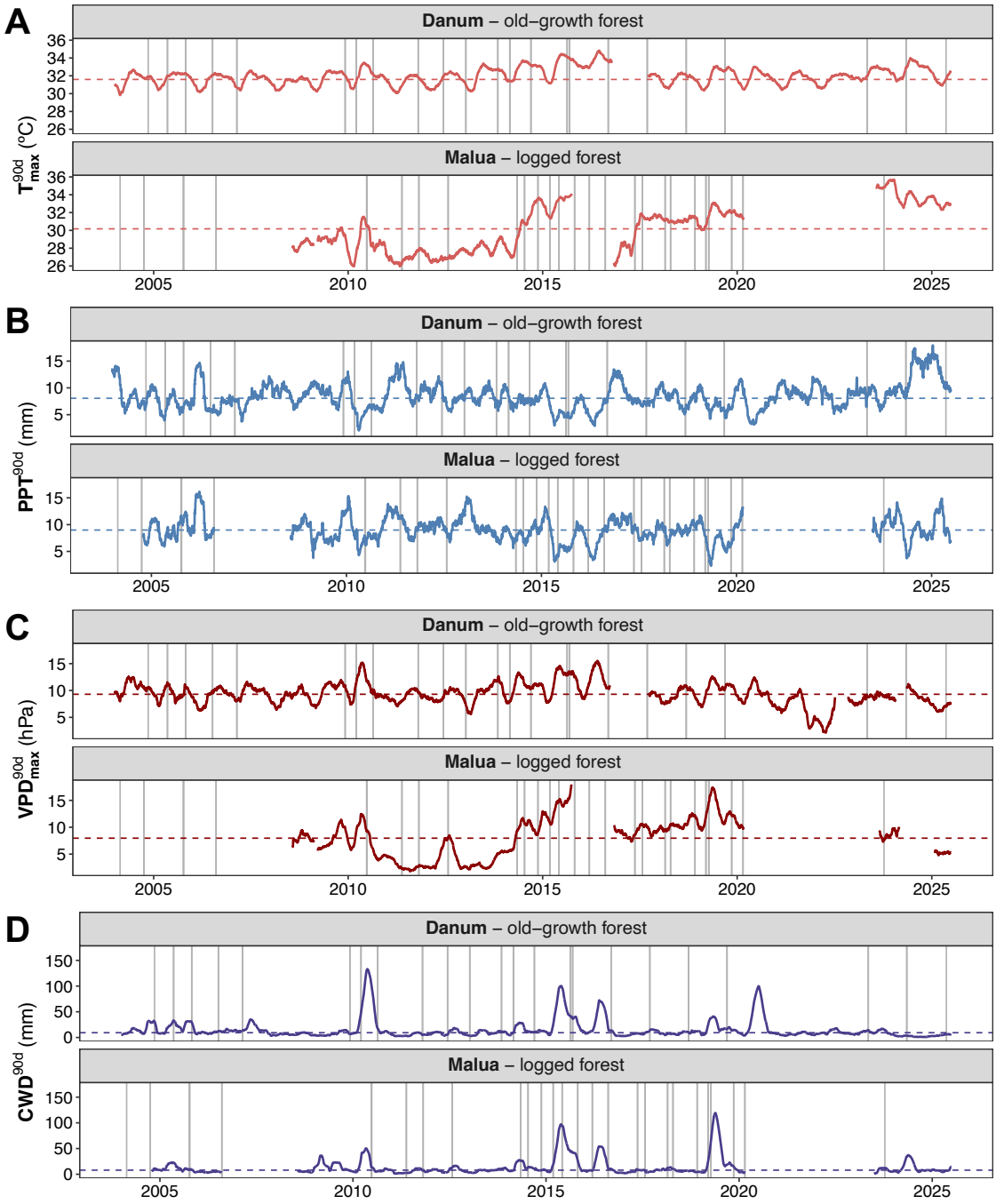


Figure S5.6, long-term microclimate dynamics at the Danum old-growth and Malua logged forest sites (top and bottom facet of each panel respectively). The graphs represent the time series of 90-day rolling averages of maximum daily temperature (T^{90d}_{max} – ºC, in light red, panel **A**), daily precipitation (PPT^{90d} – mm, in light blue, panel **B**), maximum daily vapour pressure deficit (VPD^{90d}_{max} – hPa, in dark red, panel **C**), and daily cumulative water deficit (CWD^{90d} – mm, in dark blue, panel **D**). Dashed horizontal lines denote site-specific long-term means of daily values for the corresponding variables (colour-matched) computed from all available datapoints. Vertical grey lines indicate seedling census dates, and are specific to each forest site. Gaps reflect missing rolling average data. In the old-growth forest, the most extreme interval in terms of $maxT^{90d}_{max}$ (34.4°C) and $maxVPD^{90d}_{max}$ (15.5 hPa) overlapped with the 2015-2016 El Niño, and most extreme $minPPT^{90d}$ (2.0 mm) and $maxCWD^{90d}$ (133.1 mm) occurred in 2010. In the logged forest, the most extreme $maxT^{90d}_{max}$ (33.6 °C) was observed in 2015, and the most extreme interval in terms of $minPPT^{90d}$(2.3 mm), $maxVPD^{90d}_{max}$ (17.4 hPa) and $maxCWD^{90d}$ (119.3 mm) occurred in 2019.

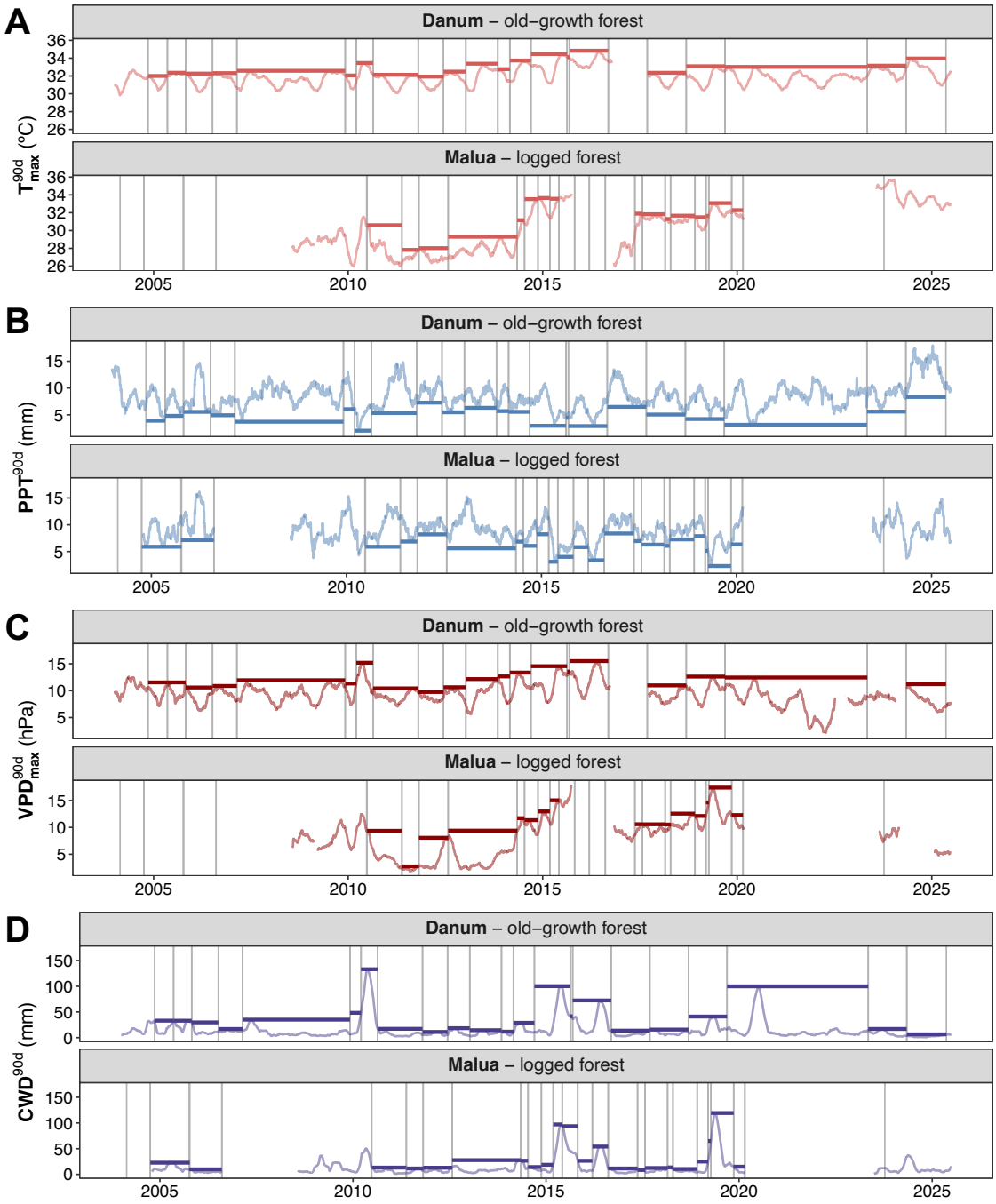


Figure S5.7, to investigate the effect of extreme climate on seedling productivity and survival, we calculated extremes of heat and drought for every census interval. **A**) maximum values of 90-day averages of maximum daily temperature ($maxT^{90d}_{max}$ – ºC, in light red). **B**) minimum values of 90-day averages of daily precipitation ($minPPT^{90d}$ – mm, in light blue). **C**) maximum values of 90-day averages of maximum daily vapour pressure deficit ($maxVPD^{90d}_{max}$ – hPa, in dark red). **D**) maximum values of 90-day averages of daily cumulative water deficit ($maxCWD^{90d}$ – mm, in dark blue). Vertical grey lines indicate seedling census dates, and are specific to each forest site. Climate extreme values for each census interval are represented by the thick horizontal lines. Timeseries of the climate running averages are also shown. Please note climate extremes were calculated independently for each seedling, that is, allowing for individual variation in census dates (median census dates are shown here for the sake of simplicity).

5.11.5. Models examining NPP_{stem} and survival across forest types

Table S5.2, summary statistics for the mixed-effects model testing if the probability of seedlings presenting non-zero stem NPP ('$Pr(NPP_{stem} > 0)$') varies as a result of log-transformed basal diameter ('$\log_{10}(D_{base})$') at both old-growth and logged forest types. The model includes an interaction term between $\log_{10}(D_{base})$ and forest type. Cohort and plot (specific to each forest type) were used as random effects to account for spatially-explicit groupings within the data. Interval and species (also specific to each forest type) were also used as random effects to account for non-independence. Please note model coefficients are expressed in the logit scale.

Formula:
$Pr(NPP_{stem} > 0) \sim \log_{10}(D_{base}) + forest\_type + forest\_type{:}\log_{10}(D_{base}) + (1|forest\_type{:}interval) + (1|forest\_type{:}cohort) + (1|forest\_type{:}plot) + (1|forest\_type{:}species)$

Family: binomial (logit link)

Fixed effects	**Estimate**	**Std. Error**	**z-value**	**Pr(>|z|)**
(Intercept)	**0.7256**	**0.3412**	**2.13**	**0.0335**
$\log_{10}(D_{base})$	**0.4567**	**0.1724**	**2.65**	**0.0081**
forest_type_logged	-0.6937	0.4437	-1.46	0.1179
$\log_{10}(D_{base})$:forest_type_logged	**0.4074**	**0.2023**	**2.01**	**0.0441**

Random effects	**Variance**	**Groups**
forest_type:interval	1.01824	41
forest_type:cohort	0.00978	3
forest_type:plot	0.02713	26
forest_type:species	0.05517	41
residual	-	15672

Table S5.3, summary statistics for the mixed-effects model testing if the log-transformed stem NPP of growing seedlings ('$\log_{10}(NPP_{stem})$') varies as a result of log-transformed basal diameter ('$\log_{10}(D_{base})$') at both old-growth and logged forest types. The model includes an interaction term between $\log_{10}(D_{base})$ and forest type. Cohort and plot (specific to each forest type) were used as random effects to account for spatially-explicit groupings within the data. Seedling identity was used to account for repeated measures. Interval and species (also specific to each forest type) were also used as random effects to account for non-independence. Please note model coefficients are expressed in the log-transformed scale.

Formula:
$\log_{10}(NPP_{stem}) \sim \log_{10}(D_{base}) + forest\_type + forest\_type{:}\log_{10}(D_{base}) + (1|forest\_type{:}interval) + (1|forest\_type{:}cohort) + (1|forest\_type{:}plot) + (1|forest\_type{:}species) + (1|seedling)$

Family: gaussian (identity link)

Fixed effects	**Estimate**	**Std. Error**	**z-value**	**Pr(>|z|)**
(Intercept)	**-4.4146**	**0.1178**	**-37.46**	**0.0000**
$\log_{10}(D_{base})$	**2.2930**	**0.0495**	**46.35**	**0.0000**
forest_type_logged	**-0.4834**	**0.1491**	**-3.24**	**0.0012**
$\log_{10}(D_{base})$:forest_type_logged	**0.3786**	**0.0527**	**7.19**	**0.0000**

Random effects	**Variance**	**Groups**
forest_type:interval	0.06266	41
forest_type:cohort	0.00565	3
forest_type:plot	0.00784	26
forest_type:species	0.00751	41
seedling	0.02622	3553
residual	0.22861	12276

Table S5.4, summary statistics for the mixed-effects model testing if the probability of seedling interval survival ('Pr(survival > 0)') varies as a result of log-transformed basal diameter ('$\log_{10}(D_{base})$') and log-transformed interval length ('$\log_{10}$(interval length)') at both old-growth and logged forest types. The model includes interaction terms between $\log_{10}(D_{base})$ and forest type and between $\log_{10}$(interval length) and forest type. Cohort and plot (specific to each forest type) were used as random effects to account for spatially-explicit groupings within the data. Interval and species (also specific to each forest type) were also used as random effects to account for non-independence. Please note model coefficients are expressed in the logit scale.

Formula:
Pr(survival > 0) ~ $\log_{10}(D_{base})$ + $\log_{10}$(interval_length) + forest_type + forest_type:$\log_{10}(D_{base})$ + forest_type:$\log_{10}$(interval_length) + (1|forest_type:interval) + (1|forest_type:cohort) + (1|forest_type:plot) + (1|forest_type:species)

Family: binomial (logit link)

Fixed effects	**Estimate**	**Std. Error**	**z-value**	**Pr(>|z|)**
(Intercept)	**6.3920**	**1.3772**	**4.64**	**0.0000**
$\log_{10}(D_{base})$	**1.9648**	**0.3078**	**6.38**	**0.0000**
$\log_{10}$(interval_length)	**-2.3355**	**0.5409**	**-4.32**	**0.0000**
forest_type_logged	0.7101	1.6130	0.44	0.6598
$\log_{10}(D_{base})$:forest_type_logged	**-0.8181**	**0.3284**	**-2.49**	**0.0127**
$\log_{10}$(interval_length):forest_type_logged	-0.1229	0.6174	0.20	0.8422

Random effects	**Variance**	**Groups**
forest_type:interval	0.32859	41
forest_type:cohort	0.04516	3
forest_type:plot	0.27330	26
forest_type:species	0.19851	41
residual	-	18399

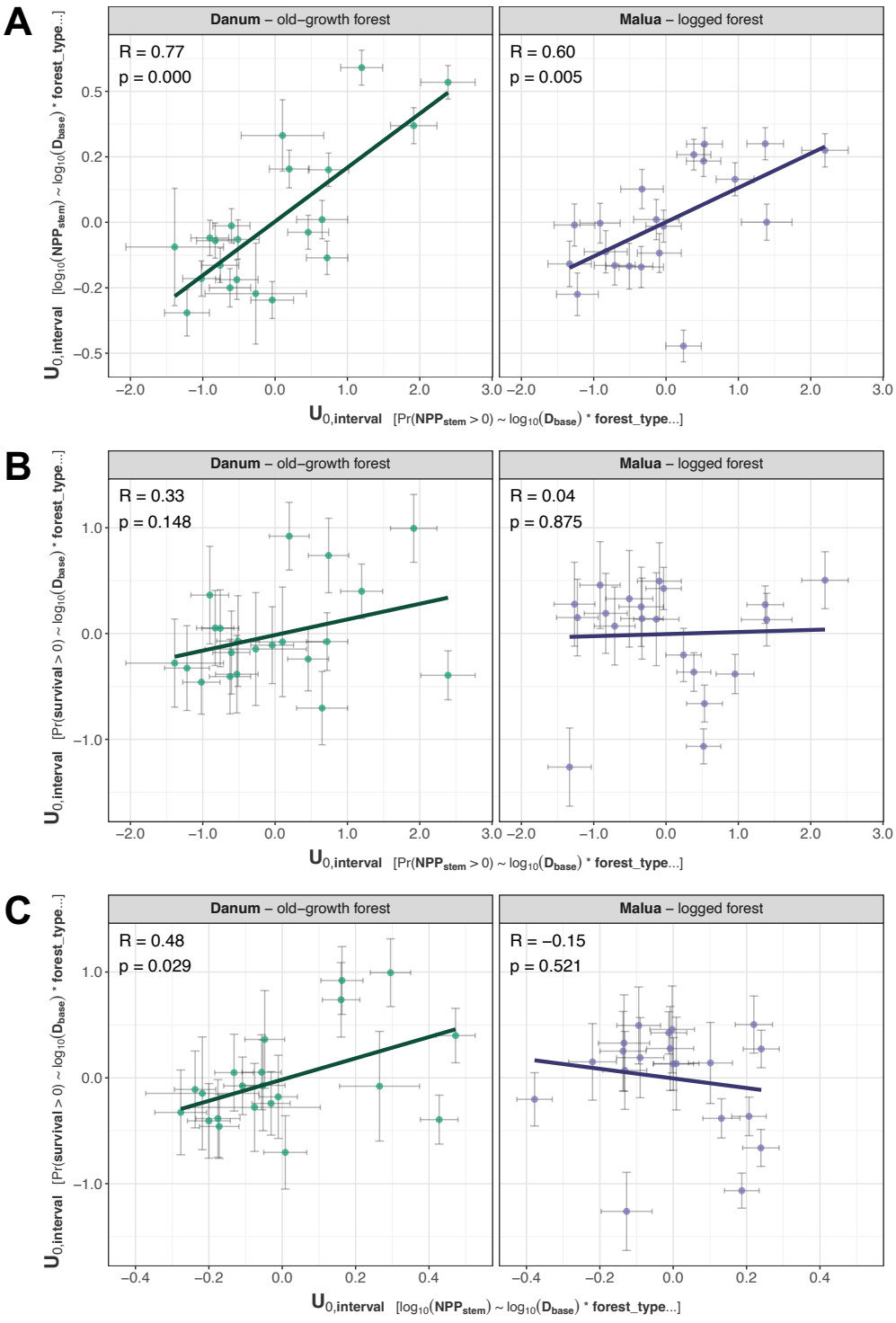


Figure S5.8, relationships among interval-level random-effect estimates from models testing whether productivity and survival vary as functions of $\log_{10}(D_{base})$ and forest type (**Table S5.2** to **Table S5.4**). Panels (faceted by forest type) show correlations between model-derived interval random effects for: **A**) $Pr(NPP_{stem} > 0)$ and $\log_{10}(NPP_{stem})$; **B**) $Pr(NPP_{stem} > 0)$ and $Pr(survival > 0)$; and **C**) $\log_{10}(NPP_{stem})$ and $Pr(survival > 0)$. Please note interval random effects remain in the transformed scales and are accompanied by error bars in the direction of both axes indicating ± standard error of estimates. Strong correlations in plot **A**) indicate that intervals with higher probability of seedlings having positive NPP_{stem} corresponded to intervals when the NPP_{stem} of growing seedlings was highest. Plot **C**) reveals intervals with higher rates of survival also corresponded to intervals when the NPP_{stem} of growing seedlings was highest, but only in the old-growth forest type.

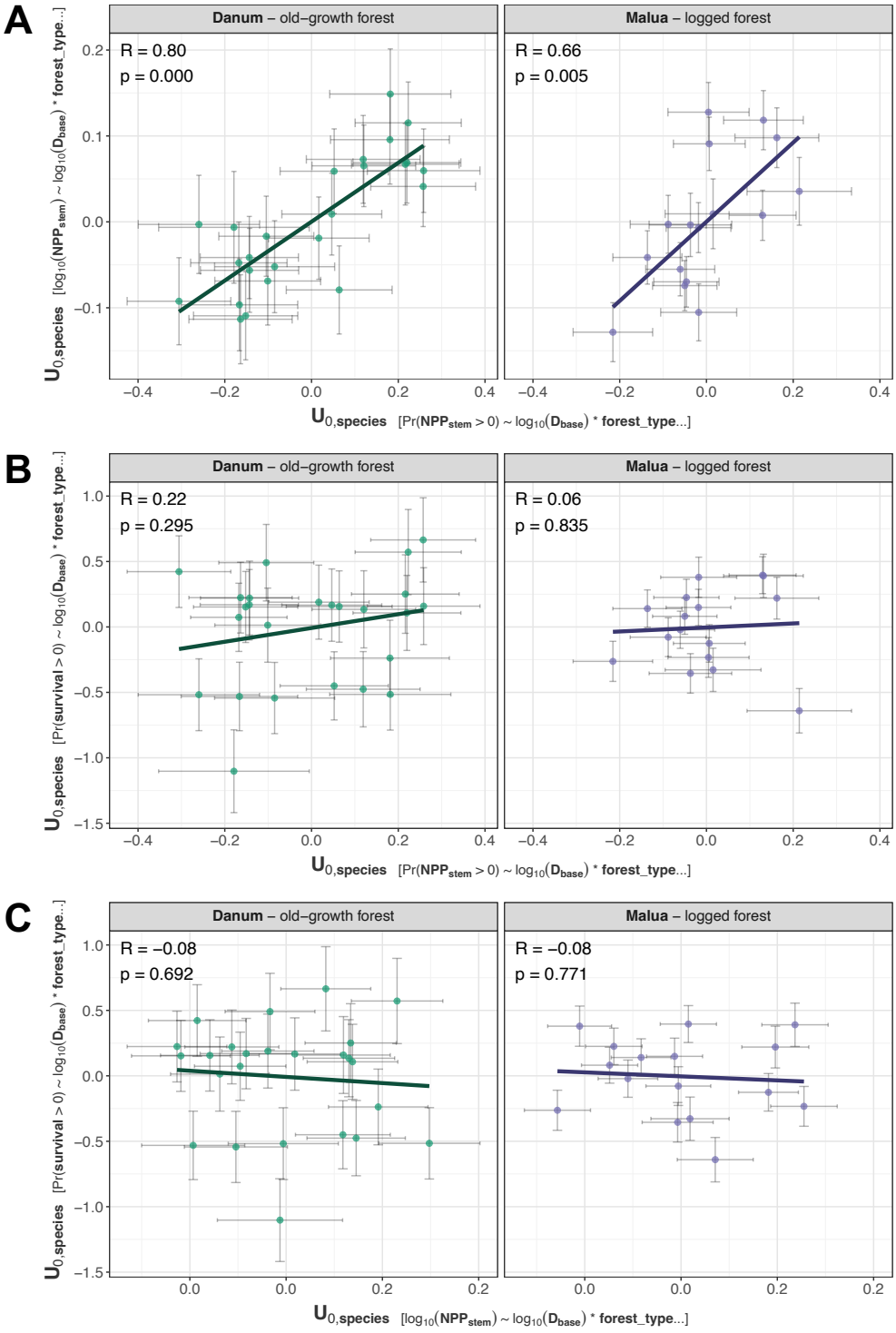


Figure S5.9, relationships among species-level random-effect estimates from models testing whether productivity and survival vary as functions of $\log_{10}(D_{base})$ and forest type (**Table S5.2** to **Table S5.4**). Panels (faceted by forest type) show correlations between model-derived species random effects for: **A**) $Pr(NPP_{stem} > 0)$ and $\log_{10}(NPP_{stem})$; **B**) $Pr(NPP_{stem} > 0)$ and Pr(survival > 0); and **C**) $\log_{10}(NPP_{stem})$ and Pr(survival > 0). Please note species random effects remain in the transformed scales and are accompanied by error bars in the direction of both axes indicating ± standard error of estimates. Strong correlations in plot **A** indicate that species with higher probability of seedlings having positive NPP_{stem} corresponded to species where growing seedlings had higher NPP_{stem} across both forest types. Survival rates at the species level remain unrelated to both the probability of attaining positive NPP_{stem} and to the degree of NPP_{stem} for growing seedlings (plots **B** and **C**).

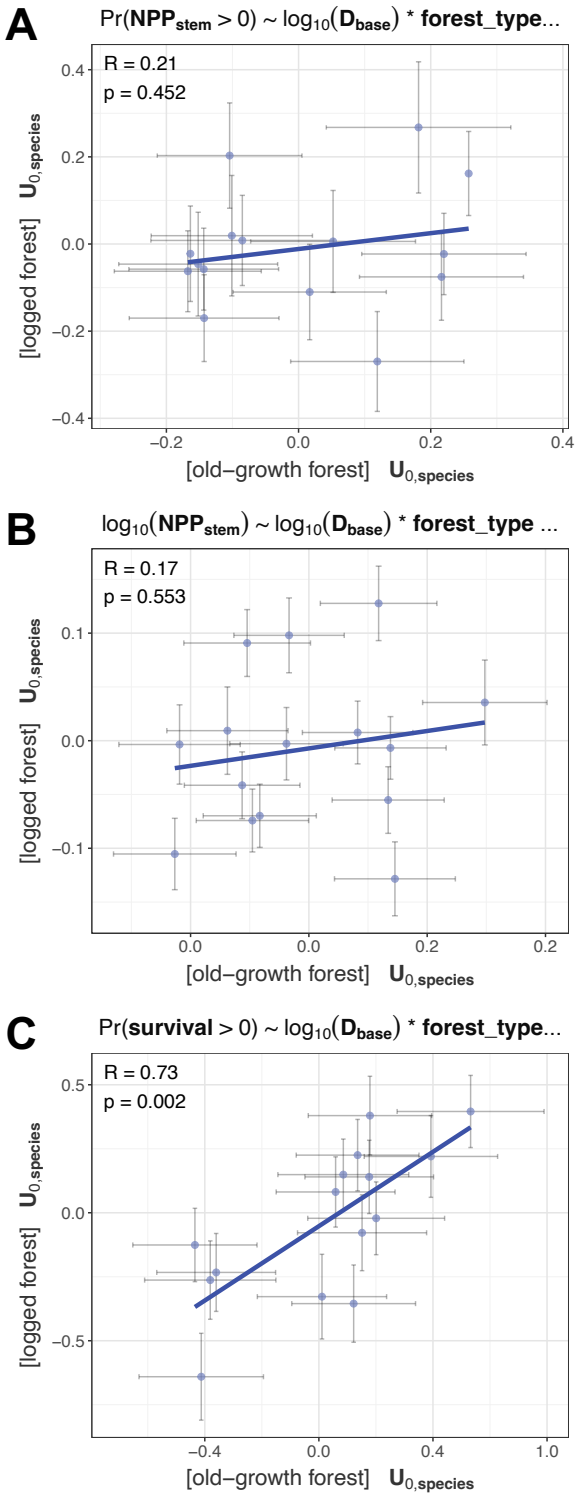


Figure S5.10, comparison of species-level random-effect estimates for old-growth vs logged forest (derived from models testing whether productivity and survival vary as functions of $\log_{10}(D_{base})$ and forest type, **Table S5.2** to **Table S5.4**). Plots show correlations between model-derived species random effects for old-growth forest (x-axis) vs logged forest (y-axis): **A**) $Pr(NPP_{stem} > 0)$; **B**) $\log_{10}(NPP_{stem})$ and **C**) Pr(survival > 0). Please note species random effects remain in the transformed scales and are accompanied by error bars in the direction of both axes indicating ± standard error of estimates. The plots reveal species with higher survival rates were consistent across forest types.

5.11.6. Models investigating the effect of climate on $Pr(NPP_{stem} > 0)$

Table S5.5, summary statistics for the mixed-effects model testing if the probability of seedlings presenting non-zero stem NPP ('$Pr(NPP_{stem} > 0)$') **within the old-growth forest at Danum** varies as a result of log-transformed basal diameter ('$\log_{10}(D_{base})$') interacted with the maximum 90-day running average of daily maximum temperature experienced by each seedling in each census interval (**$maxT^{90d}_{max}$** – ºC). Plot, census interval and species were used as random effects to account for non-independence from temporally- and spatially-explicit groupings within the data. We could not include random effect slopes for species in terms of $maxT^{90d}_{max}$ due to issues with model convergence. Please note coefficients are expressed in the logit scale.

Formula: $Pr(NPP_{stem} > 0) \sim \log_{10}(D_{base}) + maxT^{90d}_{max} + \log_{10}(D_{base}):maxT^{90d}_{max} + (1|interval) + (1|plot) + (1|species)$

Family: binomial (logit link)

Fixed effects	Estimate	Std. Error	z-value	Pr(>|z|)
(Intercept)	1.6404	12.7125	0.13	0.8973
$\log_{10}(D_{base})$	1.5762	6.0888	0.26	0.7957
$maxT^{90d}_{max}$	-0.0266	0.3875	-0.07	0.9453
$\log_{10}(D_{base}):maxT^{90d}_{max}$	-0.0343	0.1856	-0.18	0.8534

Random effects	Variance	Groups
interval	1.15480	20
plot	0.01052	20
species	0.10750	25
residual	-	4825

Table S5.6, summary statistics for the mixed-effects model testing if the probability of seedlings presenting non-zero stem NPP ('$Pr(NPP_{stem} > 0)$') **within the logged forest at Malua** varies as a result of log-transformed basal diameter ('$\log_{10}(D_{base})$') interacted with the maximum 90-day running average of daily maximum temperature experienced by each seedling in each census interval (**$maxT^{90d}_{max}$** – ºC). Plot, cohort, census interval and species were used as random effects to account for non-independence from temporally- and spatially-explicit groupings within the data. We could not include random effect slopes for species in terms of $maxT^{90d}_{max}$ due to issues with model convergence. Please note coefficients are expressed in the logit scale.

Formula: $Pr(NPP_{stem} > 0) \sim \log_{10}(D_{base}) + maxT^{90d}_{max} + \log_{10}(D_{base}):maxT^{90d}_{max} + (1|interval) + (1|cohort) + (1|plot) + (1|species)$

Family: binomial (logit link)

Fixed effects	Estimate	Std. Error	z-value	Pr(>|z|)
(Intercept)	**10.2605**	**3.2493**	**3.16**	**0.0016**
$\log_{10}(D_{base})$	0.4572	1.7333	0.26	0.7919
$maxT^{90d}_{max}$	**-0.3390**	**0.1072**	**-3.16**	**0.0016**
$\log_{10}(D_{base}):maxT^{90d}_{max}$	0.0142	0.0584	0.24	0.8084

Random effects	Variance	Groups
interval	0.23898	11
cohort	0.00326	2
plot	0.10907	6
species	0.04759	16
residual	-	5641

Table S5.7, summary statistics for the mixed-effects model testing if the probability of seedlings presenting non-zero stem NPP ('$Pr(NPP_{stem} > 0)$') **within the old-growth forest at Danum** varies as a result of log-transformed basal diameter ('$\log_{10}(D_{base})$') interacted with the minimum 90-day running average of daily precipitation experienced by each seedling in each census interval (**$\mathbf{minPPT^{90d}}$** – mm). Plot, census interval and species were used as random effects to account for non-independence from temporally- and spatially-explicit groupings within the data. We also included random effect slopes for species in terms of $minPPT^{90d}$. Please note coefficients are expressed in the logit scale.

Formula: $Pr(NPP_{stem} > 0) \sim \log_{10}(D_{base}) + minPPT^{90d} + \log_{10}(D_{base}):minPPT^{90d} + (1|interval) + (1|plot) + (1+ minPPT^{90d}|species)$

Family: binomial (logit link)

Fixed effects	**Estimate**	**Std. Error**	**z-value**	**Pr(>|z|)**
(Intercept)	**2.1806**	**0.9074**	**2.40**	**0.0163**
$\log_{10}(D_{base})$	-0.1524	0.5387	-0.28	0.7772
$minPPT^{90d}$	-0.2706	0.1672	-1.62	0.1057
$\log_{10}(D_{base}):minPPT^{90d}$	0.1053	0.0991	1.06	0.2883

Random effects	**Variance**	**Groups**
interval	1.08589	21
plot	0.01545	20
species	0.17839	25
$species:minPPT^{90d}$	0.00085	25
residual	-	4982

Table S5.8, summary statistics for the mixed-effects model testing if the probability of seedlings presenting non-zero stem NPP ('$Pr(NPP_{stem} > 0)$') **within the logged forest at Malua** varies as a result of log-transformed basal diameter ('$\log_{10}(D_{base})$') interacted with the minimum 90-day running average of daily precipitation experienced by each seedling in each census interval (**$\mathbf{minPPT^{90d}}$**– mm). Plot, cohort, census interval and species were used as random effects to account for non-independence from temporally- and spatially-explicit groupings within the data. We could not include random effect slopes for species in terms of $minPPT^{90d}$ due to issues with model convergence. Please note coefficients are expressed in the logit scale.

Formula: $Pr(NPP_{stem} > 0) \sim \log_{10}(D_{base}) + minPPT^{90d} + \log_{10}(D_{base}):minPPT^{90d} + (1|interval) + (1|cohort) + (1|plot) + (1|species)$

Family: binomial (logit link)

Fixed effects	**Estimate**	**Std. Error**	**z-value**	**Pr(>|z|)**
(Intercept)	**4.0162**	**0.9300**	**4.32**	**0.0000**
$\log_{10}(D_{base})$	-0.1765	0.4933	-0.36	0.7205
$minPPT^{90d}$	**-0.6614**	**0.1350**	**-4.90**	**0.0000**
$\log_{10}(D_{base}):minPPT^{90d}$	**0.1566**	**0.0721**	**2.17**	**0.0299**

Random effects	**Variance**	**Groups**
interval	1.60594	17
cohort	0.01574	2
plot	0.08276	6
species	0.02827	16
residual	-	7895

Table S5.9, summary statistics for the mixed-effects model testing if the probability of seedlings presenting non-zero stem NPP ('$Pr(NPP_{stem} > 0)$') **within the old-growth forest at Danum** varies as a result of log-transformed basal diameter ('$\log_{10}(D_{base})$') interacted with the maximum 90-day running average of daily maximum vapour pressure deficit experienced by each seedling in each census interval (**$\mathbf{maxVPD_{max}^{90d}}$** – hPa). Plot, census interval and species were used as random effects to account for non-independence from temporally- and spatially-explicit groupings within the data. We could not include random effect slopes for species in terms of $maxVPD_{max}^{90d}$ due to issues with model convergence. Please note coefficients are expressed in the logit scale.

Formula: $Pr(NPP_{stem} > 0) \sim \log_{10}(D_{base}) + maxVPD_{max}^{90d} + \log_{10}(D_{base}):maxVPD_{max}^{90d} + (1|interval) + (1|plot) + (1|species)$

Family: binomial (logit link)

Fixed effects	**Estimate**	**Std. Error**	**z-value**	**Pr(>|z|)**
(Intercept)	0.2077	1.9010	0.11	0.9130
$\log_{10}(D_{base})$	1.7665	0.9959	1.77	0.0761
$maxVPD_{max}^{90d}$	0.0447	0.1559	0.29	0.7741
$\log_{10}(D_{base}):maxVPD_{max}^{90d}$	-0.1063	0.0806	-1.32	0.1871

Random effects	**Variance**	**Groups**
interval	1.20834	19
plot	0.00979	20
species	0.10479	25
residual	-	4820

Table S5.10, summary statistics for the mixed-effects model testing if the probability of seedlings presenting non-zero stem NPP ('$Pr(NPP_{stem} > 0)$') **within the logged forest at Malua** varies as a result of log-transformed basal diameter ('$\log_{10}(D_{base})$') interacted with the maximum 90-day running average of daily maximum vapour pressure deficit experienced by each seedling in each census interval (**$\mathbf{maxVPD_{max}^{90d}}$** – hPa). Plot, cohort, census interval and species were used as random effects to account for non-independence from temporally- and spatially-explicit groupings within the data. We could not include random effect slopes for species in terms of $maxVPD_{max}^{90d}$ due to issues with model convergence. Please note coefficients are expressed in the logit scale.

Formula: $Pr(NPP_{stem} > 0) \sim \log_{10}(D_{base}) + maxVPD_{max}^{90d} + \log_{10}(D_{base}):maxVPD_{max}^{90d} + (1|interval) + (1|cohort) + (1|plot) + (1|species)$

Family: binomial (logit link)

Fixed effects	**Estimate**	**Std. Error**	**z-value**	**Pr(>|z|)**
(Intercept)	**-2.9250**	**0.6363**	**-4.60**	**0.0000**
$\log_{10}(D_{base})$	**0.8738**	**0.2384**	**3.66**	**0.0002**
$maxVPD_{max}^{90d}$	**0.2528**	**0.0388**	**6.52**	**0.0000**
$\log_{10}(D_{base}):maxVPD_{max}^{90d}$	-0.0024	0.0263	-0.09	0.9266

Random effects	**Variance**	**Groups**
interval	2.46724	11
cohort	0.00404	2
plot	0.09424	6
species	0.04622	16
residual	-	5641

Table S5.11, summary statistics for the mixed-effects model testing if the probability of seedlings presenting non-zero stem NPP ('$Pr(NPP_{stem} > 0)$') **within the old-growth forest at Danum** varies as a result of log-transformed basal diameter ('$\log_{10}(D_{base})$') interacted with the maximum 90-day running average of daily cumulative water deficit experienced by each seedling in each census interval (**$\mathbf{maxCWD^{90d}}$** – mm). Plot, census interval and species were used as random effects to account for non-independence from temporally- and spatially-explicit groupings within the data. We also included random effect slopes for species in terms of $maxCWD^{90d}$. Please note coefficients are expressed in the logit scale.

Formula: $Pr(NPP_{stem} > 0) \sim \log_{10}(D_{base}) + maxCWD^{90d} + \log_{10}(D_{base}):maxCWD^{90d} + (1|interval) + (1|plot) + (1+ maxCWD^{90d}|species)$

Family: binomial (logit link)

Fixed effects	**Estimate**	**Std. Error**	**z-value**	**Pr(>|z|)**
(Intercept)	**1.0474**	**0.4750**	**2.20**	**0.0275**
$\log_{10}(D_{base})$	0.3416	0.2421	1.41	0.1583
$maxCWD^{90d}$	-0.0058	0.0089	-0.66	0.5098
$\log_{10}(D_{base}):maxCWD^{90d}$	0.0009	0.0043	0.20	0.8389

Random effects	**Variance**	**Groups**
interval	1.06346	21
plot	0.01523	20
species	0.16577	25
$species:maxCWD^{90d}$	0.00001	25
residual	-	4982

Table S5.12, summary statistics for the mixed-effects model testing if the probability of seedlings presenting non-zero stem NPP ('$Pr(NPP_{stem} > 0)$') **within the logged forest at Malua** varies as a result of log-transformed basal diameter ('$\log_{10}(D_{base})$') interacted with the maximum 90-day running average of daily cumulative water deficit experienced by each seedling in each census interval (**$\mathbf{maxCWD^{90d}}$**– mm). Plot, cohort, census interval and species were used as random effects to account for non-independence from temporally- and spatially-explicit groupings within the data. We also included random effect slopes for species in terms of $maxCWD^{90d}$. Please note coefficients are expressed in the logit scale.

Formula: $Pr(NPP_{stem} > 0) \sim \log_{10}(D_{base}) + maxCWD^{90d} + \log_{10}(D_{base}):maxCWD^{90d} + (1|interval) + (1|cohort) + (1|plot) + (1+ maxCWD^{90d}|species)$

Family: binomial (logit link)

Fixed effects	**Estimate**	**Std. Error**	**z-value**	**Pr(>|z|)**
(Intercept)	**-2.3465**	**1.0665**	**-2.20**	**0.0278**
$\log_{10}(D_{base})$	**1.0026**	**0.1520**	**6.59**	**0.0000**
$maxCWD^{90d}$	**0.0761**	**0.0292**	**2.61**	**0.0092**
$\log_{10}(D_{base}):maxCWD^{90d}$	-0.0055	0.0045	-1.21	0.2256

Random effects	**Variance**	**Groups**
interval	6.08830	17
cohort	0.01525	2
plot	0.08097	6
species	0.04095	16
$species:maxCWD^{90d}$	0.00001	16
residual	-	7895

5.11.7. Models investigating the effect of climate on $log_{10}(NPP_{stem})$

Table S5.13, summary statistics for the mixed-effects model testing if the log-transformed stem NPP of growing seedlings ('$log_{10}(NPP_{stem})$') **within the old-growth forest at Danum** varies as a result of log-transformed basal diameter ('$log_{10}(D_{base})$') interacted with the maximum 90-day running average of daily maximum temperature experienced by each seedling in each census interval ($\mathbf{maxT_{max}^{90d}}$ – ºC). Seedling ID, plot, census interval and species were used as random effects to account for non-independence from repeated measures, as well as temporally- and spatially-explicit groupings within the data. We also included random effect slopes for species in terms of $maxT_{max}^{90d}$. Please note coefficients are expressed in the log-transformed scale.

Formula: $log_{10}(NPP_{stem}) \sim log_{10}(D_{base}) + maxT_{max}^{90d} + log_{10}(D_{base}):maxT_{max}^{90d} + (1|interval) + (1|plot) + (1 + maxT_{max}^{90d} | species) + (1|seedling)$

Family: gaussian (identity link)

Fixed effects	Estimate	Std. Error	z-value	Pr(>|z|)
(Intercept)	**8.8703**	**3.6684**	**2.42**	**0.0156**
$log_{10}(D_{base})$	-1.3720	1.4574	-0.94	0.3465
$maxT_{max}^{90d}$	**-0.4087**	**0.1120**	**-3.65**	**0.0003**
$log_{10}(D_{base}):maxT_{max}^{90d}$	**0.1152**	**0.0445**	**2.59**	**0.0097**

Random effects	Variance	Groups
interval	0.09616	20
plot	0.00975	20
species	4.01432	25
species:$maxT_{max}^{90d}$	0.00354	25
seedling	0.01477	473
residual	0.20814	3804

Table S5.14, summary statistics for the mixed-effects model testing if the log-transformed stem NPP of growing seedlings ('$log_{10}(NPP_{stem})$') **within the logged forest at Malua** varies as a result of log-transformed basal diameter ('$log_{10}(D_{base})$') interacted with the maximum 90-day running average of daily maximum temperature experienced by each seedling in each census interval ($\mathbf{maxT_{max}^{90d}}$ – ºC). Seedling ID, plot, cohort, census interval and species were used as random effects to account for non-independence from repeated measures, as well as temporally- and spatially-explicit groupings within the data. We also included random effect slopes for species in terms of $maxT_{max}^{90d}$. Please note coefficients are expressed in the log-transformed scale.

Formula: $log_{10}(NPP_{stem}) \sim log_{10}(D_{base}) + maxT_{max}^{90d} + log_{10}(D_{base}):maxT_{max}^{90d} + (1|interval) + (1|cohort) + (1|plot) + (1 + maxT_{max}^{90d}| species) + (1|seedling)$

Family: gaussian (identity link)

Fixed effects	Estimate	Std. Error	z-value	Pr(>|z|)
(Intercept)	**-2.5712**	**0.7720**	**-3.33**	**0.0009**
$log_{10}(D_{base})$	**2.2082**	**0.4609**	**4.79**	**0.0000**
$maxT_{max}^{90d}$	**-0.0724**	**0.0262**	**-2.76**	**0.0058**
$log_{10}(D_{base}):maxT_{max}^{90d}$	0.0123	0.0160	0.77	0.4425

Random effects	Variance	Groups
interval	0.00764	11
cohort	0.00348	2
plot	0.00677	6
species	0.20947	16
species:$maxT_{max}^{90d}$	0.00023	16
seedling	0.04007	2234
residual	0.20069	4257

Table S5.15, summary statistics for the mixed-effects model testing if the log-transformed stem NPP of growing seedlings ('$\log_{10}(NPP_{stem})$') **within the old-growth forest at Danum** varies as a result of log-transformed basal diameter ('$\log_{10}(D_{base})$') interacted with the minimum 90-day running average of daily precipitation experienced by each seedling in each census interval (**$\mathbf{minPPT^{90d}}$** – mm). Seedling ID, plot, census interval and species were used as random effects to account for non-independence from repeated measures, as well as temporally- and spatially-explicit groupings within the data. We also included random effect slopes for species in terms of $minPPT^{90d}$. Please note coefficients are expressed in the log-transformed scale.

Formula: $\log_{10}(NPP_{stem}) \sim \log_{10}(D_{base}) + minPPT^{90d} + \log_{10}(D_{base}):minPPT^{90d} + (1|interval) + (1|plot) + (1 + minPPT^{90d}|species) + (1|seedling)$

Family: gaussian (identity link)

Fixed effects	**Estimate**	**Std. Error**	**z-value**	**Pr(>|z|)**
(Intercept)	**-5.7153**	**0.2153**	**-26.54**	**0.0000**
$\log_{10}(D_{base})$	**2.5882**	**0.1278**	**20.25**	**0.0000**
$minPPT^{90d}$	**0.2483**	**0.0361**	**6.88**	**0.0000**
$\log_{10}(D_{base}):minPPT^{90d}$	**-0.0515**	**0.0237**	**-2.17**	**0.0300**

Random effects	**Variance**	**Groups**
interval	0.13671	21
plot	0.01158	20
species	0.00426	25
$species:minPPT^{90d}$	0.00003	25
seedling	0.01920	473
residual	0.20595	3912

Table S5.16, summary statistics for the mixed-effects model testing if the log-transformed stem NPP of growing seedlings ('$\log_{10}(NPP_{stem})$') **within the logged forest at Malua** varies as a result of log-transformed basal diameter ('$\log_{10}(D_{base})$') interacted with the minimum 90-day running average of daily precipitation experienced by each seedling in each census interval (**$\mathbf{minPPT^{90d}}$**– mm). Seedling ID, plot, cohort, census interval and species were used as random effects to account for non-independence from repeated measures, as well as temporally- and spatially-explicit groupings within the data. We could not include random effect slopes for species in terms of $minPPT^{90d}$ due to issues with model convergence. Please note coefficients are expressed in the log-transformed scale.

Formula: $\log_{10}(NPP_{stem}) \sim \log_{10}(D_{base}) + minPPT^{90d} + \log_{10}(D_{base}):minPPT^{90d} + (1|interval) + (1|cohort) + (1|plot) + (1|species) + (1|seedling)$

Family: gaussian (identity link)

Fixed effects	**Estimate**	**Std. Error**	**z-value**	**Pr(>|z|)**
(Intercept)	**-5.1146**	**0.1989**	**-25.72**	**0.0000**
$\log_{10}(D_{base})$	**2.8239**	**0.1240**	**22.78**	**0.0000**
$minPPT^{90d}$	0.0446	0.0274	1.63	0.1035
$\log_{10}(D_{base}):minPPT^{90d}$	-0.0329	0.0176	-1.88	0.0607

Random effects	**Variance**	**Groups**
interval	0.02549	17
cohort	0.00483	2
plot	0.00499	6
species	0.00593	16
seedling	0.03296	2800
residual	0.21961	6099

Table S5.17, summary statistics for the mixed-effects model testing if the log-transformed stem NPP of growing seedlings ('$\log_{10}(NPP_{stem})$') **within the old-growth forest at Danum** varies as a result of log-transformed basal diameter ('$\log_{10}(D_{base})$') interacted with the maximum 90-day running average of daily maximum vapour pressure deficit experienced by each seedling in each census interval (**$\mathbf{maxVPD_{max}^{90d}}$** – hPa). Seedling ID, plot, census interval and species were used as random effects to account for non-independence from repeated measures, as well as temporally- and spatially-explicit groupings within the data. We also included random effect slopes for species in terms of $maxVPD_{max}^{90d}$. Please note coefficients are expressed in the log-transformed scale.

Formula: $\log_{10}(NPP_{stem}) \sim \log_{10}(D_{base}) + maxVPD_{max}^{90d} + \log_{10}(D_{base}):maxVPD_{max}^{90d} + (1|interval) + (1|plot) + (1 + maxVPD_{max}^{90d}|species) + (1|seedling)$

Family: gaussian (identity link)

Fixed effects	**Estimate**	**Std. Error**	**z-value**	**Pr(>|z|)**
(Intercept)	**-1.9471**	**0.4755**	**-4.09**	**0.0000**
$\log_{10}(D_{base})$	**1.8709**	**0.2595**	**7.21**	**0.0000**
$maxVPD_{max}^{90d}$	**-0.2153**	**0.0394**	**-5.46**	**0.0000**
$\log_{10}(D_{base}):maxVPD_{max}^{90d}$	**0.0447**	**0.0212**	**2.11**	**0.0351**

Random effects	**Variance**	**Groups**
interval	0.09329	19
plot	0.00986	20
species	0.12713	25
$species:maxVPD_{max}^{90d}$	0.00059	25
seedling	0.01485	473
residual	0.20713	3801

Table S5.18, summary statistics for the mixed-effects model testing if the log-transformed stem NPP of growing seedlings ('$\log_{10}(NPP_{stem})$') **within the logged forest at Malua** varies as a result of log-transformed basal diameter ('$\log_{10}(D_{base})$') interacted with the maximum 90-day running average of daily maximum vapour pressure deficit experienced by each seedling in each census interval (**$\mathbf{maxVPD_{max}^{90d}}$** – hPa). Seedling ID, plot, cohort, census interval and species were used as random effects to account for non-independence from repeated measures, as well as temporally- and spatially-explicit groupings within the data. We also included random effect slopes for species in terms of $maxVPD_{max}^{90d}$. Please note coefficients are expressed in the log-transformed scale.

Formula: $\log_{10}(NPP_{stem}) \sim \log_{10}(D_{base}) + maxVPD_{max}^{90d} + \log_{10}(D_{base}):maxVPD_{max}^{90d} + (1|interval) + (1|cohort) + (1|plot) + (1 + maxVPD_{max}^{90d}|species) + (1|seedling)$

Family: gaussian (identity link)

Fixed effects	**Estimate**	**Std. Error**	**z-value**	**Pr(>|z|)**
(Intercept)	**-4.9312**	**0.1202**	**-41.04**	**0.0000**
$\log_{10}(D_{base})$	**2.5410**	**0.0504**	**50.44**	**0.0000**
$maxVPD_{max}^{90d}$	0.0126	0.0091	1.39	0.1658
$\log_{10}(D_{base}):maxVPD_{max}^{90d}$	0.0023	0.0064	0.36	0.7222

Random effects	**Variance**	**Groups**
interval	0.03667	11
cohort	0.00394	2
plot	0.00679	6
species	0.00391	16
$species:maxVPD_{max}^{90d}$	0.00001	16
seedling	0.04040	2234
residual	0.20023	4257

Table S5.19, summary statistics for the mixed-effects model testing if the log-transformed stem NPP of growing seedlings ('$\log_{10}(NPP_{stem})$') **within the old-growth forest at Danum** varies as a result of log-transformed basal diameter ('$\log_{10}(D_{base})$') interacted with the maximum 90-day running average of daily cumulative water deficit experienced by each seedling in each census interval (**$maxCWD^{90d}$** – mm). Seedling ID, plot, census interval and species were used as random effects to account for non-independence from repeated measures, as well as temporally- and spatially-explicit groupings within the data. We could not include random effect slopes for species in terms of $maxCWD^{90d}$ due to issues with model convergence. Please note coefficients are expressed in the log-transformed scale.

Formula: $\log_{10}(NPP_{stem}) \sim \log_{10}(D_{base}) + maxCWD^{90d} + \log_{10}(D_{base}):maxCWD^{90d} + (1|interval) + (1|plot) + (1|species) + (1|seedling)$

Family: gaussian (identity link)

Fixed effects	**Estimate**	**Std. Error**	**z-value**	**Pr(>|z|)**
(Intercept)	**-4.2650**	**0.1305**	**-32.69**	**0.0000**
$\log_{10}(D_{base})$	**2.3183**	**0.0620**	**37.37**	**0.0000**
$maxCWD^{90d}$	**-0.0056**	**0.0025**	**-2.26**	**0.0236**
$\log_{10}(D_{base}):maxCWD^{90d}$	0.0004	0.0009	0.51	0.6128

Random effects	**Variance**	**Groups**
interval	0.09497	21
plot	0.01065	20
species	0.00805	25
seedling	0.01834	473
residual	0.20956	3912

Table S5.20, summary statistics for the mixed-effects model testing if the log-transformed stem NPP of growing seedlings ('$\log_{10}(NPP_{stem})$') **within the logged forest at Malua** varies as a result of log-transformed basal diameter ('$\log_{10}(D_{base})$') interacted with the maximum 90-day running average of daily cumulative water deficit experienced by each seedling in each census interval (**$maxCWD^{90d}$**– mm). Seedling ID, plot, cohort, census interval and species were used as random effects to account for non-independence from repeated measures, as well as temporally- and spatially-explicit groupings within the data. We could not include random effect slopes for species in terms of $maxCWD^{90d}$ due to issues with model convergence. Please note coefficients are expressed in the log-transformed scale.

Formula: $\log_{10}(NPP_{stem}) \sim \log_{10}(D_{base}) + maxCWD^{90d} + \log_{10}(D_{base}):maxCWD^{90d} + (1|interval) + (1|cohort) + (1|plot) + (1|species) + (1|seedling)$

Family: gaussian (identity link)

Fixed effects	**Estimate**	**Std. Error**	**z-value**	**Pr(>|z|)**
(Intercept)	**-4.7668**	**0.0968**	**-49.25**	**0.0000**
$\log_{10}(D_{base})$	**2.5720**	**0.0386**	**66.62**	**0.0000**
$maxCWD^{90d}$	-0.0025	0.0021	-1.18	0.2366
$\log_{10}(D_{base}):maxCWD^{90d}$	0.0017	0.0012	1.38	0.1671

Random effects	**Variance**	**Groups**
interval	0.02483	17
cohort	0.00515	2
plot	0.00507	6
species	0.00593	16
seedling	0.03260	2800
residual	0.21996	6099

5.11.8. Models investigating the effect of climate on Pr(survival > 0)

Table S5.21, summary statistics for the mixed-effects model testing if the interval survival rate ('Pr(survival > 0)') **within the old-growth forest at Danum** varies as a result of log-transformed basal diameter ('$\log_{10}(D_{base})$') interacted with the maximum 90-day running average of daily maximum temperature experienced by each seedling in each census interval (**$\mathbf{maxT_{max}^{90d}}$** – ºC). The model also includes an additive effect of log-transformed interval length in days ('$\log_{10}$(interval length)'). Plot, census interval and species were used as random effects to account for non-independence from temporally- and spatially-explicit groupings within the data. We could not include random effect slopes for species in terms of $maxT_{max}^{90d}$ due to issues with model convergence. Please note coefficients are expressed in the logit scale.

Formula: Pr(survival > 0) ~ $\log_{10}$(interval length) + $\log_{10}(D_{base})$ + $maxT_{max}^{90d}$ + $\log_{10}(D_{base})$:$maxT_{max}^{90d}$ + (1|interval) + (1| plot) + (1| species)

Family: binomial (logit link)

Fixed effects	Estimate	Std. Error	z-value	Pr(>|z|)
(Intercept)	12.1607	15.9763	0.76	0.4466
$\log_{10}$(interval length)	**-2.2053**	**0.5548**	**-3.98**	**0.0001**
$\log_{10}(D_{base})$	7.3261	11.6871	0.63	0.5308
$maxT_{max}^{90d}$	-0.1880	0.4913	-0.38	0.7019
$\log_{10}(D_{base})$:$maxT_{max}^{90d}$	-0.1598	0.3555	-0.45	0.6531

Random effects	Variance	Groups
interval	0.32560	20
plot	0.42796	20
species	0.35012	25
residual	-	5218

Table S5.22, summary statistics for the mixed-effects model testing if the interval survival rate ('Pr(survival > 0)') **within the logged forest at Malua** varies as a result of log-transformed basal diameter ('$\log_{10}(D_{base})$') interacted with the maximum 90-day running average of daily maximum temperature experienced by each seedling in each census interval (**$\mathbf{maxT_{max}^{90d}}$** – ºC). The model also includes an additive effect of log-transformed interval length in days ('$\log_{10}$(interval length)'). Plot, cohort, census interval and species were used as random effects to account for non-independence from temporally- and spatially-explicit groupings within the data. We also included random effect slopes for species in terms of $maxT_{max}^{90d}$. Please note coefficients are expressed in the logit scale.

Formula: Pr(survival > 0) ~ $\log_{10}$(interval length) + $\log_{10}(D_{base})$ + $maxT_{max}^{90d}$ + $\log_{10}(D_{base})$:$maxT_{max}^{90d}$ + (1|interval) + (1| cohort) + (1| plot) + (1 + $maxT_{max}^{90d}$| species)

Family: binomial (logit link)

Fixed effects	Estimate	Std. Error	z-value	Pr(>|z|)
(Intercept)	-5.7295	6.0885	-0.94	0.3467
$\log_{10}$(interval length)	**-2.3560**	**0.3435**	**-6.86**	**0.0000**
$\log_{10}(D_{base})$	5.0785	3.4425	1.48	0.1401
$maxT_{max}^{90d}$	**0.4199**	**0.2051**	**2.05**	**0.0406**
$\log_{10}(D_{base})$:$maxT_{max}^{90d}$	-0.1340	0.1204	-1.11	0.2657

Random effects	Variance	Groups
interval	0.47104	11
cohort	0.05403	2
plot	0.00000	6
species	34.82088	16
species:$maxT_{max}^{90d}$	0.04343	16
residual	-	6565

Table S5.23, summary statistics for the mixed-effects model testing if the interval survival rate ('Pr(survival > 0)') **within the old-growth forest at Danum** varies as a result of log-transformed basal diameter ('$\log_{10}(D_{base})$') interacted with the minimum 90-day running average of daily precipitation experienced by each seedling in each census interval (**$\mathbf{minPPT^{90d}}$** – mm). The model also includes an additive effect of log-transformed interval length in days ('$\log_{10}$(interval length)'). Plot, census interval and species were used as random effects to account for non-independence from temporally- and spatially-explicit groupings within the data. We also included random effect slopes for species in terms of $minPPT^{90d}$. Please note coefficients are expressed in the logit scale.

Formula: $Pr(survival > 0) \sim \log_{10}(interval\ length) + \log_{10}(D_{base}) + minPPT^{90d} + \log_{10}(D_{base}):minPPT^{90d} + (1|interval) + (1|\ plot) + (1 + minPPT^{90d}|\ species)$

Family: binomial (logit link)

Fixed effects	**Estimate**	**Std. Error**	**z-value**	**Pr(>|z|)**
(Intercept)	**8.8121**	**2.0295**	**4.34**	**0.0000**
$\log_{10}$(interval length)	**-2.4780**	**0.5327**	**-4.65**	**0.0000**
$\log_{10}(D_{base})$	0.5030	1.0084	0.50	0.6179
$minPPT^{90d}$	-0.4044	0.2714	-1.49	0.1362
$\log_{10}(D_{base}):minPPT^{90d}$	0.2867	0.1962	1.46	0.1439

Random effects	**Variance**	**Groups**
interval	0.26211	21
plot	0.40345	20
species	0.42999	25
$species:minPPT^{90d}$	0.01241	25
residual	-	5382

Table S5.24, summary statistics for the mixed-effects model testing if the interval survival rate ('Pr(survival > 0)') **within the logged forest at Malua** varies as a result of log-transformed basal diameter ('$\log_{10}(D_{base})$') interacted with the minimum 90-day running average of daily precipitation experienced by each seedling in each census interval (**$\mathbf{minPPT^{90d}}$**– mm). The model also includes an additive effect of log-transformed interval length in days ('$\log_{10}$(interval length)'). Plot, cohort, census interval and species were used as random effects to account for non-independence from temporally- and spatially-explicit groupings within the data. We also included random effect slopes for species in terms of $minPPT^{90d}$. Please note coefficients are expressed in the logit scale.

Formula: $Pr(survival > 0) \sim \log_{10}(interval\ length) + \log_{10}(D_{base}) + minPPT^{90d} + \log_{10}(D_{base}):minPPT^{90d} + (1|interval) + (1|\ cohort) + (1|\ plot) + (1 + minPPT^{90d}|\ species)$

Family: binomial (logit link)

Fixed effects	**Estimate**	**Std. Error**	**z-value**	**Pr(>|z|)**
(Intercept)	**4.9898**	**1.8324**	**2.7231**	**0.0065**
$\log_{10}$(interval length)	**-2.5007**	**0.4317**	**-5.7930**	**0.0000**
$\log_{10}(D_{base})$	**3.5515**	**0.8755**	**4.0567**	**0.0000**
$minPPT^{90d}$	0.2771	0.1682	1.6473	0.0995
$\log_{10}(D_{base}):minPPT^{90d}$	**-0.3104**	**0.1219**	**-2.5464**	**0.0109**

Random effects	**Variance**	**Groups**
interval	0.39509	17
cohort	0.05090	2
plot	0.05621	6
species	1.59184	16
$species:minPPT^{90d}$	0.02307	16
residual	-	9232

Table S5.25, summary statistics for the mixed-effects model testing if the interval survival rate ('Pr(survival > 0)') **within the old-growth forest at Danum** varies as a result of log-transformed basal diameter ('$\log_{10}(D_{base})$') interacted with the maximum 90-day running average of daily maximum vapour pressure deficit experienced by each seedling in each census interval (**$\mathbf{maxVPD_{max}^{90d}}$** – hPa). The model also includes an additive effect of log-transformed interval length in days ('$\log_{10}$(interval length)'). Plot, census interval and species were used as random effects to account for non-independence from temporally- and spatially-explicit groupings within the data. We could not include random effect slopes for species in terms of $maxVPD_{max}^{90d}$ due to issues with model convergence. Please note coefficients are expressed in the logit scale.

Formula: Pr(survival > 0) ~ $\log_{10}$(interval length) + $\log_{10}(D_{base})$ + $maxVPD_{max}^{90d}$ + $\log_{10}(D_{base})$:$maxVPD_{max}^{90d}$ + (1|interval) + (1| plot) + (1| species)

Family: binomial (logit link)

Fixed effects	**Estimate**	**Std. Error**	**z-value**	**Pr(>|z|)**
(Intercept)	5.5198	3.1634	1.74	0.0810
$\log_{10}$(interval length)	**-2.2996**	**0.5695**	**-4.04**	**0.0001**
$\log_{10}(D_{base})$	3.6152	2.1643	1.67	0.0948
$maxVPD_{max}^{90d}$	0.0643	0.2499	0.26	0.7970
$\log_{10}(D_{base})$:$maxVPD_{max}^{90d}$	-0.1318	0.1787	-0.74	0.4608

Random effects	**Variance**	**Groups**
interval	0.36569	19
plot	0.42267	20
species	0.34602	25
residual	-	5210

Table S5.26, summary statistics for the mixed-effects model testing if the interval survival rate ('Pr(survival > 0)') **within the logged forest at Malua** varies as a result of log-transformed basal diameter ('$\log_{10}(D_{base})$') interacted with the maximum 90-day running average of daily maximum vapour pressure deficit experienced by each seedling in each census interval (**$\mathbf{maxVPD_{max}^{90d}}$** – hPa). The model also includes an additive effect of log-transformed interval length in days ('$\log_{10}$(interval length)'). Plot, cohort, census interval and species were used as random effects to account for non-independence from temporally- and spatially-explicit groupings within the data. We also included random effect slopes for species in terms of $maxVPD_{max}^{90d}$. Please note coefficients are expressed in the logit scale.

Formula: Pr(survival > 0) ~ $\log_{10}$(interval length) + $\log_{10}(D_{base})$ + $maxVPD_{max}^{90d}$ + $\log_{10}(D_{base})$:$maxVPD_{max}^{90d}$ + (1|interval) + (1| cohort) + (1| plot) + (1 + $maxVPD_{max}^{90d}$| species)

Family: binomial (logit link)

Fixed effects	**Estimate**	**Std. Error**	**z-value**	**Pr(>|z|)**
(Intercept)	**7.9139**	**1.3767**	**5.75**	**0.0000**
$\log_{10}$(interval length)	**-3.3337**	**0.7295**	**-4.57**	**0.0000**
$\log_{10}(D_{base})$	**1.9640**	**0.3194**	**6.15**	**0.0000**
$maxVPD_{max}^{90d}$	**0.1692**	**0.0639**	**2.65**	**0.0080**
$\log_{10}(D_{base})$:$maxVPD_{max}^{90d}$	**-0.1163**	**0.0409**	**-2.84**	**0.0044**

Random effects	**Variance**	**Groups**
interval	0.59662	11
cohort	0.05646	2
plot	0.00000	6
species	0.22524	16
species:$maxVPD_{max}^{90d}$	0.00137	16
residual	-	6565

Table S5.27, summary statistics for the mixed-effects model testing if the interval survival rate ('Pr(survival > 0)') **within the old-growth forest at Danum** varies as a result of log-transformed basal diameter ('$\log_{10}(D_{base})$') interacted with the maximum 90-day running average of daily cumulative water deficit experienced by each seedling in each census interval (**maxCWD^{90d}** – mm). The model also includes an additive effect of log-transformed interval length in days ('$\log_{10}$(interval length)'). Plot, census interval and species were used as random effects to account for non-independence from temporally- and spatially-explicit groupings within the data. We could not include random effect slopes for species in terms of maxCWD^{90d} due to issues with model convergence. Please note coefficients are expressed in the logit scale.

Formula: Pr(survival > 0) ~ $\log_{10}$(interval length) + $\log_{10}(D_{base})$ + maxCWD^{90d} + $\log_{10}(D_{base})$:maxCWD^{90d} + (1|interval) + (1| plot) + (1| species)

Family: binomial (logit link)

Fixed effects	**Estimate**	**Std. Error**	**z-value**	**Pr(>|z|)**
(Intercept)	**6.1032**	**1.4528**	**4.20**	**0.0000**
$\log_{10}$(interval length)	**-2.3244**	**0.5435**	**-4.28**	**0.0000**
$\log_{10}(D_{base})$	**2.2460**	**0.4702**	**4.78**	**0.0000**
maxCWD^{90d}	0.0092	0.0122	0.75	0.4505
$\log_{10}(D_{base})$:maxCWD^{90d}	-0.0086	0.0084	-1.03	0.3037

Random effects	**Variance**	**Groups**
interval	0.32059	21
plot	0.40128	20
species	0.36069	25
residual	-	5382

Table S5.28, summary statistics for the mixed-effects model testing if the interval survival rate ('Pr(survival > 0)') **within the logged forest at Malua** varies as a result of log-transformed basal diameter ('$\log_{10}(D_{base})$') interacted with the maximum 90-day running average of daily cumulative water deficit experienced by each seedling in each census interval (**maxCWD^{90d}**– mm). The model also includes an additive effect of log-transformed interval length in days ('$\log_{10}$(interval length)'). Plot, cohort, census interval and species were used as random effects to account for non-independence from temporally- and spatially-explicit groupings within the data. We also included random effect slopes for species in terms of maxCWD^{90d}. Please note coefficients are expressed in the logit scale.

Formula: Pr(survival > 0) ~ $\log_{10}$(interval length) + $\log_{10}(D_{base})$ + maxCWD^{90d} + $\log_{10}(D_{base})$:maxCWD^{90d} + (1|interval) + (1| cohort) + (1| plot) + (1+ maxCWD^{90d}| species)

Family: binomial (logit link)

Fixed effects	**Estimate**	**Std. Error**	**z-value**	**Pr(>|z|)**
(Intercept)	**7.0451**	**0.9394**	**7.50**	**0.0000**
$\log_{10}$(interval length)	**-2.5439**	**0.3752**	**-6.78**	**0.0000**
$\log_{10}(D_{base})$	**1.3341**	**0.2336**	**5.71**	**0.0000**
maxCWD^{90d}	0.0008	0.0157	0.05	0.9608
$\log_{10}(D_{base})$:maxCWD^{90d}	0.0024	0.0116	0.21	0.8375

Random effects	**Variance**	**Groups**
interval	0.59662	17
cohort	0.06535	2
plot	0.05672	6
species	0.08065	16
species:maxCWD^{90d}	0.00005	16
residual	-	9232

5.11.9. Correlations between species random effects for Pr(NPP_{stem} > 0) models and plant functional traits

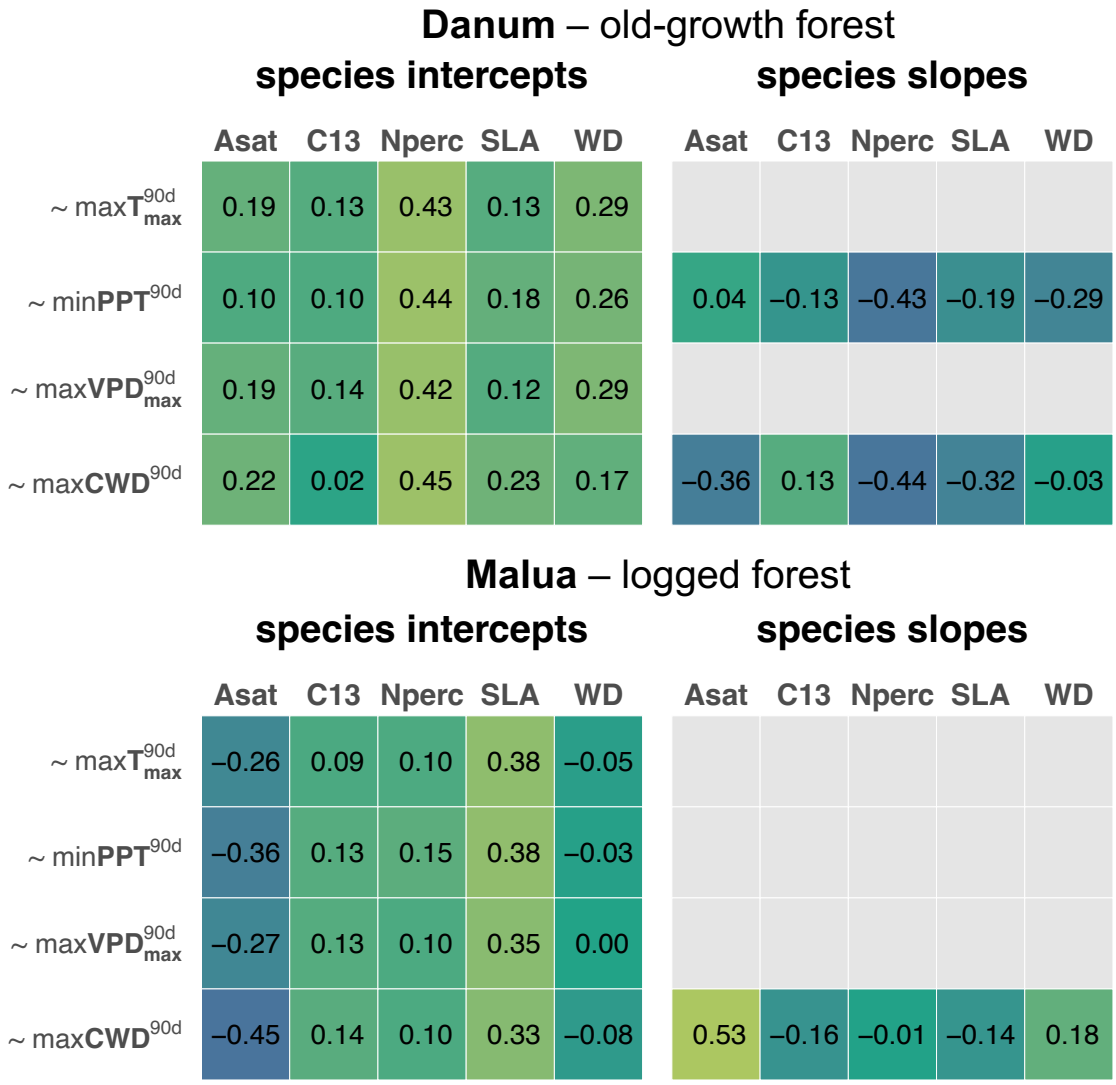


Figure S5.11, correlation matrices illustrating the relationship between species-level random-effect estimates from Pr(NPP_{stem} > 0) models and plant functional trait means. Species-level random-effect estimates (both random intercepts and slopes in terms of climate extreme variables) were derived from models investigating how the probability of seedlings attaining positive NPP_{stem} varies as a function of $\log_{10}(D_{base})$ interacted with climate extreme variables (see **Table S5.5** to **Table S5.12**). Random intercepts (left) represent the species-specific deviation from the overall model intercept, reflecting species with proportionally lower/higher Pr(NPP_{stem} > 0). Random slopes (right) represent species-specific deviations from the climate extreme variables effect on Pr(NPP_{stem} > 0), reflecting species with proportionally lower/higher climate extreme sensitivity. Each row represents the species-level random-effects derived from the models including the corresponding climate extreme variable. Columns represent each functional trait. Trait values for each species were obtained as averages from Both, Burslem *et al.* (2019). Models were specific for each forest type: correlations for the old-growth forest are shown on top, logged forest below. Correlation coefficients are indicated within each cell (blue, r = -1; yellow, r = 1). Statistically significant correlation coefficients are shown in bold (no significant relationship between species-level effects and functional traits in this case).

Chapter 6: Conclusions

In this chapter, I provide a summary of the main findings of the thesis, and outline their research significance and scientific novelty. Then, I draw some general conclusions by comparing carbon flux patterns of Cerrado savanna and lowland dipterocarp rainforests, and elaborating on common mechanisms underpinning productivity responses across both case study ecosystems. Finally, I conclude by outlining future research avenues and outstanding questions identified by this thesis.

6.1. Results synthesis

The main aim of this thesis was to investigate changes in tropical ecosystem productivity as a result of altered climate and fire regimes, and explore how these responses are influenced by plant strategies and functional traits. Specifically, in **Chapter 3 (Research Paper 1)**, I make use of a burning experiment at Serra das Araras to quantify carbon flux dynamics of Cerrado savannas across different fire regime frequencies. Long-term monitoring of ecosystem components reveals that recurrent burning within *cerrado sensu stricto* savanna increased tree mortality and led to declines in productivity, respiration and net carbon balances. Experimental burning also increased herbaceous biomass and productivity, indicating prescribed fires could be used as a management strategy for conserving endemic herbaceous biodiversity against woody encroachment (Durigan *et al*., 2020). The most dramatic shifts in vegetation structure and carbon fluxes were observed within the triennially burnt plot, which supported more intense fires leading to increased tissue damage and biomass consumption (Chiminazzo *et al*., 2025). However, canopy and belowground components showed different patterns of change across fire regimes, hinting at complex interactions between ecological processes, environmental factors and fire regime variables. Overall, this chapter demonstrates how fire regimes are key drivers of vegetation structure and ecosystem function in Cerrado savannas (Hoffmann, 2002; Reis *et al*., 2015; Le Stradic *et al*., 2018), showing that more natural fire intervals (triennial burning) can effectively restore and

maintain open-landscape processes, complementing previous studies on nutrient and herbaceous dynamics (Kauffman *et al*., 1994; Pivello *et al*., 2010; Oliveras *et al*., 2012).

The aim of **Chapter 4 (Research Paper 2)** was to comprehensively investigate fire impacts on Cerrado stem productivity and survival, with the goal of identifying the functional mechanisms influencing carbon flux dynamics across different fire frequencies. I used tree inventory data from Serra das Araras to determine how different species contribute to plot-scale stem NPP across different fire regimes, and found that generalist species disproportionately dominate productivity in fire exclusion plots, with *Tachigali vulgaris* accounting for more than 70% of NPP_{stem}. These generalist species became less dominant after burning, and were replaced by sclerophyllous and conservative savanna trees, especially in the more intense fire regimes, consistent with patterns in ecosystem-level fluxes. I then investigated changes in species-level NPP_{stem} and survival, and identified a trade-off between plant productivity and tolerance to fire, where species that were more productive before fire showed a greater long-term reduction in average NPP_{stem} after experimental burning. Functional traits strongly influenced species-level NPP_{stem} after more intense (triennial) fires, and productivity was positively associated with bark protection and light-adapted photosynthesis. These results point to the existence of shade versus fire tolerance strategies within tropical savanna, complementing studies from the broader Cerrado and other savanna regions worldwide (Gignoux *et al*., 1997; Charles-Dominique *et al*., 2018). This work goes beyond previous research in linking shifts in functional composition as a result of woody encroachment and landscape opening (e.g., Flake *et al*., 2021; Singh *et al*., 2023), with changes in tree growth and survival, ecosystem productivity, carbon-use efficiency, and biomass accumulation.

In **Chapter 5 (Research Paper 3)** I made use of two planting experiments that have been intensively monitored for over 20 years to determine if extremes of heat and drought consistently influenced rates of NPP_{stem} and survival at logged and old-growth dipterocarp rainforests, linking climate-driven changes in productivity and survival with functional plant strategies. Dry and hot climate extremes significantly reduced stem NPP in the old-growth forest, with disproportionately

strong effects on smaller individuals. In the logged forest, extreme temperatures also constrained stem productivity. Species with faster photosynthetic rates and higher foliar nitrogen were more productive, but were also more sensitive to climate extremes. Correlations between NPP_{stem} and functional traits were only observed in the logged forest, suggesting that acquisitive strategies may better translate into higher stem productivity under conditions of reduced competition. This chapter advances previous work (e.g., Miyamoto *et al*., 2021; O'Brien *et al*., 2024) by providing insight into the effects of extreme climate events across multiple variables of heat and water stress. For the first time, this thesis compares climate-productivity-trait responses across logged and old-growth dipterocarp forests. Results indicate that seedlings shift growth trajectories following enrichment planting, supporting the effectiveness of active restoration in the recovery of ecosystem functioning (Philipson *et al*., 2020).

6.2. Research significance

The work presented in this thesis addresses key geographical and temporal research gaps, and advances our understanding of ecosystem science and disturbance ecology in the context of global change. **Chapter 3 (Research Paper 1)** provides the first-ever complete carbon budget for *cerrado sensu stricto* savannas, and the second-ever carbon cycle parametrisation for the entire Cerrado region (Vourlitis *et al*., 2022). It supplements NPP estimates for *cerrado sensu stricto* and *cerradão* provided by Scalon *et al*. (2022) and Reis *et al*. (2025), as well as studies from the southern Amazon (Araujo-Murakami *et al*., 2014; Rocha *et al*., 2014) and the broader GEM network (Zhang-Zheng *et al*., 2024). **Chapter 4 (Research Paper 2)** is the first study within the Cerrado to experimentally integrate stem productivity dynamics with functional plant strategies. It fills an important knowledge gap by empirically demonstrating the existence of a growth-tolerance trade-off with respect to fire (Hoffmann *et al*., 2003), and confirms that *T. vulgaris* dominates ecosystem responses under fire suppression (Reis *et al*., 2017). Studies investigating the impacts of droughts and heatwaves on lowland dipterocarp forests have largely focused on

short-term events and experiments (e.g., Burslem *et al*., 1996; Bebber *et al*., 2004; Browne *et al*., 2021); **Chapter 5 (Research Paper 3)** thus provides exceptional long-term insight into the cumulative effects of climate change on ecological functioning (O'Brien *et al*., 2024).

This thesis also sought to refine and adapt methods for measuring and quantifying net primary productivity. In **Chapter 3 (Research Paper 1)** carbon monitoring methodologies (Malhi *et al*., 2021) were adapted to a savanna-fire context. It incorporates measurements of herbaceous productivity based on grassland monitoring of Andean *punas* (Oliveras *et al*., 2014), and develops a new method to scale up herbaceous respiration to the ecosystem level using specific leaf area and dark respiration data from Rossatto & Franco (2017). Instead of using an annual mean of air temperature, it integrates locally-sourced microclimate data to account for seasonal variations in stem and soil CO_2 efflux (Butler *et al*., 2012; Rowland *et al*., 2018). We also adapted our leaf-area-index quantification based on Ma *et al*. (2025) to account for a high proportion of dead stem area within the burnt plots. Using a soil respiration partition ratio for *cerrado sensu stricto* derived from data collected at Nova Xavantina (Butler *et al*., 2012) also helped us produce rough estimates of $R_{heterotrophic}$ and $R_{rhizosphere}$. Together, these methodologies allowed us to provide the first estimates of R_{canopy}, R_{stem} and R_{herbs} within the Cerrado, and to construct a full carbon balance for South American woodland savannas.

This thesis went further than many previous studies in statistically investigating ecosystem and stem productivity dynamics using multi-year datasets. In **Chapters 3 and 4 (Research Papers 1 and 2)**, we compared NPP estimates in burnt vs unburnt plots using a two-way ANOVA BACI framework (before-after control-impact approach; Christie *et al*., 2019), which allowed us to meet statistical assumptions, maintain interpretability and provide annual flux estimates for start and end periods. In **Chapter 4 (Research Paper 2)**, our BACI approach was extended to incorporate an interaction between census interval, fire regime and functional traits, to test if the influence of a given trait on NPP_{stem} differed from one regime to another due to the cumulative effects of burning. In **Chapter 5 (Research Paper 3)**, we used mixed-effects models that allowed us to take

advantage of climatic variation across more than 20 survey intervals as a natural heat and drought experiment (O'Brien *et al*., 2024). These analyses offer a useful framework for isolating fire and climate impacts on carbon dynamics (Dee *et al*., 2023), and provide a foundation for future studies to extend NPP monitoring protocols across other ecosystems, datasets, and disturbance regimes.

6.3. General discussion

6.3.1. Productivity of Cerrado savannas versus dipterocarp forests

Cerrado savannas and lowland dipterocarp rainforests are characterised by marked differences in vegetation structure, environmental conditions and biogeographical contexts (Banin *et al*., 2012), reflecting distinct patterns of productivity and carbon fluxes. Although this thesis did not focus on estimating total net primary productivity in dipterocarp forests, previous estimates for NPP_{total} across old-growth lowland forests in Borneo sit at 15.03 ± 0.75 MgC ha^{-1} $year^{-1}$ (Mills *et al*., 2023). In comparison, our estimate of NPP_{total} for Cerrado savanna was 3.72 ± 0.71 MgC ha^{-1} $year^{-1}$ across the unburnt plots, and 6.62 ± 2.77 MgC ha^{-1} $year^{-1}$ for *cerrado sensu stricto* at Nova Xavantina (Reis *et al*., 2025). Carbon use efficiency (CUE) was 0.43 ± 0.03 in dipterocarp forests (Mills *et al*., 2023) compared to 0.24 ± 0.05 in the Cerrado. Specific NPP components are also greater in dipterocarp forests compared to unburnt Cerrado savanna (see **Table 6.1**). For example, stem and litterfall NPP in dipterocarp forests are about six times greater than in *cerrado sensu stricto*. Despite this, the amount of carbon allocated into belowground fluxes, both productivity and respiration, is proportionally higher within Cerrado savannas (47% of NPP allocated belowground compared to 24% in dipterocarp forests, Mills *et al*., 2023). In this case, the proportion of ecosystem respiration arising from heterotrophic sources was estimated to be 20% greater in dipterocarp forests compared to the Cerrado.

Table 6.1, productivity (NPP) and respiration (R) flux components and full carbon budget for old-growth dipterocarp rainforests and unburnt Cerrado savannas. Flux estimates for lowland dipterocarp rainforests were reproduced and adapted from Mills *et al*. (2023), Proceedings of the National Academy of Sciences, 120(3): e2214462120 (https://doi.org/10.1073/pnas.2214462120) licensed under open access CC BY 4.0 (http://creativecommons.org/licenses/by/4.0/). In this case, $NPP_{aboveground}$ was calculated as a sum of $NPP_{litterfall}$, NPP_{stem} and NPP_{branch}. $NPP_{belowground}$ was calculated as a sum of $NPP_{coarse\ roots}$ and $NPP_{fine\ roots}$. $R_{rhizosphere}$ was calculated as the sum of $R_{fine\ roots}$ and $R_{coarse\ roots}$. R_{soil} was calculated as the sum of $R_{soil\ organic\ matter}$, $R_{mycorrhizae}$, R_{litter} and $R_{fine\ roots}$. Flux estimates for the unburnt *cerrado sensu stricto* plots at Serra das Araras were reproduced from **Table S3.20**. The table includes estimates of GPP (gross primary productivity; or PCE, plant carbon expenditure, in the case of Cerrado), CUE (carbon use efficiency) and NEE (net ecosystem exchange, where negative values indicate carbon accumulation). All fluxes are in MgC ha^{-1} $year^{-1}$ and are accompanied by estimated uncertainty and percentage contribution to NPP_{total} and R_{eco}.

Carbon flux (MgC ha^{-1} $year^{-1}$)	**Dipterocarp rainforest** (old-growth plots)	**Cerrado savanna** (unburnt plots)
$NPP_{litterfall}$	6.88 ± 0.40 [46%]	1.25 ± 0.20 [34%]
NPP_{stem}	3.95 ± 0.54 [26%]	0.66 ± 0.17 [18%]
NPP_{branch}	0.64 ± 0.12 [4%]	-
NPP_{herbs}	-	0.05 ± 0.01 [1%]
$NPP_{coarse\ roots}$	0.95 ± 0.14 [6%]	0.90 ± 0.65 [24%]
$NPP_{fine\ roots}$	1.21 ± 0.20 [8%]	0.86 ± 0.09 [23%]
$NPP_{aboveground}$	11.47 ± 0.68 [76%]	1.96 ± 0.26 [53%]
$NPP_{belowground}$	3.56 ± 0.47 [24%]	1.76 ± 0.67 [47%]
NPP_{total}	15.03 ± 0.75 [100%]	3.72 ± 0.71 [100%]
R_{canopy}	9.76 ± 0.46 [28%]	4.32 ± 1.02 [30%]
R_{stem}	6.18 ± 0.48 [18%]	2.42 ± 0.48 [17%]
R_{herbs}	-	0.58 ± 0.23 [4%]
$R_{rhizosphere}$	4.09 ± 0.14 [12%]	4.55 ± 0.49 [31%]
$R_{autotrophic}$	20.03 ± 0.53 [58%]	11.86 ± 1.25 [81%]
$R_{heterotrophic}$	14.32 ± 0.64 [42%]	2.71 ± 0.45 [19%]
R_{soil}	12.68 ± 0.58 [37%]	7.26 ± 0.37 [50%]
R_{eco}	34.36 ± 0.96 [100%]	14.57 ± 1.21 [100%]
GPP / PCE	35.06 ± 1.13	15.58 ± 1.44
CUE	0.43 ± 0.03	0.24 ± 0.05
NEE	-0.71 ± 1.23	-1.01 ± 0.84

Within this thesis, direct comparisons of stem NPP between Cerrado savannas and dipterocarp forests are restricted by differences in study design. **Chapters 3 and 4 (Research Papers 1 and 2)** are based on plot-level inventories, whereas **Chapter 5 (Research Paper 3)** focuses on cohorts of planted seedlings. However, comparisons can be made at the level of the average individual. When accounting for size trajectories of planted dipterocarp seedlings, the magnitude of stem NPP appears broadly comparable across study sites. For example, a rough analysis of tree survey data from Serra das Araras reveals average DBH in the first census interval (before fire) was 8.4

cm and mean individual NPP_{stem} was 0.67 KgC $year^{-1}$ (1.01 KgC $year^{-1}$ when removing negative NPP_{stem} values). If we estimate dipterocarp stem productivity for a basal diameter of 8.4 cm (using model equation 5.7, **Chapter 5**), we predict an average NPP_{stem} of 1.00 and 1.76 KgC $year^{-1}$ within our old-growth and logged forest plots respectively. Despite similar ranges of stem NPP, dipterocarps are able to attain much higher levels of NPP at larger sizes. Maximum individual NPP_{stem} for the Cerrado was 50.49 KgC $year^{-1}$ (*T. vulgaris*, initial DBH 33.4 cm), whilst maximum NPP_{stem} for dipterocarp trees was 116.04 KgC $year^{-1}$ (*Shorea mecistopteryx*, initial DBH 28.8 cm).

Although carbon flux averages are comparatively smaller in Cerrado savannas, respiration and NPP experience strong seasonal variation (Reis *et al*., 2025). Soil respiration rates at the unburnt Cerrado plots stay above 11.0 MgC ha^{-1} $year^{-1}$ during the wettest months (January-April), but fall to 6.0 MgC ha^{-1} $year^{-1}$ during the dry season (July-September). Raw estimates of $NPP_{fine\ roots}$ for the June-September trimester sit at 0.61 MgC ha^{-1} $year^{-1}$, compared to 4.35 MgC ha^{-1} $year^{-1}$ during the wet season (September-December). These patterns align with the expectation that strong water limitations in tropical savannas, compared to more aseasonal moist forests, restrict ecosystem productivity potential (Zhang-Zheng *et al*., 2024). Overall, the gross primary productivity (GPP) of dipterocarp forests is more than twice as large as that of the unburnt plots at Serra das Araras, but rates of carbon accumulation in *cerrado sensu stricto* appear to be higher than those in dipterocarp rainforests. Despite large uncertainties, the difference between GPP and R_{eco} is higher in the Cerrado as a result of woody encroachment and fire exclusion. Results suggest that on average, unburnt plots at Serra das Araras could be gaining 0.30 more megagrams of carbon annually compared to old-growth dipterocarp forests across Borneo.

6.3.2. Comparing NPP responses to changing climate and fire regimes

Although quantifying NPP components allows us to investigate ecosystem dynamics within a common currency of carbon flow, integrating productivity responses to altered climate and fire regimes across our study locations is challenging because this thesis has investigated the effects

of climate and fire separately, and because each chapter has focused on different scales of biological organisation. At the ecosystem level, comparisons of NPP are further complicated by the lack of studies investigating the effects of climate and fire on full NPP and carbon budgets within dipterocarp rainforests. Studies using ground-based methods to scale up ecosystem carbon balances have instead focused on the effects of logging (Riutta *et al*., 2018; Mills *et al*., 2023). Logging appears to drive net ecosystem carbon losses in dipterocarp forests (NEE = 3.85 ± 1.13 MgC ha^{-1} $year^{-1}$; Mills *et al*., 2023), and this trend is broadly comparable to reductions in ecosystem carbon after recurrent burning at Serra das Araras (NEE = 1.77 ± 0.51, 1.76 ± 0.58, and 0.54 ± 0.82 MgC ha^{-1} $year^{-1}$ in the triennial, biennial, and annual plots respectively, see **Figure 3.5**).

Within Cerrado savannas, changing fire regimes seem to have a stronger impact on ecosystem productivity compared to extreme climate. Total NPP for *cerrado sensu stricto* at Nova Xavantina only decreased by 0.06 MgC ha^{-1} $year^{-1}$ from 2014 to 2015 despite a reduction of ~600 mm in rainfall (Reis *et al*., 2025). In comparison, NPP_{total} at Serra das Araras was 2.80 MgC ha^{-1} $year^{-1}$ lower in the triennial plot relative to the unburnt plots (**Figure 3.5**). Other Cerrado vegetation types, however, might be more vulnerable to climate change: Reis *et al*. (2025) found that NPP_{total} for *cerradão* decreased by 2.65 MgC ha^{-1} $year^{-1}$ from 2014 to 2016. Fire and drought also have significant effects on Cerrado carbon fluxes including litterfall and fine root NPP. At Serra das Araras, $NPP_{fine\ roots}$ decreased by 1.41 and 1.46 MgC ha^{-1} $year^{-1}$ in the triennially and annually burnt plots, and $NPP_{litterfall}$ declined by 0.46, 0.62 and 1.29 MgC ha^{-1} $year^{-1}$ after triennial, biennial and annual fires (**Table S3.20**). Nardoto *et al*. (2006) found that $NPP_{litterfall}$ decreased by 1.01 MgC ha^{-1} $year^{-1}$ after six years of biennial burns at the Ecological Reserve of the IBGE, Brasília. In Nova Xavantina, Cerrado $NPP_{litterfall}$ declined by 0.27 MgC ha^{-1} $year^{-1}$ from 2014 to 2016, and $NPP_{fine\ roots}$ decreased by 0.52 MgC ha^{-1} $year^{-1}$ as a result of drought (Reis *et al*., 2025). Compared to this, $NPP_{litterfall}$ of dipterocarp forest at Lambir Hills National Park, Sarawak, increased by 1.78 MgC ha^{-1} $year^{-1}$ from 2009 to 2010 (Nakagawa *et al*., 2019) due to increased leaf shedding and fruit production during the 2009/2010 El Niño (Ichie *et al*., 2004). Despite recent advances, our understanding of root and canopy NPP responses across Borneo and the Cerrado remains limited.

Woody biomass and stem productivity dynamics, however, have received more attention across Cerrado savannas and lowland dipterocarp rainforests. **Chapters 3 and 4 (Research Papers 1 and 2)** of this thesis revealed that woody productivity of Cerrado savanna decreased by 0.22, 0.08 and 0.11 MgC ha^{-1} $year^{-1}$ after six years of triennial, biennial and annual burns as a result of shifts in functional composition and species growth rates. Comparisons of aboveground biomass estimates from de Castro & Kauffman (1998) and de Castro-Neves (2007) suggest that *cerrado sensu stricto* plots at the IBGE were losing between 0.37 and 0.89 MgC ha^{-1} $year^{-1}$ after 15 years of prescribed burning. In comparison, Toma *et al*. (2005) showed that aboveground woody biomass accumulation within logged dipterocarp forests decreased by 6.55, 6.59 and 5.64 MgC ha^{-1} $year^{-1}$ after burning in 1997. Greater absolute declines in NPP_{stem} of dipterocarp forests post-fire relative to the Cerrado could be attributed to higher rates of NPP, but also to disproportionate vulnerability to fire. Slik *et al*. (2008) reveal that aboveground biomass of dipterocarp forests continues to decline up to 7 years after fire. Notably, the authors report that herbaceous cover in once-burnt forest is twice that of unburnt forest, reflecting patterns of increased herbaceous productivity post-fire similar to those observed in the Cerrado (**Chapter 3 – Research Paper 1**).

Evidence for the effects of extreme climate on stem NPP in Cerrado savannas and dipterocarp forests remains mixed, revealing that, in some cases, species are capable of coping with heat and drought. Reis *et al*. (2025) found that NPP_{stem} for *cerrado sensu stricto* increased by 0.15 MgC ha^{-1} $year^{-1}$ after the 2015/2016 El Niño, compared to a decline of 1.62 MgC ha^{-1} $year^{-1}$ in *cerradão*. Across the Amazon-Cerrado transition, the 2015/2016 El Niño was associated with declines in species abundance and shifts in community composition (Prestes *et al*., 2024), and these patterns are somewhat comparable to post-fire changes in species dominance described in **Chapter 4 (Research Paper 2)**. Aboveground biomass in lowland dipterocarp forests remained unaffected by the 1982-1983 El Niño, but declined by 1.04 MgC ha^{-1} $year^{-1}$ during the 1997-1998 drought (Qie *et al*., 2017). Kho *et al*. (2013) also observed different patterns of change in woody NPP and mortality after the 1997-1998 El Niño in forests in clay vs sandy loam soils, and my own analyses

in **Chapter 5 (Research Paper 3)** reveal how NPP_{stem} of trees in old-growth forest declines with heat and drought, although trees in the logged forest are more likely to grow during drier periods.

In terms of woody stem NPP, this thesis reveals that dipterocarp responses to extreme climate are somewhat comparable to Cerrado responses to fire regimes when considering trees of similar sizes. **Table 6.2** includes model-based predictions for climate-driven changes in old-growth dipterocarp forest NPP_{stem} for trees of 8.4 cm basal diameter. Predicted declines in dipterocarp NPP_{stem} as a result of drought range from 0.56 to 1.43 KgC $year^{-1}$, and are similar in magnitude to fire-induced changes in species-level NPP_{stem} at Serra das Araras. For example, average NPP_{stem} for *Qualea multiflora*, *Vochysia haenkeana* and *Xylopia aromatica* respectively decreased by 0.35, 0.45 and 0.40 KgC $year^{-1}$ after 5 annual burns (**Table S4.2**). Climate-driven changes in dipterocarp NPP_{stem} are expected to be greater than those of Cerrado trees, since dipterocarp trees have the potential to reach much larger sizes, and because climate effects appear to scale non-linearly with NPP. In both cases, however, we observed variable trends of change in stem NPP across species and fire regimes (**Chapter 4 – Research Paper 2**) or across forest locations (**Chapter 5 – Research Paper 3**), indicating patterns are to be interpreted with caution and warranting further research into common functional mechanisms influencing responses to stress.

Table 6.2, example of predicted climate-driven changes in NPP_{stem} of dipterocarp trees planted within the old-growth forest at Danum Valley. NPP_{stem} estimates were derived from the mixed-effects models (equation 5.7, **Chapter 5 – Research Paper 3**) testing if the log-transformed stem NPP of growing seedlings varied as a result of log-transformed basal diameter interacted with climate extreme variables ($maxT^{90d}_{max}$, maximum 90-day running average of daily maximum temperature; $minPPT^{90d}$, minimum 90-day running average of daily precipitation; $maxVPD^{90d}_{max}$, maximum 90-day running average of daily maximum vapour pressure deficit; $maxCWD^{90d}$, maximum 90-day running average of daily cumulative water deficit). To predict NPP_{stem} values, I used a basal diameter value of 84 mm. In this case, I used the extreme climate values for the 6th and 7th census intervals at the old-growth forest (from December 2009 to March 2010 and from March 2010 to August 2010) to produce model-based predictions of NPP_{stem} during the 2009/2010 El Niño, which was associated with strong drought and heat across both forest sites (**Figure S5.6**).

Climate extremes				**Predicted NPP_{stem}** (KgC $year^{-1}$)		
Variable	**late 2009**	**early 2010**	***Difference***	**late 2009**	**early 2010**	***Difference***
$\mathbf{maxT^{90d}_{max}}$ (ºC)	32.05	33.45	1.40	1.71	0.94	-0.78
$\mathbf{minPPT^{90d}}$ (mm)	6.05	2.03	-4.02	1.48	0.37	-1.10
$\mathbf{maxVPD^{90d}_{max}}$ (hPa)	11.33	15.19	8.86	1.54	0.11	-1.43
$\mathbf{maxCWD^{90d}}$ (mm)	48.29	133.06	84.77	0.92	0.36	-0.56

6.3.3. The fast-slow spectrum as a major driver of stem productivity

After investigating how extreme climate and altered fire regimes respectively affect the productivity of lowland dipterocarp forests and Cerrado savannas, this thesis sought to explore if functional traits shape productivity responses across stressors and study locations. Our findings reveal that in both ecosystems, traits associated with resource acquisition and plant economics play an important role in determining NPP dynamics in response to changing fire regimes and extreme climate. Resource acquisition trade-offs have been identified as major drivers of plant growth, biomass accumulation and productivity (Enquist *et al*., 2007). According to optimality theory, relative growth rates can be understood as the outcome of trait syndromes that maximise carbon gain under environmental constraints, and can be mathematically described as the product of net carbon assimilation rate and investment into photosynthetic tissues (Evans, 1972; Poorter, 1989). Within this framework, acquisitive (fast) and conservative (slow) plant strategies reflect contrasting trait combinations that influence the components of growth and productivity in distinct ways (Lambers & Poorter, 1992). Acquisitive traits promote rapid carbon gain, resource capture, and fast biomass accumulation over short timescales, while conservative traits prioritise carbon retention, stress tolerance, and efficiency over long timescales (Maracahipes *et al*., 2018).

This thesis shows that in logged dipterocarp forests, species with more acquisitive resource-use were able to maximise stem productivity under favourable conditions (Wright *et al*., 2004; Reich, 2014) but were less able to sustain biomass growth during heat and drought as a result of increased photosynthetic and hydraulic risks (Ziegler *et al*., 2024; Evans *et al*., 2025; **Figure 6.1**). Resource acquisition strategies emerge as a clear predictor of NPP_{stem} and climate sensitivity, indicating that patterns in leaf carbon uptake scale up from organ-level processes to influence whole-plant carbon accumulation in the face of climate change (Trugman & Anderegg, 2025). Higher levels of productivity within logged forests are likely underpinned by more efficient acquisition under favourable conditions (Bartholomew *et al*., 2024), but increased climate variability might compromise the long-term stability of carbon assimilation and storage within these ecosystems.

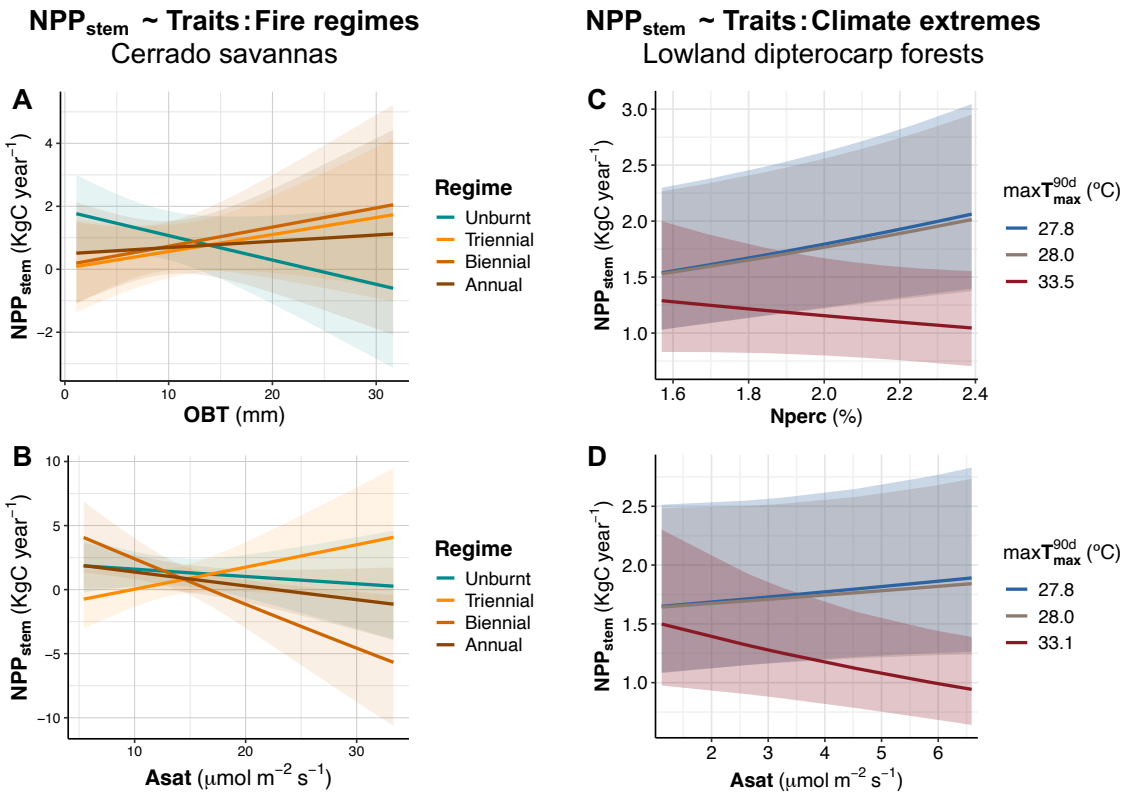


Figure 6.1, graphical visualisation of the main interactions between stem productivity (NPP_{stem}), functional traits and climate/fire stressors identified in this thesis. **A-B**) relationship of outer bark thickness (OBT, panel **A**) and light-saturated carbon assimilation (Asat, panel **B**) with NPP_{stem} of Cerrado savanna trees at Serra das Araras. Graphs illustrate NPP_{stem} predictions (alongside 95% confidence intervals) derived from mixed effect models interacting census interval, fire regime and functional traits (**Chapter 4 – Research Paper 2**, equation 4.6). Only predictions for the most recent census interval (2021-2023) are shown. **C-D**) relationship of foliar nitrogen concentrations (Nperc, panel **C**) and light-saturated assimilation (Asat, panel **D**) with NPP_{stem} of dipterocarp trees planted at the logged forest site in Malua, Malaysian Borneo. Graphs illustrate NPP_{stem} predictions (alongside 95% confidence intervals) derived from mixed effect models investigating changes in log-transformed NPP_{stem} as a function of log-transformed basal diameter interacted with the maximum 90-day running mean of daily maximum temperature for each census interval ($maxT^{90d}_{max}$), and with functional traits. Essentially, this is a version of the equation 5.10 $maxT^{90d}_{max}$ model used in **Chapter 5 (Research Paper 3)**, with an additional fixed effect for trait (used here for illustration purposes). In this case, NPP_{stem} was predicted for a basal diameter of 84 mm.

Resource acquisition traits also play a key role in mediating Cerrado stem NPP across fire regimes, although in this case, patterns of productivity are complicated by disturbance resilience trade-offs and fire tolerance constraints (Plumanns-Pouton *et al*., 2025). Notably, interactions between traits and NPP_{stem} at Serra das Araras empirically support the 'vegetation realms' framework proposed by Chiminazzo *et al*. (2025) for Cerrado fire regimes, extending its applicability to carbon flux

dynamics. In unburnt Cerrado plots, stem NPP is dominated by generalist species with lower-cost foliage, large sizes and high wood density. Although higher wood density is associated with conservative strategies, it provides structural support for large, low-cost canopies, allowing for efficient resource capture, light interception and growth competitive advantages over savanna specialists (Gignoux *et al*., 2016; Charles-Dominique *et al*., 2018; 'starving realm', Chiminazzo *et al*., 2025), which directly translate into higher rates of NPP_{stem} (Laughlin, 2023).

Across plots that are periodically burnt, productivity dynamics are dominated by shorter species that structurally invest in leaf resistance and bark thickness rather than wood density (Hoffmann *et al*., 2003; Chiminazzo *et al*., 2023; 'burning realm' Chiminazzo *et al*., 2025), optimising resource use efficiency by reducing support and maximising tissue protection (Scalon *et al*., 2020). Our triple interaction models in **Chapter 4 (Research Paper 2)** statistically confirm that bark protection and light-adapted photosynthesis allow for higher rates of NPP_{stem} after triennial burning (**Figure 6.1**). This means that within the ecophysiological and structural constraints imposed by intense fires, plants can still maximise resource acquisition and productivity by adjusting tissue investments and increasing carbon assimilation, matching patterns of stem growth observed in Australian savannas (Wright *et al*., 2019). Consequently, our results indicate that both fire tolerance and acquisitive traits underpin NPP responses in Cerrado savannas.

Taken together, this thesis shows that photosynthetic rates might be useful predictors of NPP across biomes and environmental contexts, a pattern which is consistent with the relative growth rate framework, in which higher rates of net carbon assimilation directly contribute to increased plant growth and biomass accumulation (Lambers & Poorter, 1992). Previous meta-analyses have indeed demonstrated that net carbon assimilation rates, followed by specific leaf area, are primary determinants of relative growth rates in woody species (Shipley, 2006). Surprisingly, we found no evidence for specific leaf area influencing stem productivity in Cerrado savannas or dipterocarp forests, despite its central role as a key functional trait within the leaf economics spectrum (Wright *et al*., 2004). Furthermore, our results seem to suggest that functional traits

translate into growth and productivity advantages more clearly under conditions of intense disturbance and strong environmental filtering (e.g., triennial burning or logged dipterocarp forest), and remain weakly related to species survival in the Cerrado and in logged dipterocarp forests. Conservative traits are only associated with increased survival in old-growth dipterocarp forests, potentially reflecting a trait-mediated growth-survival trade-off at the species level, but confirming functional strategies are inherently variable and heavily context-dependent (He *et al*., 2023). In light of these findings, extending the study of trait-NPP relationships into additional functional traits (e.g., plant hydraulic traits and non-structural carbohydrates) could strengthen our understanding of the functional mechanisms underpinning productivity and survival within Cerrado savannas and dipterocarp forests (O'Brien *et al*., 2020; Cruz *et al*., 2025).

6.4. Outstanding questions and future research directions

This thesis demonstrates that extreme climatic conditions and altered fire regimes can substantially affect productivity in both Cerrado savannas and lowland dipterocarp rainforests. These effects were revealed through long-term monitoring and experimental efforts, where long-term experiments such as the CERFogo Project and the Sabah Biodiversity Experiment provide a key opportunity to study ecosystem responses over ecologically-relevant timescales, allowing us to understand ecosystem dynamics beyond short-term environmental fluctuations (Hector *et al*., 2011). This is particularly important with regards to productivity, given that changes in tree growth, biomass accumulation and mortality unfold slowly, and may only become apparent after several years. Through long-term monitoring, we are able to capture delayed responses, interannual variability and cumulative impacts in the effects of fire and climate on NPP, allowing for a clearer understanding of how tropical ecosystems respond to environmental change (Malhi *et al*., 2002).

However, this thesis also reveals key challenges in designing and interpreting long-term experiments in tropical forests and savannas. Important limits to our interpretation of NPP

responses both in Cerrado savannas and dipterocarp rainforests arise from the high-degree of spatial variation in environmental conditions and vegetation structure (Blonder *et al*., 2018; Colli *et al*., 2020). For example, in the Cerrado, large heterogeneity in tree basal area between our monitoring plots prevented us from fully disentangling fire regime effects on carbon fluxes, while in Borneo, responses to extreme climate across old-growth and logged forest types were confounded by differences in planting spacing and climatic conditions. Spatial variability was further complicated by historical contingencies within our monitoring sites, given that logging and fire suppression had an important role in shaping our logged dipterocarp forest and Cerrado savanna ecosystems respectively (Durigan & Ratter, 2016; Imai *et al*., 2019), which were already found in a degraded and encroached state. Although these limitations could have been better addressed by increasing spatial coverage and plot replication, this was not possible due to significant logistical constraints, given that long-term experiments depend on continued funding, institutional capacity and equipment maintenance, which are particularly challenging to sustain within tropical areas due to remoteness and socioeconomic challenges (Phillips, 2023).

Despite these constraints this thesis provides the first carbon flux balance for Cerrado savannas across fire regimes of different frequencies, linking shifts in overall productivity to variation in stem NPP and functional traits. Taking advantage of available data, it also examines climate-driven dynamics of stem NPP in dipterocarp forests, although the effects of climate on ecosystem-level carbon balances were not addressed. Future work should therefore examine NPP responses across canopy and fine root components, to identify which aspects of dipterocarp carbon balance are most vulnerable to climate variability (Doughty *et al*., 2014). This could be effectively achieved by analysing the intensive carbon monitoring data collected at Danum Valley since 2015 (Riutta *et al*., 2018; Riutta *et al*., 2021; Mills *et al*., 2024), which could be integrated with high-resolution daily climate data recorded locally (O'Brien *et al*., 2026). In the context of this thesis, such an approach would also enable a direct comparison of how processes scale from component-level responses to whole-ecosystem dynamics under different stressors, including both fire and climate.

In relation to this, an outstanding question arising from this research relates to the extent to which changes in stem NPP act as reliable indicators of trends in total ecosystem productivity and carbon uptake. Woody biomass constitutes a substantial and relatively stable component of aboveground productivity in forests, and has been widely used to infer ecosystem carbon dynamics through tree inventories and allometric approaches (e.g., Malhi *et al*., 2004). These measurements enable relatively straightforward quantification of species-level contributions to biomass gain and facilitate links between carbon fluxes and functional traits (Enquist *et al*., 2017). However, stem NPP has important limitations as an indicator of ecosystem carbon dynamics, as it captures only a fraction of total carbon allocation (26% for dipterocarp forests, 18% for Cerrado savannas, **Table 6.1**). Large components of NPP, including litterfall, fine root and herbaceous production, may respond more rapidly to environmental variability and disturbance, shifting NPP allocation and ecosystem-scale patterns (Malhi *et al*., 2017). Previous studies have shown that NPP allocation strategies can change markedly following disturbances such as fire and logging (Rocha *et al*., 2014; Mills *et al*., 2023), a pattern that is now also confirmed for the Brazilian Cerrado. In the context of Serra das Araras, a more detailed assessment of carbon allocation patterns in relation to vegetation structure (*sensu* Riutta *et al*., 2018) would provide a robust framework for linking component-level NPP and mortality to the whole-ecosystem carbon balance.

Investigating belowground carbon flux dynamics in greater detail would also improve our understanding of global change impacts on ecosystem carbon. Characterising soil conditions in logged versus old-growth plots at Malua and Danum could help explain unexpected ecosystem responses to climatic extremes (O'Brien *et al*., 2024). In tropical savannas, belowground carbon remains markedly understudied, despite representing a substantial proportion of total carbon stocks and allocation (Grace *et al*., 2006). This gap is particularly relevant in the context of the Serra das Araras project, where both fine root NPP and soil respiration declined across all fire regimes during the monitoring period, despite frequent fire being associated with increased allocation to belowground components (Le Stradic *et al*., 2021). Improving measurements of coarse root growth would allow for a more complete quantification of belowground NPP, moving

beyond fixed root-to-shoot ratios. In this context, emerging methods such as ground-penetrating radar offer a promising and cost-effective approach for estimating root biomass and improving representation of belowground productivity (Zhou *et al*., 2022).

Although this thesis has examined the effects of fire and climate on ecosystem NPP separately, an important next step is to quantify their individual and interactive influences across Cerrado savannas and dipterocarp forests. Analysing the carbon monitoring data collected during the 2023–2024 El Niño event at Serra das Araras would provide a valuable opportunity to assess the combined impacts of heat, drought, and fire regimes on Cerrado productivity (Reis *et al*., 2025). In addition, microclimate data collected across the fire regime plots could help elucidate how fire management alters local environmental conditions, thereby influencing NPP through indirect feedbacks (Costa *et al*., 2020). Although comparable microclimatic measurements are not available across the dipterocarp forest plots at Danum and Malua, canopy-driven microclimate models could be used to estimate variables such as maximum temperature and vapour pressure deficit (Jucker *et al*., 2018). These estimates would support efforts to disentangle the interacting effects of heat and drought stress on tree growth and survival (Brown, 1993).

Finally, this thesis has shown that functional trait measurements can be useful indicators of stem productivity at the individual and species level, underpinning ecosystem carbon uptake across contrasting biomes through trade-offs between stress tolerance and resource acquisition. An important question is whether the relationships among traits, NPP, and environmental stressors are consistent across other locations. Future research could use large-scale forest plot networks (e.g., Forestplots.net, 2021) in combination with functional trait datasets to quantify species-level contributions to productivity and to scale trait-NPP relationships regionally and continentally. Such studies would strengthen the potential of trait-based frameworks to predict ecosystem responses to global change and, in the context of shifting climate and fire regimes, enhance our ability to understand and adapt to changes in ecosystem services and Earth-system functioning.

6.5. References

Araujo-Murakami, A., Doughty, C. E., Metcalfe, D. B., Silva-Espejo, J. E., Arroyo, L., Heredia, J. P., Flores, M., Sibler, R., Mendizabal, L. M., Pardo-Toledo, E., Vega, M., Moreno, L., Rojas-Landivar, V. D., Halladay, K., Girardin, C. A. J., Killeen, T. J., & Malhi, Y. (2014). The productivity, allocation and cycling of carbon in forests at the dry margin of the Amazon forest in Bolivia. *Plant Ecology & Diversity*, *7*(1–2), 55–69. https://doi.org/10.1080/17550874.2013.798364

Banin, L., Feldpausch, T. R., Phillips, O. L., Baker, T. R., Lloyd, J., Affum-Baffoe, K., Arets, E. J. M. M., Berry, N. J., Bradford, M., Brienen, R. J. W., Davies, S., Drescher, M., Higuchi, N., Hilbert, D. W., Hladik, A., Iida, Y., Salim, K. A., Kassim, A. R., King, D. A., … Lewis, S. L. (2012). What controls tropical forest architecture? Testing environmental, structural and floristic drivers. *Global Ecology and Biogeography*, *21*(12), 1179–1190. https://doi.org/10.1111/j.1466-8238.2012.00778.x

Bartholomew, D. C., Hayward, R., Burslem, D. F. R. P., Bittencourt, P. R. L., Chapman, D., Bin Suis, Mohd. A. F., Nilus, R., O'Brien, M. J., Reynolds, G., Rowland, L., Banin, L. F., & Dent, D. (2024). Bornean tropical forests recovering from logging at risk of regeneration failure. *Global Change Biology*, *30*(3), e17209. https://doi.org/10.1111/gcb.17209

Bebber, D. P., Brown, N. P., & Speight, M. R. (2004). Dipterocarp seedling population dynamics in Bornean primary lowland forest during the 1997-8 El Niño-Southern Oscillation. *Journal of Tropical Ecology*, *20*(1), 11–19. https://doi.org/10.1017/S0266467404006133

Blonder, B., Both, S., Coomes, D. A., Elias, D., Jucker, T., Kvasnica, J., Majalap, N., Malhi, Y. S., Milodowski, D., Riutta, T., & Svátek, M. (2018). Extreme and highly heterogeneous microclimates in selectively logged tropical forests. *Frontiers in Forests and Global Change*, *1*(5). https://doi.org/10.3389/ffgc.2018.00005

Brown, N. (1993). The implications of climate and gap microclimate for seedling growth conditions in a Bornean lowland rain forest. *Journal of Tropical Ecology*, *9*(2), 153–168. https://doi.org/10.1017/S0266467400007136

Browne, L., Markesteijn, L., Engelbrecht, B. M. J., Jones, F. A., Lewis, O. T., Manzané-Pinzón, E., Wright, S. J., & Comita, L. S. (2021). Increased mortality of tropical tree seedlings during the extreme 2015–16 El Niño. *Global Change Biology*, *27*(20), 5043–5053. https://doi.org/10.1111/gcb.15809

Burslem, D. F. R. P., Grubb, P. J., & Turner, I. M. (1996). Responses to simulated drought and elevated nutrient supply among shade-tolerant tree seedlings of lowland tropical forest in Singapore. *Biotropica*, *28*(4), 636–648. https://doi.org/10.2307/2389050

Butler, A., Meir, P., Saiz, G., Maracahipes, L., Marimon, B. S., & Grace, J. (2012). Annual variation in soil respiration and its component parts in two structurally contrasting woody savannas in Central Brazil. *Plant and Soil*, *352*(1–2), 129–142. https://doi.org/10.1007/s11104-011-0984-7

Castro, E. A. de, & Kauffman, J. B. (1998). Ecosystem structure in the Brazilian Cerrado: A vegetation gradient of aboveground biomass, root mass and consumption by fire. *Journal of Tropical Ecology*, *14*(3), 263–283. https://doi.org/10.1017/S0266467498000212

Charles-Dominique, T., Midgley, G. F., Tomlinson, K. W., & Bond, W. J. (2018). Steal the light: Shade vs fire adapted vegetation in forest–savanna mosaics. *New Phytologist*, *218*(4), 1419–1429. https://doi.org/10.1111/nph.15117

Chiminazzo, M. A., Bombo, A. B., Charles-Dominique, T., & Fidelis, A. (2023). Bark production of generalist and specialist species across savannas and forests in the Cerrado. *Annals of Botany*, *131*(4), 613–621. https://doi.org/10.1093/aob/mcad014

Chiminazzo, M. A., Charles-Dominique, T., Andrade, R. S., Bombo, A. B., & Fidelis, A. (2025). How do plants survive in the starving, burning, and hiding vegetation realms generated by novel fire regimes? *Perspectives in Plant Ecology, Evolution and Systematics*, *68*, 125885. https://doi.org/10.1016/j.ppees.2025.125885

Christie, A. P., Amano, T., Martin, P. A., Shackelford, G. E., Simmons, B. I., & Sutherland, W. J. (2019). Simple study designs in ecology produce inaccurate estimates of biodiversity responses. *Journal of Applied Ecology*, *56*(12), 2742–2754. https://doi.org/10.1111/1365-2664.13499

Colli, G. R., Vieira, C. R., & Dianese, J. C. (2020). Biodiversity and conservation of the Cerrado: Recent advances and old challenges. *Biodiversity and Conservation*, *29*(5), 1465–1475. https://doi.org/10.1007/s10531-020-01967-x

Costa, B. M., Pantoja, D. L., Sousa, H. C., de Queiroz, T. A., & Colli, G. R. (2020). Long-term, fire-induced changes in habitat structure and microclimate affect Cerrado lizard communities. *Biodiversity and Conservation*, *29*(5), 1659–1681. https://doi.org/10.1007/s10531-019-01892-8

Cruz, W. J. A., Machado, M. S., Navarro-Rosales, F., Carniello, M. A., Andrade, M. L. F., Oliveira, F. C., & Oliveras Menor, I. (2025). Deciphering fire tolerance of trees at the Amazonia–Cerrado transition by trait-based approach: Implications from species to communities. *American Journal of Botany*, *n/a*(n/a), e70066. https://doi.org/10.1002/ajb2.70066

Dee, L. E., Ferraro, P. J., Severen, C. N., Kimmel, K. A., Borer, E. T., Byrnes, J. E. K., Clark, A. T., Hautier, Y., Hector, A., Raynaud, X., Reich, P. B., Wright, A. J., Arnillas, C. A., Davies, K. F., MacDougall, A., Mori, A. S., Smith, M. D., Adler, P. B., Bakker, J. D., … Loreau, M. (2023). Clarifying the effect of biodiversity on productivity in natural ecosystems with longitudinal data and methods for causal inference. *Nature Communications*, *14*(1), 2607. https://doi.org/10.1038/s41467-023-37194-5

de Castro-Neves, B. M. (2007). Efeito de queimadas em áreas de *cerrado stricto sensu* e na biomassa de raízes finas. PhD Thesis. Universidade de Brasília.

Doughty, C. E., Malhi, Y., Araujo-Murakami, A., Metcalfe, D. B., Silva-Espejo, J. E., Arroyo, L., Heredia, J. P., Pardo-Toledo, E., Mendizabal, L. M., Rojas-Landivar, V. D., Vega-Martinez, M., Flores-Valencia, M., Sibler-Rivero, R., Moreno-Vare, L., Viscarra, L. J., Chuviru-Castro, T., Osinaga-Becerra, M., & Ledezma, R. (2014). Allocation trade-offs dominate the response of tropical forest growth to seasonal and interannual drought. *Ecology*, *95*(8), 2192–2201. https://doi.org/10.1890/13-1507.1

Durigan, G., & Ratter, J. A. (2016). The need for a consistent fire policy for Cerrado conservation. *Journal of Applied Ecology*, *53*(1), 11–15. https://doi.org/10.1111/1365-2664.12559

Durigan, G., Pilon, N. A. L., Abreu, R. C. R., Hoffmann, W. A., Martins, M., Fiorillo, B. F., Antunes, A. Z., Carmignotto, A. P., Maravalhas, J. B., Vieira, J., & Vasconcelos, H. L. (2020). No net loss of species diversity after prescribed fires in the Brazilian savanna. *Frontiers in Forests and Global Change*, *3*. https://doi.org/10.3389/ffgc.2020.00013

Enquist, B. J., Bentley, L. P., Shenkin, A., Maitner, B., Savage, V., Michaletz, S., Blonder, B., Buzzard, V., Espinoza, T. E. B., Farfan-Rios, W., Doughty, C. E., Goldsmith, G. R., Martin, R. E., Salinas, N., Silman, M., Díaz, S., Asner, G. P., & Malhi, Y. (2017). Assessing trait-based scaling theory in tropical forests spanning a broad temperature gradient. *Global Ecology and Biogeography*, *26*(12), 1357–1373. https://doi.org/10.1111/geb.12645

Enquist, B. J., Kerkhoff, A. J., Stark, S. C., Swenson, N. G., McCarthy, M. C., & Price, C. A. (2007). A general integrative model for scaling plant growth, carbon flux, and functional trait spectra. *Nature*, *449*(7159), 218–222. https://doi.org/10.1038/nature06061

Evans, G. C. (1972). *The quantitative analysis of plant growth*. Blackwell Scientific.

Evans, M. E. K., Hu, J., & Michaletz, S. T. (2025). Scaling plant responses to heat: From molecules to the biosphere. *Science*, *388*(6752), 1167–1173. https://doi.org/10.1126/science.adv7597

Flake, S. W., Abreu, R. C. R., Durigan, G., & Hoffmann, W. A. (2021). Savannas are not old fields: Functional trajectories of forest expansion in a fire-suppressed Brazilian savanna are driven by habitat generalists. *Functional Ecology*, *35*(8), 1797–1809. https://doi.org/10.1111/1365-2435.13818

ForestPlots.net, Blundo, C., Carilla, J., Grau, R., Malizia, A., Malizia, L., Osinaga-Acosta, O., Bird, M., Bradford, M., Catchpole, D., Ford, A., Graham, A., Hilbert, D., Kemp, J., Laurance, S., Laurance, W., Ishida, F. Y., Marshall, A., Waite, C., … Tran, H. D. (2021). Taking the pulse of Earth's tropical forests using networks of highly distributed plots. *Biological Conservation*, *260*, 108849. https://doi.org/10.1016/j.biocon.2020.108849

Gignoux, J., Clobert, J., & Menaut, J.-C. (1997). Alternative fire resistance strategies in savanna trees. *Oecologia*, *110*(4), 576–583. https://doi.org/10.1007/s004420050198

Gignoux, J., Konaté, S., Lahoreau, G., Le Roux, X., & Simioni, G. (2016). Allocation strategies of savanna and forest tree seedlings in response to fire and shading: Outcomes of a field experiment. *Scientific Reports*, *6*(1), 38838. https://doi.org/10.1038/srep38838

Grace, J., José, J. S., Meir, P., Miranda, H. S., & Montes, R. A. (2006). Productivity and carbon fluxes of tropical savannas. *Journal of Biogeography*, *33*(3), 387–400. https://doi.org/10.1111/j.1365-2699.2005.01448.x

He, N., Yan, P., Liu, C., Xu, L., Li, M., Van Meerbeek, K., Zhou, G., Zhou, G., Liu, S., Zhou, X., Li, S., Niu, S., Han, X., Buckley, T. N., Sack, L., & Yu, G. (2023). Predicting ecosystem productivity based on plant community traits. *Trends in Plant Science*, *28*(1), 43–53. https://doi.org/10.1016/j.tplants.2022.08.015

Hector, A., Philipson, C., Saner, P., Chamagne, J., Dzulkifli, D., O'Brien, M., Snaddon, J. L., Ulok, P., Weilenmann, M., Reynolds, G., & Godfray, H. C. J. (2011). The Sabah Biodiversity Experiment: A long-term test of the role of tree diversity in restoring tropical forest structure and functioning. *Philosophical Transactions of the Royal Society B: Biological Sciences*, *366*(1582), 3303–3315. https://doi.org/10.1098/rstb.2011.0094

Hoffmann, W. A. (2002). Direct and indirect effects of fire on radial growth of cerrado savanna trees. *Journal of Tropical Ecology*, *18*(1), 137–142. https://doi.org/10.1017/S0266467402002080

Hoffmann, W. A., Orthen, B., & Nascimento, P. K. V. do. (2003). Comparative fire ecology of tropical savanna and forest trees. *Functional Ecology*, *17*(6), 720–726. https://doi.org/10.1111/j.1365-2435.2003.00796.x

Ichie, T., Hiromi, T., Yoneda, R., Kamiya, K., Kohira, M., Ninomiya, I., & Ogino, K. (2004). Short-term drought causes synchronous leaf shedding and flushing in a lowland mixed dipterocarp forest, Sarawak, Malaysia. *Journal of Tropical Ecology*, *20*(6), 697–700. https://doi.org/10.1017/S0266467404001713

Imai, N., Sugau, J. B., Pereira, J. T., Titin, J., & Kitayama, K. (2019). Impacts of selective logging on spatial structure of tree species composition in Bornean tropical rain forests. *Journal of Forest Research*, *24*(6), 335–340. https://doi.org/10.1080/13416979.2019.1666958

Jucker, T., Hardwick, S. R., Both, S., Elias, D. M. O., Ewers, R. M., Milodowski, D. T., Swinfield, T., & Coomes, D. A. (2018). Canopy structure and topography jointly constrain the microclimate of human-modified tropical landscapes. *Global Change Biology*, *24*(11), 5243–5258. https://doi.org/10.1111/gcb.14415

Kauffman, J. B., Cummings, D. L., & Ward, D. E. (1994). Relationships of fire, biomass and nutrient dynamics along a vegetation gradient in the Brazilian Cerrado. *The Journal of Ecology*, *82*(3), 519. https://doi.org/10.2307/2261261

Kho, L. K., Malhi, Y., & Tan, S. K. S. (2013). Annual budget and seasonal variation of aboveground and belowground net primary productivity in a lowland dipterocarp forest in Borneo. *Journal of Geophysical Research: Biogeosciences*, *118*(3), 1282–1296. https://doi.org/10.1002/jgrg.20109

Lambers, H., & Poorter, H. (1992). Inherent variation in growth rate between higher plants: A search for physiological causes and ecological consequences. In *Advances in Ecological Research* (Vol. 34, pp. 283–362). Elsevier. https://doi.org/10.1016/S0065-2504(03)34004-8
Laughlin, D. C. (2023). *Plant Strategies: The Demographic Consequences of Functional Traits in Changing Environments*. Oxford University Press.

Le Stradic, S., Hernandez, P., Fernandes, G. W., & Buisson, E. (2018). Regeneration after fire in *campo rupestre*: Short- and long-term vegetation dynamics. *Flora, Plant Life on Campo Rupestre, a Megadiverse Neotropical Old-Growth Grassland*, *238*, 191–200. https://doi.org/10.1016/j.flora.2016.12.001

Le Stradic, S., Roumet, C., Durigan, G., Cancian, L., & Fidelis, A. (2021). Variation in biomass allocation and root functional parameters in response to fire history in Brazilian savannas. *Journal of Ecology*, *109*(12), 4143–4157. https://doi.org/10.1111/1365-2745.13786

Ma, T., Tang, M., Liu, F., Duah-Gyamfi, A., Adu-Bredu, S., Naive, M. A. K., Menor, I. O., Moore, S., Zhang, Z., Malhi, Y., Dahlsjö, C. A. L., & Zhang-Zheng, H. (2025). *An AI-based and coding-free protocol for forests Leaf Area Index (LAI) calculation* (p. 2025.07.24.666563). bioRxiv. https://doi.org/10.1101/2025.07.24.666563

Malhi, Y., Baker, T. R., Phillips, O. L., Almeida, S., Alvarez, E., Arroyo, L., Chave, J., Czimczik, C. I., Fiore, A. D., Higuchi, N., Killeen, T. J., Laurance, S. G., Laurance, W. F., Lewis, S. L., Montoya, L. M. M., Monteagudo, A., Neill, D. A., Vargas, P. N., Patiño, S., … Lloyd, J. (2004). The above-ground coarse wood productivity of 104 Neotropical forest plots. *Global Change Biology*, *10*(5), 563–591. https://doi.org/10.1111/j.1529-8817.2003.00778.x

Malhi, Y., Girardin, C. A. J., Goldsmith, G. R., Doughty, C. E., Salinas, N., Metcalfe, D. B., Huaraca Huasco, W., Silva-Espejo, J. E., del Aguilla-Pasquell, J., Farfán Amézquita, F., Aragão, L. E. O. C., Guerrieri, R., Ishida, F. Y., Bahar, N. H. A., Farfan-Rios, W., Phillips, O. L., Meir, P., & Silman, M. (2017). The variation of productivity and its allocation along a tropical elevation gradient: A whole carbon budget perspective. *New Phytologist*, *214*(3), 1019–1032. https://doi.org/10.1111/nph.14189

Malhi, Y., Girardin, C., Metcalfe, D. B., Doughty, C. E., Aragão, L. E. O. C., Rifai, S. W., Oliveras, I., Shenkin, A., Aguirre-Gutiérrez, J., Dahlsjö, C. A. L., Riutta, T., Berenguer, E., Moore, S., Huasco, W. H., Salinas, N., da Costa, A. C. L., Bentley, L. P., Adu-Bredu, S., Marthews, T. R., … Phillips, O. L. (2021). The Global Ecosystems Monitoring network: Monitoring ecosystem productivity and carbon cycling across the tropics. *Biological Conservation*, *253*, 108889. https://doi.org/10.1016/j.biocon.2020.108889

Malhi, Y., Phillips, O. l., Lloyd, J., Baker, T., Wright, J., Almeida, S., Arroyo, L., Frederiksen, T., Grace, J., Higuchi, N., Killeen, T., Laurance, W., Leaño, C., Lewis, S., Meir, P., Monteagudo, A., Neill, D., Núñez Vargas, P., Panfil, S. N., … Vinceti, B. (2002). An international network to monitor the structure, composition and dynamics of Amazonian forests (RAINFOR). *Journal of Vegetation Science*, *13*(3), 439–450. https://doi.org/10.1111/j.1654-1103.2002.tb02068.x

Maracahipes, L., Carlucci, M. B., Lenza, E., Marimon, B. S., Marimon, B. H., Guimarães, F. A. G., & Cianciaruso, M. V. (2018). How to live in contrasting habitats? Acquisitive and conservative strategies emerge at inter- and intraspecific levels in savanna and forest woody plants. *Perspectives in Plant Ecology, Evolution and Systematics*, *34*, 17–25. https://doi.org/10.1016/j.ppees.2018.07.006

Mills, M. B., Both, S., Jotan, P., Huaraca Huasco, W., Cruz, R., Pillco, M. M., Burslem, D. F. R. P., Maycock, C., Malhi, Y., Ewers, R. M., Berrio, J. C., Kaduk, J., Page, S., Robert, R., Teh, Y. A., & Riutta, T. (2024). From tree to plot: Investigating stem CO_2 efflux and its drivers along a logging gradient in Sabah, Malaysian Borneo. *New Phytologist*, *244*(1), 91–103. https://doi.org/10.1111/nph.20043

Mills, M. B., Malhi, Y., Ewers, R. M., Kho, L. K., Teh, Y. A., Both, S., Burslem, D. F. R. P., Majalap, N., Nilus, R., Huaraca Huasco, W., Cruz, R., Pillco, M. M., Turner, E. C., Reynolds, G., & Riutta, T. (2023). Tropical forests post-logging are a persistent net carbon source to the atmosphere. *Proceedings of the National Academy of Sciences*, *120*(3), e2214462120. https://doi.org/10.1073/pnas.2214462120

Miyamoto, K., Aiba, S., Aoyagi, R., & Nilus, R. (2021). Effects of El Niño drought on tree mortality and growth across forest types at different elevations in Borneo. *Forest Ecology and Management*, *490*, 119096. https://doi.org/10.1016/j.foreco.2021.119096

Nakagawa, M., Ushio, M., Kume, T., & Nakashizuka, T. (2019). Seasonal and long-term patterns in litterfall in a Bornean tropical rainforest. *Ecological Research*, *34*(1), 31–39. https://doi.org/10.1111/1440-1703.1003

Nardoto, G. B., Bustamante, M. M. da C., Pinto, A. S., & Klink, C. A. (2006). Nutrient use efficiency at ecosystem and species level in savanna areas of Central Brazil and impacts of fire. *Journal of Tropical Ecology*, *22*(2), 191–201. https://doi.org/10.1017/S0266467405002865

O'Brien, M., Hanapi, J., Reynolds, G., & Walsh, R. (2026). *Danum/Malua compiled climate data 1985 to 2025* [Dataset]. Zenodo. https://doi.org/10.5281/zenodo.18159592

O'Brien, M. J., Hector, A., Ong, R., & Philipson, C. D. (2024). Tree growth and survival are more sensitive to high rainfall than drought in an aseasonal forest in Malaysia. *Communications Earth & Environment*, *5*(1), 179. https://doi.org/10.1038/s43247-024-01335-5

O'Brien, M. J., Valtat, A., Abiven, S., Studer, M. S., Ong, R., & Schmid, B. (2020). The role of soluble sugars during drought in tropical tree seedlings with contrasting tolerances. *Journal of Plant Ecology*, *13*(4), 389–397. https://doi.org/10.1093/jpe/rtaa017

Oliveras, I., Girardin, C., Doughty, C. E., Cahuana, N., Arenas, C. E., Oliver, V., Huaraca Huasco, W., & Malhi, Y. (2014). Andean grasslands are as productive as tropical cloud forests. *Environmental Research Letters*, *9*(11), 115011. https://doi.org/10.1088/1748-9326/9/11/115011

Oliveras, I., Meirelles, S. T., Hirakuri, V. L., Freitas, C. R., Miranda, H. S., & Pivello, V. R. (2012). Effects of fire regimes on herbaceous biomass and nutrient dynamics in the Brazilian savanna. *International Journal of Wildland Fire*, *22*(3), 368–380. https://doi.org/10.1071/WF10136

Philipson, C. D., Cutler, M. E. J., Brodrick, P. G., Asner, G. P., Boyd, D. S., Moura Costa, P., Fiddes, J., Foody, G. M., van der Heijden, G. M. F., Ledo, A., Lincoln, P. R., Margrove, J. A., Martin, R. E., Milne, S., Pinard, M. A., Reynolds, G., Snoep, M., Tangki, H., Sau Wai, Y., … Burslem, D. F. R. P. (2020). Active restoration accelerates the carbon recovery of human-modified tropical forests. *Science*, *369*(6505), 838–841. https://doi.org/10.1126/science.aay4490

Phillips, O. L. (2023). Sensing forests directly: The power of permanent plots. *Plants*, *12*(21), 3710. https://doi.org/10.3390/plants12213710

Pivello, V. R., Oliveras, I., Miranda, H. S., Haridasan, M., Sato, M. N., & Meirelles, S. T. (2010). Effect of fires on soil nutrient availability in an open savanna in Central Brazil. *Plant and Soil*, *337*(1), 111–123. https://doi.org/10.1007/s11104-010-0508-x

Plumanns-Pouton, E., Santos, J. L., Aponte, C., Brotons, L., Kelly, L. T., Mason Jr., S. C., Parris, K., Ponisio, L., & Keith, D. A. (2025). The mechanisms through which fire drives population change in terrestrial biota. *Global Change Biology*, *31*(9), e70479. https://doi.org/10.1111/gcb.70479

Poorter, H. (1989). Plant growth analysis: Towards a synthesis of the classical and the functional approach. *Physiologia Plantarum*, *75*(2), 237–244. https://doi.org/10.1111/j.1399-3054.1989.tb06175.x

Prestes, N. C. C. S., Marimon, B. S., Morandi, P. S., Reis, S. M., Junior, B. H. M., Cruz, W. J. A., Oliveira, E. A., Mariano, L. H., Elias, F., Santos, D. M., Esquivel-Muelbert, A., & Phillips, O. L. (2024). Impact of the extreme 2015-16 El Niño climate event on forest and savanna tree species of the Amazonia-Cerrado transition. *Flora*, *319*, 152597. https://doi.org/10.1016/j.flora.2024.152597

Qie, L., Lewis, S. L., Sullivan, M. J. P., Lopez-Gonzalez, G., Pickavance, G. C., Sunderland, T., Ashton, P., Hubau, W., Abu Salim, K., Aiba, S.-I., Banin, L. F., Berry, N., Brearley, F. Q., Burslem, D. F. R. P., Dančák, M., Davies, S. J., Fredriksson, G., Hamer, K. C., Hédl, R., … Phillips, O. L. (2017). Long-term carbon sink in Borneo's forests halted by drought and vulnerable to edge effects. *Nature Communications*, *8*(1), 1966. https://doi.org/10.1038/s41467-017-01997-0

Reich, P. B. (2014). The world-wide 'fast–slow' plant economics spectrum: A traits manifesto. *Journal of Ecology*, *102*(2), 275–301. https://doi.org/10.1111/1365-2745.12211

Reis, S. M., de Oliveira, E. A., Elias, F., Gomes, L., Morandi, P. S., Marimon, B. S., Marimon Junior, B. H., das Neves, E. C., de Oliveira, B., & Lenza, E. (2017). Resistance to fire and the resilience of the woody vegetation of the "Cerradão" in the "Cerrado"–Amazon transition zone. *Brazilian Journal of Botany*, *40*(1), 193–201. https://doi.org/10.1007/s40415-016-0336-1

Reis, S. M., Lenza, E., Marimon, B. S., Gomes, L., Forsthofer, M., Morandi, P. S., Marimon Junior, B. H., Feldpausch, T. R., & Elias, F. (2015). Post-fire dynamics of the woody vegetation of a savanna forest (Cerradão) in the Cerrado-Amazon transition zone. *Acta Botanica Brasilica*, *29*, 408–416. https://doi.org/10.1590/0102-33062015abb0009

Reis, S. M., Malhi, Y., Marimon Junior, B. H., Schwantes Marimon, B., Zhang-Zheng, H., Araújo, I., Freitag, R., Almeida de Oliveira, E., da Silva Peixoto, K., Januário de Souza, L., Souza da Silva, E. L., Bernardes Santos, E., Parreira da Silva, K., Alves Gonçalves, M. D., Girardin, C., Dahlsjö, C., L. Phillips, O., & Oliveras Menor, I. (2025). Sensitivity of tropical woodland savannas to El Niño droughts. *Biogeosciences*, *22*(15), 3949–3964. https://doi.org/10.5194/bg-22-3949-2025

Riutta, T., Kho, L. K., Teh, Y. A., Ewers, R., Majalap, N., & Malhi, Y. (2021). Major and persistent shifts in below-ground carbon dynamics and soil respiration following logging in tropical forests. *Global Change Biology*, *27*(10), 2225–2240. https://doi.org/10.1111/gcb.15522

Riutta, T., Malhi, Y., Kho, L. K., Marthews, T. R., Huaraca Huasco, W., Khoo, M., Tan, S., Turner, E., Reynolds, G., Both, S., Burslem, D. F. R. P., Teh, Y. A., Vairappan, C. S., Majalap, N., & Ewers, R. M. (2018). Logging disturbance shifts net primary productivity and its allocation in Bornean tropical forests. *Global Change Biology*, *24*(7), 2913–2928. https://doi.org/10.1111/gcb.14068

Rocha, W., Metcalfe, D. B., Doughty, C. E., Brando, P., Silvério, D., Halladay, K., Nepstad, D. C., Balch, J. K., & Malhi, Y. (2014). Ecosystem productivity and carbon cycling in intact and annually burnt forest at the dry southern limit of the Amazon rainforest (Mato Grosso, Brazil). *Plant Ecology & Diversity*, *7*(1–2), 25–40. https://doi.org/10.1080/17550874.2013.798368

Rossatto, D. R., & Franco, A. C. (2017). Expanding our understanding of leaf functional syndromes in savanna systems: The role of plant growth form. *Oecologia*, *183*(4), 953–962. https://doi.org/10.1007/s00442-017-3815-6

Rowland, L., da Costa, A. C. L., Oliveira, A. A. R., Oliveira, R. S., Bittencourt, P. L., Costa, P. B., Giles, A. L., Sosa, A. I., Coughlin, I., Godlee, J. L., Vasconcelos, S. S., Junior, J. A. S., Ferreira, L. V., Mencuccini, M., & Meir, P. (2018). Drought stress and tree size determine stem CO_2 efflux in a tropical forest. *New Phytologist*, *218*(4), 1393–1405. https://doi.org/10.1111/nph.15024

Scalon, M. C., Maia Chaves Bicalho Domingos, F., Jonatar Alves da Cruz, W., Marimon Júnior, B. H., Schwantes Marimon, B., & Oliveras, I. (2020). Diversity of functional trade-offs enhances survival after fire in Neotropical savanna species. *Journal of Vegetation Science*, *31*(1), 139–150. https://doi.org/10.1111/jvs.12823

Scalon, M. C., Oliveras Menor, I., Freitag, R., Peixoto, K. S., Rifai, S. W., Marimon, B. S., Marimon Junior, B. H., & Malhi, Y. (2022). Contrasting strategies of nutrient demand and use between savanna and forest ecosystems in a neotropical transition zone. *Biogeosciences*, *19*(15), 3649–3661. https://doi.org/10.5194/bg-19-3649-2022

Shipley, B. (2006). Net assimilation rate, specific leaf area and leaf mass ratio: Which is most closely correlated with relative growth rate? A meta-analysis. *Functional Ecology*, *20*(4), 565–574. https://doi.org/10.1111/j.1365-2435.2006.01135.x

Singh, J., Boucher, P. B., Hockridge, E. G., & Davies, A. B. (2023). Effects of long-term fixed fire regimes on African savanna vegetation biomass, vertical structure and tree stem density. *Journal of Applied Ecology*, *60*(7), 1223–1238. https://doi.org/10.1111/1365-2664.14435

Slik, J. W. F., Bernard, C. S., Van Beek, M., Breman, F. C., & Eichhorn, K. A. O. (2008). Tree diversity, composition, forest structure and aboveground biomass dynamics after single and repeated fire in a Bornean rain forest. *Oecologia*, *158*(3), 579–588. https://doi.org/10.1007/s00442-008-1163-2

Toma, T., Ishida, A., & Matius, P. (2005). Long-term monitoring of post-fire aboveground biomass recovery in a lowland dipterocarp forest in East Kalimantan, Indonesia. *Nutrient Cycling in Agroecosystems*, *71*(1), 63–72. https://doi.org/10.1007/s10705-004-0381-1

Trugman, A. T., & Anderegg, L. D. L. (2025). Source vs sink limitations on tree growth: From physiological mechanisms to evolutionary constraints and terrestrial carbon cycle implications. *New Phytologist*, *245*(3), 966–981. https://doi.org/10.1111/nph.20294

Vourlitis, G. L., Pinto Jr., O. B., Dalmagro, H. J., Enrique Zanella de Arruda, P., de Almeida Lobo, F., & de Souza Nogueira, J. (2022). Net primary production and ecosystem carbon flux of Brazilian tropical savanna ecosystems from eddy covariance and inventory methods. *Journal of Geophysical Research: Biogeosciences*, *127*(8), e2021JG006780. https://doi.org/10.1029/2021JG006780

Wright, I. J., Cooke, J., Cernusak, L. A., Hutley, L. B., Scalon, M. C., Tozer, W. C., & Lehmann, C. E. R. (2019). Stem diameter growth rates in a fire-prone savanna correlate with photosynthetic rate and branch-scale biomass allocation, but not specific leaf area. *Austral Ecology*, *44*(2), 339–350. https://doi.org/10.1111/aec.12678

Wright, I. J., Reich, P. B., Westoby, M., Ackerly, D. D., Baruch, Z., Bongers, F., Cavender-Bares, J., Chapin, T., Cornelissen, J. H. C., Diemer, M., Flexas, J., Garnier, E., Groom, P. K., Gulias, J., Hikosaka, K., Lamont, B. B., Lee, T., Lee, W., Lusk, C., … Villar, R. (2004). The worldwide leaf economics spectrum. *Nature*, *428*(6985), 821–827. https://doi.org/10.1038/nature02403

Zhang-Zheng, H., Adu-Bredu, S., Duah-Gyamfi, A., Moore, S., Addo-Danso, S. D., Amissah, L., Valentini, R., Djagbletey, G., Anim-Adjei, K., Quansah, J., Sarpong, B., Owusu-Afriyie, K., Gvozdevaite, A., Tang, M., Ruiz-Jaen, M. C., Ibrahim, F., Girardin, C. A. J., Rifai, S., Dahlsjö, C. A. L., … Malhi, Y. (2024). Contrasting carbon cycle along tropical forest aridity gradients in West Africa and Amazonia. *Nature Communications*, *15*(1), 3158. https://doi.org/10.1038/s41467-024-47202-x

Zhou, Y., Singh, J., Butnor, J. R., Coetsee, C., Boucher, P. B., Case, M. F., Hockridge, E. G., Davies, A. B., & Staver, A. C. (2022). Limited increases in savanna carbon stocks over decades of fire suppression. *Nature*, *603*(7901), 445–449. https://doi.org/10.1038/s41586-022-04438-1

Ziegler, C., Cochard, H., Stahl, C., Foltzer, L., Gérard, B., Goret, J.-Y., Heuret, P., Levionnois, S., Maillard, P., Bonal, D., & Coste, S. (2024). Residual water losses mediate the trade-off between growth and drought survival across saplings of 12 tropical rainforest tree species with contrasting hydraulic strategies. *Journal of Experimental Botany*, *75*(13), 4128–4147. https://doi.org/10.1093/jxb/erae159